Isolation, structure elucidation and testing of secondary metabolites from fungi of the genus *Lactarius* and *Mycena*

Dissertation

To obtain the degree of Doctor of Natural Sciences

(Dr. rer. nat.)

Submitted to Department 2 (Biology/Chemistry)

of the University of Bremen

in November 2024

by

Yahya Fathhi Yousef Al Qudah

1. **Referee: Prof. Dr. Peter Spiteller**
2. **Referee: Prof. Dr. Franz-Peter Montforts**

Day of the public colloquium: December 12, 2024

Dedicated to my family.

Erklärung

Ich, Yahya Fathhi Yousef Al Qudah, Matrikelnummer 3200468, versichere an Eides Statt durch meine Unterschrift, dass ich die vorstehende Arbeit selbständig und ohne fremde Hilfe angefertigt und alle Stellen, die ich wörtlich dem Sinne nach aus Veröffentlichungen entnommen habe, als solche kenntlich gemacht habe, mich auch keiner anderen als der angegebenen Literatur oder sonstiger Hilfsmittel bedient habe.

Ich versichere an Eides Statt, dass ich die vorgenannten Angaben nach besten Wissen und Gewissen gemacht habe und dass die Angaben der Wahrheit entsprechen und ich nichts verschwiegen habe.

Die Strafbarkeit einer falschen eidesstattlichen Versicherung ist mir bekannt, namentlich die Strafandrohung gemäß § 156 StGB bis zu drei Jahren Freiheitsstrafe oder Geldstrafe bei vorsätzlicher Begehung der Tat bzw. gemäß § 161 Abs. 1 StGB bis zu einem Jahr Freiheitsstrafe oder Geldstrafe bei fahrlässiger Begehung.

Erklärungen zur elektronischen Version und zur Überprüfung einer Dissertation;

Hiermit ich gemäß §7, Abs. 7, Punkt 4, dass die zu Prüfungszwecken beigelegte elektronische Version meiner Dissertation identisch ist mit der abgegebenen gedruckten Version.

Ich bin mit der Überprüfung einer Dissertation gemäß §6 Abs. 2, Punkt 5 mit qualifizierter Software im Rahmen der Untersuchung von Plagiatsvorwürfen einverstanden.

Bremen, 05.11.2024

Ort, Datum

Declaration

I, Yahya Fathhi Yousef Al Qudah, student number 3200468, I certify under oath by my signature that I have completed the above work independently and without outside help and that I have identified all passages that I have literally taken from publications as such, and that I have not used any literature other than the specified literature or anything else used aids.

I declare under oath that I have provided the above information to the best of my knowledge and belief and that the information is true and that I have not concealed anything.

I am aware of the criminal liability of a false affidavit, namely the penalty in accordance with Section § 156 of the German Criminal Code (StGB) of up to three years imprisonment or a fine if the offence is committed intentionally, or in accordance with Section § 161 Paragraph 1 of the German Criminal Code (StGB) of up to one year imprisonment or a fine if the offence is committed negligently.

Statements on the electronic version and the review of a dissertation;

I hereby declare in accordance with Section 7, Paragraph 7, Item 4 that the electronic version of my dissertation enclosed for review purposes is identical to the printed version submitted.

I agree to the review of a dissertation in accordance with Section 6, Paragraph 2, Item 5 using qualified software as part of the investigation into allegations of plagiarism.

Bremen, 05.11.2024

Place, Date

Acknowledgements

My greatest thanks go to my family, especially my parents for the unconditional support that made my studies possible.

My sincere gratitude is sent to Prof. Dr. Peter Spiteller for sharing this fascinating subject, providing me with good assistance, allowing me tremendous freedom in creating goals and questions and creating a terrific work environment.

I would like to thank Prof. Dr. Franz-Peter Montforts from Bremen University for kindly taking over the second report and Prof. Dr. Tim Neudecker from Bremen University for leading the examining committee.

Especial thanks also to Prof. Dr. Markus Plaumann from Otto-von-Guericke-Universität Magdeburg for the valuable scientific discussions, support, and for participation in the examining committee. In addition, I would like to express my gratitude to Dr. Wieland Willker and Mr. Dipl.-Ing. Johannes Stelten for their assistance with NMR experiments and the numerous productive conversations with rational structural suggestions for unidentified metabolites. I would also like to thank Dr. Thomas Dülcks and Ms. Dipl.-Ing. Dorit Kemken for the acquisition of mass spectra and their support in the interpretation of mass spectrometric data.

I would especially like to thank Mrs. Ingrid Killer for her outstanding technical assistance and mental support throughout my doctoral work. Additionally, I would also like to thank Mrs. Dörte Riemer for her support and assistance with my bureaucratic inquiries. Also, I like to thank Miss Amelie Sprengel for her support and technical assistance.

I would like to thank all current and former colleagues in the Spiteller working group for their constant willingness to help and many discussions as well as the pleasant atmosphere. Special thanks go to Dr. Rieke Himstedt, Dr. Freya Müller, Miss Sinja Müller, Mr. Lennart Schmiedeken, Dr. Patrick Swieca, Dr. Arne Helmers, Dr. Felix Mysegaes, Dr. Hedda Schrey, Dr. Julia Lohmann, Mrs. Luisa Rebecka Plitzko, and Mr. Björn Meyer. Also, I would like to thank Mr. Markus Winkler for his valuable feedback and support and for taking part in the examining committee. As well as I would also like to thank my research interns, bachelor's and master's students, Miss Annika Hanna Drees, Mr. Mathis Kohröde, Mr. Christian Janssen, Mr. Marvin Breier, and Mr. Lennart Wunderlich for their efforts and collaboration. Also, I would like to thank Miss Simone Carola Bandte for taking part in the examining committee.

Table of contents

1 Summary – Zusammenfassung

Zusammenfassung

In dieser Arbeit geht es um die Isolierung und Strukturaufklärung bisher unerforschter Sekundärmetabolite aus Fruchtkörpern der Pilze *Lactarius circellatus*, *Lactarius trivialis* und *Mycena zephirus*.

In der Spiteller-Gruppe wurde *L. circellatus* bereits zuvor auf seinen Gehalt an Sequiterpenoiden untersucht und fünf unbekannte und mehrere bekannte Sequiterpenoide identifiziert und ihre Strukturen aufgeklärt. Allerdings konnten ihre Stereokonfiguration sowie die Protonen- und Kohlenstoffresonanzen in ihren NMR-Spektren bisher nicht vollständig zugeordnet werden.

Daher wurden erneut NMR-Spektren der zuvor isolierten Sequiterpene aufgenommen. Darüber hinaus wurden Fruchtkörper von *L. circellatus* erneut extrahiert und auf das Vorhandensein neuer Verbindungen untersucht, was zur Isolierung des bisher unbekannten Sequiterpenoids 12-Hydroxy-15-carboxyblennin A (**19**) zusammen mit Hydroxyblennin A (**34**) führte.

Eine sorgfältige Analyse der Kopplungskonstanten im ^{1}H-NMR, eine Analyse der NOE-Korrelationen in den NOESY-Spektren und eine detaillierte Analyse der Korrelationen in den HMBC-Spektren hinsichtlich ihres Diederwinkels gemäß der Karplus-Beziehung ermöglichten die Bestimmung des relativen Konfiguration aller isolierten Sequiterpenoide, einschließlich der bisher unveröffentlichten neuen Sequiterpenoide 12-Hydroxy-15-carboxyblennin A (**19**), 7,15-Dihydroxyblennin A (**20**), 2,3-Epoxylactarorufin A (**21**), 14-Carboxydesoxylactarorufin A (**22**) und 13-Hydroxy-14-carboxydesoxylactarorufin A (**23**). Um die absolute Konfiguration der isolierten Sequiterpenoide zu bestimmen, wurden CD-Spektren gemessen und mit den entsprechenden berechneten CD-Spektren verglichen. Dadurch konnte die absolute Stereochemie der Sequiterpenoide **19** bis **23** ermittelt werden. Allerdings stimmten die gemessenen und berechneten CD-Spektren von **22** und **23** nicht perfekt überein.

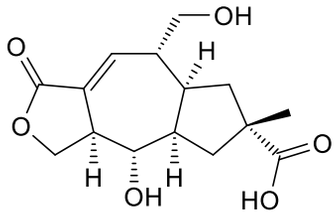

19

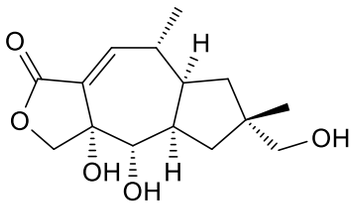

20

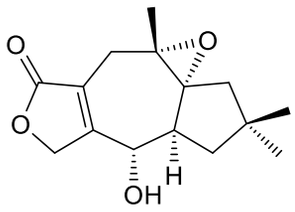

21

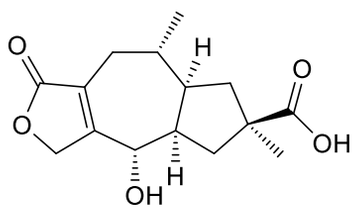

22

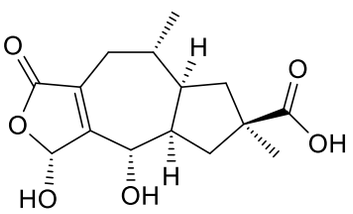

23

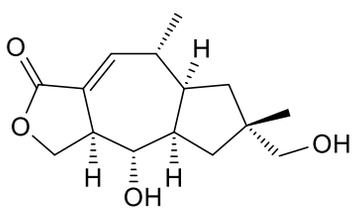

34

Bisher gibt es keine Berichte über die Farbstoffe von *L. circellatus*, obwohl dieser auf der Hutoberfläche eine graugrüne Farbe aufweist, ähnlich wie *Lactarius blennius*. Daher wurde das Pigment isoliert und seine Struktur als Blennion (**35**) aufgeklärt, das gleiche Pigment, das in *L. blennius* vorhanden ist. Es wurde festgestellt, dass Blennion (**35**) in *L. circellatus* viel häufiger vorkommt als in *L. blennius*, dem Pilz, aus dem es ursprünglich isoliert wurde. Es wurden einige biologische Tests durchgeführt, aber Blennion (**35**) zeigte keine Aktivität. Darüber hinaus wurde eine geringe Menge eines rosafarbenen Pigments in *L. blennius* gefunden, das mit Lilacinon (**37**) verwandt ist, einem rosafarbenen Pigment, das zuvor aus *L. lilacinus* isoliert und strukturell aufgeklärt wurde.

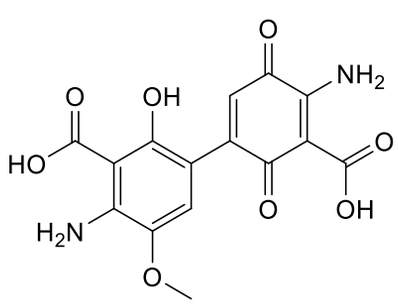

Blennione (**35**)

Frische Fruchtkörper von *Lactarius trivialis* weisen auf der Hutoberfläche eine intensive violette Farbe auf, die mit zunehmendem Alter der Fruchtkörper verblasst. Die dafür verantwortlichen Farbstoffe wurden bisher nicht untersucht. Daher wurden die Fruchtkörper von *L. trivialis* einer umfassenden Untersuchung ihrer Sekundärmetaboliten mit einem Schwerpunkt auf ihre Farbstoffen unterzogen.

Nicht ganz unerwartet erwies sich die Isolierung der Pigmente aus der Huthaut aufgrund der geringen Stabilität der Pigmente als schwierig, insbesondere wenn Methanol als Lösungsmittel verwendet wurde. Eine Extraktion mit Aceton mit anschließender Säulenchromatographie an Sephadex LH20 mit Aceton als Lösungsmittel und anschließende Reinigung der Pigmente mittels

semipräparativer HPLC führte jedoch zur Isolierung von fünf farbigen Verbindungen, die als Trivialine A (**47**), B, C, D und E bezeichnet wurden. Aufgrund ihrer HR-ESI-MS-Daten sind die fünf Pigmente der Verbindungen eng miteinander verwandt und weisen einen hohen Grad an Ungesättigtheit auf. Nur im Falle von Trivialin A (**47**) und Trivialin B reichte die isolierte Menge aus, um einen vollständigen Satz ein- und zweidimensionaler NMR-Spektren aufzunehmen. Folglich konzentrierte sich die Strukturaufklärung auf diese beiden Verbindungen, die beide die Summenformel C32H20N4O6 aufweisen. Aufgrund des hohen Ungesättigtheitsgrades und der geringen Anzahl nicht austauschbarer Protonen, die zu einem Mangel an Korrelationen im HMBC führten, erwies sich die Strukturaufklärung als sehr anspruchsvoll. Dennoch konnte für Trivialin A (**47**) eine vorläufige Struktur vorgeschlagen werden.

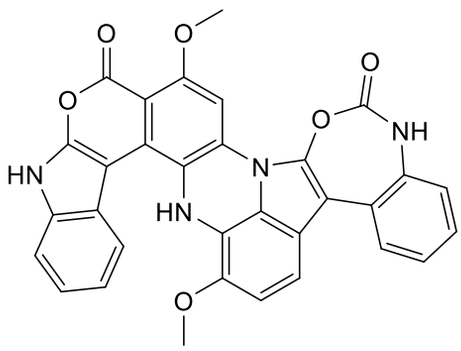

47

Darüber hinaus wurden Fruchtkörper von *L. trivialis* auf das Vorhandensein neuer Sesquiterpenoide untersucht. So wurde die neue Verbindung 14-Hydroxylactarorufin B (**53**) isoliert und ihre Struktur aufgeklärt. Darüber hinaus wurde festgestellt, dass die bereits aus anderen Pilzen bekannten Verbindungen Lactarufin B (**27**) und 14-Hydroxyblennin A (**52**) auch in *L. trivialis* vorkommen.

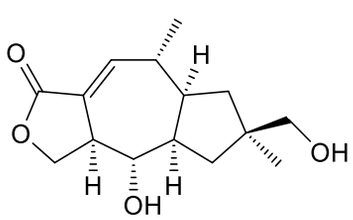

52

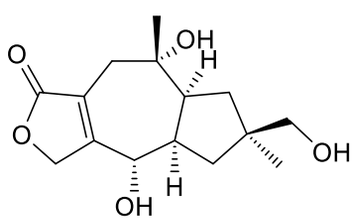

53

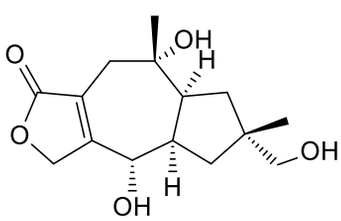

27

Bisher wurde 14-Hydroxyblennin A (**52**) nur aus *Russula sanguinea* beschrieben, die publizierten NMR-Daten passen jedoch perfekt zu 15-Hydroxyblennin A (**34**), während die NMR-Daten des entsprechenden Sesquiterpens aus *L. trivialis* sehr gut zur Struktur von 14-Hydroxyblennin A (**52**) passen. Folglich muss die Struktur im oben erwähnten Manuskript über *R. sanguinea* zu 15-Hydroxyblennin A (**34**) revidiert werden.

Neben Pilzen der Gattung *Lactarius* wurden im Rahmen dieser Arbeit auch Fruchtkörper von *Mycena zephirus* auf ihr Vorkommen an Sekundärstoffen untersucht und die Strukturen zweier Verbindungen als N^5-Isopentylglutamin (**54**) und N^5-2-Methylbutylglutamin (**55**) aufgeklärt.

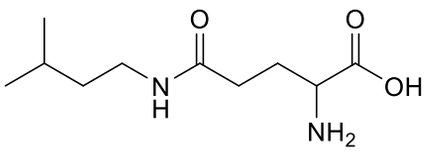

54

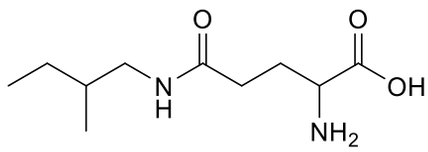

55

Summary

This thesis is about the isolation and structure elucidation of so far uninvestigated secondary metabolites from fruiting bodies of the mushrooms *Lactarius circellatus*, *Lactarius trivialis* and *Mycena zephirus*.

In the Spiteller group *L. circellatus* has already been investigated before for its content of sequiterpenoids and five unknown and several known sequiterpenoids have been identified and their structures have been elucidated. However, their stereo configuration, the proton and carbon resonances in their NMR spectra have not been fully assigned so far. Therefore, NMR spectra of the previously isolated sequiterpenes were recorded again. Moreover, fruiting bodies of *L. circellatus* were extracted again and investigated for the presence of new compounds, resulting in the isolation of the so far unknown sequiterpenoid 12-hydroxy-15-carboxyblennin A (**19**) together with hydroxyblennin A (**34**). A careful analysis of the coupling constants in the ^{1}H NMR, the analysis of the NOE correlations in the NOESY spectra, and a detailed analysis of the correlations in the HMBC spectra in respect to their dihedral angle according to the Karplus relationship allowed to determine the relative configuration of all isolated sequiterpenoids, including the so far unpublished new sequiterpenoids 12-hydroxy-15-carboxyblennin A (**19**), 7,15-dihydroxyblennin A (**20**), 2,3-epoxylactarorufin A (**21**),14-carboxy-deoxylactarorufin A (**22**), and 13-hydroxy-14-carboxy-deoxylactarorufin A (**23**). To determine the absolute configuration of the isolated sequiterpenoids, CD spectra were recorded and compared with the corresponding calculated CD spectra. By these means the absolute stereochemistry of the sequiterpenoids **19** to **23** could be determined. However, the measured and calculated CD spectra of **22** and **23** were not matching perfectly.

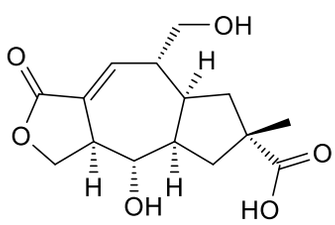

19

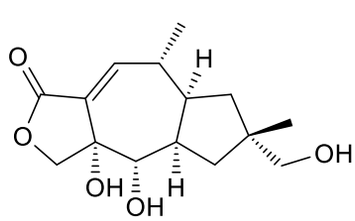

20

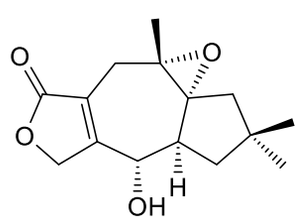

21

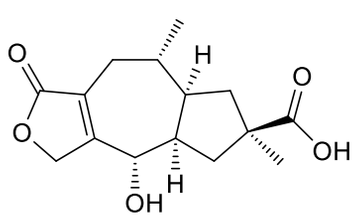

22

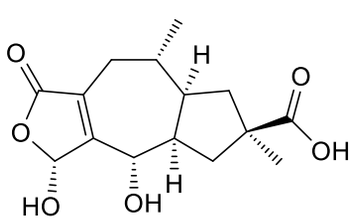

23

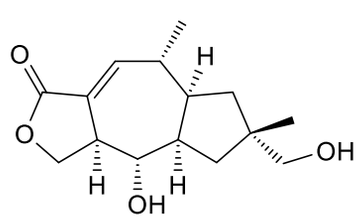

34

So far, there have been no reports about pigments from *L. circellatus*, despite the fact that it exhibits on the surface of its cap a grayish green color similarly to *L. blennius*. Consequently, the pigment was isolated and its structure elucidated to be blennione (**35**), the same pigment that is

present in *L. blennius*. Blennione (**35**) was found to be much more abundant in *L. circellatus* than in *L. blennius,* the mushroom it was originally isolated from. Some biological tests were performed but blennione (**35**) displayed no activity. In addition, tiny amount of a pink pigment from *L. blennius* was found related to lilacinone (**37**), a pink pigment that was isolated and structurally elucidated before from *L. lilacinus.*

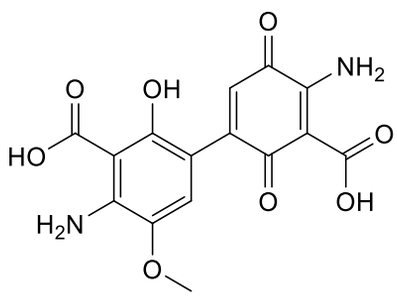

Blennione (**35**)

Fresh fruiting bodies *of Lactarius trivialis* display an intensive violet color on the cap surface that is fading away upon ageing of the fruiting bodies. The responsibe pigments have not been investigated so far. Therefore, fruiting bodies of *L. trivialis* were subjected to a comprehensive investigation of their secondary metabolites with a focus on their pigments.

Not entirely unexpectedly, the isolation of the pigments from the skin cap turned out to be difficult due to the low stability of the pigments, especially when methanol was used as a solvent. However, an extraction with acetone with subesquent column chromatography on Sephadex LH20 with acetone as a solvent followed by purification of the pigments with semi-preparative HPLC resulted in the isolation of five colored compounds, that were named trivialines A (**47**), B, C, D, and E. Due to their HR-ESI-MS data, the compounds five pigments are closely related to each other and show a high degree of unsaturation. Only in the case of trivialine A (**47**) and trivialine B the isolated amount was sufficient to record a full set of one and two dimensional NMR spectra. Consequently, the structure elucidation focussed on these two compounds, both exhibiting a molecular formula of $C_{32}H_{20}N_4O_6$. Due to the high degree of unsaturation, the low number of unexchangable protons, leading to a lack of corellations in the HMBC, the structure elucidation turned out to be very challenging. Nevertheless, for trivialine A (**47**) a tentative structure was proposed.

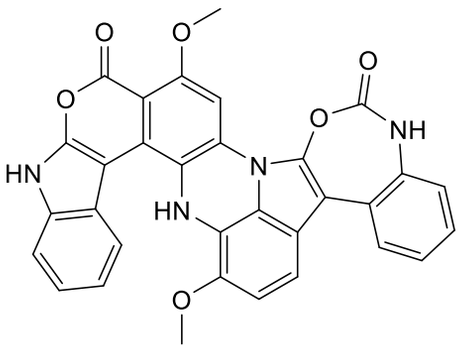

47

Moreover, fruiting bodies of *L. trivialis* were investigated for the presence of new sesquiterpenoids. Thus, the new compound 14-hydroxylactarorufin B (**53**) was isolated and its structure elucidated. In addition, the lactarorufin B (**27**) and 14-hydroxyblennin A (**52**), both known from other mushrooms, were also identified to be present in *L. trivialis*.

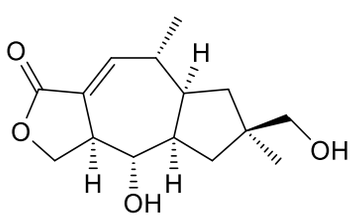

52

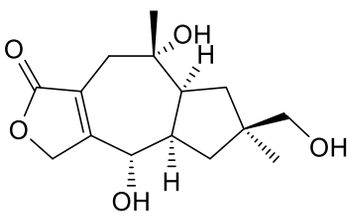

53

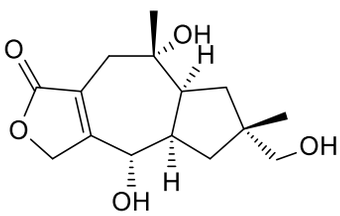

27

So far, 14-hydroxyblennin A (**52**) was reported only from *Russula sanguinea*, but the published NMR data fit perfectly to 15-hydroxyblennin A (**34**), while the NMR data from the corresponding sesquiterpene from *L. trivialis* fit very well to the structure of 14-hydroxyblennin A (**52**). Consequently, the structure in the above mentioned manuscript about *R. sanguinea* has to be revised to 15-hydroxyblennin A (**34**).

Apart from mushrooms of the genus *Lactarius*, in this thesis also fruiting bodies of *Mycena zephirus* were investigated in respect to their secondary metabolite content and the structures of two compounds were elucidated to be N^5-isopentylglutamine (**54**) and N^5-2-methylbutylglutamine (**55**), respectively.

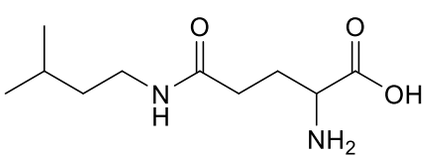

54

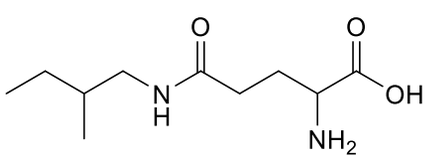

55

2 Introduction

2.1 Secondary metabolites from fungi

Secondary metabolites or specialized metabolites are compounds that are created by living things, including fungi, bacteria, plants, and animals that are not like primary metabolites directly responsible for the main metabolic functions of the organism, such as the growth, maintenance, and reproduction.[1] Nevertheless, secondary metabolites might play a very important role in the organism acting as hormones, messenger substances, pigments, and fragrances, and might be important for the chemical defence of an organism.[2] The latter occurs in mushrooms in several different forms, such as constitutive chemical defence, wound-activated chemical defence, and induced chemical defence.[3]

In pharmacy, secondary metabolites from a variety of fungal species have already been applied. The most well-known example of this is the antibiotic penicillin G (**1**), commonly known as benzylpenicillin, a β-lactam ring derivative, that was found in the mold *Penicillium rubens*.[4] Because of its antibiotic efficiency, the attention of research into bioactive secondary metabolites increased worldwide.[5] Subsequently, more antibiotics have been extracted from fungi, including cephalosporins (β-lactam ring derivatives) from the *Acremonium* fungal species, like cephalosporin C (**2**) that was isolated from *A. chrysogenum*.[6]

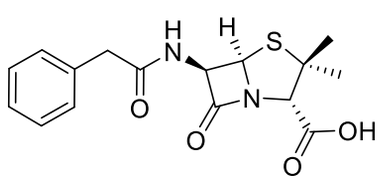

Penicillin G (**1**)

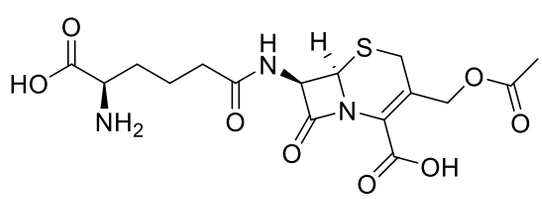

Cephalosporin C (**2**)

In addition to the medicinal benefits of naturally occurring substances isolated from fungi, some secondary metabolites from fungi also act as fungicides such as strobulin A (**3**) which was isolated from the mycelium of *Strobilurus tenacellus*.[7]

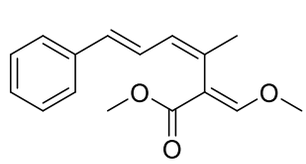

Strobilurin A (**3**)

2.2 Sesquiterpenes

Sesquiterpenes are a type of terpenes that is composed of three isoprene (**4**) molecules with a molecular formula often consisting of fifteen carbon atoms and at least twenty-four hydrogen atoms. So far, sequiterpenes with hundreds of different carbon skeletons have been isolated from natural sources, such as marine plants, terrestrial plants, fungi, and microorganisms.[8] Some of these metabolites extracted from *Lactarius* mushrooms can be considered characteristic for a distinct member of this genus.[9] Many sequiterpenes exhibit interesting biological activities, making them a great interest in research and scientific investigations.[10] For instance, some of them have shown medicinal promise in slowing the growth of cancer.[11]

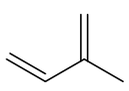

Isoprene (**4**)

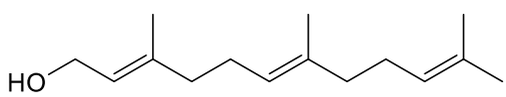

Farnesol (**5**)

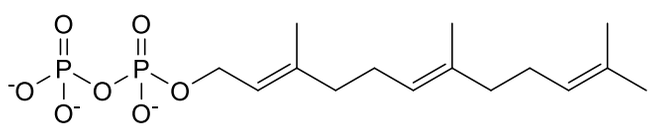

Farnesyl pyrophosphate (FPP) (**6**)

Ruzicka was the first one to propose that sesquiterpenes are products of the cyclization of an intermediate that commonly occurs or exists in living beings.[12] Initially, farnesol (**5**) was proposed to be the intermediate that forms the ring skeletons in such a group of compounds.[13] Subsequently, cyclization of the diphosphate ester farnesyl pyrophosphate (FPP) (**6**) can take place resulting in a huge variety of different terpene skeletons, (Fig. 1).[14]

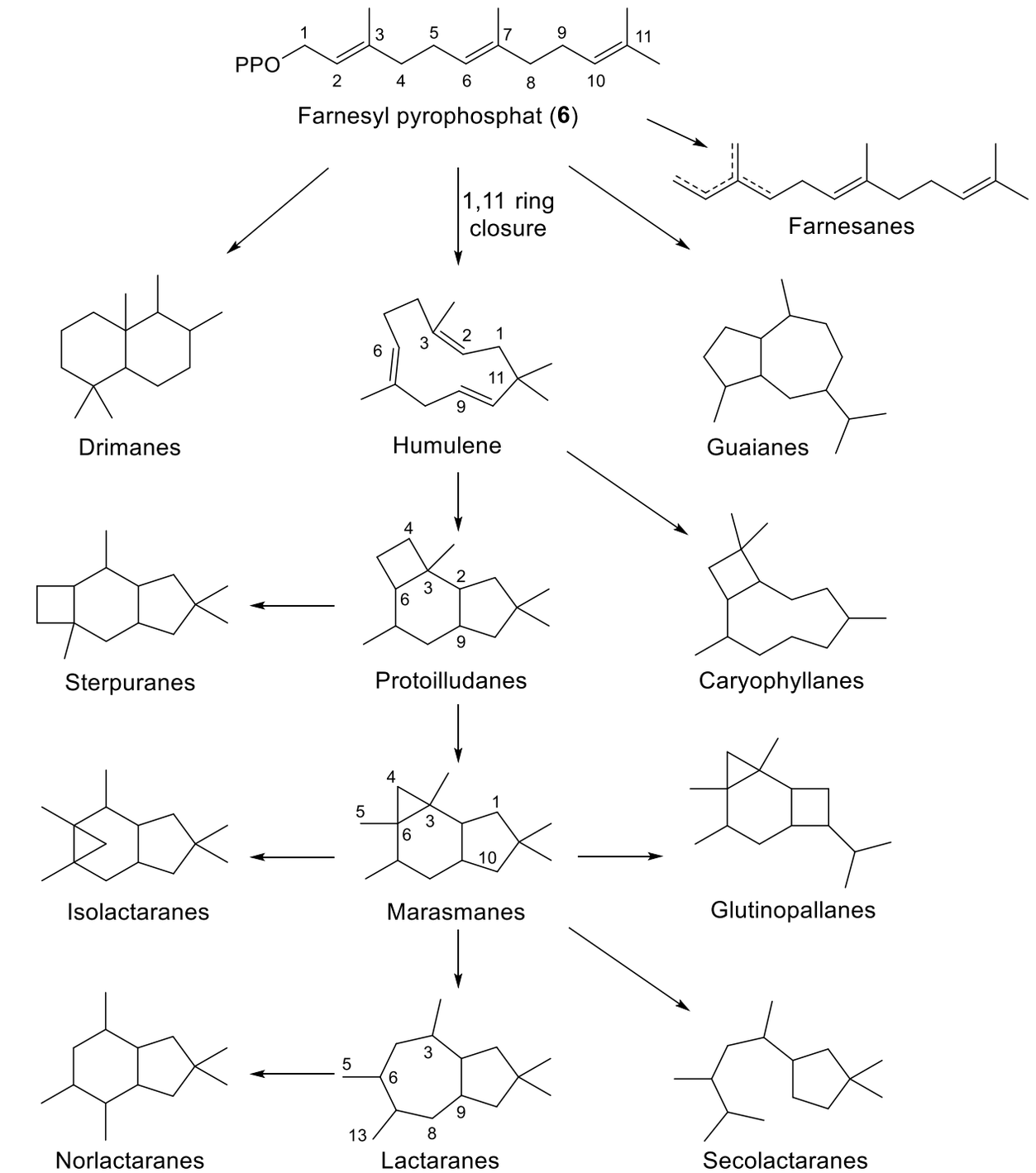

Figure. 1. Proposed biosynthesis of sesquiterpenes from *Lactarius* mushrooms, by DANIEWSKI and VIDARI in 1999.[9]

This wide variety of proposed classes of compounds was validated by the isolation of many compounds related to them from natural sources such as fungi.[9] However, not all of the skeletons above have been found in mushrooms so far. Moreover, a large number of volatile sesquiterpenes can also be produced.[15]

One of the cyclization biosynthetic pathways starting with connection of carbons 1 and 11 in **6** produces after several more steps the so-called lactarane sesquiterpenes. The oxygenated members of this class of compounds represent the majority of the sesquiterpenoids that have been isolated from *Lactarius* species.[9] [Sesquiterpenoids are a class of natural product-derived

compounds that are produced when cytochrome P450 monooxygenases oxygenate sesquiterpenes.][16]

Sesquiterpenoids isolated from *Lactarius* mushrooms consist of many classes the majority belong to the 5-lactarnolide sesquiterpenes class, (Fig. 2). Also, a significant number of the isolated sesquiterpenoids belong to furanolactarane and seco-5-lactaronlide sesquiterpenes. In this research, the focus will be on the isolated compounds from *L. circellatus* and *L. trivialis* that belong to the previously mentioned sesquiterpenoids classes.

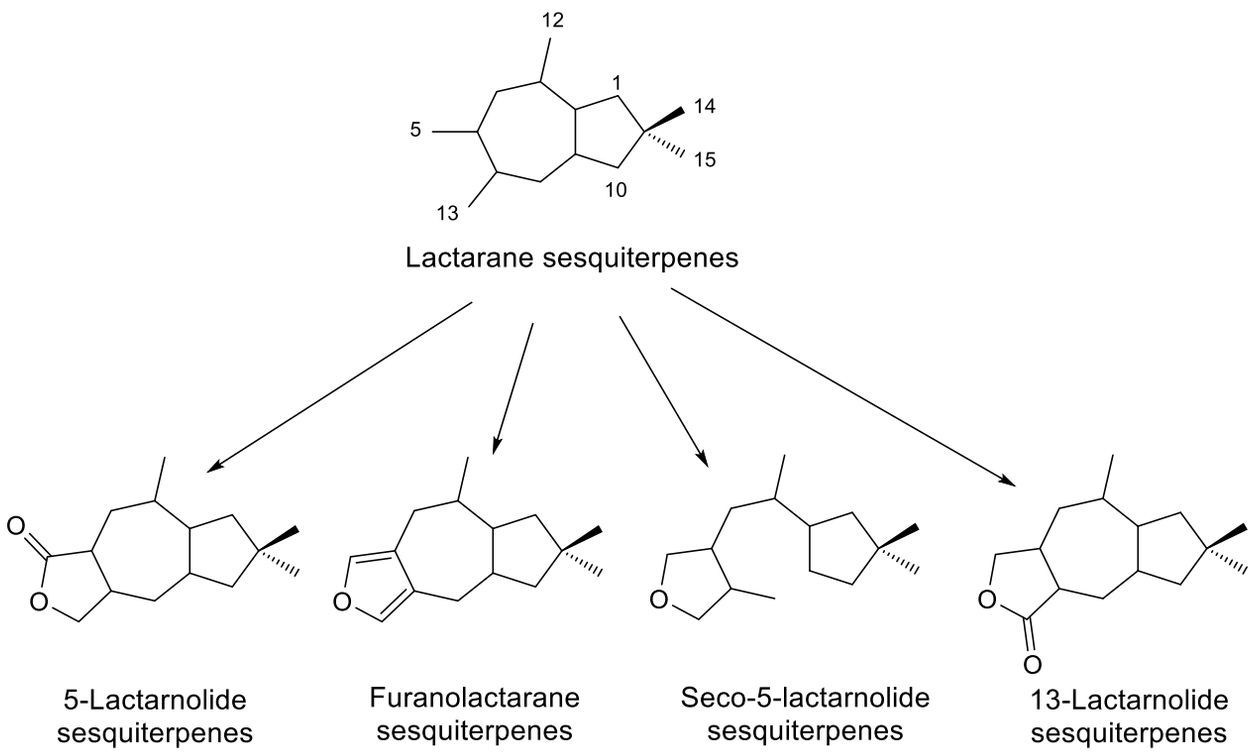

Figure. 2. Some of sesquiterpenoids classes derived from lactarane sesquiterpenes that had been isolated from *Lactarius* mushrooms.

2.3 Karplus equation

Some of the HMBC correlations of the methylene groups in the isolated sesquiterpenoids from the *Lactarius* species in this research exhibit an anomaly as one proton in the methylene group correlates with some of its neighboring carbons but not the other proton. This observation can be explained using the Karplus equation. Accordingly, such a pattern can be used to assign the stereo configuration of the methylene protons and other moieties in these compounds. Consequently, an understanding of the Karplus equation came into effect.

The Karplus equation (F1) shows the mathematical relationship between an observed coupling constant value (*J*) and the dihedral angle (φ) between two neighboring (vicinal) hydrogen atoms,[17] (Fig. 3-Left).

F1 $$J(\varphi) = A\cos^2(\varphi) + B\cos(\varphi) + C$$

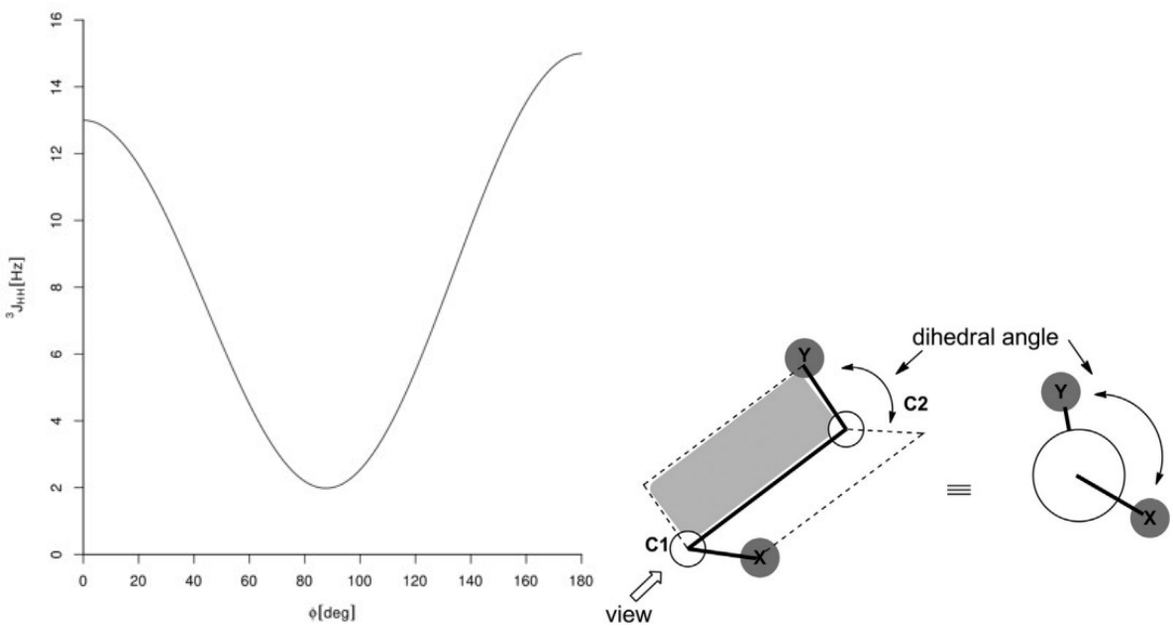

Figure. 3. Left: Karplus curve.[18] Right: Dihedral angle between atoms X and Y through atoms C1 and C2.[19]

The dihedral angle is when four atoms are connected together while the second and the third atoms bond together in the middle, then the dihedral angle will be the angle between the imaginary plane created from the bond between the first and the second atoms through this middle bond, and the other imaginary plane created from the bond between the third and the fourth atoms through the same middle bond, (Fig. 3-Right).

The Karplus equation is based on the assumption (supported by empirical data) that vicinal H-H couplings ($^3J_{HH}$) should be at their maximum for protons with dihedral angles of 180° and 0°, and that these couplings should be at their minimum for protons with 90°, which could be near zero.

These relationships can also be applied to couplings between hydrogen and carbon atoms ($^3J_{HC}$) in the 2D-NMR experiment HMBC, which will be utilized here in this research. All kinds of coupling constants will be referred to with (*J*).

3 Aim and scope of this work

The aim of this research work is to investigate, isolate, elucidate and test biologically unknown secondary metabolites from fruiting bodies of the fungi *Lactarius circellatus*, *Lactarius trivialis*, and *Mycena zephirus*.

For this purpose, extracts have to be prepared using organic solvents such as methanol or acetone. Then, the substance mixtures have to be separated using various separation methods such as liquid-liquid partitioning, solid phase extraction, HPLC and size exclusion chromatography in order to isolate the individual substances from these extracts. The structures of the isolated compounds have to be subsequently elucidated using high-resolution mass spectrometry and various NMR experiments. To evaluate the biological activity of the isolated compounds, agar diffusion assays with selected bacteria as test organisms have to be performed.

In the case of *L. circellatus*, the aim is to assign the relative configuration of the stereo centres of the new and known sesquiterpenoids isolated thereof using NMR spectroscopic methods. In addition, the proton NMR resonances of the diastereotopic protons are to be completely assigned. Moreover, CD spectra have to be recorded and compared with calculated CD spectra in order to determine the absolute configurations of the new compounds. In addition, it is intended to isolate new sesquiterpenoids as well as the dark green pigment from this mushroom.

The surface of the cap of fruiting bodies of *L. trivialis* shows a dark purple color, which has not been investigated so far and gradually, fades after collection. The color change indicates a low stability of the pigment. The structures of these previously unknown colored compounds should be isolated and their structures elucidated. In addition, this fungus should be investigated for the presence of potential new sesquiterpenoids.

No secondary metabolites have been reported from the mushroom *M. zephirus*. Therefore, potential new secondary metabolites should be isolated and structurally elucidated from fruiting bodies of this fungus.

4 Results and discussion

4.1 *Lactarius circellatus*

4.1.1 Description of *L. circellatus*

Lactarius circellatus is a toxic fungus also known as banded or/and hornbeam milkcap (Gebänderter Hainbuchenmilchling). It is a species of the family of *Russulaceae* (Täublingsverwandten).[20] The species is a mycorrhizal fungus of the hornbeam trees (Hainbuche). This means the fungus has a coexistent relationship with the tree roots as the result of a symbiotic union called mycorrhizal symbiosis, between a fungus and a plant.[21] This symbiosis occurs at the level of plant roots, where fungal hypha extends from the fungal mycelium to colonize the roots of the host plant.[22]

Figure. 4. Fruiting bodies of *Lactarius circellatus*.[23]

The mushroom has a smell of combined mild fruit-to-root aroma. The cap is between 5 to 10 cm in diameter, with a color range between grey-brown to grey-dark olive with relatively white stems that are 4 to 10 cm long, (Fig. 4). The lamellae are whitish, cream to ocher-orange colored. The fruiting bodies appear between June and October.

4.1.2 Current state of knowledge

Lactarius circellatus was investigated for the presence of sesquiterpenoids already some time ago.[24] In 1989 STERNER *et*,. *al*. were especially interested in bioactive compounds, such as velleral (**9**), vellerol (**10**), 7-*epi*-piperdial (**11**), and *epi*-piperalol (**12**), lactarorufin N (**13**), the furanol **14**, the furandiol **15**, the dihydroxyfuran **16**, lactardial (**17**), and blennin C (**18**). These compounds are probably defence agents that are generated from stearoylvelutinal (**7**) and **8** upon injury of the fruiting bodies via a wound-activated chemical defence mechanism.[24]

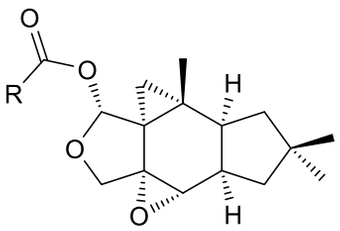

R = -$(CH_2)_{16}$-CH_3 **7**
R = -$(CH_2)_4$-CO-$(CH_2)_{11}$-CH_3 **8**

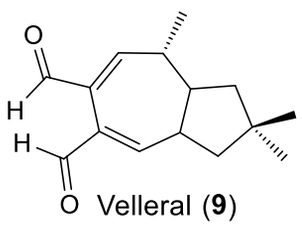

Velleral (**9**)

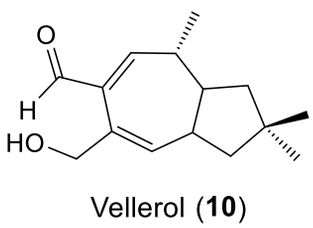

Vellerol (**10**)

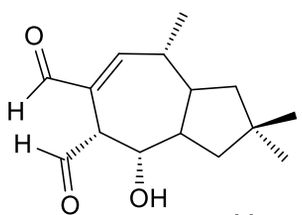

7-*epi*-Piperdial (**11**)

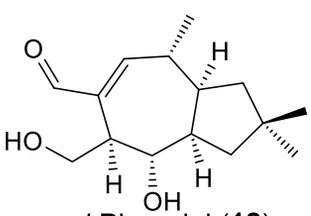

epi-Piperalol (**12**)

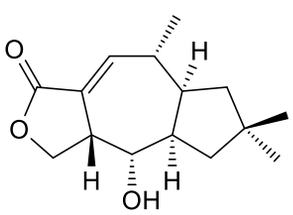

Lactarorufin N (**13**)

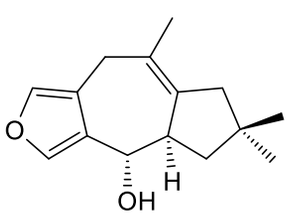

Furanol **14**

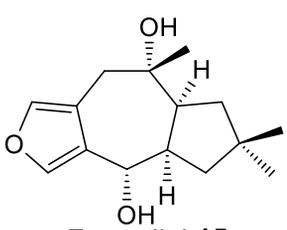

Furandiol **15**

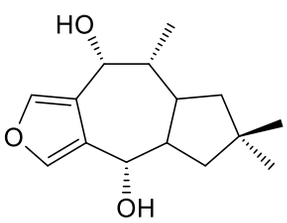

Dihydroxyfuran **16**

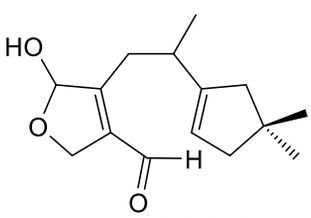

Lactardial (**17**)

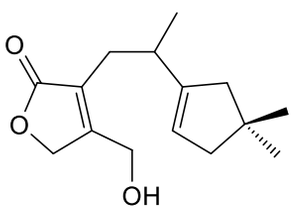

Blennin C (**18**)

The fatty acid esters stearoylvelutinal (**7**) was isolated from *Lactarius vellereus*,[25] while 6-ketostearoylvelutinal (**8**) was isolated from *Lactarius necator* before.[26] These compounds are the only sequiterpenoids that exist in intact fruiting bodies of *Lactarius* species.[24] Upon wounding of the fruiting bodies, a hydrolyase is activated, cleaving the fatty acid residue off from stearoylvelutinal (**7**) and ketostearoylvelutinal (**8**), respectively, leading to the degradation of the resulting instable sequiterpenoid to the above mentioned sequiterpenoids **9** to **18**. [24]

In the years 2016, 2017, and 2018, Dr. S. Tareq, a postdoctoral researcher in the Spiteller group, reinvestigated *L. circellatus* for the presence of so far undescribed sequiterpenoids. He isolated and elucidated the structures of the new compounds 7,15-dihydroxyblennin A (**20**), 2,3-epoxylactarorufin A (**21**), 14-carboxy-deoxylactarorufin A (**22**) and 13-hydroxy-14-carboxy-deoxylactarorufin A (**23**).* Moreover, he isolated and identified the known sequiterpenoids lactarotropone (**24**), lactarorufin A (**25**), deoxylactarorufin A (**26**), lactarorufin B (**27**), the furan alcohol **28**, the methoxyfuranalcohol **29**, 3,8-oxalactarorufin A (**30**), and 3,12-anhydrolactarorufin A (**31**) for the first time in the mushroom *L. circellatus* alongside with furandiol **15**, lactarorufin N (**13**) and blennin C (**18**) that have been reported before to be present in this mushroom.[24] However, the stereochemistry of the compounds and the resonances of the diastereotopic protons in the ^{1}H NMR have not been fully assigned so far.

* Unpublished results.

4.1.3 Isolation and structure elucidation of sesquiterpenoids

Lactarius circellatus is closely related to *L. blennius*, which is known to produce anti-inflammatory compounds.[27] Consequently, it is not astonishing that also *L. circellatus* contains interesting bioactive secondary metabolites according to a previous investigation of this mushroom in the Spiteller group by Dr. S. Tareq. Because the stereochemistry of the new compounds and the resonances in the NMR have not been not completely assigned, the fruiting bodies of *L. circellatus* were extracted, separated and spectra of the isolated compounds were recorded again to investigate the above mentioned compounds further and to find new sequiterpenoids.

Thus, the new 5-lactarnolide sesquiterpene 12-hydroxy-15-carboxyblennin A (**19**) and the known compound 15-hydroxyblennin A (**34**) were isolated and their structures elucidated.

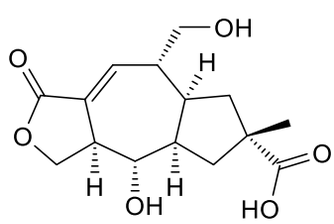

19

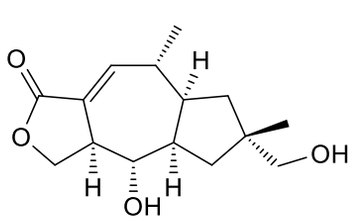

34

Moreover, the relative and the absolute configuration of most stereocenters of the above mentioned compounds were determined and the proton resonances of the diasterotopic protons were assigned. For this purpose, especially NOESY and HMBC spectra were used.

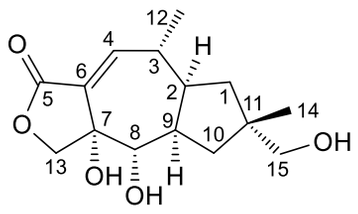

20

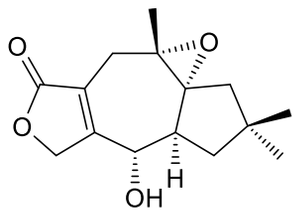

21

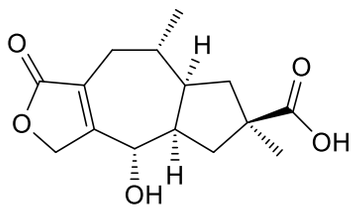

22

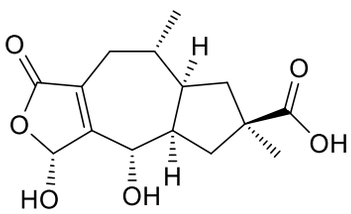

23

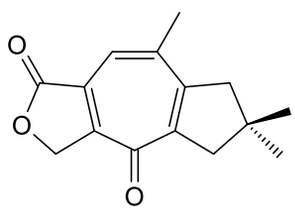

24

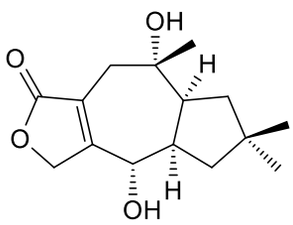

25

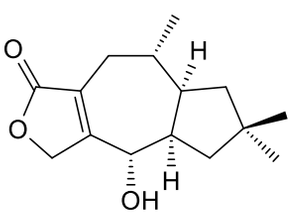

26

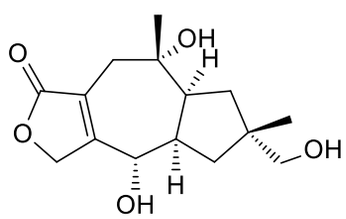

27

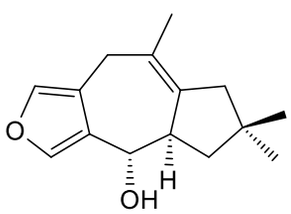

28

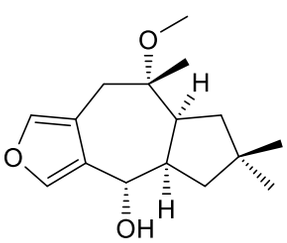

29

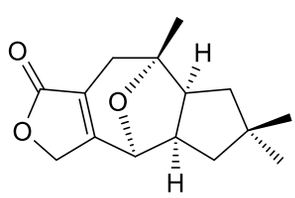

30

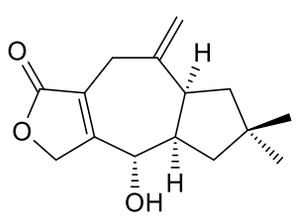

31

In addition, before this research, further investigations aiming to extract more sesquiterpenoids compounds from *L. circellatus* were pursued and the new compounds 7,15-dihydroxyblennin A (**20**), 2,3-epoxylactarorufin A (**21**), 14-carboxy-deoxylactarorufin A (**22**) and 13-hydroxy-14-carboxy-deoxylactarorufin A (**23**) were extracted and their structure elucidated. Also the known compounds, lactarotropone (**24**), lactarorufin A (**25**), deoxylactarorufin A (**26**), lactarorufin B (**27**), furan alcohol **28**, methoxyfuranalcohol **29**, 3,8-oxalactarorufin A (**30**) and 3,12-anhydrolactarorufin A (**31**) were extracted for the first time from the mushroom alongside with the already known compounds furandiol **15**, lactarorufin N (**13**) and blennin C (**18**) that were reported to be exist in this mushroom.[24]

4.1.3.1 12-Hydroxy-15-carboxyblennin A (**19**)

4.1.3.1.1 Structure elucidation

A fraction was prepared from the *Lactarius circellatus* flesh adapting the extraction method described in section 6.3.1.3, followed by SPE filtration to produce a (1:1) pre-separation fraction. This fraction was introduced to semi-preparative HPLC separation method A described in section 6.3.4.1, to produce 1.1 mg of compound **19** out of 135 g of the mushroom fruiting bodies. The separated compound was detected with a UV-detector, at a wavelength of λ 235 nm.

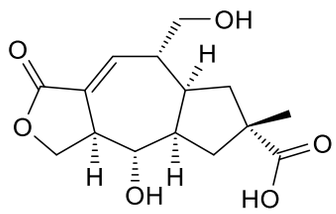

12-Hydroxy-15-carboxyblennin A
(**19**)

The HR-ESI-(+)-MS spectrum of compound **19** (Fig. 5) exhibits an $[M+H]^+$ ion at *m/z* 297.13238 and a corresponding $[2M+H]^+$ ion at *m/z* 593.25817 leading to the molecular formula $C_{15}H_{20}O_6$. Using the molecular formula, the degrees of unsaturation (DoU) can be calculated via the formula F2 to be 6 DoU for compound **19**.

F2 $\quad DoU = (2C+2+N-X-H) / 2$

- *C* is the number of carbons
- *N* is the number of nitrogens
- *X* is the number of halogens (F, Cl, Br, I)
- *H* is the number of hydrogens

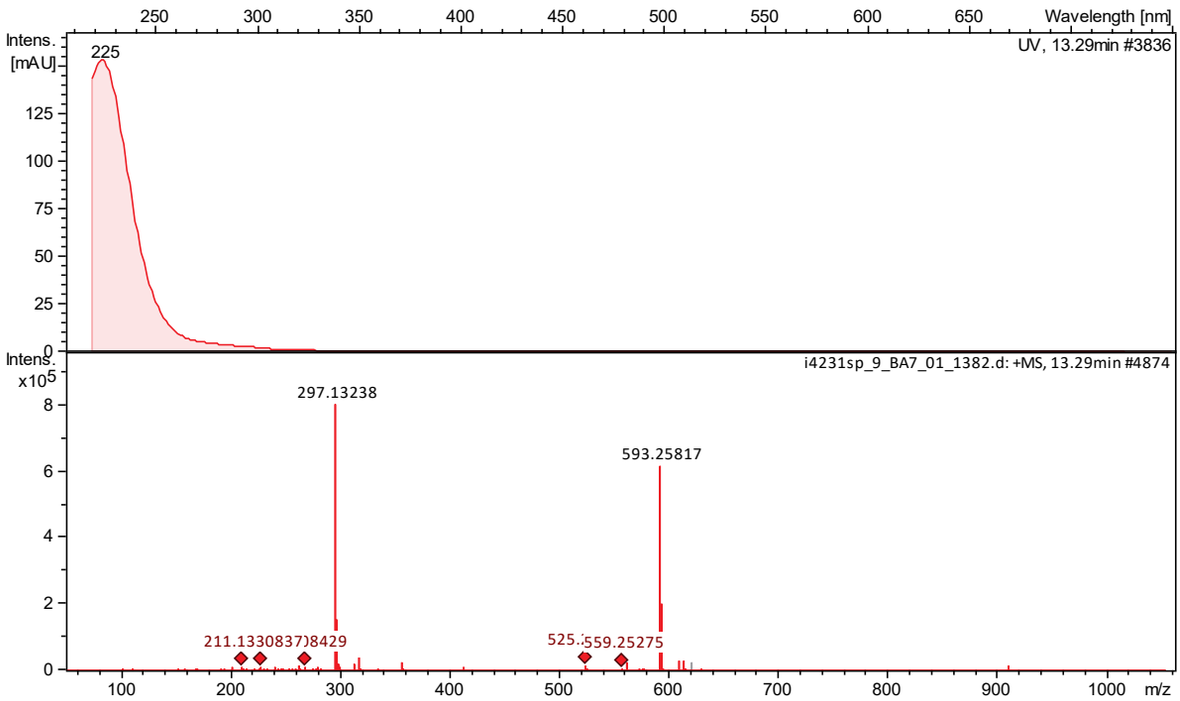

Figure. 5. HR-ESI-(+)-MS and UV/Vis-spectrums of compound **19** from *L. circellatus*.

In *Lactarius* species such a molecular formula of 15 carbon atoms and a similar number of hydrogen and oxygen atoms usually corresponds to a group of compounds called 5-lactarnolide sesquiterpenes, (Fig. 6), that are extracted from *Lactarius* species. An additional factor that is sesquiterpenes exhibit a very clear signal of $[2M+H]^+$ ion in MS spectrums. Accordingly, such a frame structure was considered.

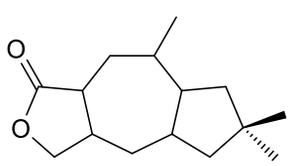

Figure. 6. 5-Lactarnolide sesquiterpenes general structure.

The ^{1}H-NMR spectrum of **19**, recorded at 297.2 K in CD_3OD (Fig. 7), exhibits 17 non-exchangeable protons. According to the HSQC and DEPT135 data, see section 9.1. The 15 signals displayed in the ^{13}C-NMR spectrum were assigned to 1 CH_3 group, 4 CH_2 groups, 6 CH groups, and four quaternary carbon atoms.

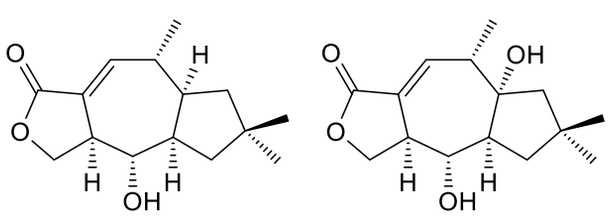

Blennin A (**32**) Blennin D (**33**)

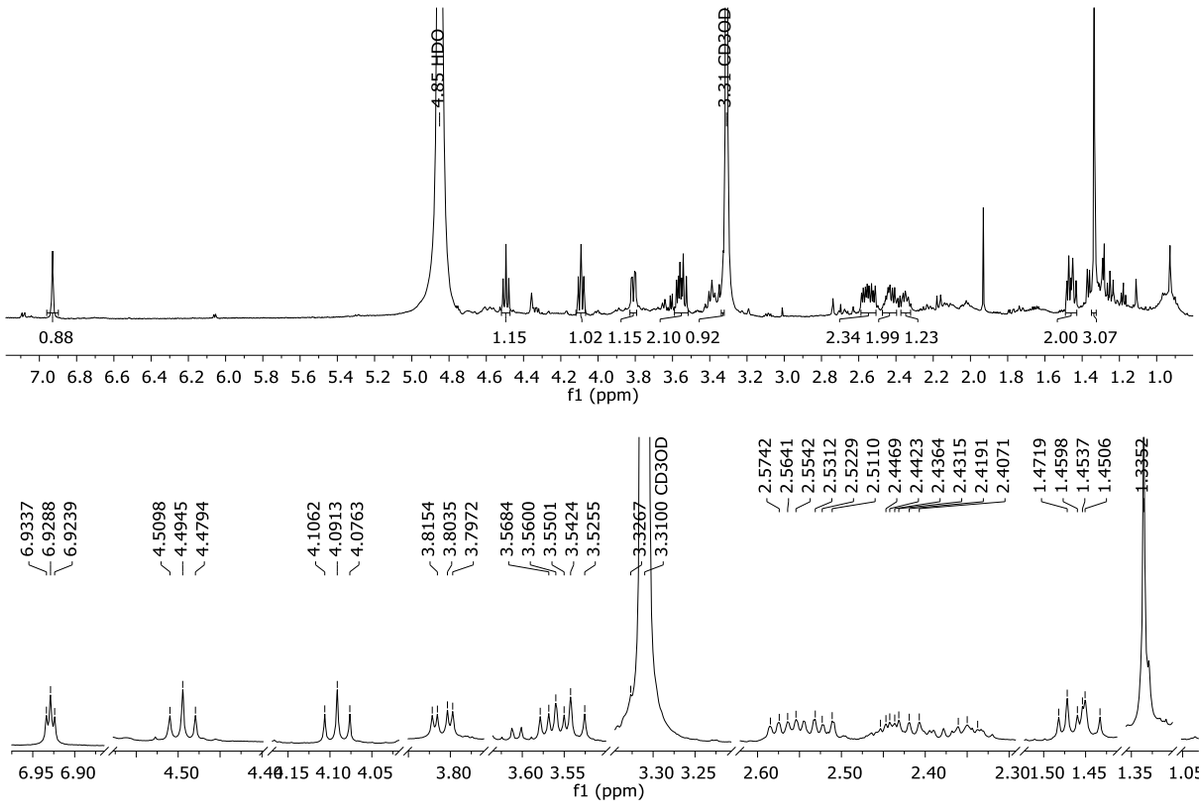

Figure. 7. ^{1}H-NMR-spectrum (600.22 MHz, CD3OD, 297.2 K) of compound **19** from *L. circellatus*.

The HSQC and COSY-spectrums revealed the presence of a C=CH–CH moiety, two separated oxygenated methylene groups CH_2–O, and two neighboring CH–CH_2–C moieties one of them coupling with a CH–CH(O)–CH fragment. The protons and carbon atoms of the C=CH–CH group exhibit chemical shifts similar to those of the corresponding C=CH–CH fragment of lactarorufin N (**13**). The vinylic proton in this moiety with chemical shifts at δ_H 6.93 couples with the proton at δ_H 2.45 that is attached to a carbon that correlates in the HMBC (Fig. 8) with the oxygenated methylene protons at δ_H 3.56 and δ_H 3.81. This corresponds also to similar spin systems in blennin A (**32**)[28] as well as blennin D (**33**)[29] and 15-hydroxyblennin A (**34**).[30] C=CH–CH fragment in lactarorufin N (**13**) has similar chemical shifts with (C-3, δ_H 2.53, δ_c 33.50), (C-4, δ_H 6.73, δ_c 146.27), and (C-6, δ_c 127.35). This assumption was verified with the existence of HMBC correlations with the carbonyl carbon at δ_C 173.94, that also one of the protons of the oxygenated methylene CH_2–O at (δ_H 4.49, δ_C 70.85) correlates with. This will locate the typical lactone ring that exists in such lactarane sesquiterpenes, accordingly assigning this carbonyl carbon to be at position 5, therefore, the vinylic proton is at carbon 4.

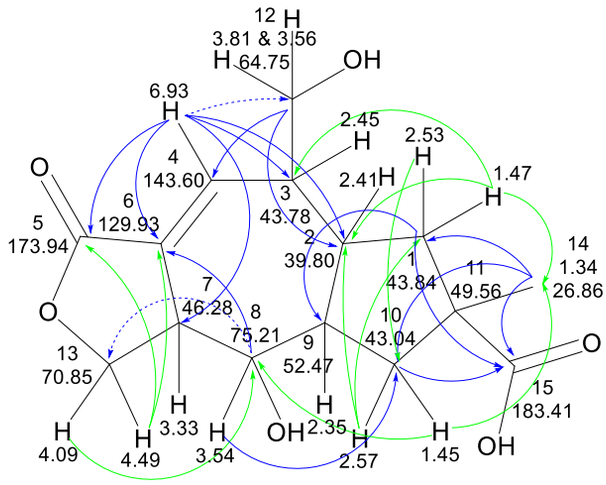

Figure. 8. Structure of compound **19** with selected HMBC correlations (⟶) and HMBC correlations with Karplus relationship (⟶), (CD_3OD).

The center proton in the CH–CH(OH)–CH fragment with the chemical shift at (δ_H 3.54, δ_C 75.21) correlates with the quaternary carbon in the C=CH–CH moiety as well as with one of the methylene carbons in the CH–CH_2–C moiety. Subsequently, this proton will be assigned to be at C-8, the quaternary carbon to be at C-6, and the methylene carbon to be at C-10. The later methylene group has correlations with the other methylene group CH–CH_2–C moiety alongside the only methyl CH_3 group in this compound also with the carboxylic acid carbon with the chemical shift at δ_C 183.41. This will form the typical cyclopentane ring in such lactarane compounds, also similar in lactarorufin N (**13**) for carbons 1 and 10 (C-1, δ_H 1.40 and 1.52, δ_C 45.58), (C-10, δ_H 1.44 and 1.66, δ_C 44.33). The previously assigned protons at C-1 from CH–CH_2–C fragment and the vinylic proton at C-4 have HMBC correlations with the carbon with chemical shift at δ_C 43.78. This will continue and connect the coupling spin system to such compound and form the seven-membered ring in the middle between the lactone ring and the cyclopentane ring, accordingly assigning this carbon at position 3.

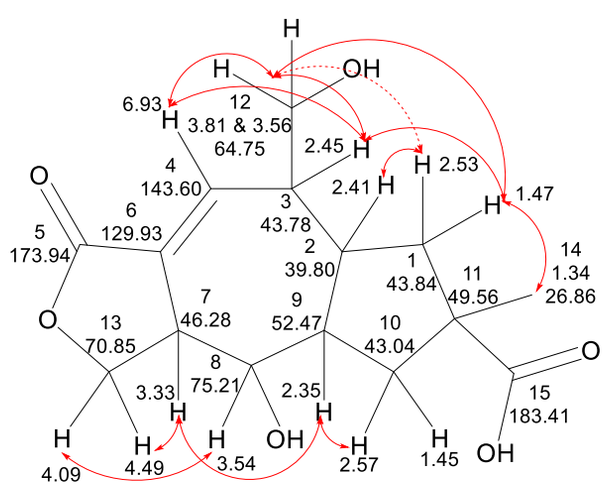

Figure. 9. Structure of compound **19** with selected NOESY correlations (↔), (CD_3OD).

NOE experiments (Fig. 9) and the Karplus relationship from the HMBC data (Fig. 8) has been used for assigning the relative stereo configuration of compound **19**.[17, 31] The two protons at the carbons connecting the cyclopentane ring and the seven-membered ring at δ_H 2.41 (C-2) and at δ_H 2.35 (C-9) exhibit both correlations in the COSY and the NOESY with its neighboring protons. The proton at δ_H 2.41 shows NOE correlation with the methylene proton at δ_H 2.53 at C-1 but not with the other at 1.47. The proton at δ_H 2.35 exhibits correlations in the NOESY with the methylene proton at δ_H 2.57 (C-10) and with the proton at δ_H 3.33 (C-7). Accordingly, the previously mentioned protons are oriented to the same side. Consequently, the proton at δ_H 1.47 (C-1) is oriented in the opposite direction.

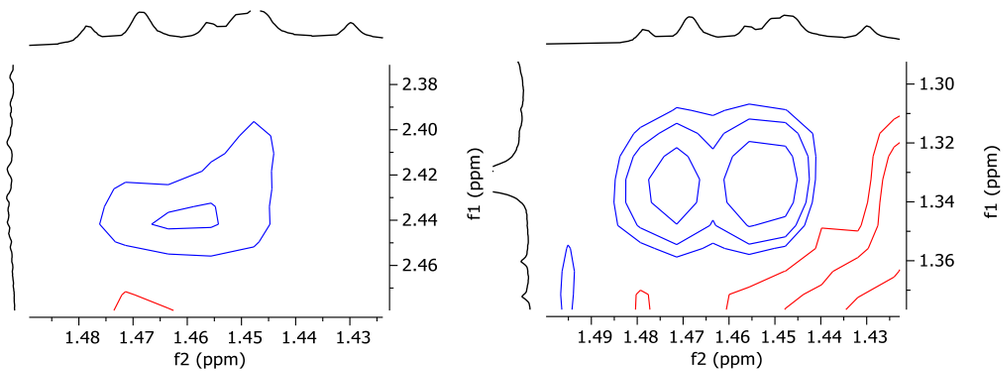

Figure. 10. NOESY expanded-spectrums of selected correlations, (CD_3OD).
Left: between protons at δ_H 1.47 and 2.45. Right: between protons at δ_H 1.47 and 1.34.

This proton shows NOESY correlations with the methyl protons at δ_H 1.34 (C-14) and the proton at δ_H 2.45 (C-3) (Fig. 10), subsequently assigning them to be on the same side of the compound. Therefore, the carboxyl group (C-15) is oriented to the opposite side as the methyl group (C-14). Also, the proton at δ_H 1.47 has an HMBC correlation with neighbor carbons in three cases but not to the other proton from this methylene group as it should be (Fig. 11), making the Karplus relationship applied here.

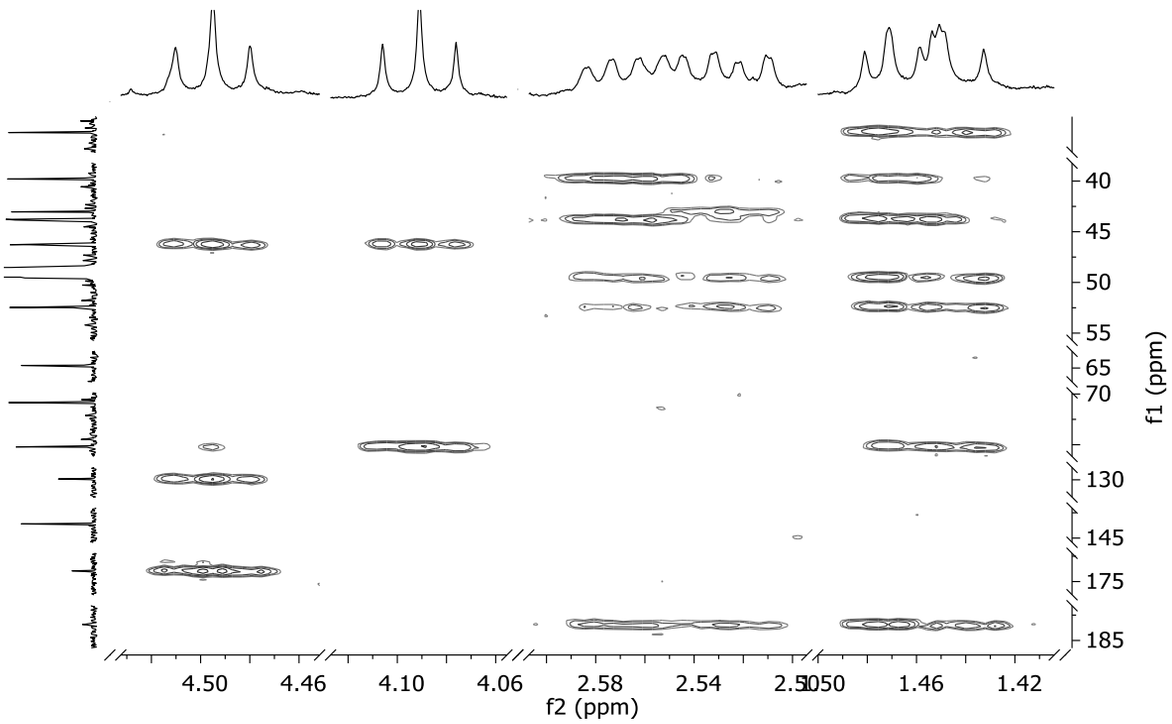

Figure. 11. HMBC concentrated-spectrum of selected correlations between protons at δ_H 1.40 and 4.6, (CD_3OD).

The pattern of lacking correlations exists with all of the three methylene groups existing in this compound. For example, the spectrum shows clearly how the two protons at δ_H 4.09 and 4.49 at δ_C 70.85 have HMBC correlations with carbon at δ_C 46.28 but only the proton at δ_H 4.09 has a clear correlation with carbon at δ_C 75.21, with only small partial correlation with the other proton in this methylene group. Also, there are two clear correlations between proton at δ_H 4.49 and carbons at δ_C 129.93 and 173.94, with no such correlations existing with the other proton at δ_H 4.09.

Similarly, protons of the methylene group at δ_C 43.84 show such a pattern as the proton at δ_H 2.53 has HMBC correlation with carbon at δ_C 43.04 but not the other proton at δ_H 1.47. Also, the later proton has three correlations with carbons at δ_C 26.86, 39.80, and 43.78 but there are no correlations between these carbons and the other proton – at δ_H 2.53 – in this methylene group.

One more example is the HMBC data from the methylene group at δ_C 43.04, as it exhibits a similar observation of the existence of correlations between one of the protons in this group with the neighboring carbons but not the other proton. Using this information, a dihedral angle of 90° was fixed between each proton and each carbon should show an HMBC correlation but it did not (Fig. 12).

Applying the Karplus relationship role made assigning the stereo configurations for protons in the methylene groups applicable to support the NOE data (Fig. 9), and even to serve as an alternative when NOE data are not decisive or absent. Accordingly, one could with ease assign the relative stereo configurations for the remaining protons.

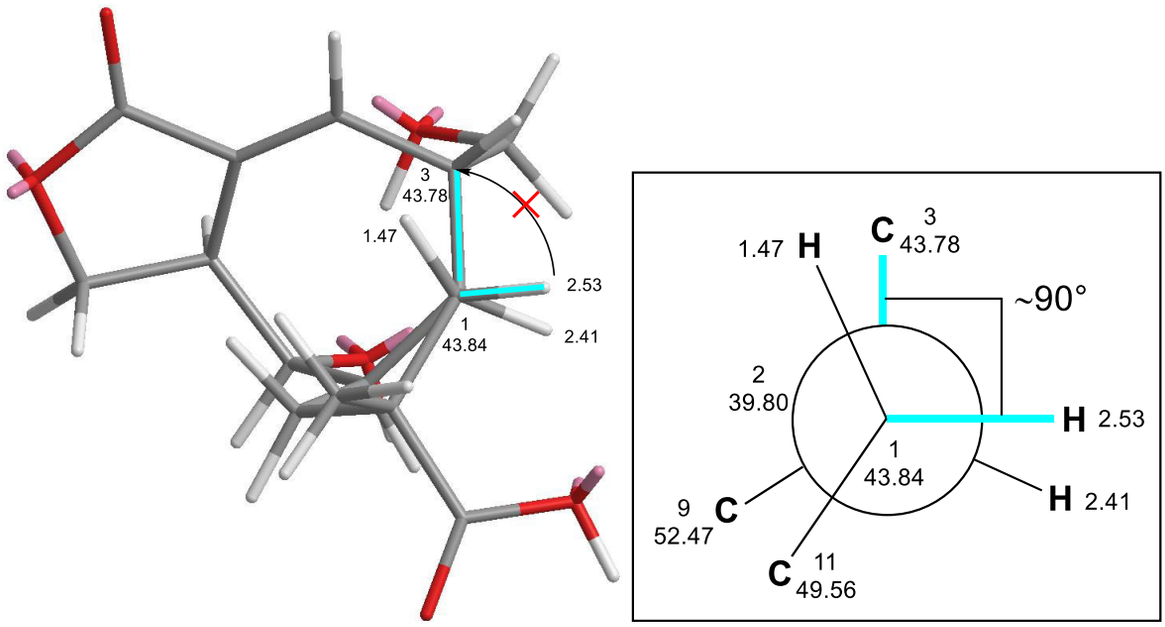

Figure. 12. Left: 3D module of compound **19** with perspective view from C-1 through C-2. Right: Newman projection with perspective view from C-1 through C-2.

Considering that the protons that have previously been assigned using the NOE data should be on the same side of the compound. These protons either exist on one side of the compound or the other, and they will be designated with an (up) configuration when moieties exist on the upper side of the drawn compound in (Fig. 16-page 29), or they will be designated with a (down) configuration when they are existing in the downside of the compound. The next step now is to consider the Karplus relationship applied observation on the HMBC data to assign the relative configuration of compound **19**.

First, a 90° dihedral angle is fixed between one of the methylene protons at δ_C 43.84 and carbon 3 at δ_C 43.78. Then matching this proposed stereo configuration with the NOE and HMBC data. Finally, fixing the proton at δ_H 2.53 with a 90° dihedral angle with the carbon at position 3 (Fig. 12) will have a consistency with the data from NOE and other HMBC correlations comply with the observed Karplus relationship. Accordingly, this proton will be in the down configuration of this compound's relative structure.

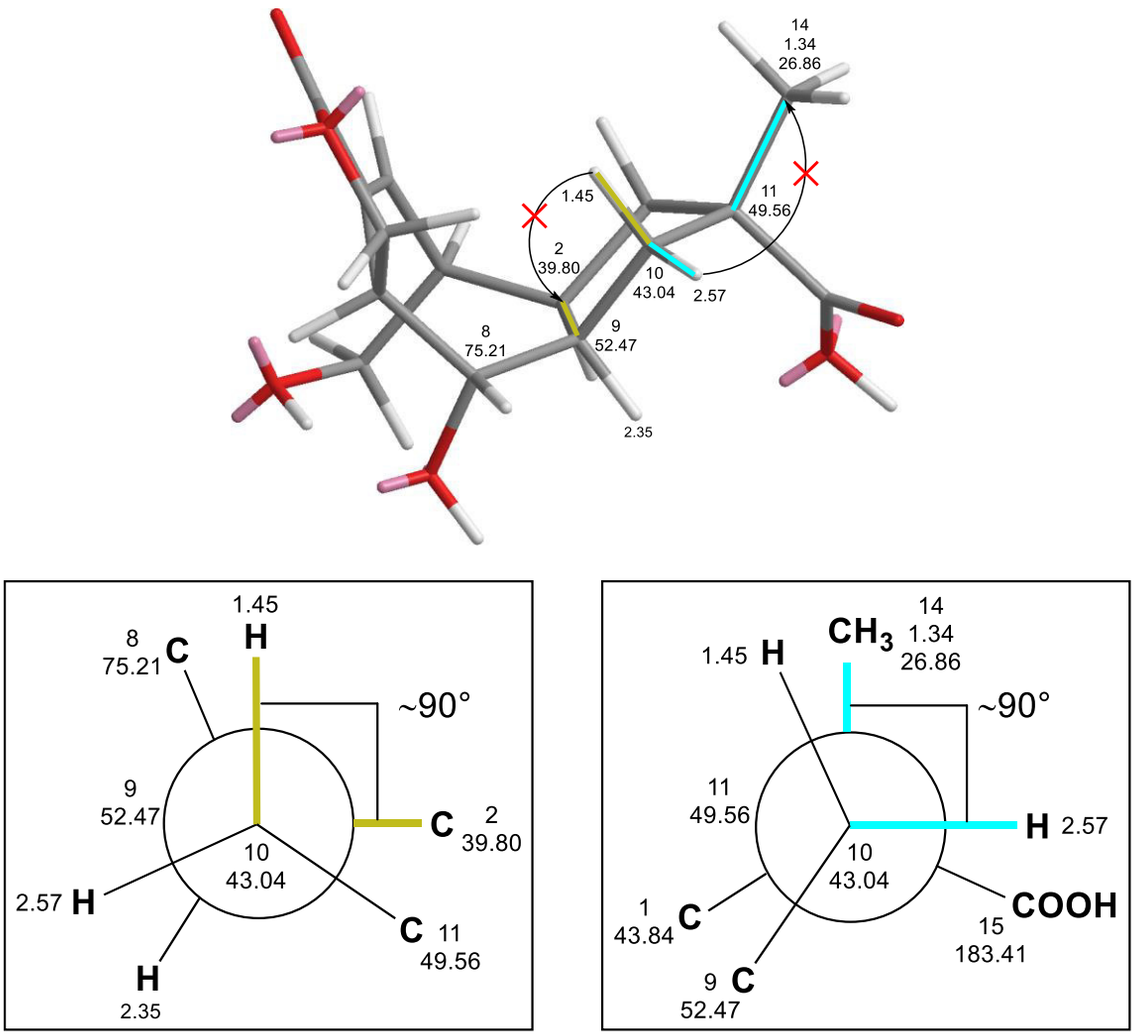

Figure. 13. Up: 3D module of compound **19**. Left down: Newman projection with perspective view from C-10 through C-9. Right down: Newman projection with perspective view from C-10 through C-11.

Similarly, methylene protons at C-10 also correspond to the Karplus relationship (Fig. 13), as the proton at δ_H 2.57 does not correlate with the methyl group carbon at δ_C 26.86 like the other proton at δ_H 1.45. Subsequently, a 90° dihedral angle is fixed between these atoms (Fig. 13). In a similar approach, such an angle is fixed between the proton at δ_H 1.45 and carbon 2 at δ_C 39.80, as there is no HMBC correlation between these atoms.

As a result, the proton at δ_H 1.45 will be in the up configuration in compound **19** relative structure. Subsequently, the proton at δ_H 2.57 will be assigned in the down configuration.

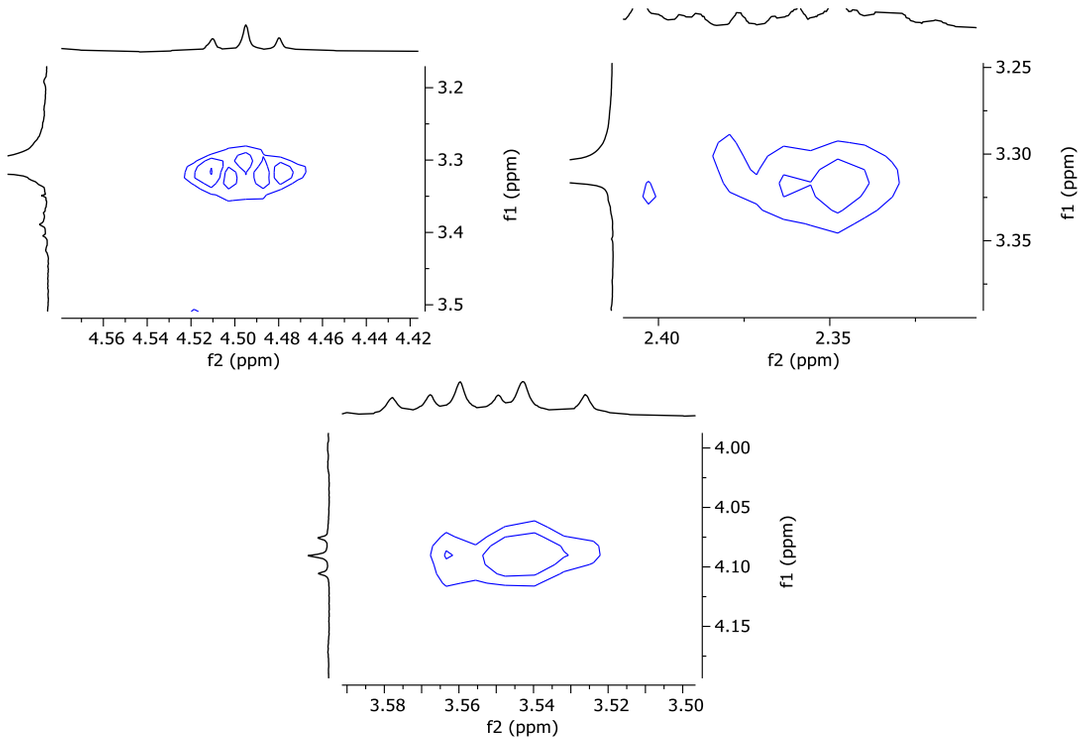

Figure. 14. NOESY expanded-spectrums of selected correlations, (CD_3OD). Up left: between protons at δ_H 3.33 and 4.49. Up right: between protons at δ_H 3.33 and 2.35. Down: between protons at δ_H 3.54 and 4.09.

The methine proton at δ_H 3.33 at C-7 with down configuration shows NOE correlation with one of the methylene protons at δ_H 4.49 at carbon 13, also there is a correlation with the proton at δ_H 2.35 at carbon 9, (Fig. 14), making them in the down configuration. And so, the other proton at δ_H 4.09 will be in the up configuration, which itself has NOE correlation with the proton of the oxygenated methine (δ_H 3.54, δ_C 75.21) at C-8 assigning it to be in the up configuration also.

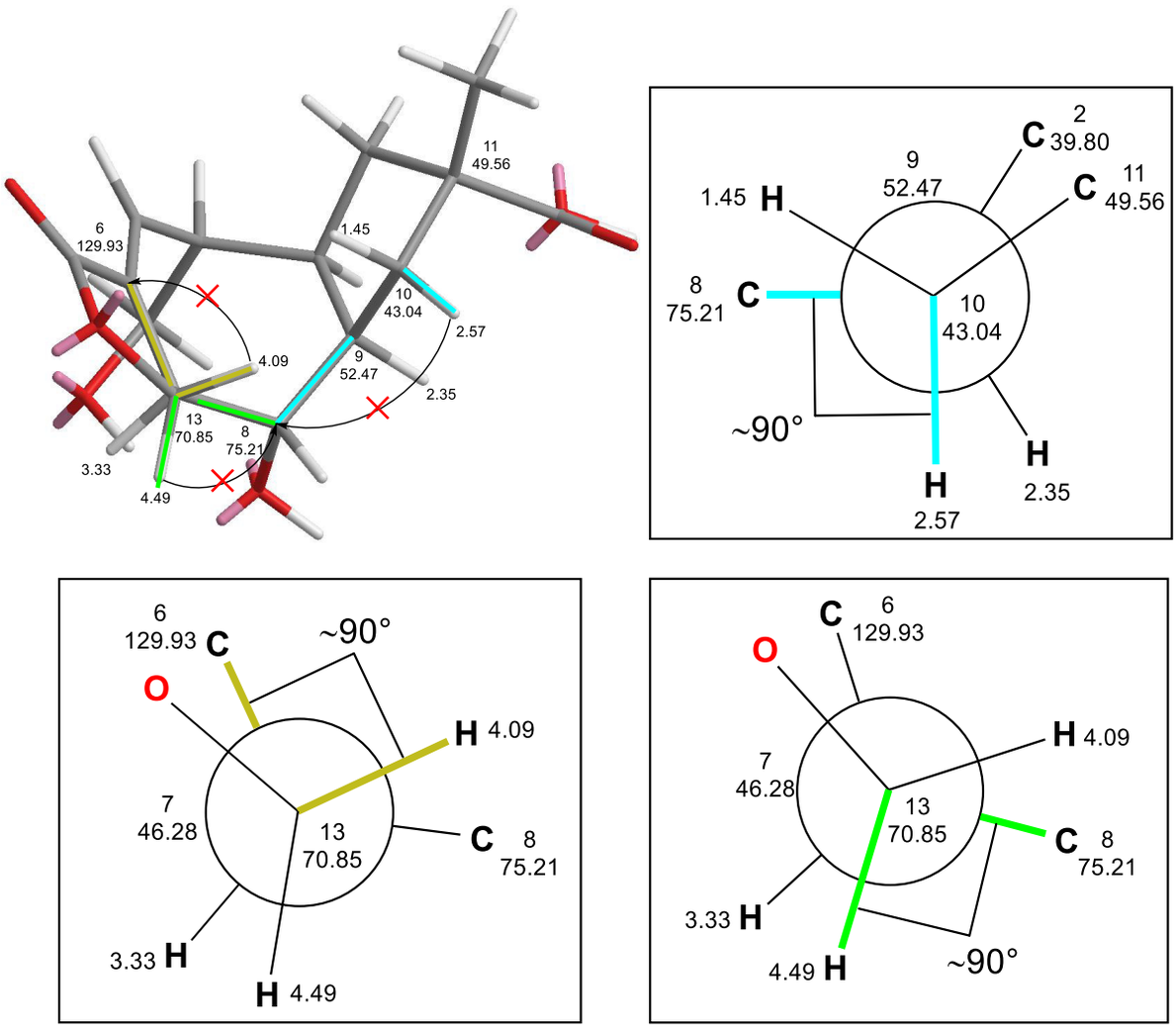

Figure. 15. Left up: 3D module of compound **19** with perspective view from C-13 through C-7. Right up: Newman projection with perspective view from C-10 through C-9. Left down: Newman projection with perspective view from C-13 through C-7. Right down: Newman projection with perspective view from C-13 through C-7**.**

For the latest assignments of protons at C-13, the Karplus relationship agrees with them firmly. As proton at δ_H 4.09 doesn't have correlations with the alkene carbon number 6 and the lactone carbonyl carbon number 5, like the other proton at δ_H 3.33 in this methylene group. Subsequently, a 90° dihedral angle is fixed between these atoms, (Fig. 15). Additionally, this proton – at δ_H 4.09 – has HMBC correlation with carbon at δ_C 75.21 at C-8 but not the other methylene proton at δ_H 4.49. And accordingly, a 90° dihedral angle is fixed between the later proton and C-8 atom. So, this proton will be assigned to be in the down configuration, and the proton at δ_H 4.09 will be in the opposite up configuration.

Also fixing the dihedral angle of 90° between the proton at δ_H 2.57 at carbon 10 with carbon 8 at δ_C 75.21 (Fig. 15) comes as compatible with the assignment of this proton to be in down configuration.

The final relative structure for compound **19** can be assigned accordingly in accordance with1D and 2D-NMR data, see (Fig. 16) and (Tab. 1). The polarimetry data was also measured for this compound in this research, $[\alpha]_{\mathrm{D}}^{25}$ –12.3 (MeOH; *c* 0.001).

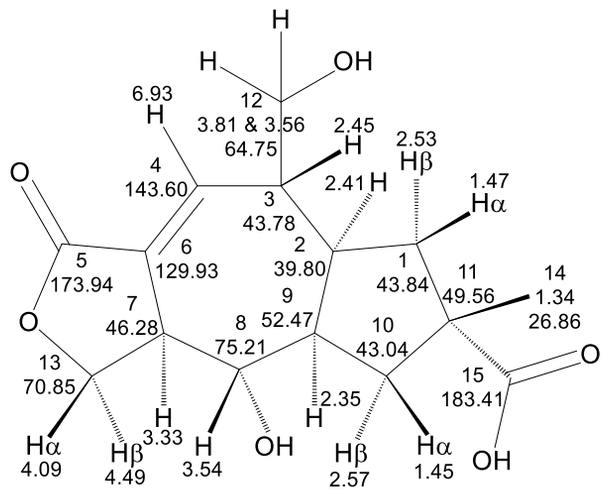

Figure. 16. Relative structure of compound **19** with assigned NMR shifts, (CD_3OD).

Table. 1: NMR data for compound **19** in CD_3OD.

position	δ_H (*J* in Hz)	δ_C
1	α:1.47 1H (dd, 13.3, 6.0) β:2.53 1H (dd, 13.3, 7.2)	43.84
2	2.41 1H (dddd, 18.0, 13.3, 6.2, 2.5)	39.80
3	2.45 1H (ddd, 18.0, 10.0, 7.0)	43.78
4	6.93 1H (dd, 2.9, 2.9)	143.60
5	-	173.94
6	-	129.93
7	3.33 1H (ddd, overlapped with CD_3OD signal)	46.28
8	3.54 1H (dd, 11.0, 6.0)	75.21
9	2.35 1H (dddd, 18.0, 14.0, 7.7, 6.0)	52.47
10	α:1.45 1H (dd appears as t, 12.3, 12.3) β:2.57 1H (dd, 12.3, 6.0)	43.04
11	-	49.56
12	3.56 1H (dd, 10.8, 3.6) 3.81 1H (dd, 10.8, 6.1)	64.75
13	α:4.09 1H (dd appears as t, 9.0, 9.0) β:4.49 1H (dd appears as t, 9.1, 9.1)	70.85
14	1.34 3H (s)	26.86
15	-	183.41

4.1.3.1.2 MS/MS considerations

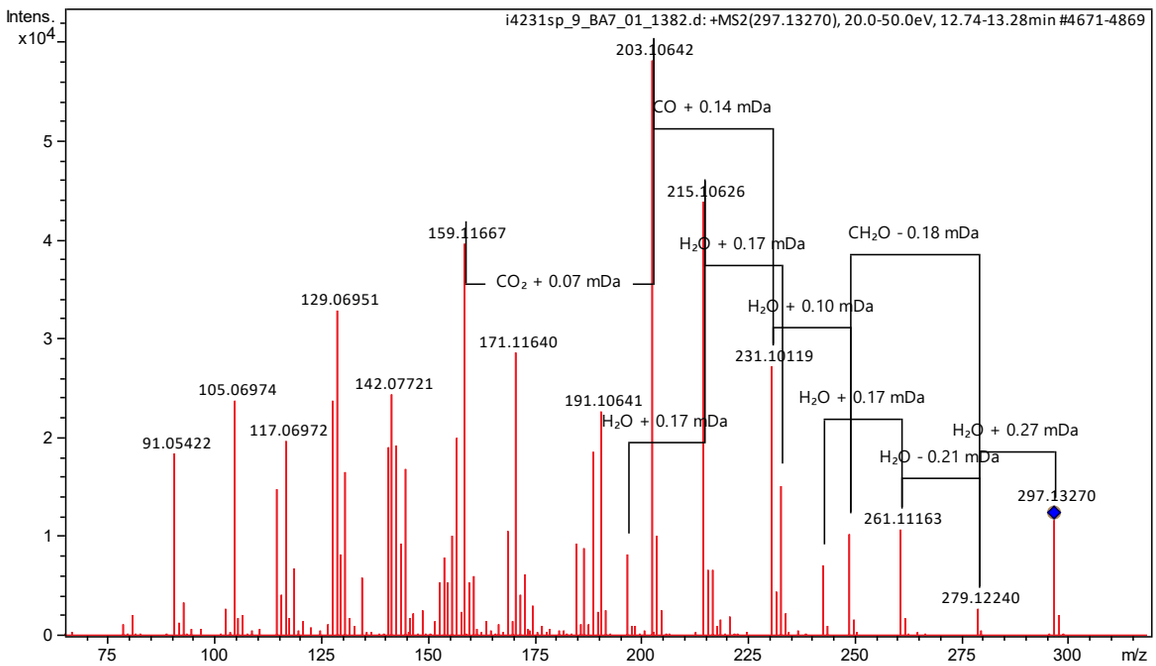

Figure. 17. HR-ESI-(+)-MS/MS-spectrum of **19**.

The MS/MS spectrum of compound **19** shows a great similarity with other MS/MS spectrums of compounds belonging to this group of sesquiterpenes. See MS/MS spectrums for compounds **25**, **34**, and **52** in sections 9.6, 9.15, and 9.16 respectively. Accordingly, such data are not even helpful to identify or characterize the compounds with the same molecular formula.

The MS/MS fragments show a gradual loss of H_2O, CO, and CO_2 moieties and parts from the precursor and sub-fragments ions. Consequently, in general, this pattern suggests a stable molecule as the fragmentation of larger parts of the molecule is not favored.

4.1.3.1.3 CD investigations

To assign the absolute structure of compound **19**, CD measurement was performed. The recorded experimental CD spectrum was then compared with the calculated spectra from the two enantiomers of the compound **19**, (Fig. 18). Tarek Scheele from Bremen University calculated the CD spectra of the enantiomers of compound **19**. The enantiomer with most moieties that have down stereo configurations of the compound will be designated with *2R,3R,7R,8S,9R,11S*-**19**, and the mirror image of it will be referred to as *2S,3S,7S,8R,9S,11R*-**19**.

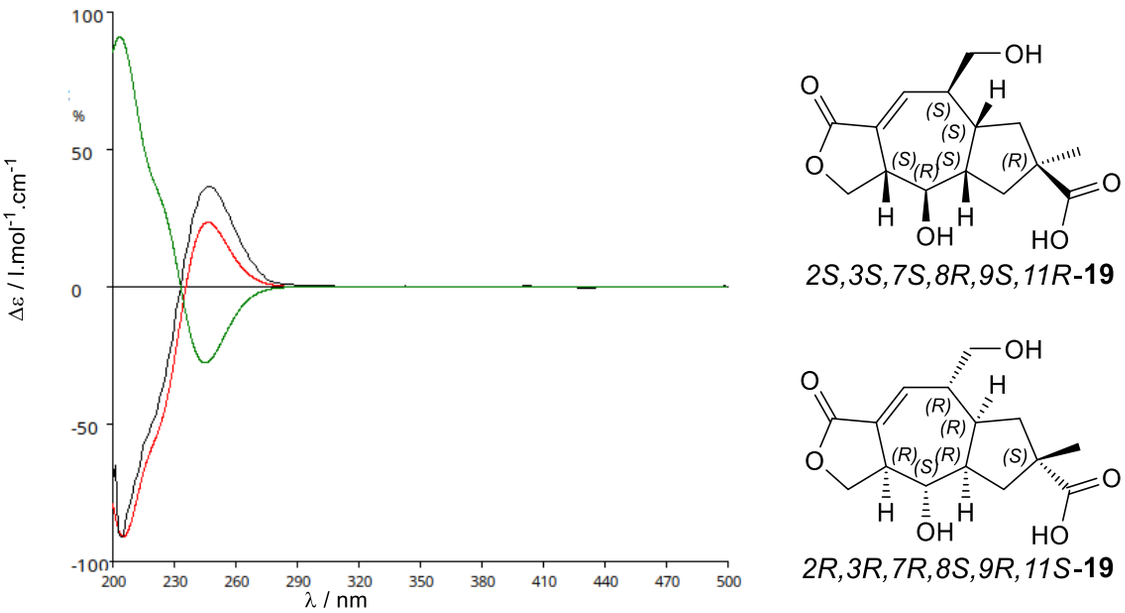

Figure. 18. Left: Comparison of the experimental CD spectrum (black) of 12-hydroxy-15-carboxylblennin A (**19**), with the calculated spectra for *2R,3R,7R,8S,9R,11S*-**19** configuration (red) and *2S,3S,7S,8R,9S,11R*-**19** configuration (green). Right: the structures of the two enantiomers of **19**.

The calculated red curve shows a high agreement with the experimental one. The comparison thus clearly shows that configuration *2R,3R,7R,8S,9R,11S* from compound **19** is representing the absolute configuration for this compound.

4.1.3.1.4 Biosynthetic considerations

Following the proposed biosynthetic pathway presented by GILARDONI *et al*. in 2014,[32] here one more step can be added to produce the compound **19**. Such a mechanism starts with the fatty acid esters **7** and/or **8** of the marasmane sesquiterpene velutinal to be converted to alcohol moiety. Rearrangements of electrons cause the ring opening of the furan part which rearranges again to produce the *epi*-piperalol (**12**). Farther rearrangements of electrons cause the formation of blennin A (**32**) that oxidizes resulting in the attachment of a hydroxyl group at the terminal methyl group attached to carbon 11 to form 15-hydroxyblennin A (**34**). Adding one more step of oxidation of the latter compound, one more hydroxyl group can be attached to the methyl group at position 12 to finally form the compound **19**, see (Fig. 19).

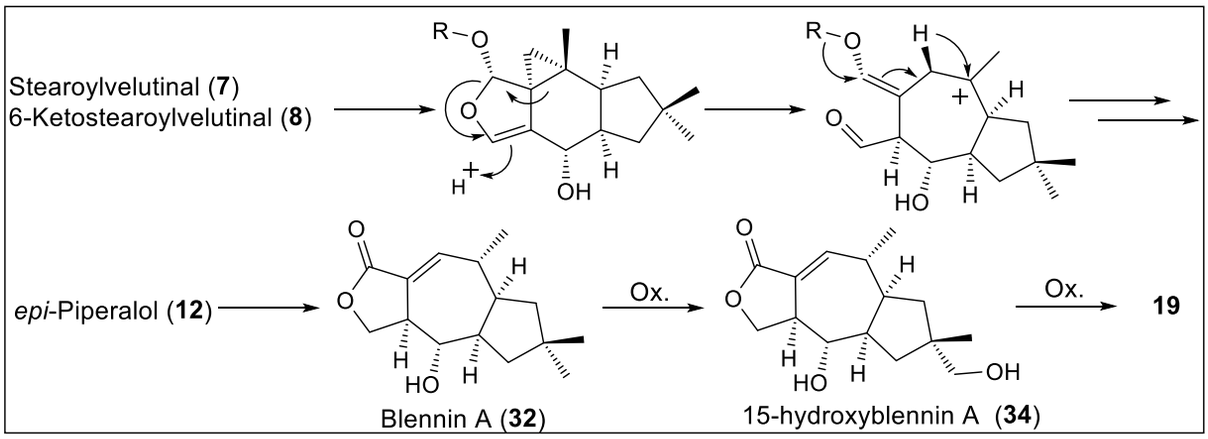

Figure. 19. Proposed biosynthetic pathway of formation of compound **19**.

4.1.3.2 7,15-Dihydroxyblennin A (**20**)

4.1.3.2.1 Own contribution to **20**

The stereo configurations assignments of the methylene groups in the already extracted and elucidated compound **20** were investigated and achieved during this research on *Lactarius circellatus* mushroom.

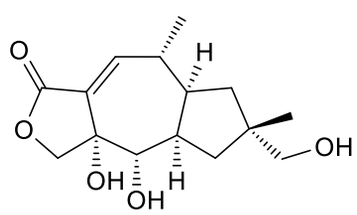

7,15-Dihydroxyblennin A (**20**)

The proposed structure of the new sesquiterpene compound **20** extracted from *L. circellatus* has partial similarity with the structure of compound **19** regarding the chemical character of carbons 1, 2, 4, 5, 6, 8, 9, 10 and 13. Such a resemblance is a usual occurrence in this group of compounds. Accordingly, Karplus relationships are proven to exist in compound **20** HMBC-NMR data for two methylene groups out of three (Fig. 20). Protons at C-1 don't resonate with these relationships. However, assigning the stereo configurations of the protons in all methylene groups in compound **20** is possible by using the same approach described in section 4.1.3.1.1.

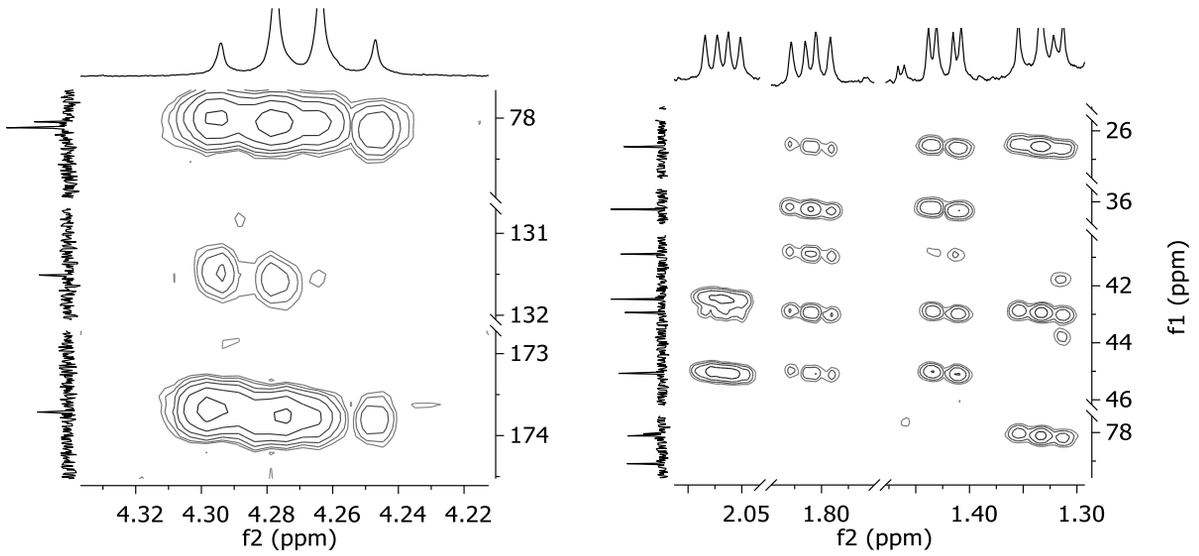

Figure. 20. HMBC concentrated-spectrums of selected correlations for, Left: protons at δ_H 4.26 and 4.28. Right: protons between δ_H 1.30 and 2.10, (CD_3OD).

The spectrum in (Fig. 20-right), shows decisively how the two protons at δ_H 1.33 and 2.07 at carbon 1 have HMBC correlations with each of the carbons at δ_C 42.94, 46.96 and 70.97, but only the proton at δ_H 1.33 has correlations with carbon 14 at δ_C 26.55 and carbon 8 at δ_C 78.12. Additionally, only the proton at δ_H 2.07 has correlations with both carbons at positions 1 and 2 at δ_C 42.46 and 45.07 respectively with only a trivial correlation between the proton at δ_H 1.33 with carbon at δ_C 42.46. This can be attributed to the dihedral angle between them is not exactly 90° but close to it.

Protons of the methylene group at C-13, δ_C 79.09 don't show coupling correlations with neighboring protons in the COSY spectrum, so in theory, they should act as an equivalent group. However, they show an observation consistent with the Karplus relationship (Fig. 21) left. An HMBC correlation between a partial part of what appears as an AB signal at δ_H 4.28 with carbon 6 at δ_C 131.51 supports this observation. Such behavior could be explained as a long distance-coupling with protons existing in two or three bonds away and there is a π system in its proximity. Similar observations usually occur with sesquiterpenes with a double bond exists between carbons in positions 6 and 7. Nevertheless, a small long-distance coupling causes the ^{1}H-NMR signal of these methylene protons not to be affected but in HMBC they show individual behavior. Also, there is NOE correlation only between the proton at δ_H 4.26 and the proton at δ_H 3.61, section 9.2-(Fig. S13). Accordingly, two ^{1}H-NMR shifts are assigned for each one of these protons at δ_H 4.26 and 4.28.

The previously assigned ^{1}H and ^{13}C-NMR shifts are shown in section 9.2-(Fig. S12).

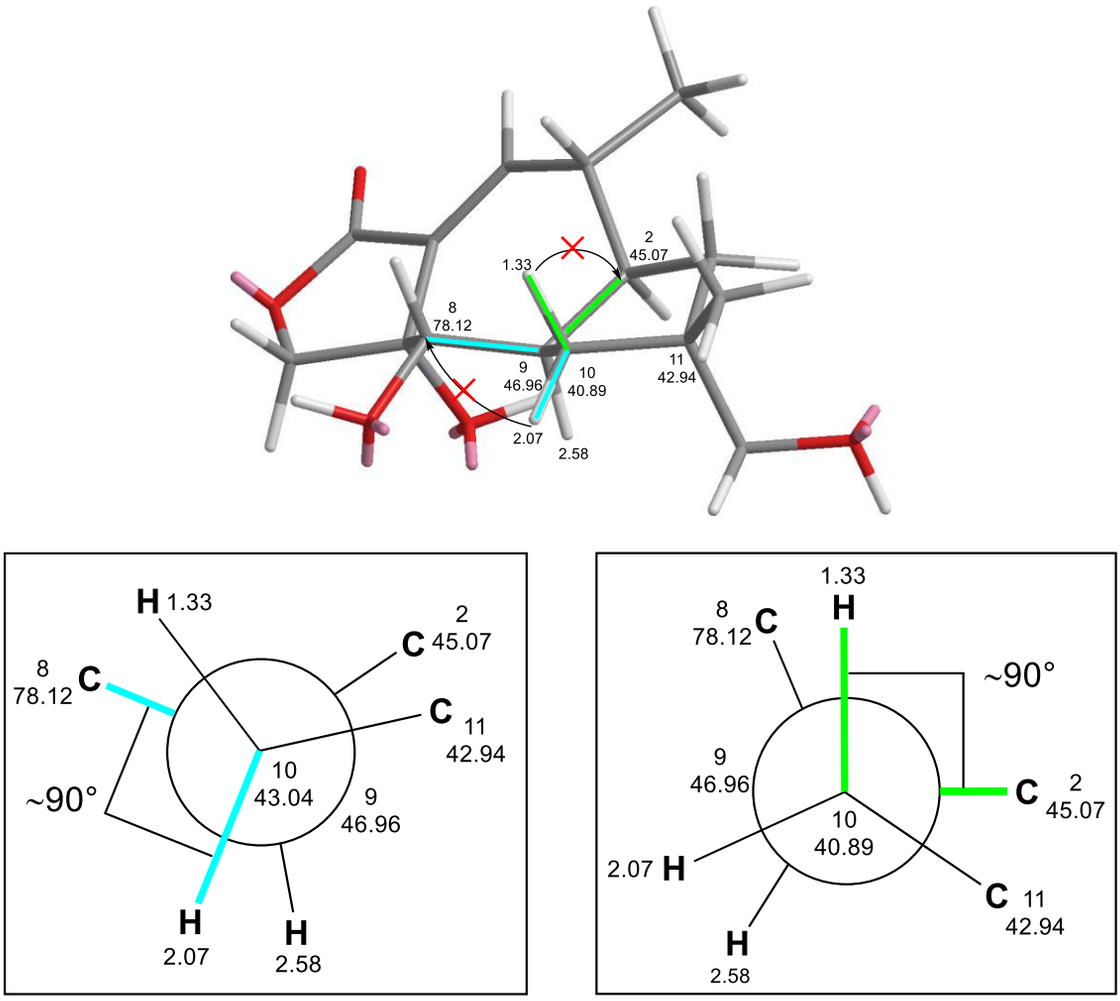

Figure. 21. Up: 3D module of compound **20** with perspective view from C-10 through C-9.
Down: Newman projections with perspective view from C-10 through C-9.

Assigning the proton at δ_H 1.33 to be in the up configuration and the proton at δ_H 2.07 to be in the down configuration agree with both HMBC and NOE-NMR data. A 90° dihedral angle is fixed between the first one and carbon 2 at δ_C 45.07, (Fig. 21-Down right), and also between the second one and carbon 8 at δ_C 78.12, (Fig. 21-Down left). This method came to remove the doubt that the proton at δ_H 1.33 is in the up configuration because both protons have NOE correlations with the proton at δ_H 3.61 at carbon 8 with the up configuration. In this case, the latest proton has a strong NOE correlation with the proton at δ_H 1.33 and a weak correlation with the proton at δ_H 2.07, accordingly the NOE data doesn't provide decisive results.

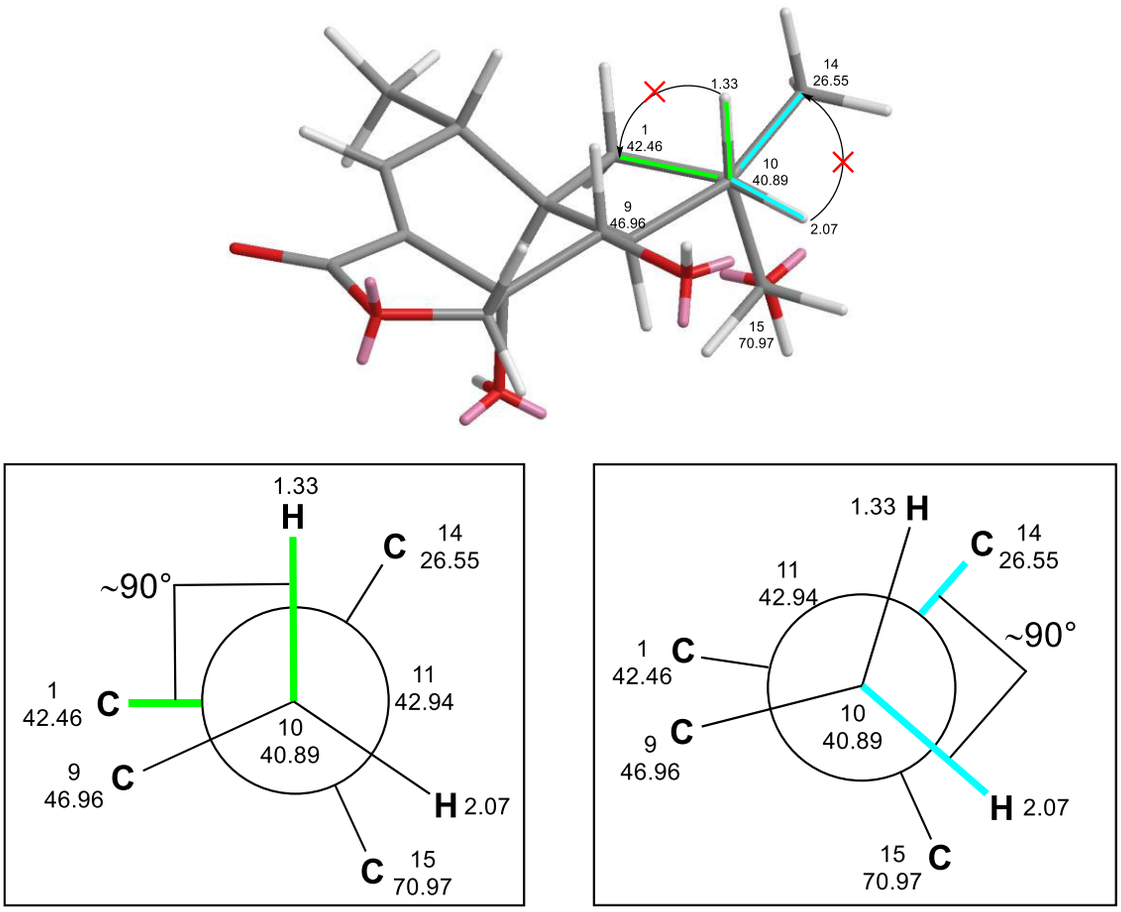

Figure. 22. Up: 3D module of compound **20** with perspective view from C-10 through C-11.
Down: Newman projections with perspective view from C-10 through C11.

Applying the previous assignments to the HMBC results regarding correlations with carbons 1 at δ_C 42.46 and 14 at δ_C 26.55 will confirm these assignments. As it's elaborated in (Fig. 22), the proton at δ_H 1.33 with the up configuration has no HMBC correlation with carbon 1 at δ_C 42.46 due to the dihedral angle between them being 90°. Moreover, the other proton – at δ_H 2.07 – shouldn't have HMBC correlation with carbon 14 at δ_C 26.55 as a result of the 90° dihedral angle between them. This was also achieved when carbon 14 was assigned to be in the up configuration and so carbon 15 in the down configuration, which in conclusion also confirmed these assignments.

For the protons in the methylene group at C-1 their stereo configurations assignments are a result of the previous assignments of the methylene group at C-10 and confirm the stereo configurations assignments of carbons 14 and 15. Therefore, the NOE correlation between protons at δ_H 1.42 and 1.10 will put this proton in the up configuration. This assignment can't be decisive as there are NOE correlations with both protons, the proton at δ_H 2.47 at carbon 3 with the up configuration and the methyl protons at δ_H 1.19 at carbon 12 with down configuration, (9.2-Fig. S13), making Karplus relationships an essential tool for assigning the stereo configurations of such protons.

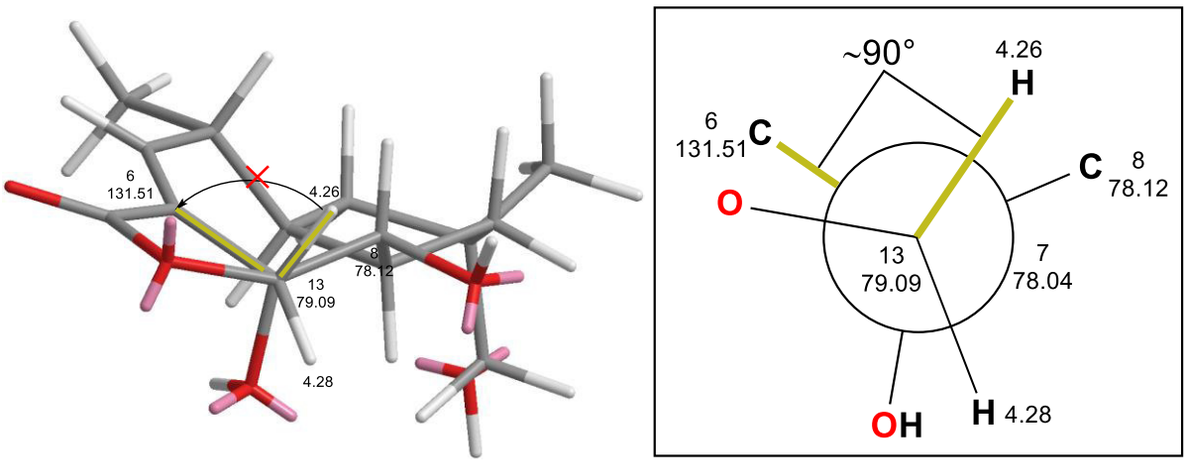

Figure. 23. Left: 3D module of compound **20** with perspective view from C-13 through C-7. Right: Newman projection with perspective view from C-13 through C-7.

Simultaneously, another example of using the Karplus relationship in assigning stereo configurations in the due compounds is assigning the hydroxyl group at C-7 to the down configuration and proton at δ_H 4.26 to be in the up configuration of the compound. This proton could have NOE correlation with proton at δ_H 3.61 at C-8 in both cases whether the hydroxyl group at carbon 7 at δ_C 78.04 is in the up configuration. But HMBC correlations give a reliable approach to the most probable stereo configuration of the hydroxyl group, as there is only HMBC correlation between the proton at δ_H 4.28 and carbon 6 at δ_C 131.51 but not the other proton from this methylene group. When applying both stereo configurations of the hydroxyl group, it becomes clear that only the down configuration allows the two protons from the methylene group at carbon 13 to exist at the right angle to produce the resulting correlation, (Fig. 23). In other words, the proton at δ_H 4.26 only exists in a dihedral angle of 90° with C-6 when the hydroxyl group at C-7 is at the down stereo configuration, resulting in the observed lack of HMBC correlation. NOE correlation between the proton at δ_H 4.26 and proton at δ_H 3.61 at carbon 8 with the up configuration supports this assignment, (9.2-Fig. S13).

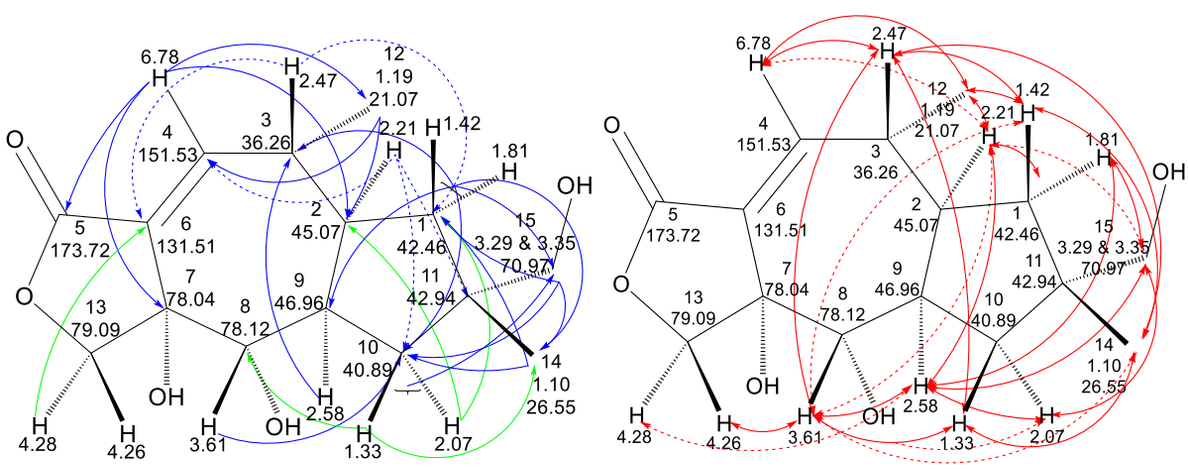

Figure. 24. Structure of compound **20**, Left: with selected HMBC correlations (⟶) and HMBC correlations with Karplus relationship (⟶). Right: With NOESY correlations (⟷), (CD_3OD).

The final relative structure of compound **20** with the assigned stereo configurations, HMBC, and NOE correlations are shown in (Fig. 24).

The polarimetry data was also measured in this research, $[\alpha]_D^{25}$ –10.3 (MeOH; *c* 0.0013). The negative sign came opposite to the results from the similar compounds **34** and **52**.

4.1.3.2.2 CD investigations

CD measurement was recorded for compound **20** to assign the absolute structure. Comparison was made between the recorded experimental CD spectrum with the calculated spectra from the most probable enantiomer of compound **20** with the two linking protons at carbons 2 and 9 to be in the down configuration *2R,3R,7S,8S,9R,11S*-**20**, (Fig. 25).

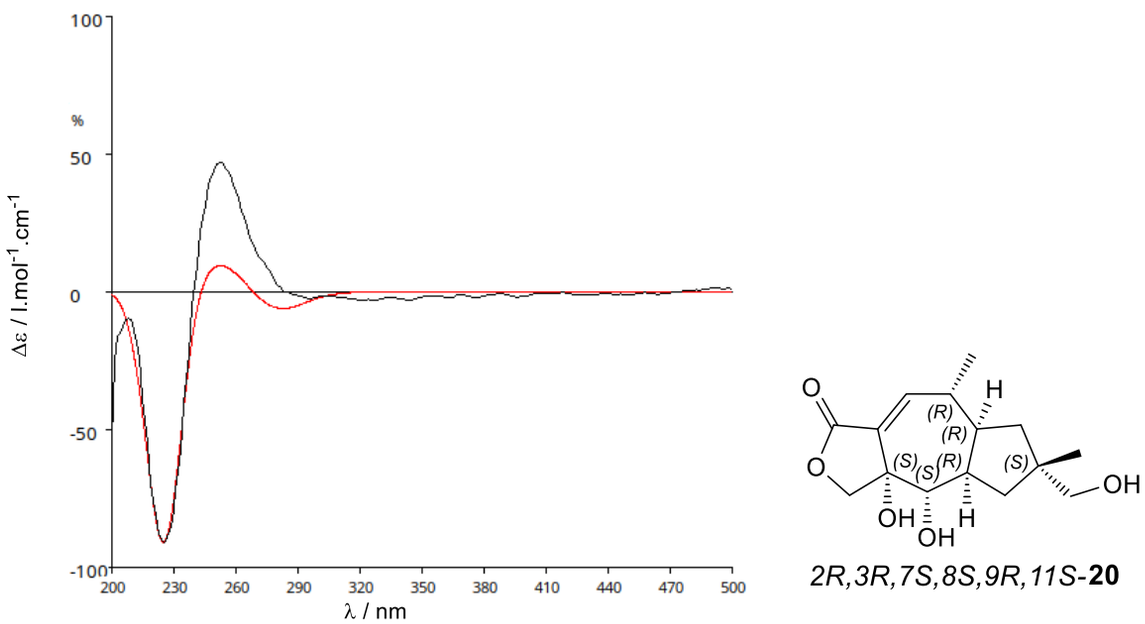

Figure. 25. Left: Comparison of the experimental CD spectrum (black) of 7,15-dihydroxyblennin A (**20**), with the calculated spectra for *2R,3R,7S,8S,9R,11S*-**20** configuration (red). Right: structure of *2R,3R,7S,8S,9R,11S*-**20**.

The comparison supports the most probable bio-synthetically *2R,3R,7S,8S,9R,11S*-**20** enantiomer, and accordingly assigning this configuration to be the absolute configuration of 7,15-dihydroxyblennin A (**20**).

4.1.3.3 2,3-Epoxylactarorufin A (**21**)

4.1.3.3.1 Own contribution to **21**

Using the same approach described in previous sections for compounds **19** and **20**, the stereo configurations of the protons in all of the four methylene groups in the new compound **21** were assigned. Three groups of them showed strong HMBC correlations that agree with Karplus

relationships but the fourth one at C-4 showed only weak correlations but were enough to use them to determine the orientation of the protons attached to this carbon. And also assigning the stereo configurations of the methyl group at δ_H 1.38 and consequently the epoxy bridge between carbons 2 and 3.

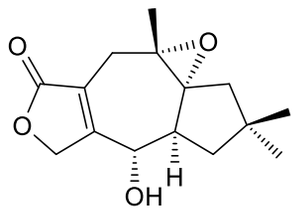

2,3-Epoxylactarorufin A (**21**)

Compound **21** that already had been extracted and measured in NMR exhibit HMBC correlations that indicate the presence of a 90° dihedral angle between protons at the methylene groups at carbons 1, 4, 10, and 13 with their neighboring carbons, (Fig. 26).

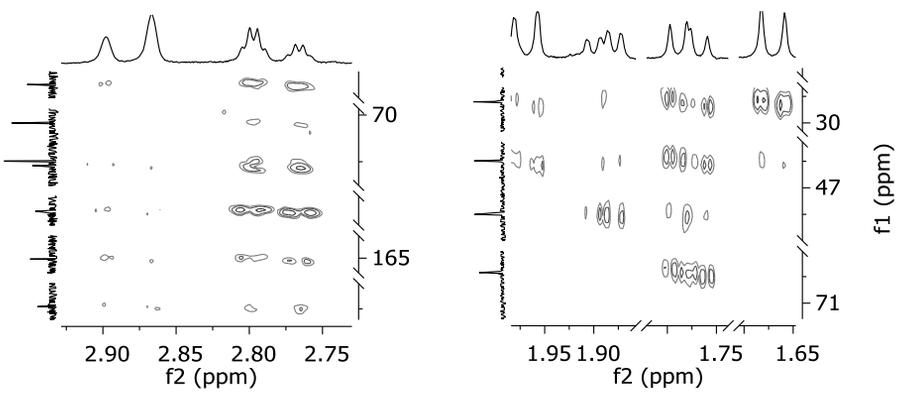

Figure. 26. HMBC concentrated-spectrums of correlations from previously extracted compound **21** from *L. circellatus*, (CD_3OD). Left: protons at δ_H 2.78 and 2.88. Right: protons between δ_H 1.65 and 2.00.

As proton at δ_H 1.67 from the methylene group at carbon 1 has a much stronger HMBC correlation with the methyl group attached to carbon 11 at δ_C 29.60 than the other geminal proton at δ_H 1.97 in this chemical group. Also, the proton at δ_H 1.78 from the methylene group at carbon 10 correlates with the oxygenated carbon 8 at δ_C 70.42 but not the other geminal proton at δ_H 1.89. A similar observation was recorded for correlation with the previously mentioned carbon at δ_C 29.60. Moreover, such a pattern was recorded for protons in the methylene group at carbon 13.

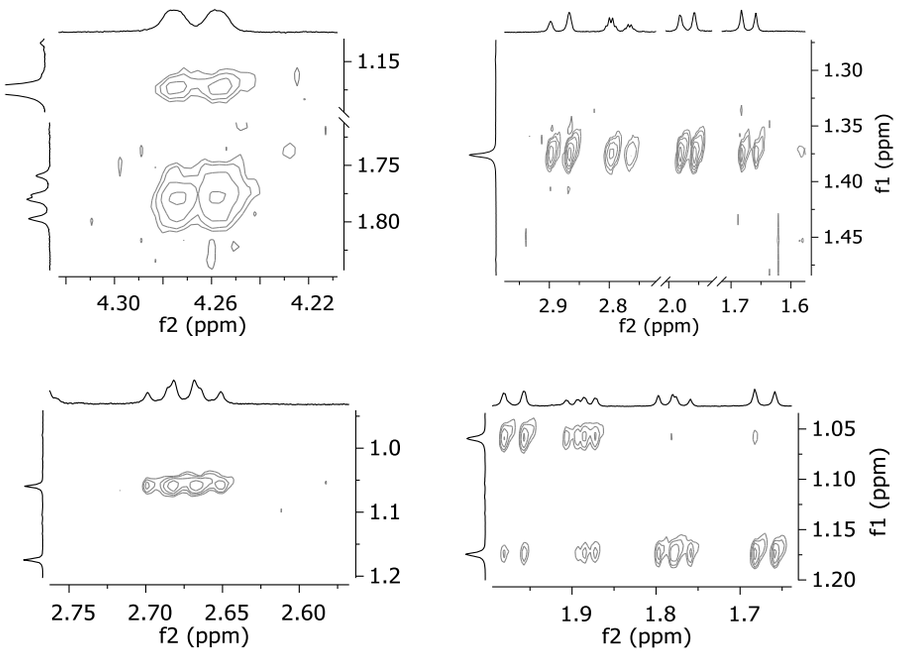

Figure. 27. NOESY expanded-spectrums of selected correlations, (CD_3OD). Up left: between protons at δ_H 4.27 and protons at δ_H 1.17 and 1.78. Up right: between proton at δ_H 1.38 and protons at carbons 1 and 4. Down left: between protons at δ_H 2.67 and 1.06. Down right: between protons at δ_H 1.06 and 1.17 and the methylene protons at C-1 and C-10.

The recorded NOE data exhibit decisive information regarding the protons at the cyclopentane part of this compound, (Fig. 27). As, there are NOE correlations between protons at δ_H 1.17, 1.67, 1.78, and 4.27 making them exist on the same side of this compound. Also, protons at δ_H 1.06, 1.89, 1.97, and 2.67 will be oriented on the opposite side of the compound structure. Following the biological pathway for this type of compound (lactarane sesquiterpene) by assigning the bridge proton at carbon 9 (at δ_H 2.67) to be in the down configuration, and consequently, the later protons group to be also on the same side of the compound and the first protons group to be in the opposite up configuration.

The protons from the methyl group attached to carbon 3 didn't show decisive NOE results. As these protons at δ_H 1.38 show NOE correlations with both protons of each methylene group at carbons 1 and 4, accordingly such data will not be attributed to assigning the stereo configurations of them, (Fig. 27-Up right). Consequently, using the HMBC correlations for proton at δ_H 2.78 although weak with carbon 2 at δ_C 72.70 to fix the dihedral angle between to be 90°. This can only occur when this proton and the epoxy bridge are in the down configuration, and accordingly, the methyl protons at δ_H 1.38 are in the up configuration.

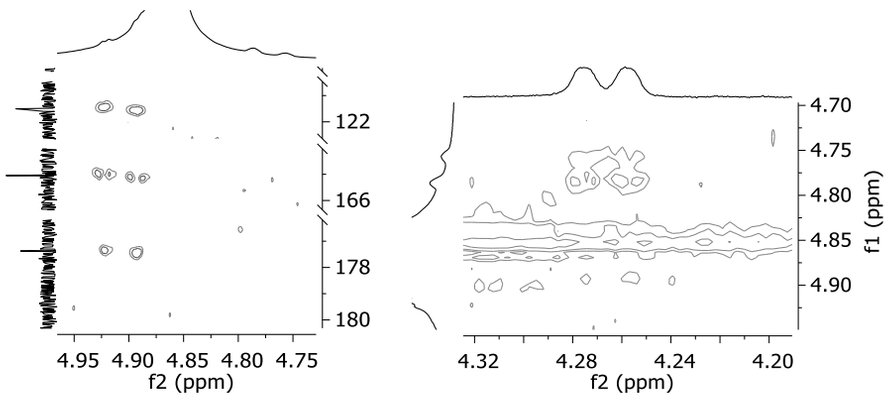

Figure. 28. Left: HMBC concentrated-spectrum of correlations from previously extracted compound **21** from *L. circellatus*, for protons at δ_H 4.77 and 4.90. Right: NOESY expanded-spectrum of correlations between proton at δ_H 4.27 and protons at δ_H 4.77 and 4.90, (CD_3OD).

For protons at carbon 13, the latter method is the only decisive approach to determine their stereo configurations, as proton at δ_H 4.77 can only exist in the up configuration in this compound to not have an HMBC correlation with its neighbouring carbons, (Fig. 28-Left). This assignment can be supported by a weak but not decisive NOE correlation with the oxygenated proton at carbon 8, (Fig. 28-Right).

The accompanied extracted information leads to assigning the relative structure of compound **21** presented in (Fig. 29). The polarimetry data was also measured for this compound in this research, $[\alpha]_D^{25}$ –16.2 (MeOH; *c* 0.001).

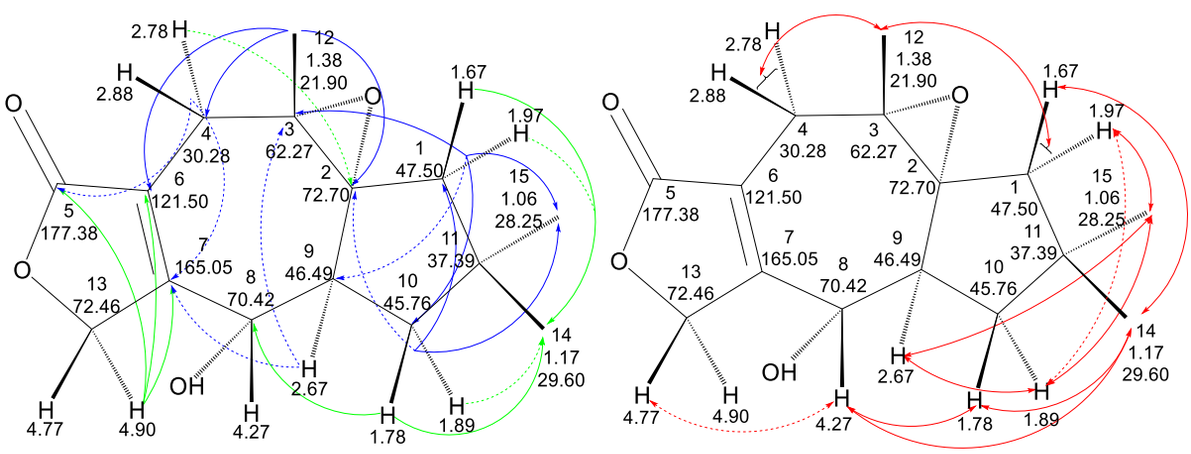

Figure. 29. Relative structure of compound **21** with assignments, (CD_3OD). Left: selected HMBC correlations (→), HMBC correlations with Karplus relationship (→). Right: NOESY correlations (↔).

4.1.3.3.2 CD investigations

Similar to the approach adopted in compounds **19** and **20** for studying the probable configuration of such types of compounds, a comparison was established between the experimental CD spectra with the calculated spectra of the two enantiomers of 2,3-epoxylactarorufin A (**21**), (Fig. 30). It becomes clear, that the calculated spectra from the enantiomer designated with *2R,3S,8S,9S*-**21**

which consist of proton at carbon 9 in the down configuration, agree with the experimental one. Such results are expected for this type of compound with biological pathways leading to protons in the linking carbons 2 and 9 to be in the down configuration of the compound structure.

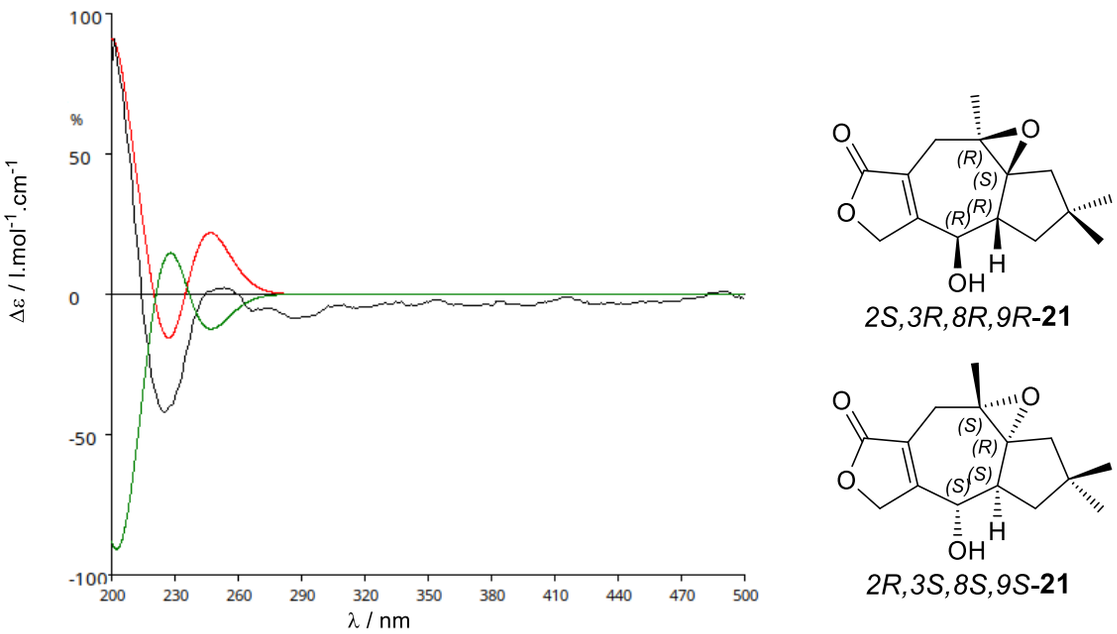

Figure. 30. Left: Comparison of the experimental CD spectrum (black) of 2,3-epoxylactarorufin A (**21**), with the calculated spectra for *2R,3S,8S,9S*-**21** configuration (red) and *2S,3R,8R,9R*-**21** configuration (green). Right: the structures of the two enantiomers of **21**.

4.1.3.4 14-Carboxy-deoxylactarorufin A (**22**)

4.1.3.4.1 Own contribution to **22**

The stereo configurations of the protons in three methylene groups out of four were assigned in this research for the new compound **22** that was extracted and measured previously in NMR in CD_3OD. Moreover, the stereo configuration of the carboxylic group attached to carbon 11 was also assigned. This was achieved using the combined NMR data from the previously measured compound fraction in CD_3OD, section 9.3 - (Fig. S16), and from the same fraction remeasured in this research in DMSO-d6, but exhibited signs of compound degradation.

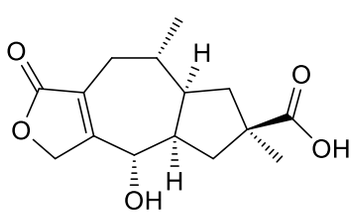

14-Carboxy-deoxylactarorufin A (**22**)

The new HMBC data shows more correlations that agree with Karplus relationships as a 90° dihedral angle can be fixed between protons in the methylene groups at carbons 1, 4, and 10 and with their neighboring carbons that should have HMBC correlations but yet they don't, (Fig. 31).

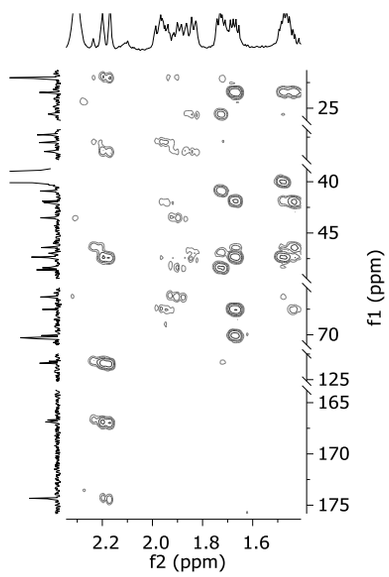

Figure. 31. HMBC concentrated-spectrums of correlations from previously extracted compound **22** from *L. circellatus*, (DMSO-d6). Protons between δ_H 1.40 and 2.40.

Proton at δ_H 1.73 at carbon 1 has HMBC correlations with both carbons 9 and 10 at δ_C 48.39 and 40.90 respectively but not the other geminal proton at δ_H 1.84. Also, the later proton has a correlation with carbon 3 at δ_C 33.90 but not the other geminal proton in this methylene group. The same observation had been noticed for the methylene protons at carbon 4 which proton at δ_H 2.18 has correlations with carbons 2, 5, 7, and 12 at δ_C 47.35, 174.33, 166.88, and 22.03 respectively but not the other proton at δ_H 1.97 in this methylene group. At last, the proton at δ_H 1.47 correlates with carbon 2 at δ_C 47.35 but not the other geminal proton at δ_H 2.30.

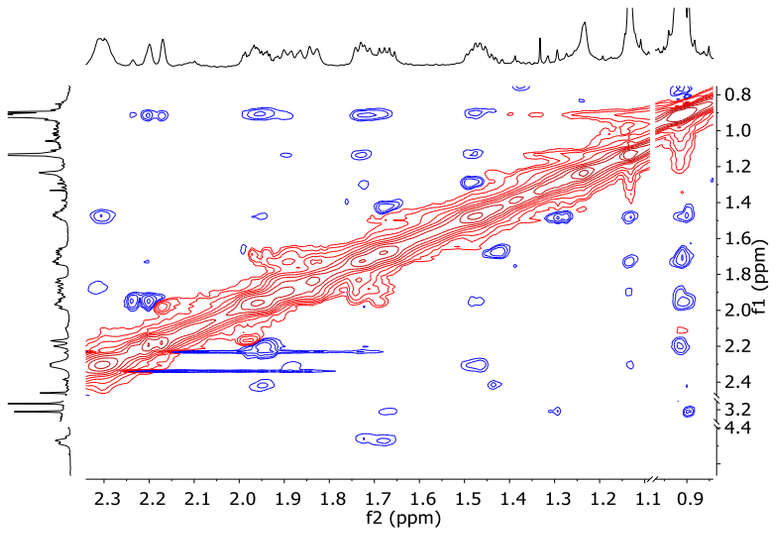

Figure. 32. NOESY concentrated-spectrum of correlations between protons at f1, δ_H 0.85 and 4.5 and f2, δ_H 0.80 and 1.17, (DMSO-d6).

NOE data show correlations between protons at δ_H 0.92, 1.13, 1.47, 1.73, and 1.90 making them oriented on the same side in this compound, (Fig. 32). Also, protons at δ_H 1.67, 2.30, and 4.48 have correlations with each other making them accordingly oriented on the opposite side of the previously mentioned protons. Consequently, the bridge protons at carbons 2 and 9 were assigned to be in the down configuration in this compound to match the expected biosynthesis outcome that was already reported for this type of compound to finally propose the relevant structure of the compound **22**. This will assign the first group of protons to be in the down configuration and the other group to be in the opposite up configuration, so the carboxylic group at carbon 11 is also in the up configuration. Regarding the methylene protons at carbon 4, the NOE correlations are proven to be indecisive as both protons are coupling with the methyl protons at δ_H 0.92, making the method described before in compounds **19** and **21** applied here. Upon testing both directions for the proton at δ_H 2.18 to agree with the data from HMBC, it can be concluded that this proton is in the down configuration. Subsequently, the relevant structure of compound **22** can be assigned, see (Fig. 33) and section 9.4 - (Fig. S16).

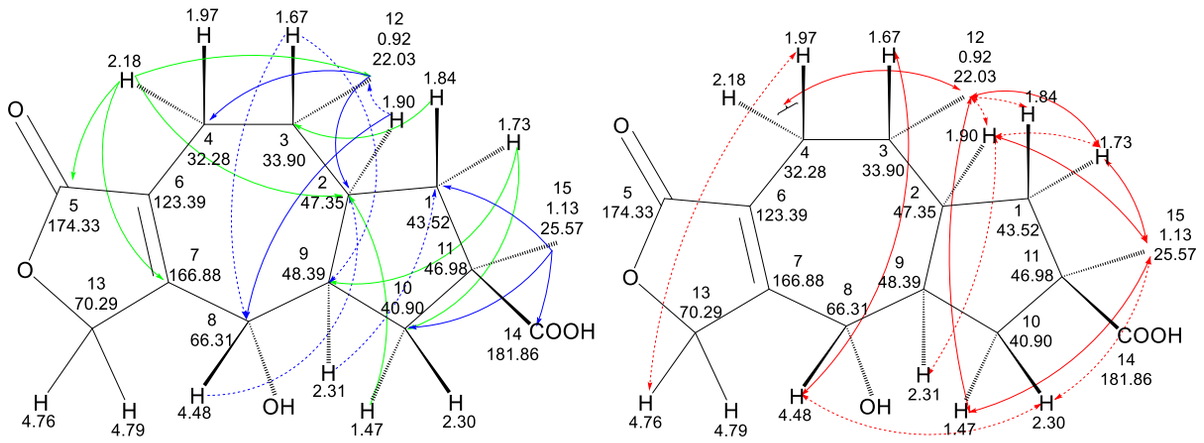

Figure. 33. Relative structure of compound **22** with assignments, (DMSO-d6). Left: selected HMBC correlations (⟶), HMBC correlations with Karplus relationship (⟶). Right: NOESY correlations (⟷).

4.1.3.5 13-Hydroxy-14-carboxy-deoxylactarorufin A (**23**)

4.1.3.5.1 Own contribution to **23**

In this research, the stereo configurations of all of the three methylene groups, the double oxygenated proton at carbon 13 and the carboxylic acid moiety at carbon 11 were assigned for the new compound 13-hydroxy-14-carboxy-deoxylactarorufin A (**23**) that was also already extracted before from *Lactarius circellatus* mushroom. This task was achieved using the combined NMR data that were already measured before and the one that was repeated in this research in CD_3OD.

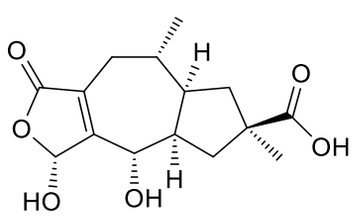

13-Hydroxy-14-carboxy-deoxylactarorufin A (**23**)

The new compound **23** is very similar to the previous new compound **22** which differs only by the presence of an additional hydroxyl group at carbon 13. This assignment was verified by taking into consideration the increased chemical shifts for both carbon 13 and the proton attached to it towards the low field area in the 1D-NMR spectrums, (δ_H 6.13, δ_C 99.04).

The new HMBC data shows more correlations for the methylene protons at carbon 4 that Karpuls relationships can interpret. These protons alongside the ones at carbon 1 show a lack of correlations with their neighboring carbons which a 90° dihedral angle can be fixed between them to explain such an occurrence, (Fig. 34).

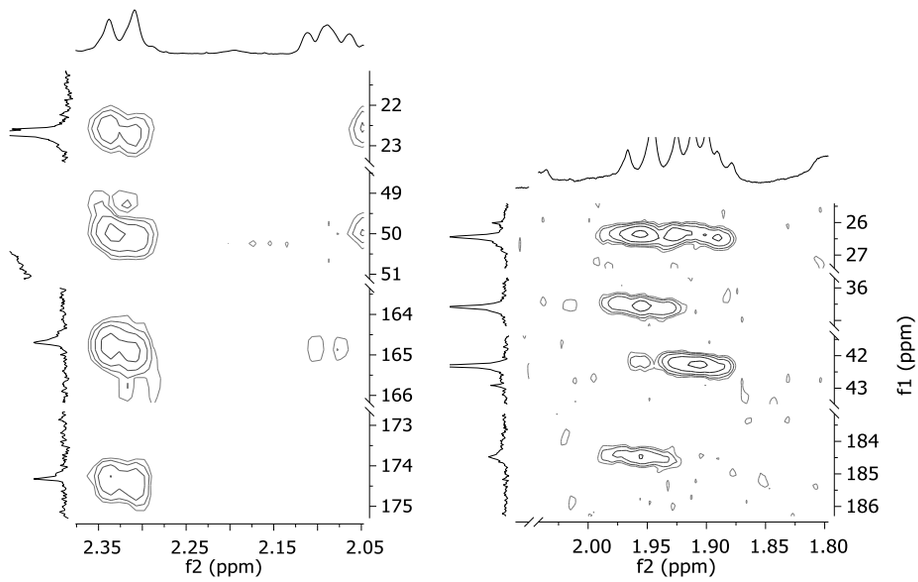

Figure. 34. HMBC concentrated-spectrums of correlations from previously extracted compound **23** from *L. circellatus*, (CD_3OD). Left: protons at δ_H 2.09 and 2.34 (repeated measurement). Right: protons at δ_H 1.90 and 1.95 (measured before).

Both protons at carbon 1 have HMBC correlations with the methyl carbon 15 at δ_C 26.44 but only the proton at δ_H 1.95 has correlations with carbons 3 and 14 but not the other geminal proton at δ_H 1.90 in this methylene group. Also, the later proton has a much stronger correlation with carbon 10 at δ_C 42.31 than the other proton in this methylene group, (Fig. 34-Right). Similar notice for the methylene group protons at carbon 4, as proton at δ_H 2.34 has correlations with carbons 2, 5, 7, and 22 at δ_C 49.69, 174.32, 164.69, and 22.69 respectively, but the other geminal proton at δ_H 2.09 either hasn't or only has a very weak correlation such as the one with carbon 7 at δ_C 164.69, (Fig. 34-Left).

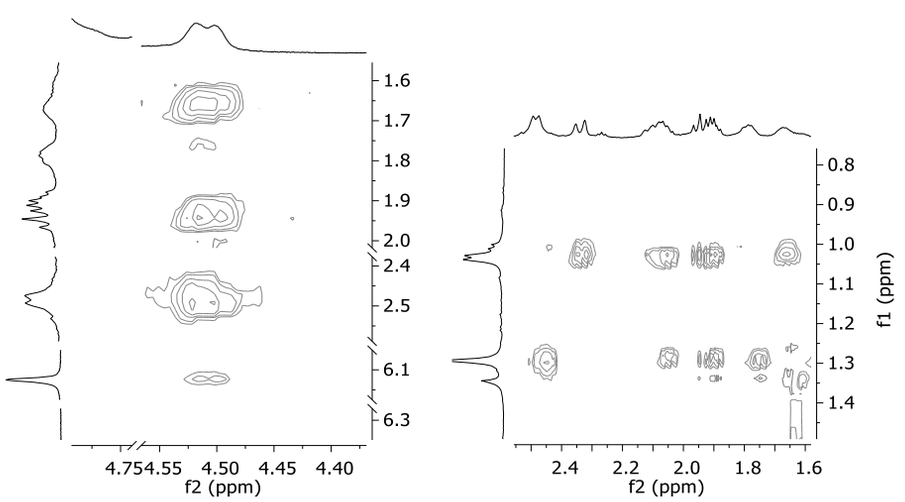

Figure. 35. NOESY expanded-spectrums of selected correlations, (CD_3OD). Left: between proton at δ_H 4.51 (f2), and protons at δ_H 1.67, 1.95, 2.48 and 6.13. Right: for methyl protons at δ_H 1.03 and 1.29 (f1).

The NOE data proved to be crucial in assigning the stereo configurations of the protons and moieties in the compound **23**. The oxygenated proton at δ_H 4.51 has NOE correlations with protons

at δ_H 1.67, 1.95, 2.48, and 6.13 making them oriented to the same side of this compound, (Fig. 35-Left). The methyl protons at δ_H 1.03 have NOE correlations with both methylene protons at carbon 1 and also with both methylene protons at carbon 4 with a stronger one with proton at δ_H 2.34. Also has a clear and pronounced correlation with the proton at δ_H 2.04 of the linking carbon 2, (Fig. 35-Right). This proton alongside with proton at δ_H 2.45 of the other linking carbon 9, has NOE correlations with the other methyl group protons at δ_H 1.29, which correlates with one of the methylene protons at carbon 10, proton at δ_H 1.79 making them all located in the same side of this compound.

Applying the previous data obtained from correlations from HMBC and NOE spectrums accompanied with the method elaborated before in sections 4.1.3.1 and 4.1.3.2, the relative structure of compound **23** can be determined. Starting from assigning both protons at δ_H 2.04 and 2.45 from the linking carbons 2 and 9 to be in the typical down configuration in compliance with the biosynthetic pathways. This will also put both of the methyl groups at δ_H 1.03 and 1.29 to be in the down configuration of this compound and so, the proton at δ_H 1.79. Consequently, the stereo configurations of the other group of protons at δ_H 1.67, 1.95, 2.48, 4.51, and 6.13 are in the up configuration side in the compound **23** and as a conclusion also the carboxylic acid group at carbon 11. Regarding the assignments of the methylene protons at δ_H 1.90 and 1.95 at carbon 1, these assignments were confirmed by applying a 90° dihedral angle between them and with the carbon atoms that should have HMBC correlations but they didn't. Which proton at δ_H 1.90 this angle with both carbons 3 and 14 at δ_C 36.58 and 184.48 respectively, when only in the down configuration of this compound with taking into consideration the NOE correlations of the other protons. The same applied to the other proton at δ_H 1.95.

The NOE results proved to be not decisive for assigning the stereo configurations of the methylene protons at carbon 4. So, the previously described method was applied here to achieve this task. Which proton at δ_H 2.09 can only be located in the up configuration of compound **23** to be compliant with the lack of HMBC correlations with carbons 5, 7, and 12 in contrast to the other geminal proton at δ_H 2.34.

Subsequently, the protons and moieties of compound **23** can be assigned and so the relative structure is shown in (Fig. 36).

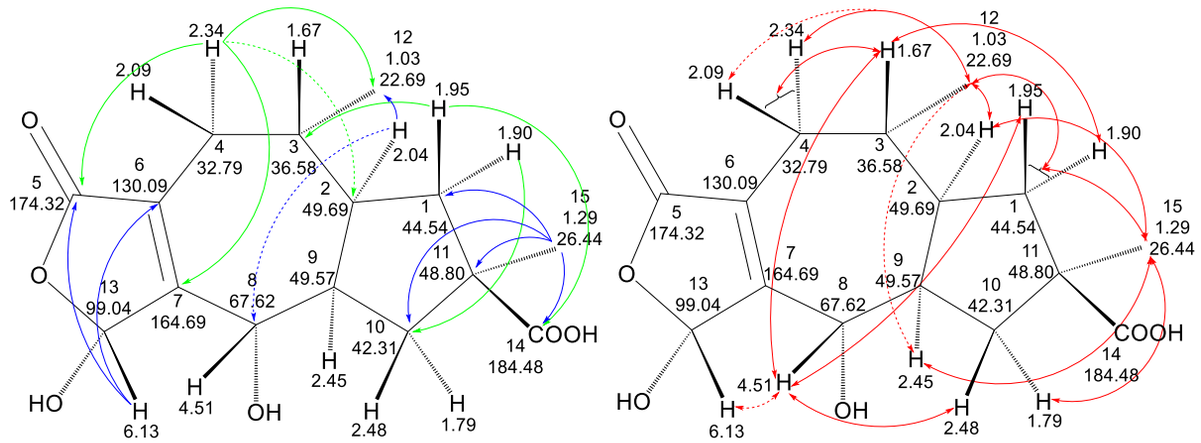

Figure. 36. Relative structure of compound **23** with assignments, **(CD_3OD)**. Left: selected HMBC correlations (⟶), HMBC correlations with Karplus relationship (⟶). Right: NOESY correlations (⟷).

4.1.3.6 Lactarotropone (**24**)

4.1.3.6.1 History of **24**

Lactarotropone was first extracted, elucidated, and named by DE BERNARDI *et al.* in 1984 from *Lactarius pallidus Persoon*,[33] also provided NMR data. Once again, BOSETTI *et al.* in 1989 extracted it from *L. scrobiculatus*[34] with a proposed biosynthetic mechanism. Finally, lactarotrpone was extracted from *Chenopodium album* Linn by QIN-GE *et al.* in 2020.[35]

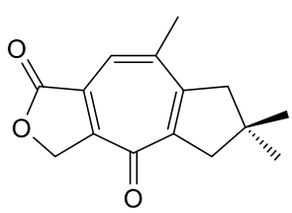

Lactarotropone (**24**)

4.1.3.6.2 Own contribution to **24**

In the already extracted and assigned compound **24** the only change was to switch assignments of data that were inquired in CD_3OD of each C-6 and C-7. Carbon atom at δ_C 154.87 is assigned to be at C-7 because protons at δ_H 5.22 at carbon 13 and proton at δ_H 2.45 at carbon 12 correlate with both carbons at δ_C 131.15 and 154.87 and it can't be distinguished between them. But only proton at δ_H 7.44 at carbon 4 correlates only with the latest carbon but not with others. So, one presumes that this shift will belong to the carbon three bonds away from the proton at δ_H 7.44. The assignments and HMBC and NOE correlations are in section 9.5 - (Fig. S18).

To inquire about more data on the highly unstable compound **24** 1D and 2D-NMR experiments were performed in DMSO-d6. This was inspired to have chemical shifts with coupling splits. Unfortunately, the new experiments didn’t express such a result, (Fig. 37), and subsequently the

stereo configurations assignment of methylene protons wasn't successful. The polarimetry was also measured, and as expected, the results proved to be trivial due to the structured nature of the compound, $[\alpha]_D^{25}$ +1.1 (MeOH; *c* 0.001).

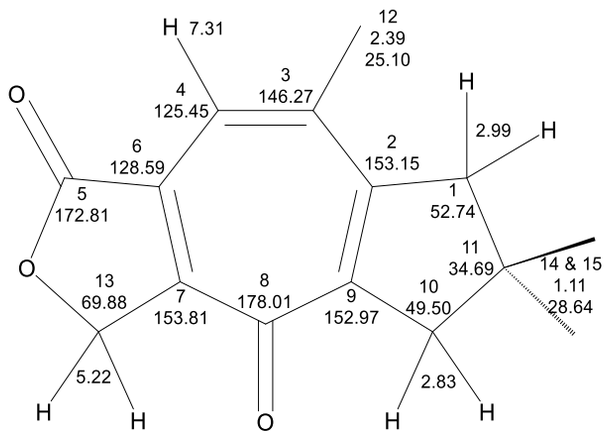

Figure. 37. Structure of compound **24** with assignments of ^{1}H-NMR, (DMSO-d6).

4.1.3.7 Lactarorufin A (**25**)

4.1.3.7.1 History of **25**

Lactarorufin A was first extracted and named by DANIEWSKI *et al.* in 1970 from *Lactarius rufus* without a proposed structure, but with only elucidated parts from the compound that could be the first attempt to introduce a structure for such a group of compounds, $[\alpha]_D^{20}$ +7.[36] Then they proposed a structure assigning the carbonyl group at C-13, and without stereo configurations assignments, but he proposed a possible biogenetic pattern of the compound formation.[37] VIDARI *et al.* in 1976 managed to extract it from *L. blennius* with an adjusted structure in which they placed the carbonyl group at the correct position at C-5 but with inverted stereo configurations assignments, $[\alpha]_D^{20}$ +12.5 ($CHCl_3$).[28] Then DANIEWSKI *et al.* in 1976 assigned the correct stereo configurations assignments afterward.[38] Then lactarorufin A was extracted from *L. trivialis* and *L. torminosus* by SEPPÄ *et al.* in 1980.[39] Also, it was extracted from *L. vellerus*[40] and *L. mitissimus*[41] by DANIEWSKI *et al.* in 1988 and 1990 respectively. Then it was extracted from *Russula emetica* by KOBATA *et al.* in 1995 providing the most recent NMR data, $[\alpha]_D^{25}$ +11.3 ($CHCl_3$; *c* 0.4).[42] Also, it was extracted from *Russula brevipes* by SURI *et al.* in 1997 but with contradicted stereo configurations assignments, $[\alpha]_D^{25}$ +18.2 (MeOH; *c* 0.1).[43] Afterword, lactarorufin A was extracted from *Russula delica* by YAOITA *et al.* in 2004,[44] *Clavicorona pyxidata* by ZHENG *et al.* in 2009,[45] *L. subvellereus* by KIM *et al.* in 2010,[46] *Russula nobilis* by MALAGÒN *et al.* in 2014,[47] *Russula nigricans* by ISAKA *et al.* in 2017,[48] *Russula aruea Pers* by ZHAO *et al.* in 2019,[49] but with contradicted stereo configurations assignments, and from *Linum numidicum Murb* and *Linum trigynum L.* by MOUNA *et al.* in 2022,[50] using LC-HRMS/MS.

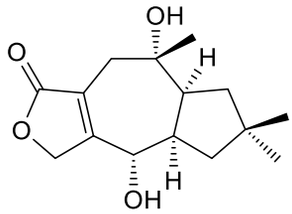

Lactarorufin A (**25**)

4.1.3.7.2 Own contribution to **25**

Stereo configuration assignments were achieved for the protons from three methylene groups in this compound out of four, moreover assigning the direction of the two methyl groups C-14 and C-15 that attached to C-11. This effort was established using NMR data from the previously extracted lactarorufin A (**25**) from *Lactarius circellatus* and *L. trivialis* in this research. The assignments were done using a similar approach described in sections 4.1.3.1.1 and 4.1.3.2.1. This compound already extracted from *L. circellatus* and measured in CD_3OD was measured again in $CDCl_3$ to compare the chemical shifts with the last reference that provided NMR data in $CDCl_3$ for this compound,[42] also to extract more 2D-correlations as much as possible. The shifts are matching but they didn't provide additional 2D data.

As expected, the Karplus relationship was observed in such a compound, (Fig. 38). For example, the proton at δ_H 1.40 at carbon 1 correlates with carbons at δ_C 30.43 and 74.03 but not the germinal proton at δ_H 1.65. At the same time, the latest proton correlates with carbon 10 at δ_C 46.27 but not the other proton in this methylene group.

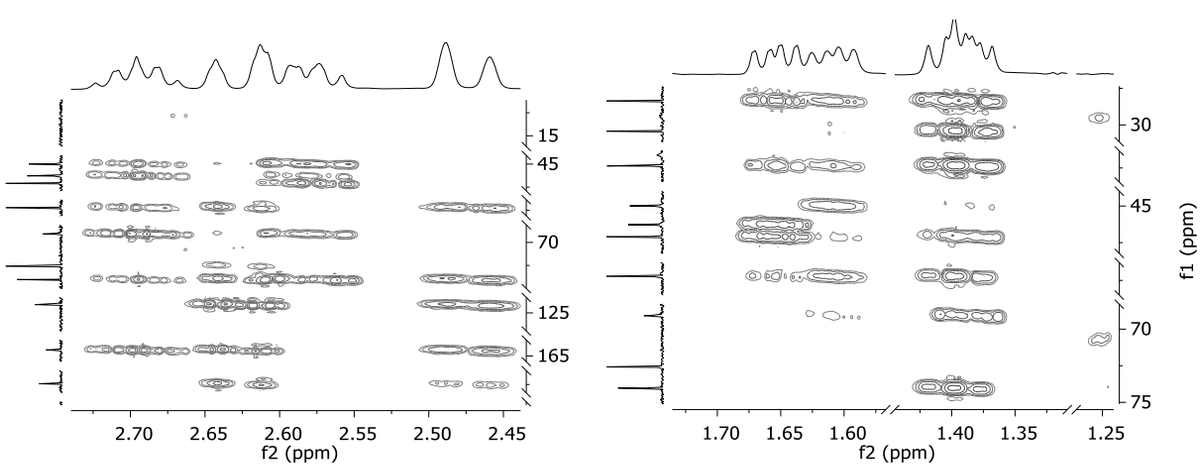

Figure. 38. HMBC concentrated-spectrums of selected correlations for compound **25** extracted from *L. trivialis*, (CD_3OD). Left: protons between δ_H 2.40 and 2.80. Right: protons between δ_H 1.35 and 1.70.

Also, such a pattern is observed in protons from the methylene group at C-10, in which the proton at δ_H 1.39 has correlations with each of the carbons at δ_C 30.43 and 69.08 but not the other. Also, the proton at δ_H 1.61 correlates with the carbons at δ_C 44.99 and 52.22 but not the other. Such relations apply also to protons at C-4. These correlations and also NOE correlations from lactarorufin A (**25**) extracted from *L. trivialis* are presented in (Fig. 39).

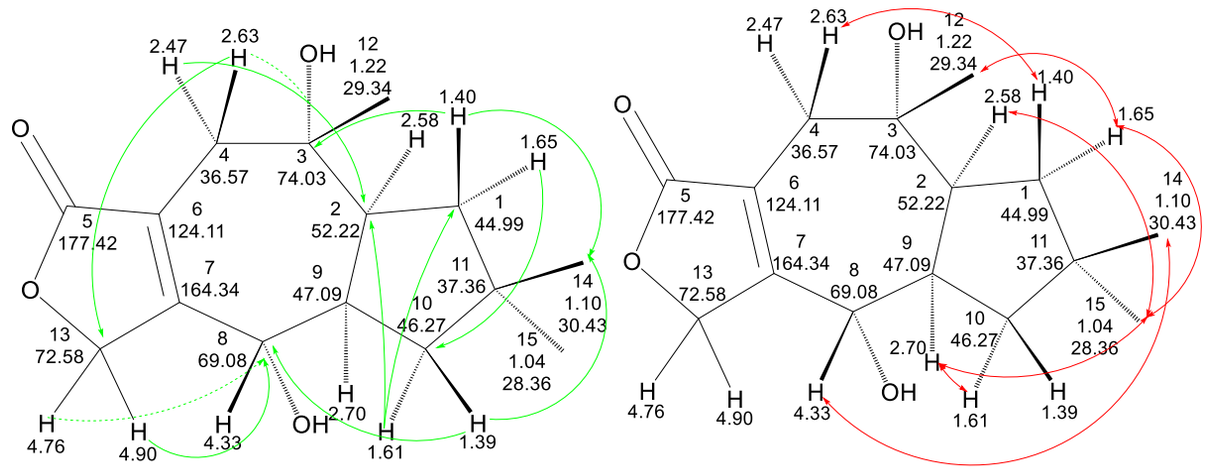

Figure. 39. Relative structure of compound **25,** Left: with HMBC correlations with Karplus relationship (⟶). Right: with NOESY correlations (↔), (CD_3OD).

Subsequently, the dihedral angle with a 90° angle was fixed between each methylene proton and carbon three bonds away, which should have HMBC correlations like the other geminal methylene proton but it didn't. Accompanied by NOE data, the stereo configurations assignments are explained for protons from methylene groups at C-1, C-4, and C-10, as well as for the two methyl groups at C-14 and C-15, (Fig. 39). The Measured polarimetry data for the compound extracted from *L. circellatus* mushroom, $[\alpha]_D^{25}$ +22.3 (MeOH; *c* 0.01) and the extracted from *L. trivialis* mushroom, $[\alpha]_D^{25}$ +23.5 (MeOH; *c* 0.005) are compatible with the reported results.

4.1.3.8 Deoxylactarorufin A (**26**)

4.1.3.8.1 History of **26**

Deoxylactarorufin A was first extracted from *Lactarius necator*, elucidated, and given the name 3-Deoxylactarorufin A by DANIEWSKI *et al.* in 1977,[51] but with an inverted stereo configuration of the methyl group at C-3, they provided ^{1}H-NMR, $[\alpha]_{578\,Hg}^{20}$ +70 ($CHCl_3$; *c* 0.1). Then he extracted it from *L. glyciosmus* and *L. subdulcis*.[52] Afterward, they changed the compound name to 3-Deosy-3-epilactarorufin A.[53] Then they managed to find and extract this compound from each of *L. vellereus*, *L. turpis*, *L. spinosulus*, *L. vietus* and *L. blennius*.[54] Then they provide the final stereo configuration of the methyl group at C-3 with it oriented into a down stereo configuration.[55] Finally, WUNDER *et al.* in 1996,[56] extracted this compound from *Lentinellus cochleatus* providing ^{13}C-NMR data but with inverted numbering positions for carbons 14 and 15, C-3, $[\alpha]_D^{23}$ +53 ($CHCl_3$; *c* 0.16).

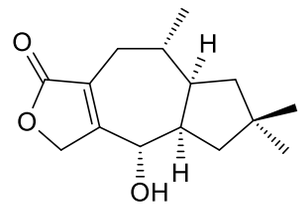

Deoxylactarorufin A (**26**)

4.1.3.8.2 Own contribution to **26**

In this research, protons from three methylene groups in this compound out of four were assigned with stereo configurations. This was achieved using already measured NMR data from the previously extracted deoxylactarorufin A from *Lactarius circellatus.* The assignments were done using a similar approach described in sections 4.1.3.1.1 and 4.1.3.2.1. To compare the chemical shifts with the previous reference that supplied NMR data in $CDCl_3$ for this compound,[56] as well as to extract as many 2D-correlations as possible, this compound that had previously been isolated from *L. circellatus* and measured in CD_3OD was measured again in $CDCl_3$. The chemical shifts lined up, and more 2D data were extracted.

In HMBC data, the Karplus relationship was noticed for protons from methylene groups at carbons 1 and 10. Although correlations of protons at C-1 are obvious, but proton at δ_H 1.75 has correlations with an area of carbon shifts that have two cramped carbons, carbon 1 at δ_C 48.74 and C-2, δ_C 48.72, (Fig. 40-Left). So, the repeated measured data in CDCl3 provided a better understanding of this correlation, (Fig. 40-Right). Due to the clearer signals of the intended carbons, it becomes understandable that the proton at δ_H 1.79 in this solvent (at δ_H 1.75 in CD_3OD solvent), has correlations with both carbons that become at δ_C 47.87 and 47.32 in this solvent.

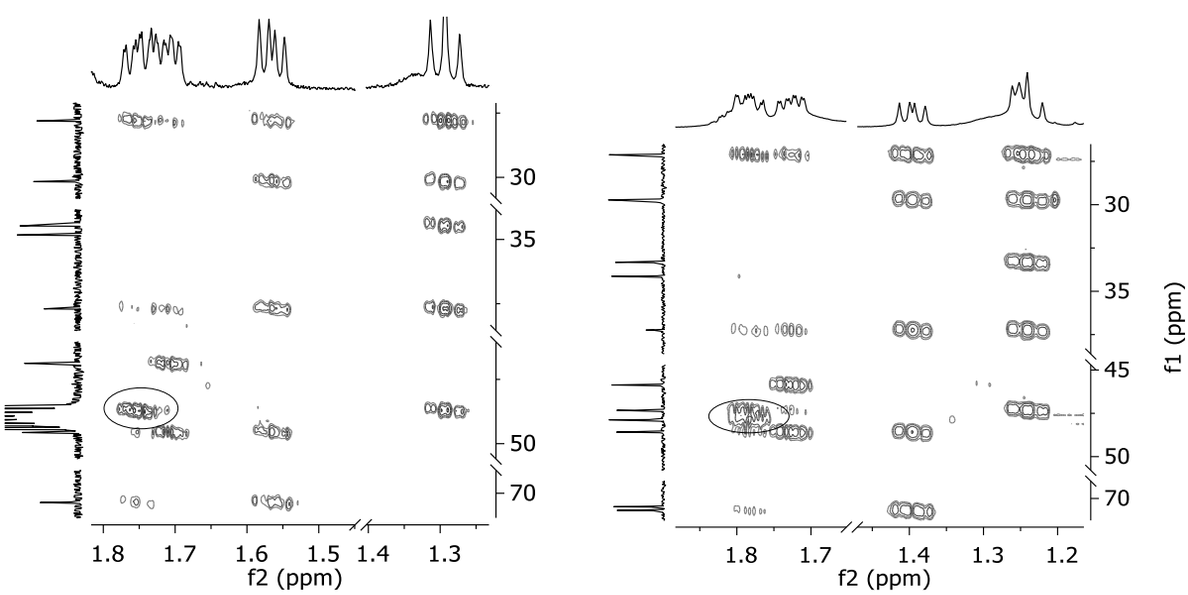

Figure. 40. HMBC concentrated-spectrums of methylene protons at C-1 and C-10 in compound **26** extracted from *L.circellatus*. Left: measured in (CD_3OD). Right: measured in ($CDCl_3$).

Once again, using these HMBC-data as the previously mentioned method accompanied with NOE-data, the stereo configurations were assigned for the methylene protons at carbons 1, 4, and 10, (Fig. 41). Also, the measured polarimetry for this compound agrees with the ones that have been reported, although it was done in a different solvent, $[\alpha]_D^{25}$ +37.3 (MeOH; *c* 0.001).

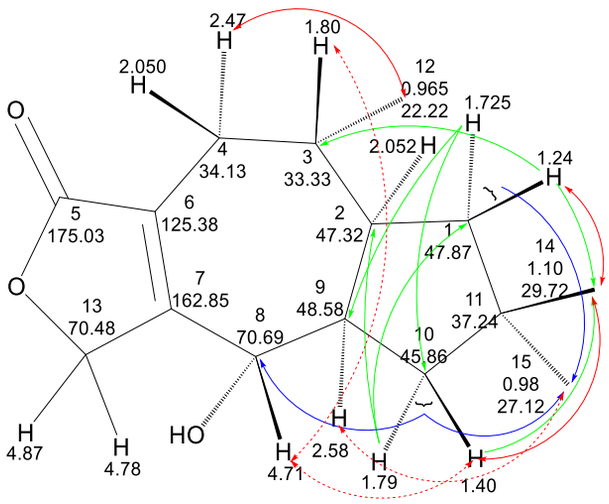

Figure. 41. Relative structure of compound **26** with assignments, selected HMBC correlations (⟶), HMBC correlations with Karplus relationship (⟶) and NOESY correlations (⟷), ($CDCl_3$).

4.1.3.9 Lactarorufin B (**27**)

4.1.3.9.1 History of **27**

Lactarorufin B (**27**) was first extracted from *Lactarius rufus* and named by DANIEWSKI *et al.* in 1970 but they didn't provide a structure for the compound, $[\alpha]_D^{20}$ +24.[36] Then they proposed a structure but assigned the carbonyl group to be at C-13.[57] Then they introduced the stereo configurations assignments for moieties in this compound.[38] Then NAWROT *et al.* in 1983 assigned the carbonyl group to be at the correct position at C-5.[58] Afterward, DANIEWSKI *et al.* in 1990 managed to extract this compound from *L. mitissimus* by providing NMR data but assigning the methyl group at C-11 to be at position 15, $[\alpha]_D^{20}$ +27 (EtOH; *c* 2.0).[41] The position of the methyl group was assigned finally to be at C-14.[59] Then, this compound was extracted from *Russula delica* by YAOITA *et al.* in 2004.[44] Finally, YAOITA *et al.* in 2004 provided an absolute structure for lactarorufin B but with inverted numbers of moieties at C-11.[60]

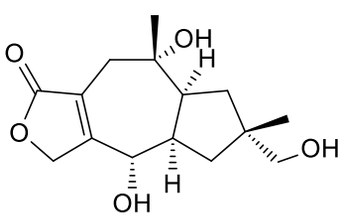

Lactarorufin B (**27**)

4.1.3.9.2 Own contribution to **27**

The stereo configuration assignments for three methylene groups in lactarorufin B were achieved in this research. This was done using the already measured NMR data in CD_3OD from the already extracted compound from *Lactarius circellatus*. Also, using NMR data measured in CD_3OD and $CDCl_3$ from this compound that was extracted as a mixture with the isomer compound **53** in this research from *L. trivialis*, section 4.2.6.2. These assignments come in agreement with the reported results by (Yaoita et al., 2004)[60] for each of the methylene groups at C-1, C-4, and C-10. Only their paper was mostly in Japanese language and such agreement was obtained from the English part. In this research, the assigning part was done using the argument described previously in sections 4.1.3.1.1 and 4.1.3.2.1.

Methylene groups at carbons 1 and 4 have HMBC correlations with the Karplus relationship. As proton at δ_H 1.36 has HMBC correlations with carbon 3 at δ_C 73.15 and carbon 14 at δ_C 26.36 but not the other proton at δ_H 1.86. Subsequently, this proton has HMBC correlation with carbon 10 at δ_C 40.40 but not the other geminal proton in this methylene group (Fig. 42-Right). Also, proton δ_H 2.48 from the methylene group at carbon 4 has HMBC correlation with carbon 12 at δ_C 30.00 but not the other geminal proton and correlates with carbon 2 at δ_C 53.44 stronger than the other correlation between the other geminal proton at δ_H 2.61 with same carbon (Fig. 42-Left).

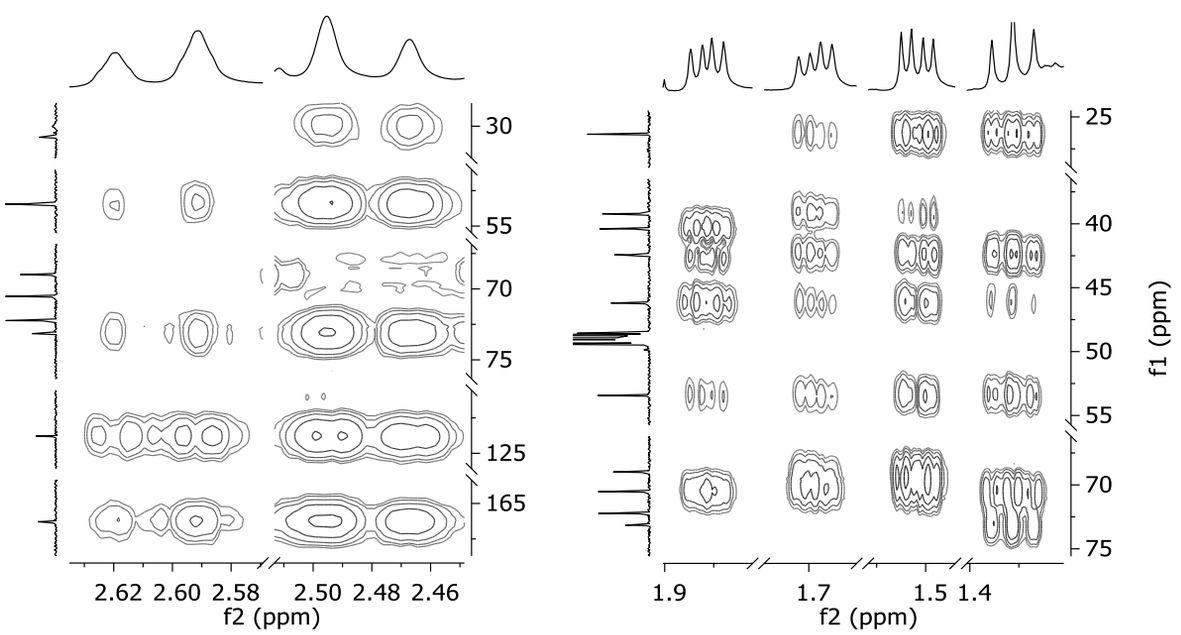

Figure. 42. HMBC concentrated-spectrums of correlations from compound **27** previously extracted *from L. circellatus*, (CD_3OD). Left: protons at δ_H 2.48 and 2.61. Right: protons between δ_H 1.30 and 1.90.

Then, using these HMBC data as the method mentioned previously accompanied with NOE data, the stereo configurations assignments were obtained for the protons at carbons 1, 4, and 10 (Fig. 43). Also, the measured polarimetry for this compound agrees with the ones that have been reported, although it was done in a different solvent, $[\alpha]_D^{25}$ +14.6 (MeOH; *c* 0.0015).

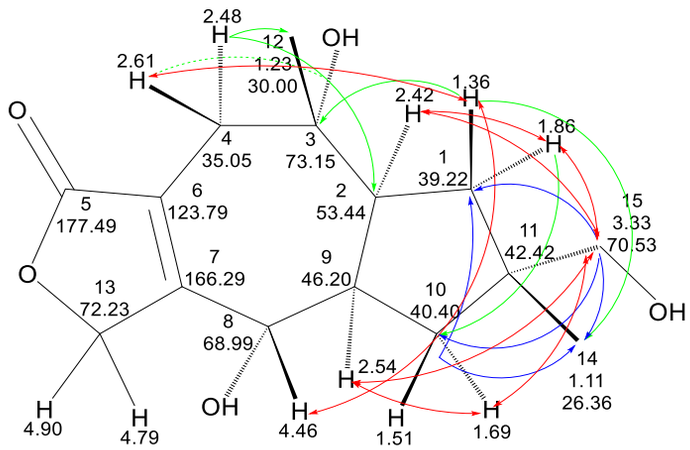

Figure. 43. Structure of compound **27** with assignments previously measured in (CD_3OD), selected HMBC correlations (⟶), HMBC correlations with Karplus relationship (⟶) and NOESY correlations (⟷).

4.1.3.10 Furandiol **15**

4.1.3.10.1 History of **15**

The furandiol **15** was first extracted and elucidated by NOZOE *et al.* in 1971 from *Fomitopsis insularis*, the proposed structure was without stereo configurations assignments.[61] Then the compound was extracted from *Lactarius scrobiculatus* by DE BERNARDI *et al.* in 1976.[62] They provide NMR data and stereo configurations assignments but it was inverted, $[\alpha]_D^{20}$ +30.8 ($CHCl_3$). Moreover, VIDARI *et al.* in 1976 extracted this compound from *L. blennius*.[28] ANDINA *et al.* in 1980 managed to extract this compound from *Russula sardonia*, they introduced the correct stereo configurations assignments.[63] Once again, DE BERNARDI *et al.* in 1984 extracted this compound from *L. pallidus Persoon*, but they suspect that such a compound is only a result of decomposition of stearoyl velutinal induced by extraction solvent.[33] Then, DANIEWSKI *et al.* in 1988 extracted the compound from *L. vellereus*.[40] Then it was extracted from *L. circellatus* and *L. necator* by STERNER in 1989, and they also have skepticism that such a compound is a result of velutinal degradation.[24] Then BOSETTI *et al.* in 1989 came and concluded that this compound that they extracted previously from *L. scrobiculatus* was not related to velutinal degradation.[34] Also, DANIEWSKI *et al.* in 1990 extracted the compound from *L. mitissimus*.[41] Then, THOMPSON *et al.* in 1992 synthesized this furandiol and provided NMR data.[64] Then, KOBATA *et al.* in 1995 succeeded in extracting this compound from *Russula emetica* and they provided the most recent NMR data of the compound but without assigning the resulted chemical shifts to the designated protons and carbons in the compound structure, $[\alpha]_D^{25}$ +31.0 ($CHCl_3$; *c* 0.1).[42] Then this compound was extracted again from *Russula delica* by YAOITA *et al.* in 2003,[65] from *L. subvellereus* by KIM *et al.* in 2010,[46] and finally from *Russula nobilis* by MALAGÒN *et al.* in 2014.[47]

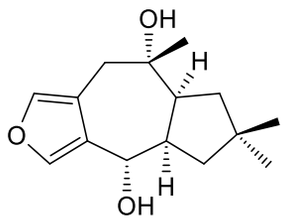

Furandiol **15**

4.1.3.10.2 Own contribution to **15**

The assignments of the stereo configurations of the three methylene groups at C-1, C-4, and C-10 in furandiol **15** were achieved in this research. This was done using the already measured NMR data in CD_3OD from the already extracted compound from *Lactarius circellatus*, also, with measuring the previous sample in $CDCl_3$. Also, using NMR data measured in CD_3OD and $CDCl_3$ from this compound that was extracted in this research from *L. trivialis*, section 4.2.6. The resulting chemical shifts come in agreement with the reported results by KOBATA *et al.* in 1995 that were measured in $CDCl_3$.[42] These assignments were done using the approach described previously in sections 4.1.3.1.1 and 4.1.3.2.1.

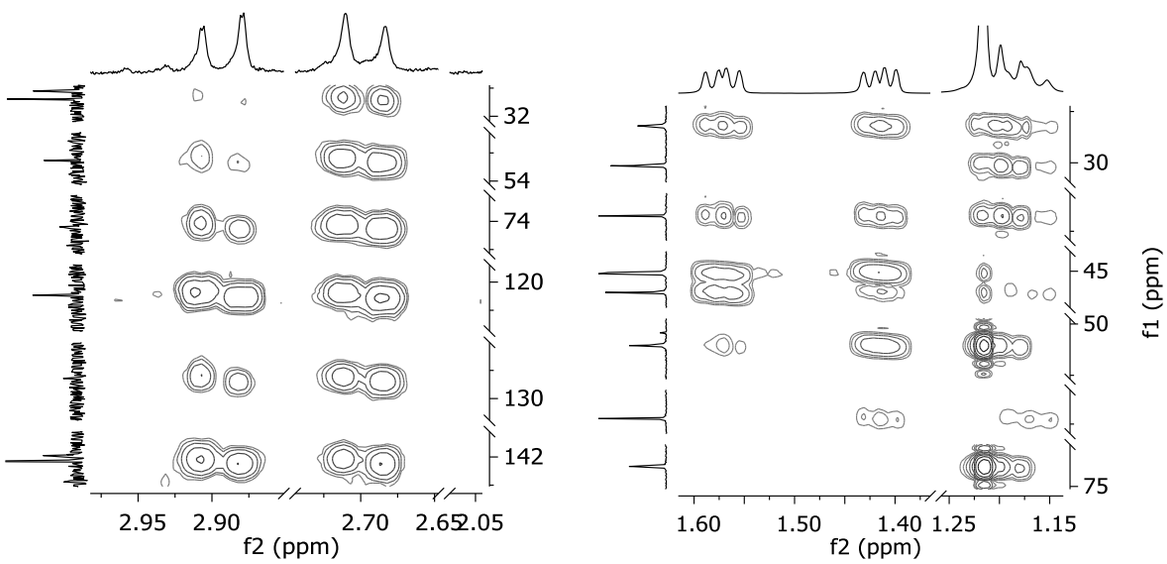

Figure. 44. HMBC concentrated-spectrums of correlations from compound **15**. Left: protons at δ_H 2.70 and 2.89, the data from previously extracted compound from *L. circellatus*, (CD_3OD). Right: protons between protons at δ_H 1.15 and 1.60, the data from compound extracted from *L. trivialis,* ($CDCl_3$).

The nature of chemical shifts in this compound made it necessary to use different deuterated solvents in the 1D and 2D-NMR experiments and use the combined results to perfect the assigning process. As methylene group at C-1 has one equivalent chemical shift for both protons at δ_H 1.48 when it's measured in CD_3OD. Section 9.9 - (Fig. S30) shows assigning stereo configurations of methylene protons only at carbons 1 and 4. These protons split into two chemical shifts at δ_H 1.17 and 1.41 when it's measured in $CDCl_3$. However, the methyl group that attached at C-11 becomes almost equivalent with one chemical shift at δ_H 0.98 when measured in $CDCl_3$. At the same time, the methylene protons at C-4 have more reliable 2D-NMR data when it's measured in CD_3OD than

when measured in $CDCl_3$ solvent, as in the later, the chemical shift of proton at δ_H 2.71 will be disturbed with the chemical shift of proton at δ_H 2.70 at carbon 9. Subsequently, the combined HMBC data from this compound resulted of using both in these deuterated solvents (Fig. 44).

Accordingly, one can infer that both protons at δ_H 1.41 and 1.57 from methylene groups at carbons 10 and 1 respectively don't have HMBC correlations with carbon 15 at δ_C 30.15 but the other geminal protons do (Fig. 44-Right). Also, oppositely, these protons have HMBC correlations with other carbons three bonds away, but not the other geminal protons. Such as, the proton at δ_H 1.57 at carbon 1 has HMBC correlations with carbons 9 and 10 at δ_C 46.03 and 45.12 respectively but not the other geminal proton at δ_H 1.20. Moreover, proton at δ_H 1.41 at carbon 10 has HMBC correlations with carbons 1 and 2 at δ_C 45.06 and 51.05 respectively but not the other geminal proton at δ_H 1.17.

Such a pattern of compliance with the Karplus relationship is also noticed with protons at carbon 4 but not so pronounced as the previously mentioned examples. As proton at δ_H 2.71 has much stronger HMBC correlations with carbons 2 and 12 at δ_C 51.05 and 31.51 respectively than the other geminal proton at δ_H 2.90 at this methylene group (Fig. 44-Left). Using this information alongside NOE data, the prober dihedral angle will be fixed between these protons and the surrounding carbons to match with the observed Karplus relationship. Accordingly, the stereo configurations assignments of the methylene protons in this compound will be reached (Fig. 45). Also, the reported results for this compound come in agreement with the measured polarimetry using a different solvent, $[\alpha]_D^{25}$ +14.6 (MeOH; *c* 0.0015).

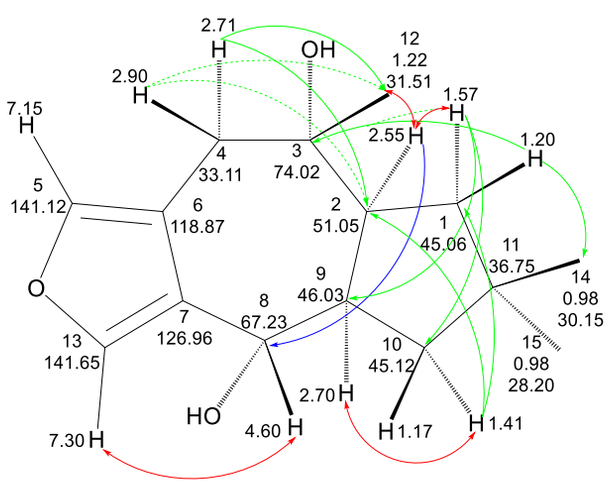

Figure. 45. Structure of compound **15** extracted from *L. trivialis* with assignments, selected HMBC correlations (⟶), HMBC correlations with Karplus relationship (⟶) and NOESY correlations (⟷), ($CDCl_3$).

4.1.3.11 Furan alcohol **28**

4.1.3.11.1 History of **28**

The furan alcohol **28** was first extracted from *Fomitopsis insularis* by NOZOE *et al.* in 1971, provided NMR data and proposed a structure but without stereo configurations assignments, $[\alpha]_D$ +69.5.[61] Then MAGNUSSON *et al.* in 1974 managed to extract this compound from *Lactarius vellereus*, *L. pergamenus*, and *L. helvus*.[66] They also provided NMR data and proposed partial stereo configuration assignments but it was inverted, $[\alpha]_D^{22}$ +123.0 (MeOH and $CHCl_3$; *c* 0.6). Then, VIDARI *et al*. in 1976 extracted this compound from *L. blennius*.[28] Then, ANDINA *et al.* in 1980 succeeded in extracting this compound from *Russula sardonia*.[63] They assigned the stereo configurations of the hydroxyl group at C-8 and the proton at C-9 to be in the down configuration. After that, STERNER in 1989 extracted this furan alcohol from *L. circellatus* and *L. nector*.[24] They refer to this compound as (hydroxyfuran) and (monohydroxyfuran). Moreover, PANG *et al.* in 1992 extracted this compound from *L. scrobiculatus* referring to it as (lactarane furan).[67] Also, THOMPSON *et al.* in 1992 reported the total synthesis of this compound also providing NMR data.[64] Afterward, DE BERNARDI *et al.* in 1993 extracted this furan alcohol from *L. chrysorrheus* and also from the previously reported *L. scrobiculatus*.[68] Finally, ALARCÓN *et al.* in 2013 extracted it from *Russula austrodelica* but they provided a contradicted structure.[69]

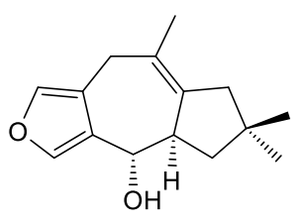

Furan alcohol **28**

4.1.3.11.2 Own contribution to **28**

The previously extracted furan alcohol **28** was dissolved in CD_3OD and run in NMR with 1D and 2D experiments to acquire the chemical shifts and correlations to elucidate and identify this compound structure. NOE data were missing, and accordingly, the compound fraction was measured again to achieve such information. The resulting data proved this compound unstable and will be degraded with time as the resulting NMR spectrums were for a mixture of compounds. Subsequently, this compound was extracted again from *Lactarius circellatus*, followed by performing 1D and 2D-NMR experiments, see section 9.10. By using the combined NMR data from both extracts, the stereo configurations assignments were achieved for the three methylene groups in this compound and also the stereo configurations of the two methyl groups attached to carbon 11 were assigned. Also, such a process came with agreement with the stereo configurations assignments for the protons at carbons 8 and 9.[64]

HMBC correlations of furan alcohol **28** show observations can be explained using the Karplus relationship. Such as the proton at δ_H 1.57 shows HMBC correlation with carbon at δ_C 29.35 but not the other geminal proton at δ_H 1.90 which itself correlates with carbon at δ_C 47.24 but not the proton at δ_H 1.57 (Fig. 46-Right). Also, protons at carbon 1 show such observation, such as the obvious lack of correlations between proton at δ_H 2.06 and carbons 9 and 10 at δ_C 49.44 and 47.40 respectively, in contrast to the other geminal proton at δ_H 2.20 in this methylene group. Also, protons at carbon 4 show a couple of set correlations that can be interpreted with the Karplus relationship, but they are less clear than the previously mentioned examples as the proton at δ_H 3.37 still shows correlations with its neighboring carbons but much weaker than the other proton in this methylene group, (Fig. 46-Left).

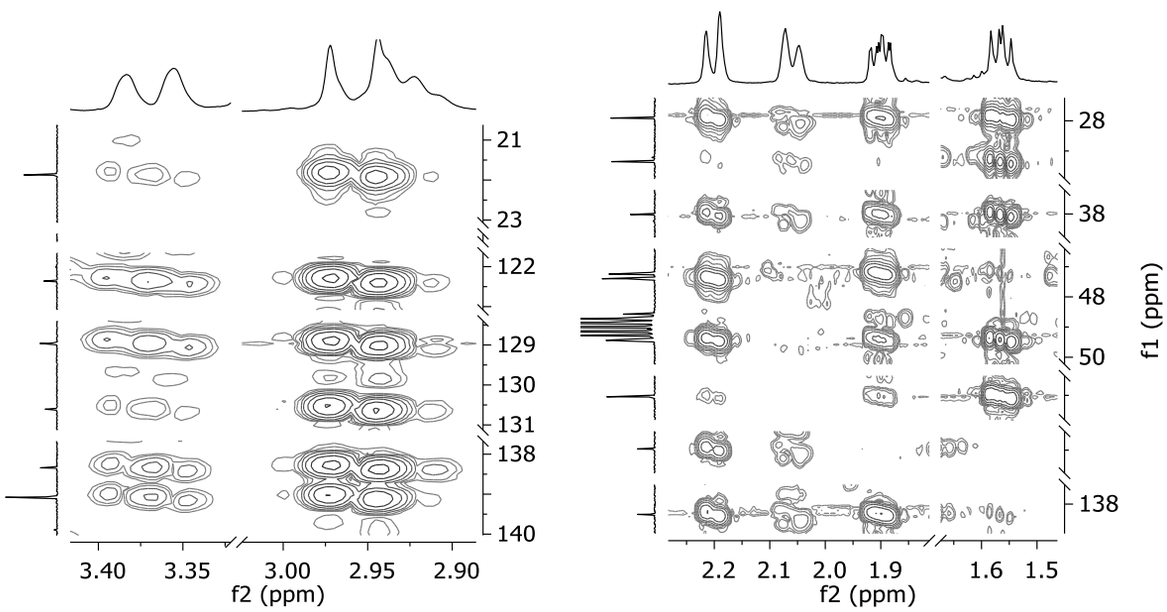

Figure. 46. HMBC concentrated-spectrums of correlations from previously extracted compound **28** from *L. circellatus*, (CD_3OD). Left: protons at δ_H 2.96 and 3.37. Right: protons between δ_H 1.50 and 2.25.

Subsequently, using a similar approach described in sections 4.1.3.1.1 and 4.1.3.2.1, the dihedral angle with 90° angle was fixed between each methylene proton and carbon three bonds away, which should have HMBC correlations like the other geminal methylene proton but it didn't. Accompanied with NOE data, the stereo configurations assignments are determined and explained for the previously mentioned moieties in this compound (Fig. 47).

Also, the measured polarimetry for this compound agrees with the ones that have been reported by the early research groups that extracted it,[61, 66] $[\alpha]_D^{25}$ +5.4 (MeOH; *c* 0.0017).

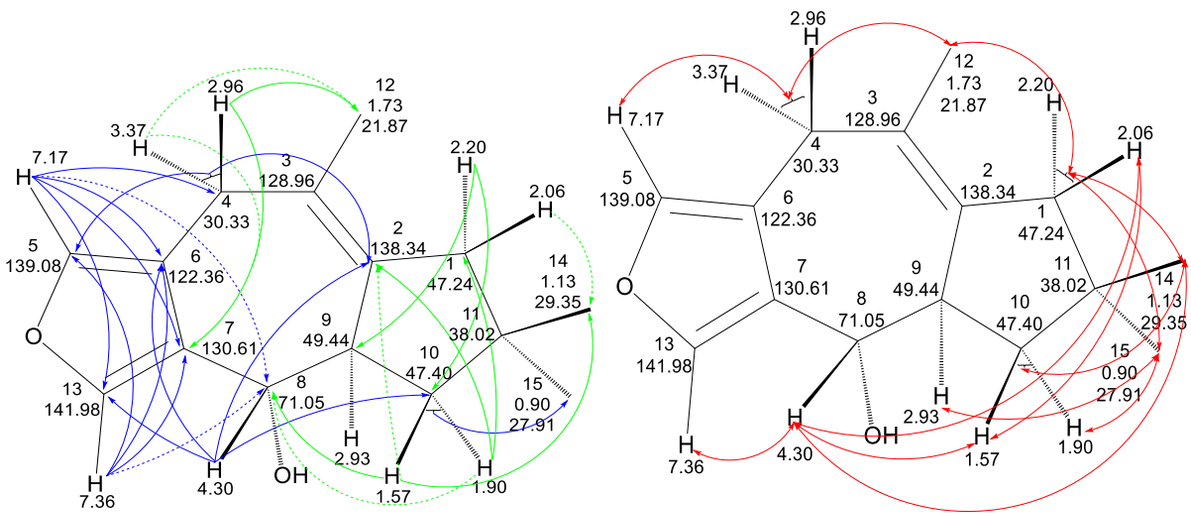

Figure. 47. Relative structure of compound **28** with assignments, (CD_3OD). Left: selected HMBC correlations (⟶), HMBC correlations with Karplus relationship (⟶). Right: NOESY correlations (⟷).

Additionally, the assignments of carbons 6 and 7 can't be proven by NMR data as the neighboring protons have extensive and similar HMBC correlations beyond the ability to conclude the exact positions of these carbons. And so, these assignments were done due to the chemical characteristics of these carbons. Carbon 7 is attached to the oxygenated carbon 8, and accordingly, it can be inferred that carbon 7 will have slightly less electron density than carbon 6 and that will cause the chemical shift of this carbon to be shifted more in the downfield direction in the NMR spectrum. This observation is noticed in the similar compounds furandiol **15** and methoxyfuranalcohol **29**.

4.1.3.12 Methoxyfuranalcohol **29**

4.1.3.12.1 History of **29**

The methoxyfuranalcohol **29** was first extracted from *Lactarius vellereus*, *L. pergamenus*, and also from *L. helvus* (*Russulaceae*), and elucidated by MAGNUSSON *et al.* in 1974.[66] They refer to it as (furan alcohol 9), and also they provided NMR data with different numbering system and with inverted stereo configurations assignments, $[\alpha]_D^{22}$ +6.0 (MeOH; *c* 0.6). Then, KABATA *et al.* in 1995 extracted the compound from *Russula emetica*.[42] They refer to it as (methoxyfuranalcohol), and they provided the most recent reported NMR data with the correct stereo configurations assignments for moieties from this compound but with inverted numbering assignments for C-14 and C-15, $[\alpha]_D^{25}$ +29.0 ($CHCl_3$; *c* 0.2). Finally, ISAKA *et al.* in 2017 extracted this compound from *R. nigricans*, $[\alpha]_D^{25}$ +5.0 (MeOH; *c* 0.32).[48]

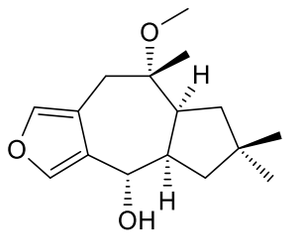

Methoxyfuranalcohol **29**

4.1.3.12.2 Own contribution to **29**

Applying the same method mentioned in sections 4.1.3.1.1 and 4.1.3.2.1, of fixating the angle between atoms in this compound to agree with the HMBC correlations that align with the Karplus relationship. This will result in assigning the stereo configurations of the protons from the three methylene groups existing in this compound. As shown in (Fig. 48), these protons will show at least once that when the compound is at the most stable structure formation, a dihedral angle of 90° between a proton and a neighboring carbon will be formed, making coupling between them missing.

For example, the proton at δ_H 2.68 from the methylene group at carbon 4 doesn't have an HMBC correlation with carbon 12 at δ_C 25.06 like the other geminal proton in this chemical group as would be expected. Another example is the protons at carbon 1. These protons will also show such an observation, as in two cases, the proton at δ_H 1.62 has correlations with carbons 9 and 10 at δ_C 48.44 and 45.20 respectively but not the other geminal proton at δ_H 1.54. Also, this proton at δ_H 1.54 has two correlations with carbons 3 and 14 at δ_C 79.23 and 31.87 respectively but not the other proton in this chemical group.

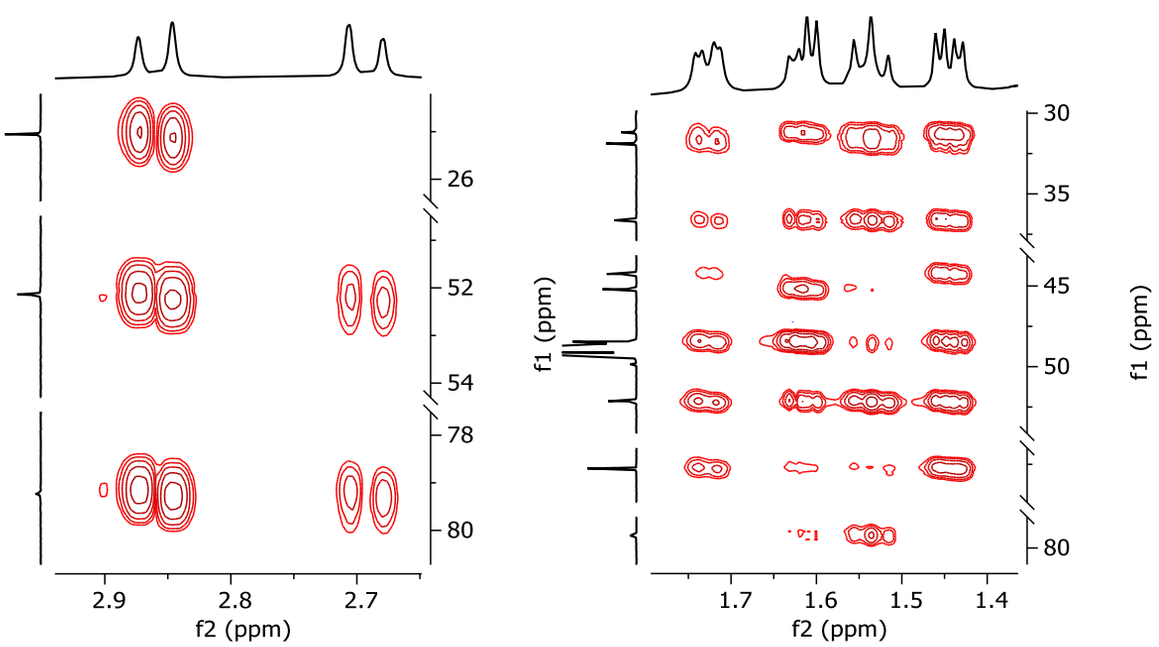

Figure. 48. HMBC concentrated-spectrums of correlations from previously extracted compound **29** from *L. circellatus*, (CD_3OD). Left: protons at δ_H 2.68 and 2.86. Right: protons between δ_H 1.40 and 1.80.

NOE data also show that protons at δ_H 4.56, 2.68, 1.54 and a methyl group at δ_H 1.12 exist on the same side of this compound. Also, in the same way, protons at δ_H 1.45, 2.468 and a methyl group at δ_H 1.07 exist in the opposite one. Adding this information from NOE data to the previously extracted information from HMBC correlations, lead to the determination of the stereo configurations of moieties in this compound as shown in the compound structure in (Fig. 49).

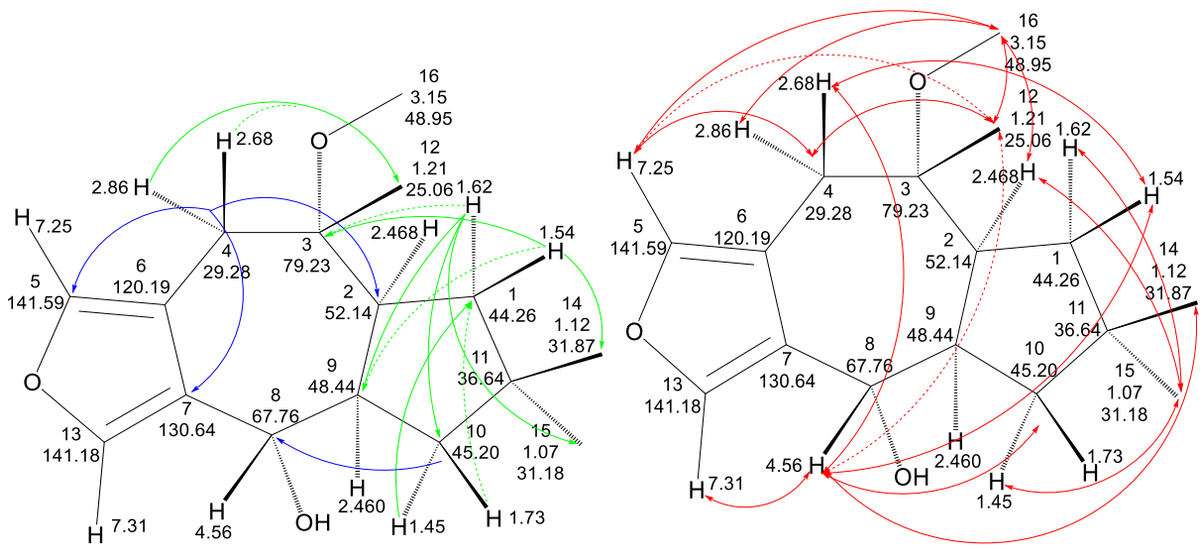

Figure. 49. Relative structure of compound **29** with assignments, (CD_3OD). Left: selected HMBC correlations (⟶), HMBC correlations with Karplus relationship (⟶). Right: NOESY correlations (⟷).

4.1.3.13 3,8-Oxalactarorufin A (**30**)

4.1.3.13.1 History of **30**

3,8-Oxa-13-hydroxy-lactar-6-en-5-oic-acid γ-lactone, was given the name 3,8-oxalactarorufin A (**30**) in this research was first introduced by DANIEWSKI *et al.* in 1971 as a product of the chemical reaction of lactarorufin A.[37] Subsequently, the assignment of the carbonyl group was at the wrong position at C-13, $[\alpha]_D^{20}$ +132. Then, they succeed in extracting this compound from *Lactarius necator* providing NMR data and the stereo configurations assignments just with inverted numbering of carbons at positions 14 and 15.[70] The epoxy bridge between C-3 and C-8 is in the down configuration, $[\alpha]_D^{20}$ +334.5 ($CHCl_3$; *c* 0.6). A similar but different compound with the name (Rufuslactone) was extracted from *L. rufus* by LUO *et al.* in 2005.[71] The compound has inverted moieties of the seven-member ring part which the epoxy bridge between C-3 and C-8 is in the up configuration. They provided NMR data for both compounds with the inverted numbering of carbons 14 and 15, $[\alpha]_D^{22.6}$ –5.87 ($CHCl_3$; *c* 0.24). After that, this compound was extracted from *Strobilurus stephanocystis* by HIRAMATSU *et al.* in 2008.[72] Finally, MALAGÒN *et al.* in 2014 extracted this compound from *Russula nobilis*.[47] They refer to it as (5-lactaranolides epoxylactone (+)).

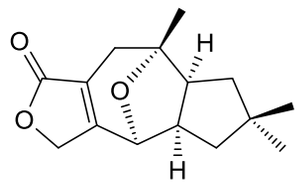

3,8-Oxalactarorufin A (**30**)

4.1.3.13.2 Own contribution to **30**

In this study, the stereo configurations of the protons of the four methylene groups in this compound at C-1, C-4, C-10, and C-13 were assigned. Also reviewing the most updated assignments of this compound.[71] This was done using the already measured NMR data in CD_3OD of the already extracted compound from the *Lactarius circellatus* mushroom. Moreover, NMR data from the previous fraction was measured in $CDCl_3$. The stereo configurations assignments were done using the approach described previously in sections 4.1.3.1.1 and 4.1.3.2.1.

The previous elucidation of this compound was based on a comparison between the resulting chemical shifts of the measured extracted compound with the reported chemical shifts of this compound done by *Luo et al.* in 2005.[71] The resulting chemical shifts come in agreement with the reported one that was measured in $CDCl_3$, but that research group still reported such data without assigning the stereo configurations for the targeted protons, also, there were mistakes in assigning some of the NMR chemical shifts from this compound. First, they exchange the carbon chemical shifts assignments between carbons 1 and 4 as they assign δ_C 31.2 to carbon 1 instead of carbon 4, and δ_C 42.0 to carbon 4 instead of carbon 1. (PS The argument here is using their reported shifts. In general, the chemical shifts are very similar to the one resulted here). The second exchange is between the carbon chemical shifts assignments of carbons 2 and 9. Also, a third wrong exchange is between assignments of carbon 12 and one of the methyl groups that attached at carbon 11. The fourth mistake is, regardless of their numbering system they assign protons of a methyl group at δ_H 0.98 to be in the up configuration and protons from the other methyl group at δ_H 1.00 to be in the down configuration of the compound, which is wrong. The opposite is the correct assignment. The process of achieving the assignments is described next.

The nature of chemical shifts in this compound made it necessary to use different deuterated solvents in the 1D and 2D-NMR experiments and use the combined results to perfect the assigning process. As methylene group at carbon 4 has one equivalent chemical shift for both protons at δ_H 2.33 when it's measured in CD_3OD. Section 9.11 - (Fig. S35) shows assigning stereo configurations of methylene protons only at carbons 1, 10, and 13. These protons split into two chemical shifts at δ_H 2.34 and 2.44 when it's measured in $CDCl_3$. However, the methylene protons at carbons 1 and 10 have similar 2D-NMR data to the one measured in CD_3OD. But protons at carbon 13 have no data at all when the compound is measured again in $CDCl_3$. This observation

is because these protons are exchanged with deuterium atoms from the deuterated solvent CD_3OD that was measured before. Such an encounter is discussed in detail in section 4.1.3.16.

Subsequently, the combined HMBC data from this compound resulting from using both of these deuterated solvents will be in use but with a focus on data from $CDCl_3$, (Fig. 50).

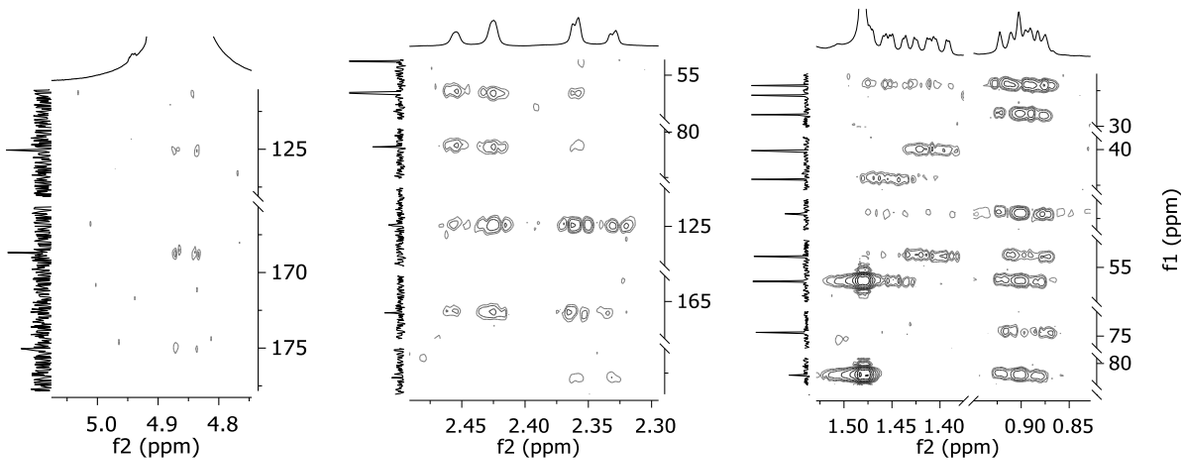

Figure. 50. HMBC concentrated-spectrums of correlations from compound **30** from *L. circellatus*. Left: previously measured in (CD_3OD), for protons at δ_H 4.85 and 4.93. Middle: protons at δ_H 2.34 and 2.44. Right: protons between δ_H 0.85 and 1.50, ($CDCl_3$).

The NMR data for compound **30** measured in $CDCl_3$ show complaint with Karplus relationship for methylene groups at carbons 1, 4, and 10 as shown in (Fig. 50-Middle and Right). For example, proton at δ_H 0.89 at carbon 10 has HMBC correlations with carbons 8 and 14 at δ_C 74.74 and 29.19 respectively but not the other geminal proton at δ_H 1.45. In the same way, the latest proton has correlations with carbons 1 and 2 at δ_C 42.08 and 55.98 respectively but not the proton at δ_H 0.89. The same observation was noticed for methylene protons at carbon 1, as proton at δ_H 0.90 correlated with carbons 3 and 14 at δ_C 80.82 and 29.19 respectively but not the other proton in this methylene group at δ_H 1.41. Also, the later proton correlates with carbons 9 and 10 at δ_C 54.22 and 40.07 respectively but not the other geminal proton. The same pattern of correlations was noticed for protons at carbon 4, as the proton at δ_H 2.44 has stronger and more pronounced correlations with its neighboring carbons than the other geminal proton at δ_H 2.34. The later proton correlates although weak with carbon 5 at δ_C 172.75 but not the other proton at δ_H 2.44.

Also using HMBC data from the previous measured fraction in CD_3OD, such observation was noticed for protons at C-13 (Fig. 50-Left). Proton at δ_H 4.85 that will be at δ_H 4.74 in data measured in $CDCl_3$ solvent has correlations with carbons 5, 6, and 7 but not the other geminal proton at δ_H 4.93 that will shift at δ_H 4.83 in measurements done with $CDCl_3$ solvent.

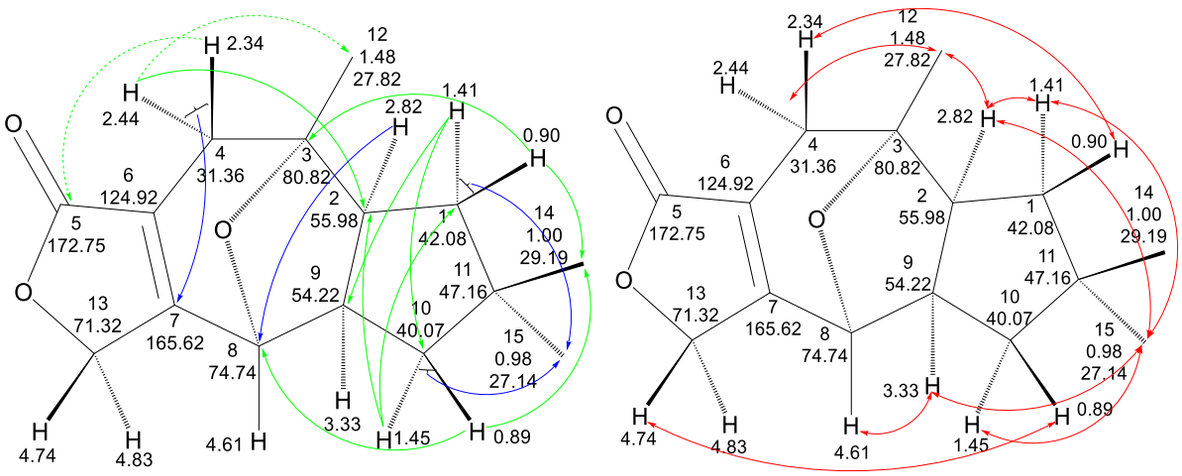

Figure. 51. Relative structure of compound **30** with assignments, ($CDCl_3$). Left: selected HMBC correlations (⟶), HMBC correlations with Karplus relationship (⟶). Right: NOESY correlations (⟷).

All together with correlations collected from NOE experiments in both deuterated solvents, and fixing the dihedral angle with 90° between the atoms that don't have HMBC correlations as expected, will finally afford assigning the stereo configurations for methylene protons and other moieties in this compound (Fig. 51). Also, the measured polarimetry data for this compound comes in agreement with the reported one, $[\alpha]_D^{25}$ +23.7 (MeOH; *c* 0.00061).

4.1.3.14 Lactarorufin N (**13**)

4.1.3.14.1 History of **13**

Lactarorufin N was first extracted from *Lactarius necator* by DANIEWSKI *et al.* in 1976.[38] They provided NMR data, $[\alpha]_D^{20}$ –15.1 ($CHCl_3$; *c* 1.0). After that, they proposed stereo configuration assignments with some contradicting assignments.[51] Then, this research group extracted this compound from *L. thejogallus*, *L. terminosus*, and *L. glyciosmus*.[52] They proposed stereo configuration assignments for the compound but with assigning proton at C-7 to be in the down configuration. This assignment is for the very similar isomer compound blennin A (**32**), which only differs from lactarorufin N (**13**) by the direction of the proton at C-7. And subsequently, has an opposite sign for the measured polarimetry, which is a positive sign for blennin A (**32**) and a negative sign for lactarorufin N (**13**). Then, this research group, DANIEWSKI *et al.* in 1981, adjusts the assignment of proton at C-7 to the correct up configuration.[53] Also, they extracted this compound from *L. vietus*.[54] Finally, STERNER in 1989 extracted lactarorufin N (**13**) from *L. circellatus*.[24]

4.1.3.14.2 Own contribution to **13**

In this study, proton and carbon chemical shifts were assigned to this compound as the last NMR data reported were from 1976.[38] Also, the stereo configurations assignments for the three

methylene groups in this compound at carbons 1, 10, and 13 were all achieved. This was done using the already measured NMR data in CD_3OD of the already extracted compound from the *Lactarius circellatus* mushroom. The NOE experiment was not performed before so this experiment was run in CD_3OD. Moreover, NMR data from this compound were measured in $CDCl_3$. The stereo configurations assignments were done using the approach described previously in sections 4.1.3.1.1 and 4.1.3.2.1.

At first glance at the NMR chemical shifts of the previously extracted fraction from *L. circellatus*, it is thought to be blennin A (**32**). This compound is a famous lactarane sesquiterpene that is already extracted from a variant of mushroom species. It was extracted from; *L. blennius*,[28] *L. torminosus*,[39] *L. thejogallus* and *L. glyciosmus*,[52] *Lentinellus cochleatus*,[56] *L. piperatus*,[73] *Strobilurus stephanocystis*,[72] *Russula sanguinea*,[74] and from *L. aurantiacus*, *L. subdulcis*, and *R. sanguinaria*.[32]

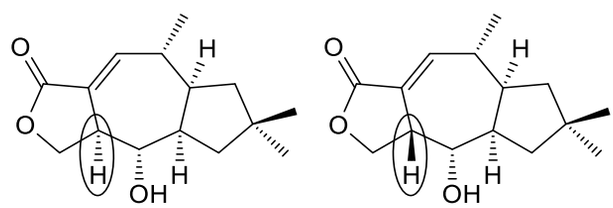

Blennin A (**32**) Lactarorufin N (**13**)

However, upon measuring and processing the NOE-NMR experiment in CD_3OD and also the data from full 1D and 2D-NMR experiments in $CDCl_3$. Moreover, the negative value for the measured polarimetry for this fraction was convincing that such a compound is lactarorufin N (**13**) the isomer of blennin A (**32**). They only differ in the stereo configuration of the proton at C-7 and in the sign of polarimetry data, which is (–) for lactarorufin N (**13**) and (+) for blennin A (**32**).

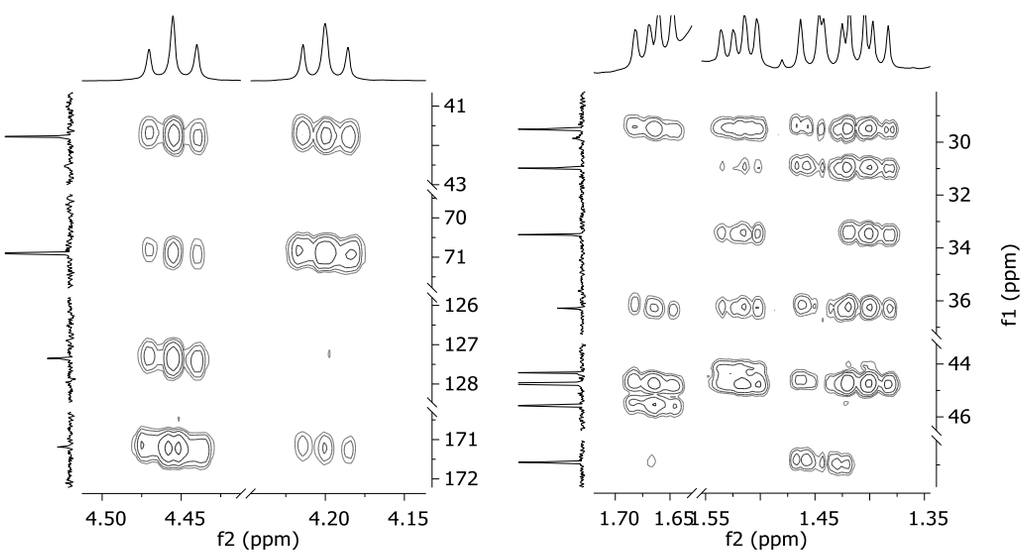

Figure. 52. HMBC concentrated-spectrums of correlations from compound **13** from *L. circellatus*, ($CDCl_3$). Left: protons at δ_H 4.20 and 4.46. Right: protons between δ_H 1.35 and 1.70.

The chemical shifts of the protons in this compound were not decisive for this research, as the protons of methylene groups at carbons 1 and 10 resulted in shifts with two protons equivalent. Section 9.12 - (Fig. 37) shows the assigning chemical shifts of this compound and the stereo configurations of methylene protons only at carbon 13. This made it necessary to use different deuterated solvents in the 1D and 2D-NMR experiments, and then use the combined results to undergo the assigning process. Indeed, the new NMR data in $CDCl_3$ were more distinguished. As methylene group at carbon 1 has now two ^{1}H-NMR shifts for their protons. These protons split into two chemical shifts at δ_H 1.40 and 1.52 when it's measured in $CDCl_3$. Also, protons at carbon 10 have now two chemical shifts at δ_H 1.44 and 1.66.

Protons at carbons 1, 10, and 13 show also observations in the HMBC-NMR data that can be explained using the Karplus relationship. As shown in (Fig. 52-Right), the proton at δ_H 1.40 has a much stronger correlation with the methyl carbon at δ_C 30.98 at carbon 14 than the other geminal proton at δ_H 1.52. Also, the later proton correlates with carbon at δ_C 44.33 at carbon 10 but not the other proton in this methylene group. Also, such notice was observed from protons at carbon 10, which proton at δ_H 1.44 has correlations with both carbons 8 and 14 at δ_C 70.90 and 30.98 respectively but not the other geminal proton at δ_H 1.66. The later proton also correlates with carbon 1 at δ_C 45.58 but not the other proton in this methylene group. Moreover, such notice is shown for the protons at carbon 13, in which the proton at δ_H 4.46 has HMBC correlation with carbon 6 at δ_C 127.35 but not the other proton at δ_H 4.20 from this methylene group, (Fig. 52-Left).

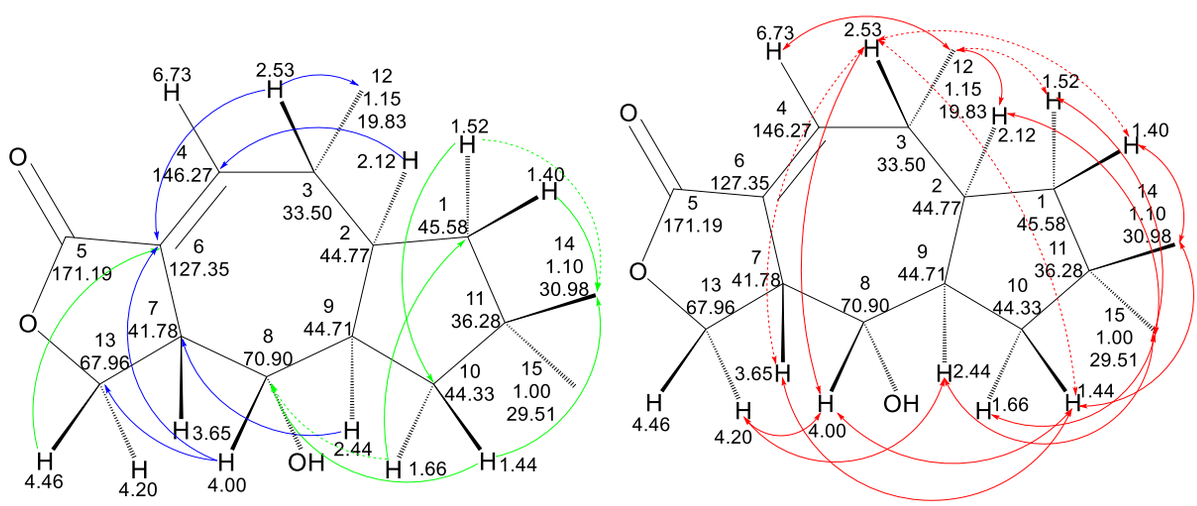

Figure. 53. Relative structure of compound **13** with assignments, ($CDCl_3$). Left: selected HMBC correlations (⟶), HMBC correlations with Karplus relationship (⟶). Right: NOESY correlations (⟷).

Applying the obtained information from HMBC to fix the dihedral angle with 90° between the atoms that has no correlations where it should be, as mentioned before, adding to it the crucial information from NOE-data one can assign all stereo configurations for protons and moieties in this compound as shown in (Fig. 53) above. Protons at δ_H 3.65 at carbon 7, δ_H 1.44 at carbon 10, δ_H 1.10 at carbon 14, δ_H 1.40 at carbon 1, and δ_H 2.53 at carbon 3 all are configured on the same side of this compound structure, which is the up configuration making this compound to be

identified as lactarorufin N. Also, the measured polarimetry data $[\alpha]_{\mathrm{D}}^{25}$ –66.8 (MeOH; *c* 0.001), comes in agreement with the reported one.[38]

4.1.3.15 Blennin C (**18**)

4.1.3.15.1 History of **18**

Blennin C was first extracted from *Lactarius necator* by DANIEWSKI *et al.* in 1975 referring to it as (lactaronecatorin A).[75] They also provided NMR data but with a different numbering system assigning the carbonyl group in the opposite carbon in the lactone ring in this compound, $[\alpha]_{\mathrm{Hg}}^{20}$ –5.56. Then, DE BERNARDI *et al.* in 1976 extracted it from *L. scrobiculatus* but still the assignments of C-5 and C-13 are inverted, also they provided NMR data, $[\alpha]_{\mathrm{D}}^{20}$ –7.3 ($CHCl_3$).[62] Then, VIDARI *et al.* in 1976 extracted the compound from *L. blennius* referring to it with the name (blennin C), also provided NMR data and assigned the carbonyl group to be at the correct position at C-5.[28] Then, SEPPÄ *et al.* in 1980 succeeded in extracting this compound from *L. trivialis* and from *L. torminosus*.[39] Also, PYYSALO *et al.* in 1980 identified it from the latest mushroom using gas chromatography (GC).[76] Afterwards, DANIEWSKI *et al.* in 1981 referring to this compound with the name (lactaronecatorin), introduced an identification method using the HPLC for this compound in mushrooms; *L. thejogallus*, *L. terminosus*, *L. glyciosmus*, *L. subdulcis* and the previously mentioned *L. necator*.[52] Then, DE BERNARDI *et al.* in 1984 extract this compound from *L. pallidus Persoon*.[33] Then, DANIEWSKI *et al.* in 1984 again using HPLC method identified this compound in *L. turpis*, *L. vellereus*, and *L. vietus*.[54] Then, DE BERNARDI *et al.* in 1986 assigned stereo configurations assignments to this compound mainly assigning the methyl group at C-3 in the up configuration.[77] Afterward, STERNER in 1989 extracted this compound from *L. circellatus* referring to it with the name (lactaronecatorin A).[24] After that, DE BERNARDI *et al.* in 1993 extracted this compound from *L. chrysorrheus*,[68] in which they also proposed a biosynthetic route to the formation of this compound. Then, WUNDER *et al.* in 1996 succeeded in extracting this compound from *Lentinellus cochleatus*,[56] but they reported positive sign of the measured polarimetry, $[\alpha]_{\mathrm{D}}^{23}$ +27.5 ($CHCl_3$; *c* 0.17). Afterward, YAOITA *et al.* in 2003 extracted the compound from *Russula delica*.[65] After that, this compound was extracted from *Strobilurus tephanocystis* by HIRAMATSU *et al.* in 2008.[72] Finally, MALAGÒN *et al.* in 2014 extracted blennin C from *R. nobilis* with a negative sign of polarimetry.[47]

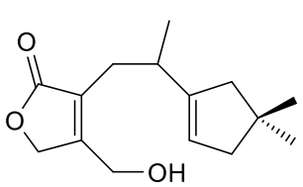

Blennin C (**18**)

4.1.3.15.2 Own contribution to **18**

NMR data measured in CD_3OD from the previously extracted blennin C from *Lactarius circellatus* didn't support the argument that is used in this research as most of the methylene groups show only one equivalent chemical shift for these protons, see section 9.13 - (Fig S39). Subsequently, the fraction of this compound was measured in $CDCl_3$ to obtain more data. Unfortunately, the results were similar and didn't provide additional data, but even the assignments of carbons 1 and 10 were not secured for sure as there is not enough data to explain the exact positions of the chemical shifts of these carbons, (Fig. 54).

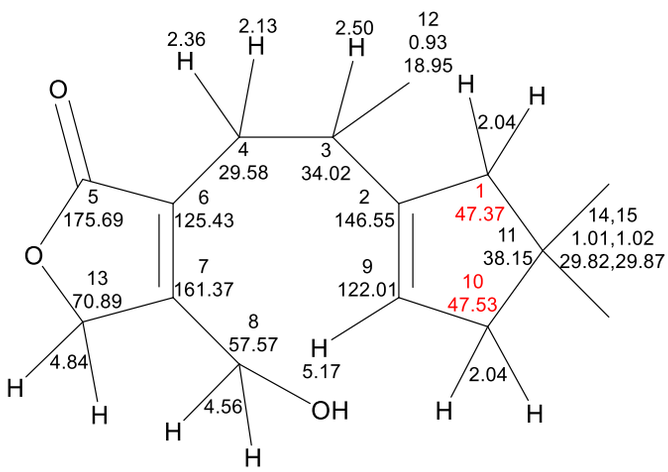

Figure. 54. Structure of compound **18** with assignments, ($CDCl_3$).

However, the results of the measured polarimetry for this compound, $[\alpha]_D^{25}$ –20.7 (MeOH; *c* 0.002), are in agreement with the negative sign data reported by DANIEWSKI *et al.* in 1975,[75] and DE BERNARDI *et al.* in 1976,[62] but don't agree with the positive sign data reported by WUNDER *et al.* in 1996.[56]

4.1.3.16 3,12-Anhydrolactarorufin A (**31**)

4.1.3.16.1 History of **31**

3,12-Anhydrolactarorufin A extracted for the first time from *Lactarius necator* by DANIEWSKI *et al.* in 1981.[52] They provided NMR data with partial stereo configurations assignments for protons at carbons 2 and 9, $[\alpha]_D^{20}$ +26.9 ($CHCl_3$; *c* 1.0). Afterward, using HPLC they identify the existence of this compound in each of the following *Lactarius* mushrooms; *L. turpis*, *L. controversus*, *L. vellereus*, *L. pergamenus*, *L. vietus*, *L. spinosulus*, and *L. blennius*.[54] Finally, this compound was extracted from *L. scrobiculatus* by BOSETTI *et al.* in 1989, assigning the stereo configurations of the hydroxyl group at C-8 to be in the down configuration.[34]

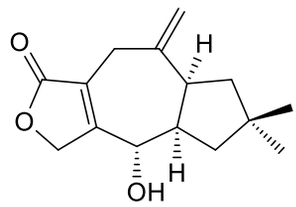

3,12-Anhydrolactarorufin A (**31**)

4.1.3.16.2 Own contribution to **31**

The stereo configuration assignments were reached in this research for three methylene groups out of the four groups that exist in this compound. This was done using the already measured NMR data in CD_3OD from the already extracted compound from *Lactarius circellatus*. Also, using NMR-data measured in DMSO-d6 for this compound. In this research, the assigning part was done using the method described previously in sections 4.1.3.1.1 and 4.1.3.2.1.

Weak HMBC correlations of the protons at C-13 made it important to repeat the measurements in the NMR experiments. Surprisingly, the resulting data don't show at all the chemical shifts and correlations of the protons in this methylene group, (Fig. 55-Middle). First, the possibility of degradation of this compound was considered, but there were no other changes in the chemical shifts of the rest of the protons in this compound. Then, after this fraction was measured in HR-LCMS it was clear that the calculated molecular formula shows the existence of two deuterium atoms in this compound instead of the normal hydrogen atoms expected in such a compound that was extracted from a natural source. This was convincing enough to accept the idea that during the previous measurements in the deuterated solvent CD_3OD, there was an unusual protons exchange with deuterium atoms. This caused the total disappearance of the chemical shifts of these protons in the NMR spectrums.

Also, one of the protons in the methylene group at carbon 1 and one of the protons in the methylene group at carbon 10, both have the same ^{1}H-chemical shift at δ_H 1.74 when compound **31** measured in CD_3OD, see section 9.14 - (Fig. S40). Accordingly, this made it necessary to use different deuterated solvents in the 1D and 2D-NMR experiments and use the combined results to produce more decisive assignments. Indeed, when using DMSO-d6 solvent the results were slightly better, as those protons become at δ_H 1.64 for the proton at carbon 1 and at δ_H 1.62 for the other proton at carbon 10.

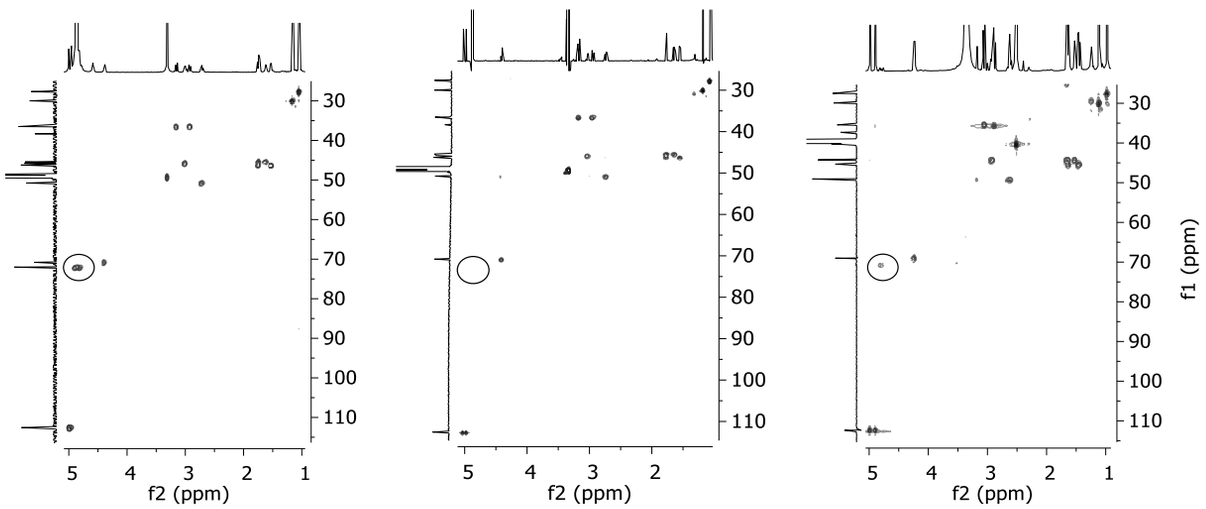

Figure. 55. HSQC-spectrums for compound **31**. Left: previously measured, (CD_3OD). Middle: repeated measurements, (CD_3OD). Right: after processing which some protons exchanged back, (DMSO-d6).

Subsequently, an attempt was made to exchange back the protons of the methylene group at carbon 13, see section 6.7.

Afterworlds, the HR-LCMS measurements show some protons exchange back but still the majority of this fraction contains deuterium atoms (Fig. 56).

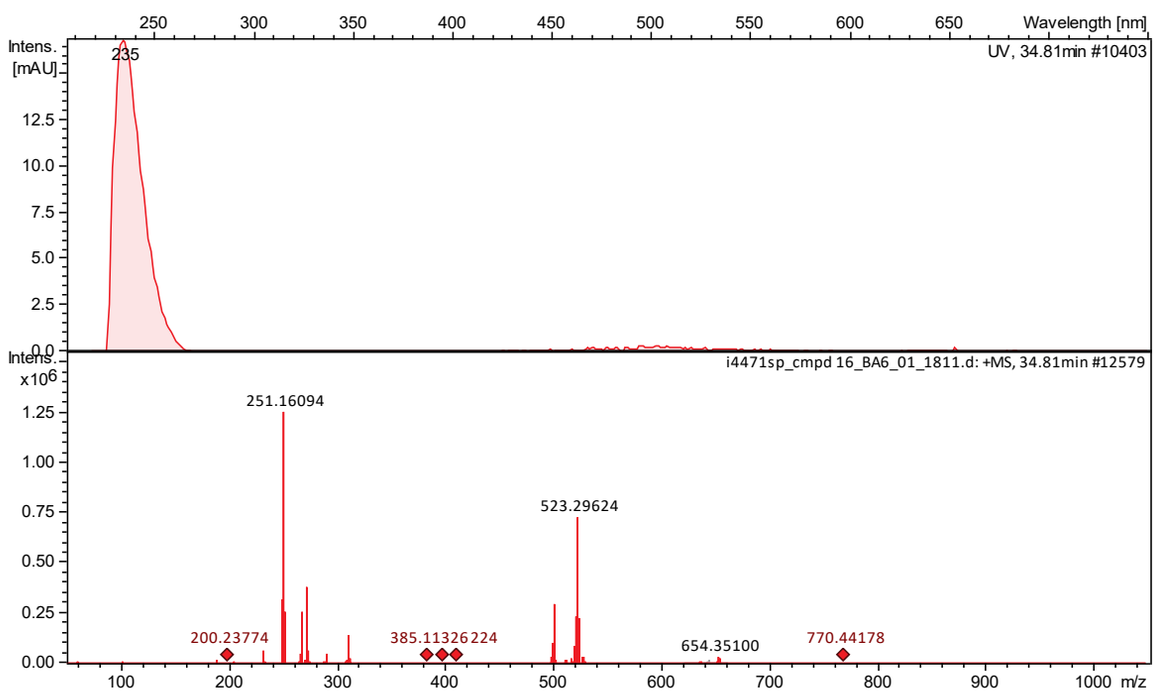

Figure. 56. HR-LCMS-spectrum view for compound **31** after treatment with aqueous alcoholic solvent.

The results show the existence of the protonated ion of compound **31** with two deuterium atoms as the major component, $[M+H]^+$ at *m/z* 251.16094, and the corresponding $[2M+H]^+$ ion at *m/z* 501.31496, not the expected ion of $[M+H]^+$ at *m/z* 249.14896. Also shows the existence of the compound with only one atom of deuterium, as there is also the ion $[M+H]^+$ at *m/z* 250.15506. The

generated molecular formulas for the previously mentioned ions and their corresponding compounds are shown in (Tab. 2).

Table. 2. Measured molecular formulas of compound **31**.

Meas. m/z	Ion Formula	Sum Formula
249.14896	$C_{15}H_{21}O_3$	$C_{15}H_{20}O_3$
250.15506	$C_{15}H_{20}DO_3$	$C_{15}H_{19}\mathbf{D}O_3$
251.16103	$C_{15}H_{19}D_2O_3$	$C_{15}H_{18}\mathbf{D_2}O_3$

Also, the signals that occasionally appear in HR-LCMS for this type of compound show agreement in calculations with the existence of one or two deuterium atoms in combination in this compound. Such as, $[M+Na]^+$ and $[2M+Na]^+$ ions at *m/z* 273.14327 and *m/z* 523.29654 respectively that correspond to compound **31** with two deuterium atoms, see section 9.14 - (Fig. S41). All these signals are major signals, indicating the compound with two exchanged deuterium atoms is the main component in this compound combination.

The proposed mechanism of this exchange of atoms is shown in (Fig. 57).

An instantaneous rearrangement of the electrons of the γ-lactone ring oxygen atoms will induce proton loss from the methylene group at carbon 13 and deuterium atom gain at the nucleophilic oxygen atom. Such an atom will be lost causing reformation of the carbonyl group and rearranging the electrons to finally attack another deuterium atom from carbon 13 to form again the methylene group that consists of one proton atom and one deuterium atom. This will put the compound in status **A**. Continued exchange presses will also lead to the replacement of the other proton in this moiety, causing the compound to reach status **B** which both protons at methylene group at carbon 13 will be replaced with deuterium atoms.

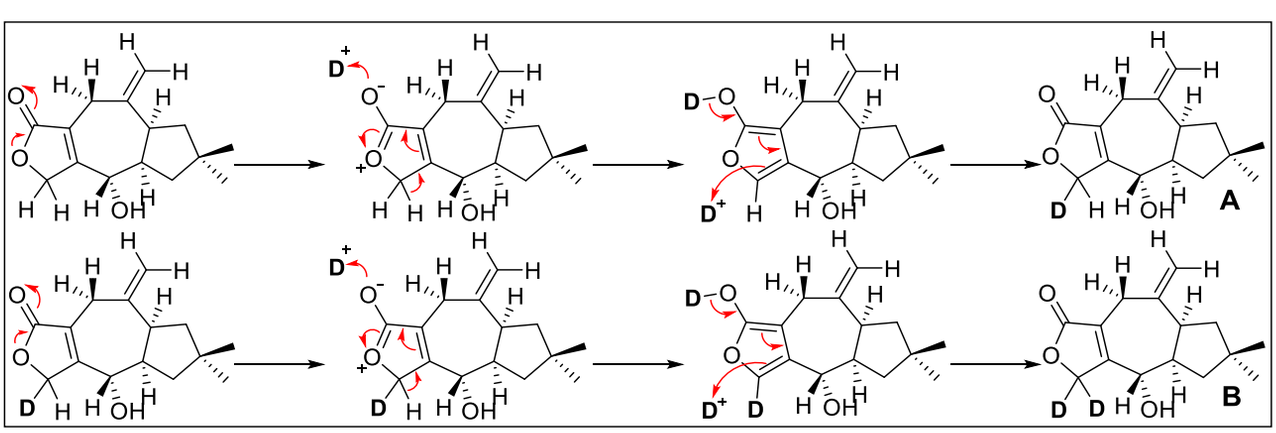

Figure. 57. Proposed mechanism of exchange protons at carbon 13 with deuterium atoms in compound **31**.
A: one atom exchanged. B: two atoms exchanged.

Nevertheless, upon measuring this fraction after exchanging back some of the protons at carbon 13, the results show the chemical shifts of these protons appear back (Fig. 55-Right). Despite the

appearance again of these chemical shifts and correlations in ^{1}H-NMR and HSQC-spectrums, it still didn't show correlations in HMBC-spectrums.

Methylene groups at carbons 1, 4, and 10 have HMBC correlations consonant with Karplus relationships. Such as proton at δ_H 1.51 at carbon 1 has HMBC correlations with carbon 9 at δ_C 48.89 and carbon 10 at δ_C 44.94 but not the other proton at δ_H 1.64. Subsequently, the later proton has HMBC correlation with carbon 13 at δ_C 145.21 and carbon 14 at δ_C 29.49 but not the other geminal proton in this methylene group (Fig. 58-Right). Also, the proton at δ_H 3.05 from the methylene group at carbon 4 has HMBC correlation with carbon 2 at δ_C 43.81 and carbon 5 at δ_C 173.85 but not the other geminal proton at δ_H 2.87 (Fig. 58-Middle). In the same manner, proton at δ_H 1.45 at carbon 10 has correlations with carbons 8 and 14 at δ_C 68.52 and 29.49 respectively but not the other geminal proton at δ_H 1.62. Also, the later proton correlates with carbon 2 at δ_C 43.81 but not the other proton in this methylene group. Protons at carbon 13 in the lactone ring in this compound have weak and indecisive HMBC correlations which can't be used in this argument (Fig. 58-Left).

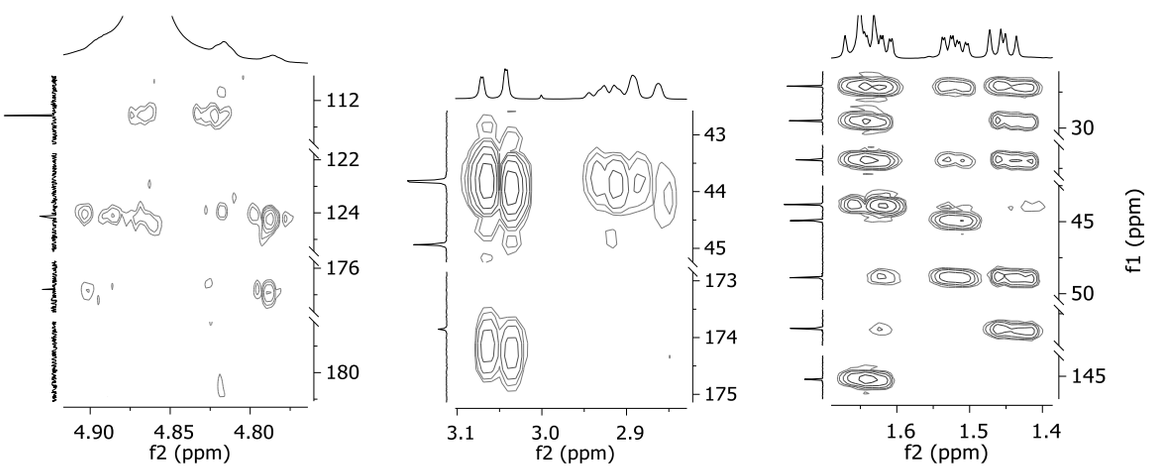

Figure. 58. HMBC concentrated-spectrums of correlations from compound **31** from *L. circellatus*.
Left: protons at δ_H 4.80 and 4.88, measured previously, (CD_3OD). Middle: protons at δ_H 2.87 and 3.05, (DMSO-d6). Right: protons between δ_H 1.40 and 1.70, (DMSO-d6).

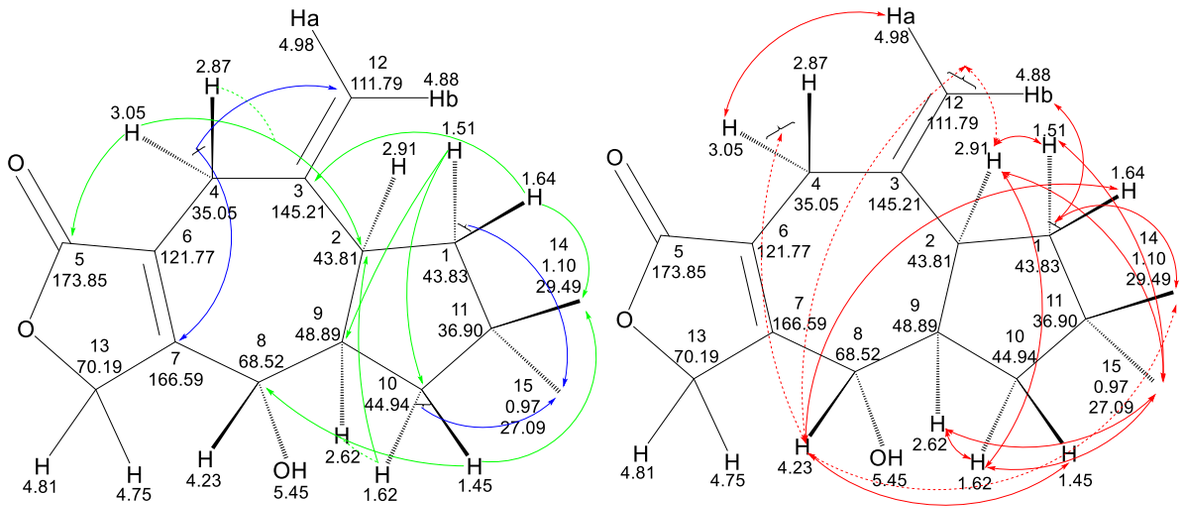

Figure. 59. Relative structure of compound **31** from *L. circellatus*, with assignments.
Left: with HMBC correlations (⟶), HMBC correlations with Karplus relationship (⟶).
Right: with NOESY correlations (⟷), (DMSO-d6).

Combining information from the HMBC correlations with the Karplus relationship with NOE correlations, one can assign the stereo configurations for protons and moieties in this compound except protons at C-13 (Fig. 59). Also, the measured polarimetry data, $[\alpha]_{\mathrm{D}}^{25}$ +22.6 (MeOH; *c* 0.001), agrees with the reported one.[52]

4.1.3.17 15-Hydroxyblennin A (**34**)

4.1.3.17.1 History of **34**

15-Hydroxyblennin A was first extracted by WIDÉN *et al.* in 1979 from *Lactarius torminosus* providing NMR data.[30] The name is derived using the numbering system that takes into account the two organic groups attached to C-11 to be in position 14 for the group in the up configuration, and accordingly, in position 15 for the other moiety in the down configuration. So, due to the hydroxyl group attached to the methylene group in the down configuration, the part (15-hydroxy) was added to the name of the compound – blennin A (**32**) – without such a moiety. Subsequently, when YAOITA *et al.* in 2012 reported extraction of the isomer compound 14-hydroxyblennin A (**52**) from *Russula sanguinea*,[74] in contradiction to the previously mentioned system. They used the numbering system of the group attached at C11 in the down configuration to be in position 14, and so, they described the already known compound 15-hydroxyblennin A (**34**). They also provided NMR and polarimetry data, $[\alpha]_{\mathrm{D}}^{19}$ +42.3 (MeOH; *c* 0.04), to this compound. Upon comparing them with data from the two compounds 14-hydroxyblennin A (**52**) and 15-hydroxyblennin A (**34**) that were extracted during this research from *L. trivialis* and *L. circellatus* respectively, it becomes clear, that the NMR data they provide are matching with the data from 15-hydroxyblennin A (**34**). This conclusion was mentioned before by GILARDONI *et al.* in 2014 in their report on lactarane

sesquiterpenes from the European mushrooms.[32] Accordingly, before this research, there is no NMR or polarimetry data were reported for compound 14-hydroxyblennin A (**52**).

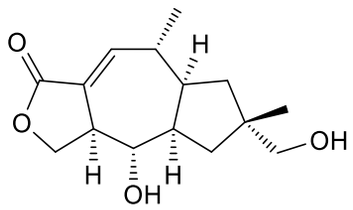

15-Hydroxyblennin A (**34**)

4.1.3.17.2 Own contribution to **34**

15-Hydroxyblennin A (**34**) was extracted from *Lactarius circellatus* during this research from the same fraction that compound **19** was extracted, section 4.1.3.1.1. Also, the stereo configurations assignments for protons of the methylene groups at carbons 1, 10, and 13 were achieved. This was done using NMR data from 1D and 2D experiments for the compound dissolved in CD_3OD. Also, 1D-NMR measurements were performed for this compound in $CDCl_3$ to compare the resulting data with the one reported from YAOITA *et al.* in 2012.[74] It's shown in (Tab. 3), the ^{1}H-NMR data measured in $CDCl_3$ for each of compound 15-hydroxyblennin A (**34**) extracted from *L. circellatus*, compound sangusulactones A extracted from *Russula sanguinea*[74] and compound 14-hydroxyblennin A (**52**) extracted from *L. trivialis*.

Table 3: ^{1}H-NMR data for compounds **34**, sangusulactones A[74], and **52** in $CDCl_3$.

position	δ_H (*J* in Hz) **34**	δ_H (*J* in Hz) sangusulactones A	δ_H **52**
1	α:1.47 1H (dd, 14.0, 5.0)	α:1.42 1H (dd, 13.9, 4.4)	1.60 2H (m)
	β:1.77 1H (dd, 13.9, 7.7)	β:1.70 1H (dd, 13.9, 7.7)	
2	2.14 1H (dddd, 10.0, 7.5, 5.0)	2.08 1H (m)	2.18 1H (m)
3	2.47 1H (dddd)	2.42 1H (m)	2.44 1H (m)
4	6.75 1H (dd appears as t, 3.0, 3.0)	6.68 1H (dd, 2.9, 2.9)	6.74 1H (dd)
5	-	-	-
6	-	-	-
7	3.32 1H (dddd)	3.29 1H (m)	3.33 1H (m)
8	3.62 1H (dd appears as t, 10.0, 10.0)	3.52 1H (dd, 10.3, 10.3)	3.63 1H (dd)
9	2.29 1H (dddd appears as tt, 10.2, 7.3)	2.23 1H (m)	2.38 1H (m)
10	α:1.33 1H (dd, 12.9, 11.0)	α:1.25 1H (dd, 12.8, 11.7)	α:1.55 1H (m)
	β:2.07 1H (dd, 13.0, 6.8)	β:2.06 1H (dd, 12.8, 6.6)	β:1.68 1H (dd)
11	-	-	-
12	1.17 3H (d, 7.3)	1.12 3H (d, 7.0)	1.14 3H (d)
13	α:4.13 1H (dd appears as t, 8.9, 8.9)	α:4.09 1H (dd, 9.2, 8.8)	α:4.13 1H (dd)
	β:4.54 1H (dd appears as t, 9.2, 9.2)	β:4.50 1H (dd, 9.2, 9.2)	β:4.53 1H (dd)
14	1.12 3H (s)	3.27 1H (d, 11.0)	3.43 2H (s)
		3.33 1H (d, 11.0)	
15	3.38 2H (AB, 10.4)	1.06 3H (s)	1.04 3H (s)

At first glance at these data, it becomes clear that such data from these very similar compounds are almost the same. This is expected from such isomers that only differ in the stereo configuration of the oxygenated carbon that is attached to carbon 11, regardless of the number given to it with any numbering system. So, one should focus more on the chemical shifts of the protons at the neighboring carbons to this moiety. Protons at carbons 1 and 10 in compound sangusulactones A show much similarity with the same protons in compound **34** rather than the ones in compound **52**. Also, it must be taken in consideration the coupling pattern of protons at carbon 1 in different deuterated solvents. which 14-hydroxyblennin A (**52**) exhibits only one chemical shift in ^{1}H-NMR for both of them at δ_H 1.60 when it's measured in deuterated chloroform (Fig. 60), but exhibits two separate signals for each one at δ_H 1.55 and 1.68 when it's measured in deuterated methanol as it shows in (Tab. 8) from section 4.2.6.1.

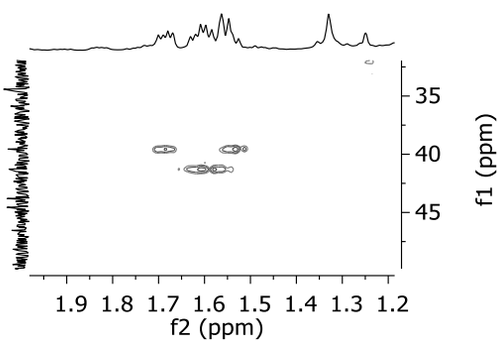

Figure. 60. HSQC expanded-spectrum for protons at C-1 and C-10 in compound **52**, extracted from *L. trivialis*, ($CDCl_3$).

Such a coupling pattern was not reported about sangusulactones A. Consequently, it can be concluded that the latter compound is actually 15-hydroxyblennin A (**34**), not 14-hydroxyblennin A (**52**). ^{13}C-NMR data for these compounds didn't provide decisive information, see (Tab. 4).

Moreover, YAOITA *et al.* proposed stereo configuration assignments for the protons in the hydroxymethyl group in question here that attached to carbon 11 using NOESY data.[74] No such results were obtained in this research for both stereoisomers. One can conclude that the bond between the sp^3 hybridized carbons 11 and 14 will rotate freely without being hindered, and the NOE correlations if any, will be equivalent with other protons in these compounds. Also, the same happens for the bond between carbons 11 and 15. It can be suggested to use temperature control NMR measurements in which a lower temperature can be tested, but no such approach has been mentioned, or the use of anything other than traditional NOE experiments.

Table 4: ^{13}C-NMR data for compounds **34**, sangusulactones A[74], and **52** in $CDCl_3$

position	δ_C **34**	δ_C sangusulactones A	δ_C **52**
1	40.77	40.5	41.27
2	44.63	44.1	43.80
3	33.92	33.7	34.41
4	146.28	146.3	145.99
5	171.88	172.2	171.89
6	126.97	126.8	126.87
7	44.30	44.1	44.56
8	75.88	75.4	75.20
9	52.03	51.7	50.97
10	39.78	39.4	39.56
11	42.11	41.8	42.39
12	20.43	20.3	20.55
13	69.27	69.3	69.33
14	26.41	70.4	71.78
15	71.08	26.2	25.07

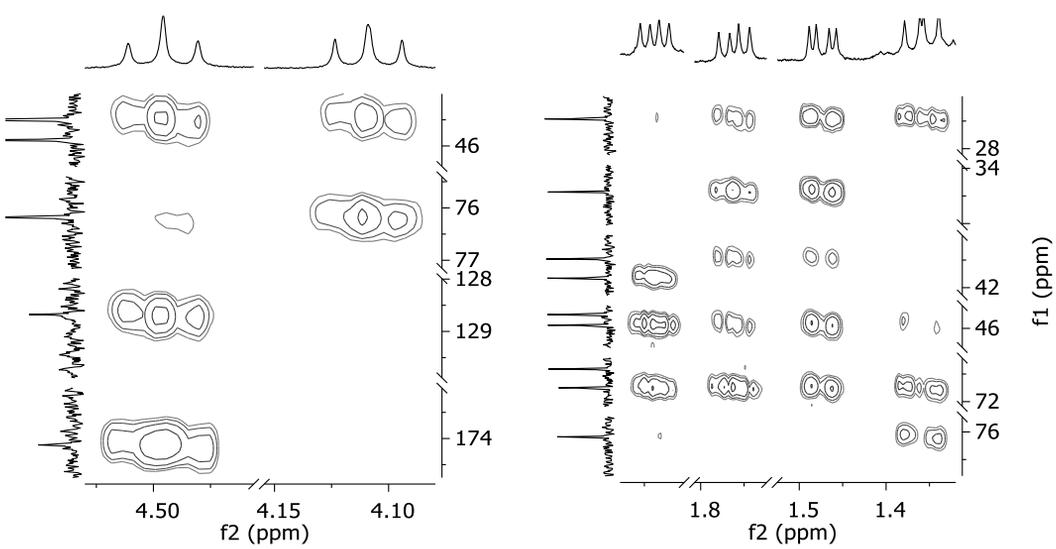

Figure. 61. HMBC concentrated-spectrums of correlations from compound **34** from *L. circellatus*, (CD_3OD). Left: protons at δ_H 4.11 and 4.50. Right: protons between δ_H 1.30 and 2.10.

Protons of the methylene groups at carbons 10 and 13 show HMBC correlations that can be explained with Karplus relationships, (Fig. 61). Which proton at δ_H 1.36 has HMBC correlations with each of carbons 8 and 14 at δ_C 76.18 and 26.92 respectively but not the other geminal proton at δ_H 2.04. Also, the later proton has correlations with carbons 1 and 2 at δ_C 41.66 and 45.89 respectively but the other geminal proton at δ_H 1.36 only has a weak correlation with the later carbon. Similarly, the proton at δ_H 4.11 from the methylene group at carbon 13 has an HMBC correlation with carbon 8 at δ_C 76.18 but the proton at δ_H 4.50 only has a very weak correlation that can discarded. Also, the later proton has clear correlations with carbons 5 and 6 at δ_C 174.12 and 128.67 but the other geminal proton in this methylene group doesn't. Accordingly, a dihedral angle with 90° was fixed between the protons and carbons that should have HMBC correlations but they didn't. Then, the information from the previous approach combined with data from NOE

correlations, will conclude which protons from this compound will be in the up or down configurations.

Subsequently, due to the correlations from NOE data, each of the protons at δ_H 4.50, 3.36, 2.29, 2.04, 3.30, 1.76, 2.12, and 1.17 should exist on the same side of this compound structure. And so, protons at δ_H 4.11, 3.51, 1.36, 1.10, 1.47, and 2.54 should exist on the opposite side of this structure. Due to the biological synthetic formation of this type of compound, one could expect the stereo configurations of protons at carbons 2 and 9 to be in the down configuration in the compound. Examining this assumption with the previously mentioned data including the fixed dihedral angles between the due atoms, will reach the relative structure of this compound (Fig. 62).

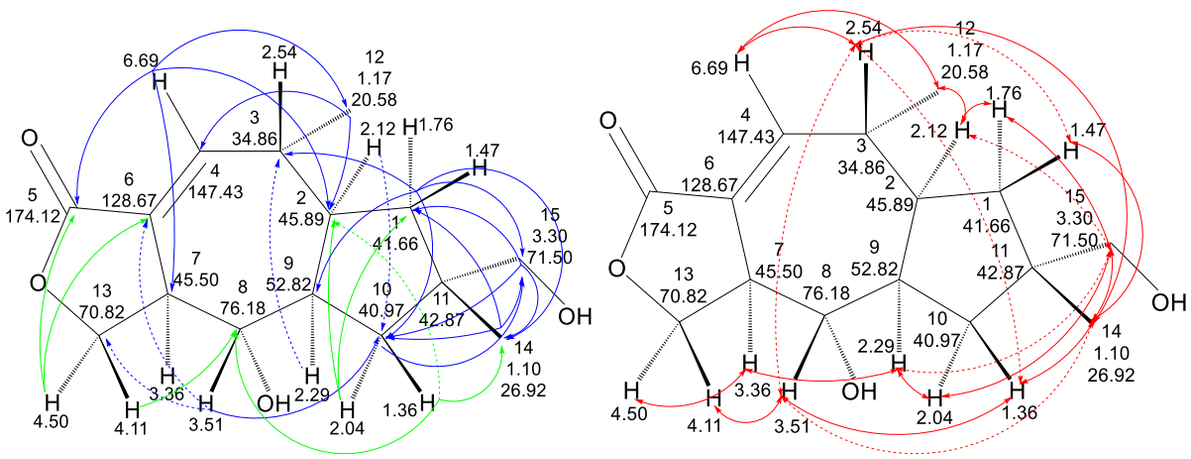

Figure. 62. Relative structure of compound **34** with assignments, (CD_3OD). Left: selected HMBC correlations (⟶), HMBC correlations with Karplus relationship (⟶). Right: NOESY correlations (⟷).

The measured polarimetry of this fraction, $[\alpha]_D^{25}$ +19.2 (MeOH; *c* 0.0005), agrees with the reported by YAOITA *et al.*.[74]

4.1.3.18 Investigation of the presence sesquiterpenes using LC-MS

With possession in hand of the sesquiterpenes compounds that were already extracted from *Lactarius circellatus* mushroom and also the ones that were extracted during this research, a comparison was performed between them and with processed samples from both mushrooms, *L. circellatus* and *L. blennius*.

A small-scale extraction was performed from the flesh of one fruiting body from each mushroom (approximately 10g), using a MeOH solvent. The raw extracts from both mushrooms were filtered through solid phase extraction (SPE) using gradients of H_2O and MeOH solvents, see section 6.3.2. The H_2O fractions were discarded, and fractions 1:1 and MeOH were used. Compound 21 exhibits great deal of degradation that it exists in a trivial quantity by the time of mesearuing the samples in HR-LCMS, (Tab. 5).

Table. 5. Sesquiterpenes compounds exist in processed samples from *L. circellatus* and *L. blennius* mushrooms.

cmpd #	*exist in:	rt (min)	exact mass	cmpd #	*exist in:	rt (min)	exact mass
19	2, 4	13.30	296.13	**27**	2, 4	13.20	282.15
20	1(more), 4	19.60	282.15	**15**	1, 3	36.96	250.16
21	none	26.40	264.14	**28**	1, 3	39.49?	232.15
22	2, 4	25.30	280.13	**30**	1, 3	30.82	248.14
23	1, 2, 4 (few)	24.12	296.13	**13**	1, 3	36.96	250.16
24	1, 3	32.45	244.11	**18**	1, 3	36.96	250.16
25	1, 3	27.43	266.15	**31**	1, 3	34.70	248.14
26	1, 3	36.17	250.16	**34**	1, 3, 4	23.0	266.15

* Sample 1: flesh extract from *L. circellatus* – SPE – MeOH fraction.
Sample 2: flesh extract from *L. circellatus* – SPE – 1:1 fraction.
Sample 3: flesh extract from *L. blennius* – SPE – MeOH fraction.
Sample 4: flesh extract from *L. blennius* – SPE – 1:1 fraction.

4.1.4 Isolation and structure elucidation of Aminobenzoquinone Derivatives

4.1.4.1 Blennione (**35**)

One of the aim targets in this project of research *Lactarius circellatus* mushroom is to investigate the presence of blennione (**35**) compound as it was suspected to be responsible for the gray-green color of the cap skin of this mushroom. Blennione (**35**) is a green pigment that was extracted and elucidated before from *L. blennius*.[78] To enable the means of convenient comparison, the green compound was extracted from both mushrooms *L. circellatus* and *L. blennius*.

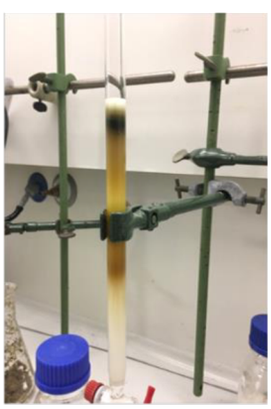

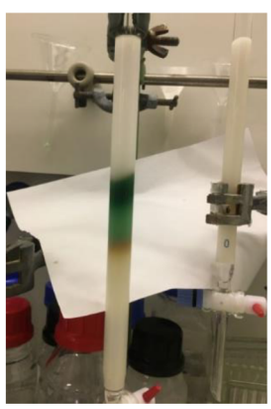

Repeated LH20 column

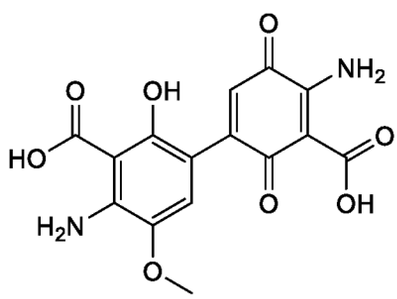

Blennione (35)

Blennione (**35**) was extracted and elucidated from *L. circellatus* during this research using a similar procedure with repeated use of LH20 column that was utilized to extract this compound from *L. blennius* mushroom with adding the use of SPE method, see section 6.3.1.2.

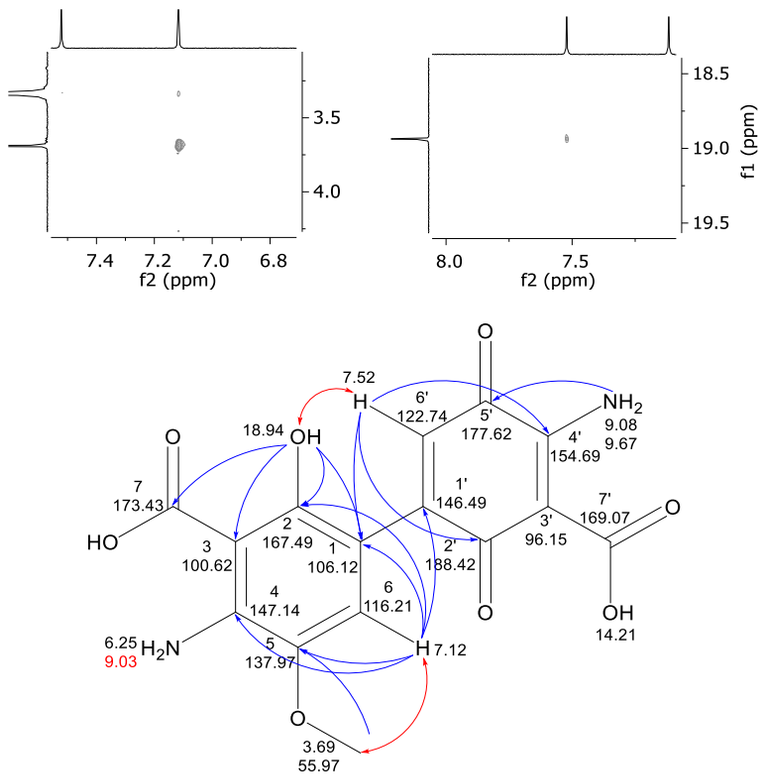

Figure. 63. Up**:** NOESY expanded-spectrums of selected correlations, (DMSO-d6), left: between protons at δ_H 3.69 and 7.12, right: between protons at δ_H 7.52 and 18.94. Down: Relative structure of compound (**35**) with assignments, with selected HMBC correlations (⟶) and with NOESY correlations (↔), (DMSO-d6).

The 1D and 2D-NMR measurements (Fig. 63), exhibit exact chemical shifts in comparison to the reported one, see section 9.18. Also, blennione (**35**) was investigated and extracted from *L. fluens* mushroom. The green compound was found to be in much higher abundance in *L. circellatus* than in *L. blennius* although the external color of the two mushrooms indicates the opposite, also much easier and more convenient to extract.

Blennione (**35**) was tested with three types of bacteria; *Azospirillum brasilense*, *Bacillus megaterium* and *Escherichia coli*. The results showed a negative effect on the mentioned bacteria.

4.1.4.2 Isolation of other colored fractions

A yellow fraction was separated from the LH20 column turned to be riboflavin (vitamin B_2) (**36**) comparing the retention time, mass, and UV data with a sample from the industrial compound.

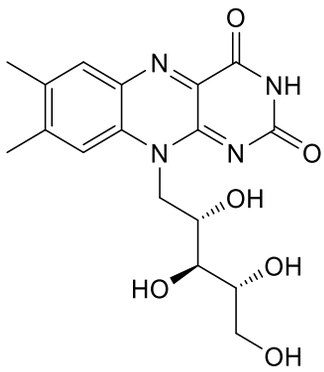

Riboflavin (vitamin B_2) (**36**)

The pink fraction was produced by applying the resulting fraction from the LH20 column to the C18-ec cartridge as a last step of purification of the crud extract from *L. blennius*, but not from *L. circellatus*. This fraction eluted with H_2O:MeOH (1:1 v/v) gradient. This fraction was obtained visually only from large-scale extractions.

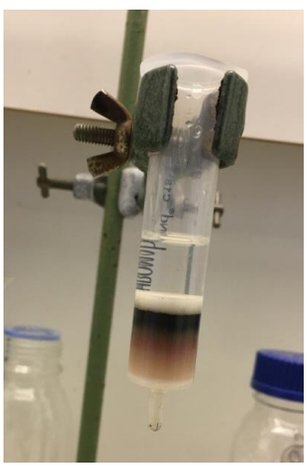

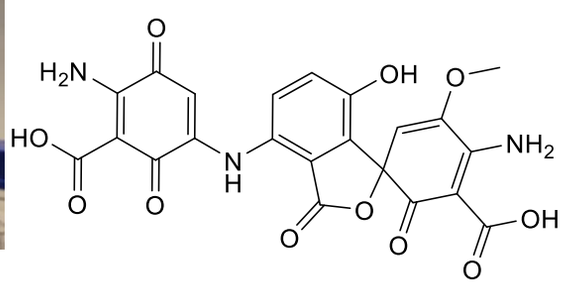

Lilacinone (**37**)

This fraction was suspected to be the compound lilacinone (**37**) a pink pigment that was isolated and elucidated from the pink mushroom *L. lilacinus*.[79]

A comparison between this fraction with a crud extract from *L. lilacinus* mushroom, showed different retention times and similar but yet different UV-spectra between the main compounds in these samples, see (Fig. 64 and 65).

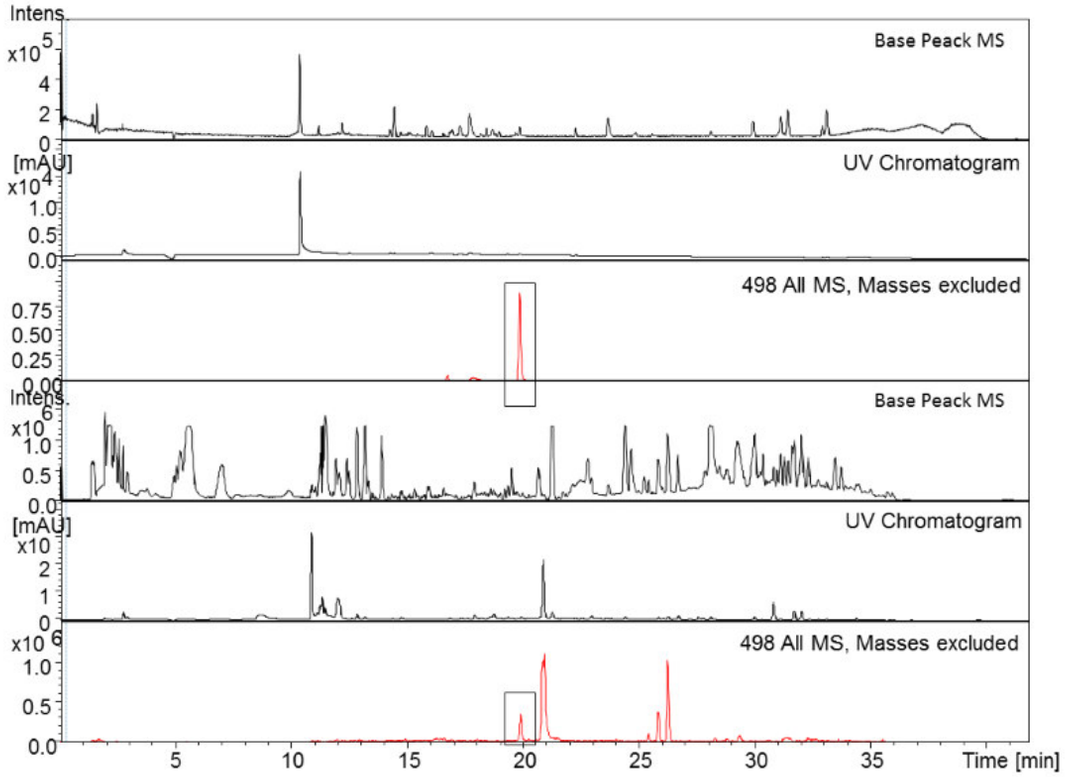

Figure. 64. LC-MS, UV and EIC of 498 $[M+H]^+$ chromatograms from up to down. Gradient (E). (1st set): the pink fraction extracted from *L. blennius*. (2nd set): crud extract from *L. lilacinus* (down).

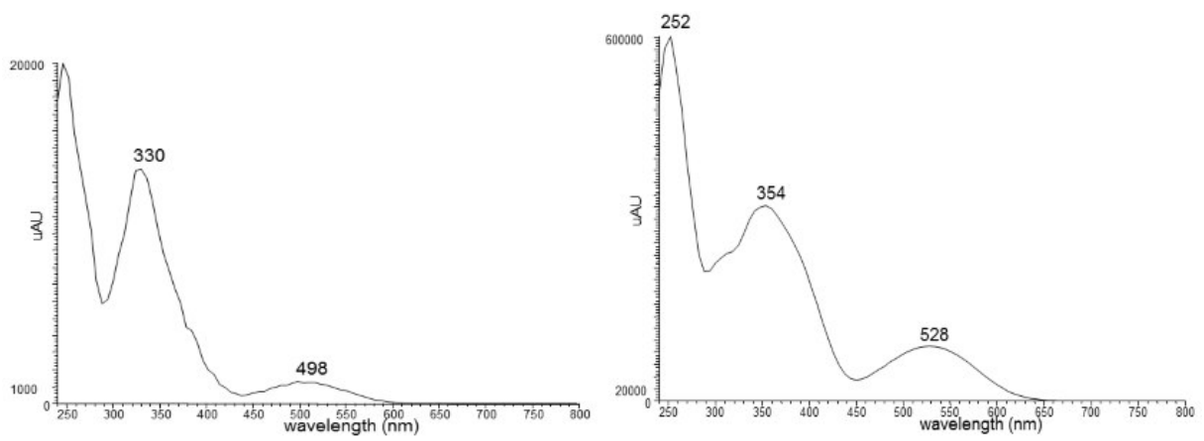

Figure. 65. UV-spectra of the pink compounds with 498 $[M+H]^+$. Left: from *L. blennius*. Right: from *L. lilacinus*.

In conclusion; there are two compounds (isomers) in *L. lilacinus* matching the molecular ion of *m/z* = 498.07 and the molecular formula of the pink compound that was extracted from *L. blennius*, one of them matches the R_t but not the UV absorption pattern, the other one (the main one) is belong to lilacinone (**37**). No compounds match such mass in *L. circellatus*.

4.2 *Lactarius trivialis*

4.2.1 Description of *L. trivialis*

Lactarius trivialis is a fungus also known as northern milkcap (Nordischer Milchling) and is a species of the family of *Russulaceae* (Täublingsverwandten). At first, it was described in 1815 as *Agaricus trivialis* and in 1838 it was placed in the genus *Lactarius* (Milchlinge), to have now its current name.[80] It has a cap 5 to 20 cm in diameter that can be flattened and spread later, and light brown to dark purple, with the stem 4 to 10 cm long and 1 to 3 cm wide and also cream-colored, (Fig. 66).[81] The lamellae of the fungus have grown and are cream to ocher in color. The flesh is whitish and has a fruity smell.

Figure. 66. Fruiting bodies of *Lactarius trivialis*.[82]

The fungus is particularly widespread in northern areas of North America and Europe.[83] As a mycorrhizal fungus, it is usually found near birch or spruce trees (Fichten) or (Birken).[81] It is therefore often found on moorlands, on the edges of moorlands, in swampy forests, and in spruce or pine forests, as well as in moist coniferous forests. The fruiting bodies of the fungus can be found from July to October. In Germany, the fungus only exists in mountainous or higher-hilly areas.[83] Due to its sharp taste,[84] however, it is considered inedible in Central Europe, whereas it is eaten after a special preparation in Eastern Europe,[85] such as parboiling or pickling.[86] ROTOLA-PUKKILA *et al.* in 2019 investigated the effect of cooking on umami compounds (umami means: nice pungent taste, which is a class of flavors in foods besides sweet, sour, salty, and bitter that correspond to the taste of glutamate, especially monosodium glutamate) in *L. trivialis* with other wild mushrooms.[87] The highest contents of such compounds were found to exist in the cooked *L. trivialis*.

4.2.2 Current state of knowledge

Lactarius trivialis was subjected to a study of the identification of volatile compounds from edible mushrooms by PYYSALO in 1976.[88] The research reveals the existence of a wide range of known alcohols, esters, and acids. In addition, the toxic stereomeric muscarines (Muscarine (**38**), *epi*-Muscarine (**39**), and *allo*-Muscarine (**40**)) were detected in the mushroom by STADELMANN *et al.* in 1976 but in very small amounts.[89]

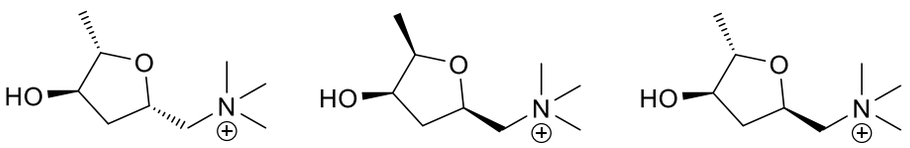

Muscarine (**38**) *epi*-Muscarine (**39**) *allo*-Muscarine (**40**)

Afterwards, the known sesquiterpenoids compounds furandiol **15**, blennin C (**18**), and lactarorufin A (**25**) were isolated from *L. trivialis* by SEPPÄ *et al.* in 1980.[39] No compounds belonging to this group of alkaloids were reported from the mushroom until this research. Also from the same year, KURKELA *et al.* in 1980 studied the presence of amino acids in the mushroom.[90] Stearoylvelutinal (**7**) and 6-ketostearoylvelutinal (**8**) were also reported to be exist in *L. trivialis* as well as *L. circellatus* by VIDARI and DANIEWSKI *et al.* in 1999.[9]

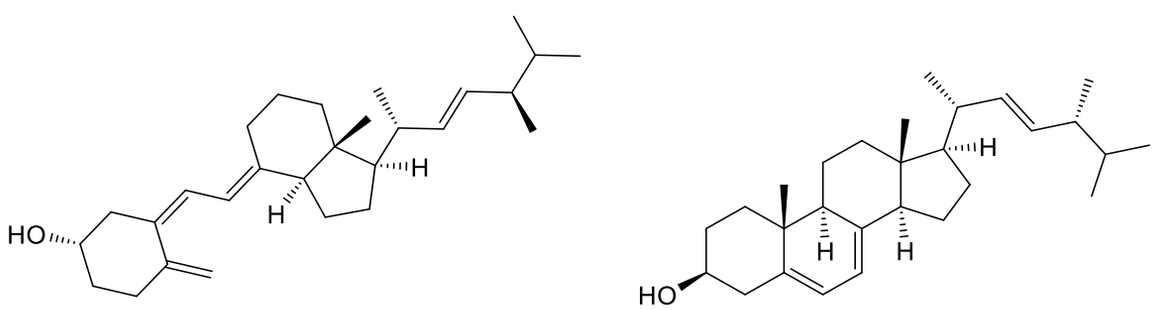

Ergocalciferol (Vitamin D_2) (**41**) Ergosterol (**42**)

Very low contents of selenium were detected in *L. trivialis* which was picked in Finland by PIEPPONEN *et al.* in 1983.[91] Also, ergocalciferol (vitamin D_2) (**41**) was detected for the first time in the mushroom by MATTILA *et al.* in 1994 using HPLC methods.[92] Ergosterol (**42**) a sterol considered to be a provitamin for vitamin D2 when exposed to UV light, was detected by MATTILA *et al.* in 2002 in *L. trivialis*.[85]

L. trivialis also went under several analytical and biological studies that are concerned about the elemental analysis in this mushroom, such as the presence of ^{137}Cs that was investigated in the mushroom from Finland among other edible natural products by KOSTIAINEN in 2007.[93] The relatively high level of the radioactive isotope of Cesium element in the natural beings that were affected by the Chernobyl accident in 1986 showed no significant change in the corresponding area of the study. This exhibits no tangible reduction of the concretions of this radioactive isotope.

Also, similar investigations and results were performed by VINICHUK *et al.* in 2010 for several fungi from Sweden among them *L. trivialis*.[94] Boron content was investigated in the mushroom by LAVOLA *et al.* in 2011.[95] Also, VINICHUK *et al.* in 2012 and 2013 investigated the metal amounts in the mushroom with other mushroom spices.[96] Finally, SHAO *et al.* in 2020 assembled and annotated a complete mitochondrial genome from *L. trivialis*.[97]

4.2.3 Motivation

The motivation for studying *Lactarius trivialis* mushrooms is that there are no reports about the distinguished secondary metabolites from the skin of this mushroom cap. As it had been previously recorded such compounds that were found in variant mushrooms from the *Lactarius* genus such as the aminobenzoquinones blennione (**35**),[78] and lilacinone (**37**),[79] extracted from *L. blennius* and *L. lilacinus* respectively. Also, necatorone (**43**),[98] and binecatorones (**44**-**46**),[99] extracted from *L. necator* and *L. atroviridis*. Such compounds are responsible for the distinguishing color of each of these mushrooms. Mainly, compounds such as sesquiterpenes were reported to be extracted from *L. trivialis*,[39] and these compounds are usually targeted in the mushroom flesh.

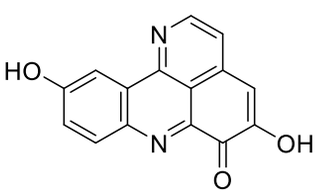

Necatorone (**43**)

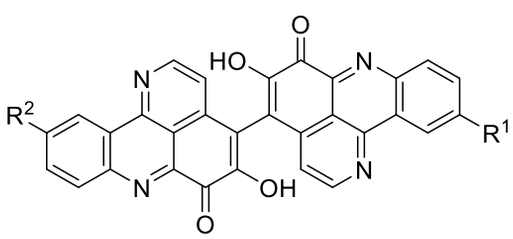

	R^1	R^2
44	OH	OH
45	OH	H
46	H	H

What also stimulated research into the skin of the mushroom is the fact that the mushroom cap change of color that had been observed when the mushroom was picked. Before picking, the mushroom had a light gray to light purple color, but then, the color began to change to be darker. This indicates that changes are occurring in the fruiting bodies of *L. trivialis* when it is picked that have a chemical nature. Therefore, it can be considered that there is a defense mechanism in this mushroom. Especially since it has been reported that this mushroom has a pungent taste,[84] and it can be considered edible but after treatment in a special way.[86] So, this may be the mechanism by which this fungus defends itself. Consequently, separate investigations were conducted targeting the flesh and the cap of this mushroom separately.

4.2.4 Initial investigations

At first, an attempt was made to extract the compounds responsible for the color in this mushroom using conventional methods, where methanol was used as a solvent, and an extract with a pink to dark red color was obtained. However, when this extract was examined in LC-MS, an unusually large number of compounds were designated as potential candidates. Believing these were the target compounds, an initial attempt was made to extract them. One of the first notes was these compounds were unstable, which was puzzling at first. Then the idea emerged that perhaps the methanol solvent played a role in this extract more than just an extraction solvent, as it might have interacted chemically with some of these compounds.

It was necessary to consider a solvent that has a low probability of interacting chemically with the targeted compounds. Because methanol and its likes contain alcoholic parts are excluded, it was necessary to think about solvents that are less reactive or even inert. Therefore, it appears that acetone solvent is the best candidate for this matter. Indeed, when the acetone solvent was used in the extraction process, it showed that the resulting extract contained compounds with colors closer to the color of the skin of the mushroom. Upon examining this extract using LC-MS, the compounds present were more specific, so that they could be limited to a certain number of compounds. When these compounds that were extracted using acetone were linked to the compounds that were extracted using methanol, a link was found showing that the targeted compounds had a methoxy added to them. Then the methanol acts not only as a solvent but as part of a chemical reaction with the target compounds even if the extraction is at room temperature. The stirring process probably acted as a catalyst in addition to the accessibility to react in the first place.

4.2.5 Isolation of trivialines

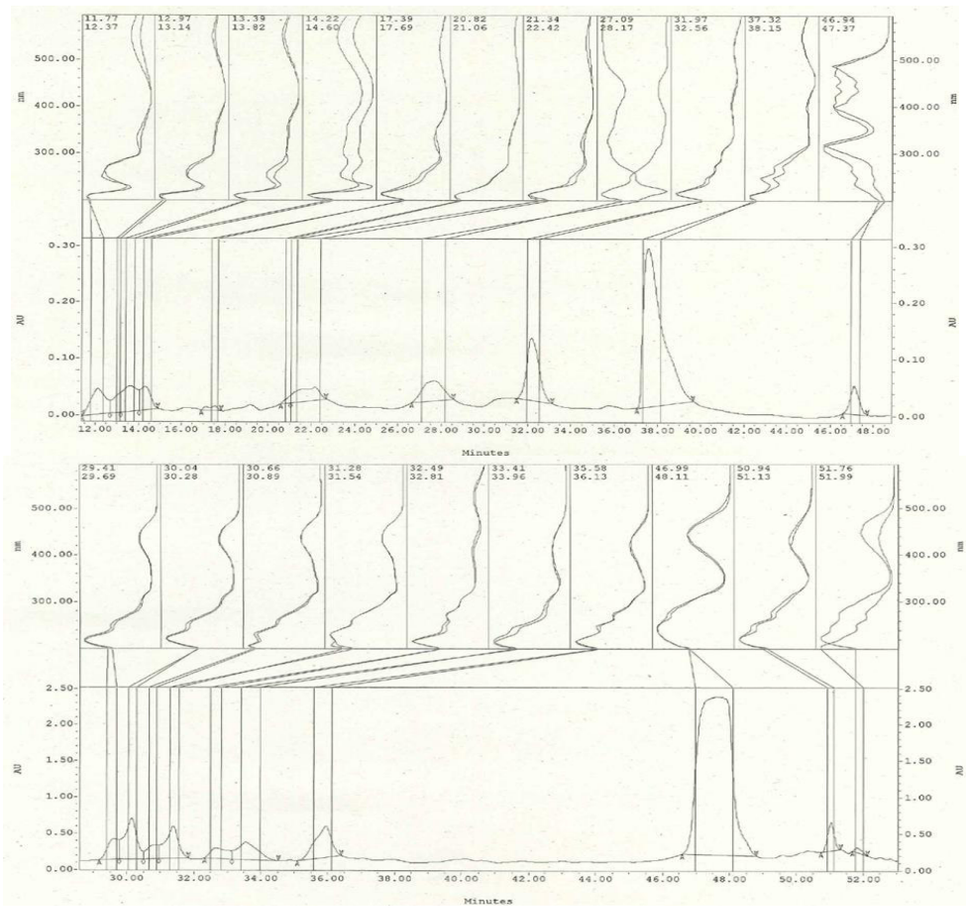

Figure. 67. Semipreparative-HPLC separation chromatograms for the (A1) SPE fraction, see section 6.3.1.1. Detection wavelengths at 550 nm (up), at 440 nm (down).

Applying the extraction method A explained in section 6.3.1.1, several fractions were isolated from the processed extraction from the cap skin of mushroom *L. trivialis*. Two different UV wavelengths were used to detect the targeted compounds, at 440 and 550 nm, (Fig. 67) shows the Semipreparative-HPLC separation chromatograms for (A1) SPE fraction.

4.2.5.1 Trivialine A (**47**)

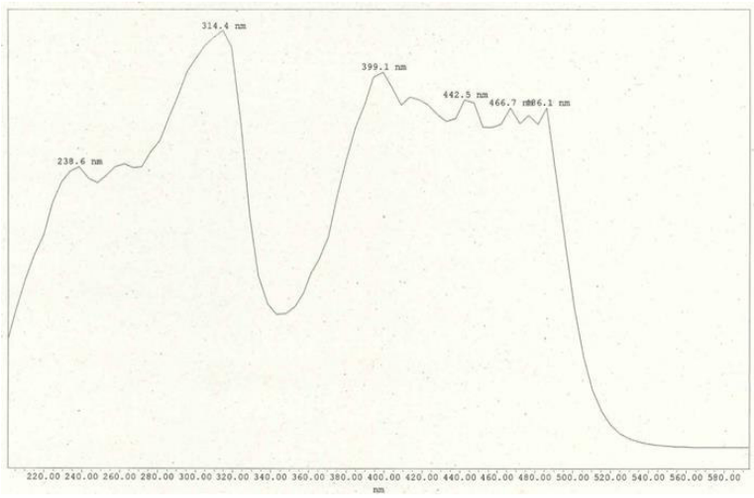

Figure. 68. UV/Vis-Spectrum of compound **47**.
The spectrum was recorded from the semi-preparative HPLC, section 6.3.4.3.

Trivialine A (**47**) a yellow solid compound, was detected using UV wavelength at 440 nm and exhibits an absorption maximum at λ= 442 nm and a shoulder at 238 nm, also, shows UV absorption at 314 nm indicating the existence of a conjugated π system in this molecule. The UV/Vis-spectrum exhibit a large degree of saturation, (Fig. 68). LCESI-(+)-MS shows ion mass of $[M+H]^+$ at *m/z* 557.02, (Fig. 69).

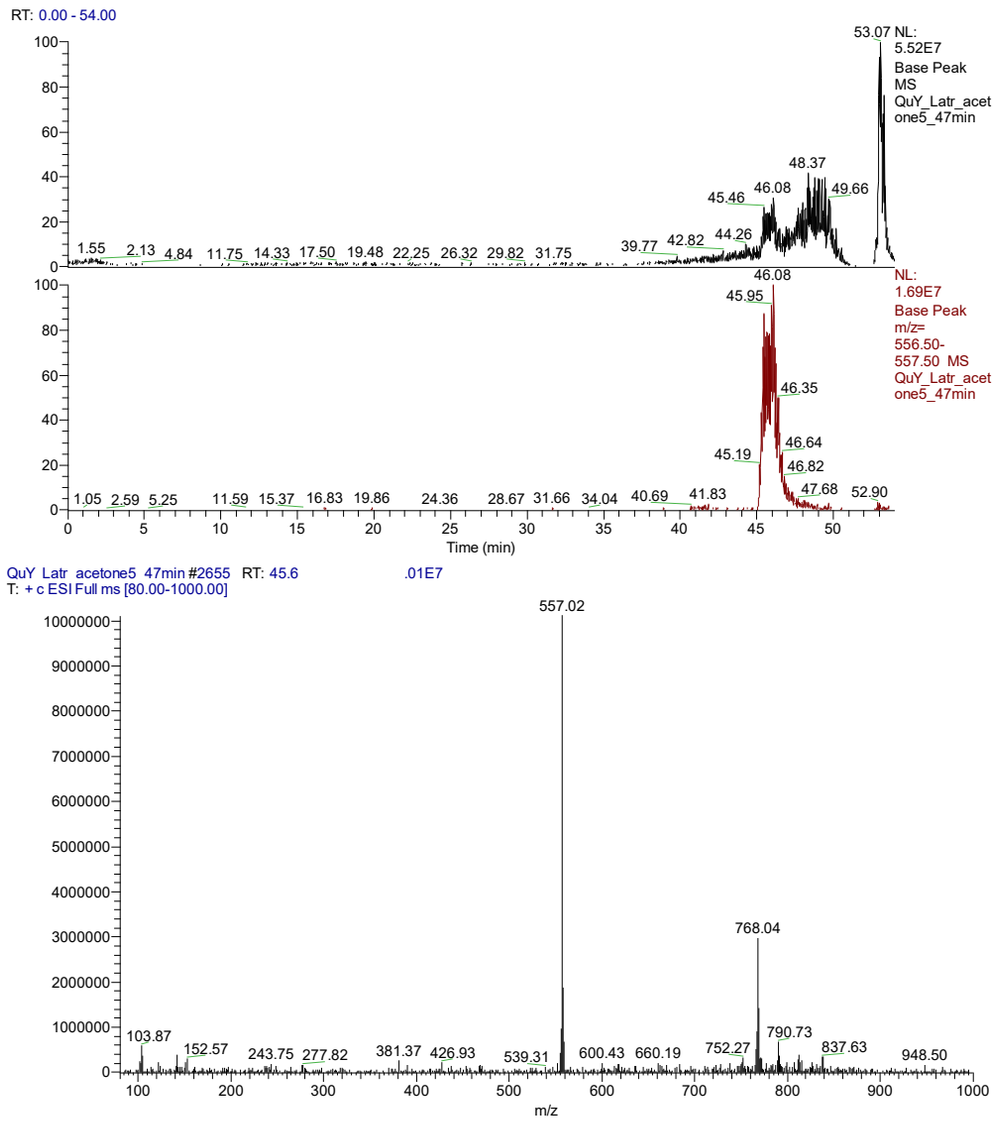

Figure. 69. (Up): LCESI-(+)-MS and excluded ion of 557 chromatograms, from up to down, for compound **47**. (Down): Molecular mass of $[M+H]^+$ at *m/z* 557.02 at the R_t of 45.65 min. Gradient is in section 6.3.4.3.

The measurement of this compound in HR-ESI-(+)-MS *was* delayed due to the unavailability of the HR-LCMS measuring device for four weeks, and although a sample from this fraction was kept in –7°, a suspected high degree of degradation or conversion occurred. Such a conclusion was made due to the already established high sensitivity of such fractions from this mushroom, and the large shift in R_t from around 47 to 34 min (Fig. 70), which is the R_t of trivialine B (**48**), see section 4.2.5.2. And the UV absorption spectrum is the same, compare (Fig. 71) with (Fig. 74). In addition, a compound *with* $[M+H]^+$ ion at *m/z* 558.12867 at R_t of 28.60 min. This compound has a molecular formula of $C_{32}H_{20}N_3O_7$ with the calculated $[M+H]^+$ ion at 558.13013 that comes in agreement with the measured one. This molecular mass and the molecular formula were found in a fraction that was isolated through the semi-preparative HPLC, see section 4.2.5.3.

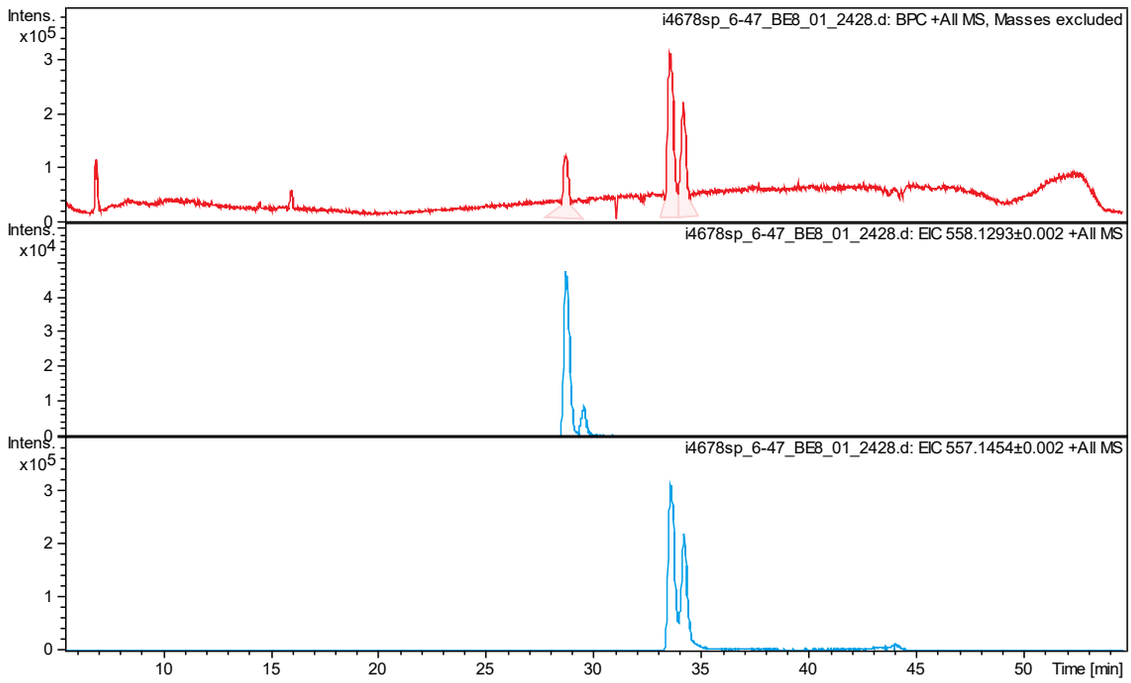

Figure. 70. (From up to down): HRESI-(+)-MS, excluded ion of 558.129 and excluded ion of 557.145 chromatograms, for compound **47**. Gradient is in section 6.3.4.3.

The resulting data show two isomers with the same mass and molecular formulas have R_t at 33.4 and 34.0 min. This observation was noted in the measured NMR experiments for this fraction with the presence of at least two isomers with similar chemical shifts and with an intensity ratio (1:9). Accordingly, the data from the more abundant isomer (R_t = 33.4 min) will be considered to be the one who represents the compound trivialine A (**47**). Subsequently, the correspondent $[M+H]^+$ experimented ion at *m/z* 557.14499 in the HR-ESI-(+)-MS *that* agrees with the calculated one with 557.14611, will suggest the molecular formula $C_{32}H_{21}N_4O_6$ for trivialine A (**47**), (Fig. 70). As a result, this compound has 25 degrees of unsaturation, see equation 2 in section 4.1.3.1.1.

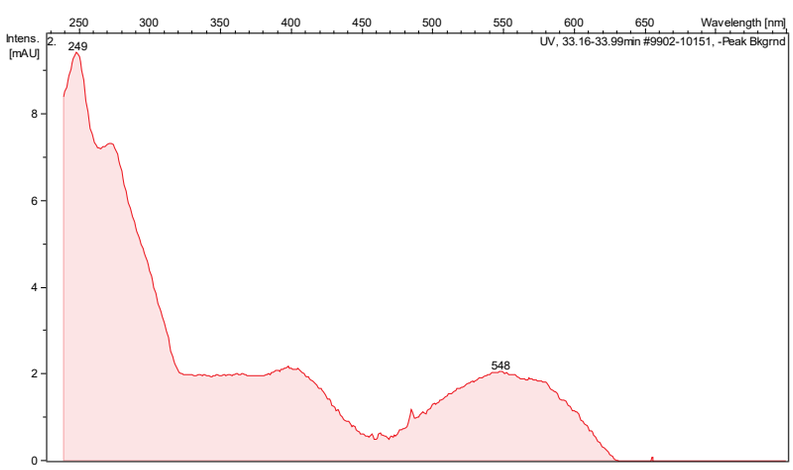

Figure. 71. UV/Vis-Spectrum of compound **47**. The spectrum was recorded from the HRESI-(+)-MS.

The molecular formula of this compound that was concluded to be $C_{32}H_{21}N_4O_6$ also using the initial measurement in LCESI-(+)-MS that shows a compound with a molecular mass of $[M+H]^+$ at 557.02 with an R_t at 45.65 min, and the data extracted from the 1D-NMR experiments that show presence

of 32 carbon atoms and 20 hydrogen atoms in compound **47**, and the great deal of similarities in chemical shifts and correlations in the 2D-NMR experiments with trivialine B (**48**). This will produce the conclusion that both compounds are related to each other meaning that the more abundant trivialine A (**47**) is the precursor of trivialine B (**48**), and the same molecular mass and formula, indicates a bio-reaction of rearrangement causes the observed convergent.

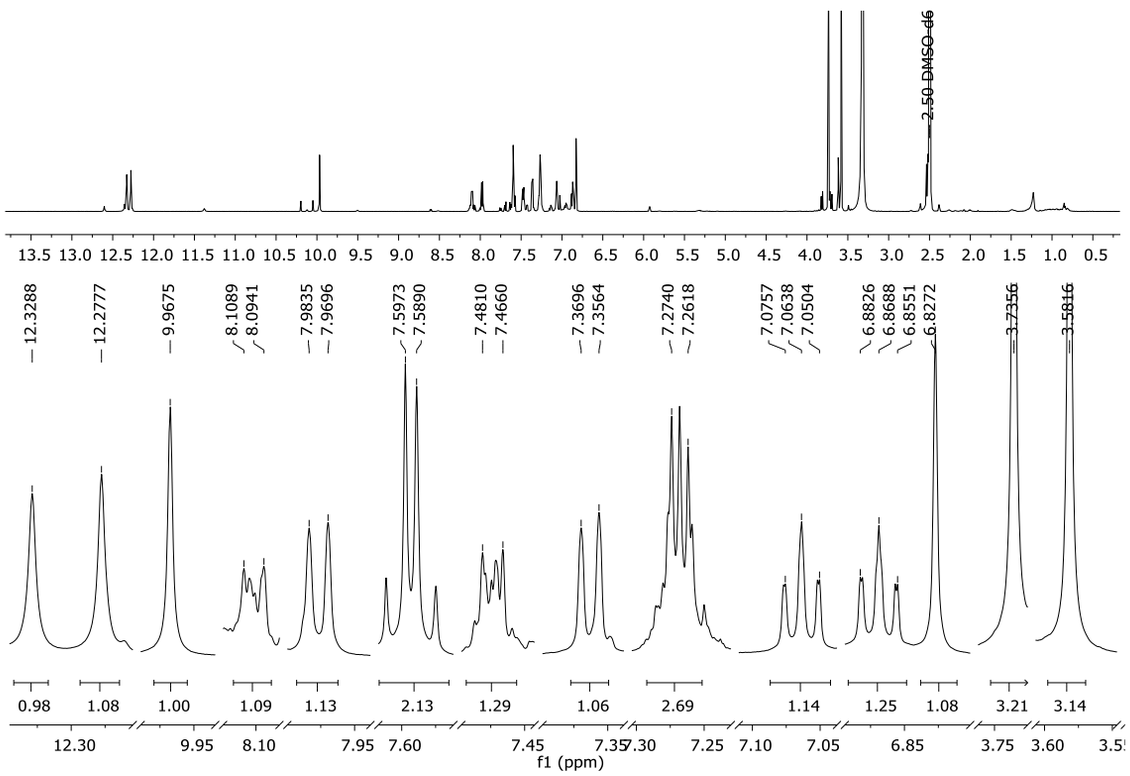

Figure. 72. ^{1}H-NMR and ^{1}H-NMR-spectrums with removed signal-free areas, (600.22 MHz, DMSO-d6, 297.1 K).

The ^{1}H-NMR spectrum was recorded at 297 K in DMSO-d6 and shows 17 non-exchangeable protons which HSQC-spectrum shows correlations that are interpreted to correspond to eleven (CH), and two (OCH_3) groups, (Fig. 72). Additionally, this compound will contain three exchangeable protons at δ_H 9.97, 12.28 and 12.33. These protons are attached to nitrogen atoms according to ^{15}N-HMBC data, (Fig. S114).

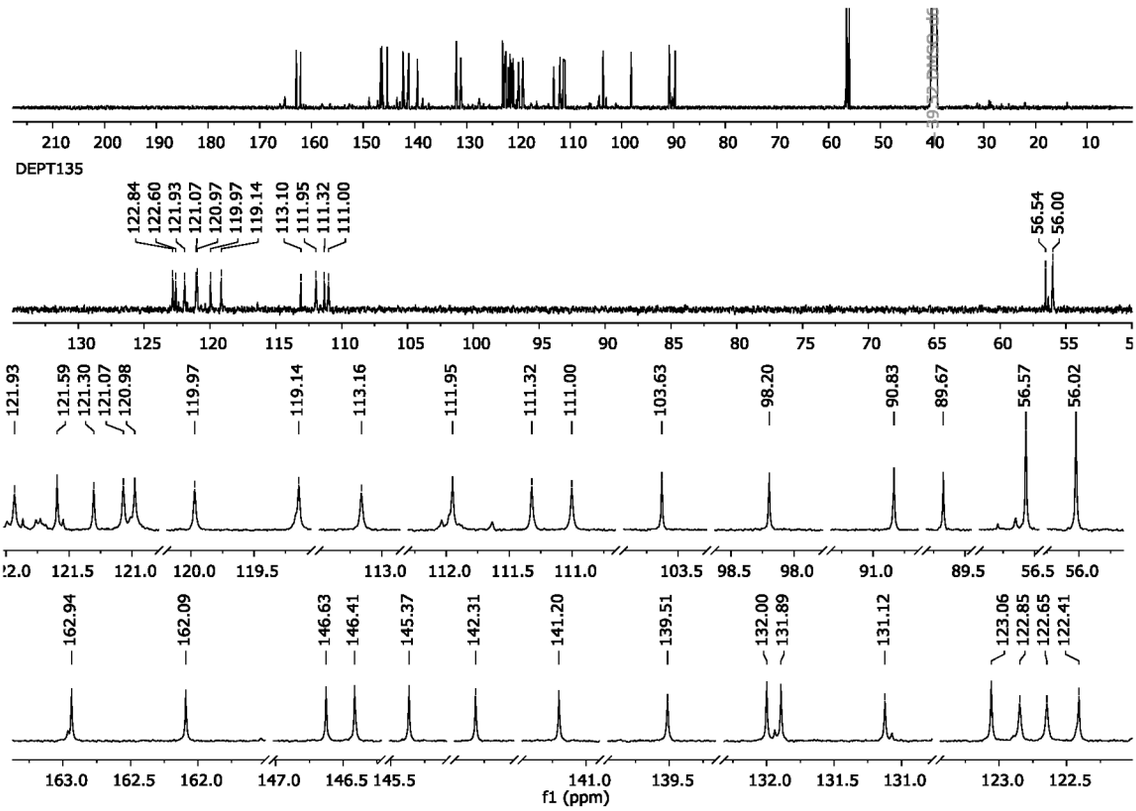

Figure. 73. ^{13}C-NMR, DEPT135 and ^{13}C-NMR-spectrums with removed signal-free areas, (150.94 MHz, DMSO-d6, 297.1 K).

The ^{13}C-NMR spectrum contained two methoxy signals at δ_C 56.02 and 56.57 and 30 carbon signals between δ_C 89.67 and 162.94, these were assigned to eleven methine groups at δ_C 111.00, 111.32, 111.95, 113.16, 119.14, 119.97, 120.98, 121.07, 121.93, 122.65, 122.85 and a staggering number of 19 quaternary carbon atoms, (Fig. 73).

The COSY-spectrum shows the presence of four distinguished spin systems and subsequently combined with the data extracted from HMBC and NOESY-spectrums, four substructures that are designated with symbols (**A**), (**B**), (**C**), and (**D**) can be identified, all of which are parts of benzene rings.

According to the COSY-spectrum, there are four aromatic protons exist in one spin system that exists in a substructure designated with symbol (**A**). The protons at δ_H 6.87 and 7.06 have COSY correlations with each other and separately each one of them has one more correlation with protons at δ_H 7.98 and 7.36 respectively.

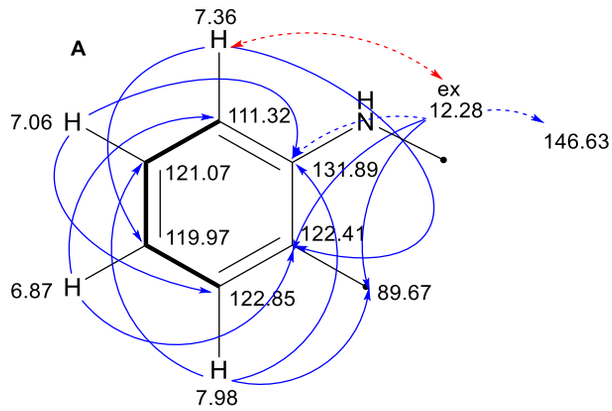

Substructure (**A**). HMBC correlations (⟶). NOESY correlation (⟷).

The later protons have only one COSY coupling suggesting that these protons are adjacent to quaternary carbons and accordingly, these four protons are neighbors to each other and connected in a continuously. Proton at δ_H 7.06 has HMBC correlations with carbons at δ_C 122.85 and 131.89. Also, proton at δ_H 7.98 correlates with the later carbon making them located at meta-position to this carbon that attached to a nitrogen atom, this conclusion was made due to its chemical shift that would be shifted more towards the low filed area in the ^{13}C NMR spectrum. Consequently, protons at δ_H 6.87 and 7.36 exist in *para* and *ortho*-positions respectively to carbon at δ_C 131.89. TOCSY data agrees with assigning the later protons to be in the same spin system, section 9.19 - (Fig. S110 and S111). Moreover, an exchangeable proton at δ_H 12.28 has HMBC correlations with carbons at δ_C 89.67, 122.41, 131.89, and 146.63 suggesting that it is located at the nitrogen atom attached to carbon at δ_C 131.89. The previous assumption was validated with a ^{15}N-HMBC NMR experiment that shows $^1J_{H\text{-}N}$ coupling between this proton and a nitrogen atom with the chemical shift at δ_N 122.9, see section 9.19 - (Fig. S114).

The singlet signal proton at δ_H 6.83 with no COSY correlations proved to be isolated. In addition, this proton has HMBC correlations with carbons at δ_C 121.30, 123.06, 141.20, and 142.31 making them located close to this proton and also suggesting that they exist in a benzene ring. Moreover, the singlet (OCH_3) protons at δ_H 3.74 correlate with carbon at δ_C 142.31 making this methoxy group attached to this carbon and a moiety in this benzene ring. Also, there is NOE correlation between this methoxy group and proton δ_H 6.83, making the later proton to be located in ortho-position to this moiety. The previous atoms are located in the proposed substructure (**B**).

The chemical shift of the carbon at δ_C 141.20 suggests that a nitrogen atom is attached to it. In a similar manner to the proposed substructure (**A**), the ^{15}N-HMBC data showed that this nitrogen atom at δ_N 90.1 is attached to it an exchangeable proton at δ_H 9.97. This proton has HMBC correlations with so many carbons which suggests a central position in this molecule. It has strong correlations with carbons at δ_C 103.63 and 145.37, also, weaker correlations with carbons at δ_C 113.16 and 121.30, and much weaker correlations with carbons at δ_C 89.67, 98.20, 122.65,

139.51, 141.20, and 162.94. In addition, it has a NOE correlation with the proton at δ_H 7.98 from the substructure (**A**). The assignments of carbons at δ_C 123.06 and 141.20 could exchange.

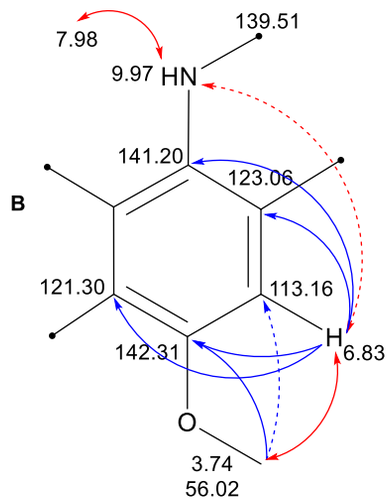

Substructure (**B**). HMBC correlations (→). NOESY correlations (↔).

In a similar coupling pattern in the protons in the substructure (**A**), protons at δ_H 7.2667, 7.2706, 7.48, and 8.10 have COSY correlations located in the same spin system. Protons at δ_H 7.2667 and 7.2706 couple with each other and separately have one more correlation with protons at δ_H 7.48 and 8.10 respectively.

Consequently, the later protons couple only with one proton each from the previously mentioned protons making them adjacent to quaternary carbons. So, this coupling pattern will suggest that all of these protons are neighbors to each other in a direct manner that suggests they are in a benzene ring. The HMBC data revealed that protons at δ_H 7.2706 and 7.48 exist in meta-position to carbon at δ_C 121.59 as they couple with this carbon and with the carbon they attached to. Accordingly, protons at δ_H 7.2667 and 8.10 exist in para and ortho-position respectively to the later carbon. Also, the sixth carbon in this benzene ring at δ_C 132.00 is attached to a hetero atom as in substructure (**A**), and the similarity of their chemical shifts suggests also that it is attached to a nitrogen atom. Subsequently, the previously mentioned atoms exist in the substructure (**C**).

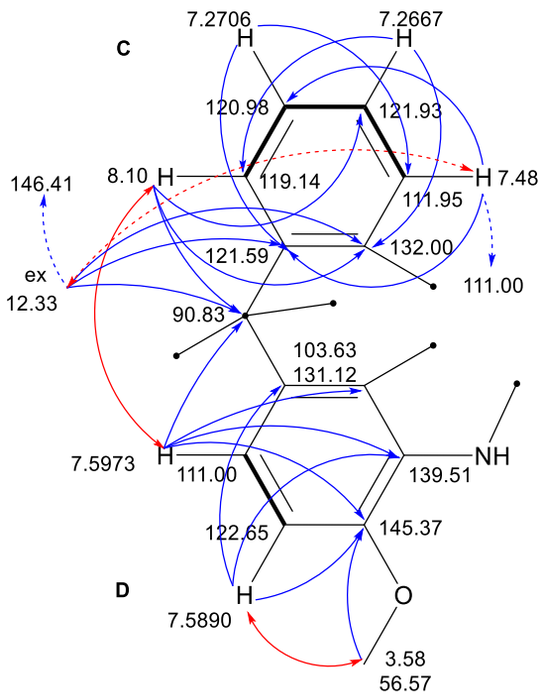

Substructures (**C**) and (**D**). HMBC correlations (⟶). NOESY correlations (⟷).

Finally, the more substituted substructure (**D**) will contain the last aromatic protons in this compound, as protons at δ_H 7.5890 and 7.5973 couple with each other in the COSY-spectrum. Also, the HMBC-spectrum revealed that the other (OCH_3) protons exist in this substructure as these protons at δ_H 3.58 coupled with carbon at δ_C 145.37 that also coupled with the mentioned previously protons. Assigning the positions of these aromatic protons related to the later oxygenated carbon proved challenging as there are long distant correlations due to the existence of the conjugated π electrons, but due to proton at δ_H 7.5973 has couplings with the more distant carbons at δ_C 90.83, this will place it in the meta-position to this carbon and the other aromatic proton in this benzene ring at the *ortho*-position. This assignment is confirmed with the existence of NOE correlation between the methoxy group at this carbon and proton at δ_H 7.5890. In this benzene ring, the other *ortho*-position will be assigned to carbon at δ_C 139.51 that will be designated to be attached to a nitrogen atom due to its chemical shift more towered low filed area. This nitrogen atom is most probably the secondary amino group linked to the substructure (B).

The latest substructures (**C**) and (**D**) have proven to be linked to each other as both protons at δ_H 7.5973 and 8.10 have HMBC correlations with the carbon at δ_C 90.83 and also, they have NOE correlation with each other. This will suggest that there is a third ring located between these substructures.

The overall assessment of the chemical shifts of trivialine A (**47**) implies that the substructures (**A**) and (**B**) are connected to form half of this compound, and the substructures (**C**) and (**D**) are also connected with a great similarity to (**A**) and (**B**) half, suggesting an occurrence of a dimerization.

4.2.5.2 Trivialine B (**48**)

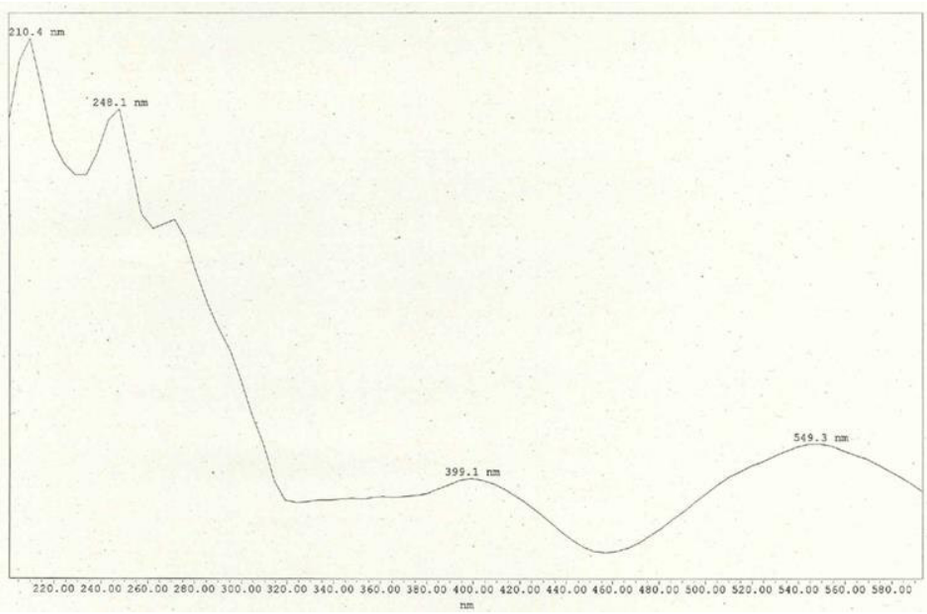

Figure. 74. UV/Vis-Spectrum of compound **48**.
The spectrum was recorded from the semi-preparative HPLC, section 6.3.4.3.

Trivialine B (**48**) a violet solid compound, was detected using UV wavelength at 550 nm and exhibits an absorption maximum at λ= 248 nm and a shoulder at 280 nm, also, at 399 and 549 nm indicating the existence of a conjugated π system in this molecule and giving the compound its violet color, (Fig. 74). LCESI-(+)-MS shows *ion* mass of $[M+H]^+$ at *m/z* 557.10, (Fig. 75).

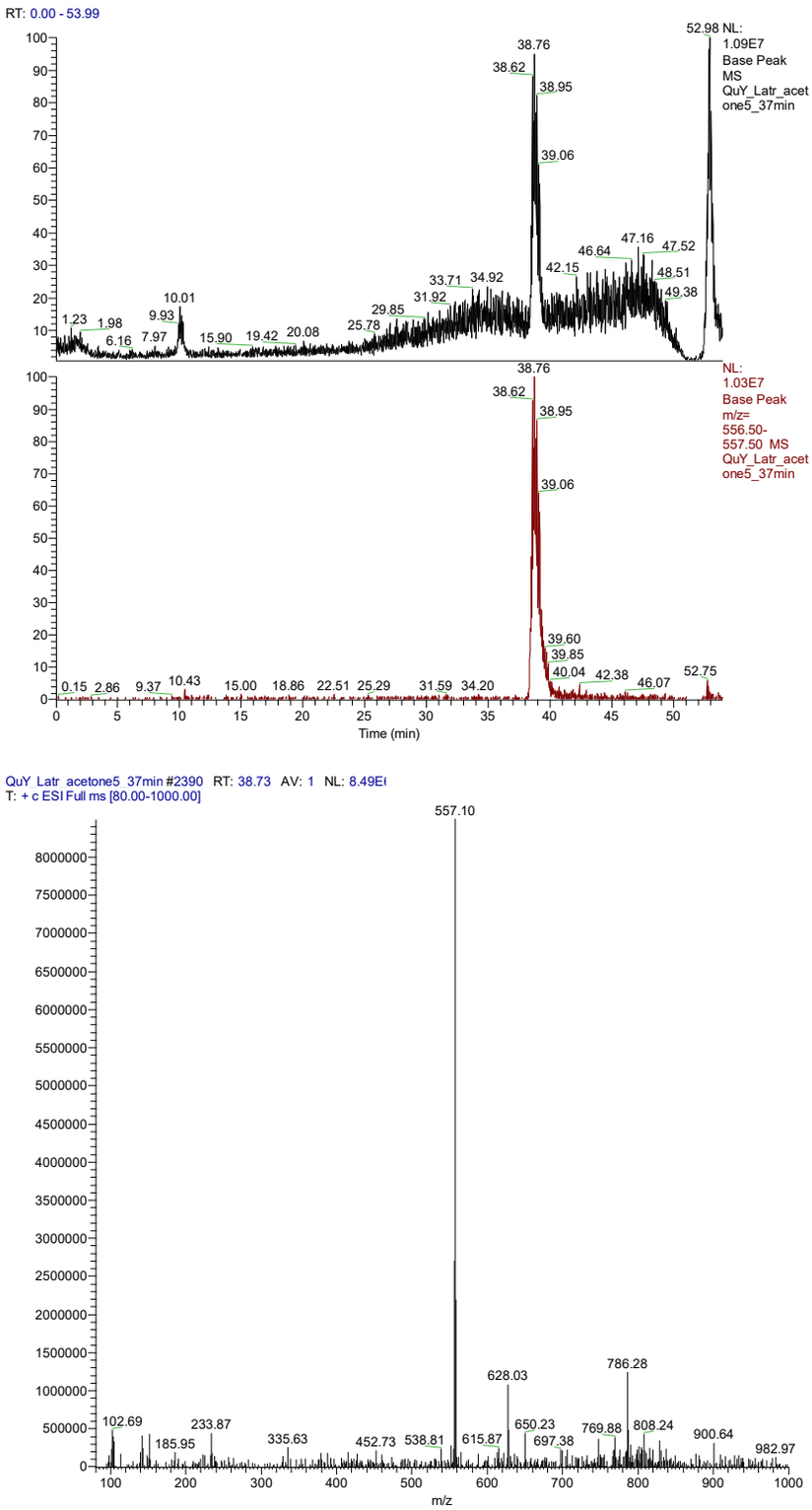

Figure. 75. (Up): LCESI-(+)-MS and excluded ion of 557 chromatograms, from up to down, for compound **48**. (Down): Molecular mass of $[M+H]^+$ at *m/z* 557.10 at the R_t of 38.73 min. Gradient is in section 6.3.4.3.

The $[M+H]^+$ ion at *m/z* 557.14480 in the HR-ESI-(+)-MS with the experimented molecular formula $C_{32}H_{21}N_4O_6$ agrees with the calculated one with 557.14611, (Fig. S116). Accordingly, this compound has 25 degrees of unsaturation, see equation in section 4.1.3.1.1.

Again, due to the self-degradation nature of such compound and due to the relatively long time until the sample measured for the HRESI-(+)-MS, the resulting chromatogram of compound **48**

shows a mixture of compounds besides the main one, mainly a compound with $[M+H]^+$ ion at *m/z* 573.14014 at R_t of 23.10 min. This compound has a molecular formula of $C_{32}H_{21}N_4O_7$ with the calculated $[M+H]^+$ ion at 573.14102 that agrees with the measured one. Such a compound was isolated separately in the semi-preparative HPLC, see section 4.2.5.4.

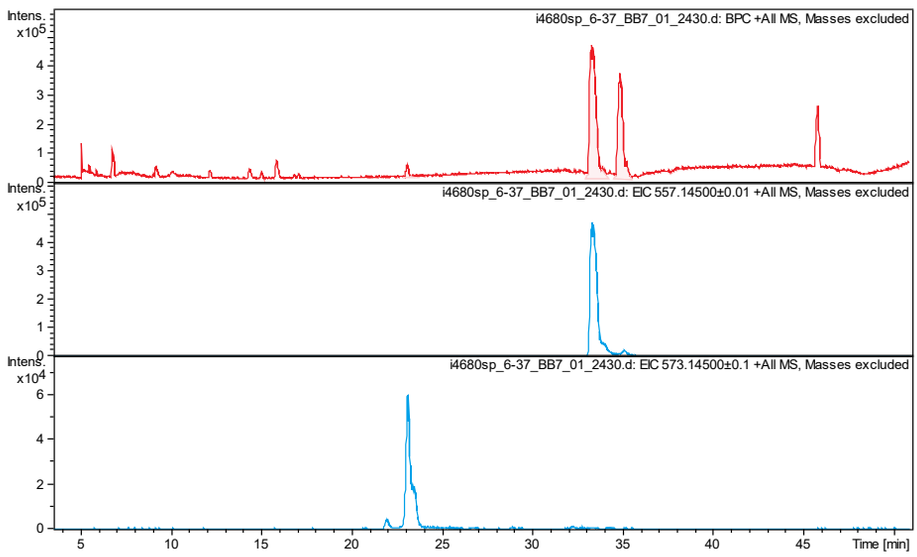

Figure. 76. (From up to down): HRESI-(+)-MS, excluded ion of 557.145 and excluded ion of 573.145 chromatograms, for compound **48**. Gradient is in section 6.3.4.3.

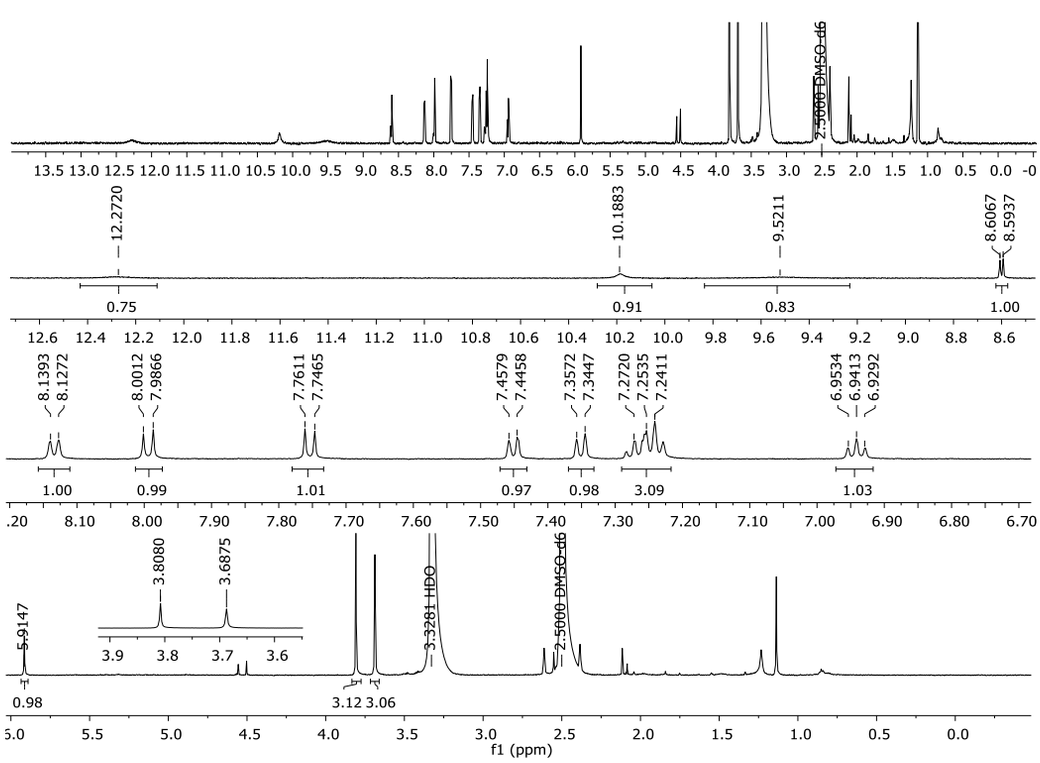

Figure. 77. Concentrated ^{1}H-NMR-spectrums of **48**, (600.22 MHz, DMSO-d6, 296.7 K).

The ^{1}H-NMR spectrum was recorded at 297 K in DMSO-d6 and shows 17 non-exchangeable protons which HSQC-spectrum shows correlations that are interpreted to correspond to eleven (CH), and two (OCH_3) groups (Fig. 77). Subsequently, this compound will contain three exchangeable protons. The ^{13}C-NMR spectrum of **48** contained two methoxy signals at δ_C 56.89

and 56.96 and 30 carbon signals between δ_C 90.32 and 166.33, these were assigned to eleven methine groups at δ_C 101.26, 112.19, 117.75, 118.92, 119.20, 120.92, 121.16, 122.01, 122.93, 126.88, 129.17 and a staggering number of 19 quaternary carbon atoms (Fig. 78).

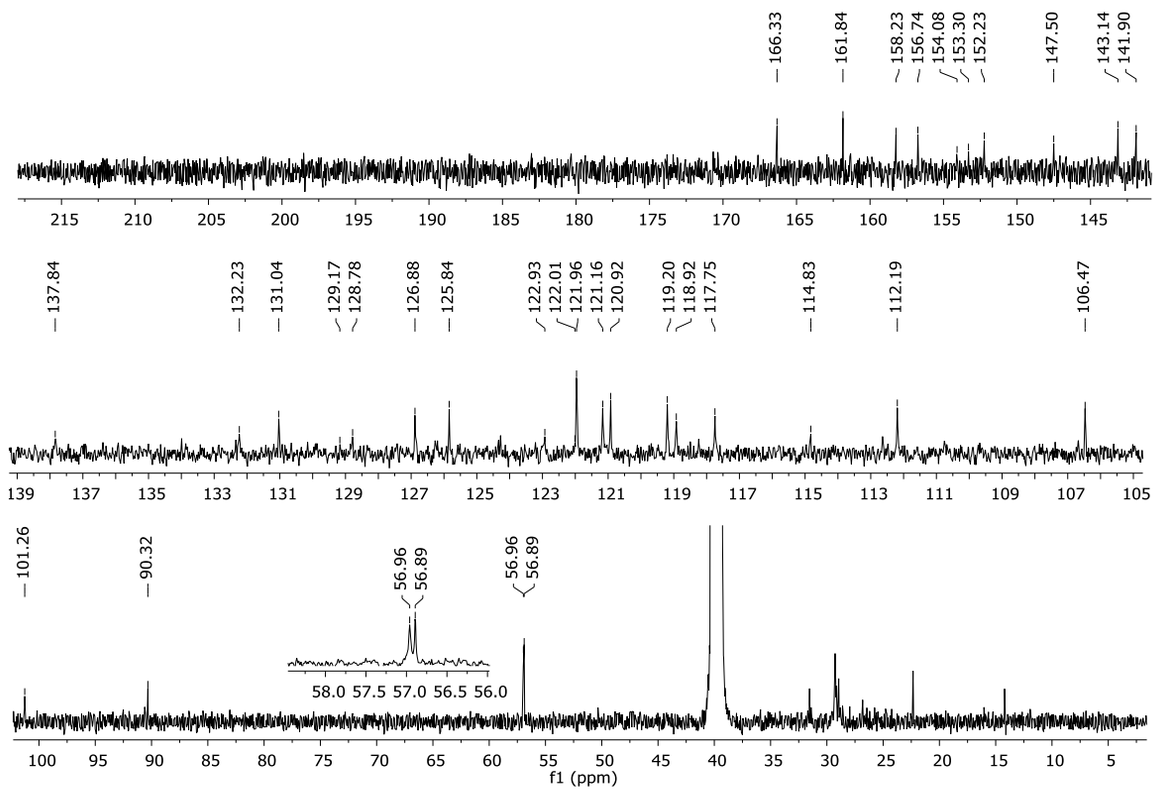

Figure. 78. Concentrated ^{13}C-NMR-spectrums of **48**, (151.01 MHz, DMSO-d6, 297.1 K).

The COSY-spectrum shows also the presence of four spin systems similar to trivialine A (**47**), and subsequently combined with the data extracted from HMBC and NOESY-spectrums, also four substructures that designated with symbols (**A**), (**B**), (**C**), and (**D**) can be identified, all of them are parts of benzene rings, see (Fig. 79).

The chemical shifts, the spin systems, and the same molecular formula in trivialine B (**48**) suggest that this compound is either a diastereomer or a constitutional isomer to trivialine A (**47**) rather than a different compound. The highly unstable nature of these compounds supports the assumption of the later suggestion, which a rearrangement could cause the formation of trivialine B (**48**) as trivialine A (**47**) will act as a precursor for more compounds in *L. trivialis* mushroom. This could be validated when the resulting data from measuring the trivialines fractions in high-resolution liquid chromatography, exhibit different degrees of degradations (or reformations) causing of appearance of compounds with related molecular formulas, see section 4.2.5.4.

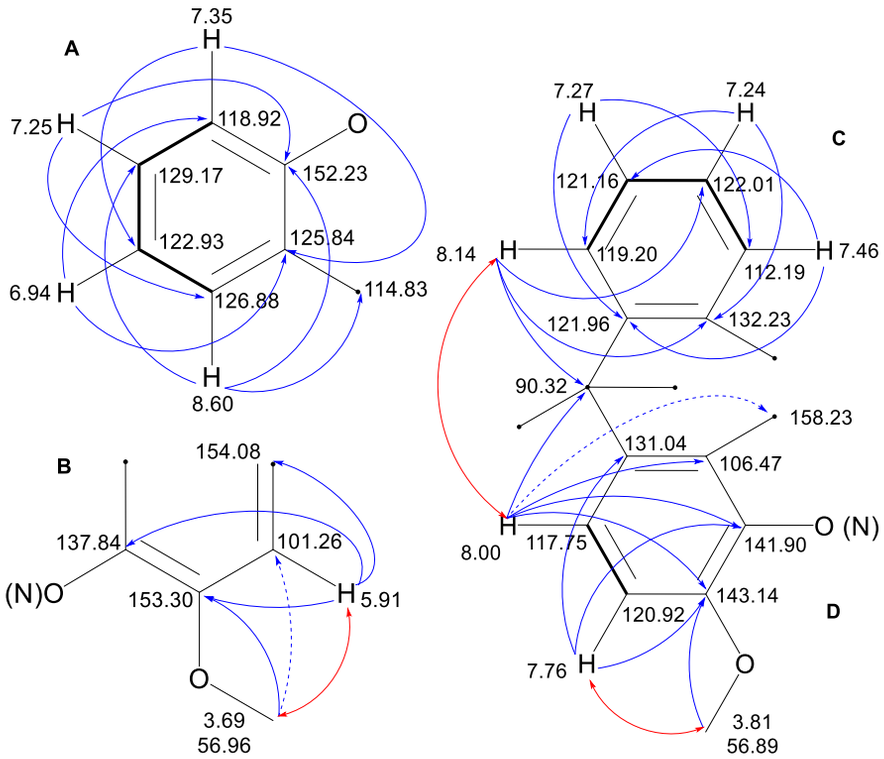

Figure. 79. Substructures (**A**), (**B**), (**C**), and (**D**).
HMBC correlations (⟶). NOESY correlation (⟷).

4.2.5.3 Trivialines C (**49**), D (**50**), and E (**51**)

More compounds belonging to the trivialines class of compounds were isolated from *L. trivialis* mushroom in this research. Consequently, the yellow trivialines C (**49**) and E (**51**) were detected using UV wavelength at 440 nm, and trivialine D (**50**) with peach color was detected using UV wavelength at 550 nm. The NMR data show a pattern and chemical shifts with a certain similarity to trivialioines A (**47**) and B (**48**), see sections 9.21, 9.22, and 9.23. Due to the isolated small masses of these compounds, the NMR data show fewer chemical shifts than the expected number of hydrogen and carbon atoms from the measured molecular formulas.

4.2.5.4 Trivialines comparisons

Trivialines were measured in high-resolution LCMS to assign their molecular formulas. The general form of the elemental formula consists of 32 carbon atoms, at least 20 hydrogen atoms, and at least 6 oxygen and 4 nitrogen atoms. The molecular formulas are varied about the presence of amino content. Moreover, each fraction exhibits a degree of degradation which shows the presence of at least one related compound that has a similar molecular formula, see (Tab. 6).

Table. 6. An overview of isolated trivialines.

Trivialines	**Color**	**UV detection, R_t** (semi-preparative HPLC)	**Molecular mass (*m/z*), R_t (min), Molecular formula** (Analytical-HR-LCMS)	
			Main compound	**Other compound(s)**
A (**47**)	Yellow	440 nm, 47 min,	557, 33-34, $\mathbf{C_{32}H_{21}N_4O_6}$	558, 29, $\mathbf{C_{32}H_{20}N_3O_7}$
B (**48**)	Violet	550 nm, 37 min	557, 33-34, $\mathbf{C_{32}H_{21}N_4O_6}$	573, 23, $\mathbf{C_{32}H_{21}N_4O_7}$
C (**49**)	Yellow	440 nm, 34 min	575, 32.5, $\mathbf{C_{32}H_{23}N_4O_7}$	557, 33-34, $\mathbf{C_{32}H_{21}N_4O_6}$ 281, 32, $\mathbf{C_{16}H_{13}N_2O_3}$ 265, 15, $\mathbf{C_{15}H_9N_2O_3}$
D (**50**)	Peach	550 nm, 32 min	573, 23, $\mathbf{C_{32}H_{21}N_4O_7}$	558, 29, $\mathbf{C_{32}H_{20}N_3O_7}$ 574, 19, $\mathbf{C_{32}H_{20}N_3O_8}$
E (**51**)	Yellow	440 nm, 29 min	573, 23, $\mathbf{C_{32}H_{21}N_4O_7}$	576, 27, $\mathbf{C_{32}H_{22}N_3O_8}$ 559, 18.5, $\mathbf{C_{32}H_{15}N_8O_3}$

The full NMR data for compounds (**47**) and (**48**), and the partial NMR data for compounds (**49**) and (**50**) suggest that (**47**) and (**49**) are structurally close to each other, hence the yellow color of both of them and the same UV absorption wavelength that they were detected at (440 nm), see (Tab. 7). Also, (**48**) and (**50**), hence the violet and peach color respectively, and as well, the same UV absorption wavelength used for detecting and isolating these compounds (550 nm). In addition, compound (**50**) exhibits a high degree of degradation or chemical change with time although the storing conditions, to the color eventually changed from peach to violet color. Compound (**51**) has much less NMR data.

In general, the MS and NMR data for the isolated trivialines suggest two proposals for their chemistry, they either two groups of compounds with very similar chemical structures, or, they all have the same chemical structure but with different hetero atoms numbers and attachments, hence the same number of carbon atoms (32), and altering numbers of oxygen and nitrogen atoms.

The noticeable changes in the chemical shifts of hydrogen and carbon atoms in trivialines A (**47**) and B (**48**) are marked in bold numbers in (Tab. 7). Most of the changes are in and around the substructure **B**.

Table. 7: NMR data for trivialines in DMSO-d6

Sub-structures	A (**47**) δ_H and (or) δ_C	B (**48**) δ_H and (or) δ_C	C (**49**) δ_H and (or) δ_C	D (**50**) δ_H and (or) δ_C
A	131.89	152.23	M	M
	7.36 111.32	7.35 118.92	7.44 112.35	M
	7.06 121.07	7.25 129.17	7.23 (2H) 121.74	M
	6.87 119.97	6.94 122.93		6.91 120.30
	7.98 122.85	8.60 126.88	8.02 121.31	8.50 125.39
	122.41	125.84	M	M
	89.67	**114.83**	M	M
	146.63	147.50	M	147.18
	162.09	161.84	M	M
B	123.06	128.78	M	M
	141.20	**154.08**	M	M
	6.83 113.16	**5.91** 101.26	6.64 110.52	5.79 99.74
	142.31	153.30	M	M
	3.74 (3H) 56.02	3.69 (3H) 56.96	3.73 (3H) 56.72	3.49 (3H) 55.59
	121.30	**137.84**	M	M
	98.20	**158.23**	M	157.88
	146.41	**156.74**	147.13	156.30
	162.94	166.33	162.62	M
C	132.00	132.23	132.33	131.90
	7.48 111.95	7.46 112.19	7.42 112.21	7.44 111.90
	7.26 121.93	7.24 122.01	7.20 (2H) 121.17 121.99	7.24 120.30
	7.27 120.98	7.27 121.16		7.27 120.95
	8.10 119.14	8.14 119.20	7.98 119.48	8.13 118.97
	121.59	121.96	M	121.71
	90.83	90.32	90.98	90.07
D	131.12	131.04	129.44	130.70
	103.63	106.47	98.95	106.00
	7.59 111.00	8.00 117.75	7.15 106.30	7.97 117.31
	7.58 122.65	7.76 120.92	7.29 117.52	7.75 120.64
	3.58 (3H) 56.57	3.81 (3H) 56.89	3.88 (3H) 56.55	3.82 (3H) 56.67
	145.37	143.14	144.22	142.20
	139.51	141.90	143.02	142.95
exchange able	12.33	12.27	12.15	12.27
	12.28	10.13	12.23	M
	9.97	9.52	5.86?	M

M: Missing chemical shift.

4.2.5.5 MS/MS considerations

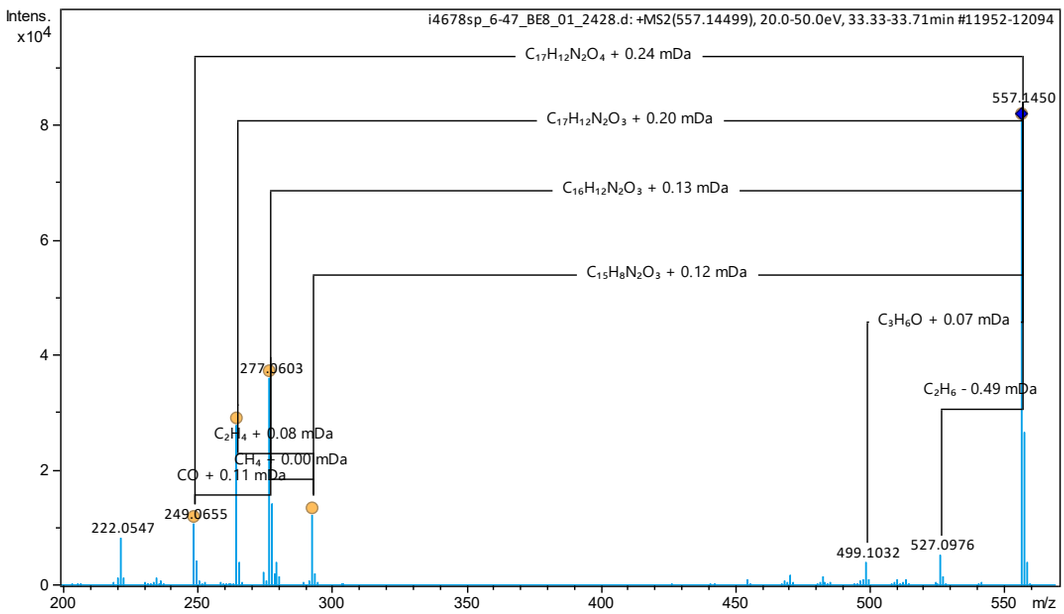

Figure. 80. HR-ESI-(+)-MS/MS-spectrum of **47**.

The MS/MS spectrum of trivialine A (**47**) exhibits a clear sign of splitting in half pattern. This suggests that there is a degree of dimerization in the structural shape of the compound **47**, (Fig. 80). Similar conclusions can be inferred from MS/MS spectrums of the other trivialines B (**48**), D (**50**), and E (**51**), see sections 9.20, 9.22, and 9.23 respectively.

4.2.5.6 Proposed structures for trivialine A (**47**)

Several proposed structures were introduced as a potential chemical structure for the yellow compound trivialine A (**47**). The most candidate structure is the proposed structure **1**. This structure exhibits the clear dimerization of two identical halves of an indol-containing moiety in a hetero chain of cycles by linking them with one secondary amino bridge, see (Fig. 81). This proposed structure can justify the very similarity in NMR chemical shifts between the substructures **A** and **B**, with the other substructures **C** and **D**. But such a structure, doesn't justify the measured chemical formula.

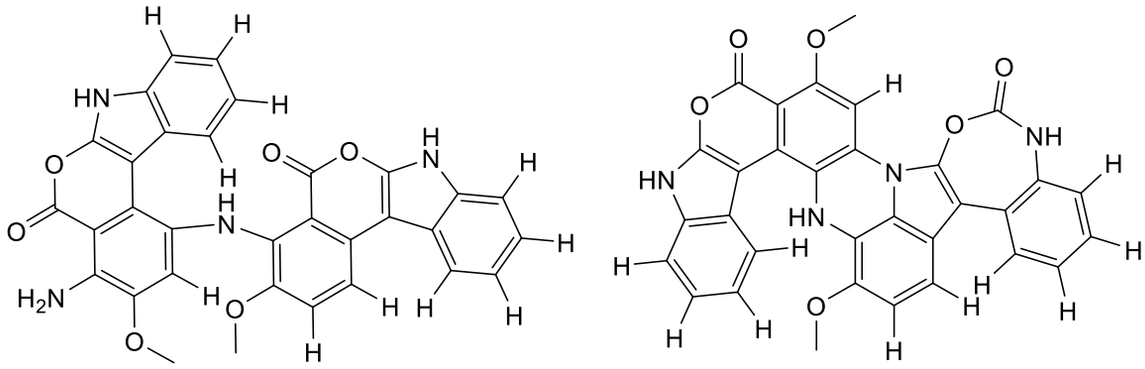

Chemical Formula: $C_{32}H_{22}N_4O_6$
Exact Mass: 558.15393
Proposed structure **1**

Chemical Formula: $C_{32}H_{20}N_4O_6$
Exact Mass: 556.13828
Proposed structure **2**

Figure. 81. Proposed structures for trivialine A (**47**).

The other proposed structure **2**, links in a similar manner two different halves through two amino bridges, one is secondary and the other is tertiary. This proposed structure matches with the measured chemical formula for trivialine A (**47**), but doesn't match entirely the NMR chemical shifts.

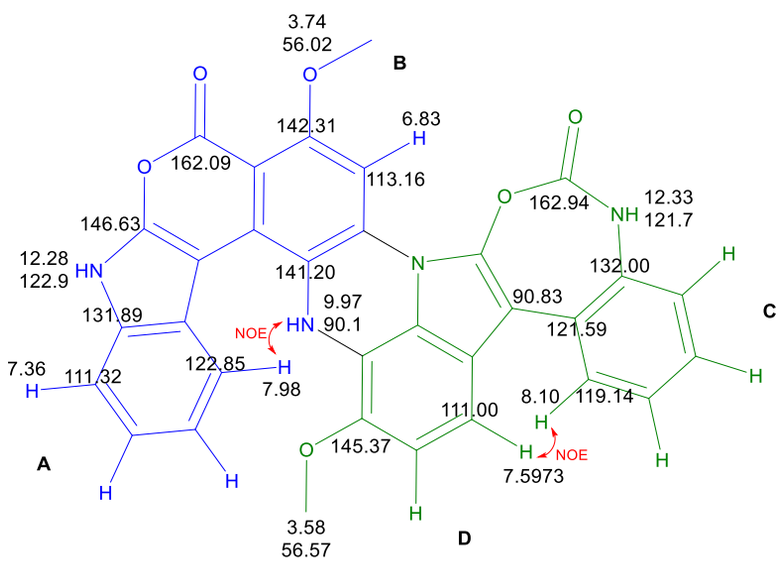

Figure. 82. Proposed structure **2** for trivialine A (**47**) with selected NMR chemical shifts.

In the proposed structure **2**, the indol containing moiety half from **1** was adapted by altering the positions of moieties in substructure **B**, see (Fig. 82). Also, the recorded NOE correlations were justified between protons at δ_H 7.98 and 9.97 in the first half (designated in color blue) and protons at δ_H 7.5973 and 8.10 in the second half (designated in green).

The chemical structure of trivialine A (**47**) is yet to be improved and configured.

4.2.6 Isolation of sesquiterpenoids

In the effort of perusing more compounds from the flesh of *L. trivialis* mushroom, known and new compounds belonging to the lactarane sesquiterpenes group of compounds were extracted. Furandiol **15** and lactarorufin A (**25**) the already known and extracted from this mushroom were extracted. Moreover, the known lactarorufin B (**27**) was also extracted and identified as a mixture with the new diastereoisomer compound 14-hydroxylactarorufin B (**53**) for the first time from *L. trivialis* mushroom. Also, compound 14-hydroxyblennin A (**52**) was extracted and elucidated from this mushroom and it has been proven that this is the first time to have recorded NMR and LC-MS data of this compound.

4.2.6.1 14-Hydroxyblennin A (**52**)

14-hydroxyblennin A (**52**) was reported to be extracted from *Russula sanguinea* by YAOITA *et al.* in 2012,[74] see section 4.1.3.17. In that research, they reported what it was believed to be compound **52**, but instead, they already reported the known compound 15-hydroxyblennin A (**34**). This was established in the previously mentioned section. This compound was extracted in this research from *Lactarius trivialis*. The close similarity between these isomers could cause confusing to differentiate between them. The difference between these isomers can be proved using the retention times in HR-LCMS and the comparison of the NMR chemical shifts of both compounds.

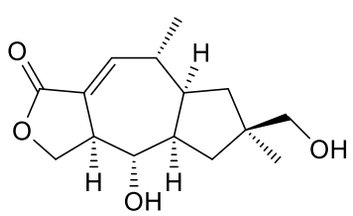

14-Hydroxyblennin A (**52**)

In section 4.1.3.17.2, such a comparison of the NMR chemical shifts was established when using $CDCl_3$ as the deuterated solvent. Also, here is a comparison was performed using CD_3OD as a solvent, see (Tab. 8).

Table 8: ^{1}H-NMR data for compound **34**, and **52** in CD_3OD.

position	δ_H (*J* in Hz) **34**	δ_H (*J* in Hz) **52**
1	α:1.47 1H (dd, 13.8, 4.9)	α:1.68 1H (dd, 14.2, 5.3)
	β:1.76 1H (dd, 13.8, 7.6)	β:1.55 1H (dd, 13.4, 8.0)
2	2.12 1H (dddd, 12.0, 7.2, 4.9)	2.18 1H (dddd, 13.2, 7.9, 5.6)
3	2.54 1H (dddd)	2.47 1H (ddd, 13.9, 7.1, 3.8)
4	6.69 1H (dd appears as t, 3.0, 3.0)	6.65 1H (dd appears as t, 2.9, 2.9)
5	-	-
6	-	-
7	3.36 1H (dddd)	3.38 1H (dddd)
8	3.51 1H (dd appears as t, 10.0, 10.0)	3.53 1H (dd appears as t, 10.0, 10.0)
9	2.29 1H (dddd appears as tt, 10.0, 7.0)	2.39 1H (dddd appears as tt, 9.9, 7.4)
10	α:1.36 1H (dd, 13.3, 10.6)	α:1.52 1H (dd appears as t, 12.0, 12.0)
	β:2.04 1H (dd, 13.2, 6.9)	β:1.72 1H (dd, 12.6, 6.5)
11	-	-
12	1.17 3H (d, 7.3)	1.14 3H (d, 7.2)
13	α:4.11 1H (dd appears as t, 9.0, 9.0)	α:4.10 1H (dd appears as t, 9.0, 9.0)
	β:4.50 1H (dd appears as t, 9.1, 9.1)	β:4.50 1H (dd appears as t, 9.1, 9.1)
14	1.10 3H (s)	3.35 2H (s)
15	3.30 2H (s)	1.04 3H (s)

Although most of the chemical shifts of these isomers are very similar to each other there is a relatively significant differences in the chemical shifts of the neighboring protons of the inverted moieties attached to carbon 11. These protons at carbons 1 and 10 show clearly that they were affected by the position of the oxygenated carbon when it's at carbon 14 and when it's at carbon 15. Although the coupling constants are similar in general, the chemical shifts are different. Such as protons at carbon 1 at δ_H 1.47 and 1.76 in 15-hydroxyblennin A (**34**) will change to be at δ_H 1.55 and 1.68 in 14-hydroxyblennin A (**52**). Also, protons at carbon 10 at δ_H 1.36 and 2.04 will change to be at δ_H 1.52 and 1.72 in these compounds respectively. These differences are understandable due to the structural nature of these asymmetrical compounds, as moieties are different on each side of these structures and so the chemical shifts will be affected in these continuous spin systems. The carbon's chemical shifts don't show such differences.

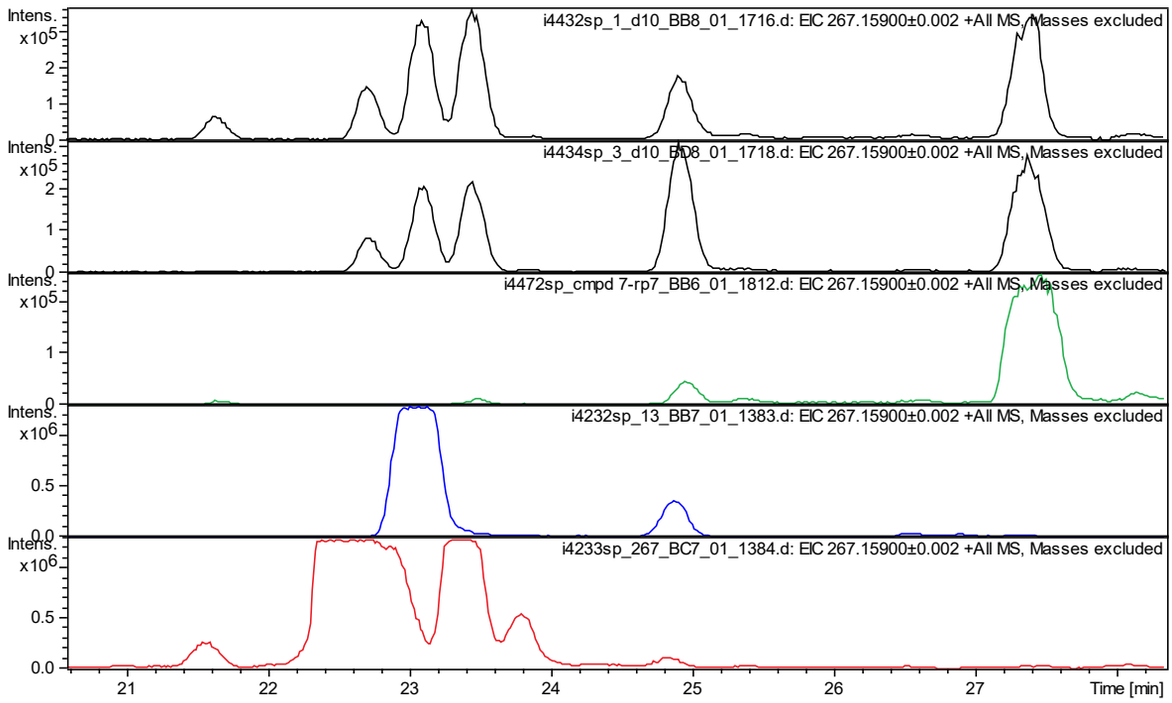

Figure. 83. The Extracted-ion chromatograms (EIC) of the exact mass 267.159 from HR-LCMS measurements for (up to down): SPE MeOH fraction from *L. circellatus* (black), SPE MeOH fraction from *L. blennius* (black), lactarorufin A (**25**) (green), 15-hydroxyblennin A (**34**) (blue), and 14-hydroxyblennin A (**52**) (red). (Gradient method F1).

Data from HR-LCMS measurements show differences in retention times although it's small. (Figure. 83) shows the Extracted-ion chromatograms (EIC) of the exact mass 267.159 from HPLC measurements results for each of the following samples, (from up to down); SPE MeOH fraction of the MeOH extract from *L. circellatus* flesh, SPE MeOH fraction of the MeOH extract from *L. blennius* flesh, compound lactarorufin A (**25**), compound 15-hydroxyblennin A (**34**), and compound 14-hydroxyblennin A (**52**). All of these three compounds have the molecular weight of 266.34 g/mol and the chemical formula of $C_{15}H_{22}O_4$, and yet a retention times are different. In the structural isomer lactarorufin A with the retention time of 27.4 min is eluting relatively later than the intended stereoisomer compounds **34** and **52**. They elute at 22.7 min and 23.0 min respectively. Yet the close retention times for these stereoisomers, but these are enough to be considered as indicators to differentiate between such isomers. Additionally, it can be inferring that compound 14-hydroxyblennin A (**52**) is exist in both mushrooms *L. circellatus* and *L. blennius* in addition to *L. trivialis*.

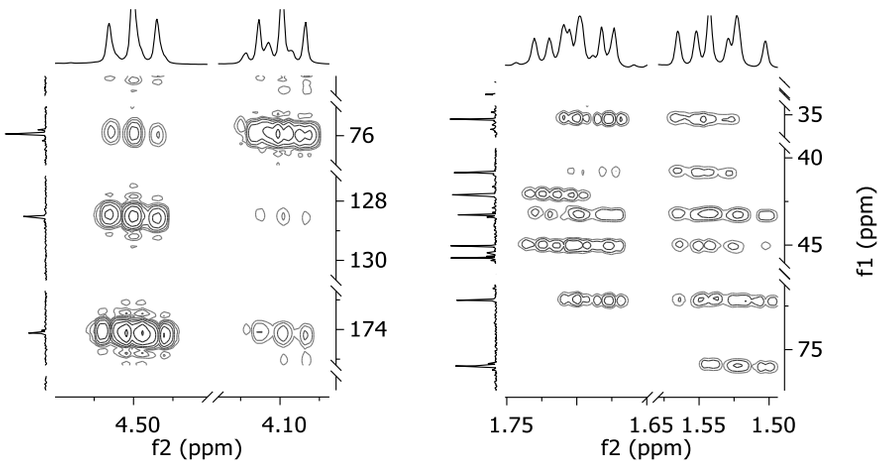

Figure. 84. HMBC concentrated-spectrums of correlations from compound **52** from *L. circellatus*, (CD_3OD). Left: protons at δ_H 4.10 and 4.50. Right: protons between δ_H 1.50 and 1.75.

For assigning the stereo configurations of the moieties and protons of the methylene groups in the compound 14-hydroxyblennin A (**52**), the approach described in sections 4.1.3.1.1 and 4.1.3.2.1 was implemented.

The protons of all methylene groups at carbons 1, 10, and 13 in this compound show HMBC correlations compatible with the Karplus relationship (Fig. 84). The proton at δ_H 1.55 at carbon 1 has a much stronger HMBC correlation with carbon 10 at δ_C 40.85 than the proton at δ_H 1.68 from this methylene group. This is an indicator that the dihedral angle between the later proton and the due carbon is not exactly 90°. Nevertheless, due to the trivial correlation, this angle is very near the 90°. However, the results from protons at carbon 10 are more decisive. Which proton at δ_H 1.52 has correlations with carbons 8 and 14 at δ_C 75.94 and 72.17 but the other geminal proton at δ_H 1.72 has not. Also, the latter proton correlates with carbon 1 at δ_C 42.12 but not the other proton in this methylene group. In the same way, similar observations from protons of methylene groups at C-13 were noticed. As proton at δ_H 4.10 has a much stronger correlation with carbon 8 at δ_C 75.94 than the other geminal proton at δ_H 4.50. Also, this proton has even stronger correlations with carbons 5 and 6 at δ_C 174.12 and 128.52 than the other geminal proton in this methylene group.

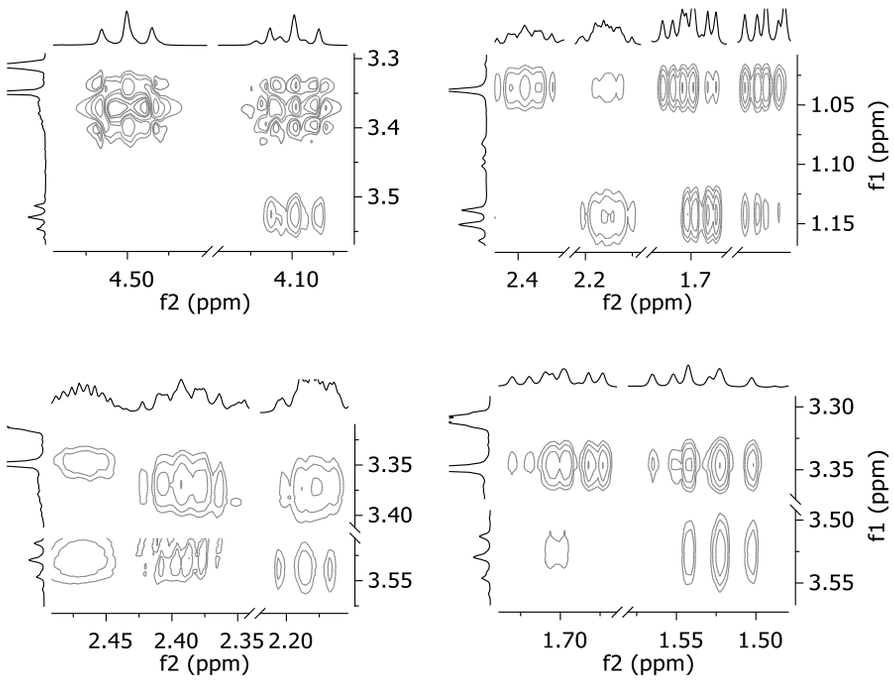

Figure. 85. NOESY expanded-spectrums of selected correlations from compound **52**, (CD_3OD). Up left: between protons at δ_H 3.35 and 4.10. Up right: for methyl protons at δ_H 1.04 and 1.14. Down left: for protons at δ_H 3.35, 3.38 and 3.53. Down right: between protons at δ_H 3.35 and 3.53 and methylene protons at C-1 and C-10.

The NOE data show sometimes less decisive results such as protons in the opposite direction will correlate with the same proton but with different intensities. In this case, only the strongest correlation among them will be initially considered. For example, the oxygenated protons at δ_H 3.35 will correlate with all protons at the methylene groups at carbons 1 and 10 (Fig. 85-Down right). So, only correlations with protons at δ_H 1.52 and 1.68 will be considered as a starter for the argument's sake. Subsequently, protons at δ_H 1.04, 1.55, 1.72, 2.18, 2.39, 1.14, and 3.38 will be assigned to be oriented towards the same side of this compound. At the same time, protons at δ_H 3.35, 1.68, 1.52, 2.47, 3.53, and 4.10 have NOE correlations between each other, and the stereo configurations of them all will also exist on the same side of the compound. By assigning the usual down configuration to protons at δ_H 2.18 and 2.39 at carbons 2 and 9 respectively, and upon combining the previously extracted data from HMBC and NOE correlations, the relative structure for compound 14-hydroxyblennin A (**52**) can be assigned.

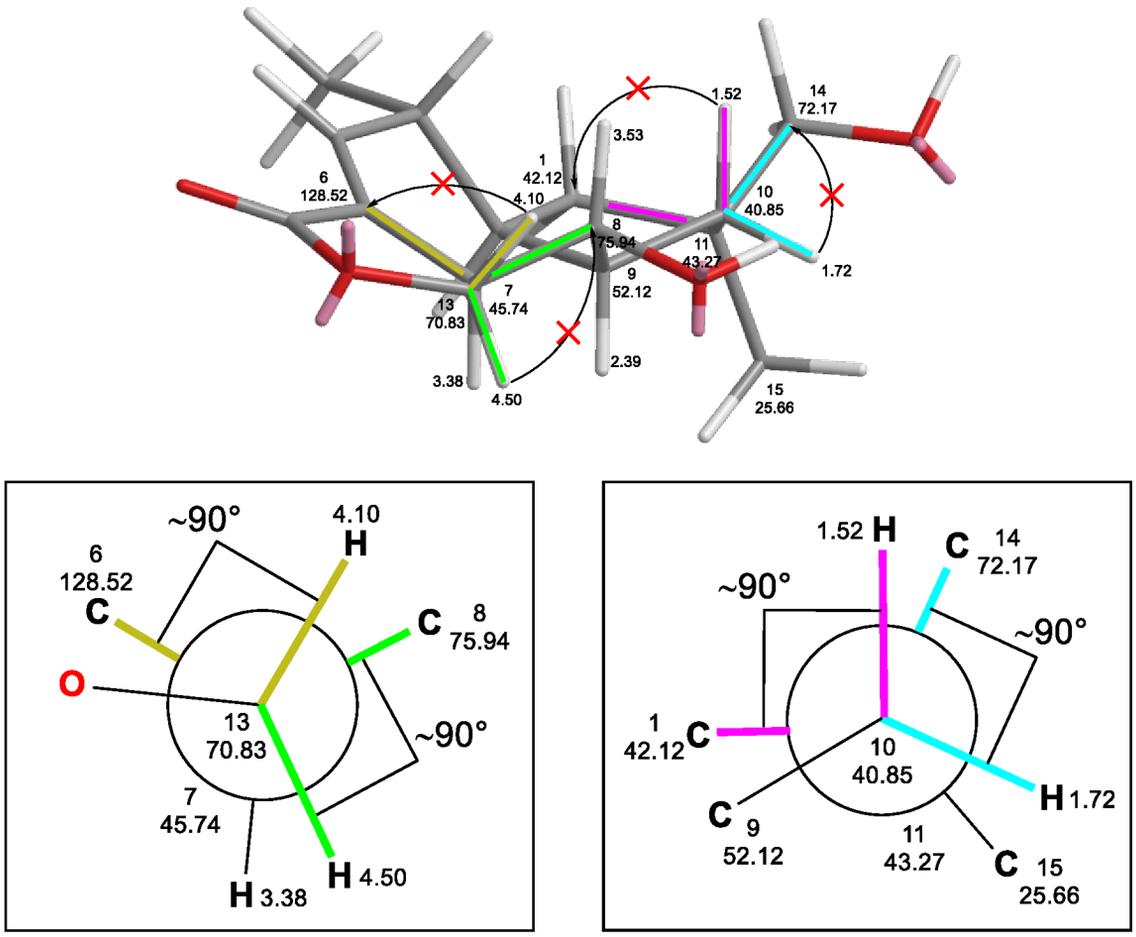

Figure. 86. Up: 3D module of compound **52**. Down left: Newman projection with perspective view from C-13 through C7. Down right: Newman projection with perspective view from C-10 through C11.

The assigning of the relative structure of such compound was performed using the same method described before, by fixing the dihedral angle with approximately a 90° between the hydrogen and carbon atoms that should have HMBC correlations but they didn't (Fig. 86-Up). Such an approach will be the answer to the not decisive NOE data, and so, is serving as a tool for assigning the stereo configurations of protons and moieties in this compound. (Fig. 86-Down left) shows Newman projection from carbon 13 through carbon 7 after applying the interpreted information from HMBC correlations. Such elaboration shows the relation between protons of the methylene group at carbon 13 with carbons 6 and 8, in which proton at δ_H 4.10 can't be in the down configuration and still has NOE correlations with proton at δ_H 3.53 that is in the up configuration, and located in the opposite side of protons at δ_H 2.39 and 3.38 that have NOE correlation between them. Similarly, (Fig. 86-Down right) shows the positions of the methylene protons at C-10 in relation to their neighboring carbons 1, 9, 14, and 15 in a manner that agrees with the Karplus relationship. So, by assigning protons at carbons 2 and 9 to be in the down configuration and then assigning the rest of the protons in accordance, the relative structure was assigned (Fig. 87). Also, if the assigning process started from any other moiety taking into consideration HMBC and NOE correlations with its neighboring atoms, then the relative structure will also be reached for this compound.

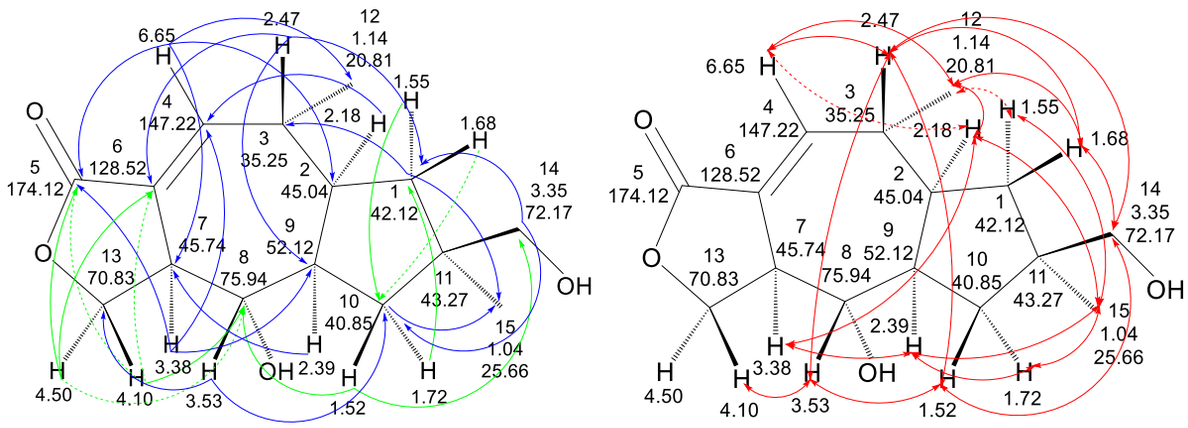

Figure. 87. Relative structure of compound **52** with assignments, (CD_3OD). Left: selected HMBC correlations (⟶), HMBC correlations with Karplus relationship (⟶). Right: NOESY correlations (⟷).

The reversed position of the oxygen-containing carbon 14 in this stereoisomer of the compound 15-hydroxyblennin A (**34**) did not drastically change the polarimetry sign, since the sign of the measured polarimetry for this compound is also positive, $[\alpha]_D^{25}$ +82 (MeOH; *c* 0.001).

4.2.6.2 Lactarorufin B (**27**) and 14-Hydroxylactarorufin B (**53**)

Lactarorufin B (**27**) and 14-hydroxylactarorufin B (**53**) were isolated from the extract of the flesh of *L. trivialis*. Gradient G was used, see section 6.3.4.7, with the mobile phase water with 0.1% acetic acid and acetonitrile and the C18-ec column. The UV/Vis absorption at 230 nm was used to isolate the substances. (Fig. 88) shows two chromatograms of the two isolated substances. The upper chromatogram already shows that the peak of the isolated substance consists of two peaks that are hardly separated from each other. A change in the gradient (lower chromatogram) makes this clearer. Therefore, instead of a single substance, two substances of equal mass were isolated. However, a renewed attempt to separate these compounds from one another using an extended adjusted gradient failed, which is why both substances were analyzed together. (5.16±0.02) mg of both compounds **27** and **53** were isolated.

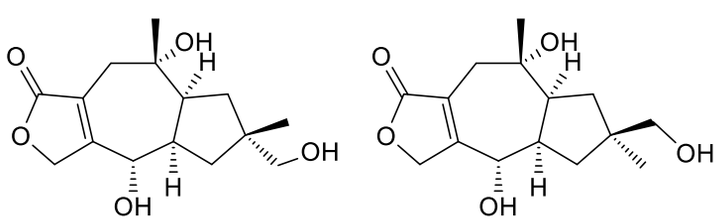

Lactarorufin B (**27**) 14-Hydroxylactarorufin B (**53**)

The naming of compound **53** came as the stereo configuration of the hydroxyl group that attached to one of the two methyl groups at carbon 11 is in the up configuration of the compound i.e. it's located at carbon 14 in contrast to the diastereomer lactarorufin B (**27**).

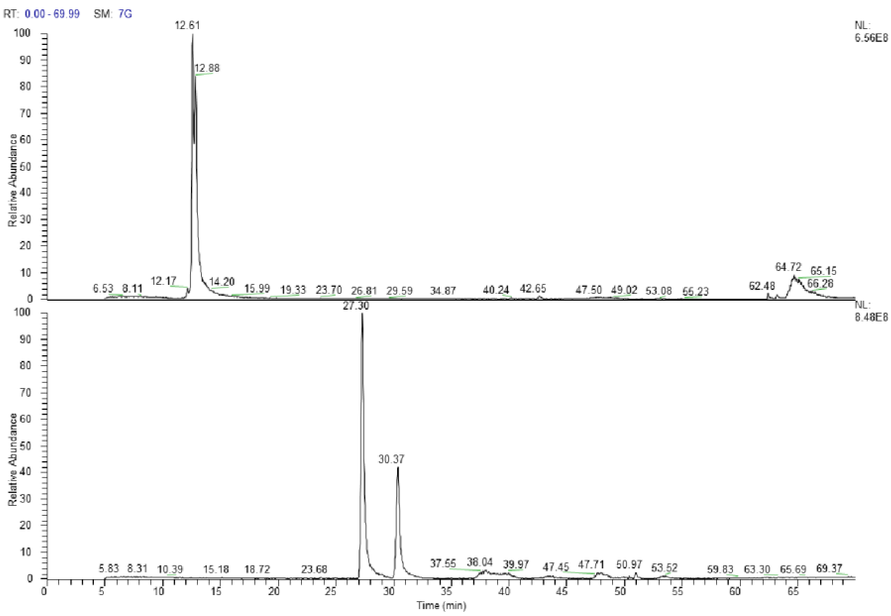

Figure. 88: Chromatograms of Compounds **27** and **53** isolated together. Above: BPC using gradient G. Below: BPC using extended gradient. The chromatograms were recorded using the LC-MS, ESI ionization method, analytical C18ec-column.

(Fig. 89) shows the UV/Vis spectrum of the colorless substances recorded during isolation of the together isolated compounds **27** and **53**. The target compounds have an absorption maximum of 223 nm.

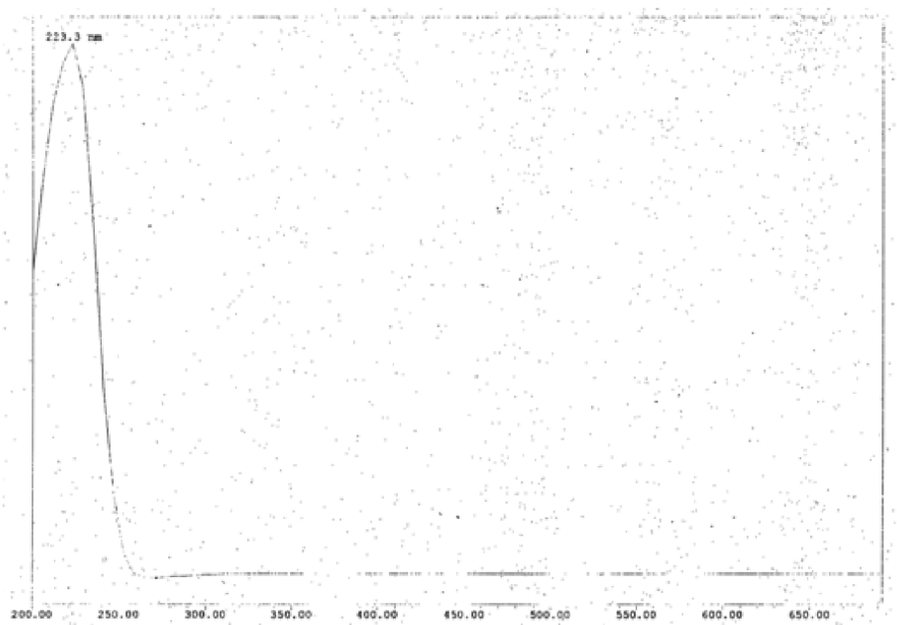

Figure. 89: UV/Vis-Spectrum of the Compounds **27** and **53**. The spectrum was recorded from the semipreparative-HPLC run with a flow rate of 5.0 mL/min and an injection volume of 250 µL.

(Fig. 90) shows the MS/MS-spectrum of the quasi-molecular ion (*m/z* 283) of compounds **27** and **53**. The quasi-molecular ion does not appear in the fragment spectrum, but can only be seen in the MS spectrum see section 9.17 - (Fig. S79 and S80). Like that of compound **53**, the spectrum shows losses of neutral parts in the form of some water molecules as well as carbon monoxide

and carbon dioxide. The MS/MS spectrum in general suggests a stable molecule, which is similar to the other lactarane sesquiterpenes compounds.

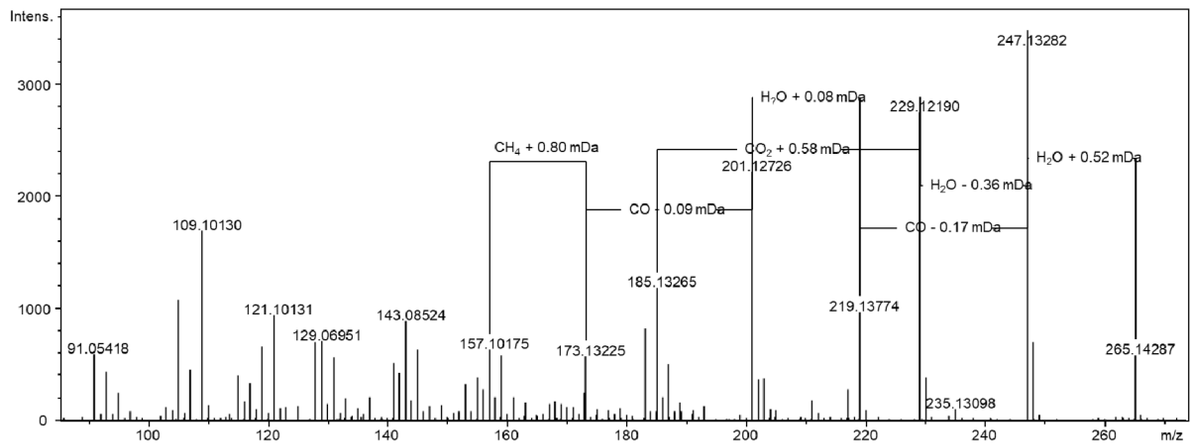

Figure. 90: MS/MS-Spectrum of the quasi-molecular ion (*m/z* 283) of Compounds **27** and **53**. The spectrum was recorded from the HR-ESI-(+)-MS run with a flow rate of 0.5 mL/min and an injection volume of 5 µL.

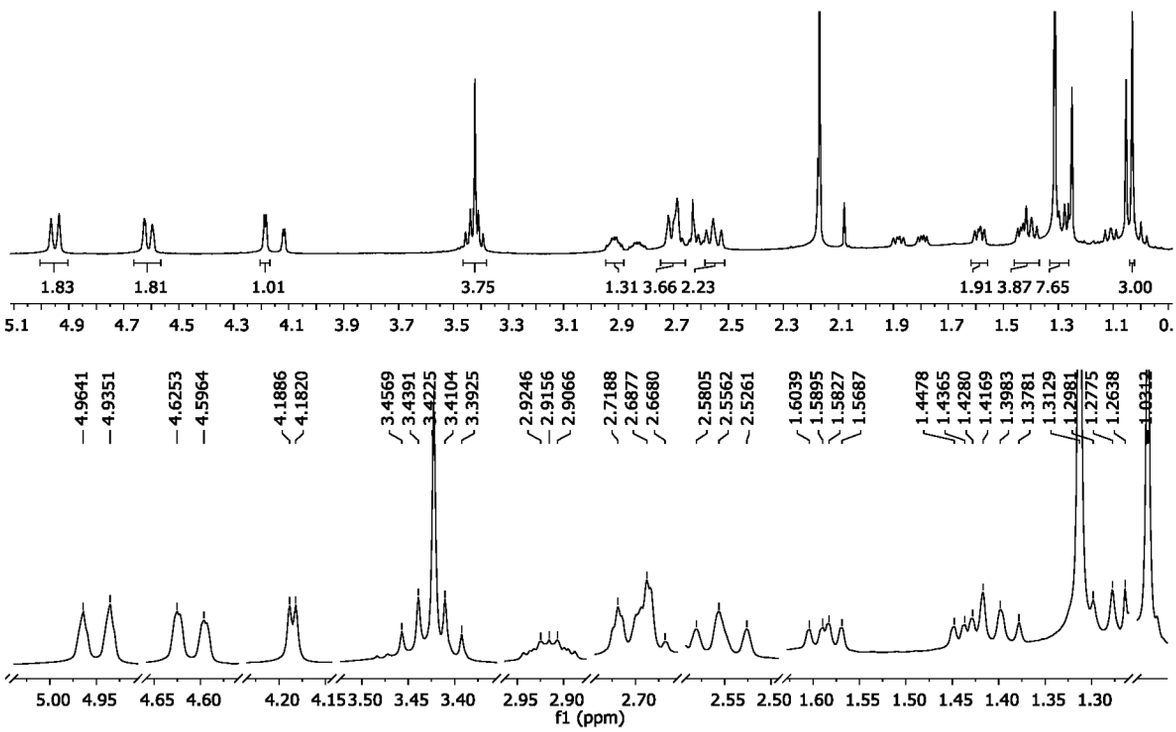

Figure. 91. ^{1}H-NMR-spectrum (600.22 MHz, $CDCl_3$, 297.2 K) of compounds **27** and **53** from *L. trivialis*.

The mixture of compounds **27** and **53** were recorded in 1D and 2D-NMR in solvents CD_3OD and $CDCl_3$. The data from both solvents were used to elucidate compound **53** with more 2D correlations recorded from the $CDCl_3$ solvent. (Fig. 91) shows the ^{1}H-NMR spectrum of the mixture fraction was recorded using $CDCl_3$ with only picked peaks of compound **53**. The rest of the NMR data are shown in section 9.17.

According to the 1D-NMR signals, the quantity of the new compound **53** is double that of lactarorufin B (**27**). Moreover, as expected, some protons and carbons have either the same or

very close chemical shifts in both ^{1}H and ^{13}C-NMR spectrums. For example, the proton signal at δ_H 3.42 belongs to protons of both oxygenated methylene groups at carbon 14 and 15 for compounds 14-haydroxylactarorufin B (**53**) and lactarorufin B (**27**) respectively. Also, proton signals at δ_H 4.76 and 4.89 are belonging to oxygenated methylene groups protons from both compounds. In the case of proton signals at δ_H 2.56 and 2.70, they belong to both methylene groups from both compounds and they are located at the same carbon atom at δ_C 34.72, (Fig. 92).

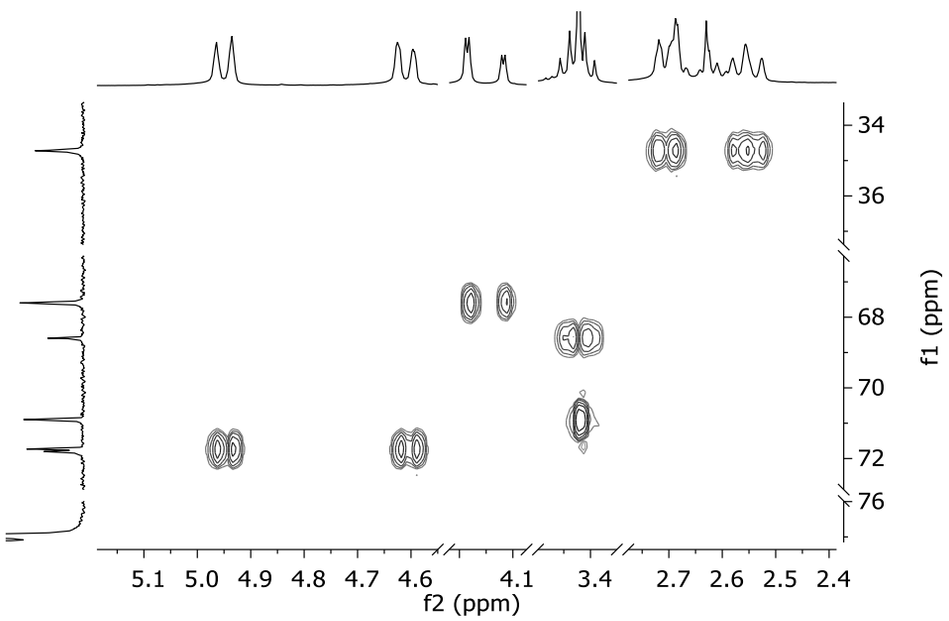

Figure. 92. HSQC concentrated-spectrum (600.50 MHz, $CDCl_3$, 297.2 K) of compounds **27** and **53** from *L. trivialis*.

The assigning of such signals was achieved by applying the bigger signals to be coupled together and assigning them to compound **53**. Also, comparing the different 2D-NMR couplings and correlations and matching them to fit with bigger signals. After that, when it had been concluded that one of the two compounds is lactarorufin B (**27**), the confirmation of assigning the bigger signals in ^{1}H and ^{13}C-NMR data to the diastereomer compound **53** was established.

For assigning the stereo configurations of methylene protons and the rest of the moieties in compound **53**, the same approach as mentioned before was used for such a type of compound, see sections 4.1.3.1.1 and 4.1.3.2.1.

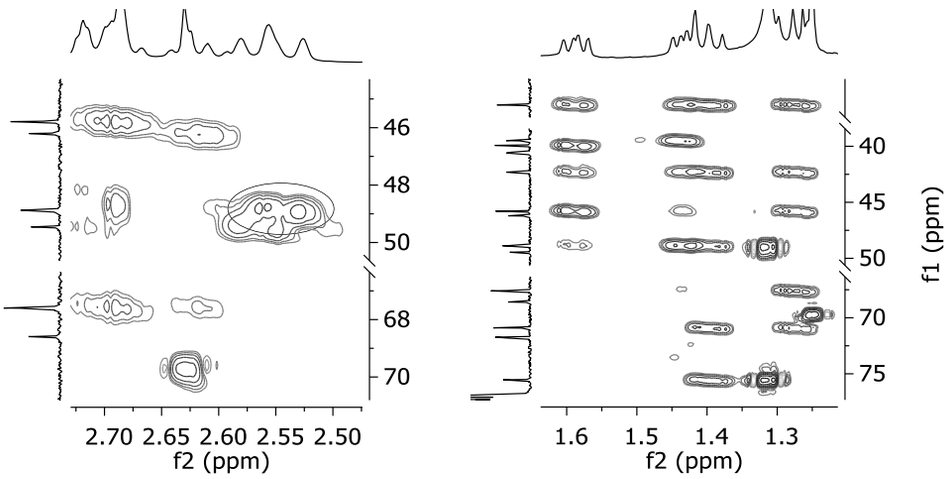

Figure. 93. HMBC concentrated-spectrums of correlations from compound **53** from *L. trivialis*, ($CDCl_3$). Left: protons at δ_H 2.56 and 2.70. Right: protons between δ_H 1.20 and 1.65.

Three methylene groups out of four in compound **53** exhibit a pattern of HMBC correlations with their neighboring carbons that can be interpreted with Karplus relationships. One of the methylene protons at δ_H 2.56 at carbon 4 has a more pronounced correlation with carbon 2 at δ_C 48.88 than the other geminal proton at δ_H 2.70, (Fig. 93-Left). Also, protons from both methylene groups at carbons 1 and 10 show similar occurrences, as the proton at δ_H 1.40 has correlations with carbons 3 and 14 at δ_C 75.54 and 70.90 respectively but not the other geminal proton at δ_H 1.59 from this methylene group at carbon 1, (Fig. 93-Right). Moreover, the later proton has HMBC correlations with carbons 9 and 10 at δ_C 45.79 and 39.92 respectively but not the other geminal proton in this moiety. Also, methylene protons at carbon 10 reveal a similar pattern as proton at δ_H 1.27 shows two explicit correlations with carbons 8 and 14 at δ_C 67.60 and 70.90 respectively but not the other proton at δ_H 1.43 in this methylene group. At the same time, the later proton has correlations with carbons 1 and 2 at δ_C 39.50 and 48.88 respectively but not the geminal proton in this group.

Such a pattern of correlations is explained using Karplus relationships, as the dihedral angle between the proton and the carbon that should have HMBC correlation but yet they don't, should be either exactly or approximately 90°.

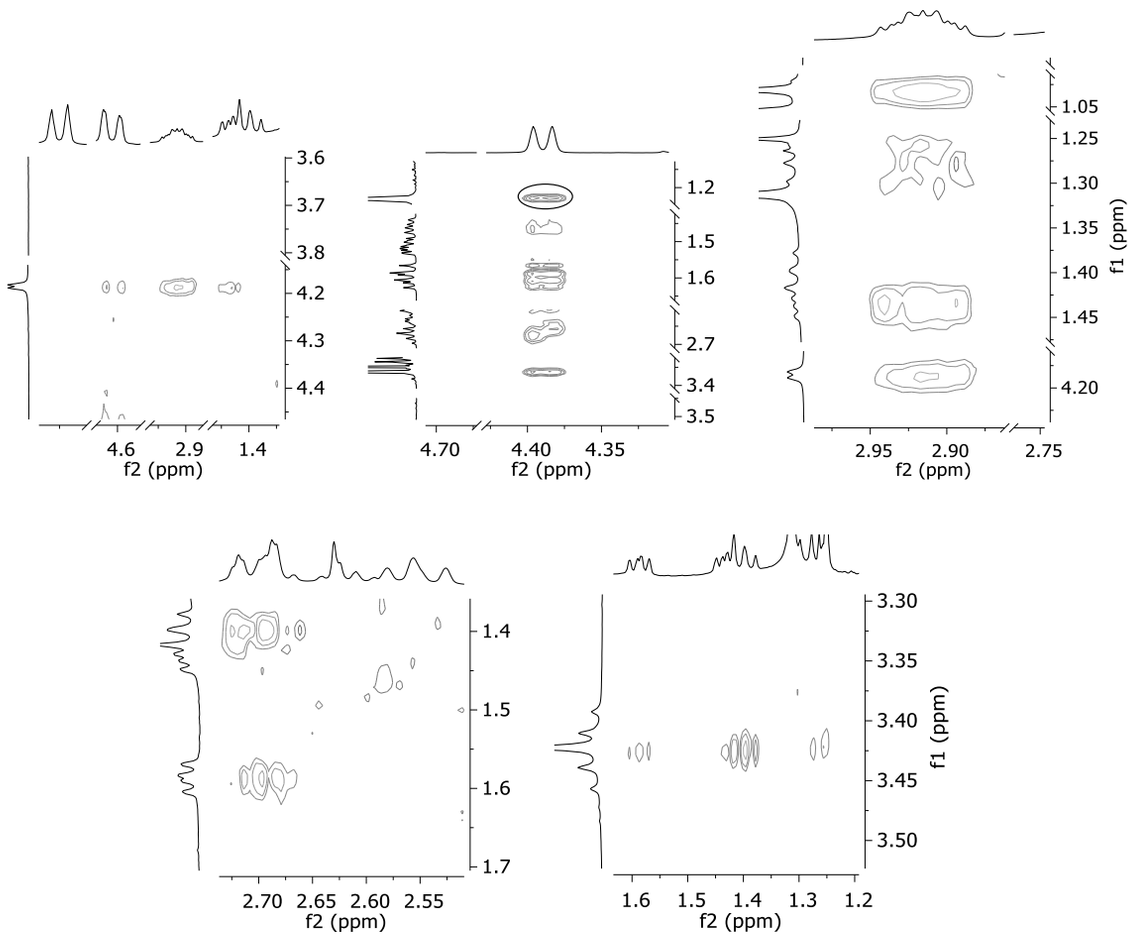

Figure. 94. NOESY expanded-spectrums of selected correlations from compound **53**, ($CDCl_3$).
Up left: for proton at δ_H 4.19. Up middle: for protons at δ_H 4.39, (CD_3OD).
Up right: for proton at δ_H 2.92. Down left: for protons at δ_H 2.69 and 2.70.
Down right: for protons at δ_H 3.428.

NOESY data of compound **53** reveal key correlations between protons in the corresponding compound. The oxygenated proton attached to carbon 8 at δ_H 4.19 has correlations with protons at δ_H 1.43, 2.92, and 4.61, (Fig. 94-Up left). The linking proton at δ_H 2.92 has also correlations with protons at δ_H 1.03 and 1.43, (Fig. 94-Up right). These correlations caused confusion at first, as the stereo configurations of the linking protons at carbons 2 and 9 in such types of compounds exist in the down configuration of the compound due to the biological synthesis pathways. Applying the information concluded from the HMBC data, it becomes clear that such correlations are possible when the compound structure is stable in a more folded formation, which put the protons at carbons 3 and 8 at δ_H 1.31 and 4.19 respectively to be the most distant from each other. This conclusion came as the same mixture fraction was measured also in CD_3OD, and the NOE data showed a clear correlation between the corresponding protons, (Fig. 94-Up middle). A similar observation was noticed for the companion compound lactarorufin B (**27**) as the corresponding protons at carbons 3 and 8 have NOE correlation when the fraction was measured in CD_3OD but didn't when it was measured in $CDCl_3$. This could be attributed to the protic and aprotic characteristics of these solvents, although it has not yet been proven. The related NMR spectrums for this mixture measured in the deuterated solvents CD_3OD and $CDCl_3$ are shown in section 9.17.

One of the methylene protons at carbon 1 at δ_H 1.40 has NOE correlations with protons at δ_H 2.70 and 3.428 of the methylene groups at carbons 4 and 14 making the stereo configurations of them are on the same side in this compound, (Fig. 94-Down spectrums).

The combined information from the HMBC and NOESY spectrums will assign protons at δ_H 1.27, 1.31, 1.40, 2.70, 3.428, 4.19, and 4.61 at carbons 10, 12, 1, 4, 14, 8, and 13 respectively to be oriented in the same side of compound **53**. At the same time, protons at δ_H 1.03, 1.43, 1.59, 2.56, 2.69, 2.92 and 4.95 at carbons 15, 10, 1, 4, 2, 9, and 13 respectively to be oriented in the opposite side of the previous protons with taking in consideration the linking protons at δ_H 2.69 and 2.92 at carbons 2 and 9 respectively to be assumed to be in the down configuration. When applying the Karplus relationship to the adherent HMBC correlations by fixing the dihedral angle with 90° between the protons and carbons atoms that should have correlations but don't, it becomes clear that the first group of protons is in the up configuration and consequently, the second group of protons to be in the opposite down configuration.

The relative structure with protons and carbons assignments in $CDCl_3$ solvent of the new compound 14-hydroxylactarorufin B (**53**) is shown in (Fig. 95).

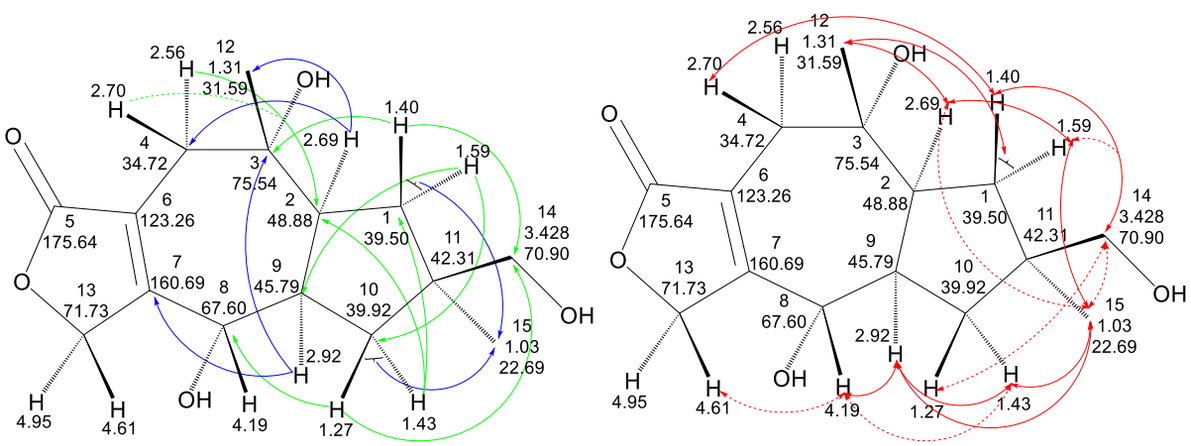

Figure. 95. Relative structure of compound **53** with assignments, ($CDCl_3$). Left: selected HMBC correlations (⟶), HMBC correlations with Karplus relationship (⟶). Right: NOESY correlations (⟷).

The chemical shifts of protons and carbons of 14-hydroxylactarorufin B (**53**) are shown in (Tab. 9).

Table. 9: NMR data for compound 14-hydroxylactarorufin B (**53**) in $CDCl_3$.

position	δ_H (J in Hz)	δ_C
1	α: 1.40 1H (dd appears as t, 11.8, 11.8) β: 1.59 1H (dd, 12.7, 8.4)	39.50
2	2.69 1H (ddd)	48.88
3	-	75.54
4	α: 2.70 1H (ddd) β: 2.56 1H (dd)	34.72
5	-	175.64
6	-	123.26
7	-	160.69
8	4.19 1H (d, 3.9)	67.60
9	2.92 1H (dddd appears as tt, 12.3, 12.3, 4.2, 4.2)	45.79
10	α:1.27 1H (dd) β:1.43 1H (dd, 11.9, 6.8)	39.92
11	-	42.31
12	1.31 3H (s)	31.59
13	α: 4.61 1H (dd appears as d, 17.2) β: 4.95 1H (ddd appears as d, 17.2)	71.73
14	3.428 2H (s)	70.90
15	1.03 3H (s)	22.69

4.3 *Mycena zephirus*

4.3.1 Description of *M. zephirus*

Mycena zephirus, also known as the rusty-spotted helmet mushroom, comes from the family of helmet mushrooms, (Fig. 96). It received its Latin name and thus its taxonomic classification from Paul Kummer in 1871.[100] In contrast to other mushrooms in the genus *Mycena*, *M. zephirus* has hardly been researched. In particular, the secondary metabolites of the mushroom have not been further investigated.

M. zephirus is found mostly in coniferous forests, especially in mountain spruce and pine forests rich in moss. In Europe, this fungus is widespread and can also be found outside Europe, for example on Ulleung Island in South Korea.[101]

Figure. 96. Fruiting bodies of *Mycena zephirus*.[102]

The fruiting bodies appear from September to November, also the mushroom is largely colorless in except for the reddish-brown spots on the top of the cap that give it its name and appear in older mushrooms, (Fig. 96). The surface color ranges from impure white to beige to gray-brown, and after a short time the reddish-brown, rust-colored spots form. As the mushroom ages, the lower half of the stem may also turn rusty brown. The cap is 2-4 cm wide. In younger mushrooms, the cap is bell-shaped. In older mushrooms, the cap is spread out and flat. The stem is 6-8 cm long and has fine scales, their color ranges from beige to gray-brown, and in older fruit bodies a brown-red coloration of the lower half of the stem is often observed. The spores are white in and are 10-13 µm long and 4-5 µm wide.[103] The mushroom is not edible, but its taste and smell are said to be reminiscent of radishes. Bioluminescence has been demonstrated in *M. zephirus*.[104]

The mushroom is largely colorless, making it difficult to study. Many methods for preparing and separating extracts from mushrooms rely on visual indicators, making the study of secondary metabolites difficult. Before secondary metabolites can be identified, a suitable separation method for the extracts must be found. The colorlessness of the mushroom may be one reason why so little research has been done. Dyes are often of great research interest, for example, the blue alkaloids sanguinones A and B alongside the red indoloquinone alkaloid sanguinolentaquinone were isolated from *M. sanguinolenta*.[105] Two red alkaloid pigments mycenarubins A and B had been also isolated from the fruiting bodies of *M. rosea*.[106] Also, the red pigments haematopodin B, mycenarubins D, E and, F were isolated from the fruiting bodies of *M. haematopus*.[107] The orange polyene pigment mycenaaurin A was isolated also from the fruiting bodies of *M. aurantiomarginata*.[108] And also the red compounds pelianthinarubins A and B that were extracted from the fruiting bodies of the mushroom *M. pelianthina*.[109] Moreover, the pigments rosellins A and B were extracted from the mushroom *M. rosella*.[110] Also, the colored compounds mycenaflavins A, B, C, and D were targeted and extracted from the mushroom *M. haematopus* on the based on of indicating interested colored pigments.[111]

4.3.2 Current state of knowledge

M. zephirus was previously targeted biologically through investigations far from any alkaloid targeting studies. For example, this mushroom was investigated among a wide range of other mushrooms to study the diversity of laccase genes in forest soil by LUIS *et al.* in 2004.[112] Also, such biological studies investigated the relevance of conidiogenesis modes in the Agaricales by WALTHER *et al.* in 2005.[113] *M. zephirus* was included in phylogenetic analysis by CHEW *et al.* in 2013.[114] Also, this mushroom was part of a systematic study of the antibacterial activity of basidiomycota reported by CLERICUZIO *et al.* in 2021.[115]

4.3.3 Initial investigations

Due to this mushroom was never investigated for secondary metabolites, and several manual techniques of separations were tested. These include the use of different extraction solvents, liquid-liquid partitioning, preparative thin layer chromatography (TLC), separations through LH20 columns, and finally solid phase extractions (SPE).

The comparison between extractions using MeOH and H_2O solvents shows indecisive results and needs to be further investigated. A similar comparison between the use of MeOH and acetone solvents in the extraction process is described in detail in section 4.3.5. Preparative-TLC was

proved to be futile as well as the use of LH20 columns, especially the colorless nature of most of the components that exist in this mushroom.

In conclusion, the typical SPE method of pre-separations was showed promising results. Although this, the even improved SPE method was developed by the use of more gradient solvents in a second separation of the resulted fractions from the first separation. This method is described in detail in section 6.3.2.1.

4.3.4 Isolated compounds from *M. zephirus*

A large-scale extraction was carried out using MeOH solvent. A detailed description of the large scale MeOH extraction can be found in the experimental section 6.3.1.4.

4.3.4.1 L-γ-glutamine derivative – N^5-isopentylglutamine (**54**)

Compound **54** was isolated using time windows between 18.00 and 18.80 min, section 6.3.4.7 from the H_2O:MeOH (1:1 v/v) fraction from the extended SPE of the methanol fraction of the first SPE carried out to the extract obtained from the methanol extraction process, (Fig. 97). An amount of 0.5 mg was obtained. The HR-ESI-(+)-MS spectrum of compound **54** exhibits an $[M+H]^+$ ion at *m/z* 217.15506. The calculated neutral molecule of $C_{10}H_{20}N_2O_3$ was derived. Subsequently, the degrees of unsaturation (DoU) for this molecular formula are 2.

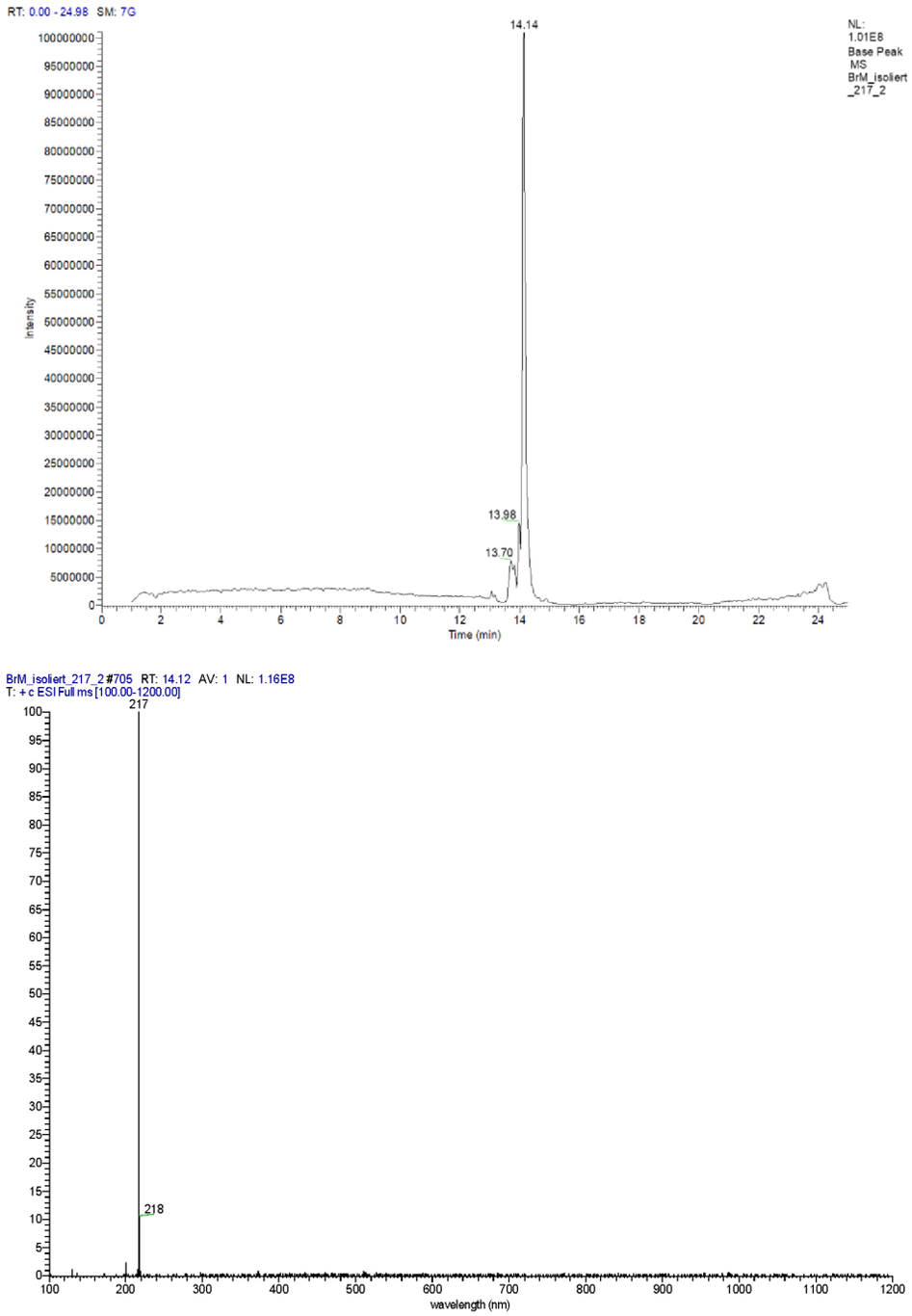

Figure. 97: The isolated compound **54**. Up**:** Base peak chromatogram; HPLC separation with gradient in section 6.3.4.6. Down: Mass spectrum at a retention time of 14.12 min.

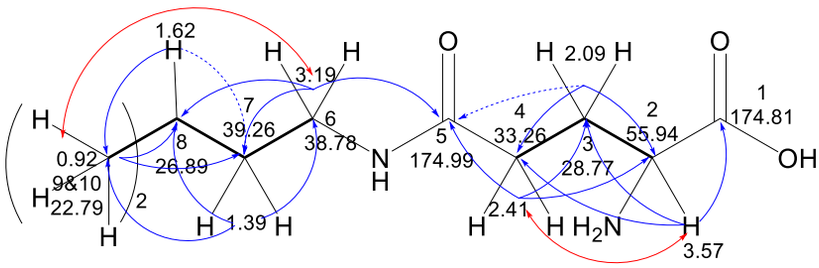

Figure. 98. Proposed structure of compound **54** with assignments, measured in CD_3OD.
With HMBC correlations (⟶), with NOESY correlations (⟷).

The ^1H NMR spectrum of **54**, recorded at 297.2 K in CD_3OD exhibits 16 non-exchangeable protons, see section 9.24. The ^{13}C-NMR spectrum shows 9 carbon signals, and according to the HSQC and DEPT135 data, were assigned to 2 equivalent CH_3 groups, 4 CH_2 groups, 2 CH groups, and 2 quaternary carbon atoms. The two equivalent methyl groups doublet signal at δ_H 0.92, (J= 6.6 Hz), show COSY correlation with the multiplet one proton at δ_H 1.62, which coupled with the triplet of doublets signal of the methylene protons at δ_H 1.39, (J= 7.1, 7.1, 7.6 Hz). The latest two groups of protons couple with the triplet methylene group at δ_H 3.19 which will indicate that it's a doublet of doublet signal, accordingly, the J coupling will be two 7.5 Hz. This will place all of the previously mentioned protons in one coupling spin system. Also, the chemical shift of the later proton at δ_H 3.19 will indicate that a nitrogen atom is attached to it. This will conclude that such a chain of $(CH_3)_2$–CH–CH_2–CH_2–N is in hand. The HMBC correlations will support such conformation. The COSY spectrum will show that a similar second spin system also exists. The triplet signal of the methine proton at δ_H 3.57, (J= 5.8, 5.8), coupled with the triplet of doublet signal of the methylene protons at δ_H 2.09, (J= 6.0, 6.0, 8.5), which itself couples with a doublet of triplet signal of the methylene protons at δ_H 2.41, (J= 1.0, 7.5, 7.5). This will place these protons in one spin system. Also, the chemical shift of the proton at δ_H 3.57 will suggest that such a proton is attached to a hetero atom. This will attach the second nitrogen atom to this proton as the three oxygen atoms in this compound belong to at least two carbonyl groups at δ_C 174.81 and 174.99. The splitting off of formic acid in MS/MS fragments is typical for amino acids, so the third oxygen will be part of a carboxylic acid moiety, (Fig. 100). Also, the Ms/Ms fragments will conclude that a pattern of losing an ammonia moiety which is usually noticed also to amino acids and their derivatives. Accordingly, the later proton is attached to a nitrogen atom similar to the proton at δ_H 3.19, with one of them attached to the NH_2 moiety. Consequently, a chain of CH_2–CH_2–CH–N also exists in this compound.

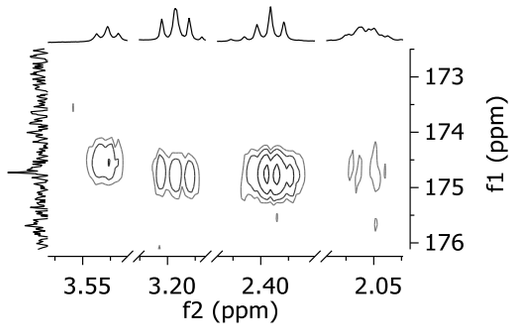

Figure. 99. HMBC concentrated-spectrum of correlations from the extracted compound **54** from *Mycena zephirus*, for protons at δ_H 2.09, 2.41, 3.19 and 3.57 with carbons at δ_C 174.81 and 174.99, (CD_3OD).

Protons at δ_H 3.19 and 2.41 from the two separated spin systems have HMBC correlations with the carbonyl group carbon at δ_C 174.99 making this carbon a linking point between them, (Fig. 99). Proton at δ_H 3.57 has also correlations with the other carbonyl group carbon at δ_C 174.81, (this carbon is located only with this HMBC correlation), then designating the second spin system in this compound to contain the amino acid part. As a result, the proposed structure of compound **54** is shown in (Fig. 98).

4.3.4.1.1 MS/MS considerations

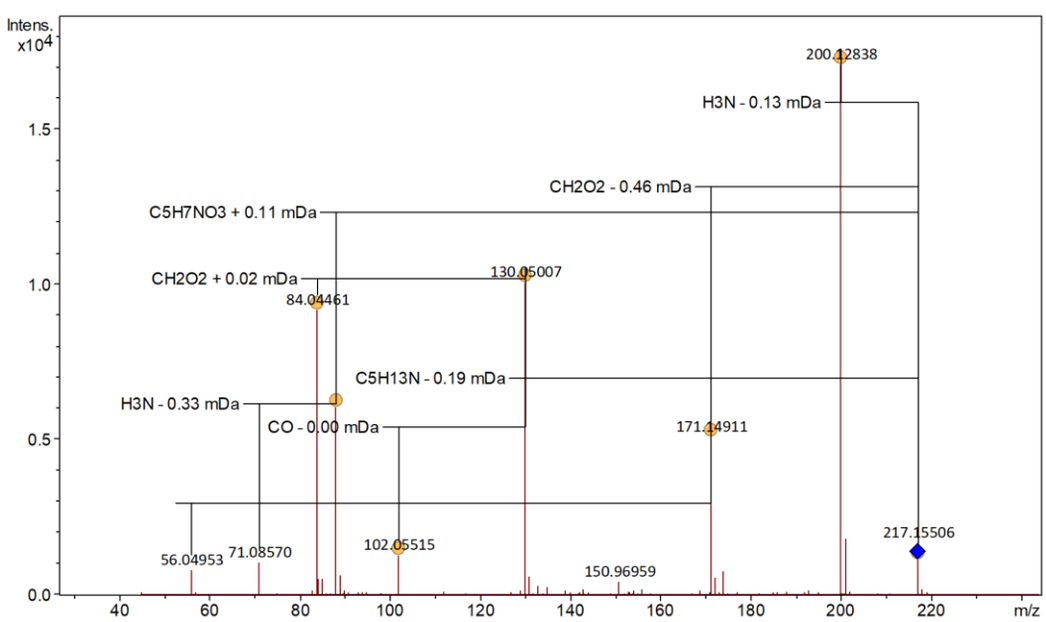

Figure. 100: ESI-MS/MS-spectrum of compound **54**.

The losses of ammonia and formic acid from the molecular ion, which can be observed in the ESI-MS/MS fragment spectrum, (Fig. 100) suggest an amino acid as a structural component. These fragments and others for the molecular ion $[M+H]^+$ were formulated to check the proposed structure.

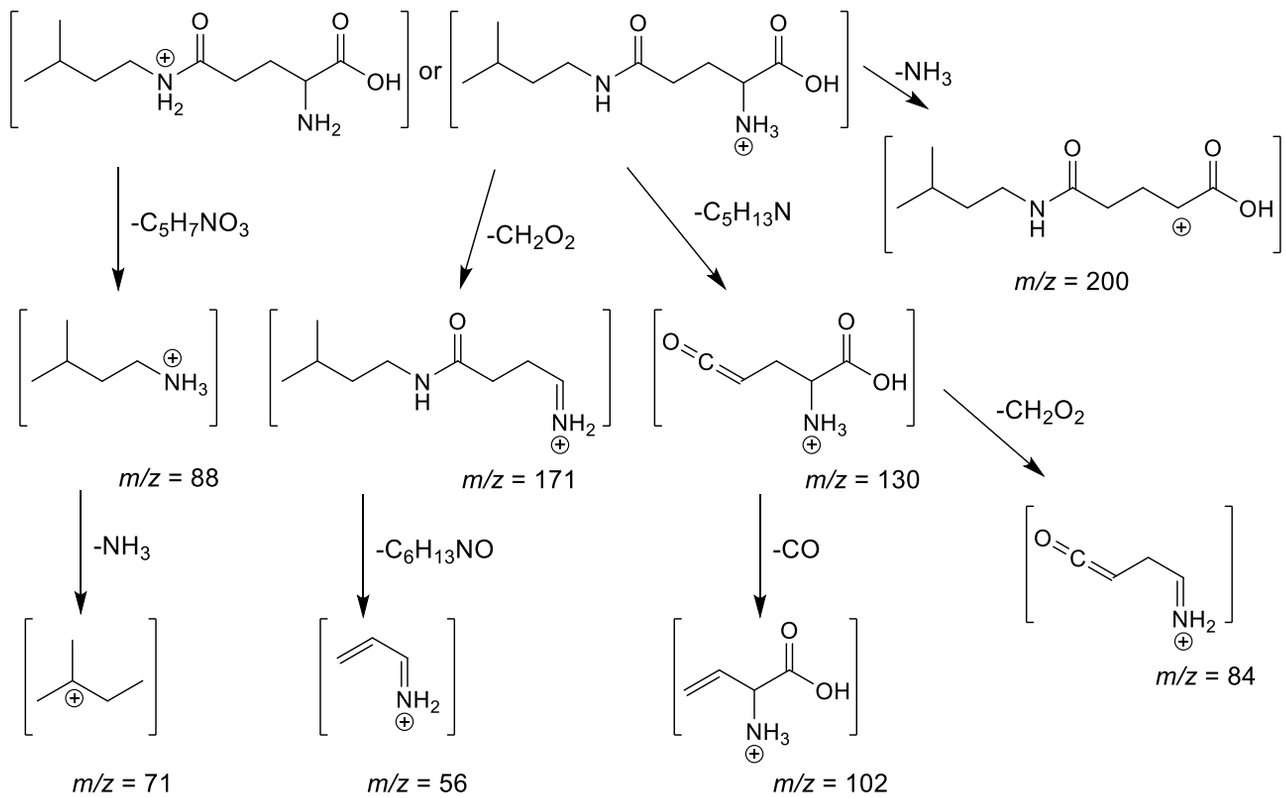

Figure. 101: Fragments for the proposed structure of compound **54**.

For all peaks appearing in the ESI-MS/MS spectrum, fragments that conform to mechanisms could be formulated for the structural proposal, (Fig. 101). The proposed structure could be biosynthetically derived from the *L*-glutamic acid and/or *L*-glutamine, so one can predict the stereo configuration of the amino moiety in compound **54** to be as similar to glutamic acid. Accordingly, the stereo configuration of the stereogenic center at carbon 2 is predicted to be (*S*).

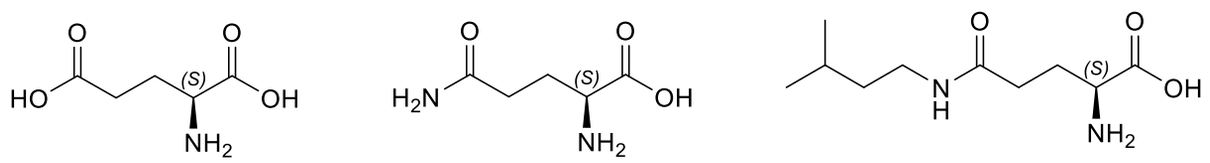

L-glutamic acid | *L*-glutamine | N^5-isopentyl-*L*-glutamine

The proposed structure of the *L*-γ-glutamine derivative compound **54** has not yet been isolated from fungi, nor are there any studies on its biosynthesis, effect, or function in metabolism. However, compound **54** is available commercially under the name of N-(3-Methylbutyl)-L-glutamine, with a relatively expensive price as one gram costs around 5000 US dollars.[116]

4.3.4.2 L-γ-glutamine derivative – N^5-2-methylbutylglutamine (**55**)

Compound **55** was isolated using time windows between 18.80 and 19.50 min from the H_2O:MeOH (1:1 v/v) fraction from the second extended SPE of the methanol fraction of the first SPE carried

out to the methanol extract like compound **54**, (Fig. 102). A total of 0.5 mg was acquired. Compound **55** has a $[M+H]^+$ ion at *m/z* 217.15398 according to its HR-ESI-(+)-MS spectra. The calculated neutral molecule of $C_{10}H_{20}N_2O_3$ was obtained. Therefore, for this chemical formula, the degrees of unsaturation (DoU) are 2.

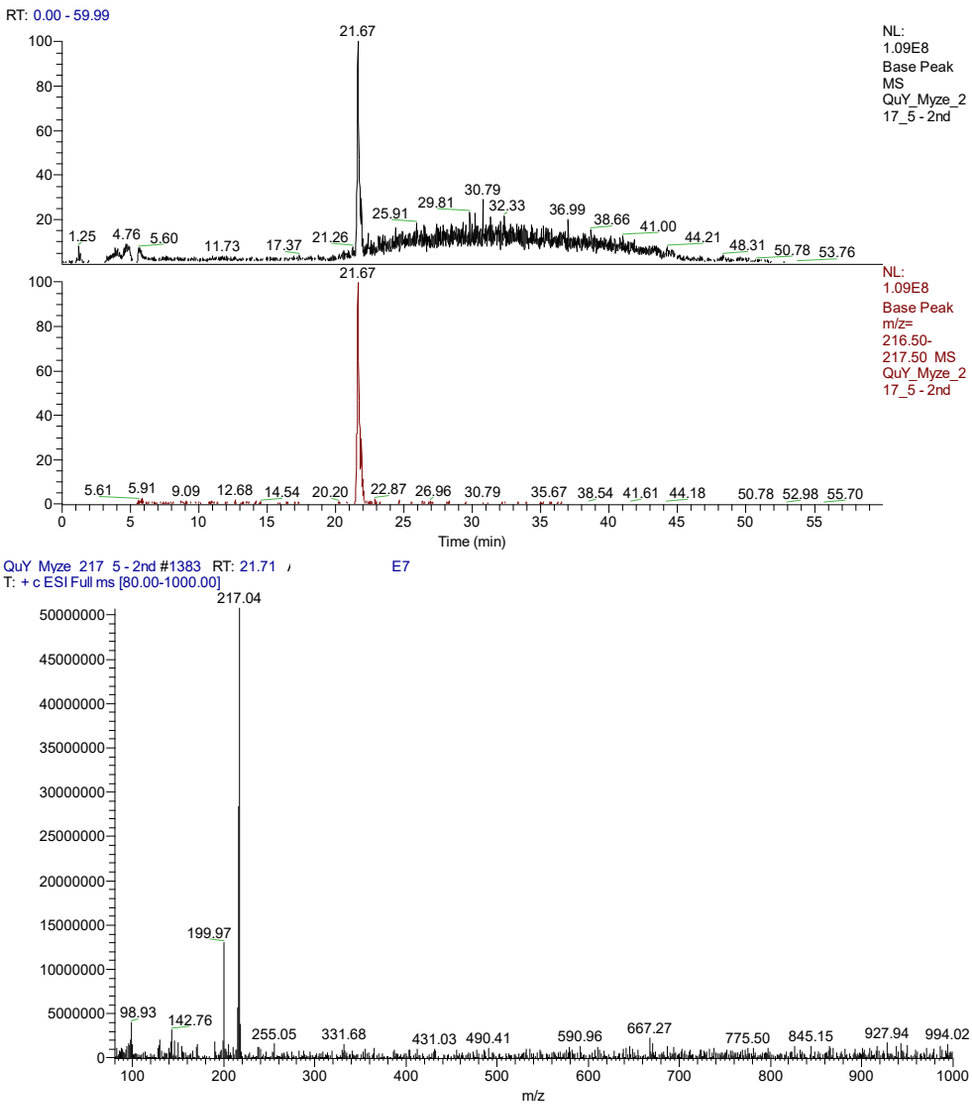

Figure. 102: The isolated compound **55**. Up**:** Base peak chromatogram; HPLC separation with gradient in section 6.3.4.7. Down: Mass spectrum at a retention time of 21.76 min.

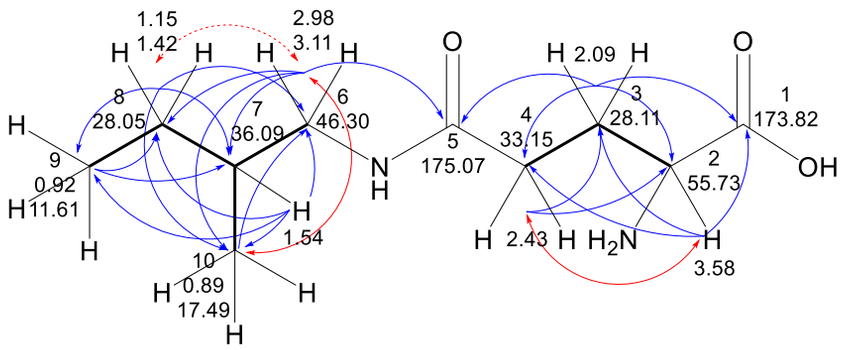

Figure. 103. Proposed structure of compound **55** with assignments, measured in CD_3OD.
With HMBC correlations (⟶), with NOESY correlations (↔).

The ^1H NMR spectrum of **55**, which was recorded at 297.2 K in CD_3OD see section 9.25, exhibits also 16 non-exchangeable protons. The ^{13}C-NMR spectrum shows 10 carbon signals, and according to the HSQC and DEPT135 data, were assigned to 2 CH_3 groups, 4 CH_2 groups, 2 CH groups, and 2 quaternary carbon atoms that according to their chemical shifts belonging to 2 carbonyl groups. The similar retention time of this compound in the preparative-HPLC separation, the same mass, the same molecular formula, and the similar ^1H and ^{13}C chemical shifts with the previous L-γ-glutamine derivative **54** will suggest that these two compounds are related structurally and accordingly, they are constitutional isomers.

The spin-spin splitting patterns of the ^1H-NMR signals of the two methyl groups in this compound will indicate that the difference between the two isomers investigated here is located in the amine half of their structures. As in compound **54** the proton signal of the two equivalent methyl groups split into doublet indicating the presence of isopropyl moiety, while one of the methyl group's proton signal in this compound splits into doublet (δ_H 0.89) and the other methyl group signal splits into triplet (δ_H 0.92). This will locate the later methyl group to exist in the terminal part of a hydrocarbon chain, and consequently, the other methyl group will be a branch in this chain. In COSY data, protons at δ_H 0.92 couple with the methylene protons at δ_H 1.15 and 1.42 that themselves couple with the methine proton at δ_H 1.54. The latter proton couples also with the other methyl group protons at δ_H 0.89 and also with the protons of α-methylene amine moiety at δ_H 2.98 and 3.11. These data alongside HMBC data will conclude the presence of (2-methylbutyl) moiety. The overall correlations will produce the relative structure of compound **55** shown in (Fig. 103).

Following the same approach proceeded for compound **54** of predicting the stereo configuration of the amino moiety in this type of compound, the stereo configuration of the stereogenic center at carbon 2 is predicted to be (*S*), reflecting on the proposed precursor *L*-glutamine.

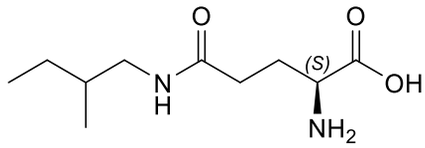

N^5-2-methylbutyl-*L*-glutamine

The proposed structure of the *L*-γ-glutamine derivative compound **55** has been subjected to a study of the involvement of enzymes in the metabolism of transglutaminase-catalyzed protein crosslinks.[117] Moreover, this compound was mentioned to be detected by high-performance liquid chromatography/quadrupole-time-of-flightmass spectrometry through its *m/z* value, characteristic MS/MS fragmentation from commercial flower buds, and the roots of *Hemerocallis citrina*.[118]

4.3.4.3 Compound **56**

Compound **56** was isolated using quarter-minute time windows from 32.00 to 34.75 min from the same extended SPE fraction used in the previous sections. The compound was isolated at 34 .00 min. An amount of 0.5 mg was obtained and some fractions with mixtures were also obtained, (Fig. 104 and 105). The HR-ESI-(+)-MS spectrum of compound **56** exhibits an $[M+H]^+$ ion at *m/z* 602.31078. Three possible molecular formulas were calculated, $C_{37}H_{40}N_5O_3$, $C_{36}H_{44}NO_7$, and $C_{28}H_{48}N_3O_9S$.

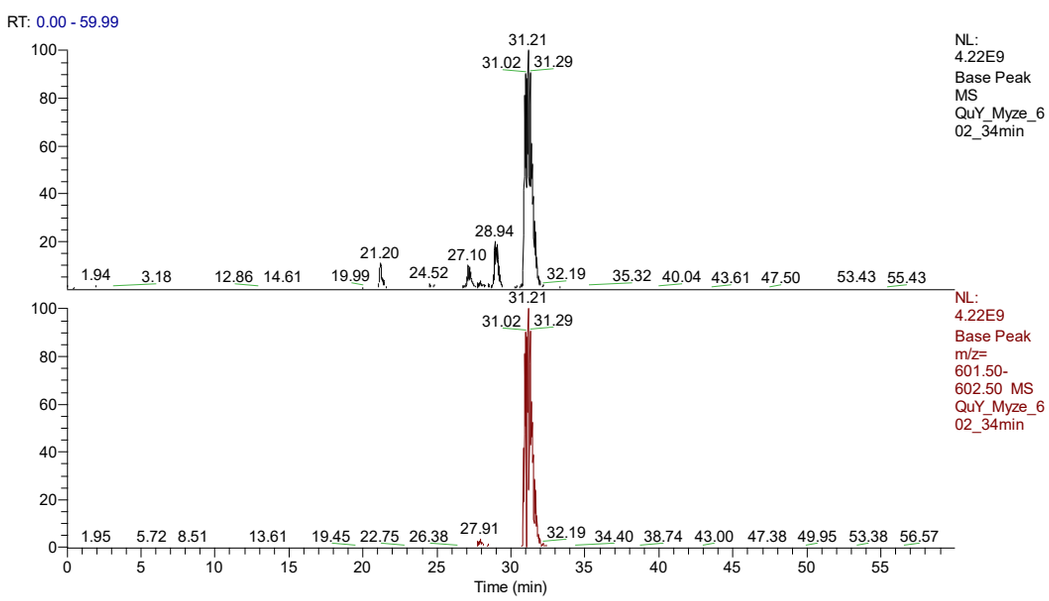

Figure. 104: Base peak chromatogram of the isolated compound **56**.
HPLC separation with gradient in section 6.3.4.7.

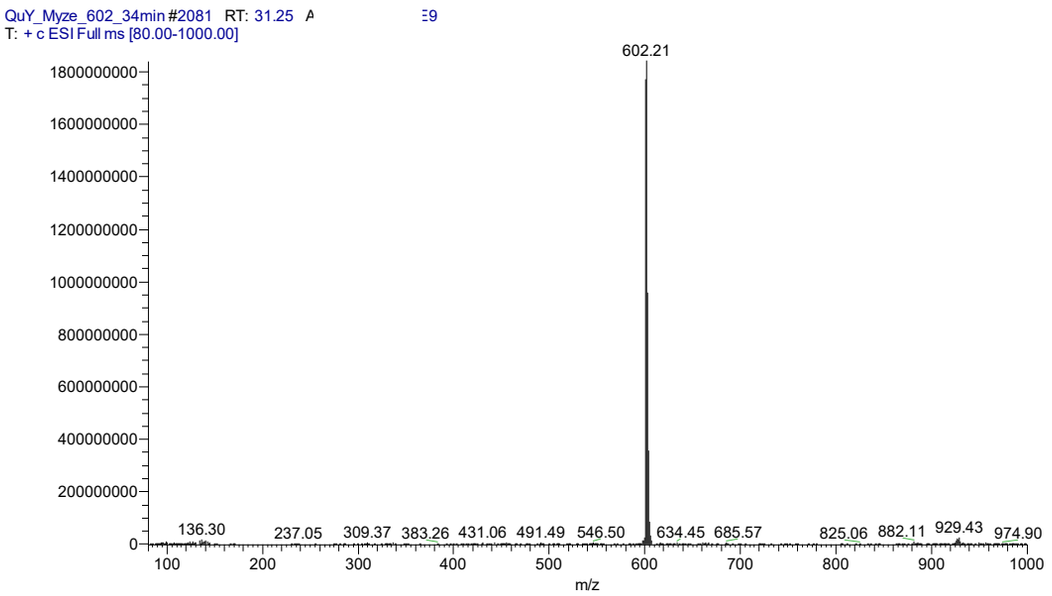

Figure. 105: Mass spectrum of the isolated compound **56** at retention time of 31.21 min.

All of the possible molecular formulas exhibit MS/MS fragments that support their elemental component, see (Fig. 106) and (Tab. 10). This great deal of uncertainty can be referred to the big molecular mass of this compound or the high quantity of impurities. The NMR data exhibits the presence of impurities that prevented the precise assignment of the proton and carbon contents in this compound.

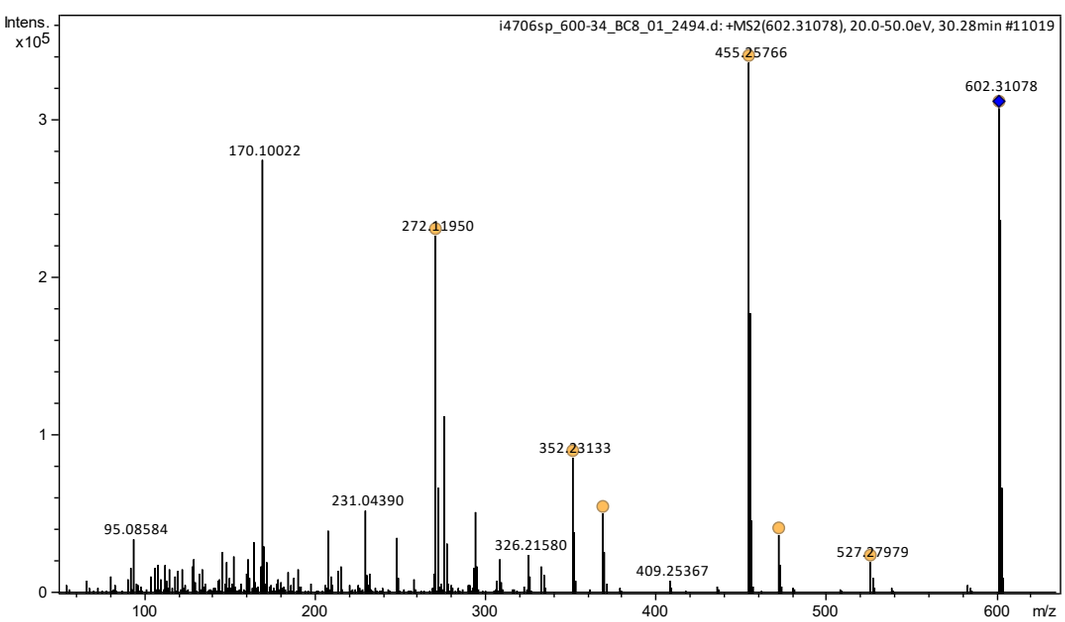

Figure. 106: ESI-MS/MS-spectrum of compound **56**.

The masses and molecular formulas of the fragments are given in (Tab. 10).

Table. 10: Masses and calculated molecular formulas of the fragments of compound **56**.

m/z	Ion Formula
602.31078	$C_{37}H_{40}N_5O_3$ $C_{36}H_{44}NO_7$ $C_{28}H_{48}N_3O_9S$
527.27979	$C_{35}H_{35}N_4O$ $C_{34}H_{39}O_5$ $C_{26}H_{43}N_2O_7S$
473.26858	$C_{32}H_{33}N_4$ $C_{31}H_{37}O_4$
455.25766	$C_{31}H_{35}O_3$ $C_{23}H_{39}N_2O_5S$
352.23133	$C_{16}H_{34}NO_7$ $C_{20}H_{34}NO_2S$
272.11950	$C_{18}H_{14}N_3$ $C_{12}H_{20}N_2O_3S$
170.09984	$C_9H_{16}NS$
95.08562	C_7H_{11}

4.3.4.4 Compound **57**

Compound **57** was isolated at 33.00 min alongside **56**, using the quarter-minute time windows. Although the small peak of this compound in the crud extract mass chromatogram, but the mass of the compound is same as the more prominent compound **57** (0.5 mg). The compound shows great deal of degradation when measured in high resolution LC-MS. The HR-ESI-(+)-MS spectrum of compound **57** exhibits $[M+H]^+$ ion at *m/z* 600.29487 with two possible molecular mass are calculated, 600.29746 for $[C_{37}H_{38}N_5O_3]^+$ and 600.29613 for $[C_{36}H_{42}NO_7]^+$. The two derived molecular formulas are similar to the first two derived molecular formulas of compound **57** indicating a possible relation to it.

The NMR data for compound **57** show the dominant presence of aliphatic protons as well as of protons attached to heteroatom, see section 6.5.3.3. Also, at least one carbonyl group and two aromatic carbons exist in this compound.

4.3.4.5 Oily green mixture

To precipitate protein residues and remove them a specific process was performed which contains a centrifugation step. An aqueous phase and a green non-polar phase were resulted, (Fig. 107-Left). Subsequently, the green (oily look-alike) phase was investigated. The green organic phase was to be separated and examined separately.

To remove polar substances that were transferred when the organic green phase was collected, water and a non-polar solvent were used as solvents in the liquid/liquid partitioning procedure. The H_2O/Hexane combination was applied, (Fig. 107-Right). Consequently, the green viscous liquid was dissolved in hexane and transferred to a separating funnel together with H_2O to perform the partitioning. The organic phase was collected and after further washing, the solvents were removed under reduced pressure.

Figure. 107: Left: Separated green phase from the crude extract. Right: H_2O and hexane liquid/liquid partitioning.

Then, size exclusion chromatography was carried out on the hexane extract to achieve further separation. A green band was collected. The green viscous liquid obtained from the hexane phase was afforded 2.49 ± 0.01 g from approximately 500 g of extracted mushroom.

Oils are generally liquids that do not mix with water and have a higher viscosity. This is the case here. Oily fats are mixtures of fatty acid triglycerides that are liquid at room temperature.[119] Since volatile oils were extracted and identified before from the edible mushrooms *Pleurotus ostreatus*, *Pleurotus eryngii*, and *Pleurotus abalones* via GC/MS among other techniques,[120] this made it suspected that such a mixture of compounds contains variant types of natural oils. Also, recently a study on the production, composition, and potential applications of mushroom oils was conducted.[121] Accordingly, it should be checked whether it is an oily fatty acid derivative to characterize it. To make an initial comparison with known vegetable oils, an IR spectrum was recorded for the green layer, as well as for sunflower oil and olive oil from Spain and Greece. Since triglycerides consist of three fatty acids esterified with glycerol, characteristic absorption maxima are to be expected in the range of 3000 to 2800 cm^{-1} caused by C–H stretching vibrations of alkanes and in the range of 1750 to 1735 cm^{-1} caused by C=O stretching vibrations of carbonyls.[122]

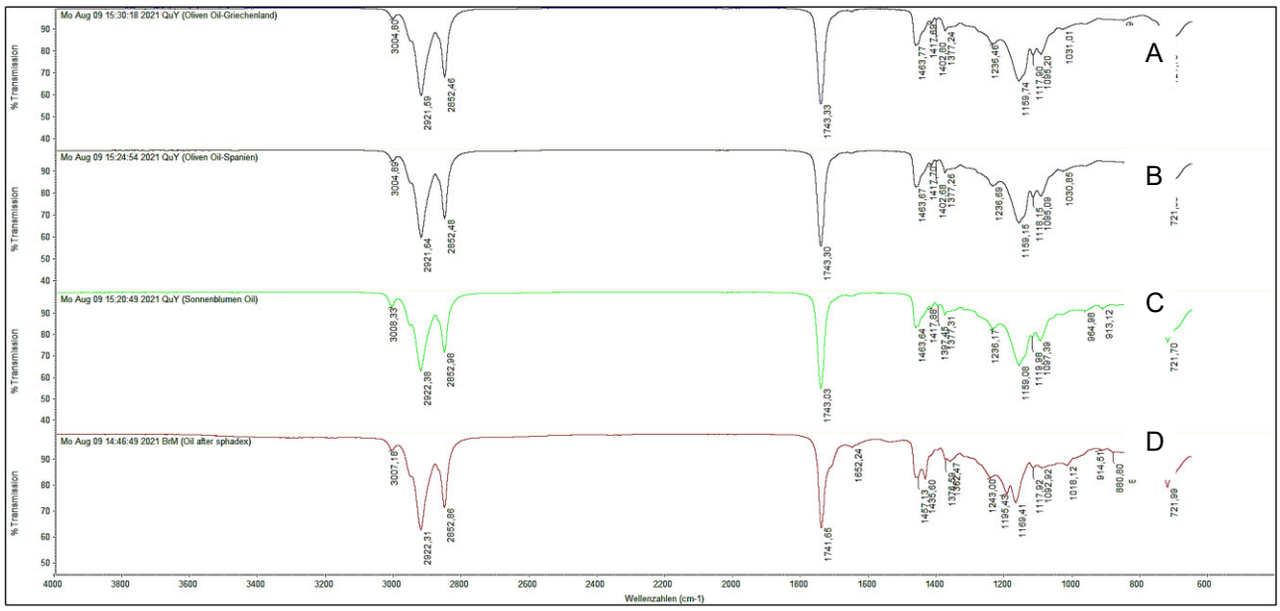

Figure. 108: IR spectra of olive oil Greece (A), Spain (B), sunflower oil (C) and the green layer (D); on the x-axis the wave number [cm^{-1}] is shown in steps from 800 to 4000.

Table. 11: Wavenumbers and assignments in the IR spectrum of the green layer.

Wavenumber [cm^{-1}]	Assignment
3007, 2922, 2852	C–H stretch - alkanes =C–H stretch - alkenes
1742	C=O stretch - carbonyls
1370	C–H rock - alkanes
1457, 1436	C–H bend - alkanes
1243, 1195, 1169, 1118, 1093	C–O stretch

It turns out that the peaks expected for fatty acids derivatives can be found not only in the vegetable oils considered here but also in the viscous liquid from *Mycena zephirus*. In a general comparison between the IR spectra, only very slight differences can be seen. Removed compounds can be expected from the purification steps for the viscous green liquid, but these differences are not visible in the recorded IR spectra. The IR spectra of the sunflower oil, the olive oil, and the green liquid from the mushroom differ only minimally in the characteristic peaks, this is probably due to the different triglycerides that occur in the oils. The similarity between the IR spectra of the green viscous liquid and the vegetable oils is an indication that this is also an oily fat, i.e. a mixture of triglycerides or related esters. An attempt to separate the green mixture was performed using HPLC but with ineffective results. However, one fraction exhibits less mixture than others and the recorded ^{1}H-NMR spectra could support that this is an esterified fatty acid, (Fig. 109).

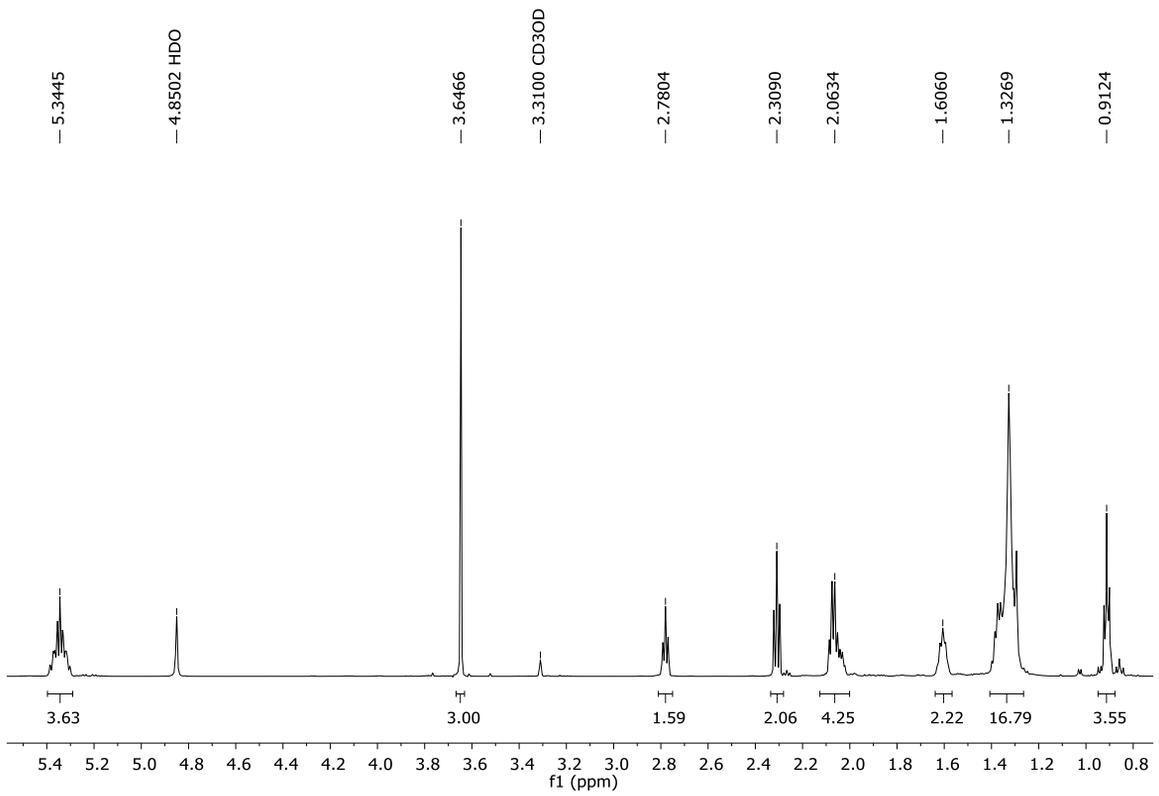

Figure. 109. ^{1}H-NMR spectrum of a fraction extracted with preparative-HPLC of the green layer, (600.50 MHz, CD_3OD, 297.1 K).

GC-MS measurement was performed for further investigation of the green layer, (Fig. 110).

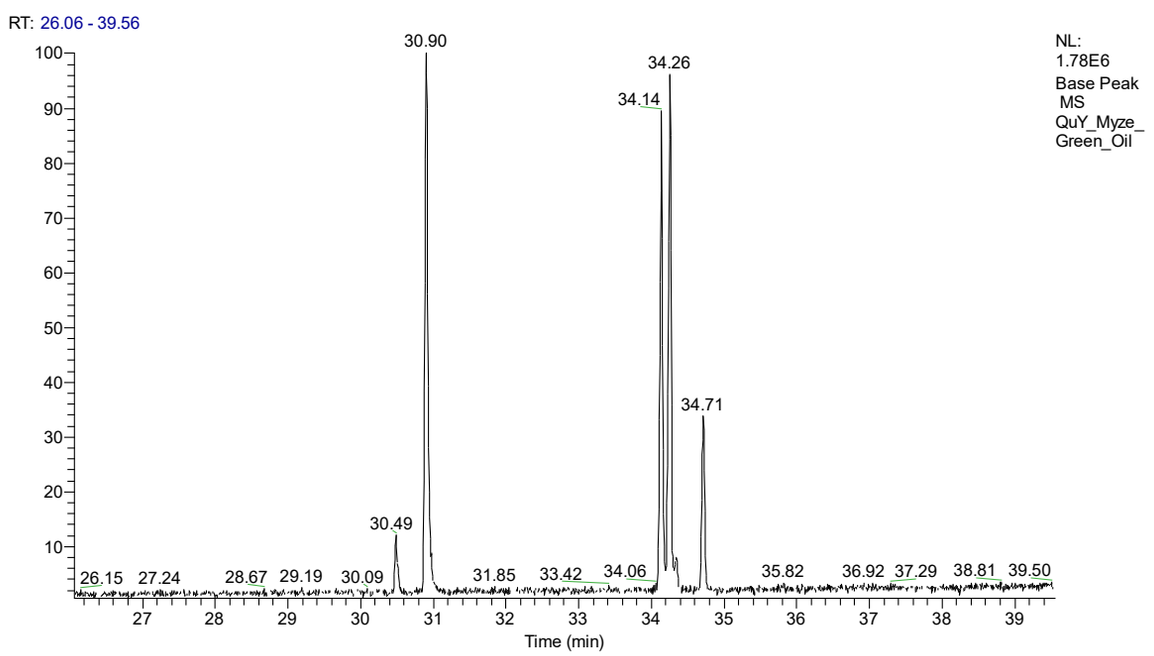

Figure. 110. GC-MS concentrated spectrum of the green layer fraction separated from *M. zephirus*. Gradient at section 6.3.4.8.

The proposed compounds in (Tab. 12) were concluded by the Xcalibur software according to the MS/MS fragments patterns compared to the ones in the software library.

Table. 12. Proposed masses and structures for compounds separated in the GC-MS measurement for the mixture of the green layer.

Peak (retention time)	Proposed structure(s)	Exact Mass (*u*)
30.48 min	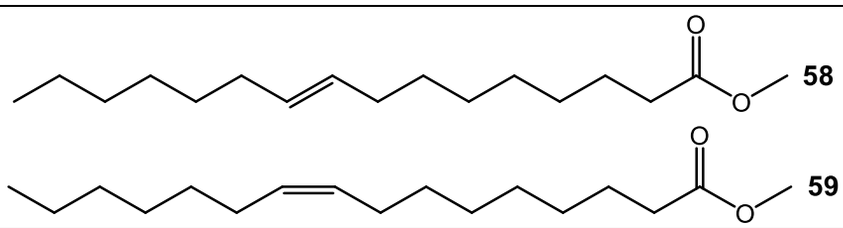 **58** **59**	268.24
30.91 min	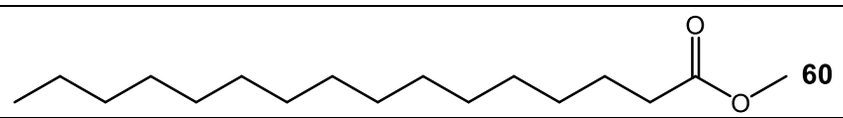 **60**	270.26
34.14 min	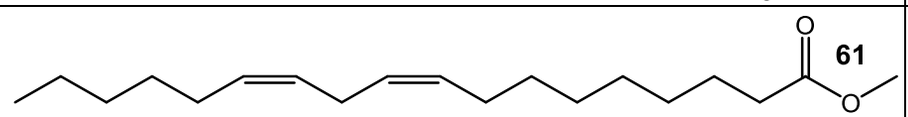 **61**	294.26
34.26 min	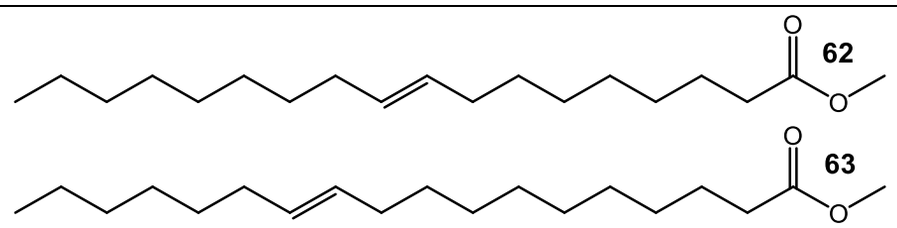 **62** **63**	296.27
34.30 min	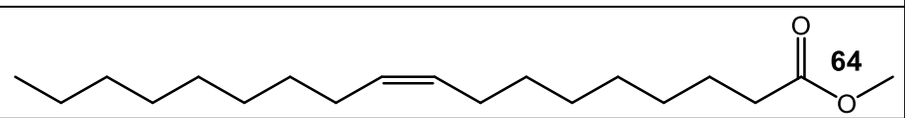 **64**	296.27
34.71 min	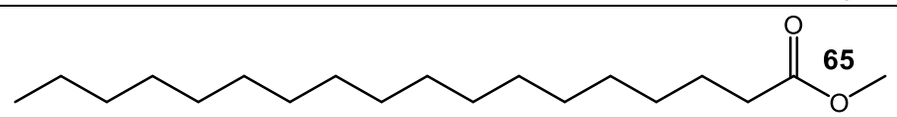 **65**	298.29

The names of the proposed compounds for peaks with retention times 30.48, 30.91, 34.14, 34.26, 34.30, and 34.71 min, are; Methyl palmitoleate (*E*) (**58**), Methyl palmitoleate (*Z*) (**59**), methyl palmitate (**60**), methyl (9*Z*,12*Z*)-octadeca-9,12-dienoate (**61**), methyl (*E*)-octadec-9-enoate (**62**), methyl (*E*)-octadec-11-enoate (**63**), methyl oleate (**64**), and methyl stearate (**65**) respectively. Such compounds come near the fatty acid that was recently reported to exist in other mushroom species.[121]

Moreover, these ester derivatives are already mentioned to exist in wild and edible mushrooms alongside corresponding fatty acids.[123]

4.3.6 Decomposition experiments

Using MeOH solvent in extraction and separation steps could interfere with the existing compounds in some mushrooms as the solvent could lead to the decomposition of various substances in the mushroom. Therefore, decomposition tests were performed using two extracts using acetone solvent with one and methanol solvent with the other one. Samples to be tested were taken directly after extraction, then after 11 days and 58 days. The period used was due to the restricted access to the laboratories. The samples were measured on the high-resolution ESI-MS/MS device and the chromatograms of the various samples were compared. When evaluating, it should be noted that the samples were not taken at exact concentrations. Differences in signal intensities can therefore occur due to concentration differences. The extracts were stored at around –8 °C. The chromatograms obtained are shown in figures (111) and (112).

At first glance at the initial chromatograms of the extracts of the two solvents used here, acetone and methanol, it becomes clear that both solvents can be used in the extraction method with preferences for methanol solvent as it shows more extracted compounds as expected from such a protic solvent, especially compounds **56** and **57** at 12.6 min.

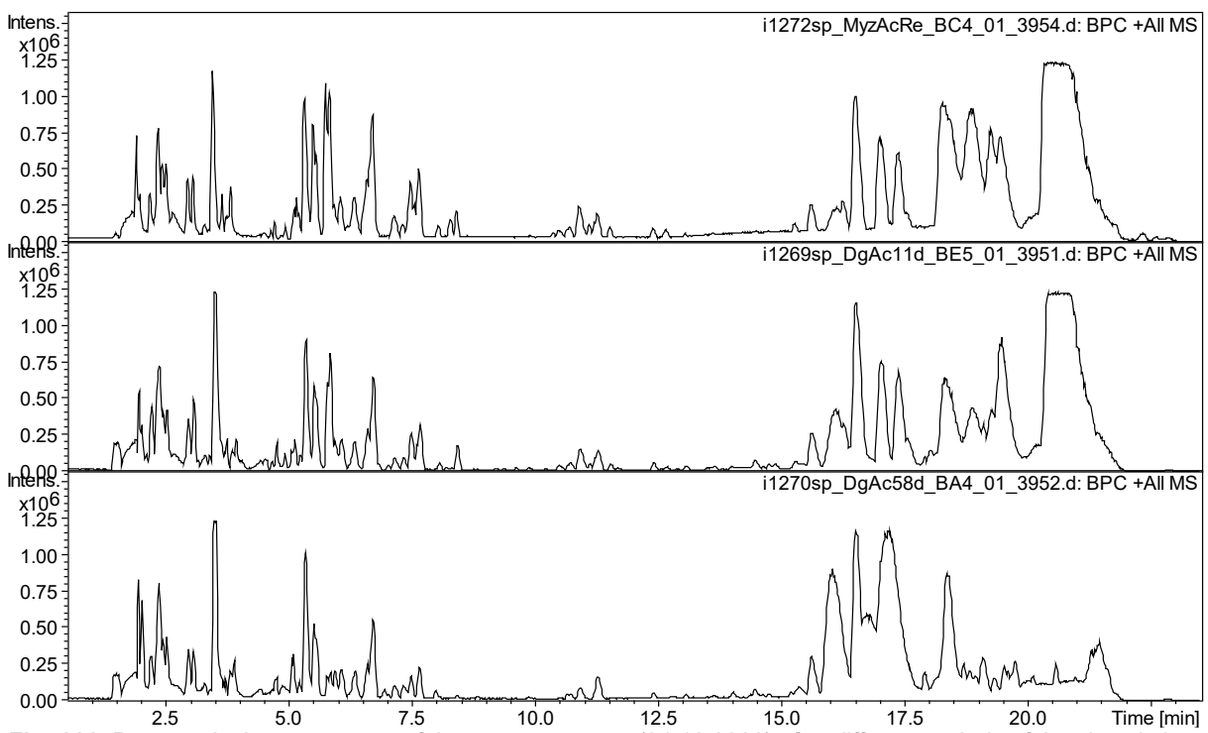

Fig. 111: Base peak chromatograms of the acetone extract (04.12.2020) after different periods of time in solution; directly dried extract (top), after 11 d (middle), after 58 d (bottom) of *M. zephirus*; HPLC-MS separation using gradient F1.

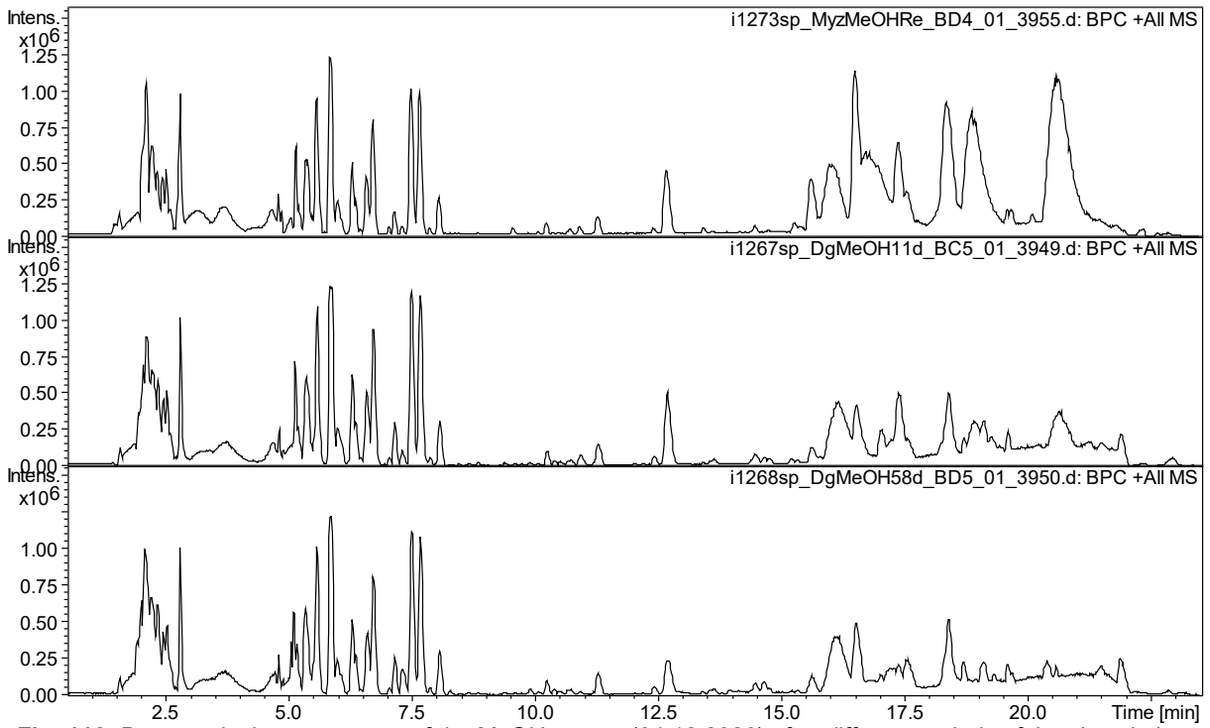

Fig. 112: Base peak chromatograms of the MeOH extract (04.12.2020) after different periods of time in solution; directly dried extract (top), after 11 d (middle), after 58 d (bottom) of *M. zephirus*; HPLC-MS separation using gradient F1.

When comparing the chromatograms, it is clear that degeneration has occurred in the non-polar areas of both solvents. The remaining signals show a slight difference over the entire period. In addition, the same masses are decomposed in both extracts. Most substances are therefore stable in acetone and methanol solvents over a longer period. Both solvents can therefore be used for further experiments with preferences of using methanol solvent.

5 Outlook

In order to evaluate the bioactivity of the so far undescribed sesquiterpenoids of *L. circellatus in more detail*, larger quantities of these secondary metabolites are required. Therefore, at least one kilogram of this mushroom should be extracted and the compounds isolated by the improved method, described in this thesis. Moreover, the extract should be investigated again for the presence of so far unidentified secondary metabolites.

The pink compound that was found in tiny amounts in *L. blennius* and that might be closely related to the known compound lilacinone (**37**) from *L. lilacinus* should be isolated in larger quantities and the isolation procedure should be optimized. Then, a full set of NMR data should be recorded to be able to elucidate its structure. Luckily, *L. blennius* is relatively widespread in Germany. Therefore, it should be no problem to upscale the extraction to several kilograms of fruiting bodies.

To elucidate the structures of the pigments isolated from *L. trivialis*, they should be reisolated according to the procedure described in this thesis. Then, a full set of NMR spectra of the trivialines B (**48**), C (**49**), D (**50**), and E (**51**) should be recorded and their structures should be elucidated. Moreover, by analysis of the data for trivialine A (**47**), the proposed tentative structure for this compound should be confirmed or revised. In addition, more biological tests should be performed with the pigments.

So far, the stereochemistry of the isolated glutamic acid derivatives **54** and **55** is unknown. To determine its stereochemistry, the compounds should be hydrolyzed and the resulting glutamic should be separated by HPLC on a suitable chiral HPLC column and the retention time compared to those of authentic samples of L-glutamic acid and D-glutamic acid. Similarly, the stereochemistry of the 2-methylbutylamine residue obtained by hydrolysis of compound **55** should be determined to fully assign the configuration of the stereocenters in compound **55**.

6 Experimental part

6.1 Chemicals

Acetonitrile: CHEMSOLUTE®, gradient grade for the LC-MS, Th. Geyer GmbH & Co. KG, Renningen

Acetic acid: ROTIPURAN® 100% p.a., Carl Roth GmbH & Co, Karlsruhe

Deionized Water: In-house treatment plant

Methanol: HiPerSolv CHROMANORM®, gradient grade for the LC-MS, VWR Chemicals, Darmstadt

Acetone: >=99.8%, Analytical reagent grade, Fisher Chemical, Loughborough

6.2 Devices

FTIR:

FTIR-Spectrometer, Nicolet iS10, Thermo Scientific. Software: OMNIC 9.6, OMNIC 9.6

NMR:

Avance NEO 600 with Prodigy TCI Probe head, Bruker

CD_3OD: Calibration for ^{1}H-NMR-Spectra δ = 3.31 ppm and for ^{13}C-NMR-Spectra δ = 49.00 ppm)

DMSO-d_6: Calibration for ^{1}H-NMR-Spectra δ = 2.50 ppm and for ^{13}C-NMR-Spectra δ = 39.52 ppm)

$CDCl_3$: Calibration for ^{1}H-NMR-Spectra δ = 7.26 ppm and for ^{13}C-NMR-Spectra δ = 77.16 ppm)

LC-MS-1:

Pump: Quaternary Pump, 1100 series G1311A, Hewlett Packard

UV-Detector: 1100 series G1314A, Hewlett Packard

Autosampler: 1100 series G1313A, Hewlett Packard

MS-Detector: Esquire-LC, Bruker

LC-MS-2:

Pump: Binary Pump, 1100 series G1312A, Hewlett Packard

UV-Detector: DAD, Hewlett Packard

Autosampler: 1100 series G1313A, Hewlett Packard

MS-Detector: LCQ Deca XP Plus, Thermo Finnigan

HR-LC-MS:

LC-Pump: Dionex Ultimate 3400 RS Pump, Thermo Scientific

UV-Detector: Dionex Ultimate 3000 RS Diode Array Detektor, Thermo Scientific

Autosampler: Dionex Ultimate 3000 RS Autosampler, Thermo Scientific

Column Oven: Dionex Ultimate 3000 RS Column Compartment

MS-Detector: Impact II, Bruker

Semipreparative HPLC:

Pump: 510 HPLC Pump, Waters

UV/Vis-Detector 1: 996 Photodiode Array Detector, Waters

UV/Vis-Detector 2: Variable Wavelength Monitor, Knauer

Analytical Balance:

SARTORIUS (1615 MP), Sartorius Lab Instruments GmbH & Co. KG (d = 0.0001 g)

Solid Phase Extraction (SPE)

CHROMABOND® C18ec 3 mL / 500 mg Cartridge, Macherey-Nagel

CHROMABOND® C18ec 15 mL / 2000 mg Cartridge, Macherey-Nagel

CHROMABOND® C18ec 45 mL / 5000 mg Cartridge, Macherey-Nagel

Columns:

Semipreparative: VP 250/10 Nucleodur 100-5 C18ec, Macherey-Nagel

Analytical: EC 250/3 Nucleodur 100-5 C18ec, Macherey-Nagel

Polarimeter:

243 Polarimeter, Perkin-Elmer

CD-Spectrometer:

Chirascan plus, Applied Photophysics

GC-MS

A mass spectrometer with a single quadrupole detector with an EI ion source Finnigan TraceDSQ from the company: THERMO FINNIGAN was used, to which a gas chromatograph Finnigan TraceGC ultra with an AS3000 autosampler with PTV injector was connected. Helium was used as the carrier gas.

Column: Optima® 5 ms Accent (15 m x 0.25 mm ID, 0.25 µm Schichtdicke) Optima® 5 Accent (30 m x 0.25 mm ID, 0.25 µm layer thickness)

Centrifugation

Two different centrifuges were used, namely a HERAEUS SEPATECH Biofuge 15 for Eppendorf cups and a coolable HETTICH Universal 16R centrifuge for larger quantities and protein precipitations (Falcon tubes 15 and 50 ml).

Freeze drying

Two lyophyllisers model Christ alpha 1-2 and Christ alpha 1-4 from JÜRGENS (HERAEUS) were used for freeze-drying aqueous samples. Rotary vane pumps, Pfeiffer

Autoclave

IBS INTEGRA BIOSCIENCES (Italy), Fedegari Autoclave type

Incubator

Heraeus B5060 EK/CO2 gassing incubator (25.6°C). Heraeus Instruments B6060 (30°C). Hereaus Instruments (38°C), Thermo SCIENTIFIC.

Sterile bench

TC 72 cleanroom workbench, GELAIRE FLOW LABORATORIES

A Fireboy Eco Bunsen burner, INTEGRA BIOSCIENCES

Device Software:

Qtof-Control 4.1

Data Analysis 3.0

Data Analysis 4.4

Thermo Xcalibur 2.0.7 SP2.48

MestReNova 11.0.4-18998

TopSpin 4.1.3

Millenium Chromatography Manager Software Version 2.10

6.3 Isolation methods

6.3.1 Extraction methods

6.3.1.1 Extraction method A

From the still frozen solid fruiting bodies of *L. trivialis* (1.0 kg), the cap skin was peeled off using a sharp blade, pictures 1 and 2.

1

2

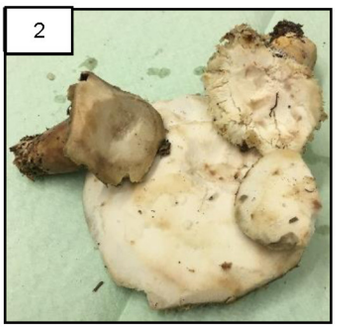

The peeled skin was crushed with mortar and pestle and then placed in a 2.5 L Erlenmeyer flask, with magnet ship for stirring and one Liter of acetone was added, and then covered with Aluminum foil, pictures 3 and 4.

3

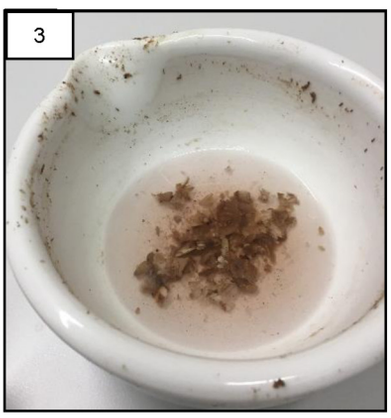

4

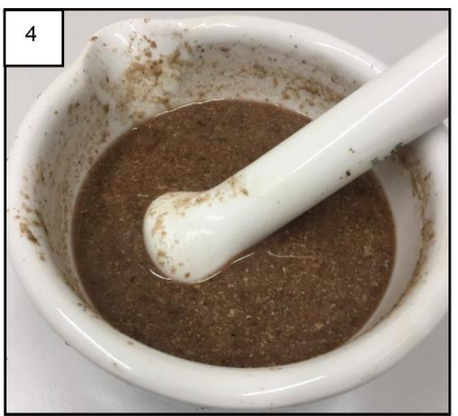

Afterward, the crushed skin was allowed to be extracted for two hours with continuous stirring under room temperature, pictures 5 and 6.

The extract was filtered using glass wool into a 2.5 L round bottom flask and the acetone solvent was evaporated to leave a non-homogeneous water mixture. This process will be repeated two times.

5

6

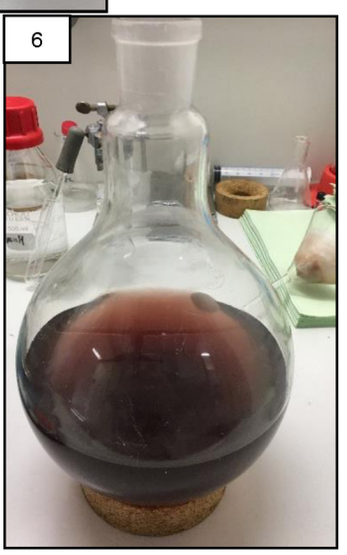

Then, the non-homogeneous water remains, will be partitioned with diethyl ether to remove the polar compounds that dissolved in water, pictures 7 and 8. No further partitioning proceeded as the sensitive nature of the targeted compounds in this mushroom prevented any unnecessary risks of exposure to the surrounding elements.

7

8

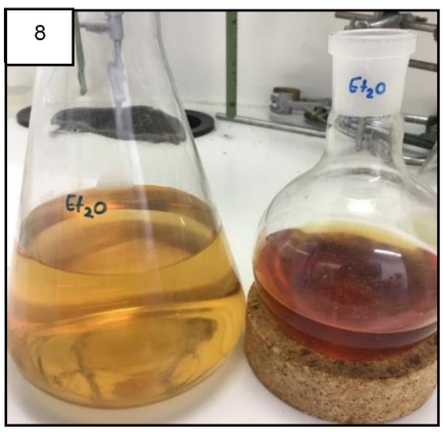

Then, the combined mixture was filtered using C18ec cartridge – SPE – see section 6.3.2, starting with H_2O to 1:1 H_2O-acetone then to acetone, to remove the water fraction and to separate the dark red-brown layer that elutes through the 45 mL cartridge using acetone gradient.

9

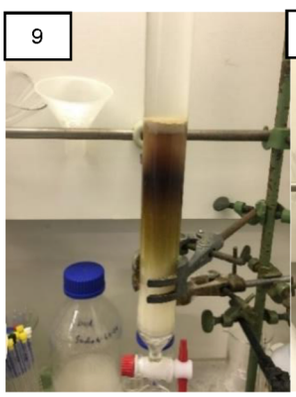

10

11

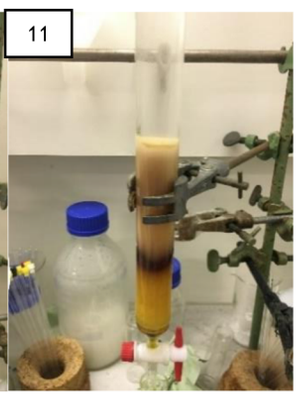

12

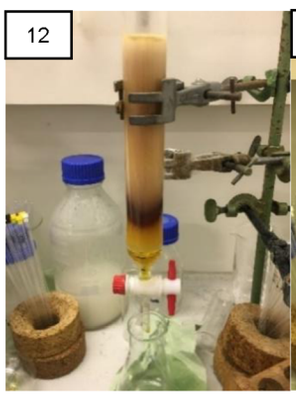

13

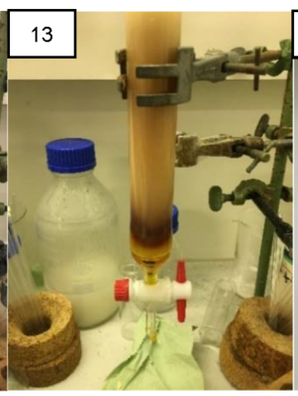

14

This fraction was run into the acetone LH20 column, see section 6.3.3-D, at the rate of three drops per minute for 18 hours to reach the reddish fraction, and within four more hours, this targeted

fraction was finally separated to be introduced for further separations and purifications, pictures 9-14. Then the targeted fraction (picture 14), will be submitted to solid phase extraction using a gradient of water and acetone see section 6.3.2, for one more step of filtration and separation. The water fraction was discarded. The water:acetone solvents gradient afforded fraction with pink color (1:1), picture 15. Using the acetone solvent afforded two fractions, the first one with brown color (A1) and the second one with violet color (A2), pictures 16 and 17 respectively.

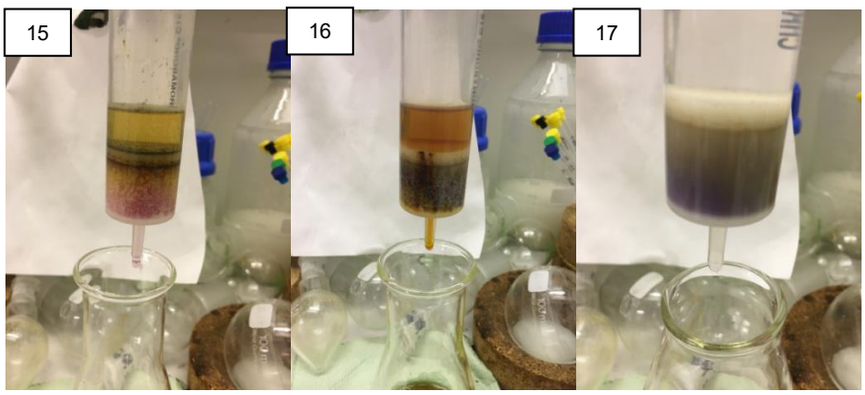

Then apply the previous SPE fractions to the semi-preparative HPLC using gradient C, see section 6.3.4.3. The resulting fractions were allowed to be set in a freezer (–30°) overnight to freeze the water part in a solvent mixture to separate any polar content of the fraction.

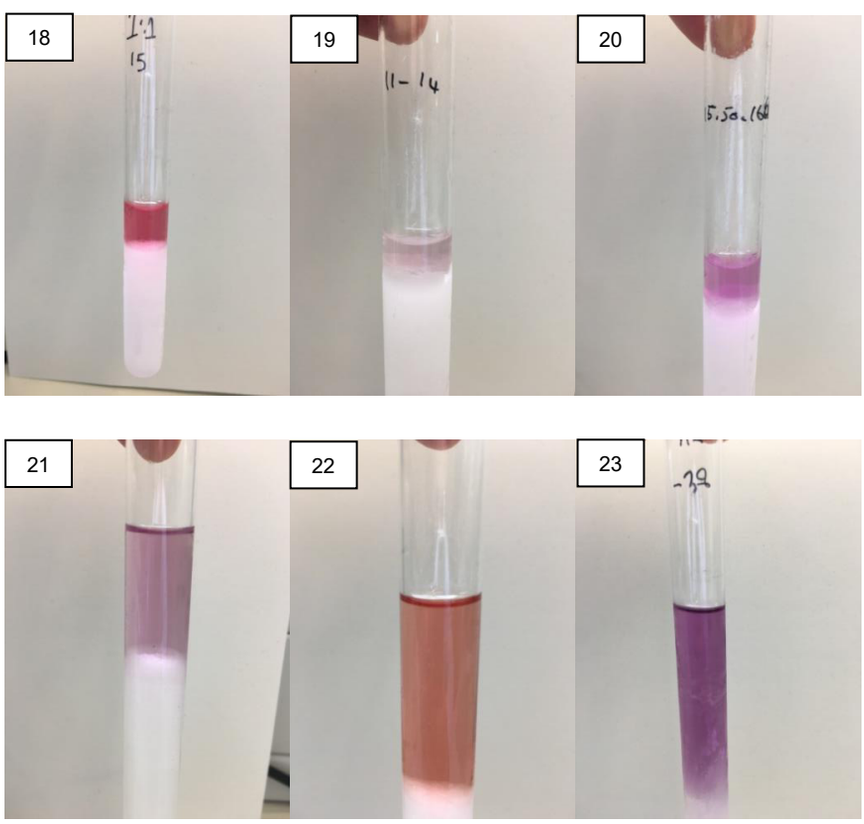

The (1:1) SPE fraction produces only one pink fraction at 15 minutes with 550 nm as the detecting wavelength, picture 18. This fraction is a mixture of compounds, possibly the halves of the dimeric designated compounds **47**-**51**.

The (A1) SPE fraction produces three fractions with a violet color and one peach color when using 550 nm as detecting wavelength at 11.00, 15.50, 21.00, and 32.00 minutes, pictures 19-22 respectively. The fraction with R_t at 32.00 min is compound **50**.

When using 440 nm as the detecting wavelength one fraction with peach color and four fractions with yellow variants colors separated at 27.00, 29.00, 34.00, 47.00, and 50.00 minutes, pictures 24-28 respectively. The fraction with R_t at 29.00 min is compound **51**. The fraction with R_t at 34.00 min is compound **49**. The fraction with R_t at 47.00 min contains compound **47** with the most abundant quantity.

The fractions with R_t at 11.00, 15.50, 21.00, 27.00, and 50.00 need further investigations to identify the main compounds in them.

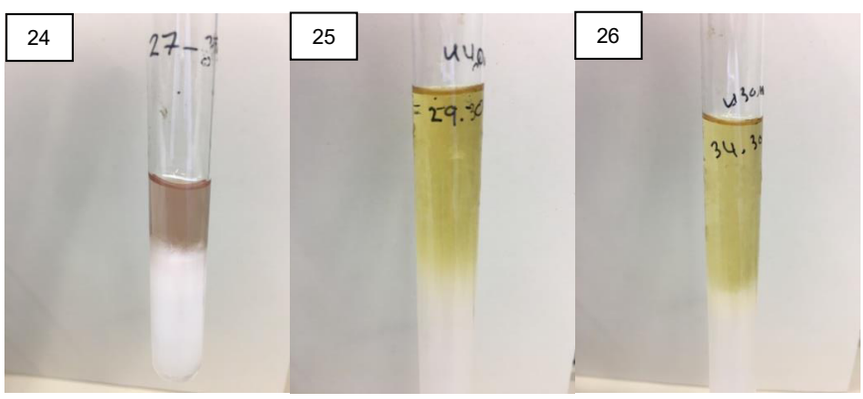

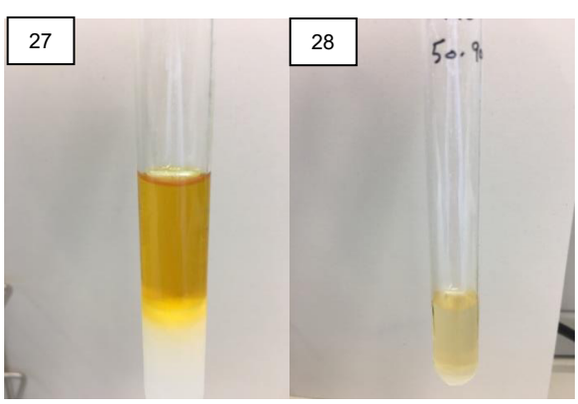

The (A2) SPE fraction produced only one violet fraction at 37.30 minutes with using 550 nm as the detecting wavelength, picture 23. This is compound **48**.

6.3.1.2 Extraction method B

As described previously, see section 6.3.1.1, from the still frozen solid fruiting bodies of *L. circellatus* (1.5 kg), the cap skin was peeled off using a sharp blade. The peeled skin was crushed with mortar and pestle and then placed in a 2.5 L Erlenmeyer flask, with magnet ship for stirring and one Liter of MeOH was added, and then covered with Aluminum foil. Afterward, the crushed skin was allowed to be extracted for two hours with continuous stirring under heating of 60°. The extract was filtered using glass wool into a 2.5 L round bottom flask and the MeOH solvent was evaporated to leave a non-homogeneous water mixture. This process will be repeated two times. Then, the combined mixture was filtered using C18ec cartridge – SPE – see section 6.3.2, starting with H_2O to 1:1 H_2O-MeOH then to MeOH, to remove the water fraction and to separate the green layer that elutes through the 45 mL cartridge using MeOH gradient. This green fraction was run into the MeOH LH20 column, see section 6.3.3-B, at the rate of three drops per minute for six hours to afford the green compound blennione (**35**).

6.3.1.3 Extraction method C

The flesh of *L. circellatus* was extracted similarly to the skin, see section 6.3.1.1, where the crushed flesh was extracted using one Liter of MeOH instead of acetone at room temperature two times. The MeOH was evaporated under reduced pressure from the extract. The non-homogeneous water remains, then will be partitioned with diethyl ether to remove the polar compounds that dissolved in water. The water layer then partitioned with ethyl acetate. The ether layer was then dried and then partitioned between Hexane and 1:4 aqueous MeOH. After that, as an additional step, the aqueous MeOH layer can be partitioned between water and butanol solvents but it proved to be futile in this case so it was skipped, but it can be useful in different cases, (Fig. 113).

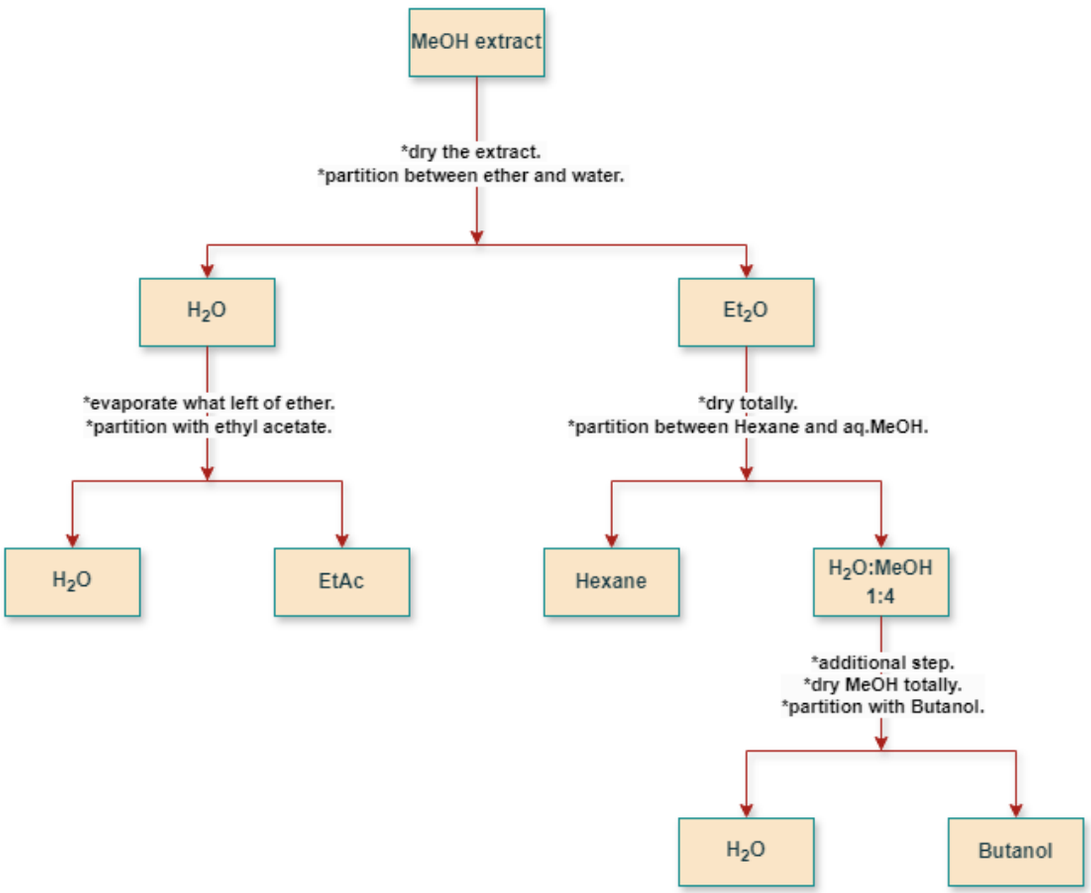

Figure. 113. Diagram of the partitioning process of the MeOH extract from *L. circellatus*.

Both solvents in the Hexane and methanolic layers were evaporated. The dried methanolic layer was filtered using SPE, water fraction was discarded. Then, the concentrated water-methanol and methanol fractions alongside the dried Hexane layer were loaded in Semi-Prep HPLC for the separation of the targeted lactarane compounds.

6.3.1.4 Extraction method D

A total mass of 506 g of *Mycena zephirus* mushroom was subjected to large-scale extraction. This was performed by gradually crashing the fruiting bodies using mortar. Afterward, the crashed mushrooms were extracted using 1 L of MeOH solvent in a 2.5 L Erlenmeyer flask at room temperature and stirring. After two hours the solution was filtered through glass wool and a new solvent was added. This was repeated three times in total until the solution showed hardly any color so that as much as possible could be extracted. It was then extracted again with acetone to test whether any substances that could not be extracted before were still dissolving. Then remove protein residues and impurities, see section 6.3.1.5. Afterward, the resulting extract was applied to the SPE technique for further separations and purifications, see section 6.3.2.

6.3.1.5 Protein contents removal

Protein precipitation by freezing:

The protein content in the mushroom extract was removed by freezing the concentrated extracts on a rotary evaporator under reduced pressure at 25 °C and dissolved in a 1:1 v/v H_2O/MeOH mixture. The extracts were completely frozen. Then extracts were thawed and centrifuged at 4000 rpm for 5 min. The solution was separated from the precipitated solid by decanting.

Protein extraction via stepwise drying:

The protein content in the mushroom extract was removed by stepwise drying by first concentrating the extract on a rotary evaporator under reduced pressure at 25 °C. As soon as white residues were visible in the flask, the liquid was transferred to a clean flask. The white residues were washed with the organic solvent used to remove any remaining substances soluble in the organic solvent and then transferred to a clean flask. These steps were repeated until no residues precipitated from the solution. The extracts were then completely dried on a rotary evaporator. Such a method is useful when large masses of mushrooms are used in the performance of large-scale extractions.

6.3.2 Solid Phase Extraction (SPE)

Solid phase extraction (SPE) was performed using a 45 mL C18ec cartridge. It can be performed in acetone or methanol solvents. Here will describe using the latter solvent.

With H_2O, H_2O-MeOH (1:1 v/v), and MeOH solvents, the cartridge was first preconditioned before the separation process, which left the packing ingredient always covered in a solvent.

Preconditioning:

- Pushing around 20 mL of MeOH through the cartridge three times. The pushing process is performed using a syringe attached to an adapter that fits exactly to the open top of the used cartridge.

- After that, also three times, 20 mL of 1:1 H_2O-MeOH solvent was pushed through the cartridge.
- Then ending with pushing three times 20 mL of H_2O solvent.

The C18ec soaked packing will act like a reverse phase column as the targeted sample of the non-homogeneous water mixture will be introduced to the preconditioned cartridge.

Separation process:

- At first, the targeted mixture sample is loaded to the surface of the upper layer of the packing material in a way not to be overloaded.
- Then, the water will be pushed out of the cartridge concentrating the intended mixture on the surface of the packing. This will follow by adding 20 mL of water and pushing it out, and by so, eluting with it the polar components of the extracted mixture.
- Afterward, 20 mL of 1:1 H_2O-MeOH will be added and pushed out. This fraction will contain compounds with medium-polar characters.
- Finally, adding 20 mL of MeOH and pushing it out will produce the fraction with the least polar compounds.

By the end of this process, three SPE fractions; H_2O, 1:1 H_2O-MeOH and MeOH will be afforded. And if to use the cartridge again, then reconditioning it back as it's described in the preconditioning part but with applying solvents only one time not three.

6.3.2.1 Extended SPE method

The MeOH extract from the mushroom *Mycena zephirus* was introduced to further separations with solid phase extraction (SPE), using gradients of H_2O and MeOH solvents, (Fig. 114). A certain degree of separation was achieved with the SPE but not all of the signals have clear separation and accordingly, not all could be isolated. Therefore, the SPE should be optimized. An extended second SPE step was performed for the MeOH fraction, which is the most eligible and promising fraction from the previous SPE step. The extended SPE method simply contains more mixtures of the H_2O and MeOH solvents.

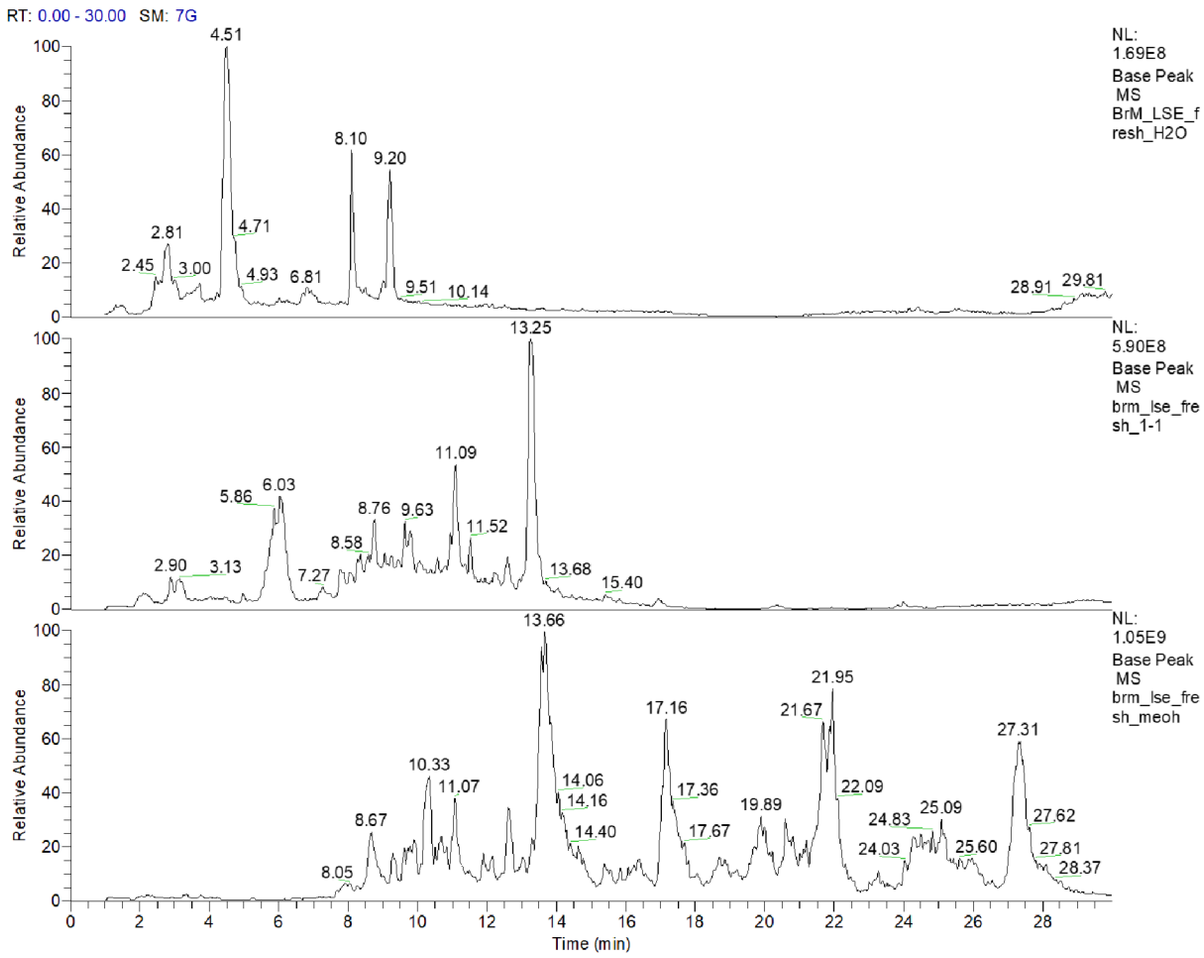

Figure. 114: Base peak chromatograms of SPE fractions, H2O (top), 1:1 (middle) and MeOH (bottom); HPLC separation with gradient in section 6.3.4.6-1.

The new step performed with decreasing polarity has seven fractions rather than three in the typical SPE method of separation and purification of the mushroom extract. The separation starts with H_2O then 8:1, then 3:1, 1:1, 1:3, 1:8 H_2O/MeOH v/v, and finally MeOH, see (Tab. 13).

Table. 13: The fractions of the extended SPE with H_2O/MeOH mixtures.

Extended SPE mixtures	Fractions symbols
H_2O/MeOH 8:1	M 1
H_2O/MeOH 3:1	M 2
H_2O/MeOH 1:1	**M 3**
H_2O/MeOH 1:3	M 4
H_2O/MeOH 1:8	M 5
MeOH	M 6

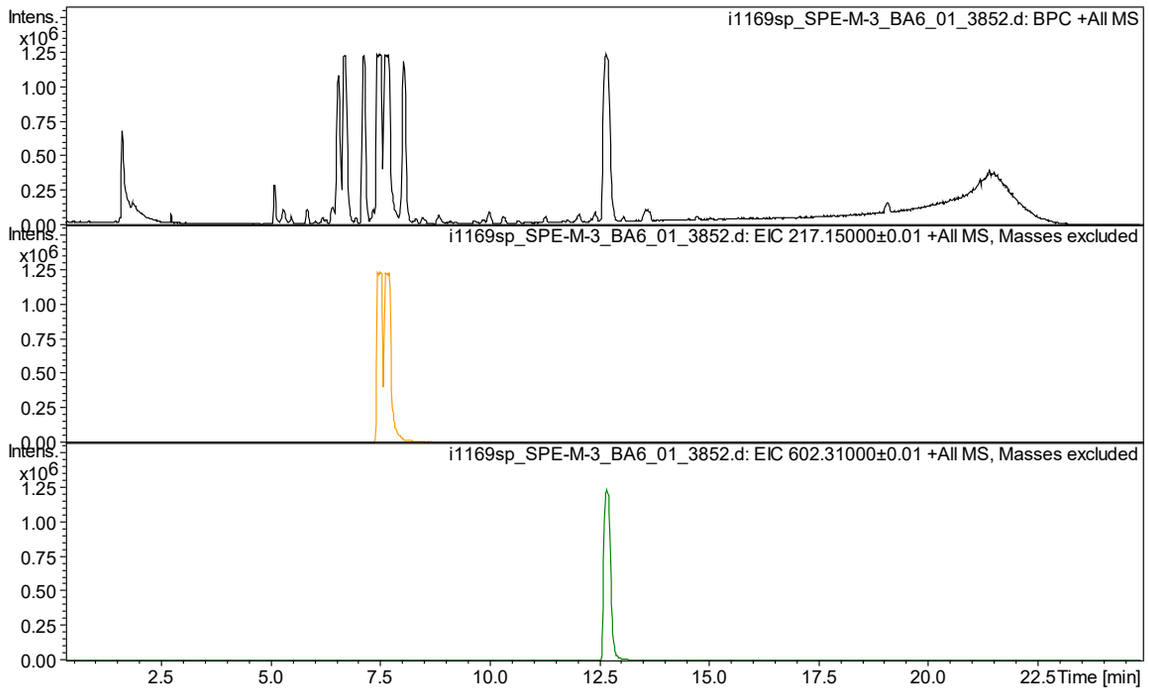

Figure. 115: Base peak chromatogram of the extended SPE fraction M 3 (top), EIC of compounds **54** and **55** (middle) and compounds **56** and **57** (bottom), from SPE fraction M 3 of the MeOH extract; HPLC-MS separation with gradient in section 6.3.4.6-2.

The extended step was proven to be useful as the targeted compounds have now better separation and therefore can perform the preparative-HPLC with a more successful outcome, (Fig. 115).

6.3.3 Size Exclusion Chromatography

A. Size exclusion chromatography used Sephadex LH-20 as the stationary phase and methanol as the mobile phase. The column material was slurred with the eluent and placed as a suspension in a glass column (30 cm×1.5 cm). The column material was then conditioned for 30 min. The samples were then dissolved in the eluent and loaded onto the column. The drop rate was 2 to 3 drops per minute.

B. Size exclusion chromatography used Sephadex LH-20 as the stationary phase and methanol as the mobile phase. The column material was slurred with the eluent and placed as a suspension in a glass column (55 cm×3.0 cm). The column material was then conditioned for 20 min. The samples were then dissolved in the eluent and loaded onto the column. The drop rate was 2 to 3 drops per minute.

C. Size exclusion chromatography used Sephadex LH-20 as the stationary phase and acetone as the mobile phase. The column material was slurred with the eluent and placed as a suspension in a glass column (30 cm×1.5 cm). The column material was then conditioned for 30 min. The

samples were then dissolved in the eluent and loaded onto the column. The drop rate was 2 to 3 drops per minute.

D. Size exclusion chromatography used Sephadex LH-20 as the stationary phase and acetone as the mobile phase. The column material was slurred with the eluent and placed as a suspension in a glass column (55 cm×3.0 cm). The column material was then conditioned for 20 min. The samples were then dissolved in the eluent and loaded onto the column. The drop rate was 2 to 3 drops per minute.

6.3.4 Separation methods

6.3.4.1 Separation method A

Gradient - RP18 - (Semi-Preparative HPLC):

Time [min]	H_2O + 0.1%HOAc	MeOH
0	90%	10%
50	30%	70%
60	0%	100%

The separation was carried out at room temperature with a C18ec column, (Nucleodur, 100 Å, 5 µm, 10 x 250 mm, Macherey-Nagel). The loaded samples were eluted with a flow rate of 3.5 mL/min, and the targeted fractions were separated using a UV-detector at a wavelength of λ 235 nm.

6.3.4.2 Separation method B

Gradient - RP18 - (Analytical HPLC):

Time [min]	H_2O + 0.1%HOAc	MeOH
0	90%	10%
50	0%	100%

The separation was carried out on an analytical HR-LC-ESI-(+)-MS at room temperature with a C18ec column, (Nucleodur, 100 Å, 5 µm, 3 x 250 mm, Macherey-Nagel). The loaded samples were eluted with a flow rate of 0.66 mL/min, and the injection volume = 5 µL from the diluted samples. The targeted compounds were detected using a wavelength range of λ 130-600 nm.

6.3.4.3 Separation method C

Gradient - RP18:

Time [min]	H_2O + 0.1%HOAc	Acetonitrile
0	100%	0%
5	65%	35%
42	33%	67%
50	0%	100%

(Semi-Preparative HPLC): The separation was carried out at room temperature with a C18ec column, (Nucleodur, 100 Å, 5 µm, 10 x 250 mm, Macherey-Nagel). The loaded samples were eluted with a flow rate of 4.0 mL/min, and the targeted fractions were separated using a UV-detector at a wavelength of λ 230 nm for compounds extracted from the mushroom flesh and at a wavelength of λ 440, 530, and 550 nm for compounds extracted from the mushroom skin.

(Analytical HPLC): The separation was carried out at room temperature with a C18ec column, (Nucleodur, 100 Å, 5 µm, 3 x 250 mm, Macherey-Nagel). The loaded samples were eluted with a flow rate of 0.5 mL/min. The targeted compounds were detected using a wavelength range of λ 130-600 nm.

6.3.4.4 Separation method D

Gradient - RP18 - (Analytical HPLC):

Time [min]	H_2O + 0.1%HOAc	Acetonitrile
0	100%	0%
5	80%	20%
30	70%	30%
35	0%	100%

The separation was carried out at room temperature with a C18ec column, (Nucleodur, 100 Å, 5 µm, 3 x 250 mm, Macherey-Nagel). The loaded samples were eluted with a flow rate of 0.5 mL/min. The targeted compounds were detected using a wavelength range of λ 130-600 nm.

6.3.4.5 Separation method E

Gradient - RP18 - (Analytical HPLC):

Time [min]	H_2O + 0.1%HOAc	Acetonitrile
0	100%	0%
50	0%	100%

The separation was carried out at room temperature with C18ec column, (Nucleodur, 100 Å, 5 µm, 3 x 250 mm, Macherey-Nagel). The loaded samples were eluted with a flow rate of 0.5 mL/min. The targeted compounds were detected using a wavelength range of λ 130-800 nm.

6.3.4.6 Separation method F

Gradient - RP18 - (Analytical HPLC) - 1:

Time [min]	H_2O + 0.1%HOAc	Acetonitrile
0	100%	0%
30	0%	100%

Gradient - RP18 - (Analytical HPLC) - 2:

Time [min]	H_2O + 0.1%HOAc	Acetonitrile
0	100%	0%
25	0%	100%

The separation was carried out at room temperature with a C18ec column, (Nucleodur, 100 Å, 5 µm, 3 x 250 mm, Macherey-Nagel). The loaded samples were eluted with a flow rate of 0.5 mL/min. The targeted colorless compounds were not able to be detected using UV-detector.

6.3.4.7 Separation method G

Gradient - RP18:

Time [min]	H_2O + 0.1%HOAc	Acetonitrile
0	100%	0%
60	0%	100%

(Semi-Preparative HPLC): The separation was carried out at room temperature with a C18ec column, (Nucleodur, 100 Å, 5 µm, 10 x 250 mm, Macherey-Nagel). The loaded samples were eluted with a flow rate of 5.0 mL/min. The targeted colorless compounds were not able to be detected using a UV-detector, so, these compounds were separated using separating different fractions with definite time windows, then testing the collected fractions in LCMS to finally narrow the time windows to only contain the targeted compounds.

6.3.4.8 Separation method H

Gradient on DB-5ms column (GCMS):

Time [min]	°C
0	50
1	50
55	320
70	320

The separations were carried out with the specified temperature gradient on the GC-MS device. The separation was carried out on a fused silica capillary column type DB-5ms (30 m x 0.25 mm, 0.25 µm) from Macherey-Nagel. The injection volumes were 0.5 µl.

6.4 Sample Material

The used fungus was collected by Prof. Peter Spiteller and stored at -30°C.

6.4.1 *Lactarius circellatus*

Table. 14: *L. circellatus* mushroom collections are used for large-scale extraction.

Mushroom collection number	Place/date of collection	Mass (g)
140/19	Leutstetten 22.09.2004	300 g

6.4.2 *Lactarius trivialis*

Table. 15: *L. trivialis* mushroom collections are used for initial investigations and large-scale extraction for the isolation of sesquiterpenoids.

Mushroom collection number	Place/date of collection	Mass (g)
139/17	Leutstetten 25.09.2017	100
184/17	Leutstetten 08.10.2017	108
57/18	Leutstetten 22.09.2018	170
54/18	Leutstetten 22.09.2018	105
17/19	Leutstetten 09.2004	117
45/20	Leutstetten 09.2014	70
		In total 670 g

Table. 16: *L. trivialis* mushroom collections are used for large-scale extraction for the isolation of trivialines.

Mushroom collection number	Place/date of collection	Mass (g)
51/04	Hohenbirken / Penzberg 09.2004	140
116/04	Leutstetten 09.2004	150
17/20	Leutstetten 28.09.2020	321
45/20	Leutstetten 30.09.2020	140
105/21	Leutstetten 09.2021	62
31/21	Pilzausstellung 19.09.2021	187
01/22	Mühltal 09.2022	392
44/22	Pilzausstellung München 18.09.2022	219
		In total 1611 g

6.4.3 *Mycena zephirus*

Table. 17: *M. zephirus* mushroom collections are used for large-scale extraction.

Mushroom collection number	Place/date of collection	Mass (g)
165/05	Reisberg 14.10.2005	108
124/07	Studentenwald BT 19.09.2007	128
117/07	Studentenwald BT 16.09.2007	59
127/09	Bayreuth 11.10.2009	98
139/20	Breitbrunn 25.10.2020	46
060/11	Wellenburg 26.09.2011	67
		In total 506 g

6.5 Experimental Data

6.5.1 Compounds from *Lactarius circellatus*

6.5.1.1 12-Hydroxy-15-carboxyblennin A (**19**)

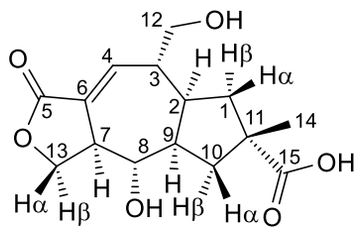

19

Colorless oil - 1.0 mg from 300 g from the flesh of the frozen fruiting bodies.

HPLC	R_t = 13.30 min / analytical - gradient at section 6.3.4.2 R_t = 24.37 min / semi-preparative - gradient at section 6.3.4.1
UV/Vis (H_2O/MeOH)	λ_{max} (log ε): 200 (2.5), 260 nm (0.4 $mol^{-1}dm^3cm^{-1}$)
CD (MeOH)	λ ($\Delta\varepsilon$): 205 (–1.1), 220 (–0.6), 245 nm (+0.42 $mol^{-1}dm^3cm^{-1}$)
$[\alpha]_D^{25}$	–12.3 (MeOH; *c* 0.001)
LCESI-(+)-MS	*m/z* = 297.132 $[M + H]^+$, 593.258 $[2M + H]^+$
HRESI-(+)-MS	*m/z* = 297.13270 $[M + H]^+$, calculated 297.13381 for $[C_{15}H_{21}O_6]^+$
HRESI-(+)-MSMS	(Precursor ion *m/z* (%) = 297.13270 (11.5)), qTOF 20-50 eV) *m/z* (%) = 279.12240 (3.5), calculated 279.12320 for $[C_{15}H_{19}O_5]^+$; 261.11163 (10.0), calculated 261.11270 for $[C_{15}H_{17}O_4]^+$; 249.11166 (9.0), calculated 249.11270 for $[C_{14}H_{17}O_4]^+$; 231.10119 (15.0), calculated 231.10210 for $[C_{14}H_{15}O_3]^+$; 215.10626 (42.5), calculated 215.10720 for $[C_{14}H_{15}O_2]^+$; 203.10642 (55.2), calculated 203.10720 for $[C_{13}H_{15}O_2]^+$
^{1}H-NMR	(600.22 MHz, 297.2 K, CD_3OD): δ_H = 6.93 (1 H, dd, *J* = 2.9, 2.9 Hz, H-4), 4.49 (1 H, dd appears as t, *J* = 9.1, 9.1 Hz, Hβ-13), 4.09 (1 H, dd appears as t, *J* = 9.0, 9.0 Hz, Hα-13), 3.81 (1 H, dd, *J* = 6.1, 10.8 Hz, H-

12), 3.56 (1 H, dd, *J* = 3.6, 10.8 Hz, H-12), 3.54 (1 H, dd, *J* = 6.0, 11.0 Hz, H-8), 3.33 (1 H, ddd, H-7), 2.57 (1 H, dd, *J* = 6.0, 12.3 Hz, Hβ-10), 2.53 (1 H, dd, *J* = 7.2, 13.3 Hz, Hβ-1), 2.45 (1 H, ddd, 7.0, 10.0, 18.0 Hz, H-3), 2.41 (1 H, dddd, *J* = 2.5, 6.2, 13.3, 18.0 Hz, H-2), 2.35 (1 H, dddd, *J* = 6.0, 7.7, 14.0, 18.0 Hz, H-9), 1.47 (1 H, dd, *J* = 6.0, 13.3 Hz, Hα-1), 1.45 (1 H, dd appears as t, *J* = 12.3, 12.3 Hz, Hα-10), 1.34 (3 H, s, H-14)

^{13}C-NMR (151.01 MHz, 297.2 K, CD_3OD): δ_C = 183.41 (C-15), 173.94 (C-5), 143.60 (C-4), 129.93 (C-6), 75.21 (C-8), 70.85 (C-13), 64.75 (C-12), 52.47 (C-9), 49.56 (C-11), 46.28 (C-7), 43.84 (C-1), 43.78 (C-3), 43.04 (C-10), 39.80 (C-2), 26.86 (C-14)

6.5.1.2 7,15-Dihydroxyblennin A (**20**)

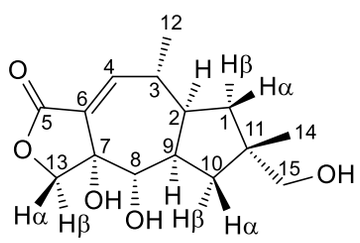

20

HPLC R_t = 19.61 min / analytical - gradient at section 6.3.4.2

UV/Vis (H_2O/MeOH) λ_{max} (log ε): 200 nm (1.1 $mol^{-1}dm^3cm^{-1}$)

CD (MeOH) λ (Δε): 210 (–0.2), 225 (–0.9), 250 nm (+0.3 $mol^{-1}dm^3cm^{-1}$)

$[\alpha]_D^{25}$ –10.3 (MeOH; *c* 0.0013)

LCESI-(+)-MS *m/z* = 283.153 $[M + H]^+$, 565.300 $[2M + H]^+$

HRESI-(+)-MS *m/z* = 283.15419 $[M + H]^+$, calculated 283.15455 for $[C_{15}H_{23}O_5]^+$

HRESI-(+)-MSMS (Precursor ion *m/z* (%) = 283.15419 (15.6)), qTOF 20-50 eV) *m/z* (%) = 265.14382 (17.3), calculated 265.14398 for $[C_{15}H_{21}O_4]^+$; 247.13315 (45.5), calculated 247.13342 for $[C_{15}H_{19}O_3]^+$; 229.12263 (47.1), calculated 229.12285 for $[C_{15}H_{17}O_2]^+$

^{1}H-NMR	(600.22 MHz, 300 K, CD_3OD)*: δ_H = 6.78 (1 H, d, *J* = 2.2 Hz, H-4), 4.28 (1 H, dd appears as t, *J* = 10.0, 10.0 Hz, Hβ-13), 4.26 (1 H, dd appears as t, *J* = 10.0, 10.0 Hz, Hα-13), 3.61 (1 H, d, *J* = 9.8 Hz, H-8), 3.29, 3.35 (2 H, AB, *J* = 10.7 Hz, H-15), 2.58 (1 H, dddd, *J* = 7.0, 7.5, 12.1, 16.2 Hz, H-9), 2.47 (1 H, ddd, 2.0, 7.2, 10.0, H-3), 2.21 (1 H, dddd, *J* = 3.9, 4.5, 8.0, 14.5 Hz, H-2), 2.07 (1 H, dd, *J* = 6.8, 13.0 Hz, Hβ-10), 1.81 (1 H, dd, *J* = 8.0, 13.8 Hz, Hβ-1), 1.42 (1 H, dd, *J* = 4.4, 13.8 Hz, Hα-1), 1.33 (1 H, dd appears as t, *J* = 12.5, 12.5 Hz, Hα-10), 1.19 (3 H, d, *J* = 7.3 Hz, H-12), 1.10 (3 H, s, H-14)
^{13}C-NMR	(150.94 MHz, 300 K, CD_3OD)*: δ_C = 173.72 (C-5), 151.53 (C-4), 131.51 (C-6), 79.09 (C-13), 78.12 (C-8), 78.04 (C-7), 70.97 (C-15), 46.96 (C-9), 45.07 (C-2), 42.94 (C-11), 42.46 (C-1), 40.89 (C-10), 36.26 (C-3), 26.55 (C-14), 21.07 (C-12)

*: These data are from the already extracted and measured compound from *L. circellatus*.

6.5.1.3 2,3-Epoxylactarorufin A (**21**)

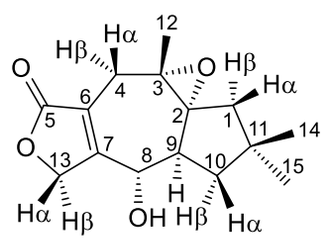

21

HPLC	R_t = 26.40 min / analytical - gradient at section 6.3.4.2
UV/Vis (H_2O/MeOH)	λ_{max} (log ε): 200 nm (0.6 $mol^{-1}dm^3cm^{-1}$)
CD (MeOH)	λ (Δε): 200 (+1.5), 225 (–1.2), 250 nm (–0.4 $mol^{-1}dm^3cm^{-1}$)
$[\alpha]_D^{25}$	–16.2 (MeOH; *c* 0.001)
^{1}H-NMR	(600.22 MHz, 300 K, CD_3OD)*: δ_H = 4.90 (1 H, dddd appears as dd, *J* = 3.2, 17.5 Hz, Hβ-13), 4.77 (1 H, dddd appears as d, *J* = 17.4 Hz, Hα-13), 4.27 (1 H, ddddd, *J* = 10.7 Hz, H-8), 2.88 (1 H, dddd appears as d, *J* = 18.7 Hz, Hα-4), 2.78 (1 H, dddd appears as dq, *J* = 3.0, 3.0, 3.0,

18.7 Hz, Hβ-4), 2.67 (1 H, dddd appears as td, *J* = 8.0, 8.0, 12.3, Hz, H-9), 1.97 (1 H, dd, *J* = 0.87, 14.2 Hz, Hβ-1), 1.89 (1 H, ddd appears as dd, *J* = 8.0, 12.6 Hz, Hβ-10), 1.78 (1 H, dddd appears as dd, *J* = 10.2, 12.6 Hz, Hα-10), 1.67 (1 H, dd appears as d, *J* = 14.2 Hz, Hα-1), 1.38 (3 H, s, H-12), 1.17 (3 H, d appears as s, H-14), 1.06 (3 H, ddd appears as s, H-15)

^{13}C-NMR (150.94 MHz, 300 K, CD_3OD)*: δ_C = 177.38 (C-5), 165.05 (C-7), 121.50 (C-6), 72.70 (C-2), 72.46 (C-13), 70.42 (C-8), 62.27 (C-3), 47.50 (C-1), 46.49 (C-9), 45.76 (C-10), 37.39 (C-11), 30.28 (C-4), 29.60 (C-14), 28.25 (C-15), 21.90 (C-12)

*: These data are from the already extracted and measured compound from *L. circellatus*.

6.5.1.4 14-Carboxyl-deoxylactarorufin A (**22**)

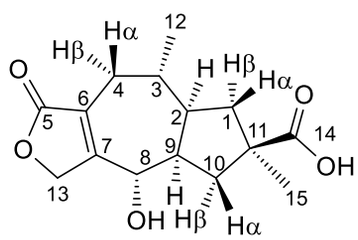

22

HPLC R_t = 25.31 min / analytical - gradient at section 6.3.4.2

UV/Vis (H_2O/MeOH) λ_{max} (log ε): 200 (1.5), 2.15 (1.8), 260 nm (0.5 $mol^{-1}dm^3cm^{-1}$)

CD (MeOH) λ (Δε): 200 (+1.6), 220 (–0.5), 245 nm (+0.40 $mol^{-1}dm^3cm^{-1}$)

$[\alpha]_D^{25}$ +25.6 (MeOH; *c* 0.003)

LCESI-(+)-MS *m/z* = 281.137 $[M + H]^+$, 561.269 $[2M + H]^+$

HRESI-(+)-MS *m/z* = 281.13840 $[M + H]^+$, calculated 281.13890 for $[C_{15}H_{21}O_5]^+$

HRESI-(+)-MSMS (Precursor ion *m/z* (%) = 281.13840 (66.1)), qTOF 20-50 eV) *m/z* (%) = 263.12785 (87.3), calculated 263.12833 for $[C_{15}H_{19}O_4]^+$; 245.11734 (21.5), calculated 245.11777 for $[C_{15}H_{17}O_3]^+$; 235.13290 (42.0), calculated 235.13342 for $[C_{14}H_{19}O_3]^+$; 217.12234 (100.0),

calculated 217.12285 for $[C_{14}H_{17}O_2]^+$; 199.11175 (25.1), calculated 199.11229 for $[C_{14}H_{15}O]^+$

^{1}H-NMR (600.22 MHz, 300 K, CD_3OD)*: δ_H = 4.88 (1 H, ddd appears as d, *J* = 18.5 Hz, Hβ-13), 4.81 (1 H, ddd appears as d, *J* = 17.5 Hz, Hα-13), 4.62 (1 H, ddd appears as d, *J* = 11.3 Hz, H-8), 2.46 (1 H, ddd, H-9), 2.39 (1 H, dd, *J* = 5.0, 13.5 Hz, Hα-10), 2.33 (1 H, d, *J* = 17.3 Hz, Hβ-4), 2.05 (1 H, dddd, Hα-4), 2.03 (1 H, dddd, H-2), 1.95 (1 H, dd appears as t, *J* = 12.5, 12.5 Hz, Hα-1), 1.92 (1 H, dd, *J* = 8.1, 12.5 Hz, Hβ-1), 1.77 (1 H, ddd, H-3), 1.70 (1 H, dd, *J* = 7.5, 13.5 Hz, Hβ-10), 1.27 (3 H, s, H-15), 1.02 (3 H, d, *J* = 6.3 Hz, H-12)

(600.51 MHz, 298.2 K, DMSO-d6)**: δ_H = 4.79 (1 H, ddd appears as d, *J* = 19.0 Hz, Hβ-13), 4.76 (1 H, ddd appears as d, *J* = 18.3 Hz, Hα-13), 4.48 (1 H, dddd appears as d, *J* = 10.6 Hz, H-8), 2.31 (1 H, ddd, H-9), 2.30 (1 H, dd, Hα-10), 2.18 (1 H, dddd appears as d, *J* = 17.6 Hz, Hβ-4), 1.97 (1 H, dddd, Hα-4), 1.90 (1 H, ddd, H-2), 1.84 (1 H, dd, Hα-1), 1.73 (1 H, dd, *J* = 7.0, 12.0 Hz, Hβ-1), 1.67 (1 H, dd, *J* = 7.0, 13.4 Hz, H-3), 1.47 (1 H, d, Hβ-10), 1.13 (3 H, s, H-15), 0.92 (3 H, d, *J* = 6.3 Hz, H-12)

^{13}C-NMR (151.94 MHz, 300 K, CD_3OD)*: δ_C = 185.81 (C-14), 177.38 (C-5), 167.80 (C-7), 126.00 (C-6), 72.05 (C-13), 68.72 (C-8), 50.06 (C-9), 49.57 (C-11), 49.28 (C-2), 45.06 (C-1), 42.29 (C-10), 35.73 (C-3), 33.67 (C-4), 26.17 (C-15), 22.58 (C-12)

(151.01 MHz, 298.1 K, DMSO-d6)**: δ_C = 181.86 (C-14), 174.33 (C-5), 166.88 (C-7), 123.39 (C-6), 70.28 (C-13), 66.31 (C-8), 48.39 (C-9), 47.35 (C-2), 46.98 (C-11), 43.52 (C-1), 40.90 (C-10), 33.90 (C-3), 32.28 (C-4), 25.57 (C-15), 22.03 (C-12)

*: These data are from the already extracted and measured compound from *L. circellatus*.
**: These data are from the same compound with repeated measurements in different solvent.

6.5.1.5 13-Hydroxy-14-carboxyl-deoxylactarorufin A (**23**)

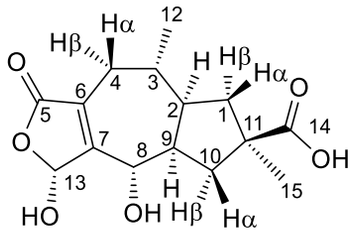

23

HPLC	R_t = 24.00 min / analytical - gradient at section 6.3.4.2
UV/Vis (H_2O/MeOH)	λ_{max} (log ε): 200 (1.3), 220 nm (1.0 $mol^{-1}dm^3cm^{-1}$)
CD (MeOH)	λ ($\Delta\varepsilon$): 205 (+4.0), 225 (–2.5), 250 nm (+1.5 $mol^{-1}dm^3cm^{-1}$)
$[\alpha]_D^{25}$	+44.1 (MeOH; *c* 0.0026)
LCESI-(+)-MS	*m/z* = 297.132 $[M + H]^+$, 593.257 $[2M + H]^+$
HRESI-(+)-MS	*m/z* = 297.22137 $[M + H]^+$, calculated 297.13381 for $[C_{15}H_{21}O_6]^+$
HRESI-(+)-MSMS	(Precursor ion *m/z* (%) = 297.22137 (1.1)), qTOF 20-50 eV) *m/z* (%) = 279.12243 (17.3), calculated 279.12325 for $[C_{15}H_{19}O_5]^+$; 261.11193 (70.5), calculated 261.11268 for $[C_{15}H_{17}O_4]^+$; 243.10133 (15.8), calculated 243.10212 for $[C_{15}H_{15}O_3]^+$; 233.11701 (58.6), calculated 233.11777 for $[C_{14}H_{17}O_3]^+$; 215.10654 (100.0), calculated 215.10720 for $[C_{14}H_{15}O_2]^+$; 187.11156 (50.0), calculated 187.11229 for $[C_{13}H_{15}O]^+$
^{1}H-NMR	(600.22 MHz, 300 K, CD_3OD)*: δ_H = 6.13 (1 H, ddd appears as s, H-13), 4.51 (1 H, ddd appears as d, *J* = 9.2 Hz, H-8), 2.48 (1 H, d, Hα-10), 2.45 (1 H, ddd, H-9), 2.34 (1 H, d, *J* = 17.7 Hz, Hβ-4), 2.09 (1 H, dddd, Hα-4), 2.04 (1 H, dddd, H-2), 1.95 (1 H, dd appears as t, *J* = 12.3, 12.3 Hz, Hα-1), 1.90 (1 H, dd, *J* = 7.0, 12.2 Hz, Hβ-1), 1.79 (1 H, dd, Hβ-10), 1.67 (1 H, ddd, H-3), 1.29 (3 H, s, H-15), 1.03 (3 H, d, *J* = 6.1 Hz, H-12)
	(600.22 MHz, 297.1 K, DMSO-d6)**: δ_H = 6.01 (1 H, ddd appears as s, H-13), 4.34 (1 H, dddd, H-8), 2.47 (1 H, d, Hα-10), 2.18 (1 H, ddd, H-9), 2.13 (1 H, dddd appears as d, *J* = 17.4 Hz, Hβ-4), 2.00 (1 H, dddd,

Hα-4), 1.86 (1 H, dd, Hα-1), 1.83 (1 H, dddd, H-2), 1.70 (1 H, dd, Hβ-1), 1.48 (1 H, ddd, H-3), 1.32 (1 H, dd, Hβ-10), 1.13 (3 H, s, H-15), 0.93 (3 H, d, *J* = 5.9 Hz, H-12)

^{13}C-NMR (150.94 MHz, 300 K, CD_3OD)*: δ_C = 184.48 (C-14), 174.32 (C-5), 164.69 (C-7), 130.09 (C-6), 99.04 (C-13), 67.62 (C-8), 49.69 (C-2), 49.57 (C-9), 48.80 (C-11), 44.54 (C-1), 42.31 (C-10), 36.58 (C-3), 32.79 (C-4), 26.44 (C-15), 22.69 (C-12)

(150.94 MHz, 297.1 K, DMSO-d6)**: δ_C = 183.08 (C-14), 171.98 (C-5), 164.90 (C-7), 127.32 (C-6), 97.42 (C-13), 64.55 (C-8), 49.30 (C-9), 48.77 (C-2), 47.48 (C-11), 43.74 (C-1), 40.64 (C-10), 35.55 (C-3), 31.07 (C-4), 27.57 (C-15), 22.11 (C-12)

*: These data are from the already extracted and measured compound from *L. circellatus*.
**: These data are from the same compound with repeated measurements in different solvent.

6.5.1.6 Lactarotropone (**24**)

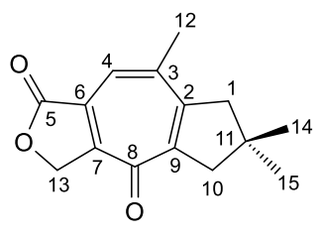

24

HPLC R_t = 32.45 min / analytical - gradient at section 6.3.4.2

$[\alpha]_D^{25}$ +1.1 (MeOH; *c* 0.001)

LCESI-(+)-MS *m/z* = 245.117 $[M + H]^+$

HRESI-(+)-MS *m/z* = 245.11701 $[M + H]^+$, calculated 245.11777 for $[C_{15}H_{17}O_3]^+$

HRESI-(+)-MSMS (Precursor ion *m/z* (%) = 245.11701 (40.0)), qTOF 20-50 eV) *m/z* (%) = 217.12110 (2.0), calculated 217.12285 for $[C_{14}H_{17}O_2]^+$; 201.12712 (2.0), calculated 201.12794 for $[C_{14}H_{17}O]^+$; 173.09542 (2.0), calculated 173.09664 for $[C_{12}H_{13}O]^+$; 159.07984 (4.0), calculated 159.08099 for $[C_{11}H_{11}O]^+$

^{1}H-NMR (600.22 MHz, 300 K, CD_3OD)*: δ_H = 7.44 (1 H, H-4), 5.22 (2 H, H-13), 3.06 (2 H, H-1), 2.94 (2 H, H-10), 2.45 (3 H, H-12), 1.18 (6H, H-14, H-15)

(600.22 MHz, 297.2 K, DMSO-d6)**: δ_H = 7.31 (1 H, H-4), 5.22 (2 H, H-13), 2.99 (2 H, H-1), 2.83 (2 H, H-10), 2.39 (3 H, H-12), 1.11 (6H, H-14, H-15)

^{13}C-NMR (150.94 MHz, 300 K, CD_3OD)*: δ_C = 180.42 (C-8), 174.56 (C-5), 156.09 (C-2), 155.13 (C-9), 154.87 (C-7), 148.51 (C-3), 131.15 (C-6), 127.65 (C-4), 71.10 (C-13), 54.50 (C-1), 50.72 (C-10), 36.21 (C-11), 29.09 (C-14, C-15), 25.81 (C-12)

(150.94 MHz, 297.1 K, DMSO-d6)**: δ_C = 178.01 (C-8), 172.81 (C-5), 153.81 (C-7), 153.15 (C-2), 152.97 (C-9), 146.27 (C-3), 128.59 (C-6), 125.45 (C-4), 69.88 (C-13), 52.74 (C-1), 49.50 (C-10), 34.69 (C-11), 28.64 (C-14, C-15), 25.10 (C-12)

*: These data are from the already extracted and measured compound from *L. circellatus*.
**: These data are from the same compound with repeated measurements in different solvent.

6.5.1.7 Lactarorufin A (**25**)

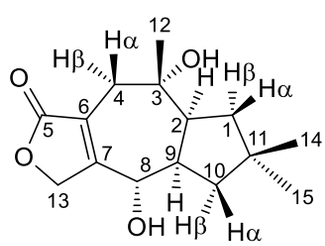

25

HPLC R_t = 27.45 min / analytical - gradient at section 6.3.4.2
R_t = 13.47 min / semi-preparative - gradient at section 6.3.4.3, when the compound was extracted from *L. trivialis*.

UV/Vis (H_2O/MeOH) λ_{max} (log ε): 200 (0.7), 220 nm (0.45 $mol^{-1}dm^3cm^{-1}$)

CD (MeOH) λ ($\Delta\varepsilon$): 200 (+3.0), 220 (–3.1), 240 nm (+1.2 $mol^{-1}dm^3cm^{-1}$)

$[\alpha]_{\mathrm{D}}^{25}$	+23.5 (MeOH; *c* 0.005)
LCESI-(+)-MS	*m/z* = 267.159 $[M + H]^+$, 289.141 $[M + Na]^+$, 533.313 $[2M + H]^+$
HRESI-(+)-MS	*m/z* = 267.15691 $[M + H]^+$, calculated 267.15963 for $[C_{15}H_{23}O_4]^+$
HRESI-(+)-MSMS	(Precursor ion *m/z* (%) = 267.15691 (1.0)), qTOF 20-50 eV) *m/z* (%) = 249.14911 (19.0), calculated 249.14907 for $[C_{15}H_{21}O_3]^+$; 231.13799 (70.5), calculated 231.13850 for $[C_{15}H_{19}O_2]^+$; 213.12764 (10.1), calculated 213.12794 for $[C_{15}H_{17}O]^+$; 203.14323 (18.2), calculated 203.14359 for $[C_{14}H_{19}O]^+$; 187.14830 (50.1), calculated 187.14868 for $[C_{14}H_{19}]^+$
^{1}H-NMR	(600.50 MHz, 297.1 K, CD_3OD)*: δ_H = 4.90 (1 H, ddd appears as d, *J* = 17.8 Hz, H-13), 4.76 (1 H, ddd appears as d, *J* = 17.8 Hz, H-13), 4.33 (1 H, dd appears as d, *J* = 7.0 Hz, H-8), 2.70 (1 H, dddd appears as quintet, *J* = 8.2, 8.2, 8.2, 8.2 Hz, H-9), 2.63 (1 H, ddd appears as d, *J* = 18.0 Hz, Hα-4), 2.58 (1 H, ddd appears as q, *J* = 9.2, 9.2, 9.2 Hz, H-2), 2.47 (1 H, ddd appears as d, *J* = 17.8 Hz, Hβ-4), 1.65 (1 H, dd, *J* = 7.4, 12.3 Hz, Hβ-1), 1.61 (1 H, dd, *J* = 7.2, 12.3 Hz, Hβ-10), 1.40 (1 H, dd appears as t, *J* = 12.2, 12.2 Hz, Hα-1), 1.39 (1 H, dd, *J* = 9.2, 12.3 Hz, Hα-10), 1.22 (3 H, s, H-12), 1.10 (3 H, s, H-14), 1.04 (3 H, s, H-15) (600.50 MHz, 297.1 K, $CDCl_3$)**: δ_H = 4.92 (1 H, H-13), 4.56 (1 H, H-13), 4.07 (1 H, H-8), 2.88 (1 H, H-9), 2.66 (1 H, H-2), 2.65 (1 H, Hα-4), 2.52 (1 H, Hβ-4), 1.64 (1 H, Hβ-1), 1.49 (1 H, Hβ-10), 1.27 (3 H, H-12), 1.12 (1 H, Hα-1), 1.02 (3 H, H-14), 1.00 (1 H, Hα-10), 0.98 (3 H, H-15)
^{13}C-NMR	(150.94 MHz, 297.2 K, CD_3OD)*: δ_C = 177.42 (C-5), 164.34 (C-7), 124.11 (C-6), 74.03 (C-3), 72.58 (C-13), 69.08 (C-8), 52.22 (C-2), 47.09 (C-9), 46.27 (C-10), 44.99 (C-1), 37.36 (C-11), 36.57 (C-4), 30.43 (C-14), 29.34 (C-12), 28.36 (C-15) (151.01 MHz, 297.1 K, $CDCl_3$)**: δ_C = 175.87 (C-5), 160.28 (C-7), 123.45 (C-6), 75.29 (C-3), 71.93 (C-13), 67.28 (C-8), 49.18 (C-2), 46.25 (C-9), 45.62 (C-10), 45.42 (C-1), 37.01 (C-11), 34.91 (C-4), 31.51 (C-12), 29.32 (C-14), 26.56 (C-15)

*: These data are from the already extracted and measured compound from *L. circellatus*.
**: These data are from the same compound with repeated measurements in different solvent.

6.5.1.8 Deoxylactarorufin A (**26**)

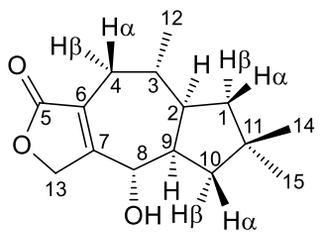

26

HPLC	R_t = 36.22 min / analytical - gradient at section 6.3.4.2
UV/Vis (H_2O/MeOH)	λ_{max} (log ε): 200 (0.6), 220 nm (0.3 $mol^{-1}dm^3cm^{-1}$)
CD (MeOH)	λ ($\Delta\varepsilon$): 200 (+4.0), 220 (–2.0), 240 nm (+0.3 $mol^{-1}dm^3cm^{-1}$)
$[\alpha]_D^{25}$	+37.3 (MeOH; *c* 0.001)
LCESI-(+)-MS	*m/z* = 251.163 $[M + H]^+$, 523.301 $[2M + H]^+$
HRESI-(+)-MS	*m/z* = 251.16372 $[M + H]^+$, calculated 251.16472 for $[C_{15}H_{23}O_3]^+$
HRESI-(+)-MSMS	(Precursor ion *m/z* (%) = 251.16372 (25.7)), qTOF 20-50 eV) *m/z* (%) = 233.15334 (40.2), calculated 233.15415 for $[C_{15}H_{21}O_2]^+$; 215.14290 (5.5), calculated 215.14359 for $[C_{15}H_{19}O]^+$; 205.15857 (10.1), calculated 205.15924 for $[C_{14}H_{21}O]^+$; 187.14783 (18.9), calculated 187.14868 for $[C_{14}H_{19}]^+$
^{1}H-NMR	(600.22 MHz, 300 K, CD_3OD)*: δ_H = 4.87 (1 H, H-13), 4.81 (1 H, H-13), 4.63 (1 H, H-8), 2.56 (1 H, H-9), 2.36 (1 H, Hβ-4), 2.05 (1 H, H-2), 2.00 (1 H, Hα-4), 1.84 (1 H, H-3), 1.75 (1 H, Hβ-10), 1.71 (1 H, Hβ-1), 1.56 (1 H, Hα-10), 1.29 (1 H, Hα-1), 1.10 (3 H, H-14), 0.99 (3 H, H-15), 0.98 (3 H, H-12)
	(600.50 MHz, 297.1 K, $CDCl_3$)**: δ_H = 4.87 (1 H, H-13), 4.78 (1 H, H-13), 4.71 (1 H, H-8), 2.58 (1 H, H-9), 2.47 (1 H, Hβ-4), 2.052 (1 H, H-

2), 2.050 (1 H, Hα-4), 1.80 (1 H, H-3), 1.79 (1 H, Hβ-10), 1.725 (1 H, Hβ-1), 1.40 (1 H, Hα-10), 1.24 (1 H, Hα-1), 1.10 (3 H, H-14), 0.98 (3 H, H-15), 0.965 (3 H, H-12)

^{13}C-NMR	(150.94 MHz, 300 K, CD_3OD)*: δ_C = 177.44 (C-5), 167.58 (C-7), 125.50 (C-6), 72.05 (C-13), 70.36 (C-8), 49.57 (C-9), 48.74 (C-1), 48.72 (C-2), 46.87 (C-10), 37.70 (C-11), 34.83 (C-4), 34.47 (C-3), 30.17 (C-14), 27.81 (C-15), 22.56 (C-12)
	(151.01 MHz, 297.2 K, $CDCl_3$)**: δ_C = 175.03 (C-5), 162.85 (C-7), 125.38 (C-6), 70.69 (C-8), 70.48 (C-13), 48.58 (C-9), 47.87 (C-1), 47.32 (C-2), 45.86 (C-10), 37.24 (C-11), 34.13 (C-4), 33.33 (C-3), 29.72 (C-14), 27.12 (C-15), 22.22 (C-12)

*: These data are from the already extracted and measured compound from *L. circellatus*.
**: These data are from the same compound with repeated measurements in different solvent.

6.5.1.9 Lactarorufin B (**27**)

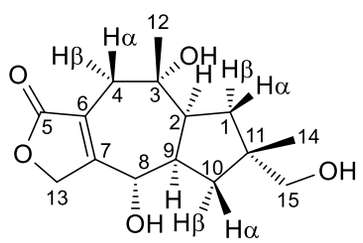

27

HPLC	R_t = 13.24 min / analytical - gradient at section 6.3.4.2 R_t = 7.34 min / semi-preparative - gradient at section 6.3.4.3, when the compound was extracted as a mixture with compound **53** from *L. trivialis*.
UV/Vis (H_2O/MeOH)	λ_{max} (log ε): 200 (0.6), 220 nm (0.25 $mol^{-1}dm^3cm^{-1}$)
CD (MeOH)	λ (Δε): 200 (+1.8), 220 (–1.25), 240 nm (+0.4 $mol^{-1}dm^3cm^{-1}$)
$[\alpha]_D^{25}$	+14.6 (MeOH; *c* 0.0015)
LCESI-(+)-MS	*m/z* = 283.153 $[M + H]^+$, 305.135 $[M+Na]^+$, 565.300 $[2M + H]^+$
HRESI-(+)-MS	*m/z* = 283.15141 $[M + H]^+$, calculated 283.15455 for $[C_{15}H_{23}O_5]^+$

HRESI-(+)-MSMS	(Precursor ion *m/z* (%) = 283.15141 (0.5)), qTOF 20-50 eV) *m/z* (%) = 265.14274 (0.7), calculated 265.14398 for $[C_{15}H_{21}O_4]^+$; 247.13182 (9.0), calculated 247.13342 for $[C_{15}H_{19}O_3]^+$; 229.12144 (13.5), calculated 229.12285 for $[C_{15}H_{17}O_2]^+$; 185.13179 (18.1), calculated 185.13303 for $[C_{14}H_{17}]^+$
^{1}H-NMR	(600.50 MHz, 297.2 K, CD_3OD)*: δ_H = 4.90 (1 H, H-13), 4.79 (1 H, H-13), 4.46 (1 H, H-8), 3.33 (2 H, H-15), 2.61 (1 H, Hα-4), 2.54 (1 H, H-9), 2.48 (1 H, Hβ-4), 2.42 (1 H, H-2), 1.86 (1 H, Hβ-1), 1.69 (1 H, Hβ-10), 1.51 (1 H, Hα-10), 1.36 (1 H, Hα-1), 1.23 (3 H, H-12), 1.11 (3 H, H-14)
	(600.22 MHz, 297.2 K, $CDCl_3$)**: δ_H = 4.95 (1 H, H-13), 4.61 (1 H, H-13), 4.12 (1 H, H-8), 3.422 (2 H, H-15), 2.83 (1 H, H-9), 2.70 (1 H, Hβ-4), 2.62 (1 H, H-2), 2.56 (1 H, Hα-4), 1.88 (1 H, Hβ-1), 1.79 (1 H, Hβ-10), 1.31 (3 H, H-12), 1.11 (1 H, Hα-1), 1.05 (3 H, H-14), 1.00 (1 H, Hα-10)
^{13}C-NMR	(151.01 MHz, 297.1 K, CD_3OD)*: δ_C = 177.49 (C-5), 166.29 (C-7), 123.79 (C-6), 73.15 (C-3), 72.23 (C-13), 70.53 (C-15), 68.99 (C-8), 53.44 (C-2), 46.20 (C-9), 42.42 (C-11), 40.40 (C-10), 39.22 (C-1), 35.05 (C-4), 30.00 (C-12), 26.36 (C-14)
	(150.94 MHz, 297.1 K, $CDCl_3$)**: δ_C = 175.54 (C-5), 160.26 (C-7), 123.32 (C-6), 75.54 (C-3), 71.80 (C-13), 68.59 (C-15), 67.57 (C-8), 49.46 (C-2), 46.21 (C-9), 42.36 (C-11), 40.60 (C-10), 40.53 (C-1), 34.72 (C-4), 31.65 (C-12), 24.52 (C-14)

*: These data are from the repeated measurements of the already extracted compound from *L. circellatus*.
**: These data are from the mixture fraction from *L. trivialis*.

6.5.1.10 Furandiol **15**

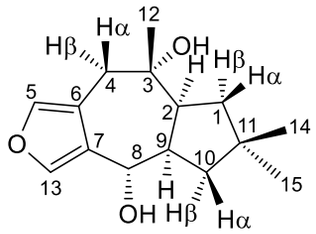

15

HPLC	R_t = 36.96 min / analytical - gradient at section 6.3.4.2
UV/Vis (H_2O/MeOH)	λ_{max} (log ε): 200 nm (0.8 $mol^{-1}dm^3cm^{-1}$)
CD (MeOH)	λ ($\Delta\varepsilon$): 200 (+0.9), 225 (–0.65), 250 nm (–0.25 $mol^{-1}dm^3cm^{-1}$)
$[\alpha]_D^{25}$	+14.6 (MeOH; *c* 0.0015))
LCESI-(+)-MS	*m/z* = 251.164 $[M + H]^+$
HRESI-(+)-MS	*m/z* = 251.16360 $[M + H]^+$, calculated 251.16472 for $[C_{15}H_{23}O_3]^+$
HRESI-(+)-MSMS	(Precursor ion *m/z* (%) = 251.16360 (18.5)), qTOF 20-50 eV) *m/z* (%) = 233.15323 (40.0), calculated 233.15415 for $[C_{15}H_{21}O_2]^+$; 215.14290 (35.5), calculated 215.14359 for $[C_{15}H_{19}O]^+$; 195.10133 (22.1), calculated 195.10212 for $[C_{11}H_{15}O_3]^+$
^{1}H-NMR	(600.22 MHz, 300 K, CD_3OD)*: δ_H = 7.34 (1 H, dddd appears as s, H-13), 7.23 (1 H, dddd appears as s, H-5), 4.59 (1 H, ddd appears as d, *J* = 7.0 Hz, H-8), 2.89 (1 H, dd, *J* = 1.3, 16.1 Hz, Hα-4), 2.70 (1 H, dd appears as d, *J* = 16.1 Hz, Hβ-4), 2.61 (1 H, dddd appears as quintet, *J* = 7.6, 7.6, 7.6, 7.6 Hz, H-9), 2.51 (1 H, ddd appears as dt, *J* = 7.8, 12.3, 12.3 Hz, H-2), 1.60 (1 H, dd, *J* = 7.3, 12.5 Hz, Hβ-1), 1.48 (2 H, d, *J* = 7.6 Hz, H-10), 1.40 (1 H, dd appears as t, *J* = 12.3, 12.3 Hz, Hα-1), 1.23 (3 H, H-12), 1.06 (3 H, H-14), 1.05 (3 H, H-15)
	(600.50 MHz, 297.2 K, $CDCl_3$)**: δ_H = 7.30 (1 H, s, H-13), 7.15 (1 H, dd appears as s, H-5), 4.60 (1 H, d, *J* = 5.1 Hz, H-8), 2.90 (1 H, d, *J* = 16.8 Hz, Hα-4), 2.71 (1 H, d, *J* = 16.8 Hz, Hβ-4), 2.70 (1 H, dddd, H-9), 2.55 (1 H, ddd appears as q, *J* = 9.4, 9.4, 9.4 Hz, H-2), 1.57 (1 H, dd, *J* =

7.9, 12.3 Hz, Hβ-1), 1.41 (1 H, dd, *J* = 6.8, 12.3 Hz, Hβ-10), 1.22 (3 H, s, H-12), 1.20 (1 H, dd, Hα-1), 1.17 (1 H, dd, Hα-10), 0.98 (3 H, s, H-14), 0.98 (3 H, s, H-15)

^{13}C-NMR (150.94 MHz, 300 K, CD_3OD)*: δ_C = 142.16 (C-5), 141.95 (C-13), 129.29 (C-7), 120.46 (C-6), 74.19 (C-3), 68.04 (C-8), 53.27 (C-2), 47.75 (C-9), 45.72 (C-10), 45.10 (C-1), 37.19 (C-11), 34.11 (C-4), 31.39 (C-12), 31.10 (C-14), 29.73 (C-15)

(151.01 MHz, 297.1 K, $CDCl_3$)**: δ_C = 141.65 (C-13), 141.12 (C-5), 126.96 (C-7), 118.87 (C-6), 74.02 (C-3), 67.23 (C-8), 51.05 (C-2), 46.03 (C-9), 45.12 (C-10), 45.06 (C-1), 36.75 (C-11), 33.11 (C-4), 31.51 (C-12), 30.15 (C-14), 28.20 (C-15)

*: These data are from the already extracted and measured compound from *L. circellatus*.
**: These data are from the compound that was extracted from *L. trivialis*.

6.5.1.11 Furan alcohol **28**

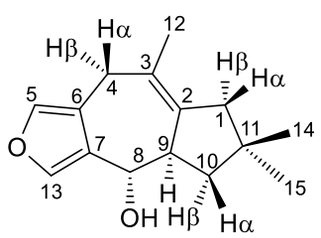

28

HPLC R_t = 39.86 min / analytical - gradient at section 6.3.4.2

UV/Vis (H_2O/MeOH) λ_{max} (log ε): 200 nm (0.8 $mol^{-1}dm^3cm^{-1}$)

CD (MeOH) λ (Δε): 205 (+5.0), 250 (–0.5), 300 nm (–1.2 $mol^{-1}dm^3cm^{-1}$)

$[\alpha]_D^{25}$ +5.4 (MeOH; *c* 0.0017)

LCESI-(+)-MS *m/z* = 233.153 $[M + H]^+$

HRESI-(+)-MS *m/z* = 233.15330 $[M + H]^+$, calculated 233.15415 for $[C_{15}H_{21}O_2]^+$

HRESI-(+)-MSMS (Precursor ion *m/z* (%) = 233.15330 (22.2)), qTOF 20-50 eV) *m/z* (%) = 215.14229 (4.0), calculated 215.14359 for $[C_{15}H_{19}O]^+$; 187.14821 (6.5), calculated 187.14868 for $[C_{14}H_{19}]^+$; 177.09027 (3.5), calculated 177.09155 for $[C_{11}H_{13}O_2]^+$

^{1}H-NMR (600.22 MHz, 300 K, CD_3OD)*: δ_H = 7.36 (1 H, H-13), 7.17 (1 H, H-5), 4.30 (1 H, H-8), 3.37 (1 H, Hβ-4), 2.96 (1 H, Hα-4), 2.93 (1 H, H-9), 2.20 (1 H, Hβ-1), 2.06 (1 H, Hα-1), 1.90 (1 H, Hβ-10), 1.73 (3 H, H-12), 1.57 (1 H, Hα-10), 1.13 (3 H, H-14), 0.90 (3 H, H-15)

^{13}C-NMR (150.94 MHz, 300 K, CD_3OD)*: δ_C = 141.98 (C-13), 139.08 (C-5), 138.34 (C-2), 130.61 (C-6,7), 128.96 (C-3), 122.36 (C-6,7), 71.05 (C-8), 49.44 (C-9), 47.40 (C-10), 47.24 (C-1), 38.02 (C-11), 30.33 (C-4), 29.35 (C-14), 27.91 (C-15), 21.87 (C-12)

*: These data are from the already extracted and measured compound from *L. circellatus*.

6.5.1.12 Methoxyfuranalcohol **29**

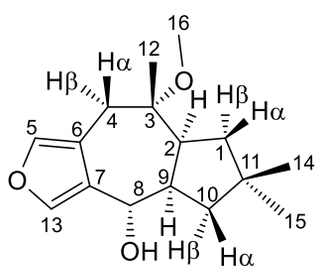

29

^{1}H-NMR (600.22 MHz, 297.2 K, CD_3OD)*: δ_H = 7.31 (1 H, H-13), 7.25 (1 H, H-5), 4.56 (1 H, H-8), 3.15 (3 H, H-16), 2.86 (1 H, Hβ-4), 2.68 (1 H, Hα-4), 2.460 (1 H, H-9), 1.73 (1 H, Hα-10), 1.62 (1 H, Hβ-1), 1.54 (1 H, Hα-1), 1.45 (1 H, Hβ-10), 1.21 (3 H, H-12), 1.12 (3 H, H-14), 1.07 (3 H, H-15)

^{13}C-NMR (150.94 MHz, 297.2 K, CD_3OD)*: δ_C = 141.59 (C-5), 141.18 (C-13), 130.64 (C-7), 120.19 (C-6), 79.23 (C-3), 67.76 (C-8), 52.14 (C-2), 48.95 (C-16), 48.44 (C-9), 45.20 (C-10), 44.26 (C-1), 36.64 (C-11), 31.87 (C-14), 31.18 (C-15), 29.28 (C-4), 25.06 (C-12)

*: These data are from the compound that extracted again and measured from *L. circellatus*.

6.5.1.13 3,8-Oxalactarorufin A (**30**)

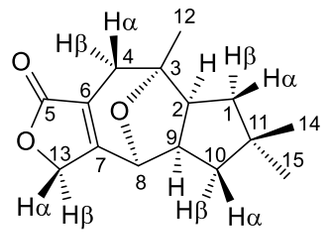

30

HPLC	R_t = 30.81 min / analytical - gradient at section 6.3.4.2
UV/Vis (H_2O/MeOH)	λ_{max} (log ε): 200 nm (0.7 $mol^{-1}dm^3cm^{-1}$)
CD (MeOH)	λ ($\Delta\varepsilon$): 210 (+5.1), 230 (–4.5), 245 nm (+1.9 $mol^{-1}dm^3cm^{-1}$)
$[\alpha]_D^{25}$	+23.7 (MeOH; *c* 0.00061)
LCESI-(+)-MS	*m/z* = 249.148 $[M + H]^+$
HRESI-(+)-MS	*m/z* = 249.14686 $[M + H]^+$, calculated 249.14907 for $[C_{15}H_{21}O_3]^+$
HRESI-(+)-MSMS	(Precursor ion *m/z* (%) = 249.14686 (88.2)), qTOF 20-50 eV) *m/z* (%) = 231.13699 (61.1), calculated 231.13850 for $[C_{15}H_{19}O_2]^+$; 221.15221 (60.0), calculated 221.15415 for $[C_{14}H_{21}O_2]^+$; 213.12635 (20.0), calculated 213.12794 for $[C_{15}H_{17}O]^+$; 203.14159 (79.0), calculated 203.14359 for $[C_{14}H_{19}O]^+$; 185.13157 (78.2), calculated 185.13303 for $[C_{14}H_{17}]^+$
^{1}H-NMR	(600.22 MHz, 300 K, CD_3OD)*: δ_H = 4.93 (1 H, Hβ-13), 4.85 (1 H, Hα-13), 4.69 (1 H, H-8), 3.35 (1 H, H-9), 2.85 (1 H, H-2), 2.33 (2 H, H-4), 1.50 (1 H, Hβ-10), 1.45 (3 H, H-12), 1.44 (1 H, Hβ-1), 1.010 (3 H, H-15), 1.007 (3 H, H-14), 0.97 (1 H, Hα-10), 0.90 (1 H, Hα-1)
	(600.50 MHz, 297.1 K, $CDCl_3$)**: δ_H = 4.83 (1 H, Hβ-13), 4.74 (1 H, Hα-13), 4.61 (1 H, H-8), 3.33 (1 H, H-9), 2.82 (1 H, H-2), 2.44 (1 H, Hβ-4), 2.34 (1 H, Hα-4), 1.48 (3 H, H-12), 1.45 (1 H, Hβ-10), 1.41 (1 H, Hβ-1), 1.00 (3 H, H-14), 0.98 (3 H, H-15), 0.90 (1 H, Hα-1), 0.89 (1 H, Hα-10)

^{13}C-NMR	(150.94 MHz, 300 K, CD_3OD)*: δ_C = 175.04 (C-5), 168.68 (C-7), 125.05 (C-6), 81.88 (C-3), 75.95 (C-8), 73.39 (C-13), 57.16 (C-2), 55.50 (C-9), 47.74 (C-11), 43.17 (C-1), 40.98 (C-10), 31.98 (C-4), 29.45 (C-14), 27.87 (C-12), 27.36 (C-15)
	(151.01 MHz, 297.1 K, $CDCl_3$)**: δ_C = 172.75 (C-5), 165.62 (C-7), 124.92 (C-6), 80.82 (C-3), 74.74 (C-8), 71.32 (C-13), 55.98 (C-2), 54.22 (C-9), 47.16 (C-11), 42.08 (C-1), 40.07 (C-10), 31.36 (C-4), 29.19 (C-14), 27.82 (C-12), 27.14 (C-15)

*: These data are from the already extracted and measured compound from *L. circellatus*.
**: These data are from the same compound with repeated measurements in different solvent.

6.5.1.14 Lactarorufin N (**13**)

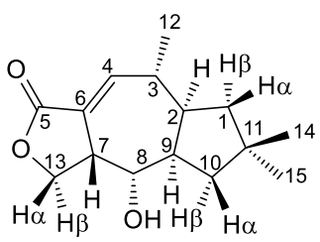

13

HPLC	R_t = 37.03 min / analytical - gradient at section 6.3.4.2
UV/Vis (H_2O/MeOH)	λ_{max} (log ε): 200 (0.9), 225 nm (0.55 $mol^{-1}dm^3cm^{-1}$)
CD (MeOH)	λ ($\Delta\varepsilon$): 200 (+0.3), 240 nm (–1.19 $mol^{-1}dm^3cm^{-1}$)
$[\alpha]_D^{25}$	–66.8 (MeOH; *c* 0.001)
LCESI-(+)-MS	*m/z* = 251.164 $[M + H]^+$, 523.303 $[2M + Na]^+$
HRESI-(+)-MS	*m/z* = 251.16425 $[M + H]^+$, calculated 251.16472 for $[C_{15}H_{23}O_3]^+$
HRESI-(+)-MSMS	(Precursor ion *m/z* (%) = 251.16425 (83.4)), qTOF 20-50 eV) *m/z* (%) = 233.15363 (41.5), calculated 233.15415 for $[C_{15}H_{21}O_2]^+$; 215.14283 (11.0), calculated 215.14359 for $[C_{15}H_{19}O]^+$; 195.10147 (52.6), calculated 195.10212 for $[C_{11}H_{15}O_3]^+$; 169.08577 (36.8), calculated 169.08647 for $[C_9H_{13}O_3]^+$

^{1}H-NMR

(600.22 MHz, 300 K, CD_3OD)*: δ_H = 6.62 (1 H, dd, *J* = 3.2, 5.6 Hz, H-4), 4.44 (1 H, dd appears as t, *J* = 9.0, 9.0 Hz, Hα-13), 4.18 (1 H, dd appears as t, *J* = 7.6, 8.8 Hz, Hβ-13), 3.92 (1 H, dd, *J* = 4.5, 7.0 Hz, H-8), 3.67 (1 H, dddd appears as m, H-7), 2.60 (1 H, m, H-3), 2.41 (1 H, qd, *J* = 7.5, 7.5, 10.0 Hz, H-9), 2.14 (1 H, qd, *J* = 7.3, 7.3, 10.7 Hz, H-2), 1.61 (2 H, d, *J* = 8.9 Hz, H-10), 1.49 (2 H, dd, *J* = 3.6, 6.8 Hz, H-1), 1.16 (3 H, d, *J* = 6.8 Hz, H-12), 1.11 (3 H, s, H-14), 1.01 (3 H, s, H-15)

(600.50 MHz, 297.1 K, $CDCl_3$)**: δ_H = 6.73 (1 H, dd, *J* = 3.2, 5.6 Hz, H-4), 4.46 (1 H, dd appears as t, *J* = 9.1, 9.1 Hz, Hα-13), 4.20 (1 H, dd appears as t, *J* = 8.4, 8.4 Hz, Hβ-13), 4.00 (1 H, dddd appears as m, H-8), 3.65 (1 H, dddd appears as m, H-7), 2.53 (1 H, ddd appears as m, H-3), 2.44 (1 H, dddd appears as qd, *J* = 7.7, 7.7, 7.7, 10.0 Hz, H-9), 2.12 (1 H, dddd appears as qd, *J* = 7.9, 7.9, 7.9, 10.0 Hz, H-2), 1.66 (1 H, dd, *J* = 7.7, 12.6 Hz, Hβ-10), 1.52 (1 H, dd, *J* = 6.7, 13.0 Hz, Hβ-1), 1.44 (1 H, dd, *J* = 10.1, 12.6 Hz, Hα-10), 1.40 (1 H, dd, *J* = 8.4, 12.9 Hz, Hα-1), 1.15 (3 H, d, *J* = 6.8 Hz, H-12), 1.10 (3 H, s, H-14), 1.00 (3 H, s, H-15)

^{13}C-NMR

(150.94 MHz, 300 K, CD_3OD)*: δ_C = 173.73 (C-5), 147.02 (C-4), 129.29 (C-6), 70.95 (C-8), 69.77 (C-13), 46.48 (C-9), 46.48 (C-1), 45.89 (C-2), 45.05 (C-10), 42.77 (C-7), 36.70 (C-11), 34.50 (C-3), 31.40 (C-14), 30.32 (C-15), 20.05 (C-12)

(151.01 MHz, 297.2 K, $CDCl_3$)**: δ_C = 171.19 (C-5), 146.27 (C-4), 127.35 (C-6), 70.90 (C-8), 67.96 (C-13), 45.58 (C-1), 44.77 (C-2), 44.71 (C-9), 44.33 (C-10), 41.78 (C-7), 36.28 (C-11), 33.50 (C-3), 30.98 (C-14), 29.51 (C-15), 19.83 (C-12)

*: These data are from the already extracted and measured compound from *L. circellatus*.
**: These data are from the same compound with repeated measurements in different solvent.

6.5.1.15 Blennin C (**18**)

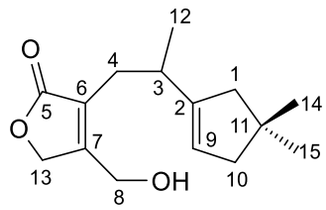

18

HPLC	R_t = 36.94 min / analytical - gradient at section 6.3.4.2
$[\alpha]_D^{25}$	–20.7 (MeOH; *c* 0.002)
LCESI-(+)-MS	*m/z* = 251.164 $[M + H]^+$, 523.302 $[2M + Na]^+$
HRESI-(+)-MS	*m/z* = 251.16285 $[M + H]^+$, calculated 251.16472 for $[C_{15}H_{23}O_3]^+$
HRESI-(+)-MSMS	(Precursor ion *m/z* (%) = 251.16285 (80.0)), qTOF 20-50 eV) *m/z* (%) = 233.15251 (32.0), calculated 233.15415 for $[C_{15}H_{21}O_2]^+$; 215.14178 (9.4), calculated 215.14359 for $[C_{15}H_{19}O]^+$
^{1}H-NMR	(600.22 MHz, 300.1 K, CD_3OD)*: δ_H = 5.22 (1 H, H-9), 4.85 (2 H, H-13), 4.52 (2 H, H-8), 2.56 (1 H, H-3), 2.41 (1 H, H-4), 2.21 (1 H, H-4), 2.10 (2 H, H-1), 2.08 (2 H, H-10), 1.07 (3 H, H-14,15), 1.06 (3 H, H-14,15), 0.99 (3 H, H-12) (600.50 MHz, 297.2 K, $CDCl_3$)**: δ_H = 5.17 (1 H, H-9), 4.84 (2 H, H-13), 4.56 (2 H, H-8), 2.50 (1 H, H-3), 2.36 (1 H, H-4), 2.13 (1 H, H-4), 2.04 (2 H, H-1,10), 2.04 (2 H, H-1,10), 1.02 (3 H, H-14,15), 1.01 (3 H, H-14,15), 0.93 (3 H, H-12)
^{13}C-NMR	(150.94 MHz, 300 K, CD_3OD)*: δ_C = 177.27 (C-5), 163.59 (C-7), 148.08 (C-2), 126.18 (C-6), 123.01 (C-9), 72.00 (C-13), 58.00 (C-8), 48.37 (C-10), 48.29 (C-1), 39.10 (C-11), 35.50 (C-3), 30.38 (C-4), 30.22 (C-14), 30.22 (C-15), 19.42 (C-12) (151.01 MHz, 297.2 K, $CDCl_3$)**: δ_C = 175.69 (C-5), 161.37 (C-7), 146.55 (C-2), 125.43 (C-6), 122.01 (C-9), 70.89 (C-13), 57.57 (C-8),

47.53 (C-1,10), 47.37 (C-1,10), 38.15 (C-11), 34.02 (C-3), 29.87 (C-14,15), 29.82 (C-14,15), 29.58 (C-4), 18.95 (C-12)

*: These data are from the already extracted and measured compound from *L. circellatus*.
**: These data are from the same compound with repeated measurements in different solvent.

6.5.1.16 3,12-Anhydrolactarorufin A (**31**)

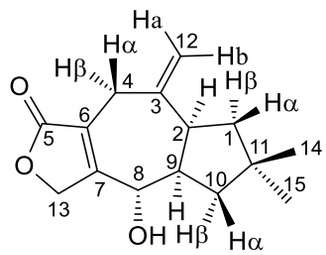

31

HPLC	R_t = 34.81 min / analytical - gradient at section 6.3.4.2
UV/Vis (H_2O/MeOH)	λ_{max} (log ε): 200 (0.7), 220 nm (0.35 $mol^{-1}dm^3cm^{-1}$)
CD (MeOH)	λ ($\Delta\varepsilon$): 200 (+0.6), 220 (–2.2), 235 (–1.0), 260 nm (–0.3 $mol^{-1}dm^3cm^{-1}$)
$[\alpha]_D^{25}$	+22.6 (MeOH; *c* 0.001)
LCESI-(+)-MS	*m/z* = 249.148 $[M + H]^+$, 498.296 $[2M + H]^+$
HRESI-(+)-MS	*m/z* = 249.14778 $[M + H]^+$, calculated 249.14907 for $[C_{15}H_{21}O_3]^+$
HRESI-(+)-MSMS	(Precursor ion *m/z* (%) = 249.14778 (37.1)), qTOF 20-50 eV) *m/z* (%) = 231.13674 (42.6), calculated 231.13850 for $[C_{15}H_{19}O_2]^+$; 213.12739 (19.0), calculated 213.12794 for $[C_{15}H_{17}O]^+$; 203.14193 (78.1), calculated 203.14359 for $[C_{14}H_{19}O]^+$; 175.14742 (40.0), calculated 175.14868 for $[C_{13}H_{19}]^+$
^{1}H-NMR	(600.22 MHz, 300 K, CD_3OD)*: δ_H = 5.00 (1 H, s, Ha-12), 4.95 (1 H, s, Hb-12), 4.88 (1 H, dd appears as d, *J* = 18.2 Hz, H-13), 4.80 (1 H, dtd appears as d, *J* = 1.3, 2.7, 18.2 Hz, H-13), 4.39 (1 H, dddd appears as dq, *J* = 1.6, 11.3 Hz, H-8), 3.15 (1 H, ddt appears as d, *J* = 1.8, 3.1, 17.3 Hz, Hβ-4), 3.00 (1 H, ddd appears as td, *J* = 6.9, 11.2, 11.6 Hz, H-2),

2.92 (1 H, dd appears as d, *J* = 17.2 Hz, Hα-4), 2.71 (1 H, dddd appears as tdd, *J* = 7.4, 9.1, 10.9 Hz, H-9), 1.74 (1 H, dd appears as t, *J* = 11.5, 11.5 Hz, Hα-1), 1.74 (1 H, dd, *J* = 6.0, 12.7 Hz, Hβ-10), 1.61 (1 H, ddd, *J* = 2.4, 6.9, 12.4 Hz, Hβ-1), 1.52 (1 H, dd, *J* = 9.2, 13.0 Hz, Hα-10), 1.15 (3 H, s, H-14), 1.04 (3 H, s, H-15)

(600.22 MHz, 297.1 K, DMSO-d6)**: δH = 4.98 (1 H, s, Ha-12), 4.88 (1 H, s, Hb-12), 4.81 (1 H, H-13), 4.75 (1 H, H-13), 4.23 (1 H, dddd appears as d, *J* = 11.3 Hz, H-8), 3.05 (1 H, ddt appears as d, *J* = 17.2 Hz, Hβ-4), 2.91 (1 H, H-2), 2.87 (1 H, dd appears as d, *J* = 17.6 Hz, Hα-4), 2.62 (1 H, H-9), 1.64 (1 H, dd appears as t, *J* = 11.8, 11.8 Hz, Hα-1), 1.62 (1 H, ddd, *J* = 2.0, 7.5, 13.1 Hz, Hβ-10), 1.51 (1 H, ddd, *J* = 2.1, 6.9, 12.3 Hz, Hβ-1), 1.45 (1 H, dd, *J* = 9.2, 12.9 Hz, Hα-10), 1.10 (3 H, s, H-14), 0.97 (3 H, s, H-15)

^{13}C-NMR

(150.94 MHz, 300 K, CD_3OD)*: δ_C = 176.80 (C-5), 167.93 (C-7), 146.51 (C-3), 124.12 (C-6), 112.57 (C-12), 72.01 (C-13), 70.80 (C-8), 50.76 (C-9), 46.22 (C-10), 45.79 (C-2), 45.43 (C-1), 38.32 (C-11), 36.49 (C-4), 29.99 (C-14), 27.65 (C-15)

(150.94 MHz, 297.2 K, DMSO-d6)**: δ_C = 173.85 (C-5), 166.59 (C-7), 145.21 (C-3), 121.77 (C-6), 111.79 (C-12), 70.19 (C-13), 68.52 (C-8), 48.89 (C-9), 44.94 (C-10), 43.83 (C-1), 43.81 (C-2), 36.90 (C-11), 33.05 (C-4), 29.49 (C-14), 27.09 (C-15)

*: These data are from the already extracted and measured compound from *L. circellatus*.
**: These data are from the same compound with repeated measurements in different solvent.

6.5.1.17 15-Hydroxyblennin A (**34**)

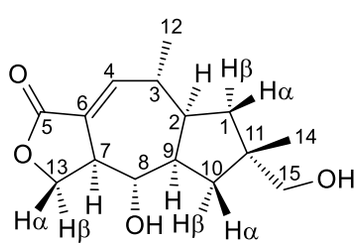

34

Colorless oil - 0.5 mg from 300 g from the flesh of the frozen fruiting bodies.

HPLC	R_t = 23.00 min / analytical - gradient at section 6.3.4.2 R_t = 31.67 min / semi-preparative - gradient at section 6.3.4.1
UV/Vis (H_2O/MeOH)	λ_{max} (log ε): 227 nm (1.5 $mol^{-1}dm^3cm^{-1}$)
CD (MeOH)	λ ($\Delta\varepsilon$): 205 (–1.6), 220 (–0.5), 250 nm (+0.55 $mol^{-1}dm^3cm^{-1}$)
$[\alpha]_D^{25}$	+19.2 (MeOH; *c* 0.0005)
LCESI-(+)-MS	*m/z* = 267.159 $[M + H]^+$, 533.311 $[2M + H]^+$
HRESI-(+)-MS	*m/z* = 267.15912 $[M + H]^+$, calculated 267.15963 for $[C_{15}H_{23}O_4]^+$
HRESI-(+)-MSMS	(Precursor ion *m/z* (%) = 267.15912 (18.5)), qTOF 20-50 eV) *m/z* (%) = 249.14852 (40.0), calculated 249.14907 for $[C_{15}H_{21}O_3]^+$; 231.13799 (35.5), calculated 231.13850 for $[C_{15}H_{19}O_2]^+$; 219.13797 (22.1), calculated 219.13850 for $[C_{14}H_{19}O_2]^+$; 203.14302 (27.4), calculated 203.14360 for $[C_{14}H_{19}O]^+$; 189.09098 (25.3), calculated 189.09160 for $[C_{12}H_{13}O_2]^+$; 185.13249 (35.6), calculated 185.13300 for $[C_{14}H_{17}]^+$
^{1}H-NMR	(600.22 MHz, 297.2 K, CD_3OD): δ_H = 6.69 (1 H, dd appears as t, *J* = 3.0, 3.0 Hz, H-4), 4.50 (1 H, dd appears as t, *J* = 9.1, 9.1 Hz, Hβ-13), 4.11 (1 H, dd appears as t, *J* = 9.0, 9.0 Hz, Hα-13), 3.51 (1 H, dd appears as t, *J* = 10.0, 10.0 Hz, H-8), 3.36 (1 H, dddd, H-7), 3.32 & 3.27 (2 H, AB, *J* = 10.6, 10.6 Hz, H-15), 2.54 (1 H, dddd, H-3), 2.29 (1 H, dddd appears as tt, *J* = 7.0, 10.0 Hz, H-9), 2.12 (1 H, dddd, *J* = 4.9, 7.2, 12.0 Hz, H-2), 2.04 (1 H, dd, *J* = 6.9, 13.2 Hz, Hβ-10), 1.76 (1 H, dd, *J* = 7.6, 13.8 Hz, Hβ-1), 1.47 (1 H, dd, *J* = 4.9, 13.8 Hz, Hα-1), 1.36 (1 H, dd, *J* = 10.6, 13.3 Hz, Hα-10), 1.17 (3 H, d, *J* = 7.3 Hz, H-12), 1.10 (3 H, s, H-14) (600.22 MHz, 297.2 K, $CDCl_3$): δ_H = 6.75 (1 H, dd appears as t, *J* = 3.0, 3.0 Hz, H-4), 4.54 (1 H, dd appears as t, *J* = 9.2, 9.2 Hz, Hβ-13), 4.13 (1 H, dd appears as t, *J* = 8.9, 8.9 Hz, Hα-13), 3.62 (1 H, dd appears as t, *J* = 10.0, 10.0 Hz, H-8), 3.40 & 3.36 (2 H, AB, *J* = 10.4, 10.4 Hz, H-15),

3.32 (1 H, dddd, H-7), 2.47 (1 H, dddd, H-3), 2.29 (1 H, dddd appears as tt, *J* = 7.3, 10.2 Hz, H-9), 2.14 (1 H, dddd, *J* = 5.0, 7.5, 10.0 Hz, H-2), 2.07 (1 H, dd, *J* = 6.8, 13.0 Hz, Hβ-10), 1.77 (1 H, dd, *J* = 7.7, 13.9 Hz, Hβ-1), 1.47 (1 H, dd, *J* = 5.0, 14.0 Hz, Hα-1), 1.33 (1 H, dd, *J* = 11.0, 12.9 Hz, Hα-10), 1.17 (3 H, d, *J* = 7.3 Hz, H-12), 1.12 (3 H, s, H-14)

^{13}C-NMR (151.01 MHz, 297.2 K, CD_3OD): δ_C = 174.12 (C-5), 147.43 (C-4), 128.67 (C-6), 76.18 (C-8), 71.50 (C-15), 70.82 (C-13), 52.82 (C-9), 45.89 (C-2), 45.50 (C-7), 42.87 (C-11), 41.66 (C-1), 40.97 (C-10), 34.86 (C-3), 26.92 (C-14), 20.58 (C-12)

(151.01 MHz, 297.2 K, $CDCl_3$): δ_C = 171.88 (C-5), 146.28 (C-4), 126.97 (C-6), 75.88 (C-8), 71.08 (C-15), 69.27 (C-13), 52.03 (C-9), 44.63 (C-2), 44.30 (C-7), 42.11 (C-11), 40.77 (C-1), 39.78 (C-10), 33.92 (C-3), 26.41 (C-14), 20.43 (C-12)

6.5.1.18 Blennione (**35**)

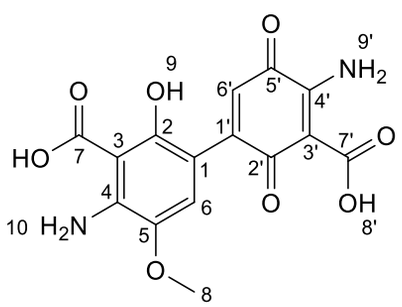

35

Organism	*Activity
Escherichia coli	–
Azospirillum brasilense	–
Bacillus megaterium	–

*: Applying 1.0 µmol from the compound.

Green solid - 0.35 mg from 28 g from the skin of the frozen fruiting bodies of *L. blennius*. 1.74 mg from 11 g from the skin of the frozen fruiting bodies of *L. circellatus*.

HPLC R_t = 23.5 min / analytical - gradient at section 6.3.4.5

UV/Vis (H_2O/MeOH)	λ_{max} (log ε): 252, 342, 426 and 672 nm
LCESI-(–)-MS	*m/z* = 347 $[M - H]^+$
^{1}H-NMR	(600.51 MHz, 294.7 K, DMSO-d6): δ_H = 18.94 (1 H, s, H-9 (OH)), 14.21 (1 H, s, H-8' (OH)), 9.67 (1 H, s, H-9' (NH)), 9.08 (1 H, s, H-9' (NH)), 9.03 (1 H, by integration, H-10 (NH)), 7.52 (1 H, s, H-6'), 7.12 (1 H, s, H-6), 6.25 (1 H, s, H-10 (NH)), 3.69 (3 H, s, H-8)
^{13}C-NMR	(151.01 MHz, 2947 K, DMSO-d6): δ_C = 188.42 (C-2'), 177.62 (C-5'), 173.43 (C-7), 169.07 (C-7'), 167.49 (C-2), 154.69 (C-4'), 147.14 (C-4), 146.49 (C-1'), 137.97 (C-5), 122.74 (C-6'), 116.21 (C-6), 106.12 (C-1), 100.62 (C-3), 96.15 (C-3'), 55.97 (C-8)

6.5.2 Compounds Isolated from *Lactarius trivialis*

6.5.2.1 Trivialine A (**47**)

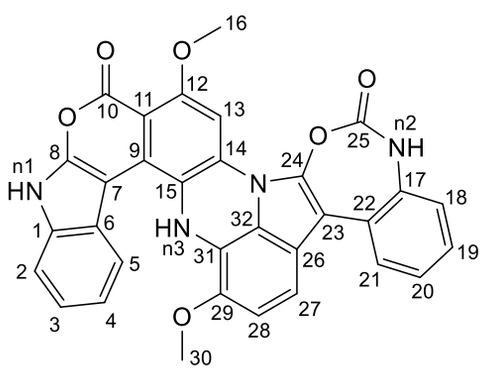

Proposed structure **2** of **47**

Organism	*Activity
Escherichia coli	–
Aspergillus restrictus	–
Bacillus subtilis	–
Bacillus megaterium	–
Bacillus pumilus	–

*: Applying 1.0 µmol from the compound.

Yellow solid - 3.5 mg from the skin of 1611 g of the frozen fruiting bodies.

HPLC	R_t = 46.00 min / analytical - (low resolution) gradient at section 6.3.4.3 R_t* = 33.40 and 34.00 min / analytical - (high resolution) gradient at section 6.3.4.3 R_t = 47.00 min / semi-preparative - gradient at section 6.3.4.3
UV/Vis (H_2O/MeCN)	λ_{max} (%): 238 (60), 314 (70), 442 nm (90)
LCESI-(+)-MS	*m/z* = 557.02 $[M + H]^+$
HRESI-(+)-MS*	*m/z* = 557.14499 $[M + H]^+$, calculated 557.14611 for $[C_{32}H_{21}N_4O_6]^+$
HRESI-(+)-MSMS	(Precursor ion *m/z* (%) = 557.14499 (80.1)), qTOF 20-50 eV) *m/z* (%) = 293.09162 (18.3), calculated 293.09262 for $[C_{17}H_{13}N_2O_3]^+$; 277.06032 (38.0), calculated 277.06132 for $[C_{16}H_9N_2O_3]^+$; 265.06040 (35.0), calculated 265.06132 for $[C_{15}H_9N_2O_3]^+$; 249.06552 (15.0), calculated 2249.06640 for $[C_{15}H_9N_2O_2]^+$
^{1}H-NMR	(600.22 MHz, 297.1 K, DMSO-d6): δ_H = 12.33 (1 H, s, NH-n2), 12.28 (1 H, s, NH-n1), 9.97 (1 H, s, NH-n3), 8.10 (1 H, d**, H-21), 7.98 (1 H, d, *J* = 8.3 Hz, H-5), 7.5973 (1 H, d, *J* = 8.5 Hz, H-27), 7.5890 (1 H, d, *J* = 8.5 Hz, H-28), 7.48 (1 H, d**, H-18), 7.36 (1 H, d, *J* = 7.9 Hz, H-2), 7.2706 (1 H, dd**, H-20), 7.2667 (1 H, dd**, H-19), 7.06 (1 H, dt, *J* = 0.8, 7.6, 7.6, Hz, H-3), 6.87 (1 H, dt, *J* = 0.9, 7.8, 7.8 Hz, H-4), 6.83 (1 H, s, H-13), 3.74 (3 H, s, H-16), 3.58 (3 H, s, H-30)
^{13}C-NMR	(150.94 MHz, 297.1 K, DMSO-d6): δ_C = 162.94 (C-25), 162.09 (C-10), 146.63 (C-8), 146.41 (C-24), 145.37 (C-29), 142.31 (C-12), 141.20 (C-15), 139.51 (C-31), 132.00 (C-17), 131.89 (C-1), 131.12 (C-32), 123.06 (C-14), 122.85 (C-5), 122.65 (C-28), 122.41 (C-6), 121.93 (C-19), 121.59 (C-22), 121.30 (C-11), 121.07 (C-3), 120.98 (C-20), 119.97 (C-4), 119.14 (C-21), 113.16 (C-13), 111.95 (C-18), 111.32 (C-2), 111.00 (C-27), 103.63 (C-26), 98.20 (C-9), 90.83 (C-23), 89.67 (C-7), 56.57 (C-30), 56.02 (C-16)
^{15}N-HMBC	(600.50, 60.85 MHz, 297.2 K, DMSO-d6): $^1J_{H\text{-}N}$ = 12.33-121.7 (NH-n2), 12.28-122.9 (NH-n1), 9.97-90.1 (NH-n3). $^3J_{H\text{-}N}$ = 6.83-90.1.

*: The fraction was measured after four weeks of isolation resulting in a certain degree of degradation.
**: The signals shapes are disturbed with signals from the other isomer. COSY spectrum shows clear coupling correlations.

6.5.2.2 Trivialine B (**48**)

Violet solid - 0.4 mg from the skin of 1611 g of the frozen fruiting bodies.

HPLC	R_t = 38.76 min / analytical (low resolution) - gradient at section 6.3.4.3 R_t* = 33.50 min / analytical (high resolution) - gradient at section 6.3.4.3 R_t = 37.30 min / semi-preparative - gradient at section 6.3.4.3
UV/Vis (H_2O/MeCN)	λ_{max} (%): 210 (90), 248 (80), 280 (70), 399 (25), 549 nm (35)
LCESI-(+)-MS	*m/z* = 557.10 $[M + H]^+$
HRESI-(+)-MS	*m/z* = 557.14480 $[M + H]^+$ and 579.12698 $[M + Na]^+$, calculated 579.12805 for $[C_{32}H_{20}N_4O_6Na]^+$
HRESI-(+)-MSMS	(Precursor ion *m/z* (%) = 557.14480 (95.1) calculated 557.14611 for $[C_{32}H_{21}N_4O_6]^+$), qTOF 20-50 eV) *m/z* (%) = 293.09156 (25.2), calculated 293.09262 for $[C_{17}H_{13}N_2O_3]^+$; 277.06016 (35.2), calculated 277.06132 for $[C_{16}H_9N_2O_3]^+$; 265.06027 (30.0), calculated 265.06132 for $[C_{15}H_9N_2O_3]^+$; 249.06563 (20.2), calculated 249.06640 for $[C_{15}H_9N_2O_2]^+$; 222.05478 (20.0), calculated 222.05550 for $[C_{14}H_8NO_2]^+$
^{1}H-NMR	(600.22 MHz, 296.7 K, DMSO-d6): δ_H = 12.27 (1 H, broad signal, NH,OH), 10.19 (1 H, s, NH,OH), 9.52 (1 H, broad signal, NH,OH), 8.60 (1 H, d, *J* = 8.0 Hz), 8.14 (1 H, d, *J* = 7.6 Hz), 8.00 (1 H, d, *J* = 8.7 Hz), 7.76 (1 H, d, *J* = 8.7 Hz), 7.46 (1 H, d, *J* = 7.6 Hz), 7.35 (1 H, d, *J* = 7.6 Hz), 7.27 (1 H, dd appears as t, *J* = 7.3, 7.3 Hz), 7.25 (1 H, dd), 7.24 (1 H, dd), 6.94 (1 H, dd, appears as t, *J* = 7.7, 7.7 Hz), 5.91 (1 H, s), 3.81 (3 H, s), 3.69 (3 H, s)
^{13}C-NMR	(151.01 MHz, 297.1 K, DMSO-d6): δ_C = 166.33, 161.84, 158.23, 156.74, 154.08, 153.30, 152.23, 147.50, 143.14, 141.90, 137.84, 132.23, 131.04, 129.17, 128.78, 126.88, 125.84, 122.93, 122.01, 121.96, 121.16, 120.92, 119.20, 118.92, 117.75, 114.83, 112.19, 106.47, 101.26, 90.32, 56.96, 56.89

*: The fraction was measured after four weeks of isolation resulting in a certain degree of degradation.

6.5.2.3 Trivialine C (**49**)

Yellow solid - 1.0 mg from the skin of 1611 g of the frozen fruiting bodies.

HPLC	R_t = 34.80 min / analytical - (low resolution) gradient at section 6.3.4.3 R_t* = 32.50 min / analytical - (high resolution) gradient at section 6.3.4.3 R_t = 34.00 min / semi-preparative - gradient at section 6.3.4.3
UV/Vis (H_2O/MeCN)	λ_{max} (%): 255 (80), 360 shoulder (360), 433 nm (35)
LCESI-(+)-MS	*m/z* = 575.03 $[M + H]^+$
HRESI-(+)-MS	*m/z* = 575.15571 $[M + H]^+$ and 597.13744 $[M + Na]^+$, calculated 597.13862 for $[C_{32}H_{22}N_4O_7Na]^+$
HRESI-(+)-MSMS	(Precursor ion *m/z* (%) = 575.15571 (70.1)), qTOF 20-50 eV) *m/z* 471.14479 (85.1), calculated 471.14571 for $[C_{29}H_{19}N_4O_3]^+$; 428.12310 (90.0), calculated 428.12464 for $[C_{24}H_{18}N_3O_5]^+$; 251.08100 (10.0), calculated 251.08205 for $[C_{15}H_{11}N_2O_2]^+$
^{1}H-NMR**	(600.51 MHz, 297.2 K, DMSO-d6): δ_H = 12.15 (1 H, s, NH), 8.02 (1H), 7.98 (1 H, d***), 7.44 (1H), 7.23 (2H), 7.42 (1 H, d***), 7.29 (1 H, d, *J* = 8.25 Hz), 7.20 (2 H****, dd***), 7.15 (1 H, d, J = 8.25 Hz), 6.64 (1H), 5.86 (1 H, s), 3.88 (3 H, s), 3.73 (3 H, s)
^{13}C-NMR**	(151.01 MHz, 297.1 K, DMSO-d6)*****: δ_C = 162.62, 147.13, 144.22, 143.02, 132.33, 129.44, 121.99, 121.74, 121.31, 121.17, 119.48, 117.52, 112.35, 112.21, 110.52, 106.30, 98.95, 90.98, 56.72, 56.55

*: The fraction was measured after four weeks of isolation resulting in a certain degree of degradation.
**: The reported chemical shifts are less than the expected in accordance to the calculated molecular formula.
***: The signals shapes are disturbed with the signals from the other isomer, with clear couplings in COSY spectrum.
****: Numbers of hydrogen atoms according to integration.
*****: The chemical shifts of ^{13}C are extracted from ^{13}C, DEPT135, and HMBC NMR experiments.

6.5.2.4 Trivialine D (**50**)

Peach colored solid - 1.8 mg from the skin of 1611 g of the frozen fruiting bodies.

HPLC	R_t = 31.65 min / analytical (low resolution) - gradient at section 6.3.4.3 R_t* = 23.50 min / analytical (high resolution) - gradient at section 6.3.4.3 R_t = 32.00 min / semi-preparative - gradient at section 6.3.4.3
UV/Vis (H_2O/MeCN)	λ_{max} (%): 250 (55), 271 (50), 300 (40), 394 (30), 520 nm (30)
LCESI-(+)-MS	*m/z* = 573.12 $[M + H]^+$
HRESI-(+)-MS	*m/z* = 573.14084 $[M + H]^+$, calculated 573.14102 for $[C_{32}H_{21}N_4O_7]^+$
HRESI-(+)-MSMS	(Precursor ion *m/z* (%) = 573.14084 (95.0)), qTOF 20-50 eV) *m/z* (%) = 293.09172 (17.3), calculated 293.09262 for $[C_{17}H_{13}N_2O_3]^+$; 280.08400 (20.7), calculated 280.08479 for $[C_{16}H_{12}N_2O_3]^+$; 265.06040 (75.4), calculated 265.06132 for $[C_{15}H_9N_2O_3]^+$
^{1}H-NMR**	(600.51 MHz, 297.1 K, DMSO-d6): δ_H = 12.27 (1 H, s, NH,OH), 8.50 (1 H, d, *J* = 7.7 Hz), 8.13 (1 H, d, *J* = 7.5 Hz), 7.97 (1 H, d, *J* = 8.7 Hz), 7.75 (1 H, d, *J* = 8.7 Hz), 7.44 (1 H, d, *J* = 7.8 Hz), 7.27 (1 H, m), 7.24 (1 H, m), 7.07 (1 H, m), 7.05 (1 H, m), 6.91 (1H), 5.79 (1H, s), 3.82 (3 H, s), 3.49 (3H, s)
^{13}C-NMR**	(150.94 MHz, 297.2 K, DMSO-d6): δ_C = 157.88, 156.30, 147.18, 142.95, 142.20, 131.90, 130.70, 125.39, 121.71, 120.95, 120.64, 120.30, 118.97, 117.31, 111.90, 106.00, 99.74, 90.07, 56.67, 55.59

*: The fraction was measured after four weeks of isolation resulting in a certain degree of degradation.
**: The reported chemical shifts are less than the expected in accordance to the calculated molecular formula.

6.5.2.5 Trivialine E (**51**)

Yellow solid - 1.0 mg from the skin of 1611 g of the frozen fruiting bodies.

HPLC	R_t = 27.21 min / analytical - (low resolution) gradient at section 6.3.4.3 R_t* = 23.30 min / analytical - (high resolution) gradient at section 6.3.4.3 R_t = 29.00 min / semi-preparative - gradient at section 6.3.4.3

UV/Vis (H_2O/MeCN) λ_{max} (%): 250 (70), 310 sholuder (22), 432.9 nm (30)

LCESI-(+)-MS *m/z* = 573.23 $[M + H]^+$

HRESI-(+)-MS *m/z* = 573.14016 $[M + H]^+$, calculated 573.14102 for $[C_{32}H_{21}N_4O_7]^+$

HRESI-(+)-MSMS (Precursor ion *m/z* (%) = 573.14016 (85.2)), qTOF 20-50 eV) *m/z* (%) = 293.09169 (20.0), calculated 293.09262 for $[C_{17}H_{13}N_2O_3]^+$; 280.08371 (22.0), calculated 280.08345 for $[C_{14}H_{10}N_5O_2]^+$; 265.06003 (85.0), calculated 265.06132 for $[C_{15}H_9N_2O_3]^+$; 250.08500 (0.7), calculated 250.08680 for $[C_{16}H_{12}NO_2]^+$

^{1}H-NMR** (600.22 MHz, 297.2 K, DMSO-d6): δ_H = 8.03 (1 H, m), 7.45 (1 H, m), 7.23 (1 H, m), 3.72 (3 H, s), 3.47 (3 H, s)

^{13}C-NMR** (150.94 MHz, 297.2 K, DMSO-d6): δ_C = 153.37, 148.69, 146.22, 142.95, 130.44, 125.12, 123.97, 121.61, 121.52, 120.89, 119.11, 111.90, 93.32, 90.56, 56.78, 56.18

*: The fraction was measured after four weeks of isolation resulting in a certain degree of degradation.
**: The reported chemical shifts are less than the expected in accordance to the calculated molecular formula.

6.5.2.6 14-Hydroxyblennin A (**52**)

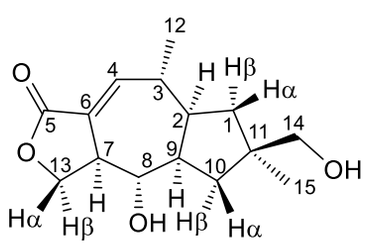

52

Colorless oil - 2.1 mg from 243 g of the flesh of the frozen fruiting bodies.

HPLC R_t = 22.71 min / analytical - gradient at section 6.3.4.2
R_t = 9.60 min / semi-preparative - gradient at section 6.3.4.3

UV/Vis (H_2O/MeCN) λ_{max} (log ε): 220 nm (2.6 $mol^{-1}dm^3cm^{-1}$)

CD (MeOH)	λ (Δε): 205 (–1.2), 220 (0.1), 245 nm (+1.75 $mol^{-1}dm^3cm^{-1}$)
$[\alpha]_D^{25}$	+82 (MeOH; *c* 0.001)
LCESI-(+)-MS	*m/z* = 267.159 $[M + H]^+$, 533.312 $[2M + H]^+$
HRESI-(+)-MS	*m/z* = 267.15966 $[M + H]^+$, calculated 267.15963 for $[C_{15}H_{23}O_4]^+$
HRESI-(+)-MSMS	(Precursor ion *m/z* (%) = 267.15966 (22.5)), qTOF 20-50 eV) *m/z* (%) = 249.14903 (38.3), calculated 249.14907 for $[C_{15}H_{21}O_3]^+$; 231.13849 (62.4), calculated 231.13850 for $[C_{15}H_{19}O_2]^+$; 219.13839 (24.1), calculated 219.13850 for $[C_{14}H_{19}O_2]^+$; 213.12780 (21.7), calculated 213.12794 for $[C_{15}H_{17}O]^+$; 203.14337 (37.3), calculated 203.14359 for $[C_{14}H_{19}O]^+$; 189.09132 (25.2), calculated 189.09155 for $[C_{12}H_{13}O_2]^+$; 185.13283 (45.2), calculated 185.13303 for $[C_{14}H_{17}]^+$; 177.09140 (9.7), calculated 177.09155 for $[C_{11}H_{13}O_2]^+$
^{1}H-NMR	(600.50 MHz, 297.2 K, CD_3OD): δ_H = 6.65 (1 H, dd appears as t, *J* = 2.9, 2.9 Hz, H-4), 4.50 (1 H, dd appears as t, *J* = 9.1, 9.1 Hz, Hβ-13), 4.10 (1 H, dd appears as t, *J* = 9.0, 9.0 Hz, Hα-13), 3.53 (1 H, dd appears as t, *J* = 10.0, 10.0 Hz, H-8), 3.38 (1 H, dddd, H-7), 3.35 (2 H, s, H-14), 2.47 (1 H, ddd, *J* = 3.8, 7.1, 13.9 Hz, H-3), 2.39 (1 H, dddd appears as tt, *J* = 7.4, 9.9 Hz, H-9), 2.18 (1 H, dddd, *J* = 5.6, 7.9, 13.2 Hz, H-2), 1.72 (1 H, dd, *J* = 6.5, 12.6 Hz, Hβ-10), 1.68 (1 H, dd, *J* = 5.3, 14.2 Hz, Hα-1), 1.55 (1 H, dd, *J* = 8.0, 13.4 Hz, Hβ-1), 1.52 (1 H, dd appears as t, *J* = 12.0, 12.0 Hz, Hα-10), 1.14 (3 H, d, *J* = 7.2 Hz, H-12), 1.04 (3 H, s, H-15) (600.50 MHz, 297.2 K, $CDCl_3$): δ_H = 6.74 (1 H, dd, H-4), 4.53 (1 H, dd appears as t, *J* = 8.9, 8.9 Hz, Hβ-13), 4.13 (1 H, dd appears as t, *J* = 9.0, 9.0 Hz, Hα-13), 3.63 (1 H, dd appears as t, *J* = 10.0, 10.0 Hz, H-8), 3.43 (2 H, s, H-14), 3.33 (1 H, m, H-7), 2.44 (1 H, m, H-3), 2.38 (1 H, m, H-9), 2.18 (1 H, m, H-2), 1.68 (1 H, dd, *J* = 6.0, 12.0 Hz, Hβ-10), 1.60 (2 H, m, H-1), 1.55 (1 H, m, Hα-10), 1.14 (3 H, d, *J* = 7.1 Hz, H-12), 1.04 (3 H, s, H-15)

^{13}C-NMR (151.01 MHz, 297.1 K, CD_3OD): δ_C = 174.12 (C-5), 147.22 (C-4), 128.52 (C-6), 75.94 (C-8), 72.17 (C-14), 70.83 (C-13), 52.12 (C-9), 45.74 (C-7), 45.04 (C-2), 43.27 (C-11), 42.12 (C-1), 40.85 (C-10), 35.25 (C-3), 25.66 (C-15), 20.81 (C-12)

(151.01 MHz, 296.9 K, $CDCl_3$): δ_C = 171.89 (C-5), 145.99 (C-4), 126.87 (C-6), 75.20 (C-8), 71.78 (C-14), 69.33 (C-13), 50.97 (C-9), 44.56 (C-7), 43.80 (C-2), 42.39 (C-11), 41.27 (C-1), 39.56 (C-10), 34.41 (C-3), 25.07 (C-15), 20.55 (C-12)

6.5.2.7 14-Hydroxylactarorufin B (**53**)

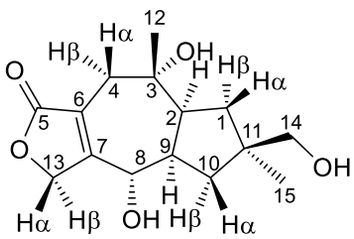

53

Colorless oil - 5.1 mg mixture with lactarorufin B (**27**), from 243 g of the flesh of the frozen fruiting bodies.

HPLC R_t = 12.61 min / analytical - gradient at section 6.3.4.3
R_t = 27.30 min / analytical - gradient at section 6.3.4.4
R_t = 7.34 min / semi-preparative - gradient at section 6.3.4.3

UV/Vis (H_2O/MeCN) λ_{max} (log ε): 220 nm

CD (MeOH) λ ($\Delta\varepsilon$): 205 (5.7), 220 (–3.5), 240 nm (+2.9 $mol^{-1}dm^3cm^{-1}$)

LCESI-(+)-MS *m/z* = 283.15 $[M + H]^+$, 565.30 $[2M + H]^+$

HRESI-(+)-MS *m/z* = 283.15440 $[M + H]^+$, calculated 283.15455 for $[C_{15}H_{23}O_5]^+$

HRESI-(+)-MSMS (Precursor ion *m/z* = 283.15440), qTOF 20-50 eV) *m/z* = 265.14367, calculated 265.14398 for $[C_{15}H_{21}O_4]^+$

^{1}H-NMR (600.50 MHz, 297.1 K, CD_3OD):): δ_H = 4.89 (1 H, ddd appears as d,

J = 17.9 Hz, H-13), 4.76 (1 H, dd appears as d, *J* = 17.9 Hz, H-13), 4.39 (1 H, d, *J* = 7.6 Hz, H-8), 3.36 (2 H, s, H-14), 2.67 (1 H, dddd appears as quintet, *J* = 8.0, 8.0, 8.0, 8.0 Hz, H-9), 2.62 (1 H, d, 17.1 Hz, H-4), 2.56 (1 H, ddd, H-2), 2.49 (1 H, d, *J* = 171 Hz, H-4), 1.61 (1 H, dd, *J* = 8.0, 13.0 Hz, Hα-10), 1.59 (1 H, dd appears as t, *J* = 12.3, 12.3 Hz, Hα-1), 1.52 (1 H, dd, *J* = 7.4, 12.3 Hz, Hβ-1), 1.46 (1 H, dd, *J* = 7.2, 13.0 Hz, Hβ-10), 1.229 (3 H, s, H-12), 1.04 (3 H, s, H-15)

(600.22 MHz, 297.2 K, $CDCl_3$): δ_H = 4.95 (1 H, ddd appears as d, *J* = 17.2 Hz, Hβ-13), 4.61 (1 H, dd appears as d, *J* = 17.2 Hz, Hα-13), 4.19 (1 H, d, *J* = 3.9 Hz, H-8), 3.428 (2 H, s, H-14), 2.92 (1 H, dddd appears as tt, *J* = 4.2, 4.2, 12.3, 12.3 Hz, H-9), 2.70 (1 H, ddd, Hα-4), 2.69 (1 H, ddd, H-2), 2.56 (1 H, dd, Hβ-4), 1.59 (1 H, dd, *J* = 8.4, 12.7 Hz, Hβ-1), 1.43 (1 H, dd, *J* = 6.8, 11.9 Hz, Hβ-10), 1.40 (1 H, dd appears as t, *J* = 11.8, 11.8 Hz, Hα-1), 1.31 (3 H, s, H-12), 1.27 (1 H, dd, Hα-10), 1.03 (3 H, s, H-15)

^{13}C-NMR

(151.00 MHz, 297.2 K, CD_3OD): δ_C = 177.45 (C-5), 165.04 (C-7), 124.03 (C-6), 73.84 (C-3), 72.45 (C-13), 71.55 (C-14), 68.94 (C-8), 52.07 (C-2), 46.43 (C-9), 42.91 (C-11), 40.57 (C-10), 39.22 (C-1), 35.98 (C-4), 29.68 (C-12), 24.44 (C-15).

(150.94 MHz, 297.1 K, $CDCl_3$): δ_C = 175.64 (C-5), 160.69 (C-7), 123.26 (C-6), 75.54 (C-3), 71.73 (C-13), 70.90 (C-14), 67.60 (C-8), 48.88 (C-2), 45.79 (C-9), 42.31 (C-11), 39.92 (C-10), 39.50 (C-1), 34.72 (C-4), 31.59 (C-12), 22.69 (C-15)

6.5.3 Compounds Isolated from *Mycena zephirus*

6.5.3.1 N^5-isopentylglutamine (**54**)

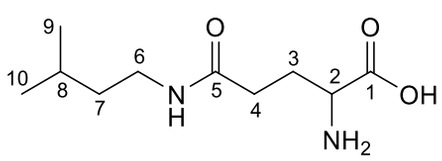

54

Colorless solid - 0.5 mg from 506 g of the frozen fruiting bodies.

HPLC	R_t = 14.14 min / analytical - (low resolution) gradient at section 6.3.4.6 R_t* = 12.90 min / analytical - (high resolution) gradient at section 6.3.4.7 R_t = 18.30-18.80 min / semi-preparative - gradient at section 6.3.4.
LCESI-(+)-MS	*m/z* = 217 $[M + H]^+$
HRESI-(+)-MS	*m/z* = 217.15506 $[M + H]^+$, calculated 217.15522 for $[C_{15}H_{21}N_2O_3]^+$
HRESI-(+)-MSMS	(Precursor ion *m/z* (%) = 217.15506 (2.5)), qTOF 20-50 eV) *m/z* (%) = 200.12838 (17.0), calculated 200.12867 for $[C_{10}H_{18}NO_3]^+$; 171.14911 (6.0), calculated 171.14974 for $[C_9H_{19}N_2O]^+$; 130.05007 (10.0), calculated 130.05042 for $[C_5H_8NO_3]^+$; 102.05515 (2.0), calculated 102.05550 for $[C_4H_8NO_2]^+$; 84.04461 (9.5), calculated 84.04494 for $[C_4H_6NO]^+$; 71.08570 (1.2), calculated 71.08607 for $[C_5H_{11}]^+$; 56.04953 (1.0), calculated 56.05002 for $[C_3H_6N]^+$
^{1}H-NMR	(600.22 MHz, 298.1 K, CD_3OD): δ_H = 3.57 (1 H, t, *J* = 5.8, 5.8 Hz, H-2), 3.19 (2 H, dd appears as t, *J* = 7.5, 7.5 Hz, H-6), 2.41 (2 H, dt, *J* = 1.0, 7.5, 7.5 Hz, H-4), 2.09 (2 H, td, *J* = 6.0, 6.0, 8.5 Hz, H-3), 1.62 (1 H, m, H-8), 1.39 (2 H, td, *J* = 7.1, 7.1, 7.6 Hz, H-7), 0.92 (6 H, d, *J* = 6.6 Hz, H-9&10).
^{13}C-NMR	(151.01 MHz, 297.1 K, CD_3OD): δ_C = 174.99 (C-5), 174.81 (C-1), 55.94 (C-2), 39.26 (C-7), 38.78 (C-6), 33.26 (C-4), 28.77 (C-3), 26.89 (C-8), 22.79 (C-9&10).

*: The fraction exhibits a great deal of degradation.

6.5.3.2 N^5-2-methylbutylglutamine (**55**)

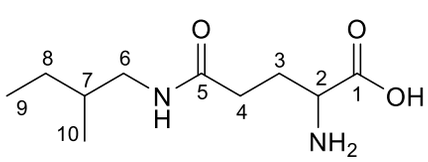

55

Colorless oil - 0.5 mg from 506 g of the frozen fruiting bodies.

HPLC	R_t = 21.67 min / analytical - (low resolution) gradient at section 6.3.4.7

	R_t = 13.48 min / analytical - (high resolution) gradient at section 6.3.4.7 R_t = 18.80-19.50 min / semi-preparative - gradient at section 6.3.4.7
LCESI-(+)-MS	*m/z* = 217.04 $[M + H]^+$
HRESI-(+)-MS	*m/z* = 217.15398 $[M + H]^+$, calculated 217.15522 for $[C_{10}H_{21}N_2O_3]^+$
HRESI-(+)-MSMS	(Precursor ion *m/z* (%) = 217.15398 (1.5)), qTOF 20-50 eV) *m/z* (%) = 200.12774 (90.0), calculated 200.12867 for $[C_{10}H_{18}NO_3]^+$; 171.14873 (25.7), calculated 171.14974 for $[C_9H_{19}N_2O]^+$; 130.04966 (55.6), calculated 130.05042 for $[C_5H_8NO_3]^+$; 88.11213 (33.8), calculated 88.11262 for $[C_5H_{14}N]^+$; 84.04441 (40.0), calculated 84.04494 for $[C_4H_6NO]^+$
^{1}H-NMR	(600.50 MHz, 296.1 K, CD_3OD): δ_H = 3.58 (1 H, t, *J* = 6.0, 6.0 Hz, H-2), 3.11 (1 H, dd, *J* = 6.2, 13.2 Hz, H-6), 2.98 (1 H, dd, *J* = 7.2, 13.2 Hz, H-6), 2.43 (2 H, t, *J* = 7.2, 7.2 Hz, H-4), 2.09 (2 H, td, *J* = 6.0, 6.0, 8.4 Hz, H-3), 1.54 (1 H, m, H-7), 1.42 (1 H, m, H-8), 1.15 (1 H, m, H-8), 0.92 (3 H, t, *J* = 7.5, 7.5 Hz, H-9), 0.89 (3 H, d, *J* = 6.7 Hz, H-10)
^{13}C-NMR	(151.01 MHz, 296.2 K, CD_3OD): δ_C = 175.07 (C-5), 173.82 (C-1), 55.73 (C-2), 46.30 (C-6), 36.09 (C-7), 33.15 (C-4), 28.11 (C-3), 28.05 (C-8), 17.49 (C-10), 11.61 (C-9)

6.5.3.3 Compound **56**

Colorless oil - 0.5 mg from 506 g of the frozen fruiting bodies.

HPLC	R_t = 31.21 min / analytical - (low resolution) gradient at section 6.3.4.7 R_t = 30.20 min / analytical - (high resolution) gradient at section 6.3.4.7 R_t = 34.00 min / semi-preparative - gradient at section 6.3.4.7
LCESI-(+)-MS	*m/z* = 602.21 $[M + H]^+$
HRESI-(+)-MS	*m/z* = 602.31078 $[M + H]^+$, two possible molecular mass are calculated; 602.31312 for $[C_{37}H_{40}N_5O_3]^+$ and 602.31178 for $[C_{36}H_{44}NO_7]^+$
HRESI-(+)-MSMS	(Precursor ion *m/z* (%) = 602.31078 (90.0)), qTOF 20-50 eV) *m/z* (%) = 527.27979 (10.0), calculated 527.28109 for $[C_{35}H_{35}N_4O]^+$ or

527.27975 for $[C_{34}H_{39}O_5]^+$; 473.26858 (15.0), calculated 473.27052 for $[C_{32}H_{33}N_4]^+$ or 473.26919 for $[C_{31}H_{37}O_4]^+$; 455.25766 (95.0), calculated 455.25862 for $[C_{31}H_{35}O_3]^+$; 352.23133 (25.5), calculated 352.23353 for $[C_{16}H_{34}NO_7]^+$; 272.11950 (60.4), calculated 272.11877 for $[C_{18}H_{14}N_3]^+$

6.5.3.4 Compound **57**

Colorless oil - 0.5 mg from 506 g of the frozen fruiting bodies.

HPLC	R_t = 30.70 min / analytical - (low resolution) gradient at section 6.3.4.7 R_t = 29.04 min / analytical - (high resolution) gradient at section 6.3.4.7 R_t = 33.00 min / semi-preparative - gradient at section 6.3.4.7
LCESI-(+)-MS	*m/z* = 600.01 $[M + H]^+$
HRESI-(+)-MS	*m/z* = 600.29487 $[M + H]^+$, two possible molecular mass are calculated; 600.29746 for $[C_{37}H_{38}N_5O_3]^+$ and 600.29613 for $[C_{36}H_{42}NO_7]^+$
HRESI-(+)-MSMS	(Precursor ion *m/z* (%) = 600.29487 (11.5)), qTOF 20-50 eV) *m/z* (%) = 525.26341 (3.5), calculated 525.26544 for $[C_{35}H_{33}N_4O]^+$ or 525.26410 for $[C_{34}H_{37}O_5]^+$; 471.25286 (9.0), calculated 471.25487 for $[C_{32}H_{31}N_4]^+$ or 471.25354 for $[C_{31}H_{35}O_4]^+$; 453.24182 (42.5), calculated 453.24297 for $[C_{31}H_{33}O_3]^+$; 231.04382 (55.2), calculated 231.04460 for $[C_{16}H_7O_2]^+$
^{1}H-NMR	(600.50 MHz, 297.2 K, CD_3OD): δ_H = 5.70 (1 H, m), 5.70 (1 H, m), 4.04 (1 H, dd), 3.92 (1 H, dd), 3.44 (1 H, m), 2.2 (3 H, t), 1.63-150 (9 H, m), 1.35-1.28 (25 H, s), 0.91 (6 H, dt)
^{13}C-NMR	(151.01 MHz, 297.1 K, CD_3OD): δ_C = 180.92, 136.64, 130.95, 76.58, 75.71, 703.14, 38.34, 37.60, 33.58, 33.14, 30.57, 27.13, 26.90, 26.59, 26.26, 23.73, 14.44, 14.41

6.6 Method for biological activity

Bio Test Procedure

Preparation of mediums and plates

- Two bottles each of 500 mL were prepared; the first one consisted of 10 g of LB Broth an d 7.5 g of Agar dissolved in 500 mL water. The second consists of 5 g of LB Broth dissolv ed in 250 mL water.
- The bottles were sterilized alongside any tool that would be used in the process. The steri lization proceeds in the (Auto claver) which it's like a press pot in it the water will be heate d until vaporization under 120 C° then the steam sterilizes the objects inside. The process will be done throw 110 minutes, approximately two hours.
- The sterilized tools and bottles were transferred to the UV-sterilized hood. After that, the s till-hot liquid from the first bottle will be poured into the (circled plastic test plates), just eno ugh to cover a third of the plate's capacity. The plates should be kept uncovered as the h ot liquid will form water drops to condense inside a covered one. The plates were left to c ool down for half an hour then were covered with clean covers, were sealed in parafilm, a nd were stored for several hours.

Preparation of bacteria

- The preparation of bacteria is achieved through two methods.
  The first one:

  Adding 20 µL from bacteria containers to the circled plates then adding 200 µL from the first bottle prepared earlier (that contains LB Broth and Agar). Then a triangle-shaped head metal rod that was previously sterilized through heating with a gas torch was used to mix the bacteria with the LB liquid and spread it equally on the surface of the test plates.

  The second method:

  Adding µL from bacteria to test tubes that already contain 2 mL of LB Broth (from the second bottle). This is the preferable method to use as it provides an easy source of ready-to-use bacteria as they are already in liquid form.

  Now firmly the containers used for bacteria were closed and left in the incubator for several days until the bacteria grew and spread enough to be used as a source of bacteria in the biological test.

Preparation of test samples

- On a small circular paper (produced using a paper puncher on filter paper), 10 µL of antib iotic material called (Gentamicin Sulfate-50 mg/mL) was added, then was left to dry for th ree hours as it dissolved in water and needed extra time to dry. This plate is characterize d by a positive sign (+).
- A solution of 0.1 mol/L (from the targeted compound that is targeted to be tested) was pre

pared. Then, 10 µL from this solution was piped out and added to the small circular paper , and left to dry. And like that, the amount taken from the sample is 1.0 µmol.

- The same procedure was performed on the solvent used to dissolve the sample, which wi ll take also 10 µL from it to the plates that will be characterized with a negative sign (–).

Performing the bioactivity test

- For each type of bacteria applied to the test, three dry plates (LB + Agar) are used, the (+), the (sample), and the (–). To each plate 20 µL from the designated bacteria in the midd le, then 200 µL from the LB liquid (the second bottle) was added and all that was spread e qually on the plate surface using the triangle-shaped head metal rod. After that, it was left to dry.
- Then using sterilized forceps, the small circular papers that were prepared before were a dded to the middle of each plate as the sign designated. The antibiotics paper on the (+) p late, the sample paper on the (sample) plate, and the solvent paper on the (–) plate.
- The plates were covered and placed in the incubator for one day and the effect of the sm all papers on the bacteria in the plates was observed, See (Fig. 116).

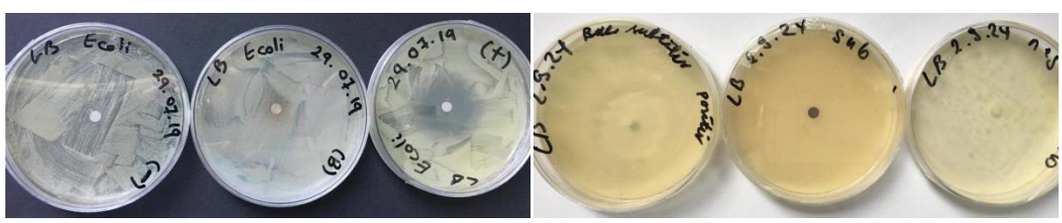

Figure. 116. Left: biological test for the activity of blennione (**35**) against *Escherichia coli*. Right: biological test for the activity of trivialine A (**47**) against *Bacillus subtilis*.

6.7 Procedure of exchange deuterium atoms with hydrogen atoms

Procedure of exchange deuterium atoms with hydrogen atoms in compound **31**.

The fraction was dissolved in 20 mL of a 1:1 mixture of H_2O and methanol and placed in a 50 mL round bottom flask. The solution was left to stir gently under room temperature for one hour, and then the solvent was evaporated under reduced pressure. This process was repeated two times.

The reason why no more harsh conditions were implemented is to avoid the risk of degradation or even react with the alcoholic solvent especially due to the existence of the alkene moiety in this compound

7 List of abbreviations

Abs.	absorption
Ac	acetyl
AcOH	acetic acid
amu	atomic mass unit
AU	absorbance Unit
BPC	base peak chromatogram
c	concentration
°C	degrees Celsius
C18ec	HPLC-column packing with (193nipolar) C18 endcapping
COSY	correlation spectroscopy
CD	circular dichroism
$CDCl_3$	deuterated chloroform
CD_3OD	deuterated methanol
D_2O	deuterated H_2O
d	doublet
dd	doublet of doublet
dt	doublet of triplet
DAD	diode array detector
DMSO-D_6	deuterated dimethyl sulfoxide
DEPT135	distortionless enhancement by polarization transfer angle 135° (CH and CH_3 opposite to CH_2)
δ_C	chemical shifts of ^{13}C
δ_H	chemical shifts of ^{1}H
EIC	extracted ion chromatogram
ESI	electrospray ionization
EtOAc	ethyl acetate
EtOH	ethanol
eV	electron volts
g	gram
GC	gas chromatography
H_2O	water
HPLC	high performance liquid chromatography
HR	high resolution
HSQC	heteronuclear single quantum coherence
HMBC	heteronuclear multiple bond correlation
Hz	hertz
h	hour
IUPAC	international union of pure and applied chemistry
J	coupling constant
K	kelvin
L	liter
λ	wavelength
m	multiplet
M	molecular weight
Me	methyl
MeCN	acetonitrile
MeOH	methanol
min	minute
ml	milliliter
MS	mass spectrometry, mass spectrometer, mass spectrum

m/z	mass-to-charge ratio
MS/MS or MS^2	tandem mass spectrometry experiment
M-fraction	SPE methanol fraction
nm	nanometer
NMR	nuclear magnetic resonance
NOESY	nuclear overhauser effect spectroscopy
PDA	photo diode array
ppm	parts per million
R_t	retention time
ROESY	rotating-frame nuclear overhauser effect spectroscopy
RP	reversed phase
RT	room temperature
rpm	rounds per minute
s	singlet
SPE	solid phase extraction
sp.	Species
t	triplet
td	triplet of doublet
θ	measured ellipticity
TOCSY	total correlation spectroscopy
UV	ultraviolet
Vis	visible light
WM-fraction	SPE water/methanol fraction
W-fraction	SPE water fraction

8 References

[1] a) R. N. Bennett, R. M. Wallsgrove, *New Phytologist* **1994**, *127*, 617-633; b) A. Crozier, M. N. Clifford, H. Ashihara, *Plant secondary metabolites*, Blackwell Publishers, **2006**.

[2] T. Costa, R. F. Vieira, H. R. Bizzo, D. Silveira, M. A. Gimenes, in *Chromatography and Its Applications* **2012**, pp. 131-164.

[3] P. Spiteller, *Chemistry–A European Journal* **2008**, *14*, 9100-9110.

[4] A. Fleming, *British Journal of Experimental Pathology* **1929**, *10*, 226-236.

[5] D. A. Dias, S. Urban, U. Roessner, *Metabolites* **2012**, *2*, 303-336.

[6] a) E. Torok, E. Moran, F. Cooke, *Oxford Handbook of Infectious Diseases and Microbiology*, OUP Oxford, **2009**; b) E. Abraham, G. Newton, *Biochemical Journal* **1961**, *79*, 377-393; c) Y. Hu, B. Zhu, *Synthetic and Systems Biotechnology* **2016**, *1*, 143-149.

[7] a) T. Anke, F. Oberwinkler, W. Steglich, G. Schramm, *The Journal of Antibiotics* **1977**, *30*, 806-810; b) D. W. Bartett, J. M. Clough, C. R. Godfrey, J. R. Godwin, A. A. Hall, S. P. Heaney, S. J. Maund, *Pesticide Outlook* **2001**, *12*, 143-148.

[8] a) D. E. Cane, *Chemical Reviews* **1990**, *90*, 1089-1103; b) J. S. Glasby, *Encyclopaedia of Terpenoids*, Wiley: Chichester, **1982**; c) A. I. Scott, T. Devon, *Handbook of Naturally Occurring Compounds*, Academic Press, **1972**.

[9] W. Ayer, E. Brandt, J. Coetzee, W. M. Daniewski, D. Ferreira, E. Malan, L. Trifonov, G. Vidari, *Progress in the Chemistry of Organic Natural Products*, Springer-Verlag Wien GmbH, **1999**.

[10] E. Rodriguez, G. H. N. Towers, J. C. Mitchell, *Phytochemistry* **1976**, *15*, 1573-1580.

[11] A. Modzelewska, S. Sur, S. K. Kumar, S. R. Khan, *Current Medicinal Chemistry-Anti-Cancer Agents* **2005**, *5*, 477-499.

[12] a) L. Ruzicka, M. Stoll, *Helvetica Chimica Acta* **1922**, *5*, 923-936; b) L. Ruzicka, *Experientia* **1953**, *9*, 357-367; c) L. Ruzicka, in *Proceedings of the Chemical Society, Vol. 341*, London, **1959**.

[13] a) J. B. Hendrickson, *Tetrahedron* **1959**, *7*, 82-89; b) J. H. Richards, J. B. Hendrickson, *The Biosynthesis of Steroids, Terpenes, and Acetogenins*, W. A. Benjamin, New York, **1964**.

[14] W. Parker, J. S. Roberts, R. Ramage, *Quarterly Reviews, Chemical Society* **1967**, *21*, 331-363.

[15] R. Kramer, W.-R. Abraham, *Phytochemistry Reviews* **2012**, *11*, 15-37.

[16] T.-D. Nguyen, G. MacNevin, D.-K. Ro, in *Methods in enzymology, Vol. 517*, Elsevier, **2012**, pp. 261-278.

[17] M. Karplus, *The Journal of Chemical Physics* **1959**, *30*, 11-15.

[18] C. B.-S. By Gringer - Own work, https://commons.wikimedia.org/w/index.php?curid=18436896.

[19] A. V. Karnik, M. Hasan, in *Stereochemistry A Three-Dimensional Insight*, Stereochemistry **2021**, p. 9.

[20] https://www.123pilzsuche.de/daten/details/GebaendHainMilch.htm.

[21] http://archive.bio.ed.ac.uk/jdeacon/microbes/mycorrh.htm.

[22] P. Bonfante, A. Genre, *Nature Communications* **2010**, *1*, 48.

[23] https://www.pilz-baden.ch/galerie/wissenschaftlich/lactarius-67/lactarius_circellatus-188.

[24] O. Sterner, *Acta Chemica Scandinavica* **1989**, *43*, 694-697.

[25] G. Magnusson, S. Thorén, T. Drakenberg, *Tetrahedron* **1973**, *29*, 1621-1624.

[26] O. Sterner, R. Bergman, E. Kesler, L. Nilsson, J. Oluwadiya, B. Wickberg, *Tetrahedron Letters* **1983**, *24*, 1415-1418.

[27] K. Lorenzen, T. Anke, *Current Organic Chemistry* **1998**, *2*, 329-364.

[28] G. Vidari, M. De Bernardi, P. Vita-Finzi, G. Fronza, *Phytochemistry* **1976**, *15*, 1953-1955.

[29] M. De Bernardi, G. Fronza, G. Mellerio, G. Vidari, P. Vitafinzi, *Phytochemistry* **1980**, *19*, 99-101.

[30] K.-G. Widén, E.-L. Seppä, *Phytochemistry* **1979**, *18*, 1226-1227.

[31] M. J. Minch, *Concepts in Magnetic Resonance* **1994**, *6*, 41-56.

[32] G. Gilardoni, O. Malagòn, S. Tosi, M. Clericuzio, G. Vidari, *Natural Product Communications* **2014**, *9*, 319-322.
[33] M. De Bernardi, G. Fronza, G. Mellerio, V. Valla, G. Vidari, P. Vita-Finzi, *Gazzetta Chimica Italiana* **1984**, *114*, 163-168.
[34] A. Bosetti, G. Fronza, G. Vidari, P. Vita-Finzi, *Phytochemistry* **1989**, *28*, 1427-1431.
[35] Q.-G. Ma, R.-R. Wei, X.-D. Zhang, Z.-P. Sang, J.-H. Dong, Q.-X. Lu, H.-F. Huang, D.-M. Guo, L. Jiang, *Fitoterapia* **2020**, *146*, 104733.
[36] W. M. Daniewski, M. Kocór, *Bulletin De L'Academie Polonaise Des Sciences-Serie Des Sciences Chimiques* **1970**, *18*, 585-593.
[37] W. M. Daniewski, M. Kocór, *Bulletin De L'Academie Polonaise Des Sciences-Serie Des Sciences Chimiques* **1971**, *19*, 553-561.
[38] W. M. Daniewski, M. Kocór, J. Król, *Roczniki Chemii* **1976**, *50*, 2095-2100.
[39] E.-L. Seppä, K.-G. Widén, in *Annales Botanici Fennici*, **1980**, pp. 56-60.
[40] W. M. Daniewski, W. Kroszczynski, P. Skibicki, M. De Bernardi, G. Fronza, G. Vidari, P. Vita-Finzi, *Phytochemistry* **1988**, *27*, 187-191.
[41] W. M. Daniewski, M. Gumulka, P. Skibicki, *Phytochemistry* **1990**, *29*, 527-529.
[42] K. Kobata, S. Kano, H. Shibata, *Bioscience, Biotechnology, and Biochemistry* **1995**, *59*, 316-318.
[43] O. P. Suri, R. Shah, N. K. Satti, K. A. Suri, *Phytochemistry* **1997**, *45*, 1453-1455.
[44] Y. Yaoita, N. Watanabe, D. Takano, M. Kikuchi, *Natural Medicines* **2004**, *58*, 235.
[45] Y. Zheng, Y. Shen, *Organic Letters* **2009**, *11*, 109-112.
[46] K. H. Kim, H. J. Noh, S. U. Choi, K. M. Park, S.-J. Seok, K. R. Lee, *Bioorganic & Medicinal Chemistry Letters* **2010**, *20*, 5385-5388.
[47] O. Malagòn, A. Porta, M. Clericuzio, G. Gilardoni, D. Gozzini, G. Vidari, *Phytochemistry* **2014**, *107*, 126-134.
[48] M. Isaka, A. Yangchum, S. Wongkanoun, S. Kongthong, *Phytochemistry Letters* **2017**, *21*, 174-178.
[49] T. Zhao, M. Sun, L. Kong, R. Wang, G. S. S. Njateng, G. Cheng, *Biochemical Systematics and Ecology* **2019**, *86*, 103912.
[50] R. Mouna, A. Broisat, A. Ahmed, M. Debiossat, A. Boumendjel, C. Ghezzi, Z. Kabouche, *Pharmaceutical Biology* **2022**, *60*, 1491-1501.
[51] W. M. Daniewski, M. kocór, J. Król, *Roczniki Chemii* **1977**, *51*, 1395-1398.
[52] W. M. Daniewski, M. Kocór, T. Januszewski, A. Rymkiewicz, *Polish Journal of Chemistry* **1981**, *55*, 807-812.
[53] W. M. Daniewski, J. Król, *Polish Journal of Chemistry* **1981**, *55*, 1247-1252.
[54] W. M. Daniewski, W. Kroszczyński, A. Wawrzuń, A. Rymkiewicz, *Journal of liquid chromatography* **1984**, *7*, 2915-2920.
[55] W. M. Daniewski, M. Gumułka, K. Ptaszyńska, P. Skibicki, U. Jacobsson, T. Norin, *Phytochemistry* **1992**, *31*, 3933-3936.
[56] A. Wunder, T. Anke, D. Klostermeyer, W. Steglich, *Zeitschrift für Naturforschung* **1996**, *51c*, 493-499.
[57] W. M. Daniewski, M. Kocór, B. Zółtowska, *Bulletin De L'Academie Polonaise Des Sciences-Serie Des Sciences Chimiques* **1973**, *21*, 785-792.
[58] J. Nawrot, E. Bloszyk, H. Grabarczyk, B. Drozdz, W. M. Daniewski, M. Holub, *Prace Naukowe Instytutu Ochrony Roślin* **1983**, *25*, 91-98.
[59] W. M. Daniewski, M. Gumulka, K. Ptaszynska, P. Skibicki, E. Bloszyk, B. Drozdz, S. Stromberg, T. Norin, M. Holub, *European Journal of Entomology* **1993**, *90*, 65-70.
[60] Y. Yaoita, M. Kikuchi, *Journal of Tohoku Pharmaceutical University* **2004**, *51*, 35-40.
[61] S. Nozoe, H. Matsumoto, S. Urano, *Tetrahedron Letters* **1971**, *12*, 3125-3126.
[62] M. De Bernardi, G. Fronza, G. Vidari, P. Vita-Finzi, *La Chimica E L'Industria* **1976**, *58*, 177-178.
[63] D. Andina, M. De Bernardi, A. Del Vecchio, G. Fronza, G. Mellerio, G. Vidari, P. Vita-Finzi, *Phytochemistry* **1980**, *19*, 93-97.

[64] S. K. Thompson, C. H. Heathcock, *The Journal of Organic Chemistry* **1992**, *57*, 5979-5989.
[65] Y. Yaoita, H. Ono, M. Kikuchi, *Chemical and Pharmaceutical Bulletin* **2003**, *51*, 1003-1005.
[66] G. Magnusson, S. Thorén, J. Dahmén, K. Leander, *Acta Chemica Scandinavica* **1974**, *28*, 841-846.
[67] Z. Pang, F. Bocchio, O. Sterner, *Tetrahedron Letters* **1992**, *33*, 6863-6866.
[68] M. De Bernardi, L. Garlaschelli, L. Toma, G. Vidari, P. Vita-Finzi, *Tetrahedron* **1993**, *49*, 1489-1504.
[69] J. Alarcón, N. Villalobos, C. Lamilla, C. L. Céspedes, *Boletín Latinoamericano y del Caribe de Plantas Medicinales y Aromáticas* **2013**, *12*, 493-498.
[70] W. M. Daniewski, M. Gumuka, E. Pankowska, K. Ptaszyńska, E. Boszyk, U. Jacobsson, T. Norin, *Phytochemistry* **1993**, *32*, 1499-1502.
[71] D.-Q. Luo, F. Wang, X.-Y. Bian, J.-K. Liu, *The Journal of Antibiotics* **2005**, *58*, 456-459.
[72] F. Hiramatsu, T. Murayama, T. Koseki, Y. Shiono, *Natural Product Research* **2008**, *22*, 1001-1006.
[73] Y. Wang, S. P. Yang, J. M. Yue, S. Chow, W. Kitching, *Helvetica Chimica Acta* **2003**, *86*, 2424-2433.
[74] Y. Yaoita, M. Hirao, M. Kikuchi, K. Machida, *Natural Product Communications* **2012**, *7*, 1133-1135.
[75] W. M. Daniewski, M. Kocór, J. Król, *Bulletin De L'Academie Polonaise Des Sciences-Serie Des Sciences Chimiques* **1975**, *23*, 637-641.
[76] H. Pyysalo, E.-L. Seppa, K.-G. Widén, *Journal of Chromatography* **1980**, *190*, 466-470.
[77] M. De Bernardi, G. Fronza, A. Scilingo, G. Vidari, P. Vita-Finzi, *Tetrahedron* **1986**, *42*, 4277-4283.
[78] P. Spiteller, W. Steglich, *Journal of Natural Products* **2002**, *65*, 725-727.
[79] P. Spiteller, N. Arnold, M. Spiteller, W. Steglich, *Journal of Natural Products* **2003**, *66*, 1402-1403.
[80] J. Heilmann-Clausen, A. Verbeken, J. Vesterholt, *Danish Mycological Society, Copenhagen* **1998**.
[81] a) E. Gerhardt, *Der große BLV Pilzführer für unterwegs: 1200 Arten· 1000 Farbfotos*, BLV Buchverlag GmbH & Company KG, **2016**; b) H. E. Laux, *Der große Kosmos Pilzführer*, Kosmos, **2022**.
[82] https://commons.wikimedia.org/wiki/File:2006-09-09_Lactarius_trivialis.jpg#/media/Datei:2006-09-09_Lactarius_trivialis.jpg.
[83] G. J. Krieglsteiner, *Die Großpilze Baden-Württembergs*, **2000**.
[84] https://www.123pilzsuche.de/daten/details/NordischerMilchling.htm.
[85] P. Mattila, A.-M. Lampi, R. Ronkainen, J. Toivo, V. Piironen, *Food Chemistry* **2002**, *76*, 293-298.
[86] O. Sterner, R. Bergman, E. Kesler, G. Magnusson, L. Nilsson, B. Wickberg, E. Zimerson, G. Zetterberg, *Mutation Research/Elsevier Biomedical Press* **1982**, *101*, 269-281.
[87] M. Rotola-Pukkila, B. Yang, A. Hopia, *Food Chemistry* **2019**, *278*, 56-66.
[88] H. Pyysalo, *Acta Chemica Scandinavica B* **1976**, *30*, 235-244.
[89] R. J. Stadelmann, E. Müller, C. H. Eugster, *Helvetica Chimica Acta* **1976**, *59*, 2432-2436.
[90] R. Kurkela, J. Koivurinta, R. Kuusinen, *Food Chemistry* **1980**, *5*, 109-130.
[91] S. Piepponen, H. Liukkonen-Lilja, T. Kuusi, *Zeitschrift für Lebensmittel-Untersuchung und-Forschung* **1983**, *177*, 257-260.
[92] P. H. Mattila, V. I. Piironen, E. J. Uusi-Rauva, P. E. Koivistoinen, *Journal of Agricultural and Food Chemistry* **1994**, *42*, 2449-2453.
[93] E. Kostiainen, *Boreal Environment Research* **2007**, *12*, 23-28.
[94] M. Vinichuk, A. Taylor, K. Rosén, K. Johanson, *Science of the Total Environment* **2010**, *408*, 2543-2548.
[95] A. Lavola, P. J. Aphalo, T. Lehto, *Mycorrhiza* **2011**, *21*, 155-165.

[96] a) M. Vinichuk, *International Scholarly Research Network/Ecololgy* **2012**, *2012*, 521582; b) M. M. Vinichuk, *Journal of Environmental Science and Health, Part A* **2013**, *48*, 980-987.
[97] S.-C. Shao, Y. Luo, W.-B. Yu, *Mitochondrial DNA Part B* **2020**, *5*, 2078-2079.
[98] aB. Fugmann, B. Steffan, W. Steglich, *Tetrahedron letters* **1984**, *25*, 3575-3578; bC. S. Hilger, B. Fugmann, W. Steglich, *Tetrahedron letters* **1985**, *26*, 5975-5978.
[99] J.-D. Klamann, B. Fugmann, W. Steglich, *Phytochemistry* **1989**, *28*, 3519-3522.
[100] P. Kummer, *Luppe's Buchhandlung, Zerbst* **1871**.
[101] M. S. Park, H. J. Cho, N. K. Kim, J. Y. Park, H. Lee, K. H. Park, M.-J. Kim, J.-J. Kim, C. Kim, Y. W. Lim, *Mycobiology* **2017**, *45*, 286-296.
[102] https://commons.wikimedia.org/wiki/File:2012-10-18_Mycena_zephirus_319638.jpg#/media/Datei:2012-10-18_Mycena_zephirus_319638.jpg.
[103] M. Bon, J. Wilkinson, *Pareys Buch der Pilze: über 1500 Pilze Europas*, Kosmos, **2005**.
[104] D. E. Desjardin, A. G. Oliveira, C. V. Stevani, *Photochemical & Photobiological Sciences* **2008**, *7*, 170-182.
[105] S. Peters, P. Spiteller, *Journal of Natural Products* **2007**, *70*, 1274-1277.
[106] S. Peters, P. Spiteller, *European Journal of Organic Chemistry* **2007**, 1571-1576.
[107] S. Peters, R. J. Jaeger, P. Spiteller, *European Journal of Organic Chemistry* **2008**, 319-323.
[108] R. J. Jaeger, P. Spiteller, *Journal of Natural Products* **2010**, *73*, 1350-1354.
[109] A. Pulte, S. Wagner, H. Kogler, P. Spiteller, *Journal of natural products* **2016**, *79*, 873-878.
[110] J. S. Lohmann, M. von Nussbaum, W. Brandt, J. Muelbradt, W. Steglich, P. Spiteller, *Tetrahedron* **2018**, *74*, 5113-5118.
[111] J. S. Lohmann, S. Wagner, M. von Nussbaum, A. Pulte, W. Steglich, P. Spiteller, *Chemistry–A European Journal* **2018**, *24*, 8609-8614.
[112] P. Luis, G. Walther, H. Kellner, F. Martin, F. Buscot, *Soil Biology and Biochemistry* **2004**, *36*, 1025-1036.
[113] G. Walther, S. Garnica, M. WEI, *Mycological Research* **2005**, *109*, 525-544.
[114] A. L. Chew, Y.-S. Tan, D. E. Desjardin, M. Y. Musa, V. Sabaratnam, *Mycologia* **2013**, *105*, 1325-1335.
[115] M. Clericuzio, M. Bivona, E. Gamalero, E. Bona, G. Novello, N. Massa, F. Dovana, E. Marengo, E. Robotti, *Antibiotics* **2021**, *10*, 1424.
[116] https://chemazone.com/Cart.asp.
[117] T. E. Bowser, M. L. Trawick, *Amino Acids* **2013**, *44*, 143-150.
[118] J. Liu, X. Zhong, Y. Jiang, L. Yu, X. Huang, Z. Dong, S. Yang, W. He, J. Zeng, Z. Qing, *Journal of Pharmaceutical and Biomedical Analysis* **2020**, *186*, 113314.
[119] a) R. Timms, *Journal of the American Oil Chemists' Society* **1985**, *62*, 241-249; b) O. Fasina, M. Craig-Schmidt, Z. Colley, H. Hallman, *LWT-Food Science and Technology* **2008**, *41*, 1501-1505; c) S. K. Ramamoorthy, D. Åkesson, M. Skrifvars, B. Baghaei, *Handbook of composites from renewable materials, physico-chemical and mechanical characterization* **2017**, *3*, 425-458.
[120] A. Usami, R. Motooka, H. Nakahashi, S. Marumoto, M. Miyazawa, *Chemistry & Biodiversity* **2015**, *12*, 1734-1745.
[121] T. R. Yeong, Z. Ilham, W. A. A. Q. I. Wan, S. A. Halim-Lim, S. R. A. Usuldin, R. Ahmad, M. Adlim, *Heliyon* **2024**, e31594.
[122] https://www.scribd.com/document/432355477/IR-Spectrum-Table-Chart-Sigma-Aldrich.
[123] a) B. Ribeiro, P. G. de Pinho, P. B. Andrade, P. Baptista, P. Valentão, *Microchemical Journal* **2009**, *93*, 29-35; b) P. C. Phan ChiaWei, L. G. Lee GuanSerm, I. Macreadie, S. Malek, D. Pamela, V. Sabaratnam, *Natural Product Communications* **2013**, *8*, 1763-1765; c) R. K. Saini, A. Rauf, A. A. Khalil, E.-Y. Ko, Y.-S. Keum, S. Anwar, A. Alamri, K. R. Rengasamy, *South African Journal of Botany* **2021**, *141*, 344-356.

9 Attachments

9.1 12-Hydroxy-15-carboxyblennin A (**19**)

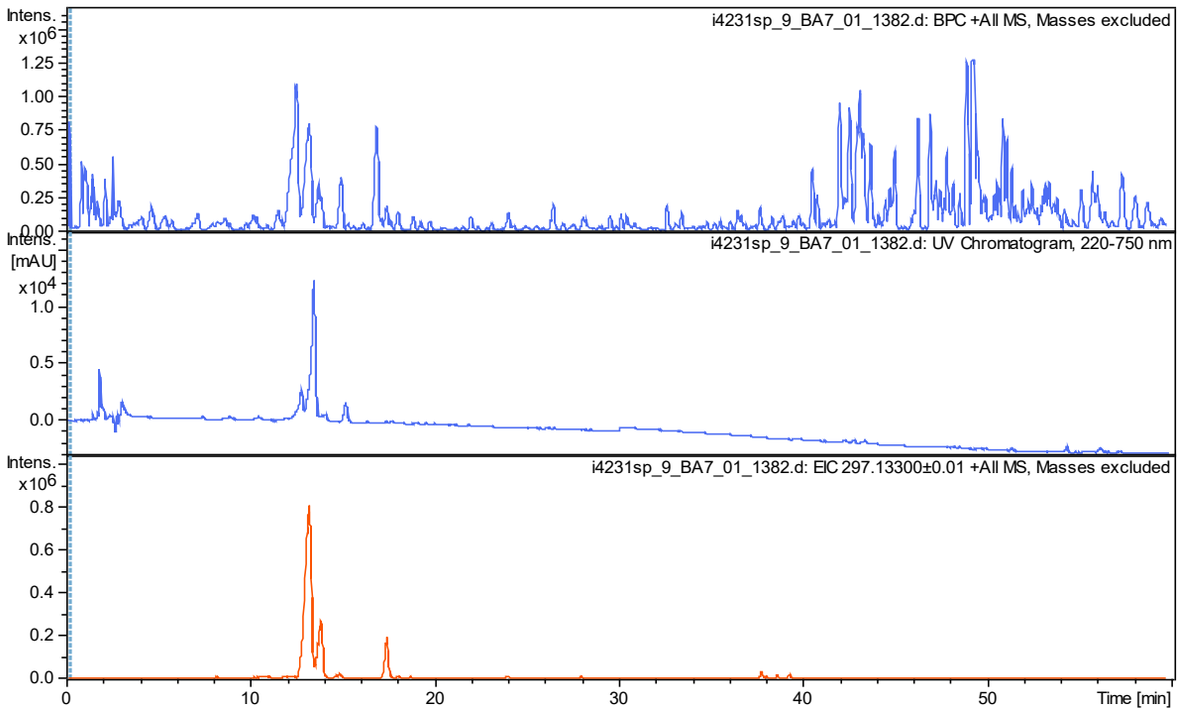

Figure. S1. HR-ESI-(+)-MS, UV/Vis and mass excluded chromatograms.

Table. S1. MS/MS fragments with molecular formula for compound **19**.

Meas. *m/z*	Ion Formula	Sum Formula
297.13270	**$C_{15}H_{21}O_6$**	**$C_{15}H_{20}O_6$**
279.12240	$C_{15}H_{19}O_5$	
261.11163	$C_{15}H_{17}O_4$	
249.11166	$C_{14}H_{17}O_4$	
231.10119	$C_{14}H_{15}O_3$	
215.10626	$C_{14}H_{15}O_2$	
203.10642	$C_{13}H_{15}O_2$	

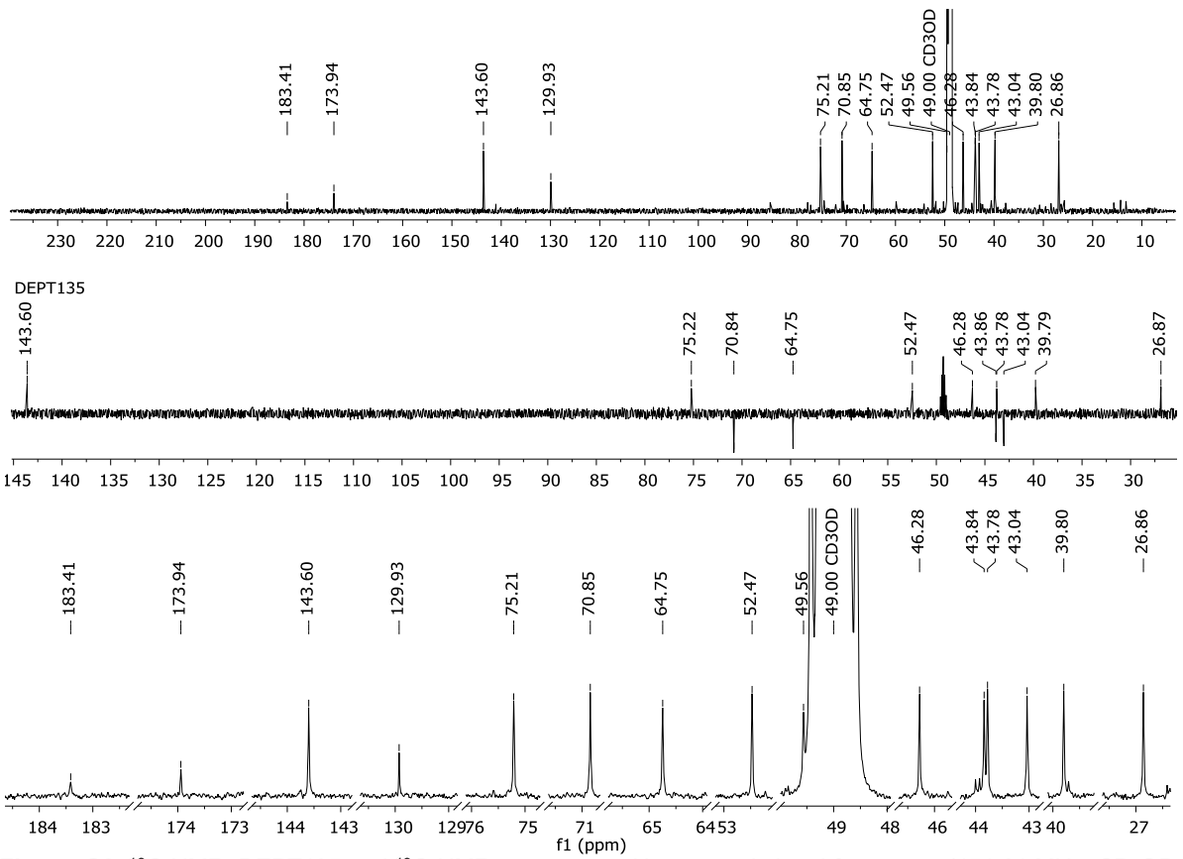

Figure. S2. ^{13}C-NMR, DEPT135 and ^{13}C-NMR-spectrums with removed signal-free areas (151.01 MHz, CD_3OD, 297.2 K).

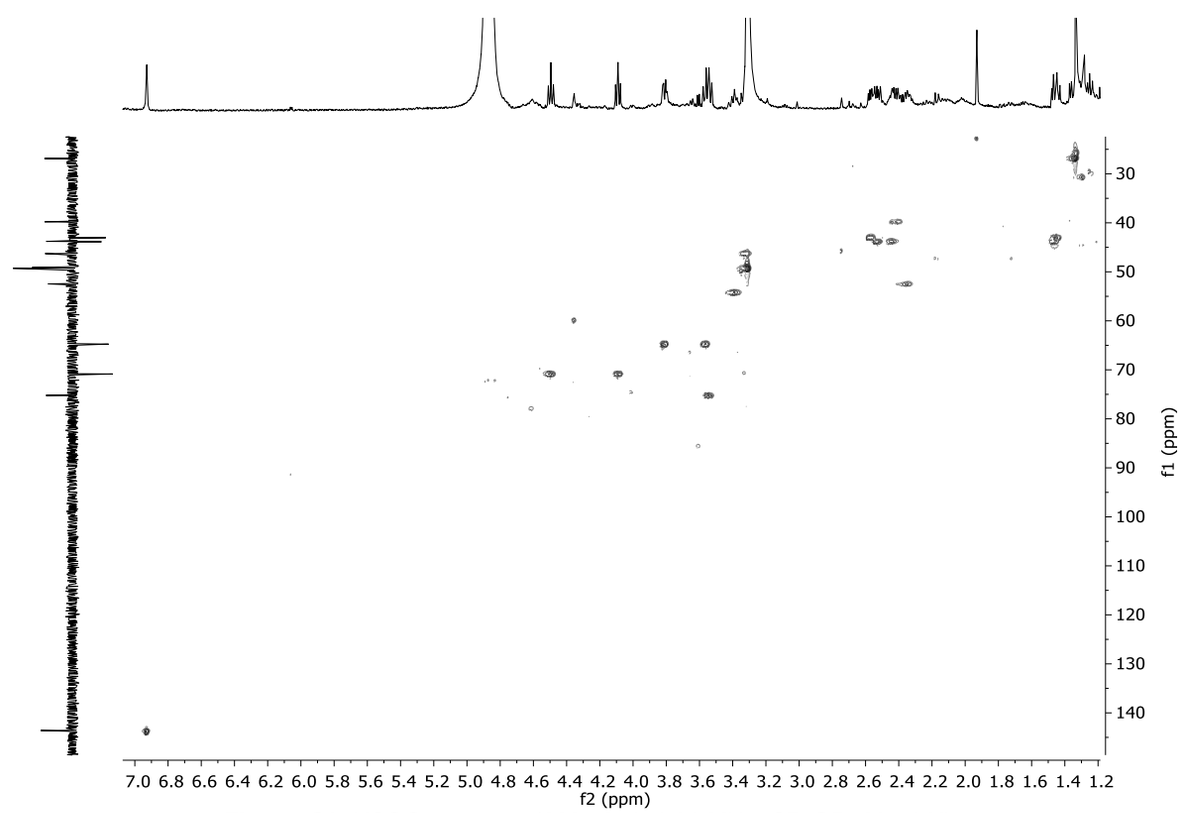

Figure. S3. HSQC-spectrum (600.50, 151.01 MHz, CD_3OD, 297.1 K).

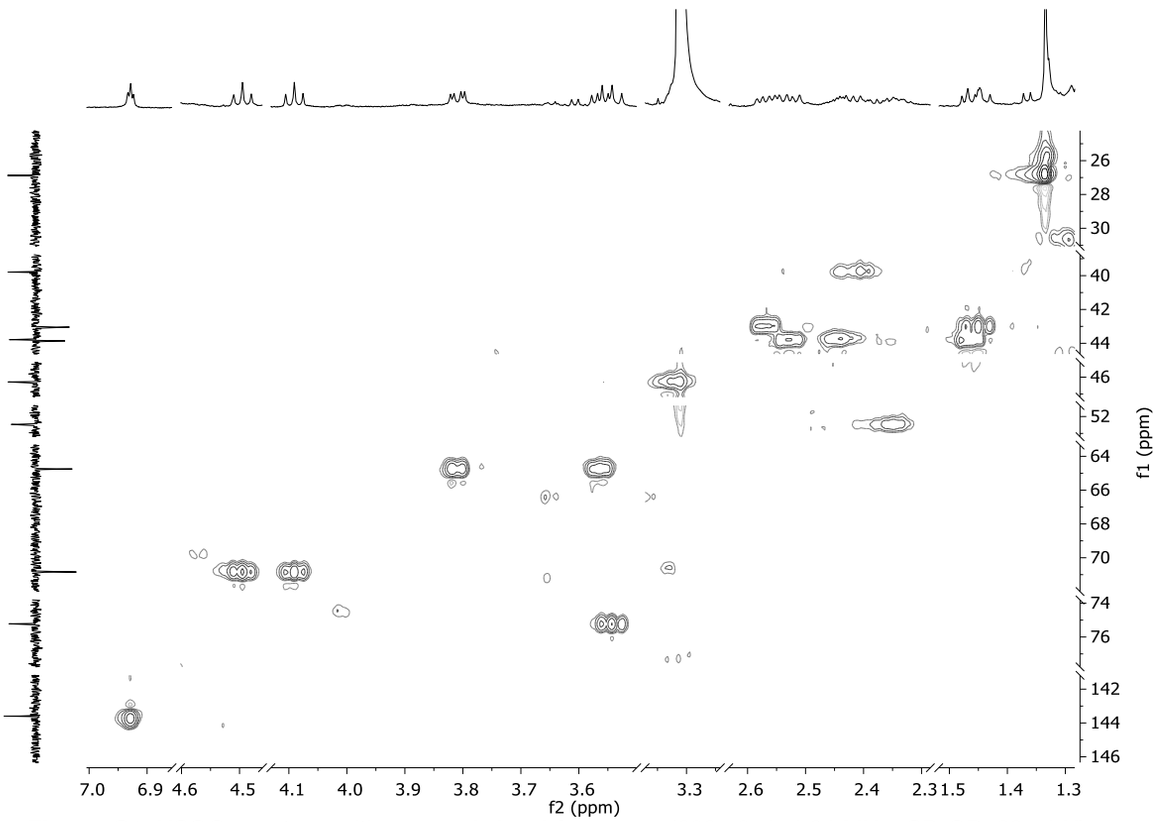

Figure. S4. HSQC-spectrum with removed signal-free areas (600.50, 151.01 MHz, CD_3OD, 297.1 K).

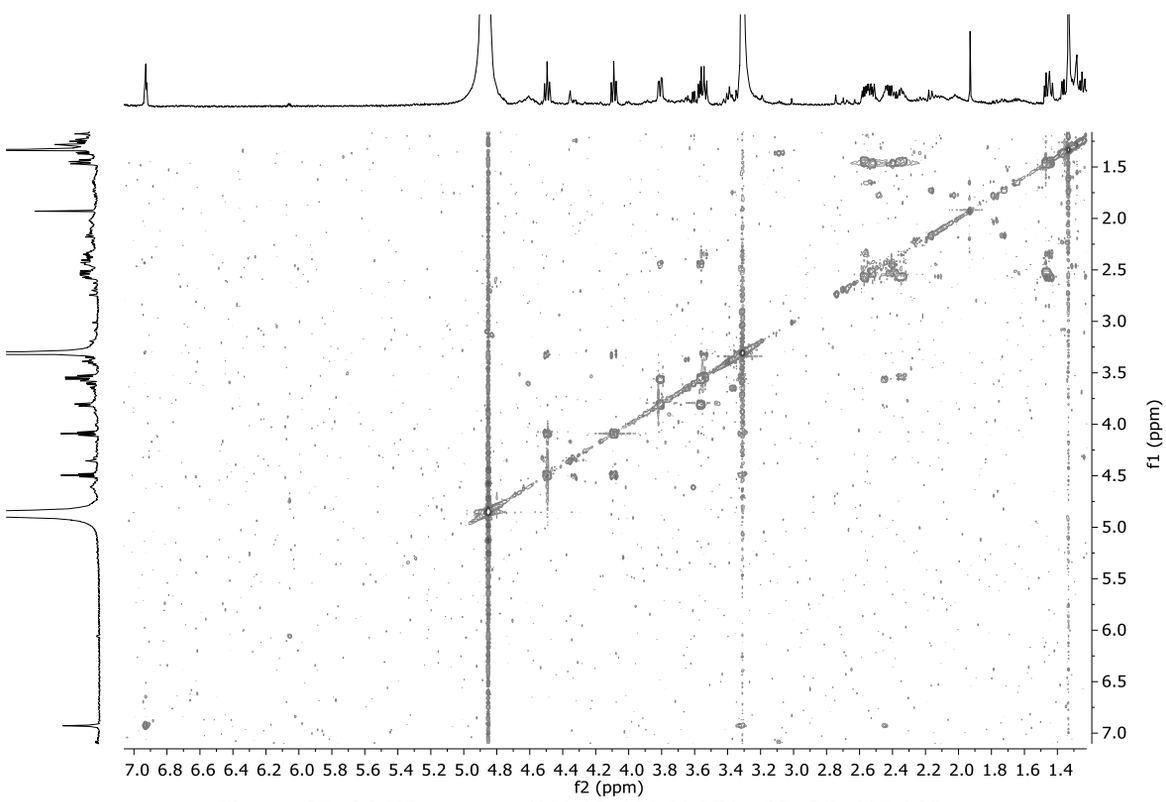

Figure. S5. COSY-spectrum (600.22, 600.22 MHz, CD_3OD, 297.1 K).

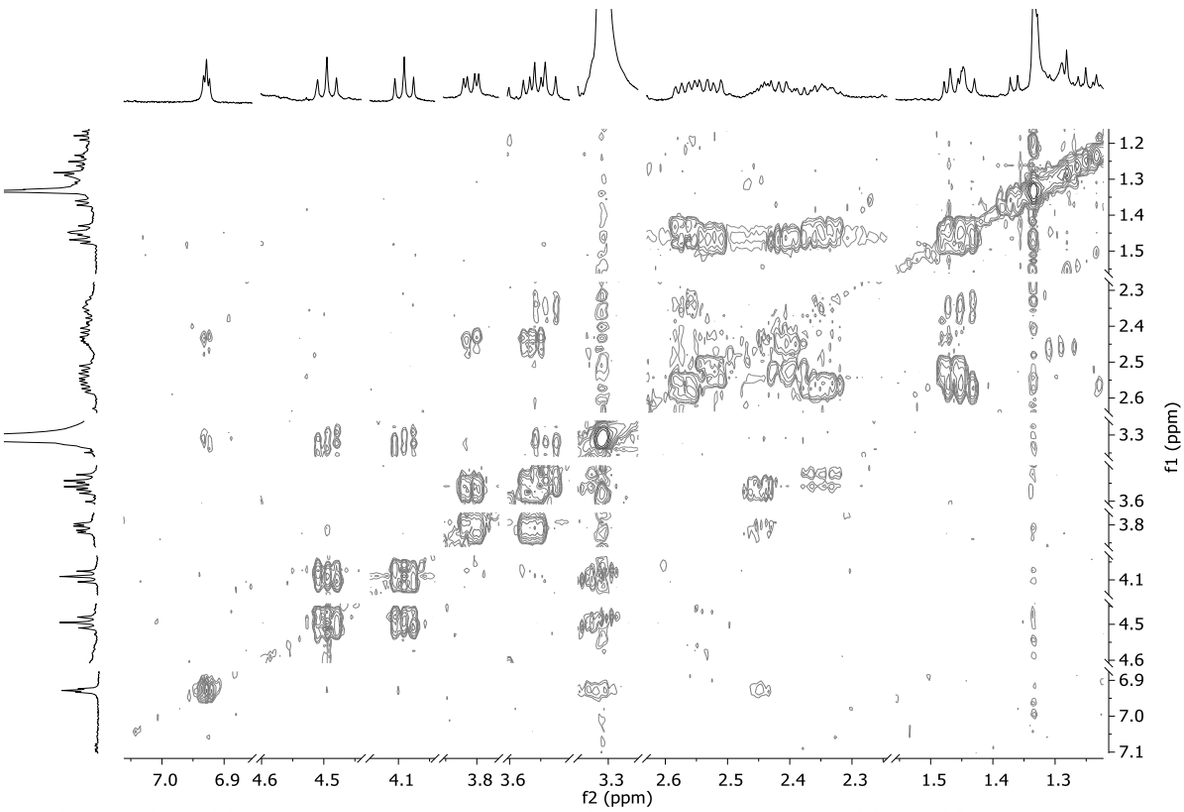

Figure. S6. COSY-spectrum with removed signal-free areas (600.22, 600.22 MHz, CD_3OD, 297.1 K).

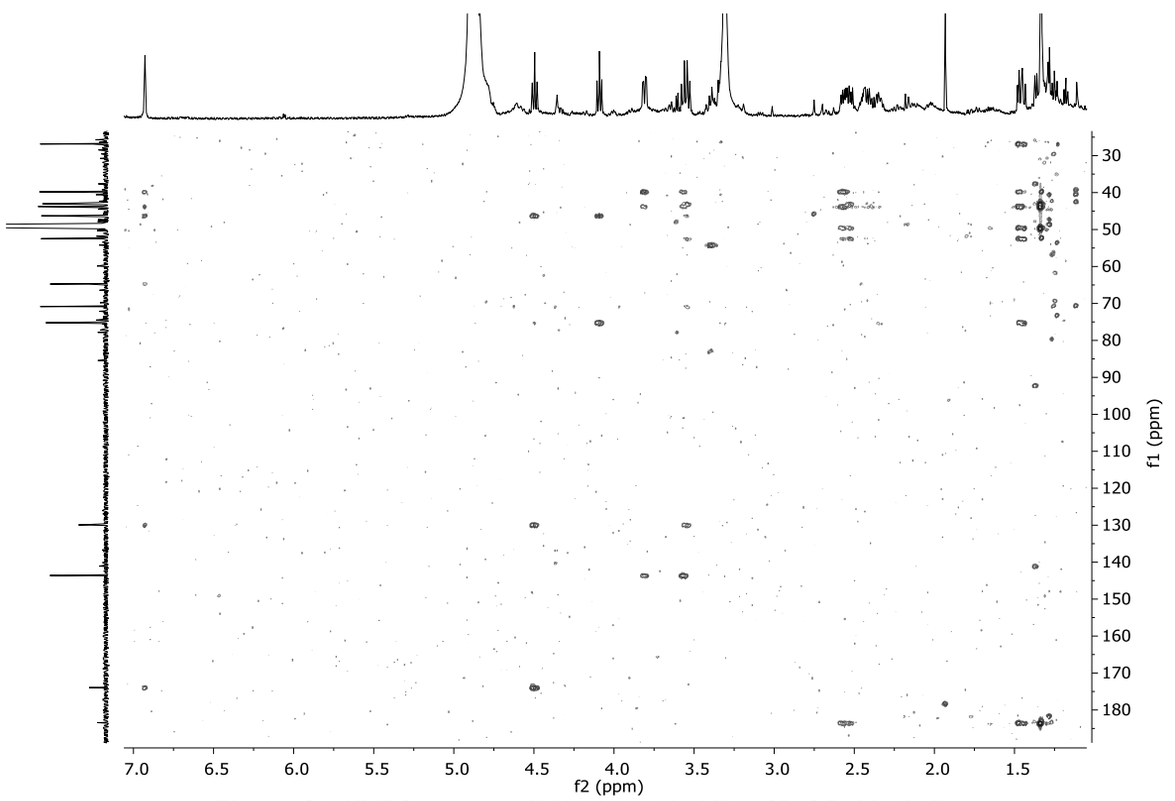

Figure. S7. HMBC-spectrum (600.50, 151.01 MHz, CD_3OD, 297.2 K).

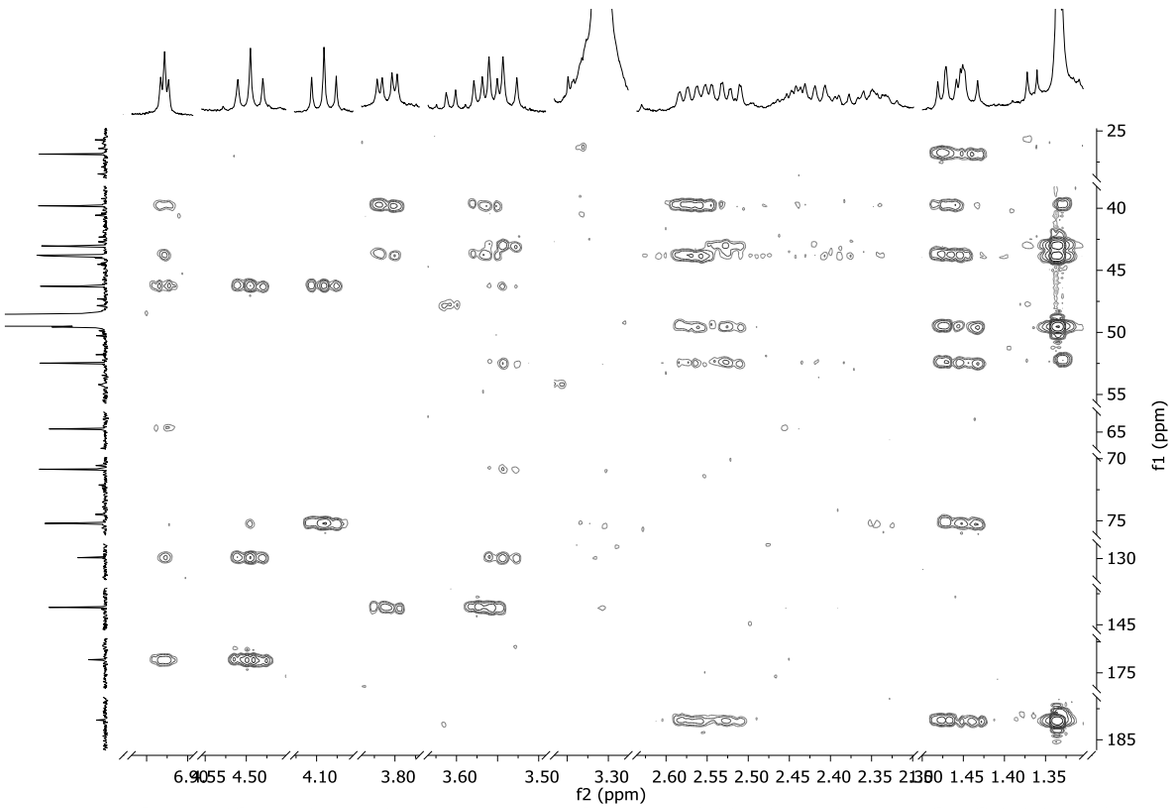

Figure. S8. HMBC-spectrum with removed signal-free areas (600.50, 151.01 MHz, CD_3OD, 297.2 K).

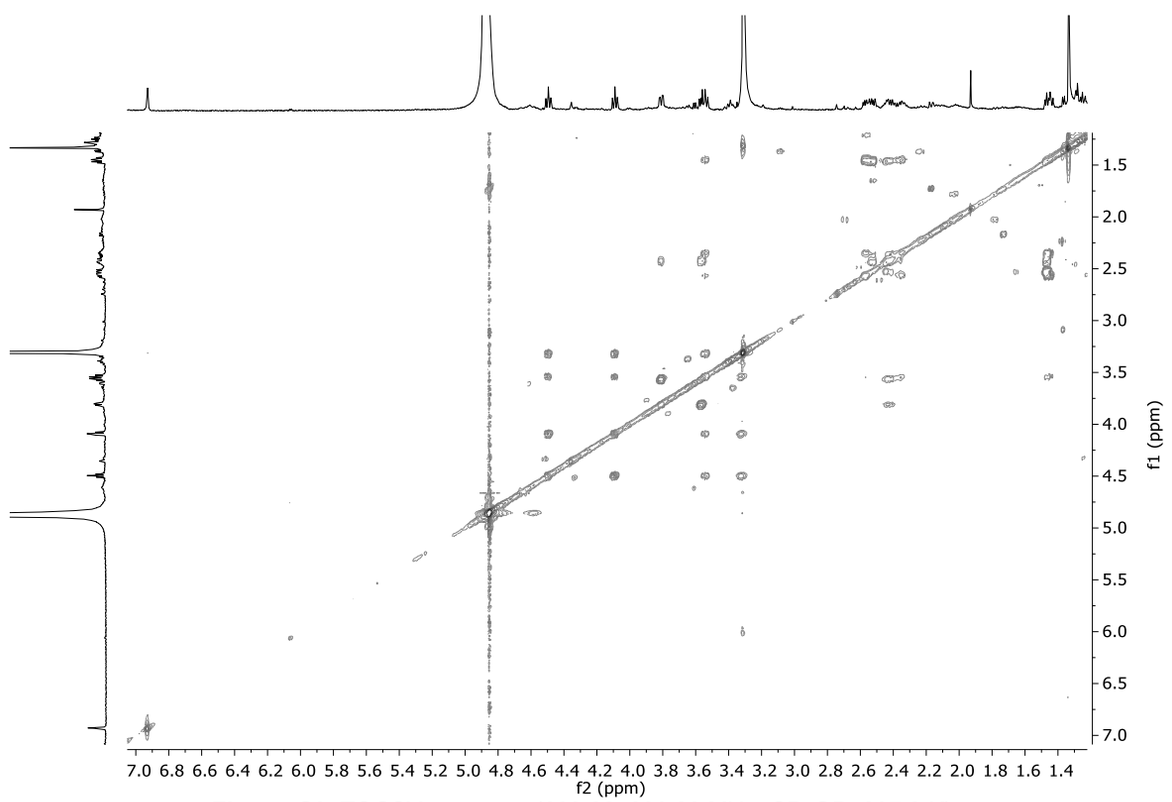

Figure. S9. TOCSY-spectrum (600.22, 600.22 MHz, CD_3OD, 297.2 K).

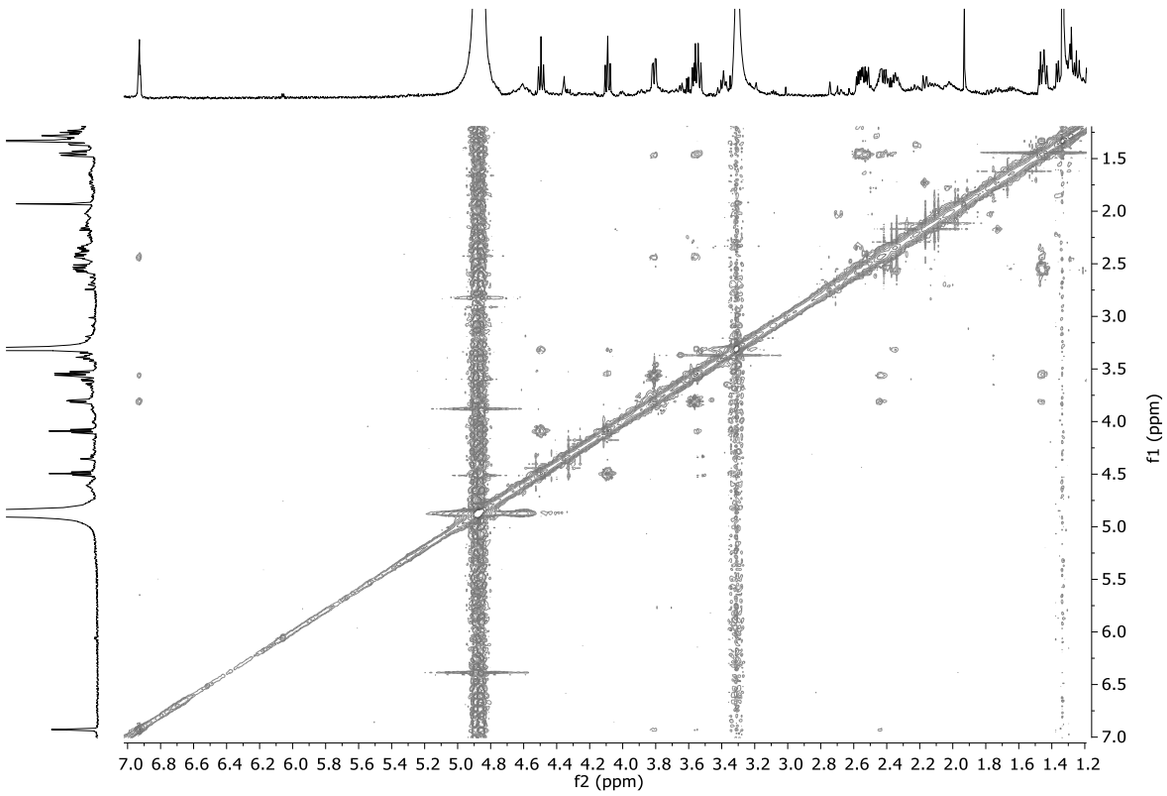

Figure. S10. NOESY-spectrum (600.50, 600.50 MHz, CD_3OD, 297.2 K).

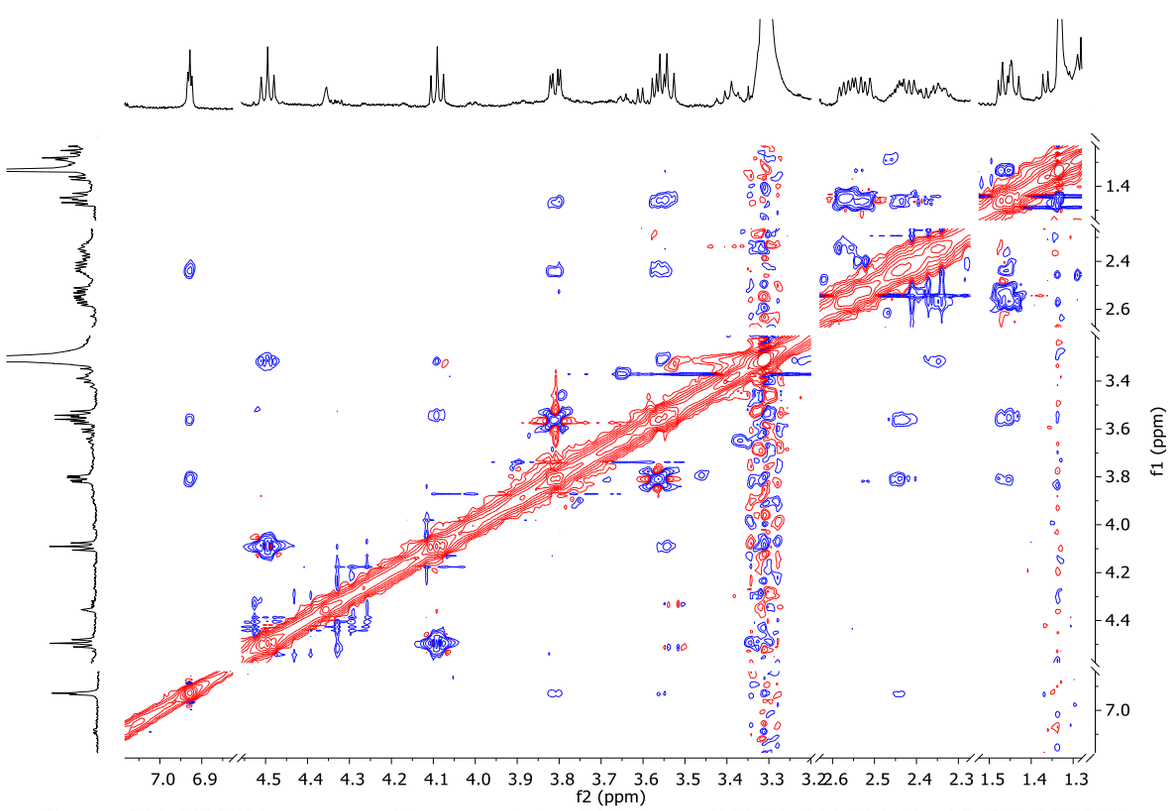

Figure. S11. NOESY-spectrum with removed signal-free areas (600.50, 600.50 MHz, CD_3OD, 297.2 K).

9.2 7,15-Dihydroxyblennin (**20**)

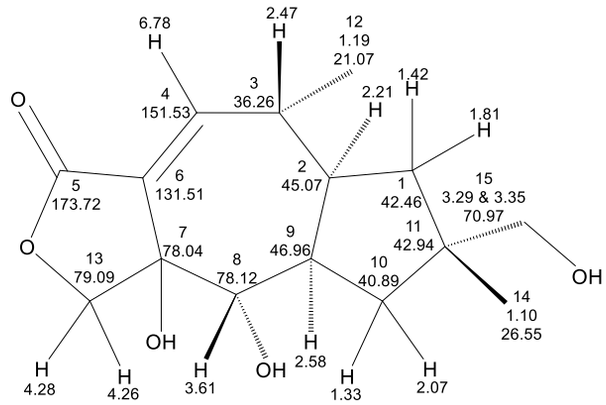

Figure. S12. Structure of compound **20** with assignments done previously, (CD_3OD).

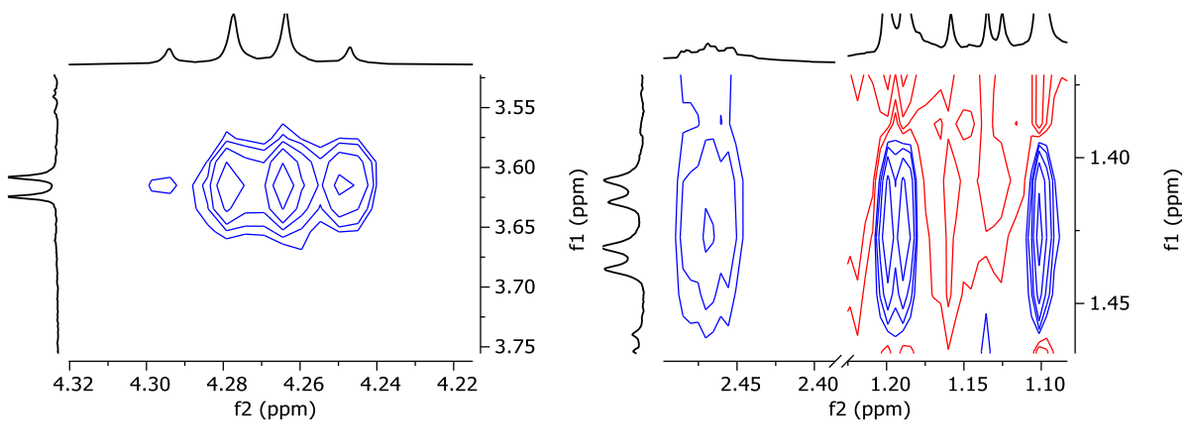

Figure. S13. ROESY expanded-spectrums of selected correlations, (CD_3OD).
Left: between δH 3.61 and 4.26 ppm. Right: between δH 1.42 and 2.47, 1.19, 1.10 ppm.

9.3 14-Carboxyl-deoxylactarorufin A (**22**)

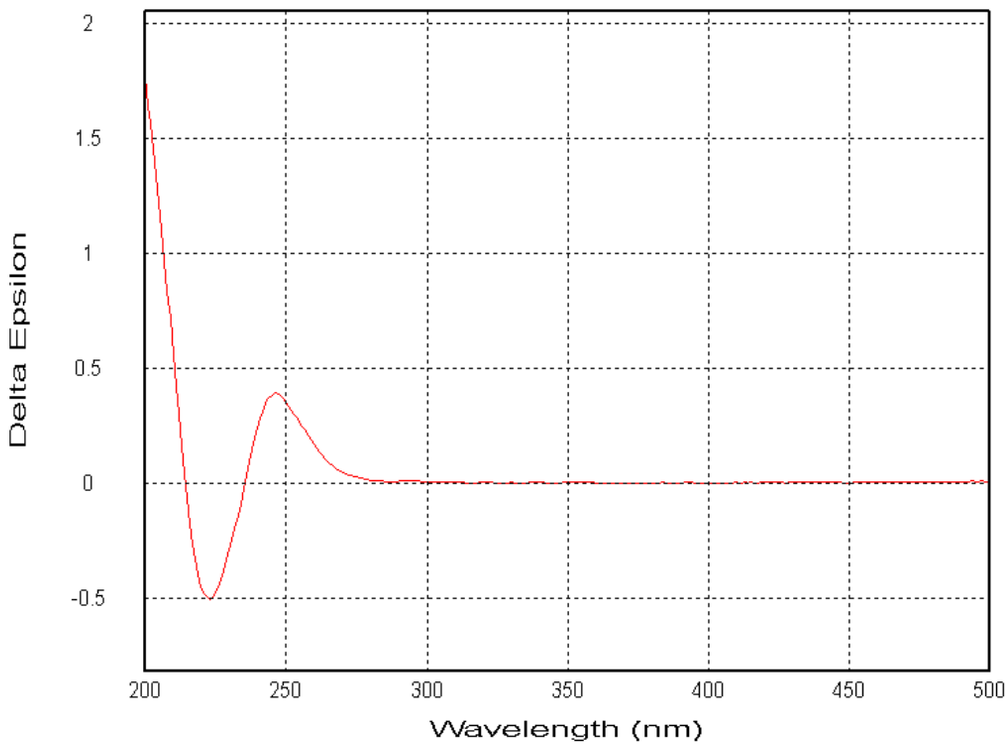

Figure. S14. CD-spectrum of the experimental measurement.

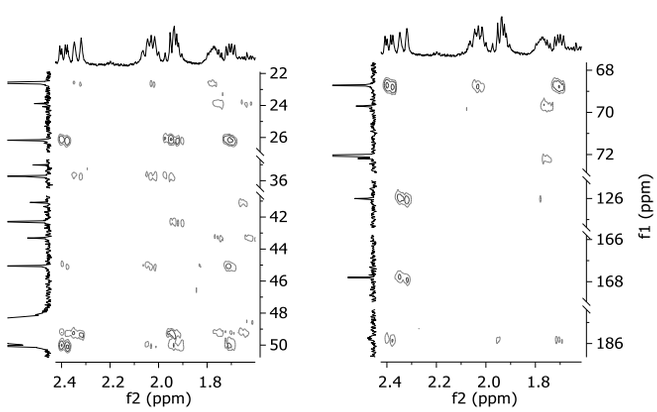

Figure. S15. HMBC concentrated-spectrums of correlations from previously extracted compound **22** from *L. circellatus*, (CD_3OD). Protons between δ_H 1.60 and 2.50 correlate with, left: carbons between δ_C 22.0 and 52.0, right: carbons between δ_C 68.0 and 186.3.

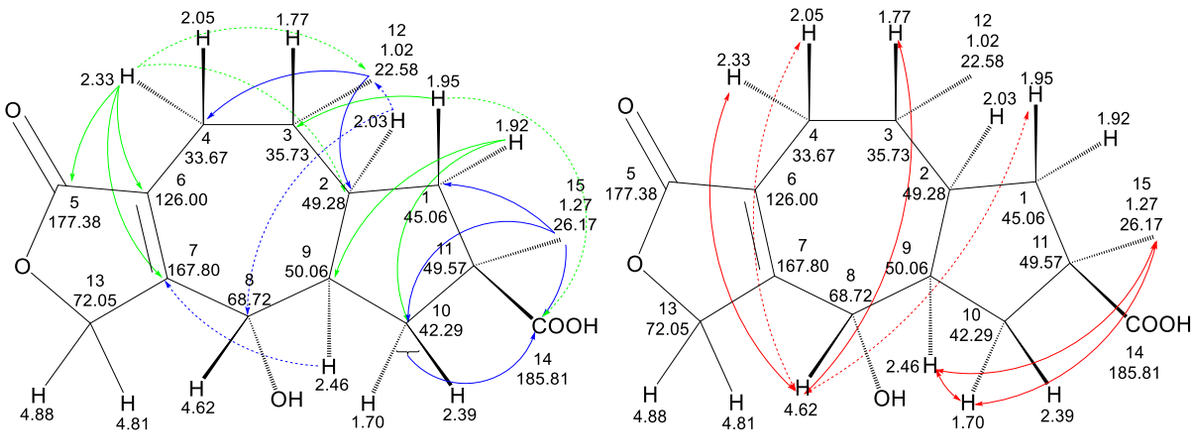

Figure. S16. Relative structure of compound **22** with assignments, measured in CD_3OD. Left: selected HMBC correlations (→), HMBC correlations with Karplus relationship (→). Right: NOESY correlations (↔).

9.4 13-Hydroxy-14-carboxyl-deoxylactarorufin A (**23**)

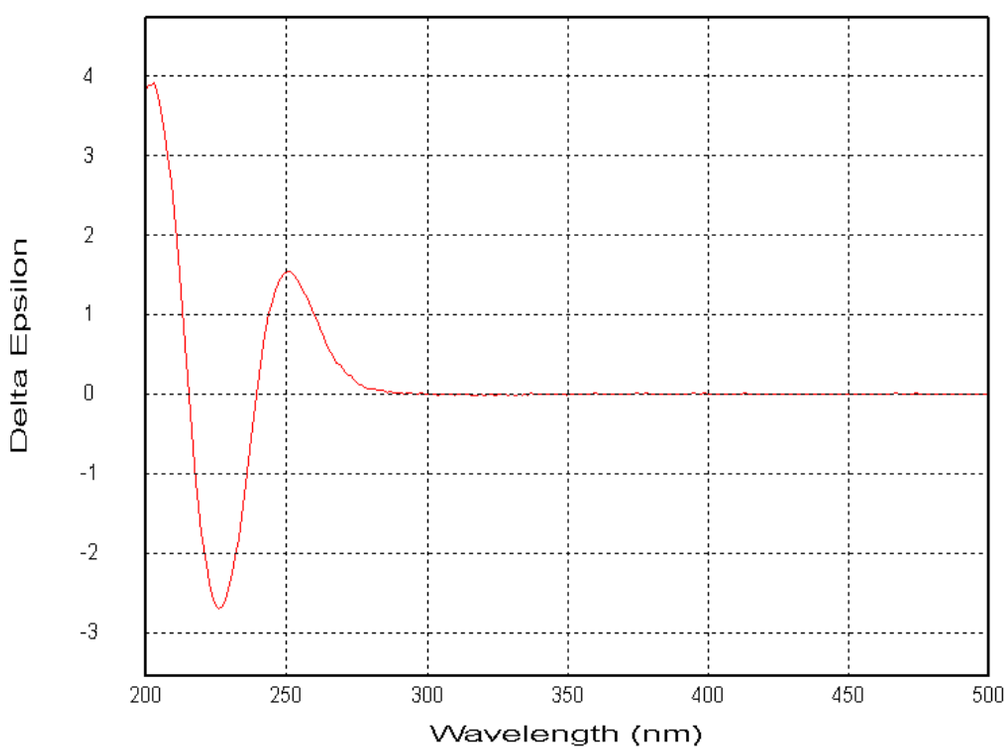

Figure. S17. CD-spectrum of the experimental measurement.

9.5 Lactaropone (**24**)

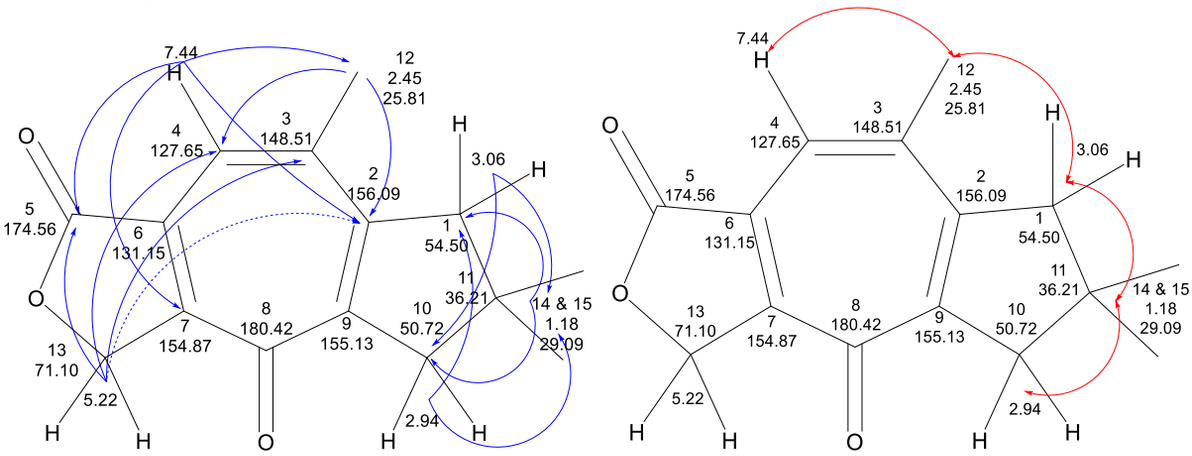

Figure. S18. Structure of compound **24** with assignments done previously of ^{1}H and ^{13}C-NMR, (CD_3OD). Left: with selected HMBC correlations (⟶). Right: with NOE correlations (⟷).

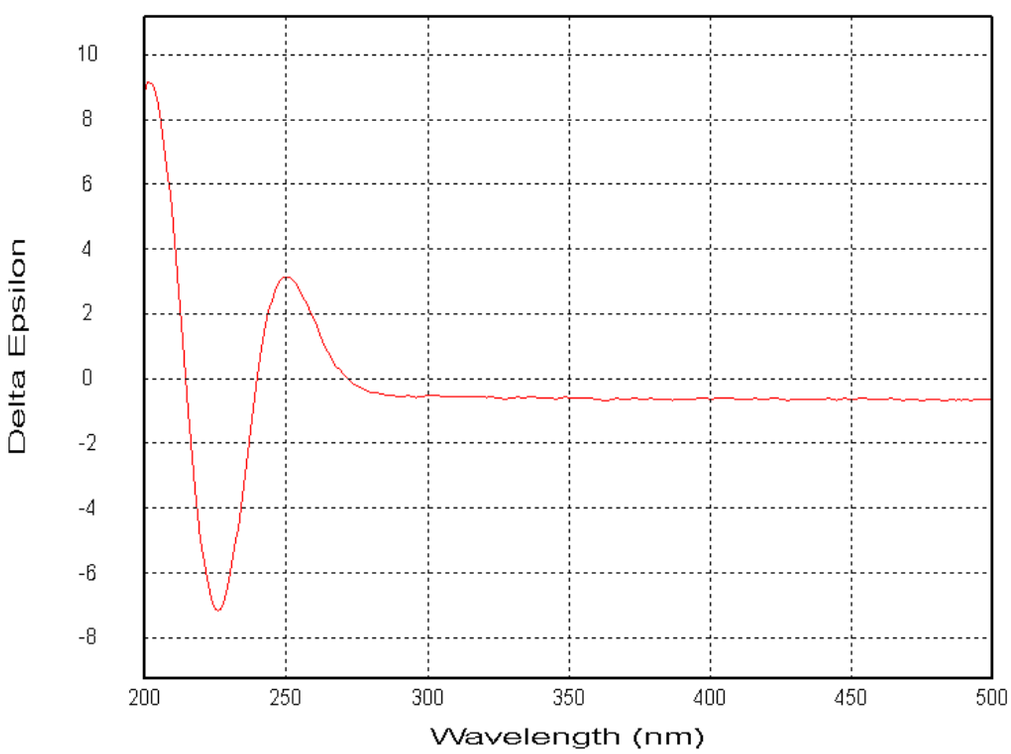

Figure. S19. CD-spectrum of the experimental measurement.

9.6 Lactarorufin A (**25**)

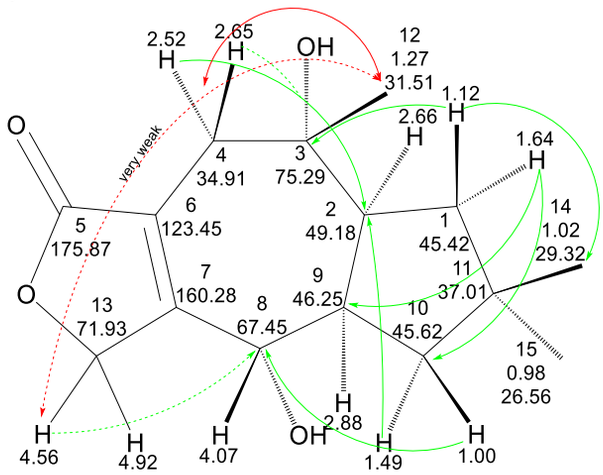

Figure. S20. Structure of compound **25** with assignments of ^{1}H and ^{13}C-NMR extracted from *L. circellatus*, ($CDCl_3$). With HMBC correlations with Karplus relationship (→). With NOE correlations (↔).

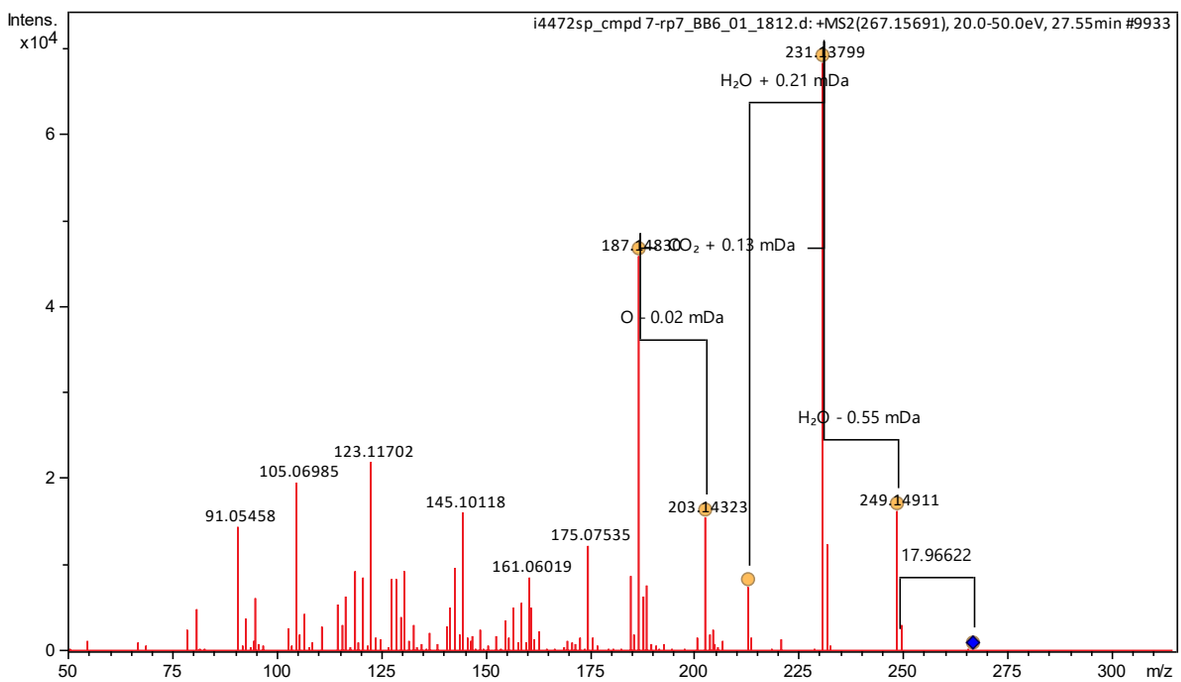

Figure. S21. HR-ESI-(+)-Ms/Ms-spectrum.

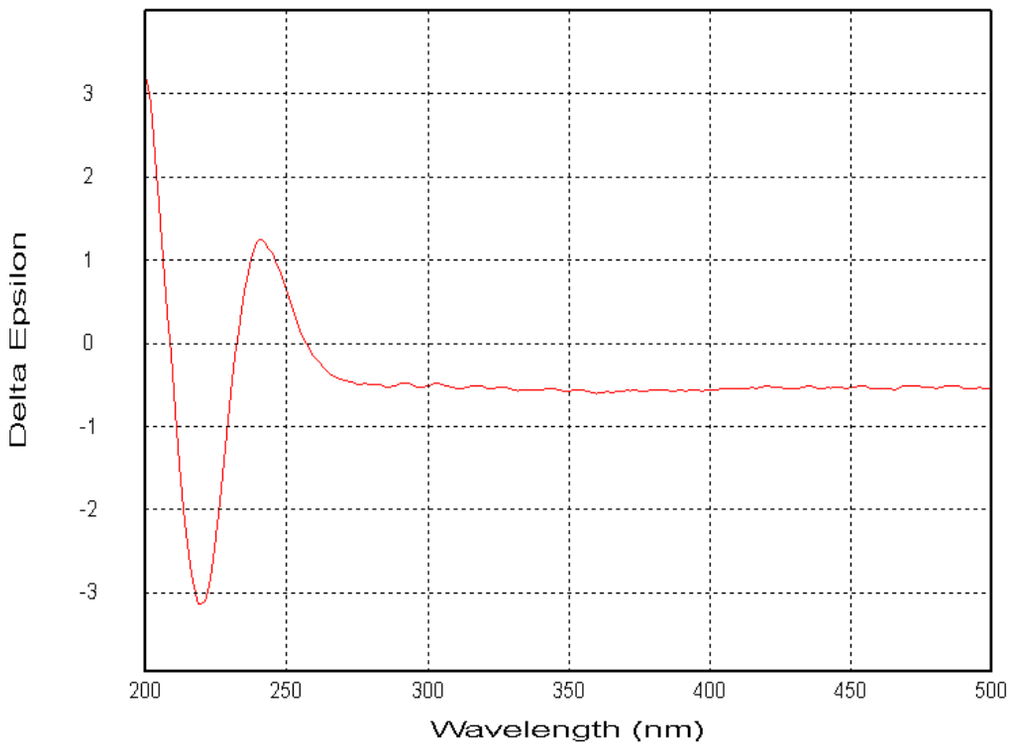

Figure. S22. CD-spectrum of the experimental measurement.

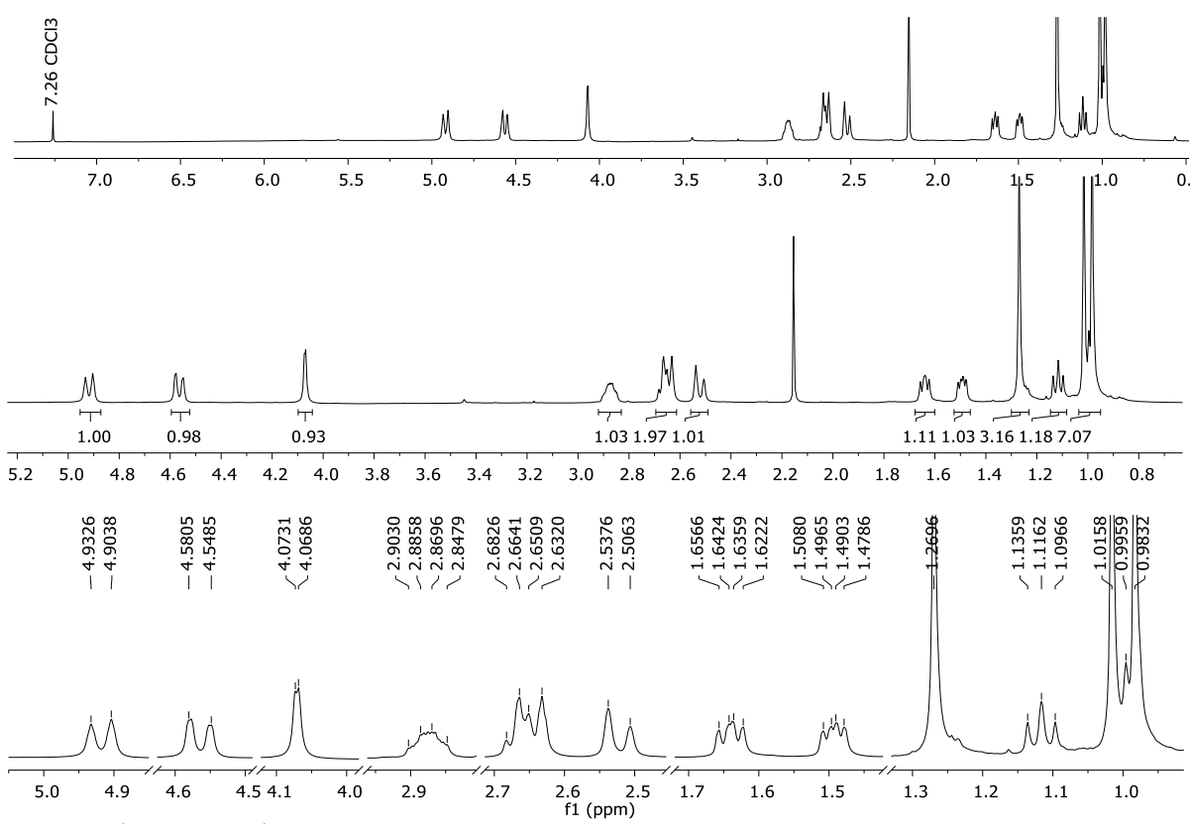

Figure. S23. ^{1}H-NMR and ^{1}H-NMR-spectrums with removed signal-free areas (600.22 MHz, $CDCl_3$, 297.2 K). From *L. circellatus*.

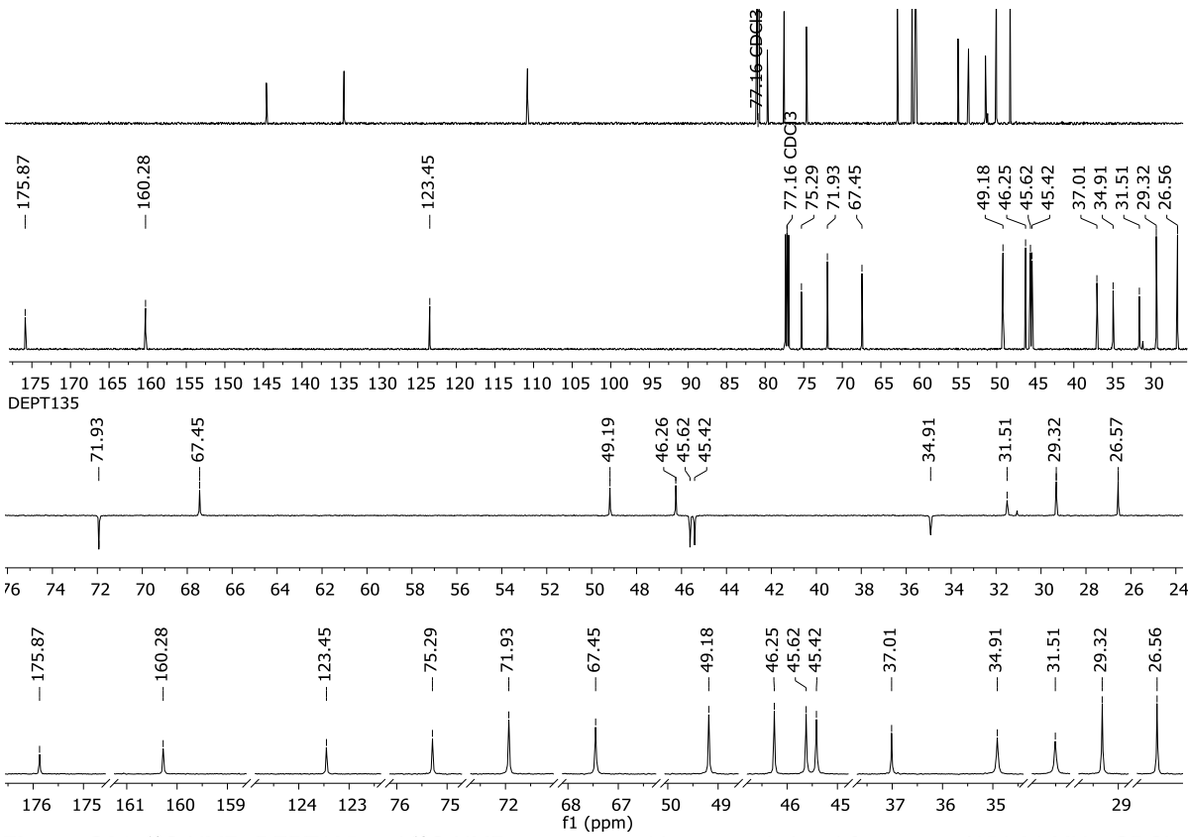

Figure. S24. ^{13}C-NMR, DEPT135 and ^{13}C-NMR-spectrums with removed signal-free areas (151.01 MHz, $CDCl_3$, 297.2 K). From *L. circellatus*.

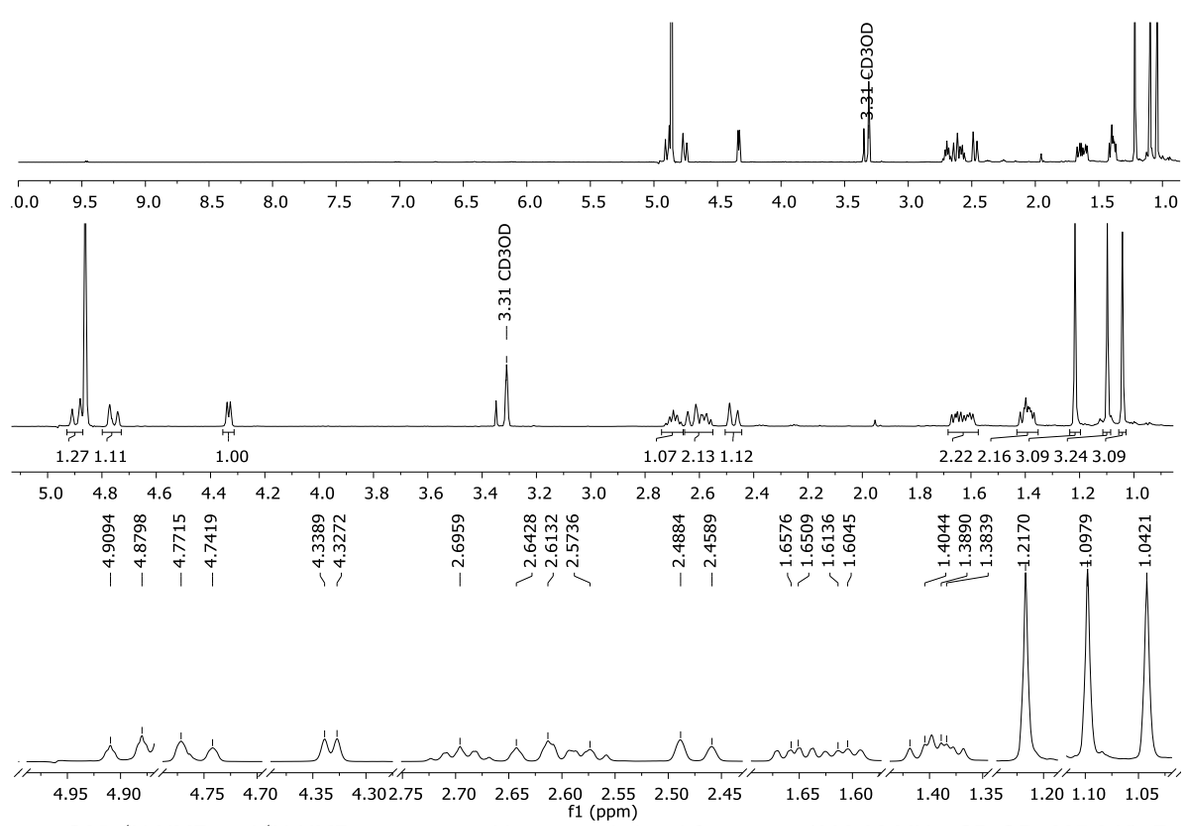

Figure. S25. ^{1}H-NMR and ^{1}H-NMR-spectrums with removed signal-free areas (600.22 MHz, CD_3OD, 297.2 K). From *L. trivialis*.

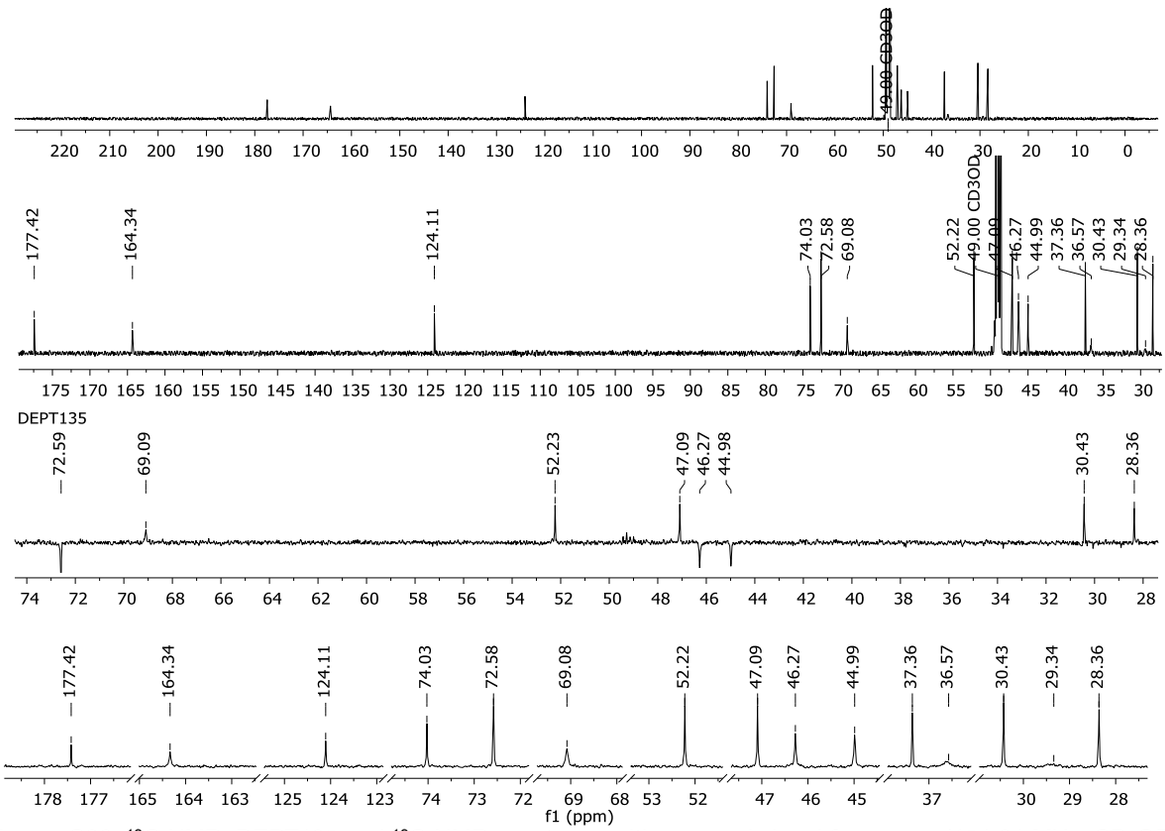

Figure. S26. ^{13}C-NMR, DEPT135 and ^{13}C-NMR-spectrums with removed signal-free areas (151.01 MHz, CD_3OD, 297.2 K). From *L. trivialis*.

9.7 Deoxylactarorufin A (**26**)

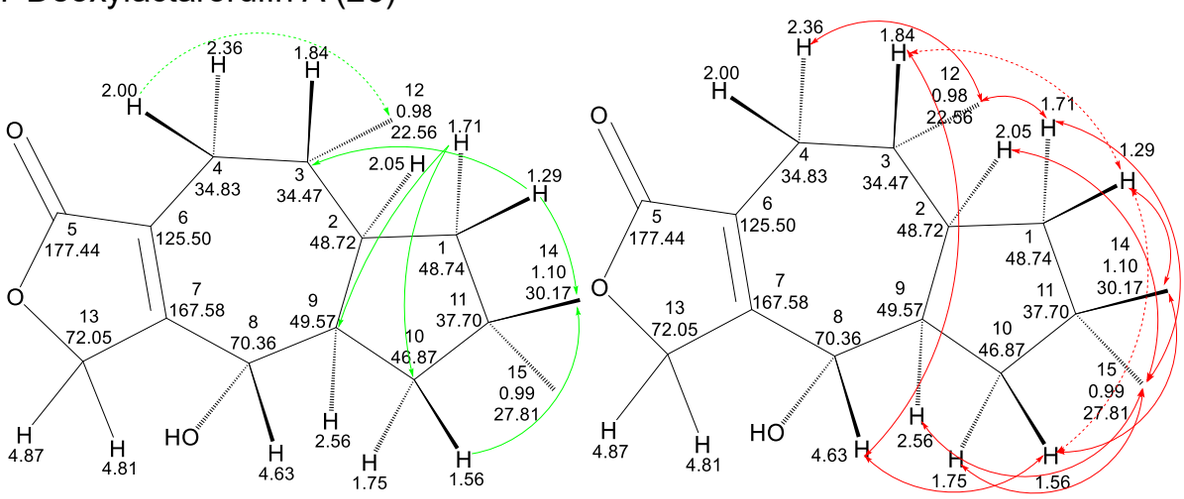

Figure. S27. Structure of compound **26** with assignments already measured in ($CDCl_3$). Left: with HMBC correlations with Karplus relationship (⟶). Right: with NOESY correlations (⟷).

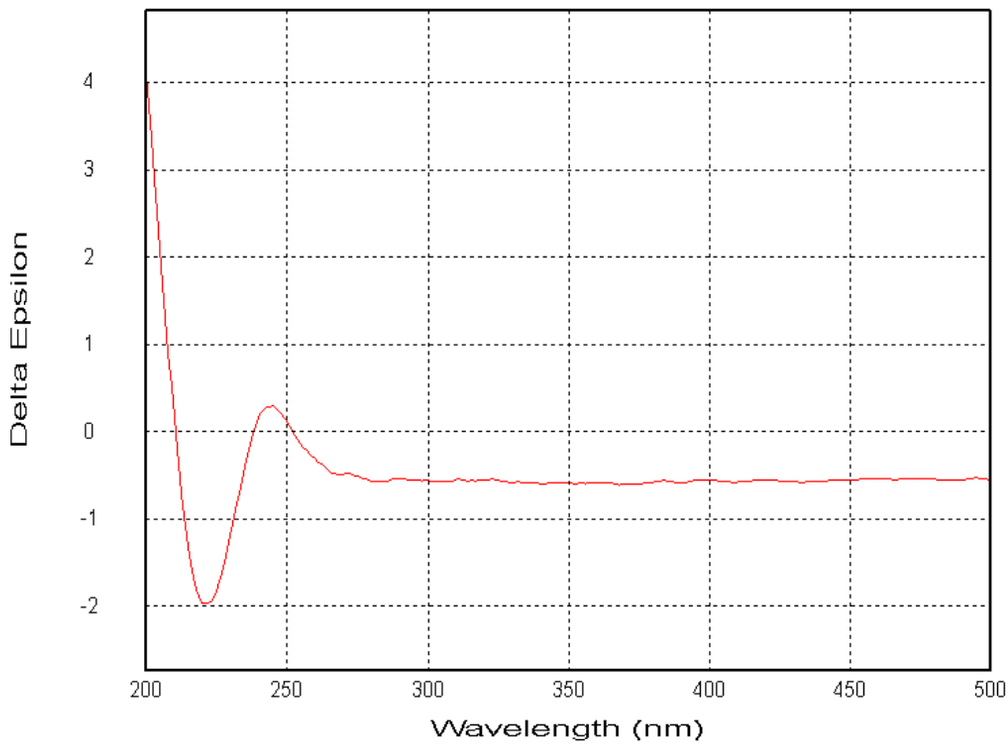

Figure. S28. CD-spectrum of the experimental measurement.

9.8 Lactarorufin B (**27**)

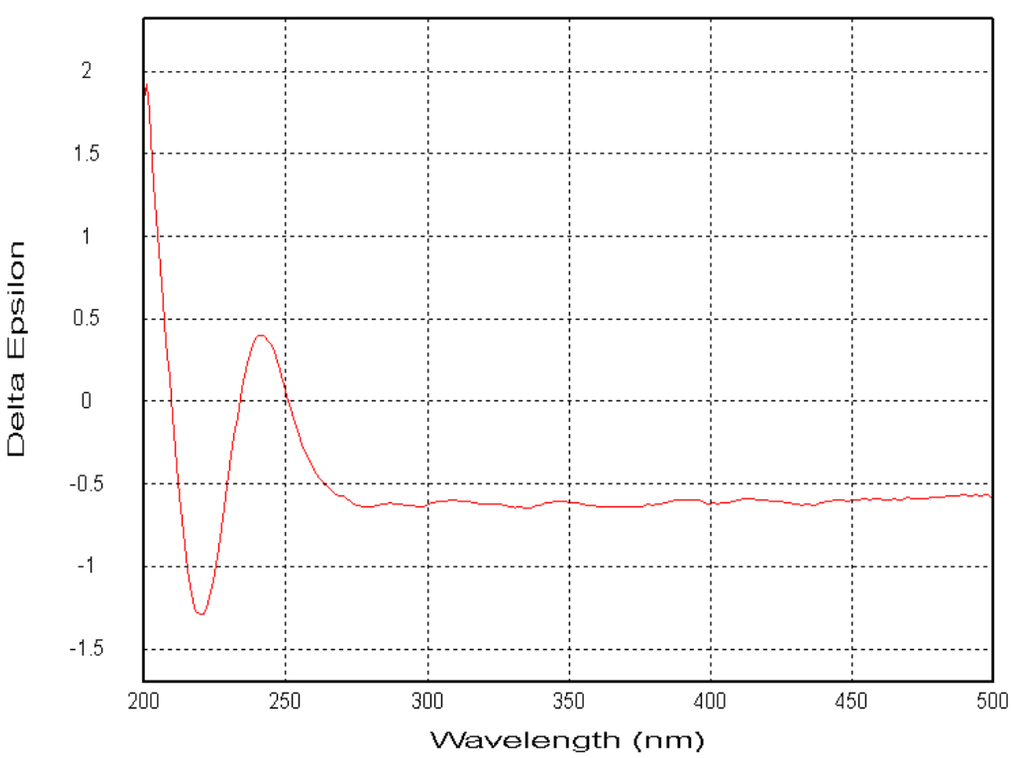

Figure. S29. CD-spectrum of the experimental measurement.

9.9 Furandiol **15**

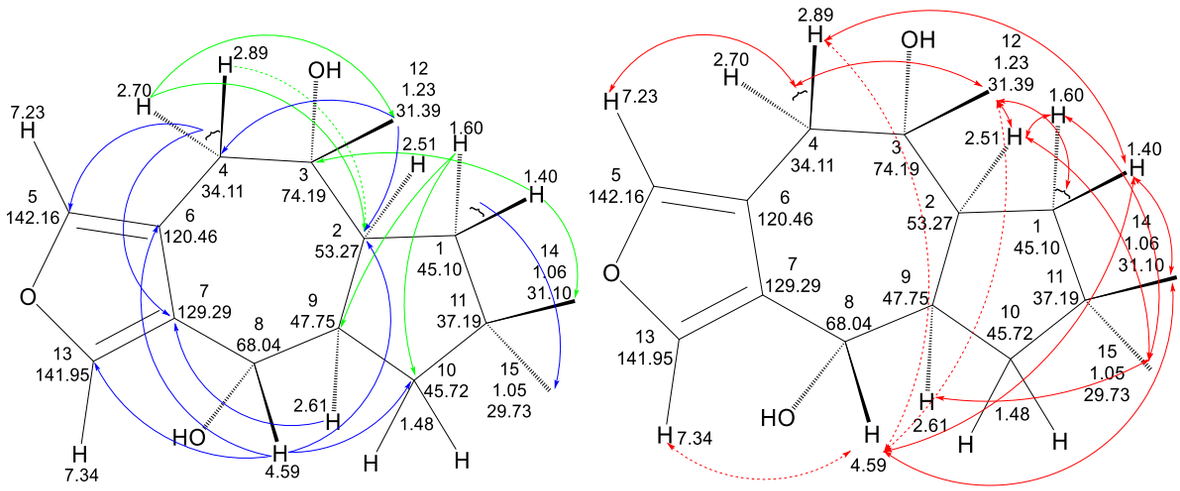

Figure. S30. Structure of the previously extracted compound **15** from *L. circellatus*, assignments.
Left: with HMBC correlations (→), HMBC correlations with Karplus relationship (→).
Right: with NOESY correlations (↔), (CD_3OD).

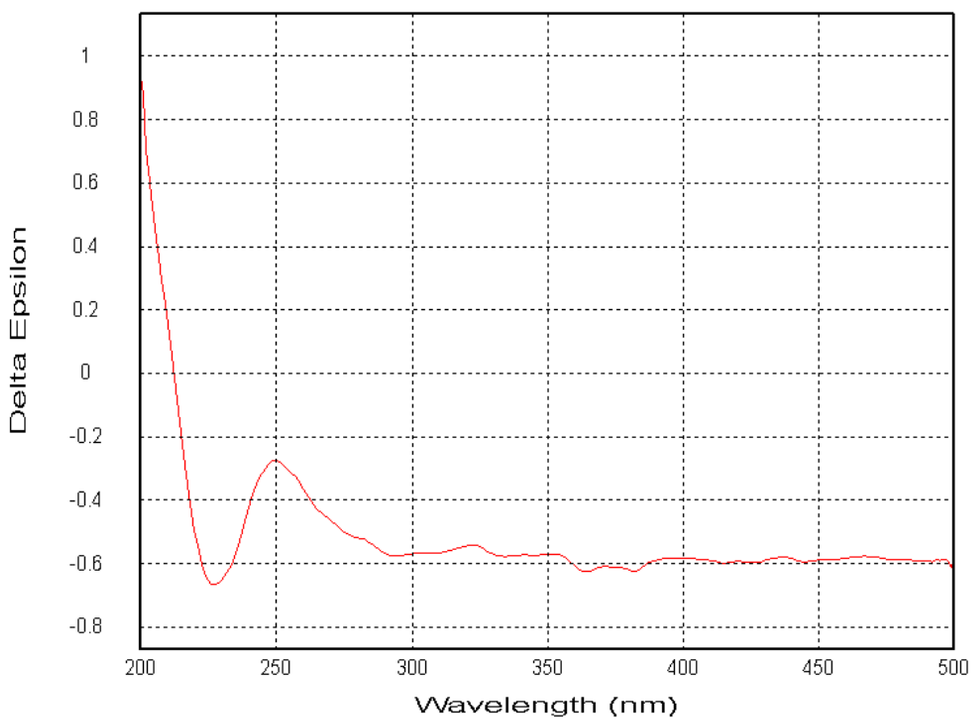

Figure. S31. CD-spectrum of the experimental measurement.

9.10 Furan alcohol **28**

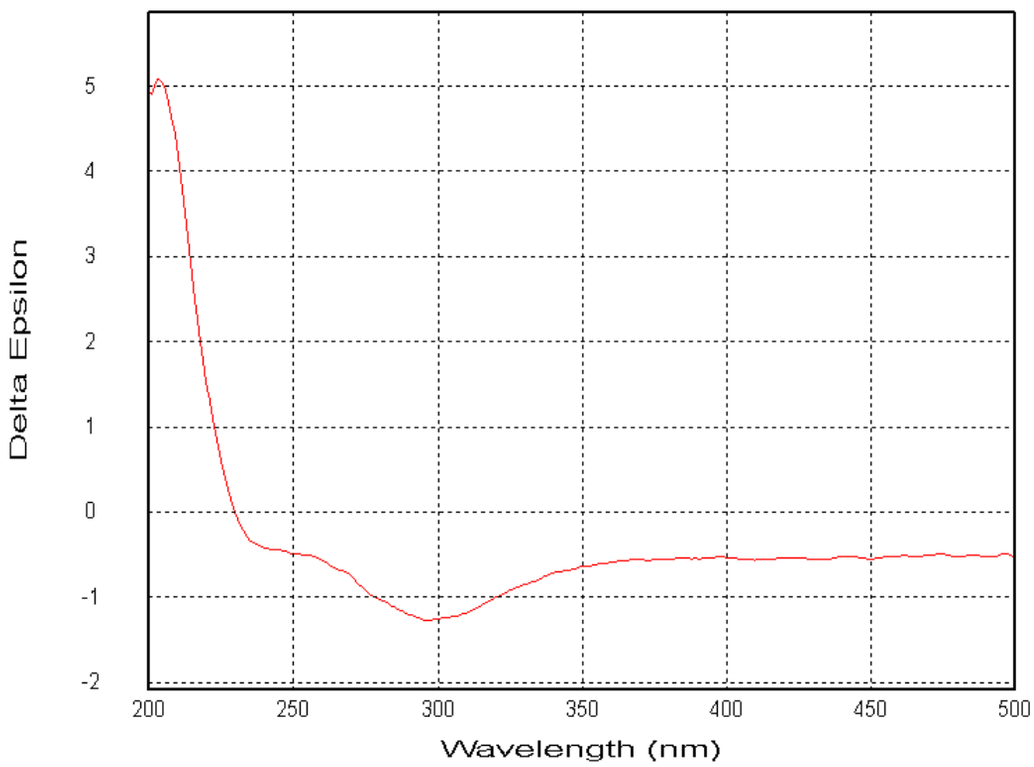

Figure. S32. CD-spectrum of the experimental measurement.

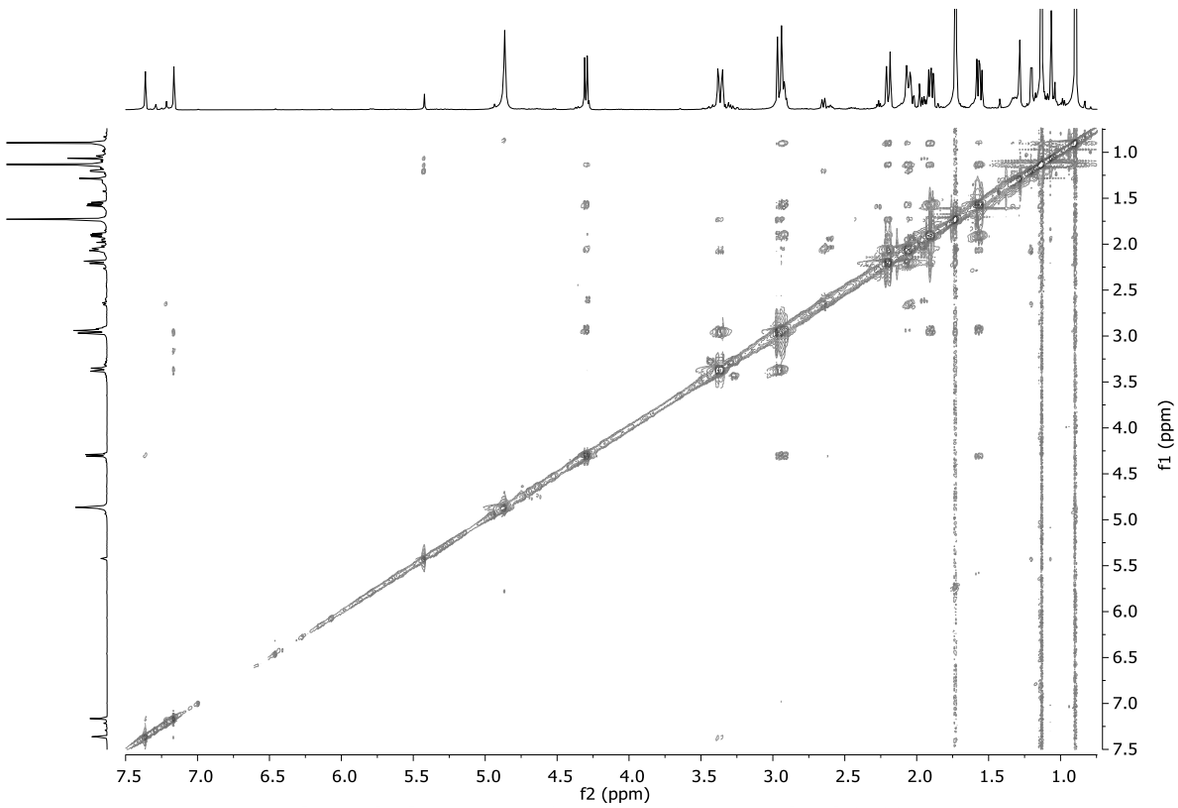

Figure. S33. NOESY-spectrum (600.50, 600.50 MHz, CD_3OD, 297.2 K).

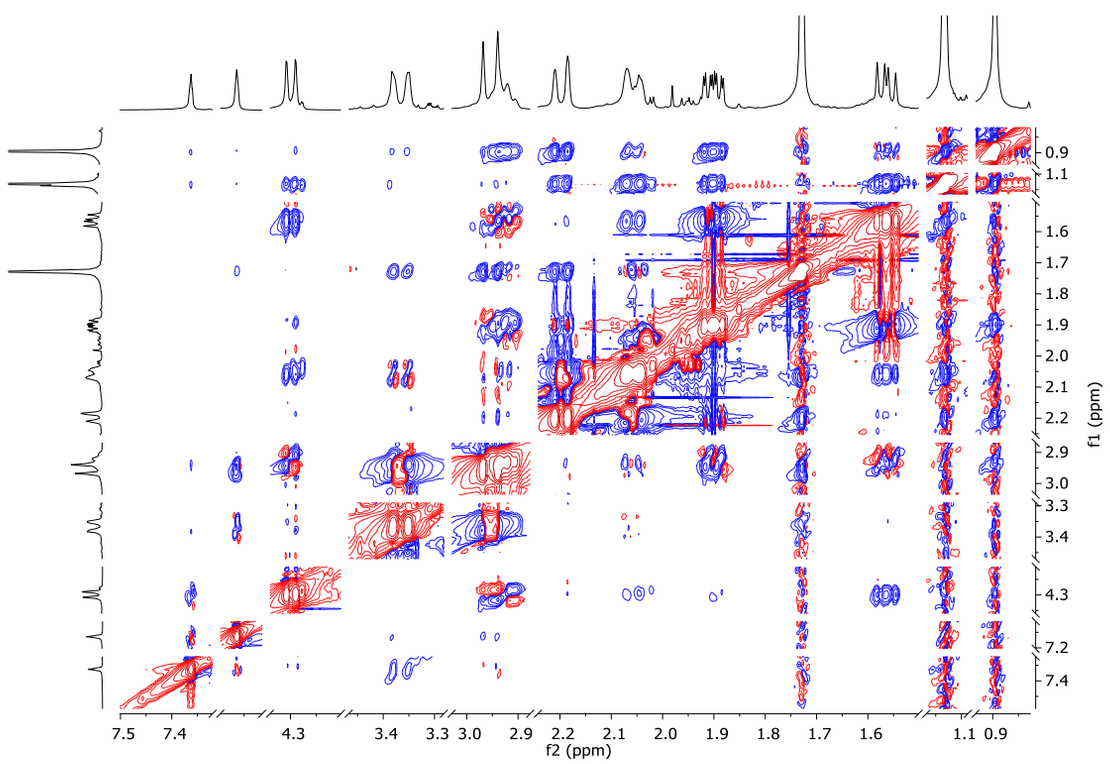

Figure. S34. NOESY-spectrum with removed signal-free areas (600.50, 600.50 MHz, CD_3OD, 297.2 K).

9.11 3,8-Oxalactarorufin A (**30**)

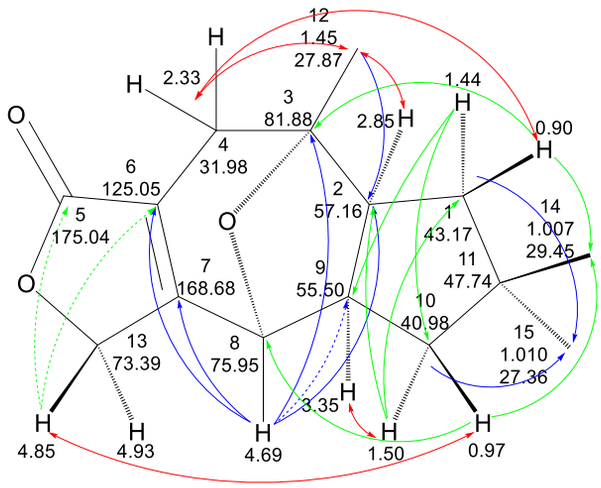

Figure. S35. Structure of the previously extracted compound **30** from *L. circellatus*, with assignments, with HMBC correlations (→), HMBC correlations with Karplus relationship (→) and with NOESY correlations (↔), (CD_3OD).

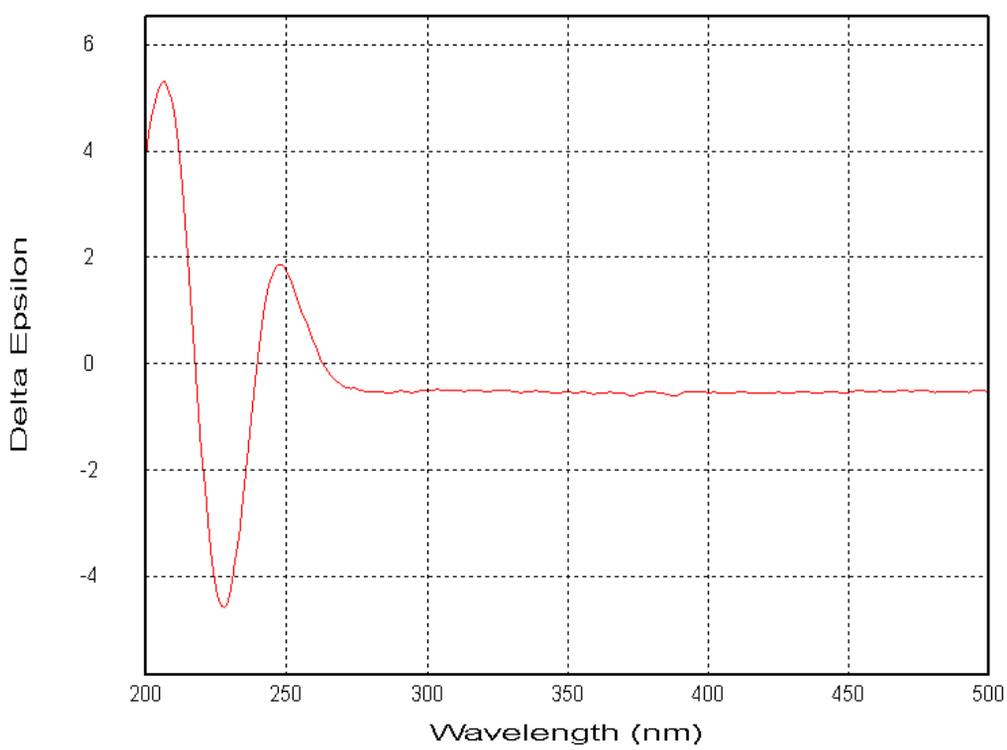

Figure. S36. CD-spectrum of the experimental measurement.

9.12 Lactarorufin N (**13**)

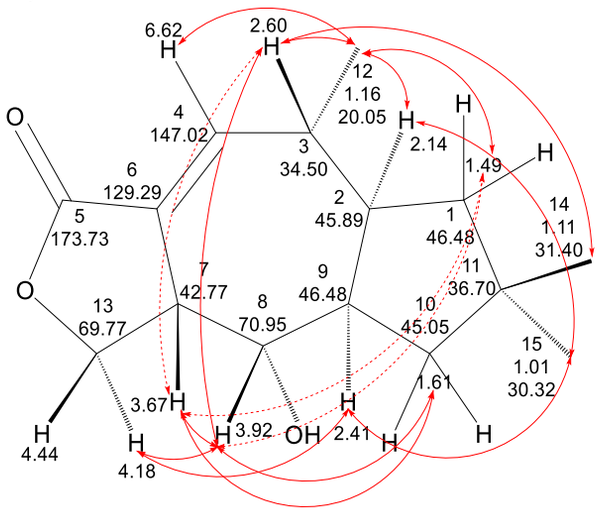

Figure. S37. Structure of the previously extracted compound **13** from *L. circellatus*, with assignments, with NOESY correlations (↔), (CD_3OD).

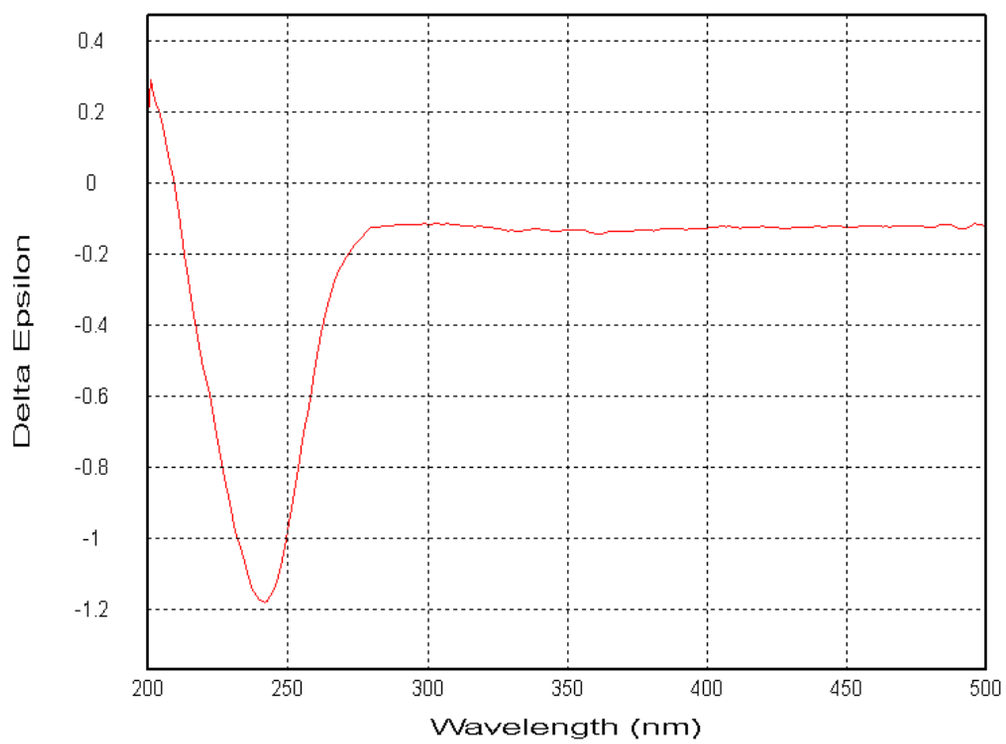

Figure. S38. CD-spectrum of the experimental measurement.

9.13 Blennin C (**18**)

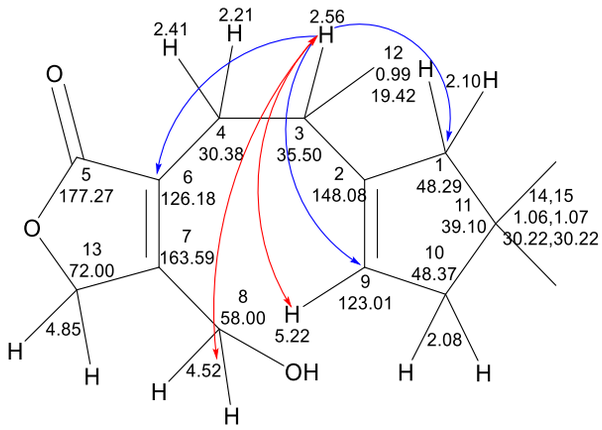

Figure. S39. Structure of the previously extracted compound **18** from *L. circellatus*, with assignments, with HMBC correlations (⟶) and with NOESY correlations (⟷), (CD_3OD).

9.14 3,12-Anhydrolactarorufin A (**31**)

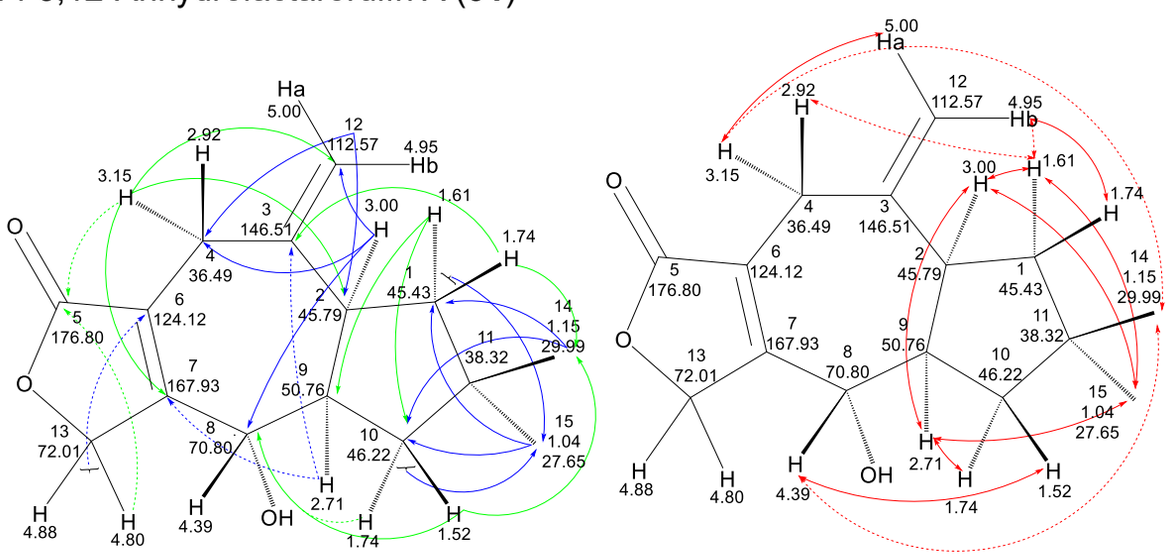

Figure. S40. Structure of the previously extracted compound **31** from *L. circellatus*, assignments.
Left: with HMBC correlations (⟶), HMBC correlations with Karplus relationship (⟶).
Right: with NOESY correlations (⟷), (CD_3OD).

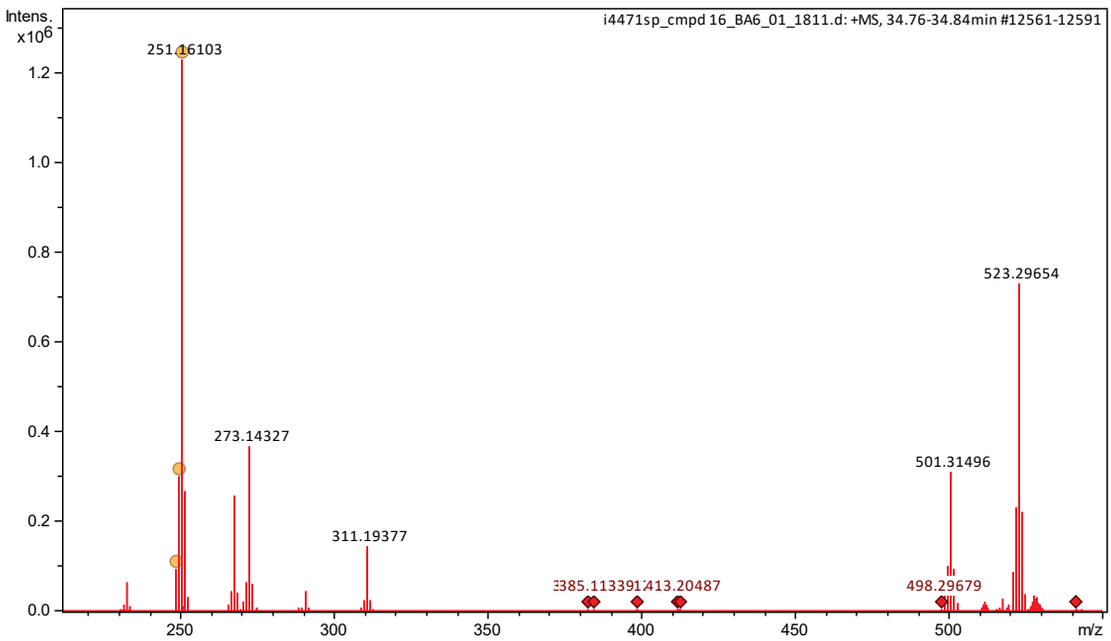

Figure. S41. Mass signal from HR-LCMS for compound **31**.

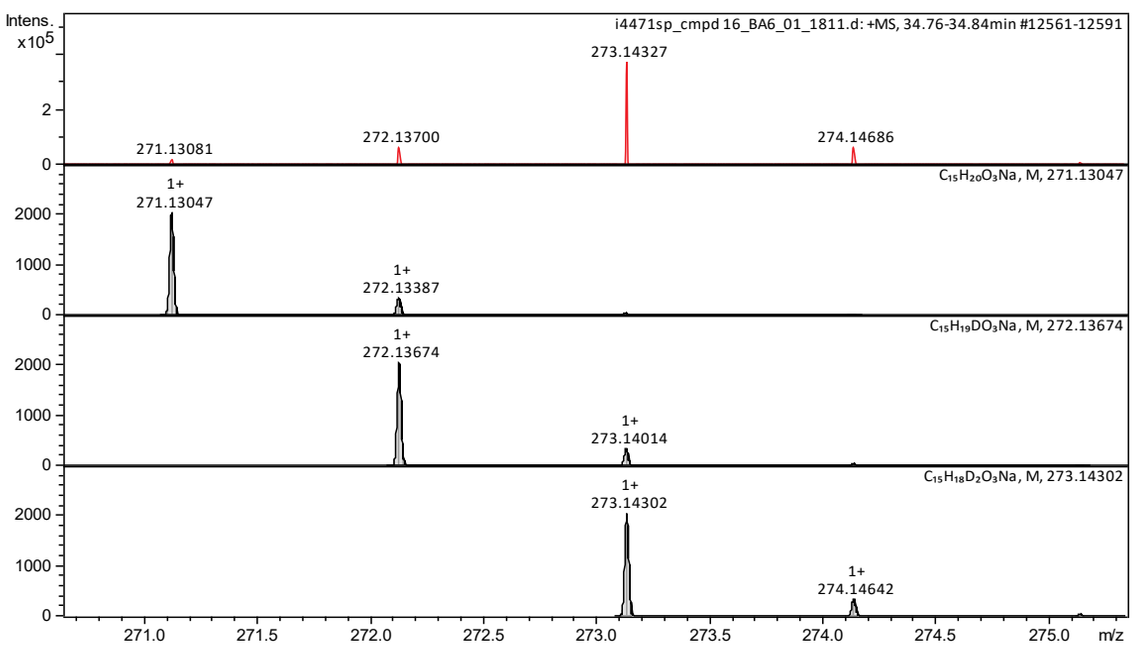

Figure. S42. From up to down: Mass signal from HR-LCMS for compound **31**. Generated ion with compound attached to Na atom, $[M+Na]^+$. Generated ion with compound with one deuterium atom attached to Na atom, $[MD+Na]^+$. Generated ion with compound with two deuterium atoms attached to Na atom, $[MD_2+Na]^+$.

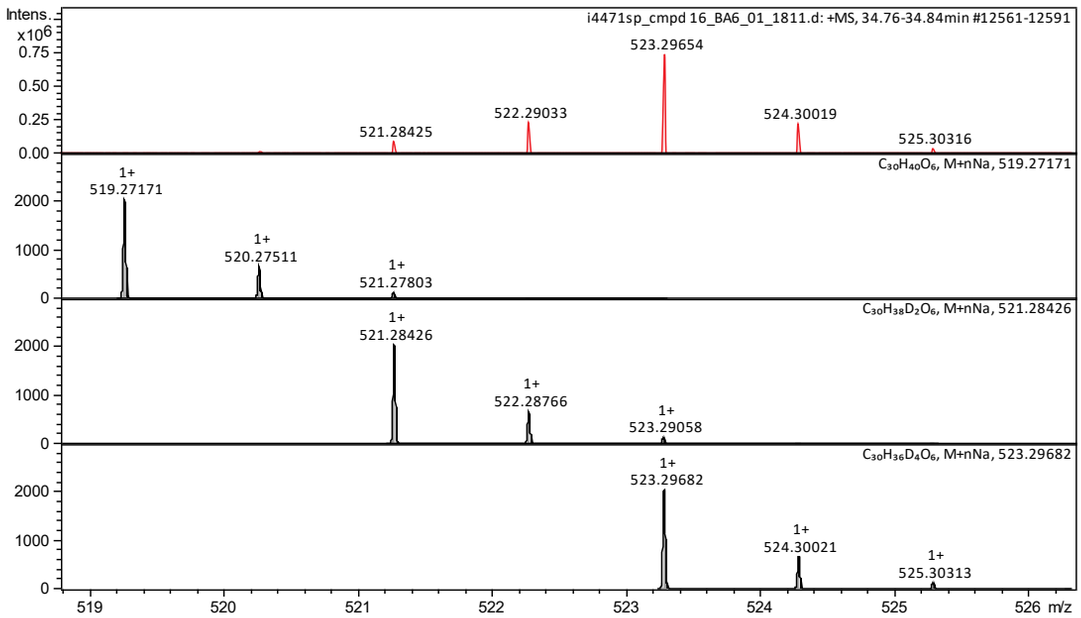

Figure. S43. From up to down: Mass signal from HR-LCMS for compound **31**. Generated ion with compound attached to Na atom, $[2M+Na]^+$. Generated ion with compound with one deuterium atom attached to Na atom, $[2MD+Na]^+$. Generated ion with compound with two deuterium atoms attached to Na atom, $[2MD_2+Na]^+$.

9.15 15-Hydroxyblennin A (**34**)

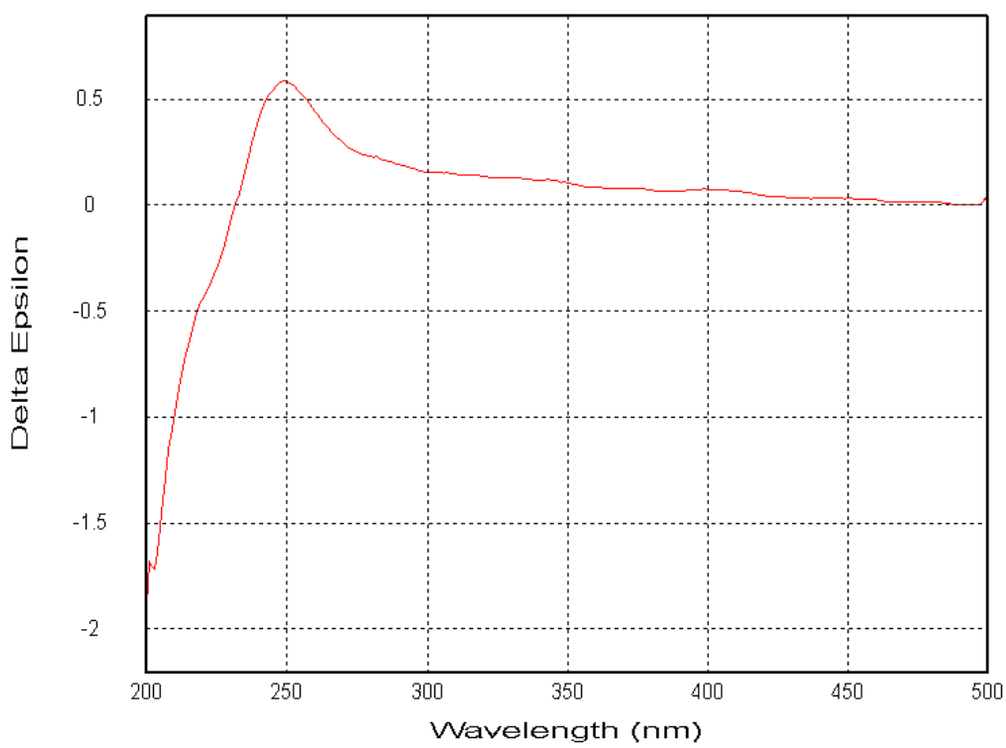

Figure. S44. CD-spectrum of the experimental measurement.

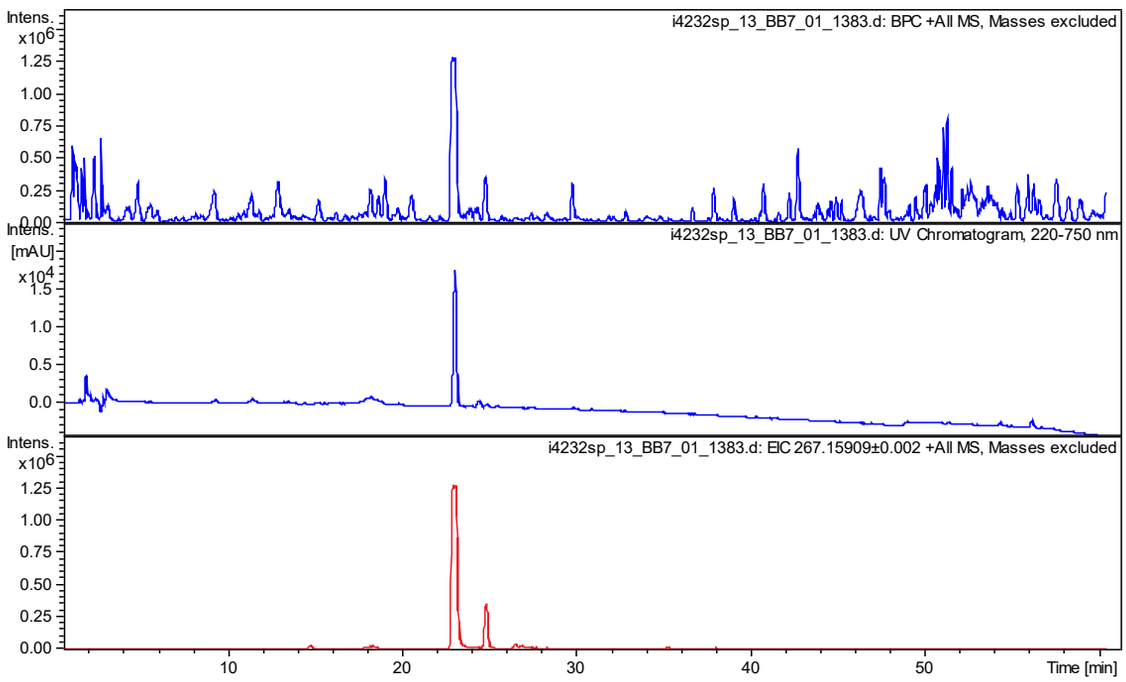

Figure. S45. HR-ESI-(+)-MS, UV/Vis and mass excluded chromatograms, gradient in section 6.3.4.7.

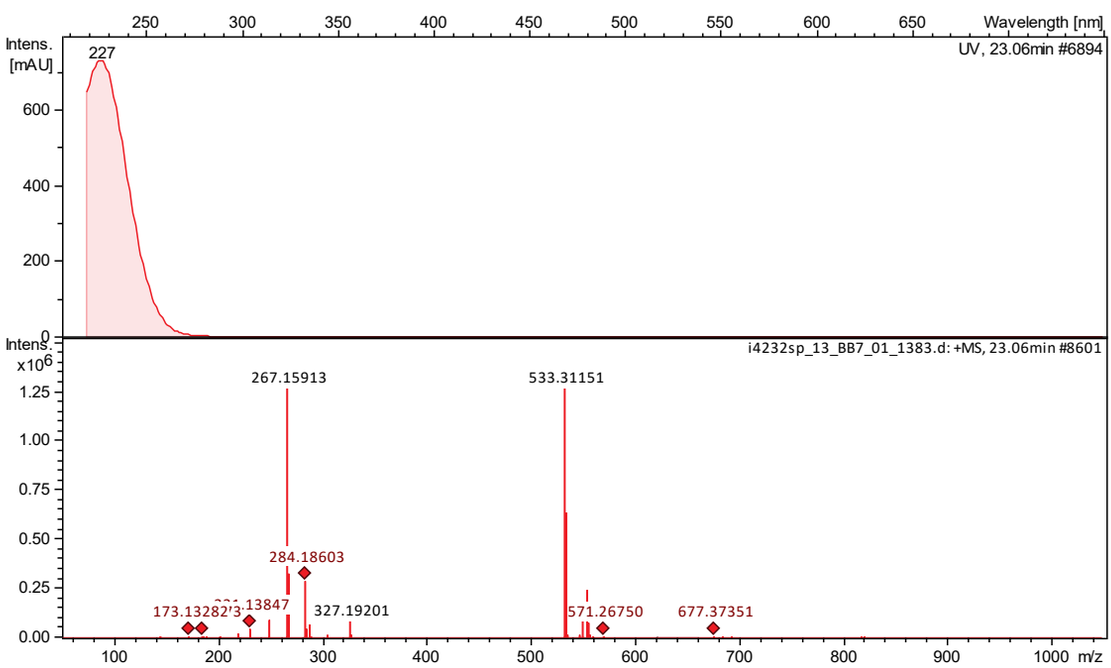

Figure. S46. HR-ESI-(+)-MS and UV/Vis-spectrums of compound **34** from *L. circellatus*.

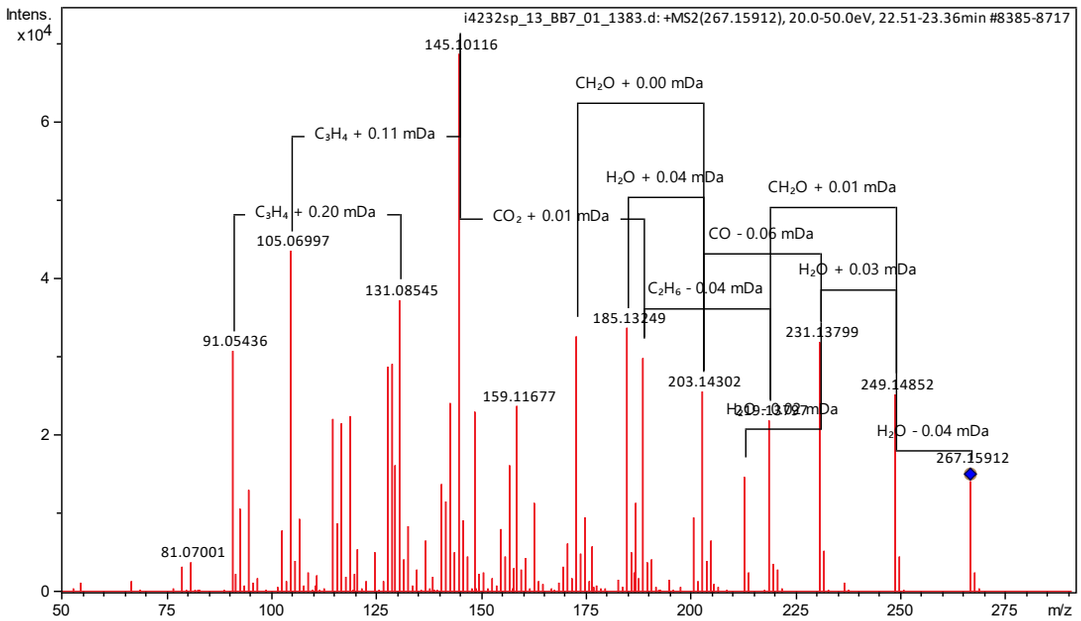

Figure. S47. HR-ESI-(+)-MS/MS-spectrum.

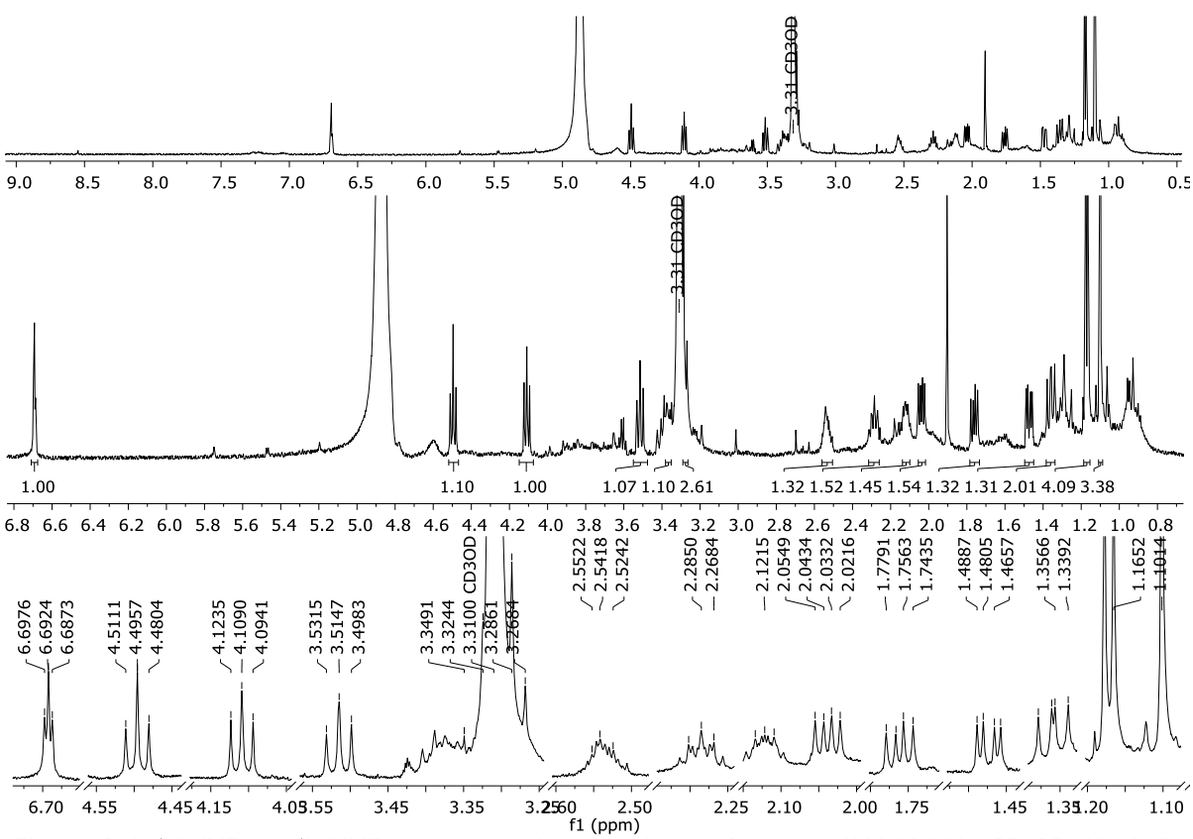

Figure. S48. ^{1}H-NMR and ^{1}H-NMR-spectrums with removed signal-free areas (600.22 MHz, CD_3OD, 297.2 K).

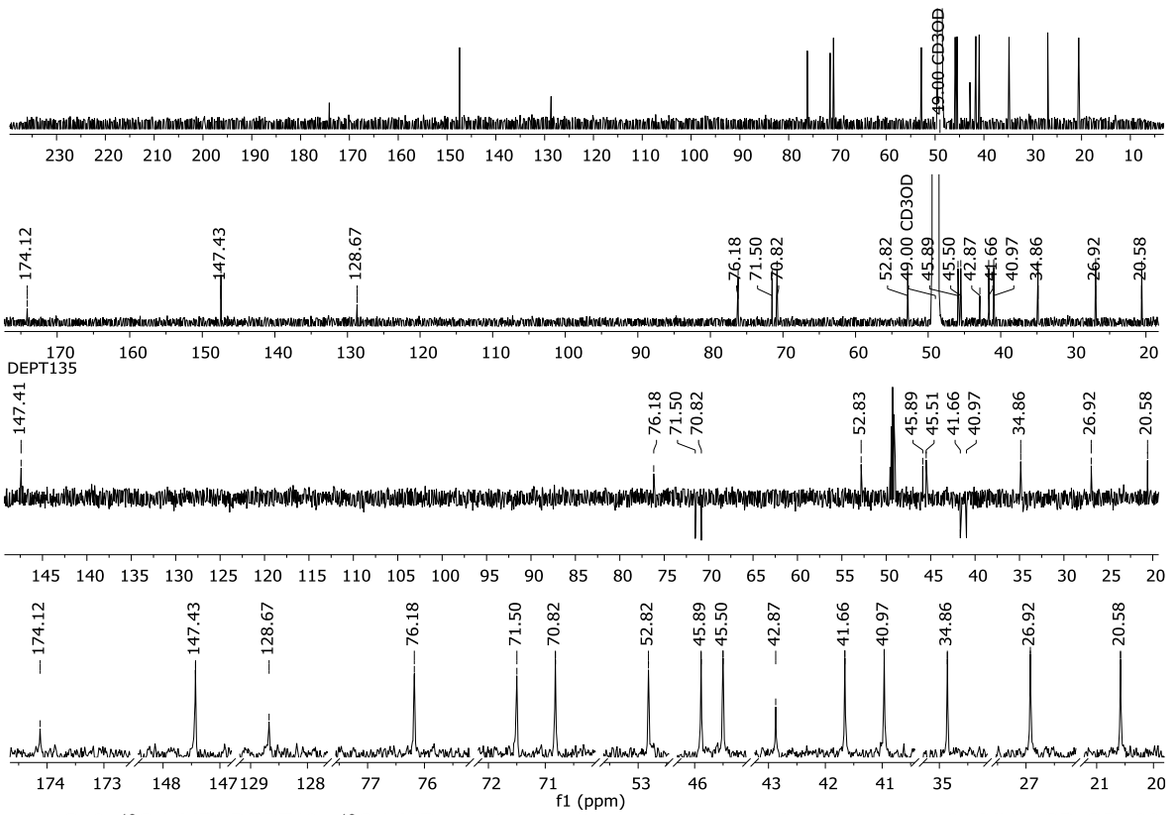

Figure. S49. ^{13}C-NMR, DEPT135 ^{13}C-NMR-spectrums with removed signal-free areas (151.01 MHz, CD_3OD, 297.2 K).

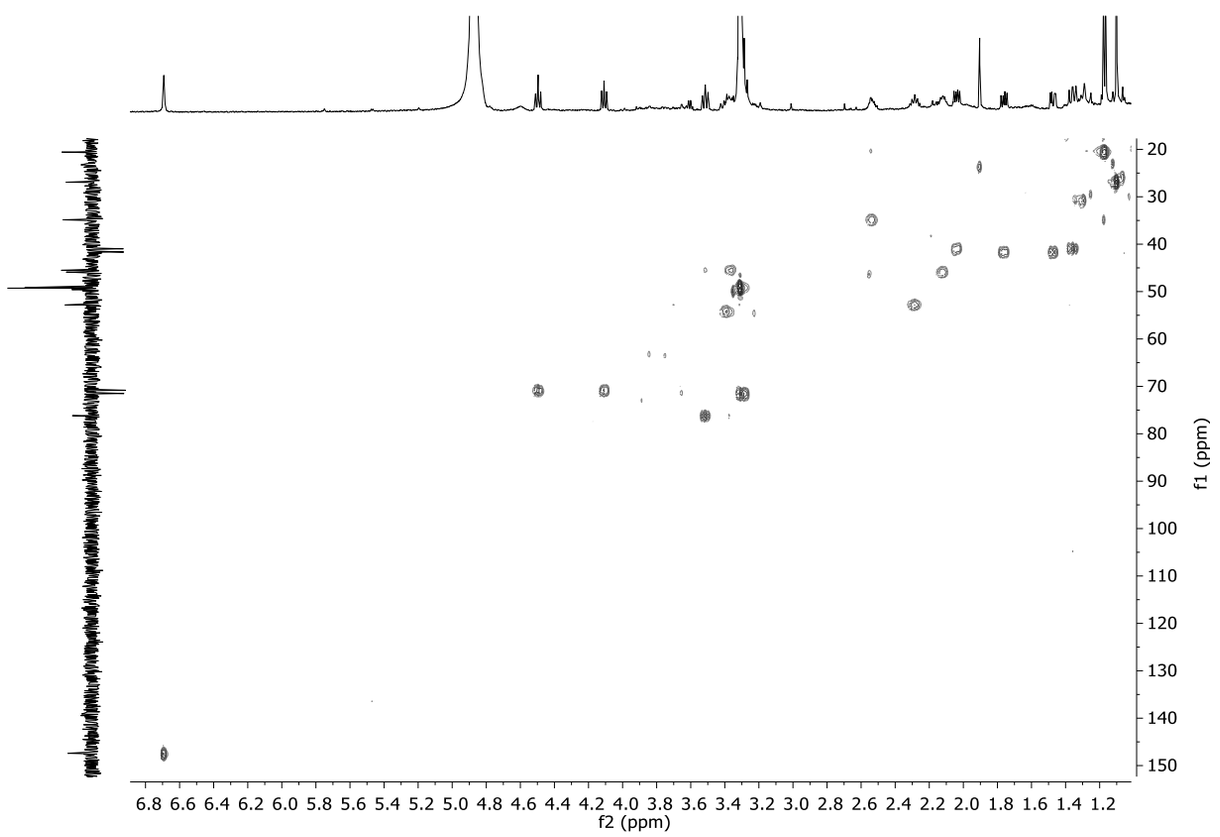

Figure. S50. HSQC-spectrum (600.50, 151.01 MHz, CD3OD, 297.1 K).

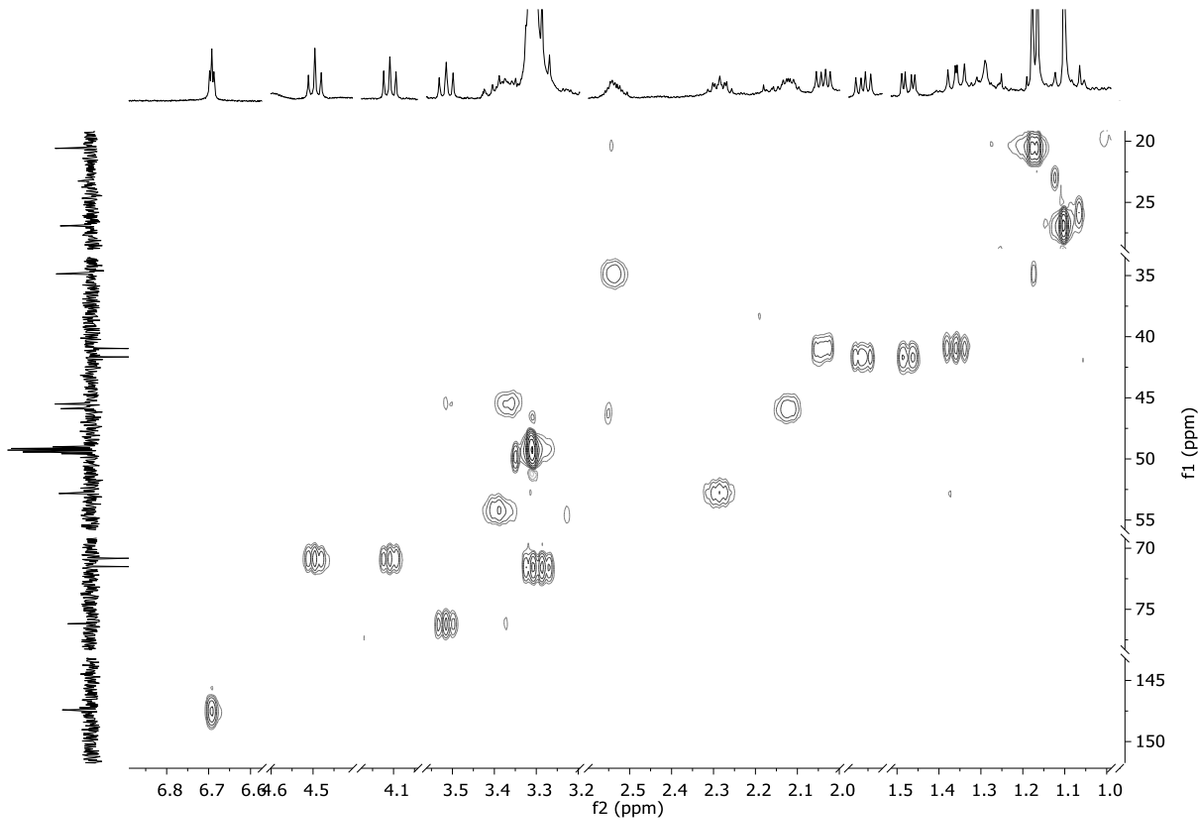

Figure. S51. HSQC-spectrum with removed signal-free areas (600.50, 151.01 MHz, CD3OD, 297.1 K).

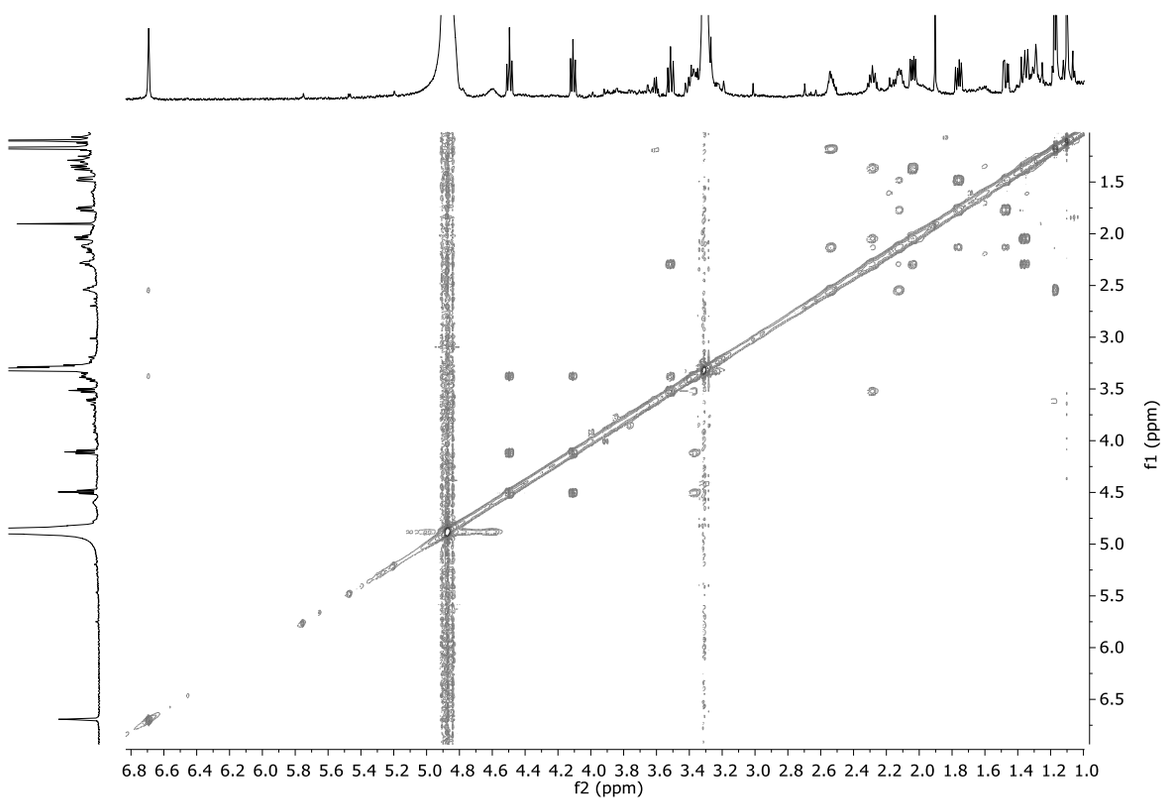

Figure. S52. COSY-spectrum (600.22, 600.22 MHz, CD3OD, 297.1 K).

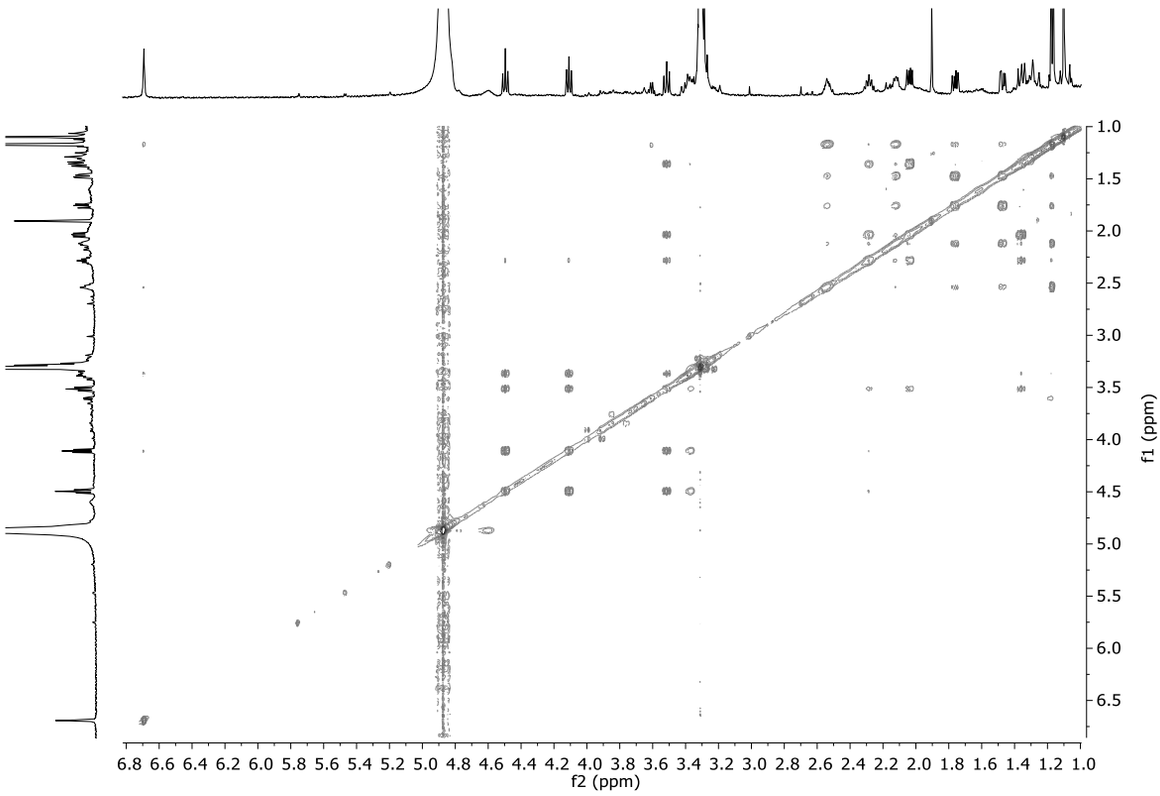

Figure. S53. TOCSY-spectrum (600.22, 600.22 MHz, CD3OD, 297.1 K).

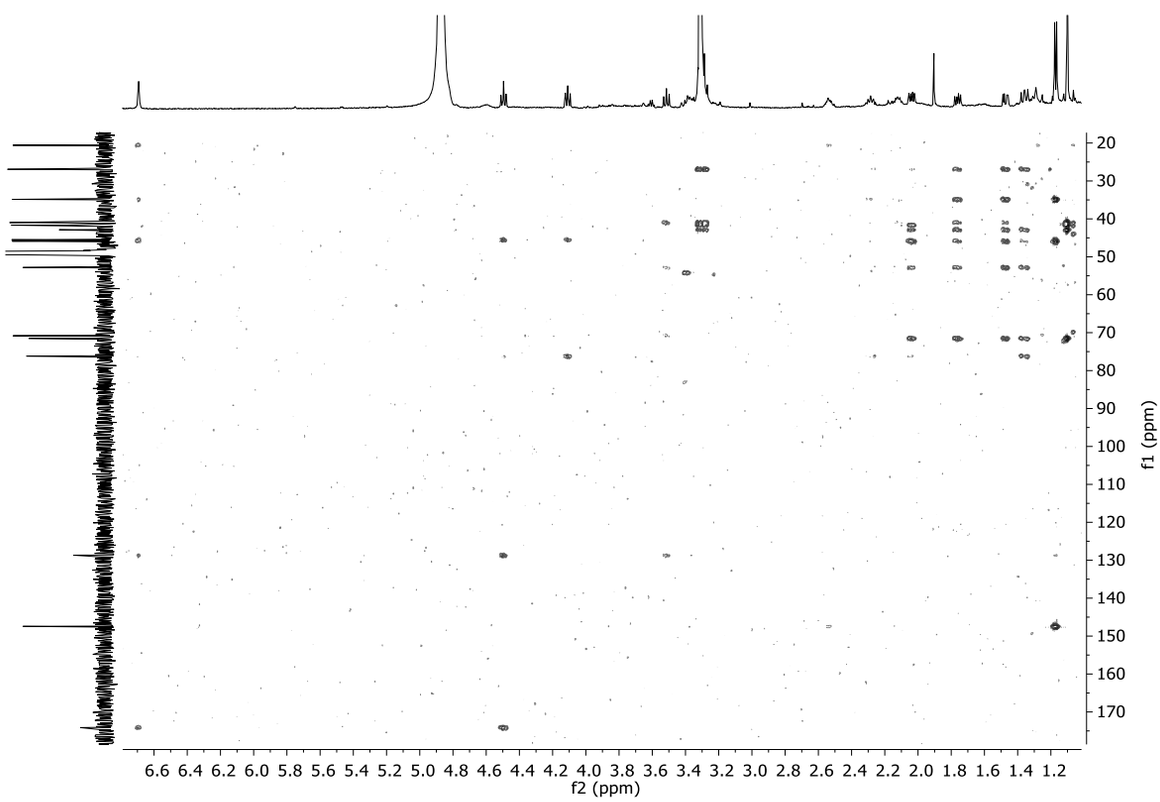

Figure. S54. HMBC-spectrum (600.50, 151.01 MHz, CD3OD, 297.2 K).

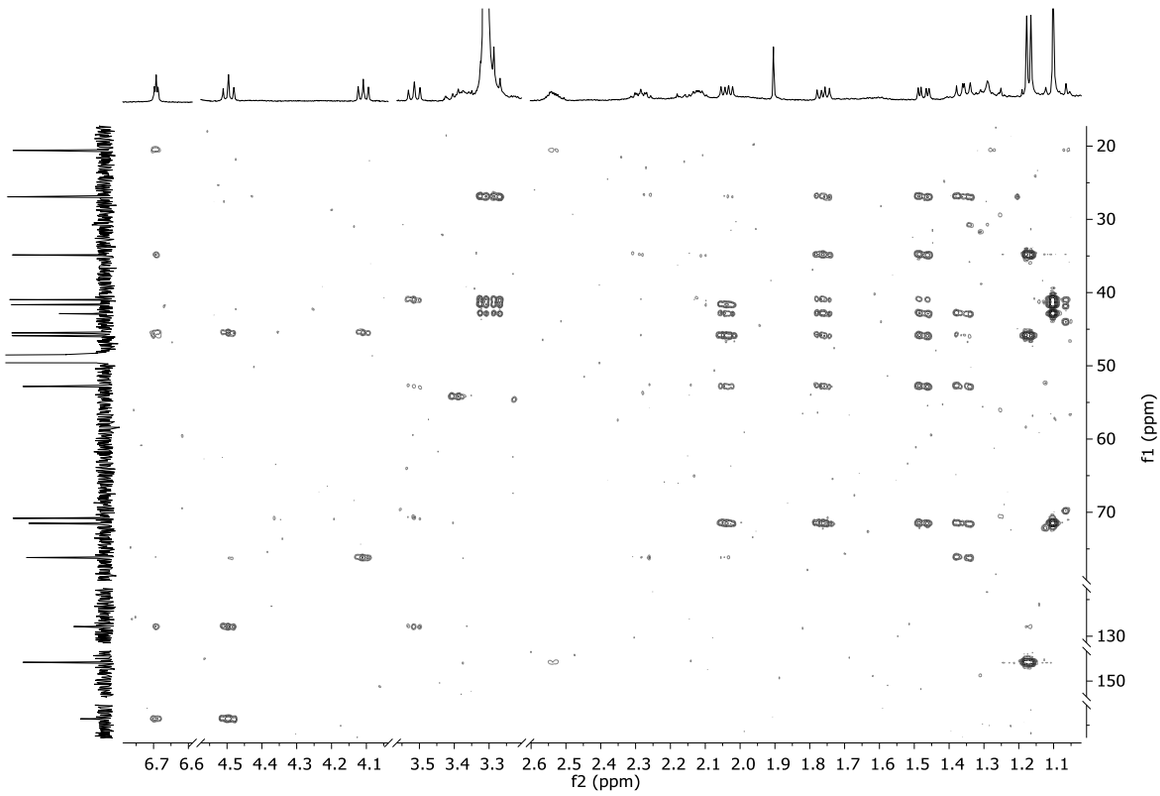

Figure. S55. HMBC-spectrum with removed signal-free areas (600.50, 151.01 MHz, CD3OD, 297.2 K).

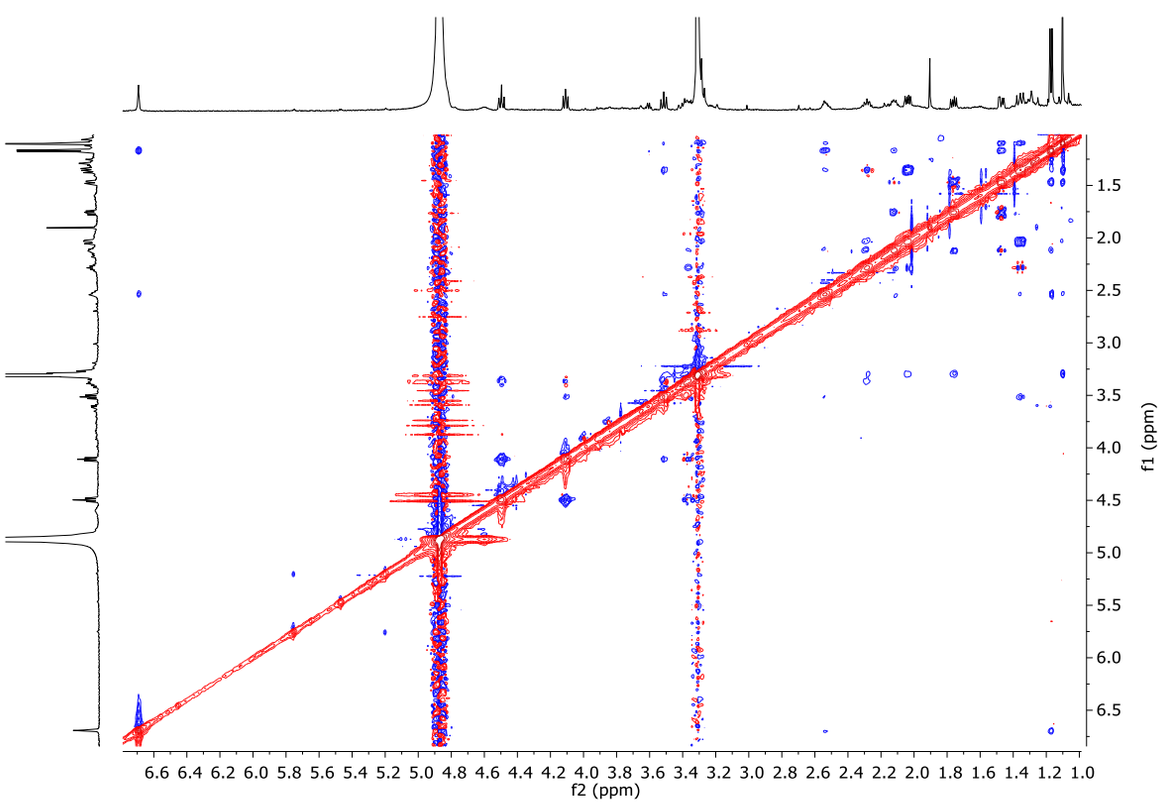

Figure. S56. NOESY-spectrum (600.50, 600.50 MHz, CD3OD, 297.2 K).

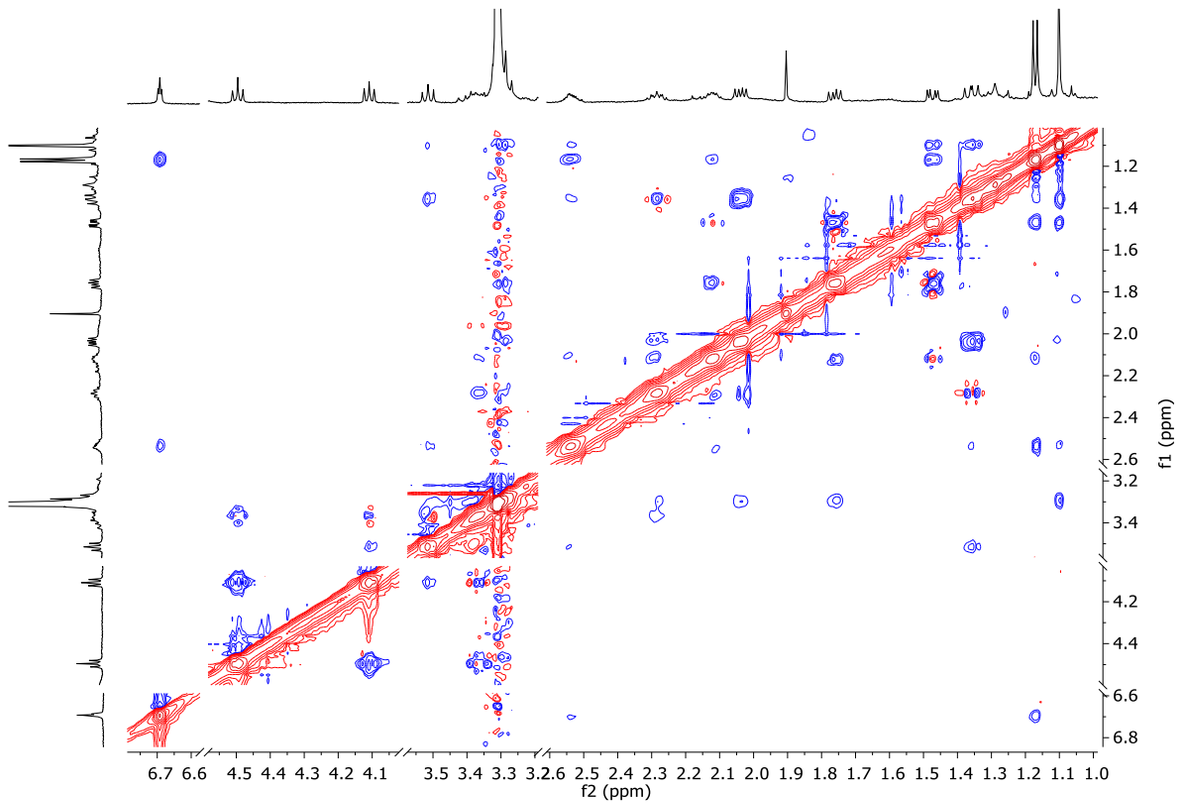

Figure. S57. NOESY-spectrum with removed signal-free areas (600.50, 600.50 MHz, CD3OD, 297.2 K).

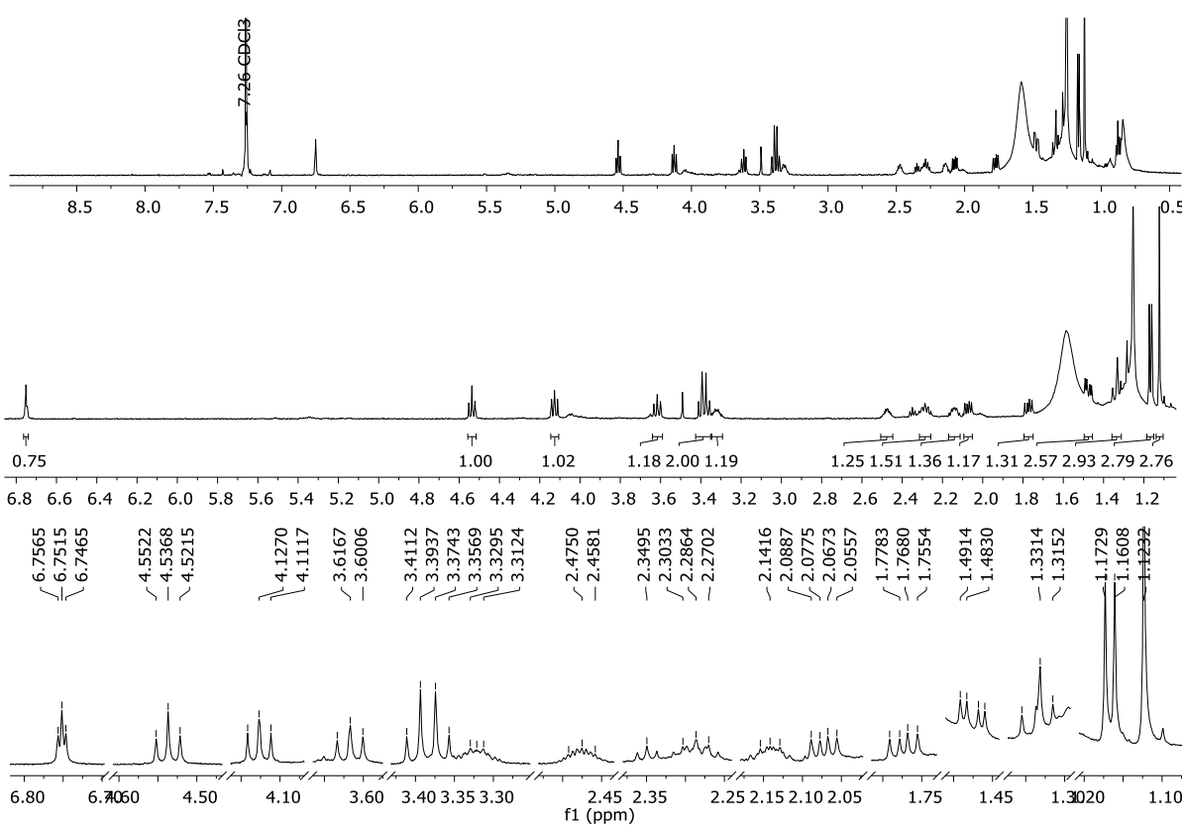

Figure. S58. ^{1}H-NMR and ^{1}H-NMR-spectrums with removed signal-free areas (600.22 MHz, $CDCl_3$, 297.2 K).

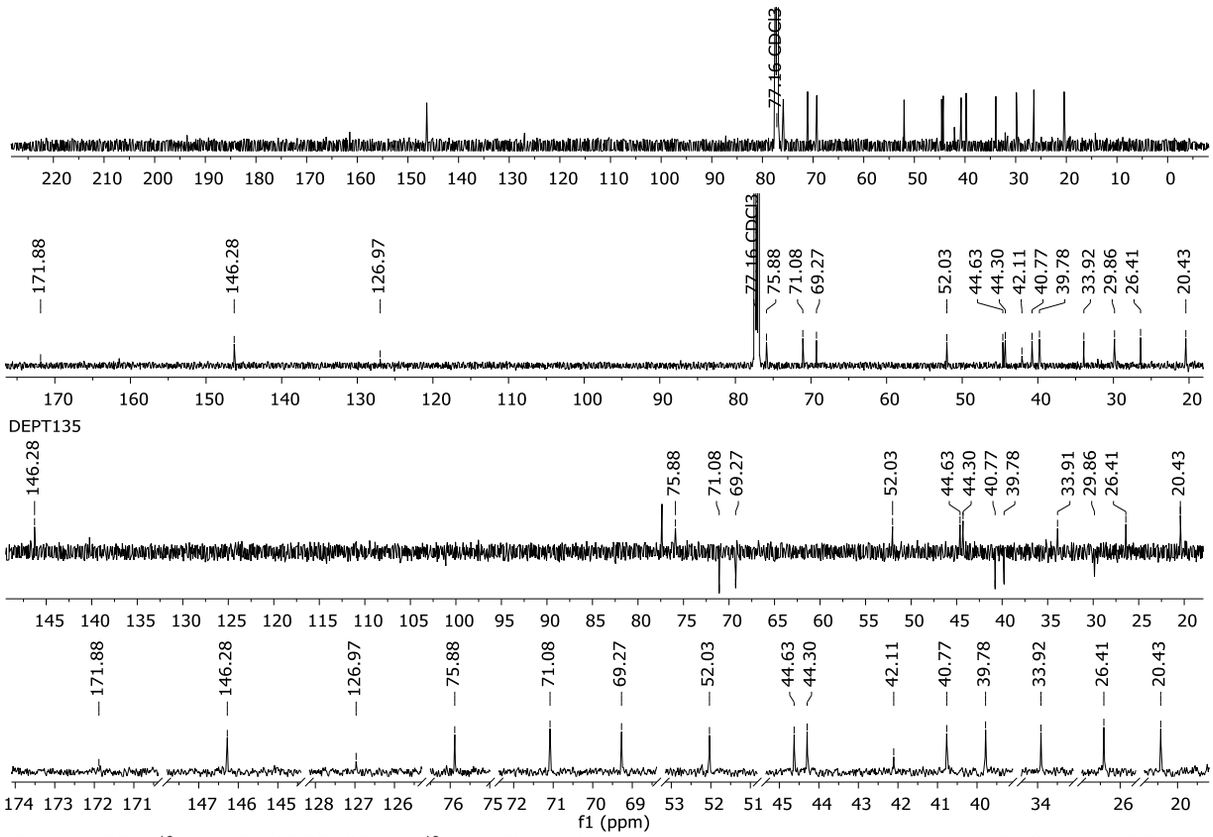

Figure. S59. ^{13}C-NMR, DEPT135 and ^{13}C-NMR-spectrums with removed signal-free areas (151.01 MHz, $CDCl_3$, 297.2 K).

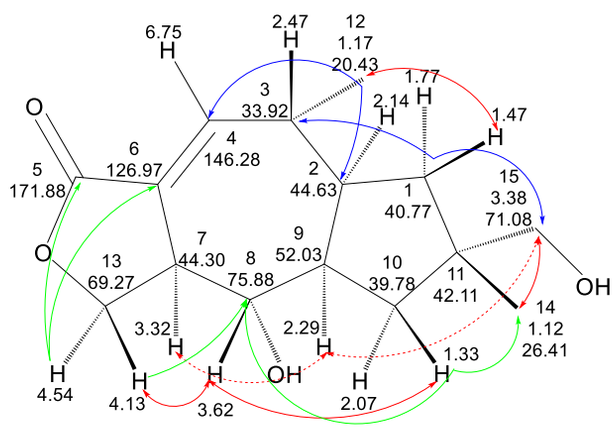

Figure. S60. Structure of the previously extracted compound **34** from *L. circellatus*, ($CDCl_3$). With assignments, with HMBC correlations (→), HMBC correlations with Karplus relationship (→) and with NOESY correlations (→).

9.16 14-Hydroxyblennin A (**52**)

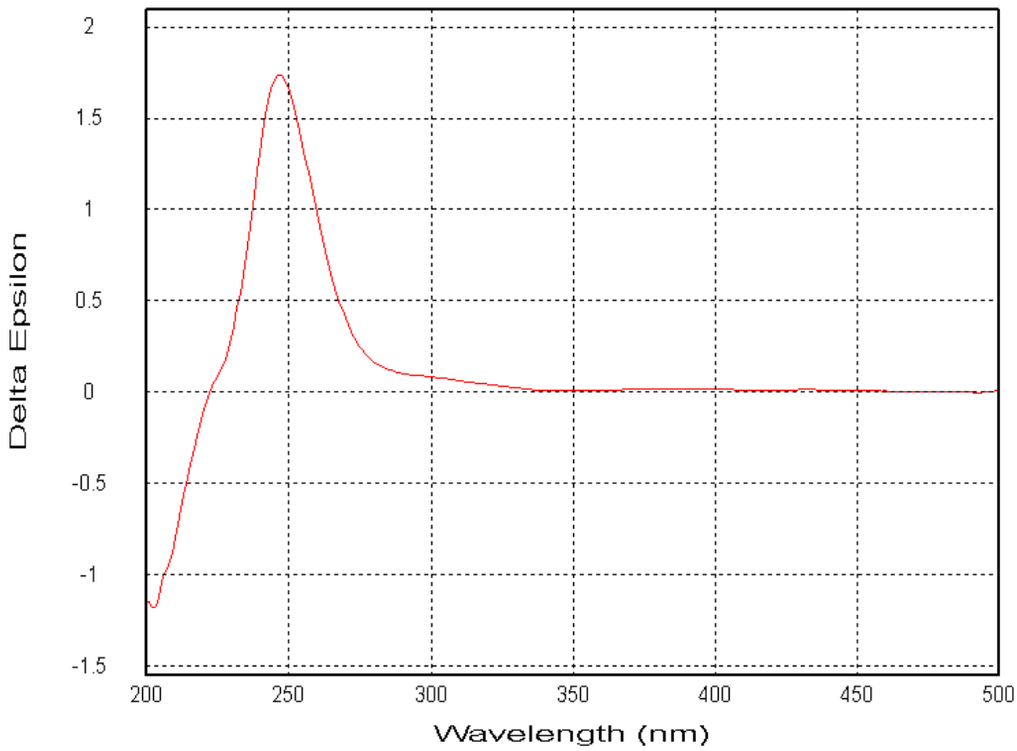

Figure. S61. CD-spectrum of the experimental measurement.

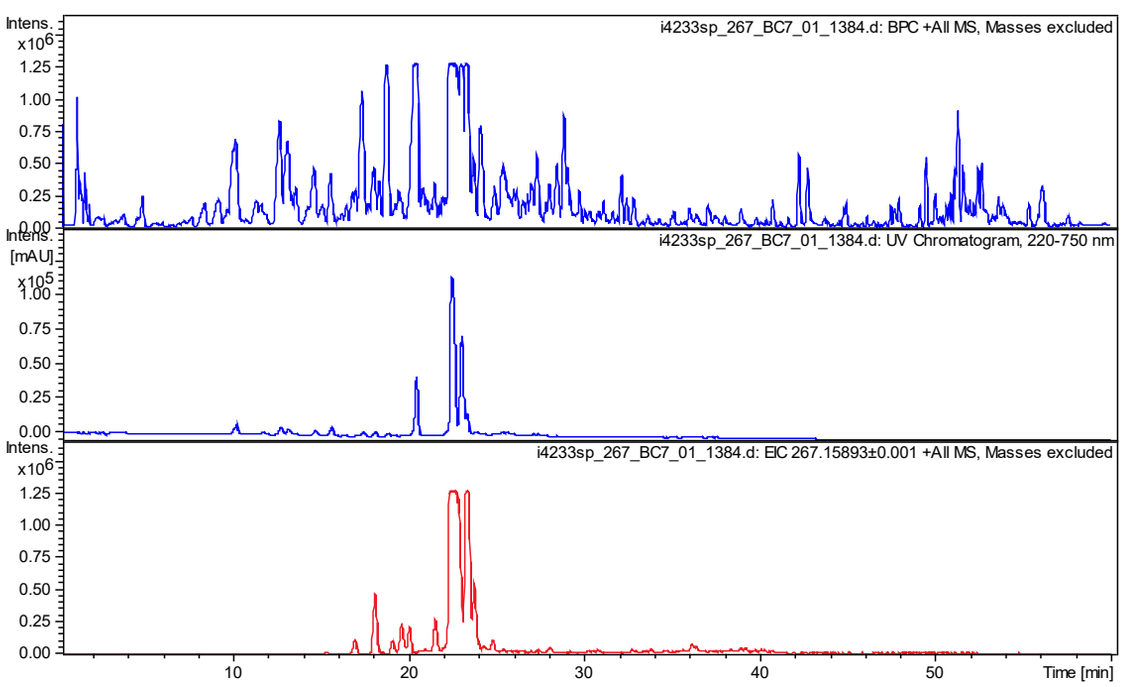

Figure. S62. HR-ESI-(+)-MS, UV/Vis and mass excluded chromatograms.

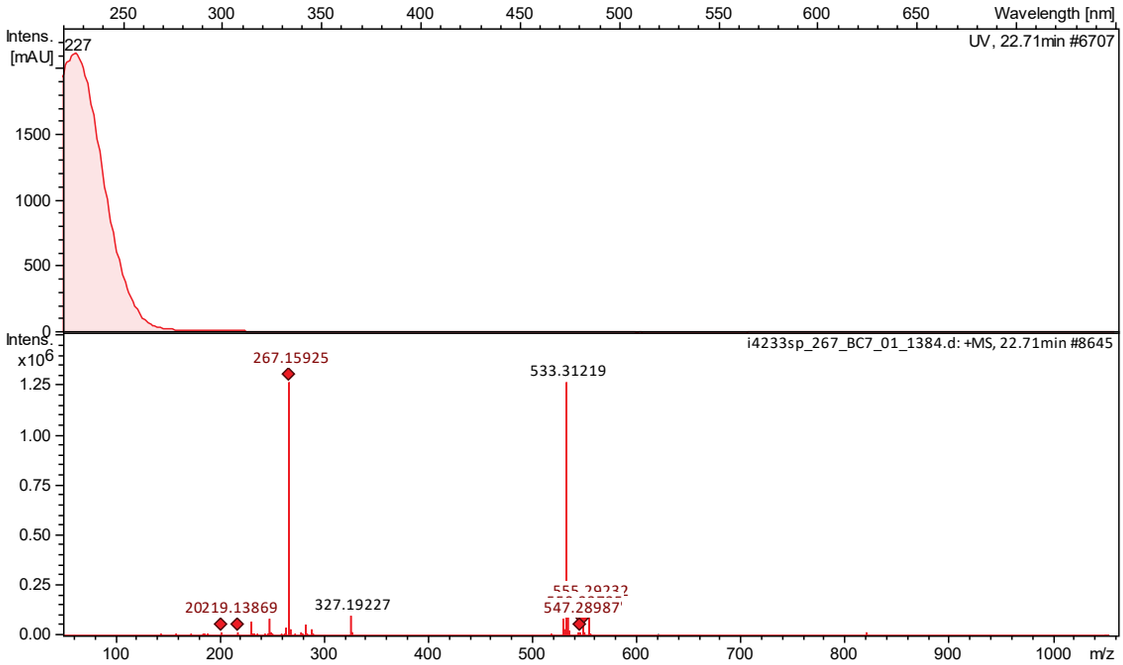

Figure. S63. HR-ESI-(+)-MS and UV/Vis-spectrums of compound **52** from *L. trivialis*, gradient in section 6.3.4.2.

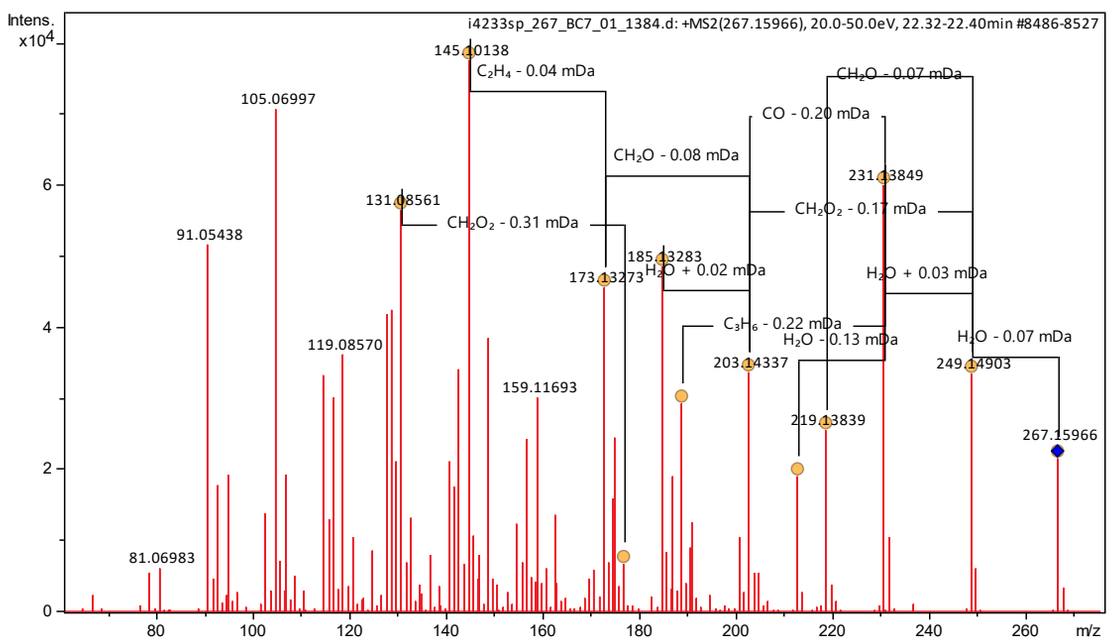

Figure. S64. HR-ESI-(+)-MS/MS-spectrum.

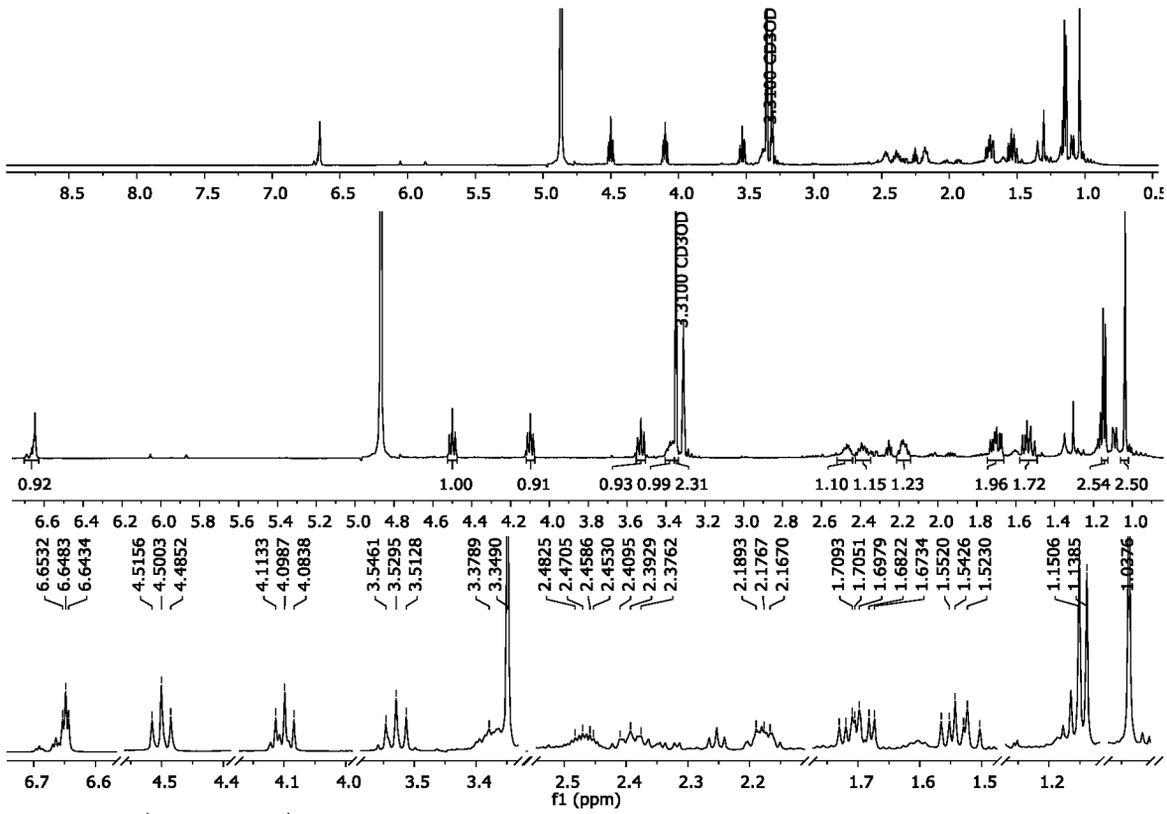

Figure. S65. ^{1}H-NMR and ^{1}H-NMR-spectrums with removed signal-free areas (600.22 MHz, CD_3OD, 297.2 K).

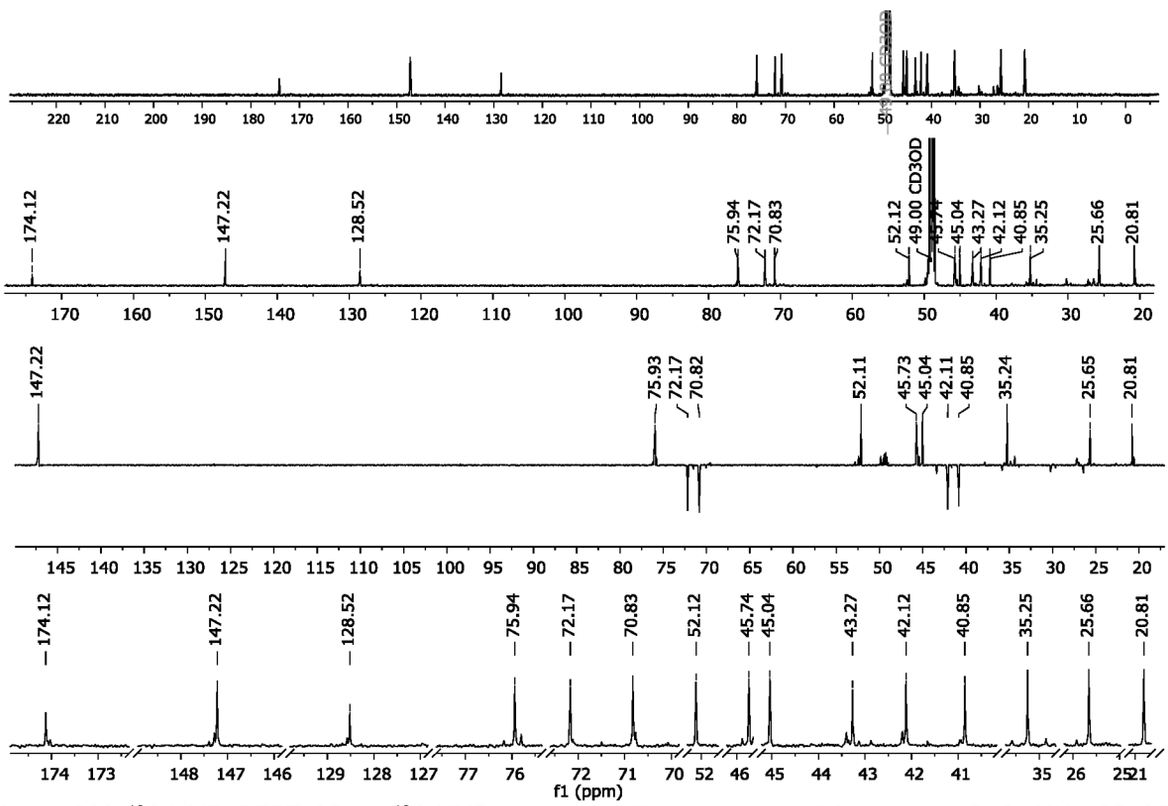

Figure. S66. ^{13}C-NMR, DEPT135 and ^{13}C-NMR-spectrums with removed signal-free areas (151.01 MHz, CD_3OD, 297.2 K).

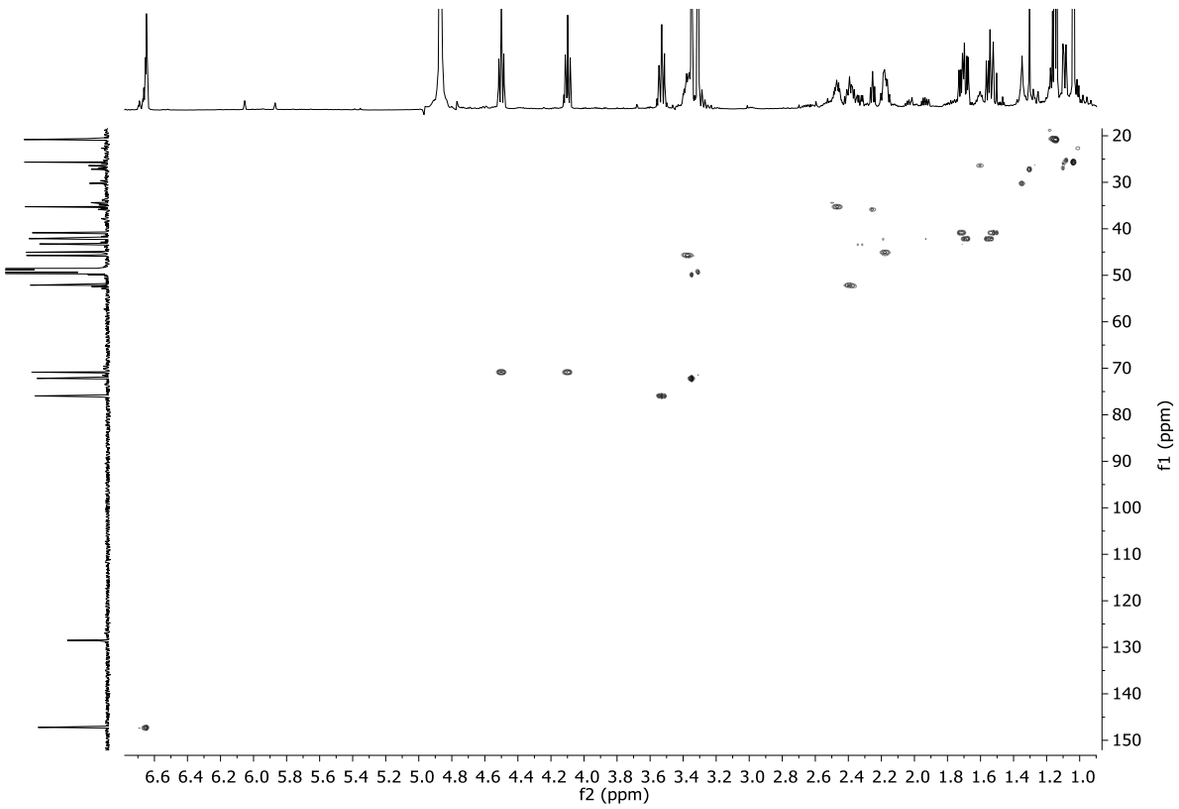

Figure. S67. HSQC-spectrum (600.50, 151.01 MHz, CD_3OD, 297.1 K).

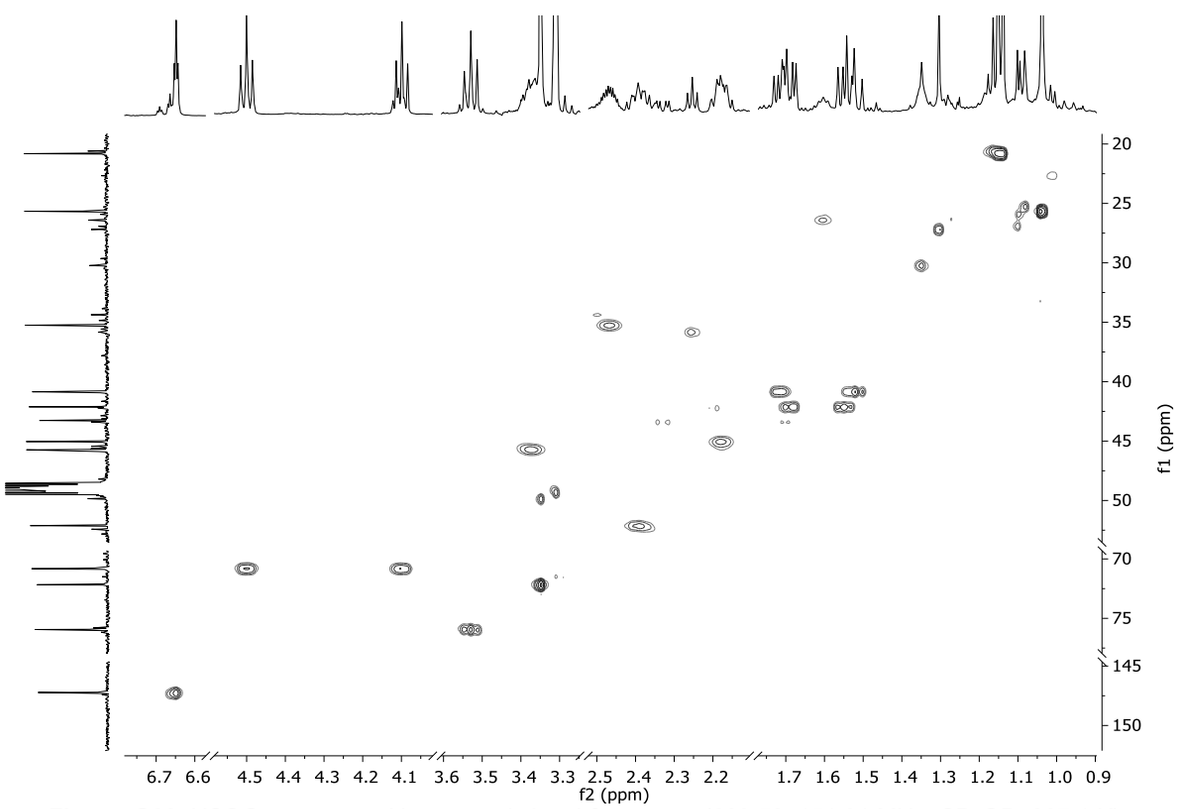

Figure. S68. HSQC-spectrum with removed signal-free areas (600.50, 151.01 MHz, CD_3OD, 297.1 K).

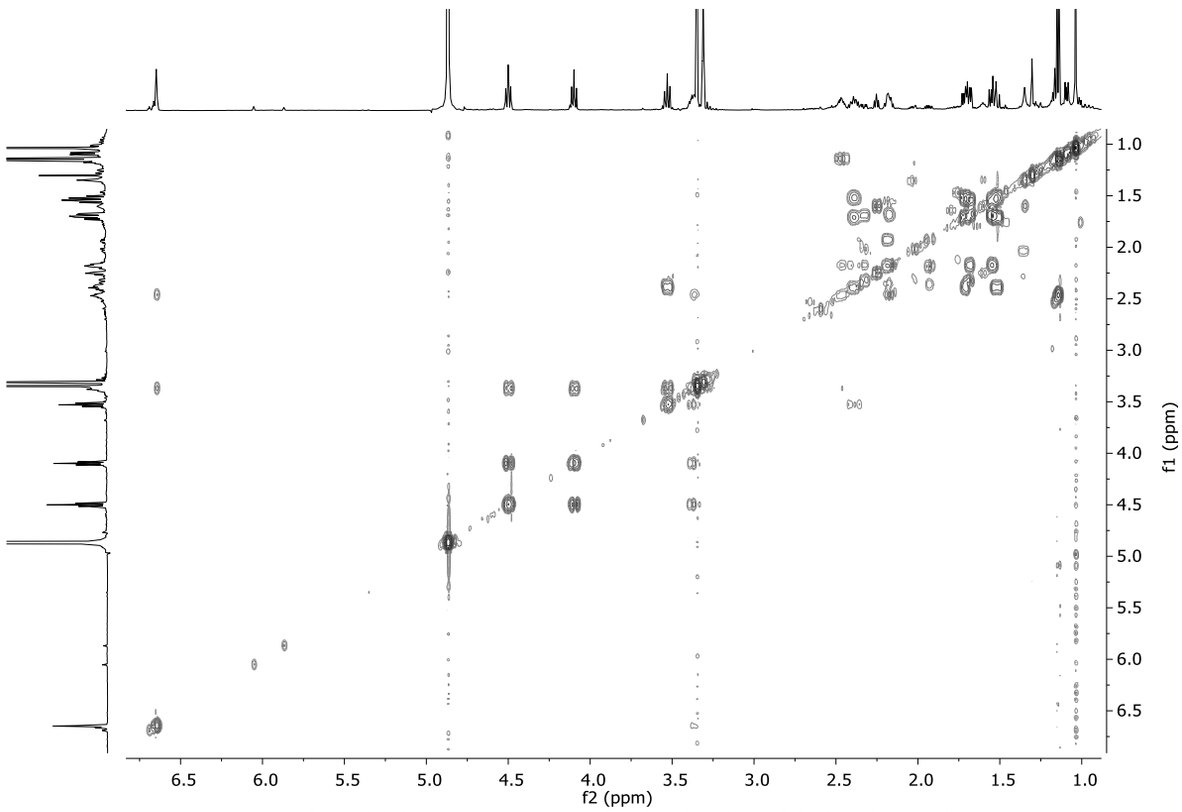

Figure. S69. COSY-spectrum (600.22, 600.22 MHz, CD_3OD, 297.1 K).

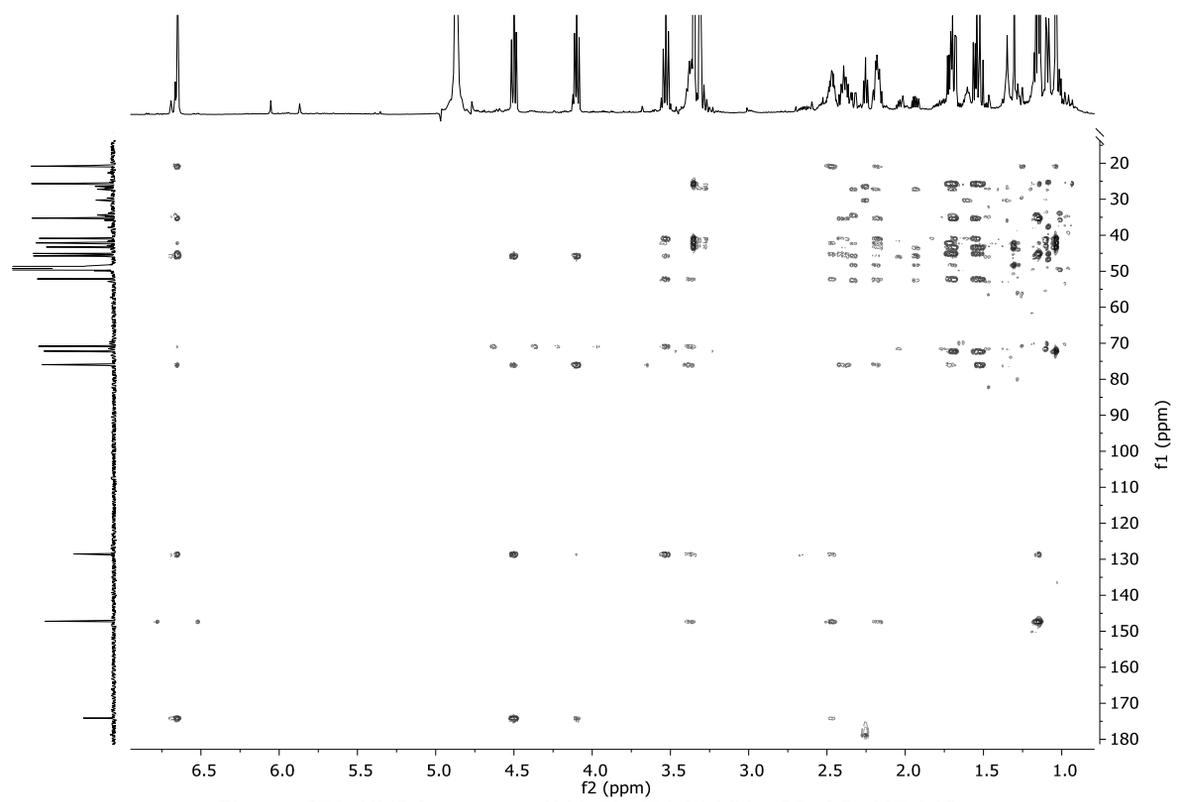

Figure. S70. HMBC-spectrum (600.50, 151.01 MHz, CD_3OD, 297.2 K).

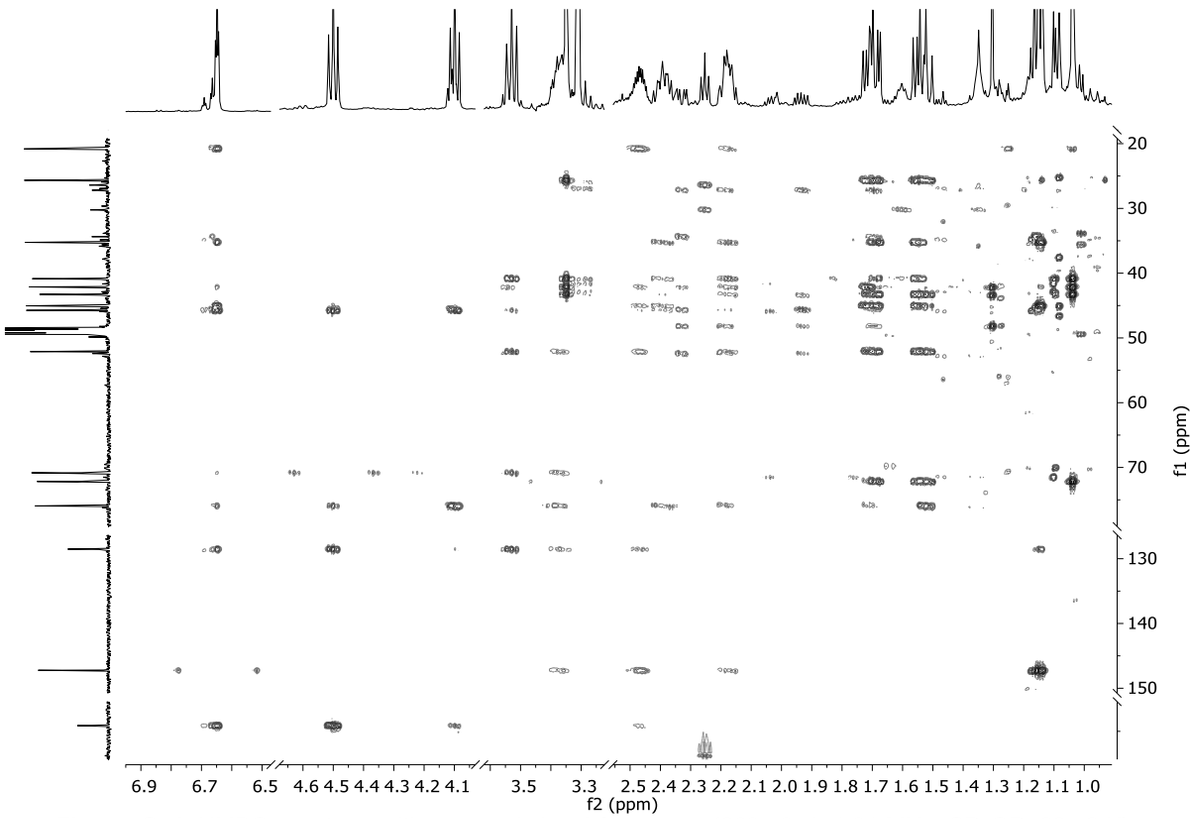

Figure. S71. HMBC-spectrum with removed signal-free areas (600.50, 151.01 MHz, CD_3OD, 297.2 K).

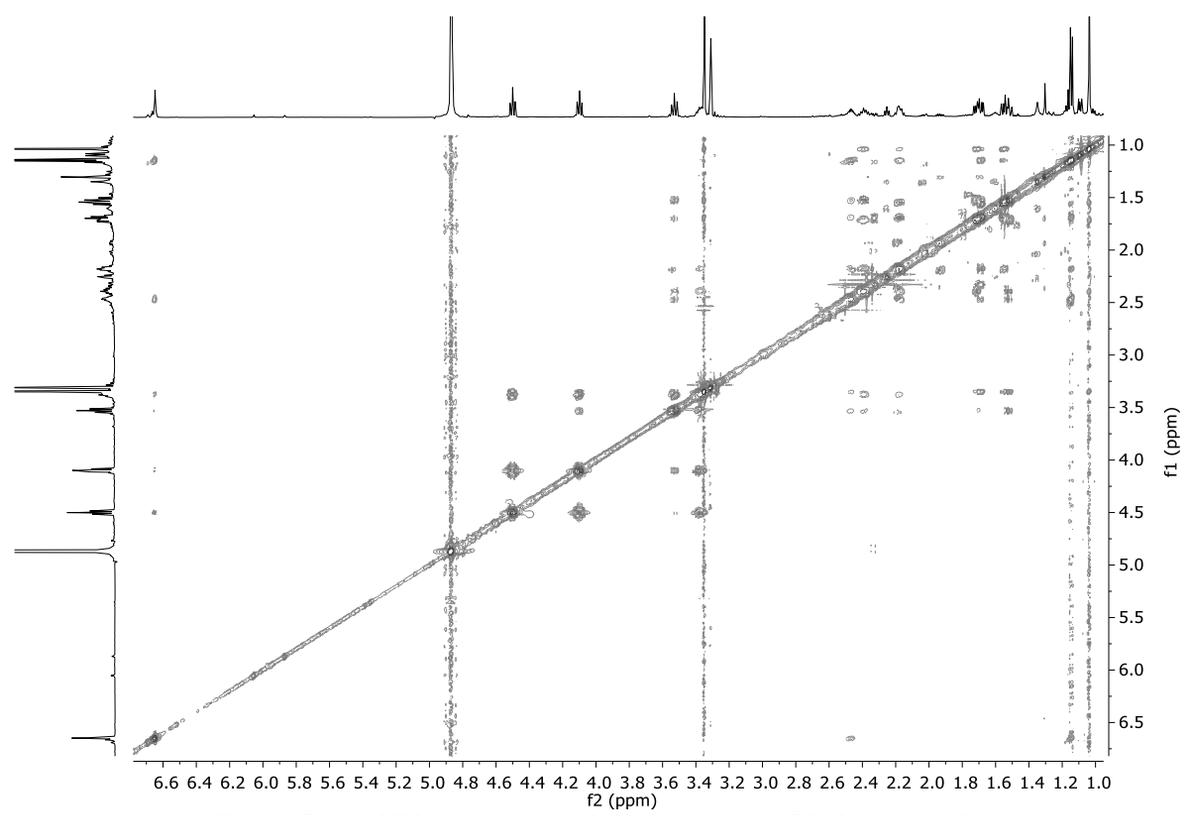

Figure. S72. NOESY-spectrum (600.50, 600.50 MHz, CD_3OD, 297.2 K).

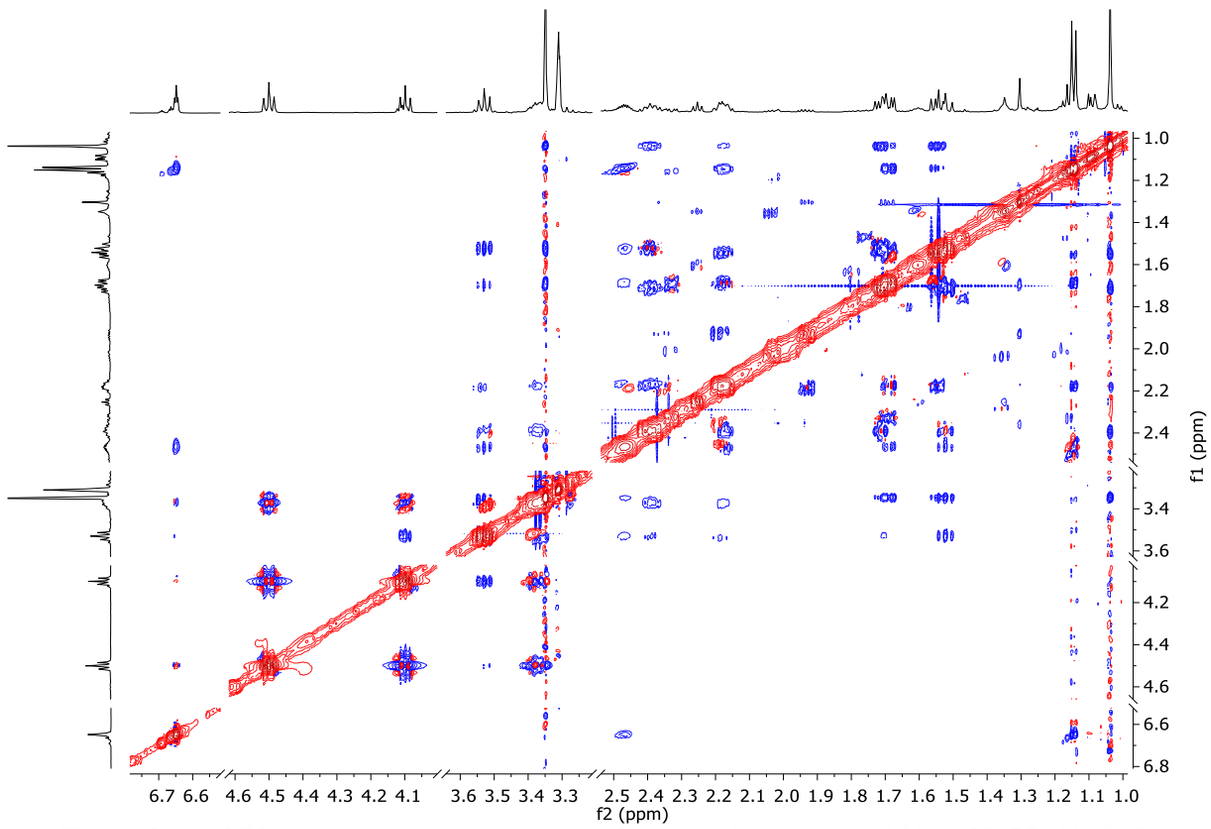

Figure. S73. NOESY-spectrum with removed signal-free areas (600.50, 600.50 MHz, CD_3OD, 297.2 K).

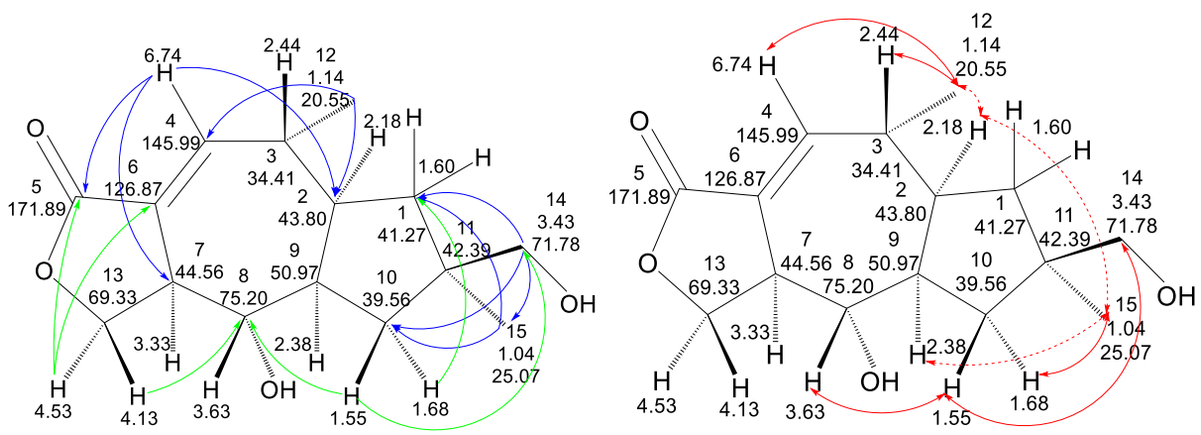

Figure. S74. Relative structure of compound **52** with assignments, ($CDCl_3$). Left: selected HMBC correlations (→), HMBC correlations with Karplus relationship (→). Right: NOESY correlations (↔).

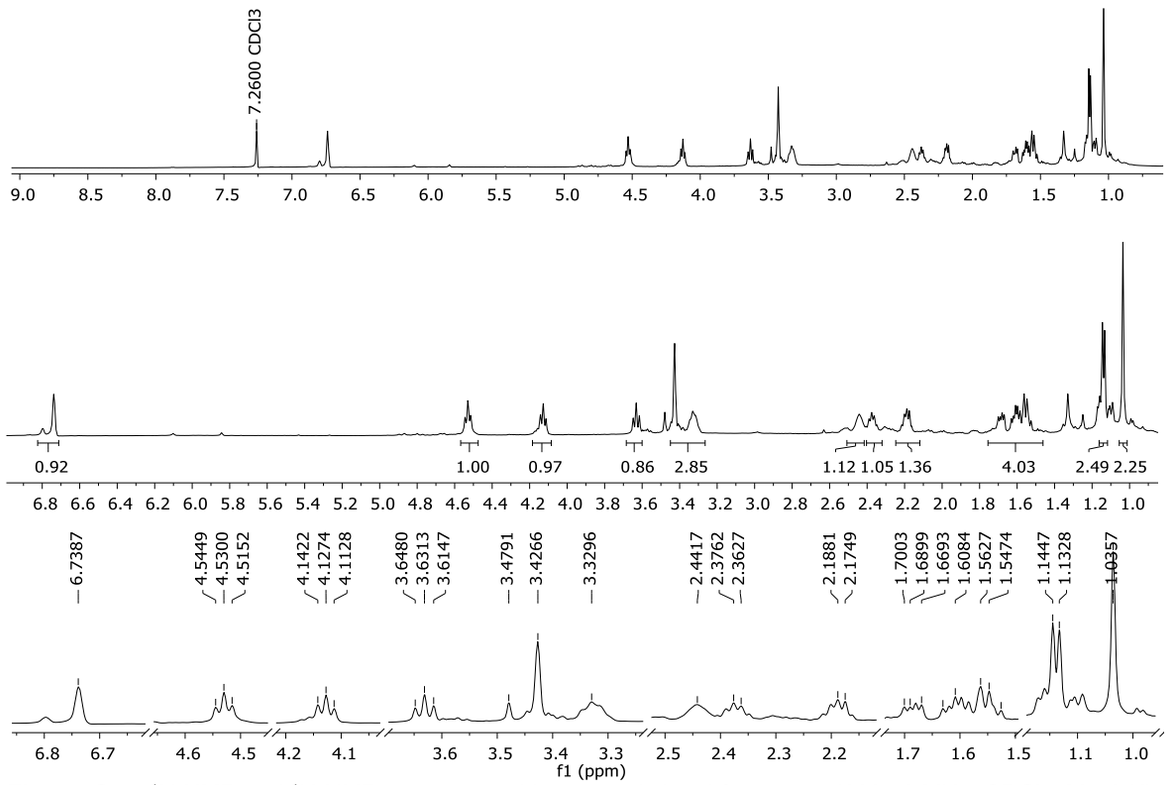

Figure. S75. ^{1}H-NMR and ^{1}H-NMR-spectrums with removed signal-free areas (600.50 MHz, $CDCl_3$, 297.2 K).

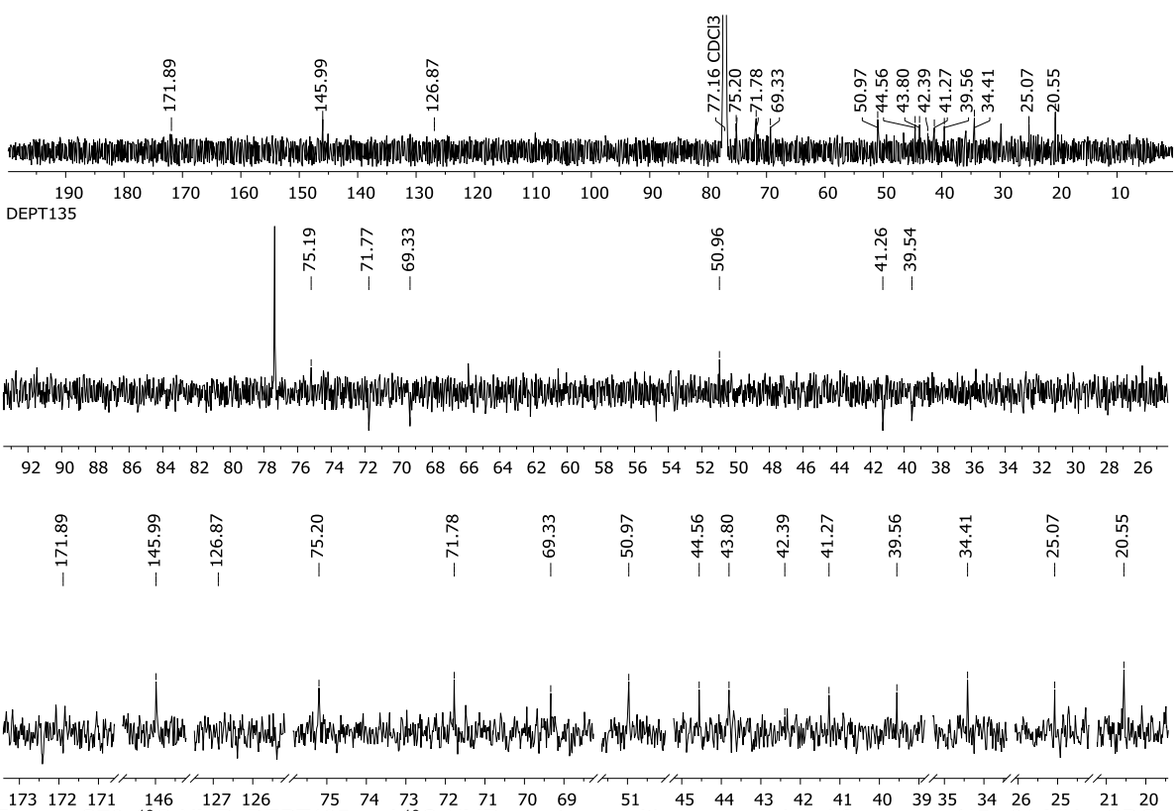

Figure. S76. ^{13}C-NMR, DEPT135 and ^{13}C-NMR-spectrums with removed signal-free areas (151.01 MHz, $CDCl_3$, 296.9 K).

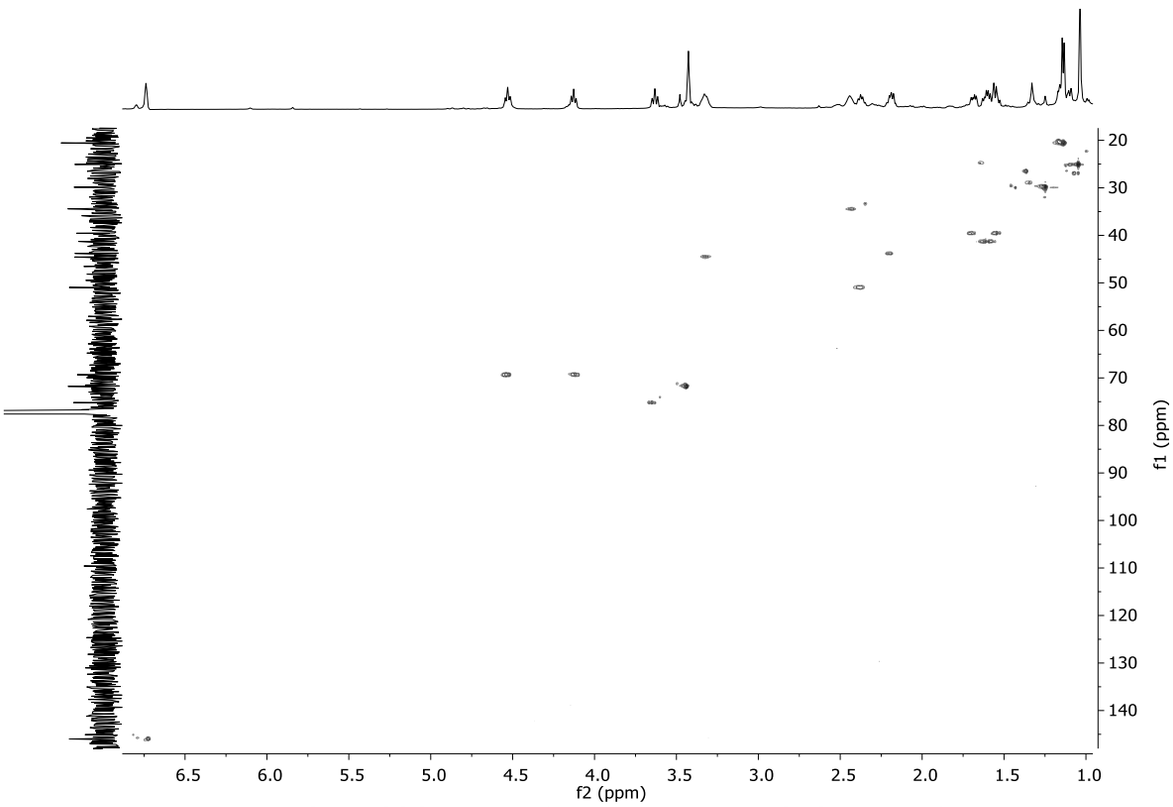

Figure. S77. HSQC-spectrum (600.50, 151.01 MHz, $CDCl_3$, 297.3 K).

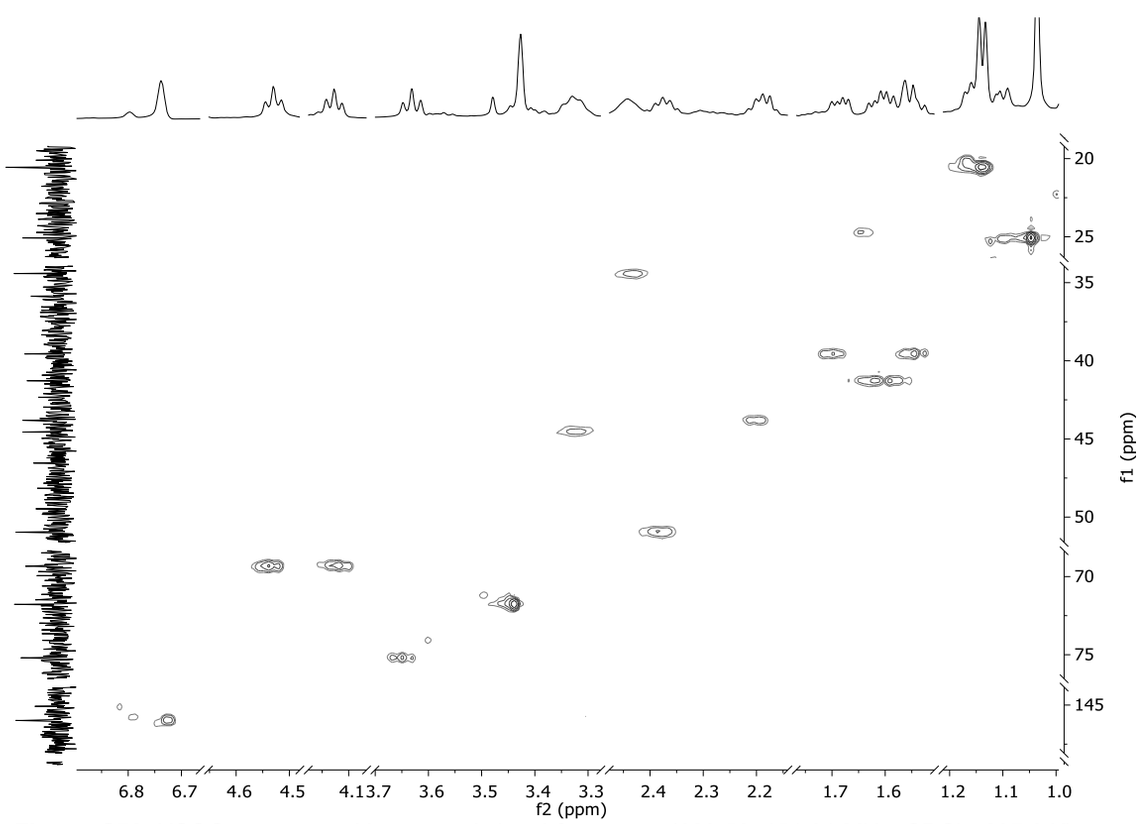

Figure. S78. HSQC-spectrum with removed signal-free areas (600.50, 151.01 MHz, $CDCl_3$, 297.3 K).

9.17 14-Hydroxylactarorufin B (**53**) and Lactarorufin B (**27**) mixture

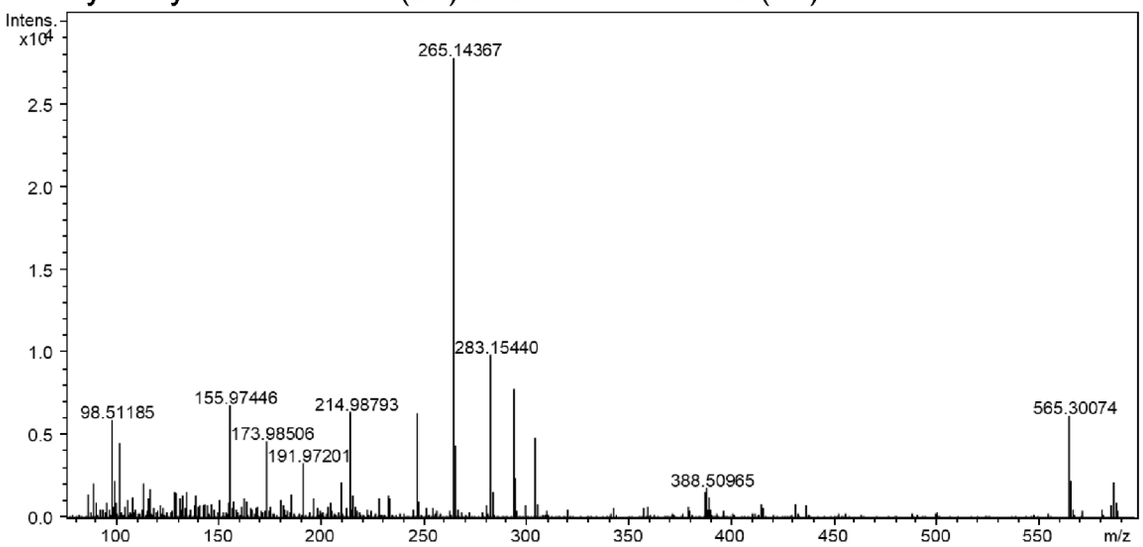

Figure. S79: Mass-Spectrum of Compound **27**.

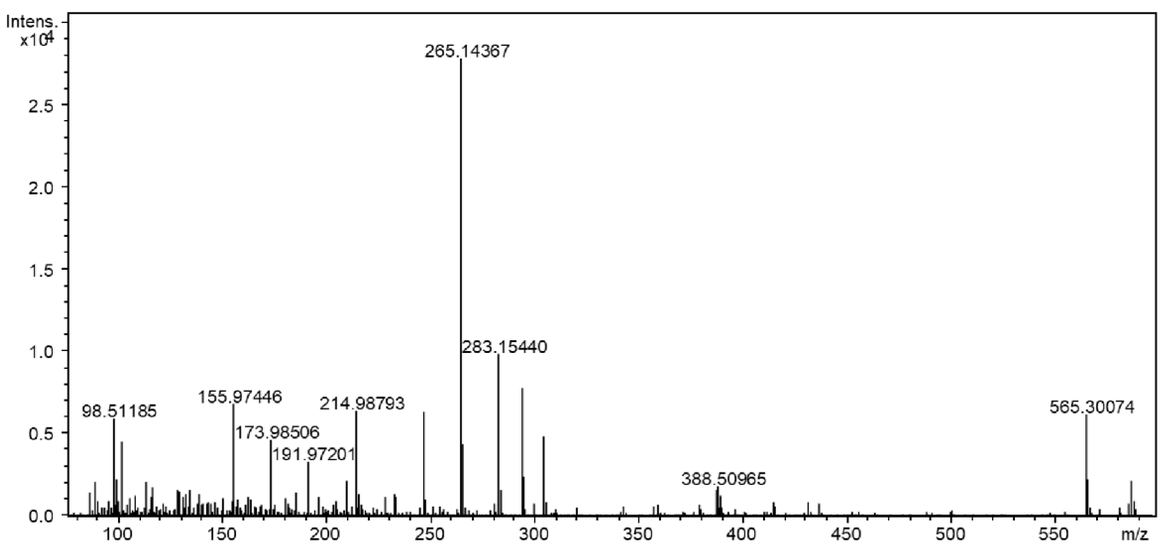

Figure. S80: Mass-Spectrum of Compound **53**.

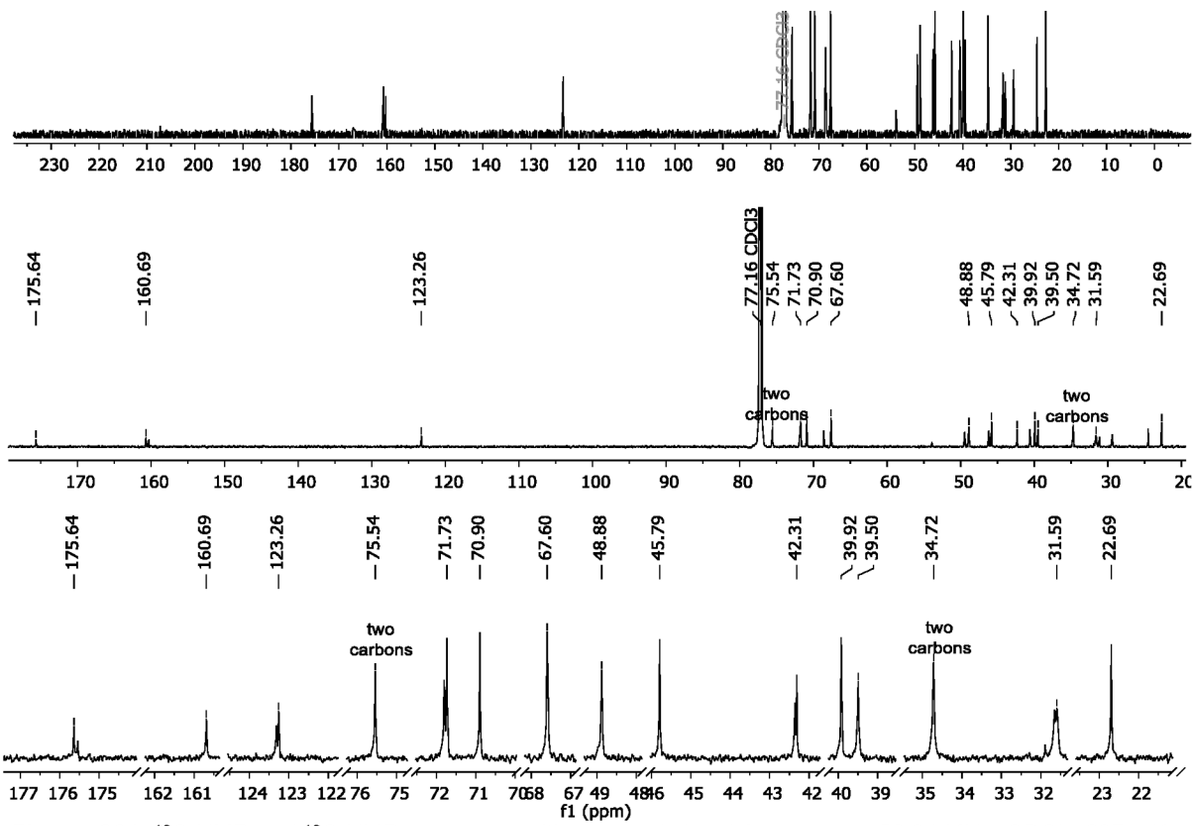

Figure. S81. ^{13}C-NMR and ^{13}C-NMR-spectrums with removed signal-free areas (150.94 MHz, $CDCl_3$, 297.1 K).

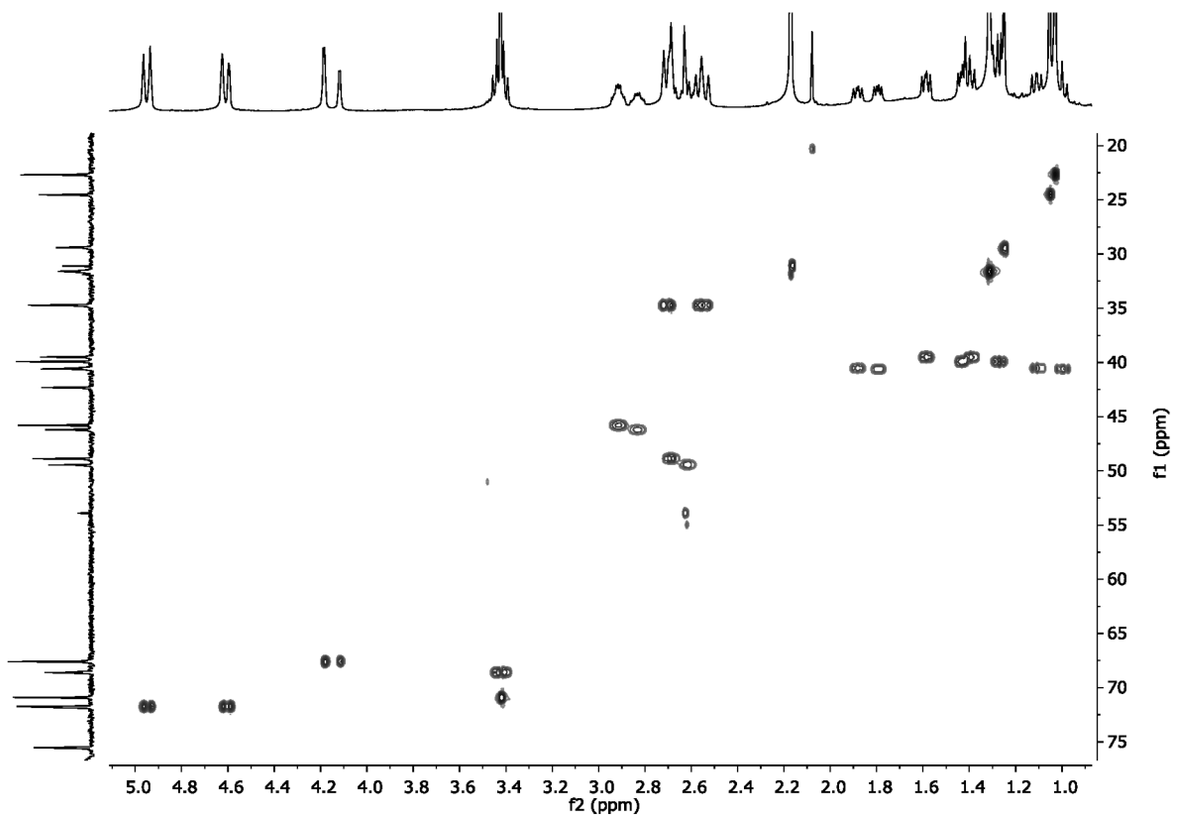

Figure. S82. HSQC-spectrum (600.50, 151.01 MHz, $CDCl_3$, 297.2 K).

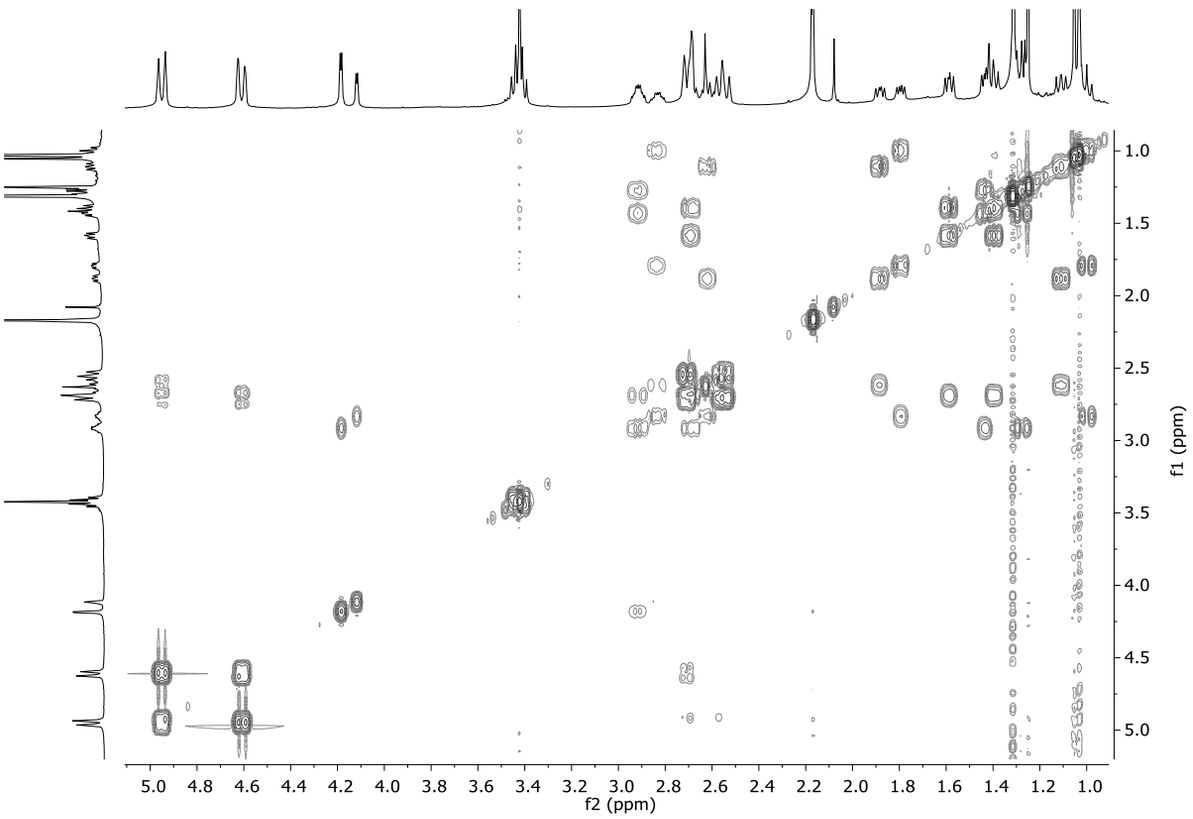

Figure. S83. COSY-spectrum (600.50, 600.50 MHz, $CDCl_3$, 297.1 K).

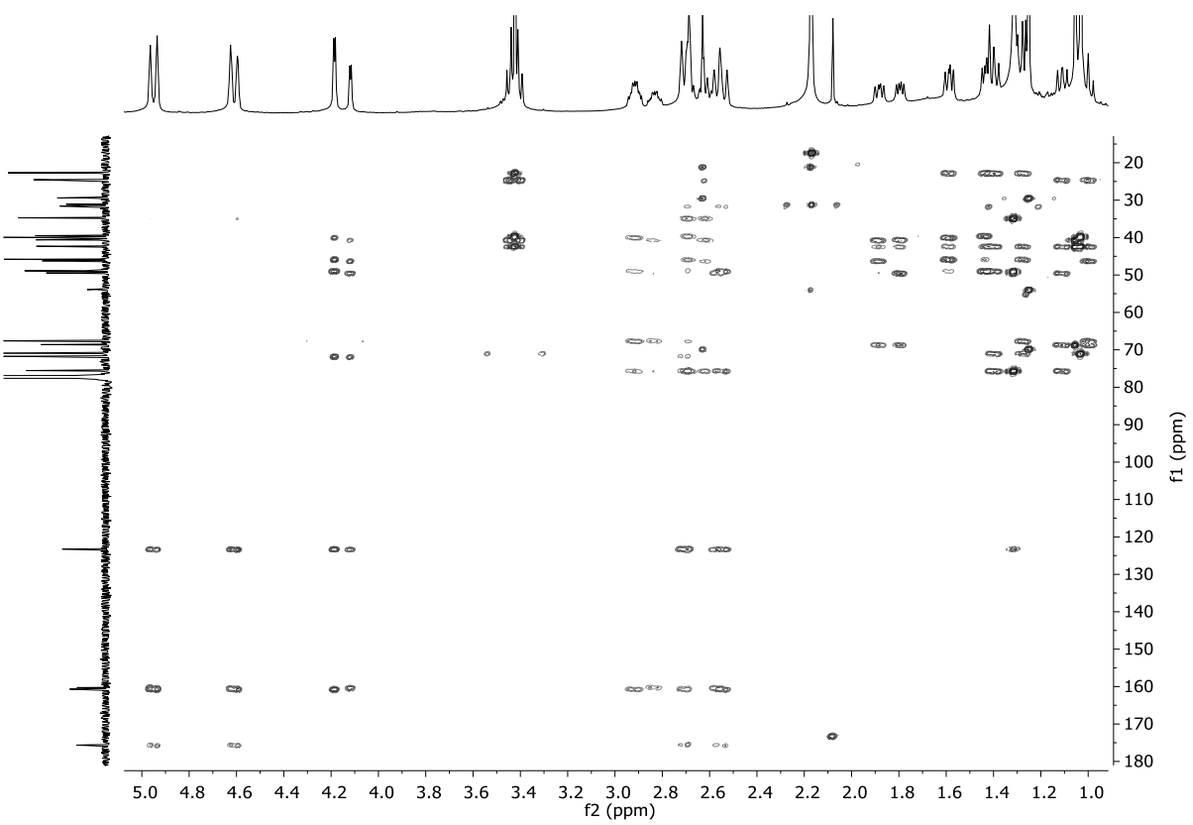

Figure. S84. HMBC-spectrum (600.50, 151.01 MHz, $CDCl_3$, 297.1 K).

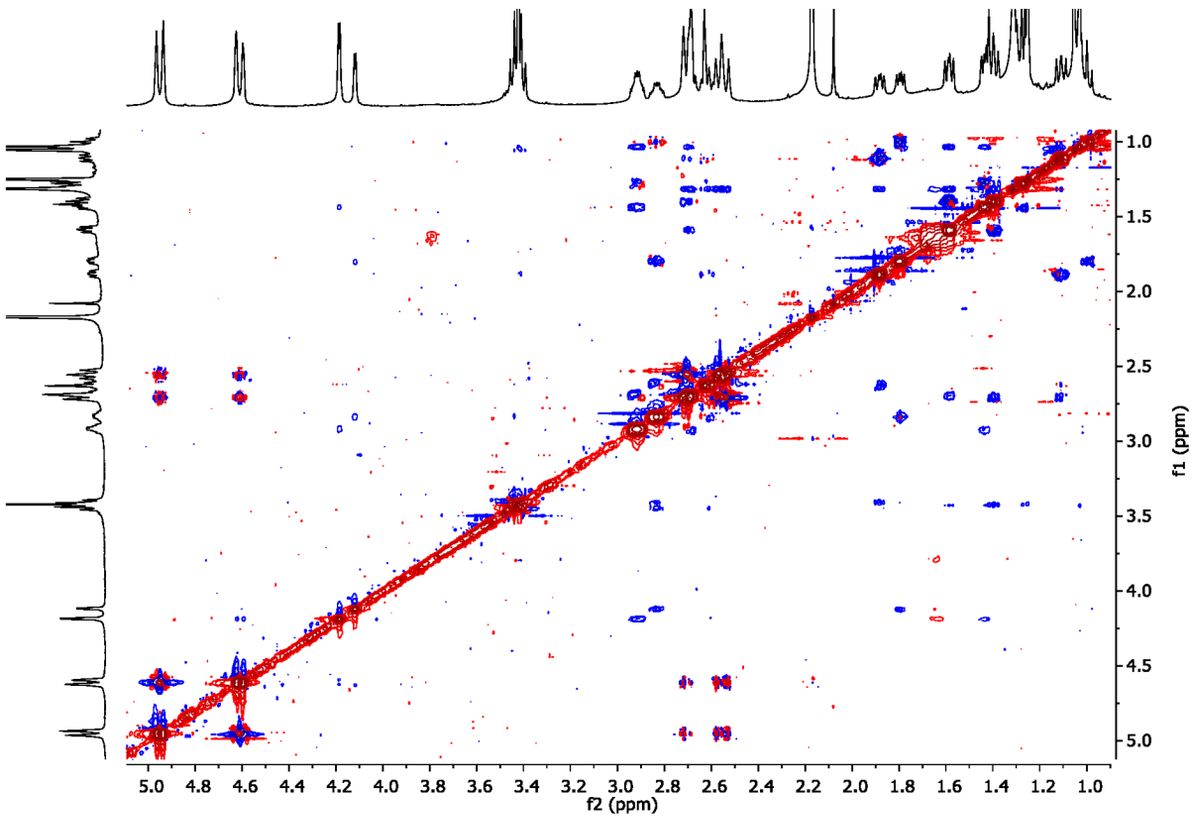

Figure. S85. NOESY-spectrum (600.50, 600.50 MHz, $CDCl_3$, 297.1 K).

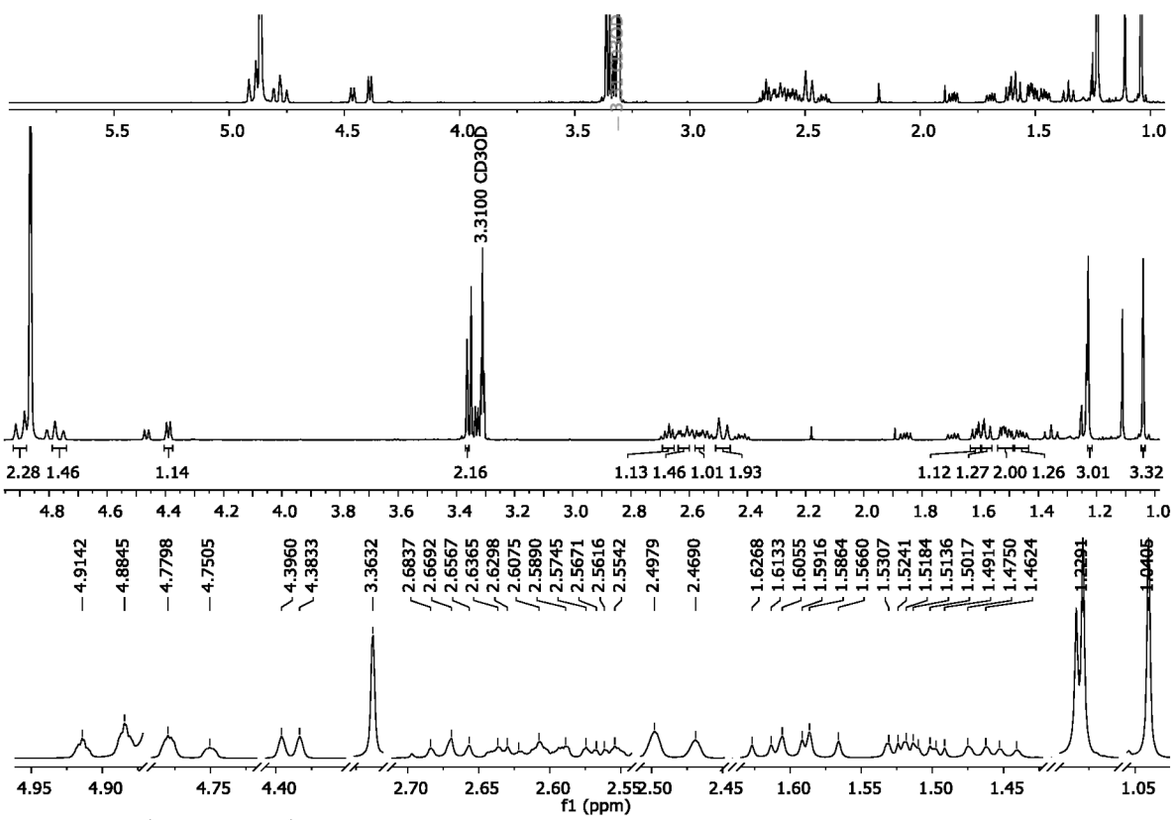

Figure. S86. ^{1}H-NMR and ^{1}H-NMR-spectrums with removed signal-free areas (600.50 MHz, CD_3OD, 297.1 K).

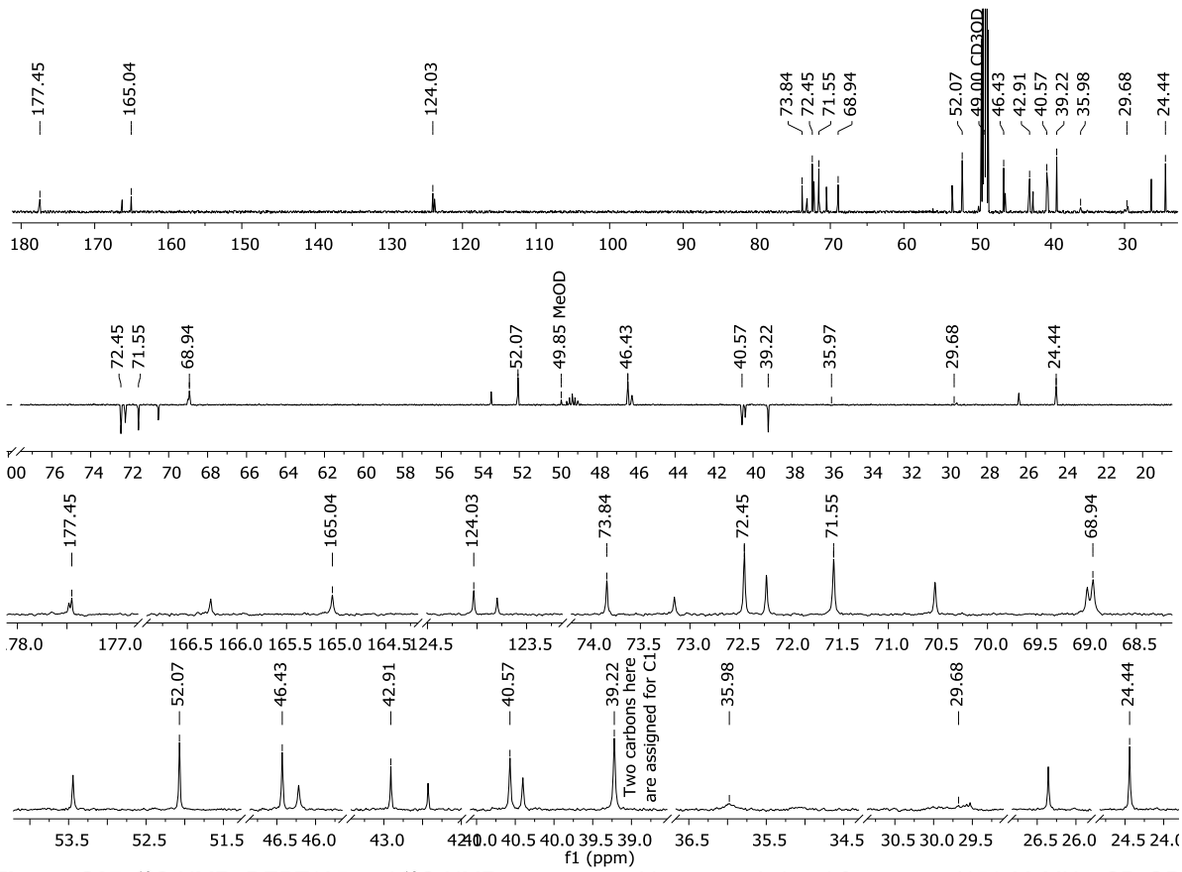

Figure. S87. ^{13}C-NMR, DEPT135 and ^{13}C-NMR-spectrums with removed signal-free areas (151.00 MHz, CD_3OD, 297.2 K).

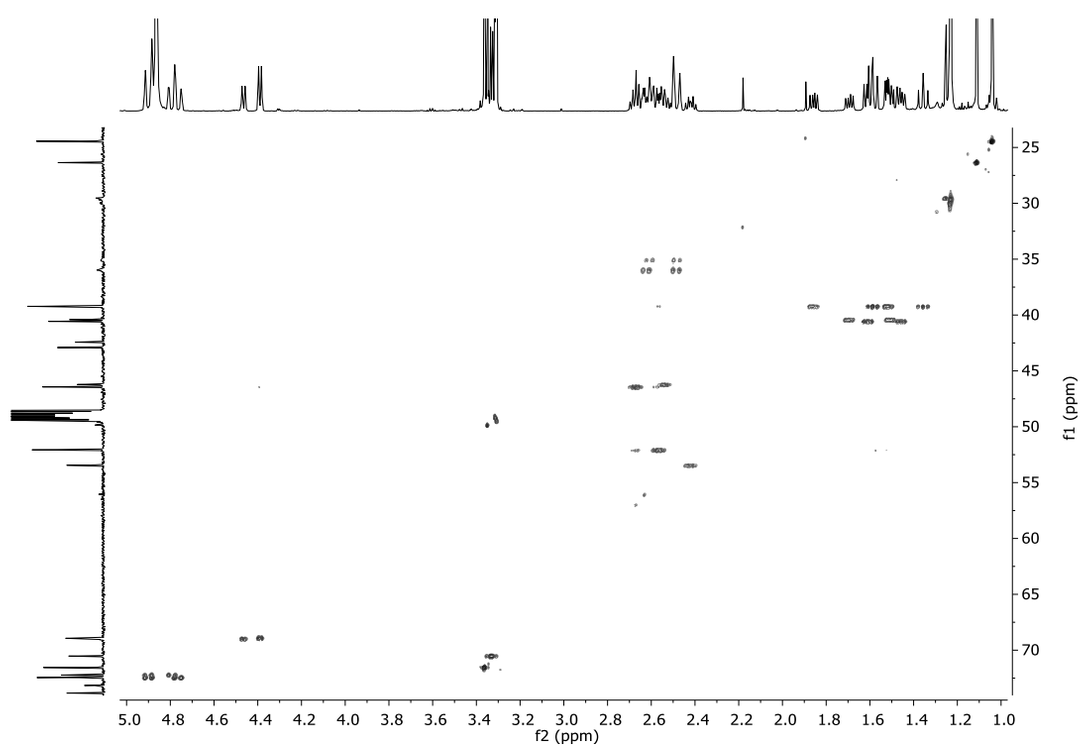

Figure. S88. HSQC-spectrum (600.50, 151.00 MHz, CD_3OD, 297.1 K).

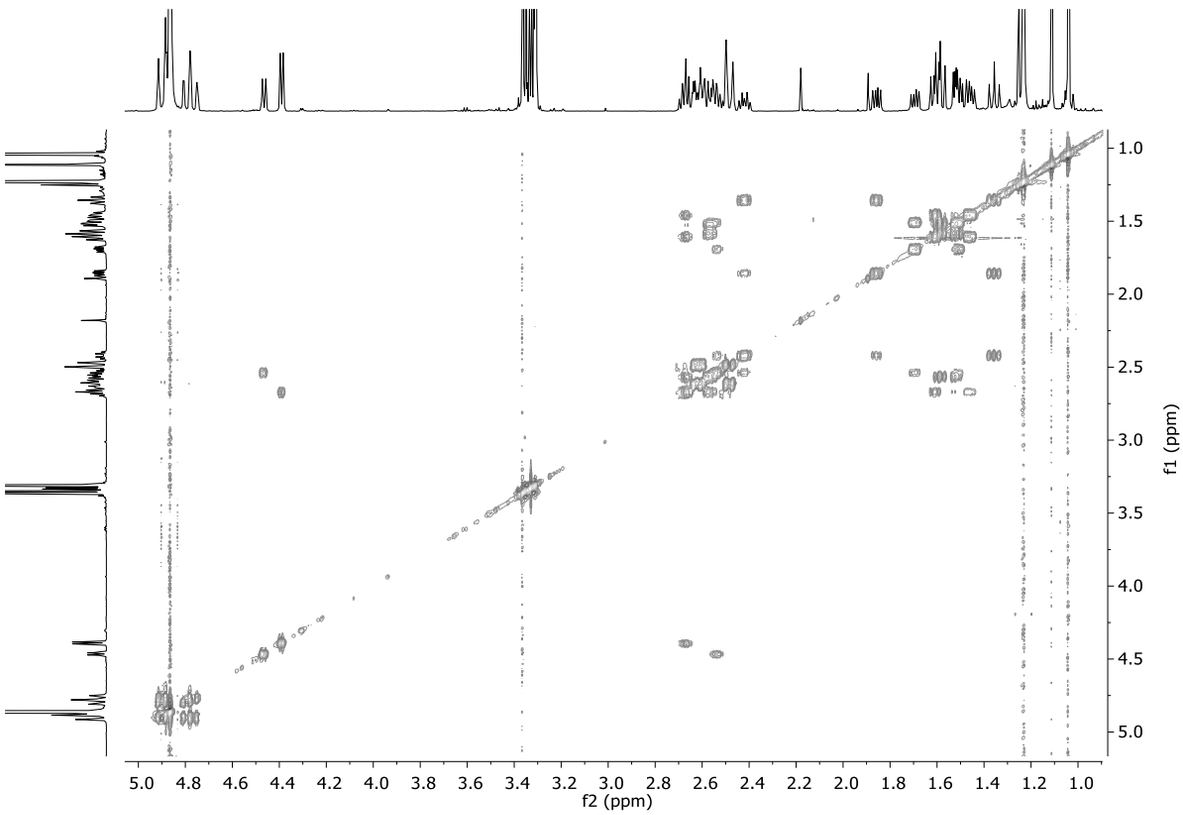

Figure. S89. COSY-spectrum (600.50, 600.50 MHz, CD_3OD, 297.1 K).

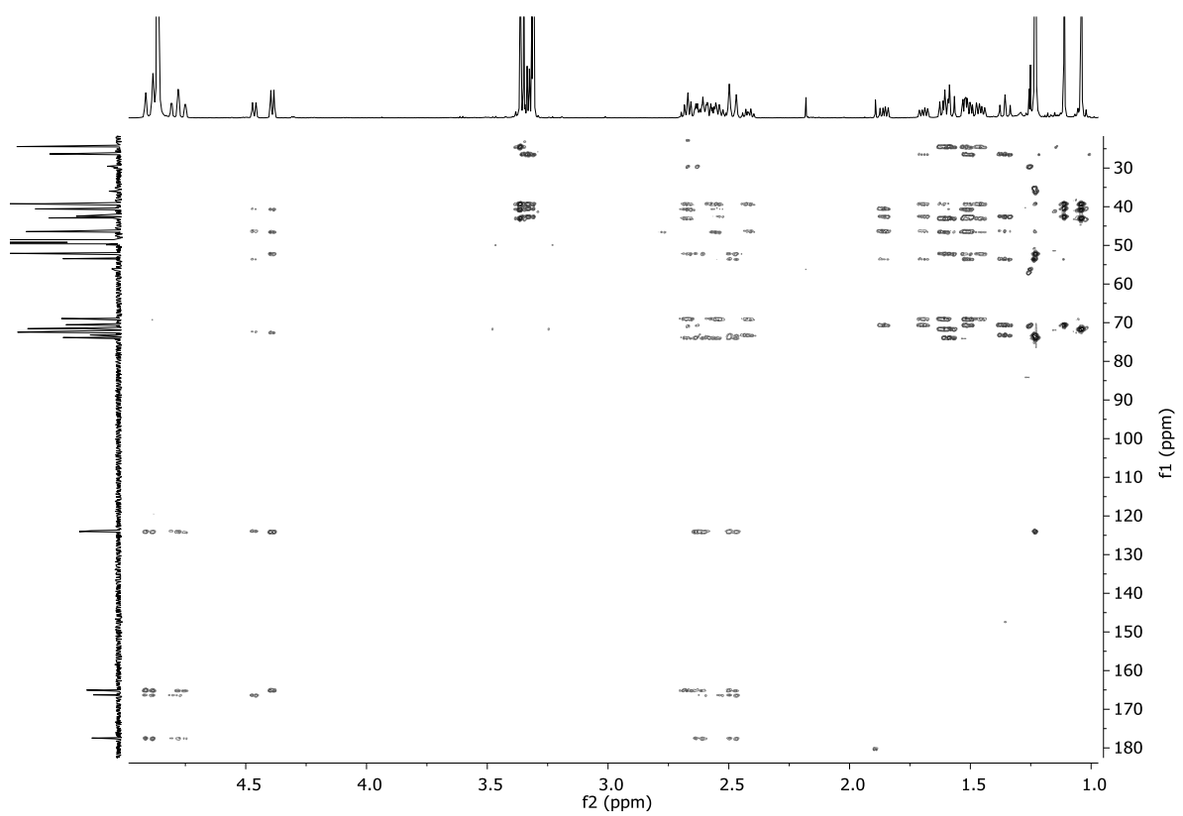

Figure. S90. HMBC-spectrum (600.50, 151.01 MHz, CD_3OD, 297.2 K).

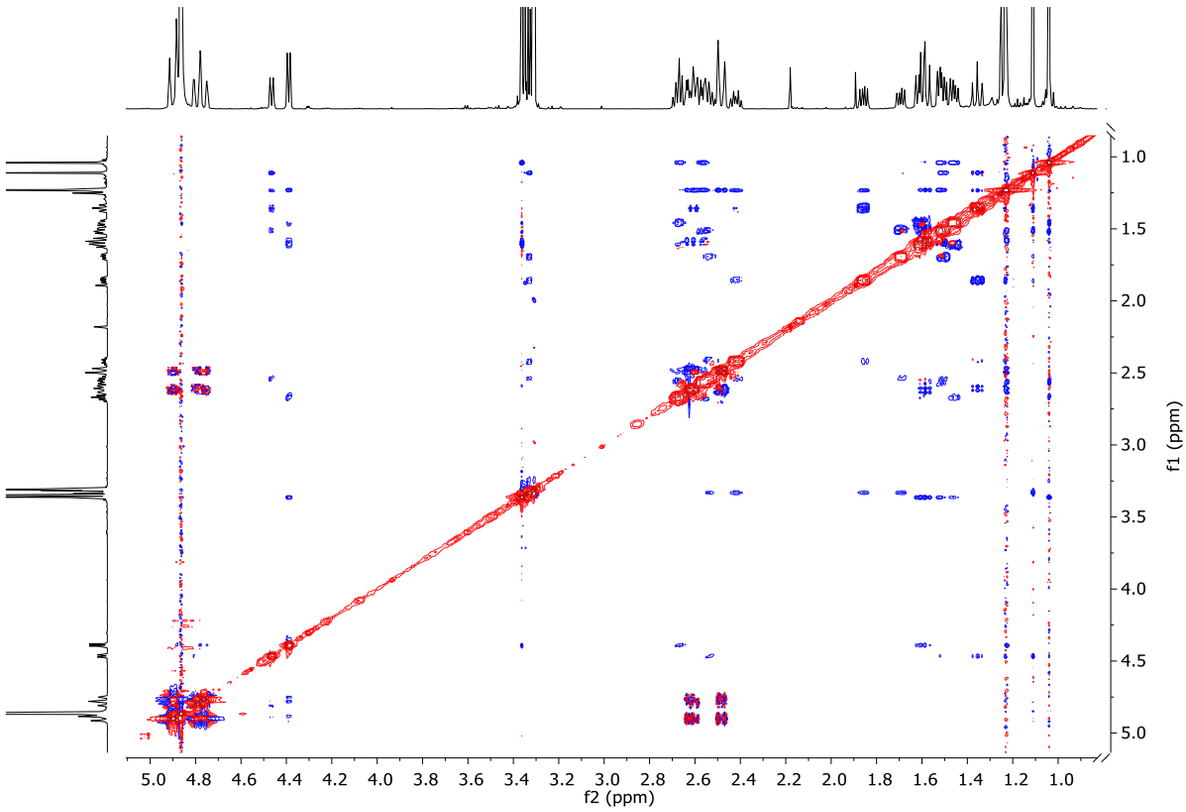

Figure. S91. NOESY-spectrum (600.50, 600.50 MHz, CD_3OD, 297.2 K).

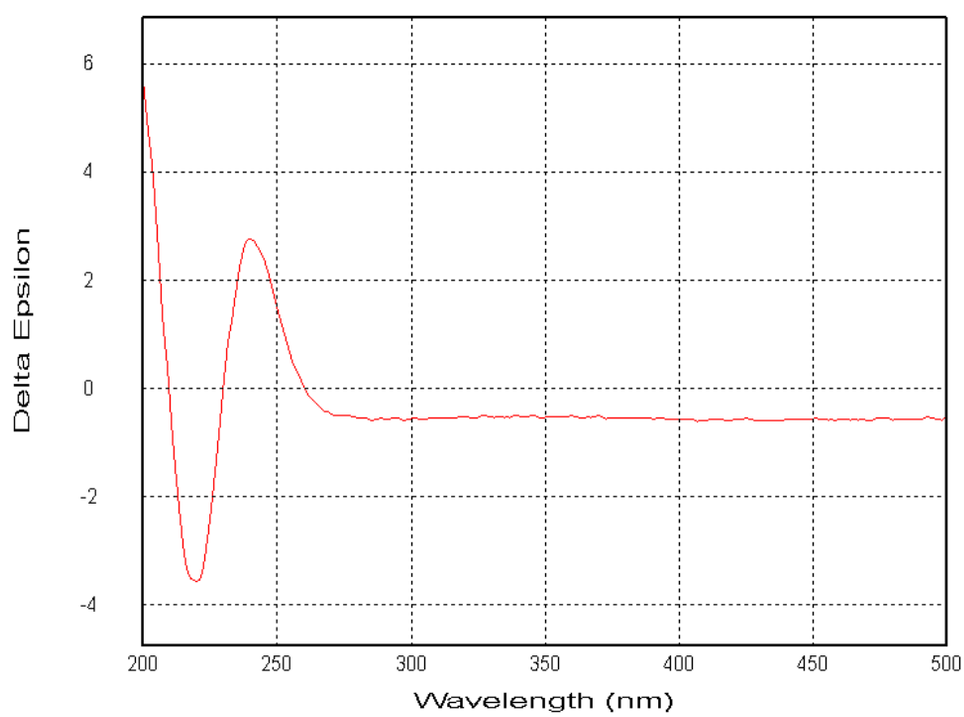

Figure. S92. CD-spectrum of the experimental measurement.

9.18 Blennione (**35**)

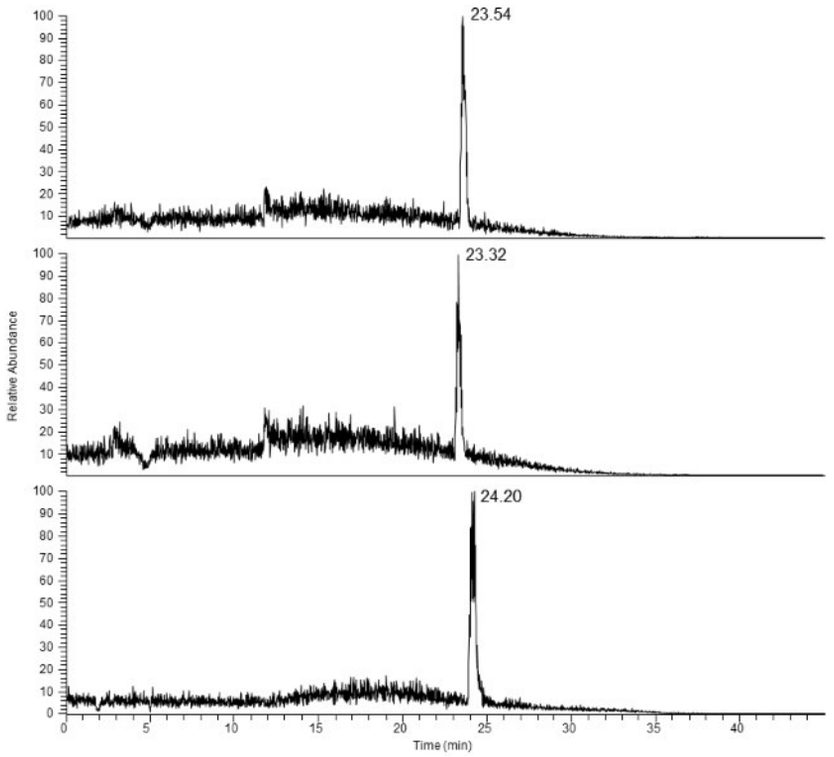

Figure. S93. LC-MS-spectrums of the extracted blennione (**35**), (gradient E). Up to down: from *L. circellatus*, *L. fluens* and from *L. blennius* stems.

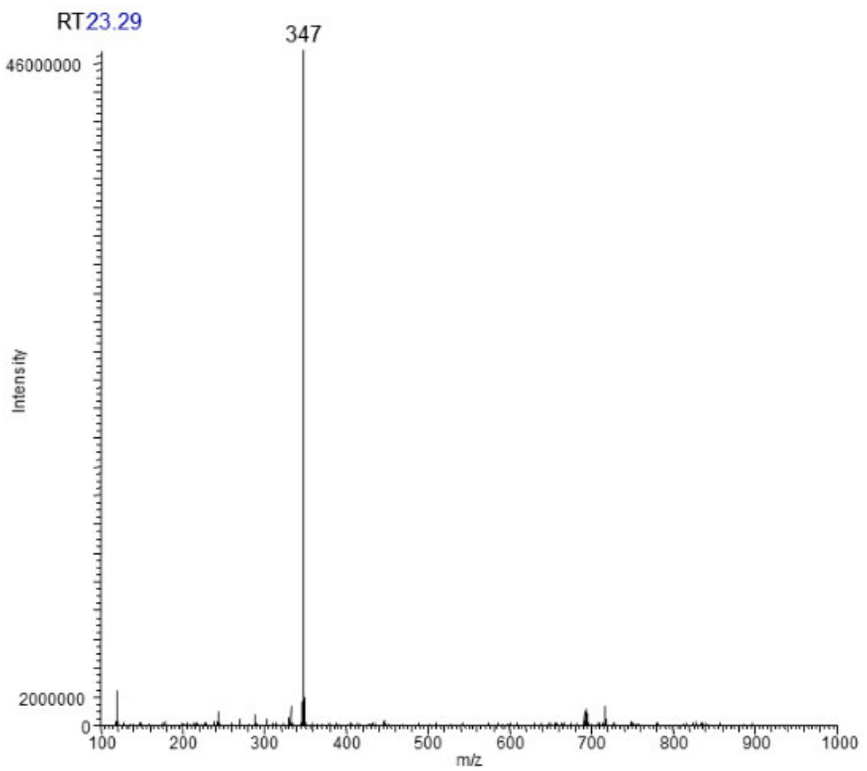

Figure. S94. Moleculer mass of blennione (**35**), (-ve mode).

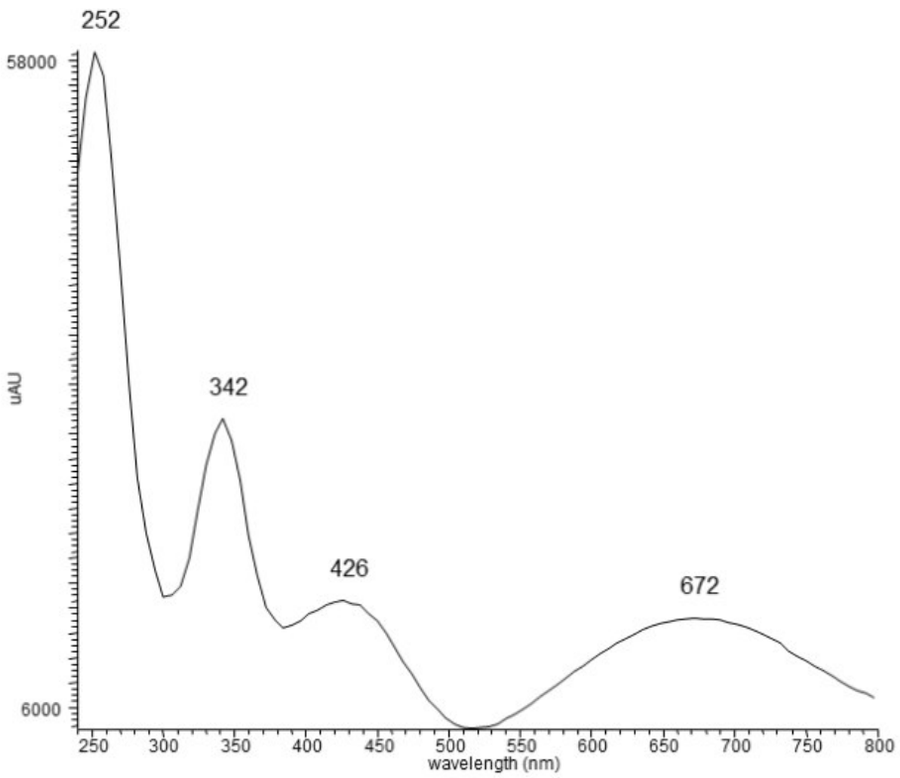

Figure. S95. UV-spectra of blennione (**35**).

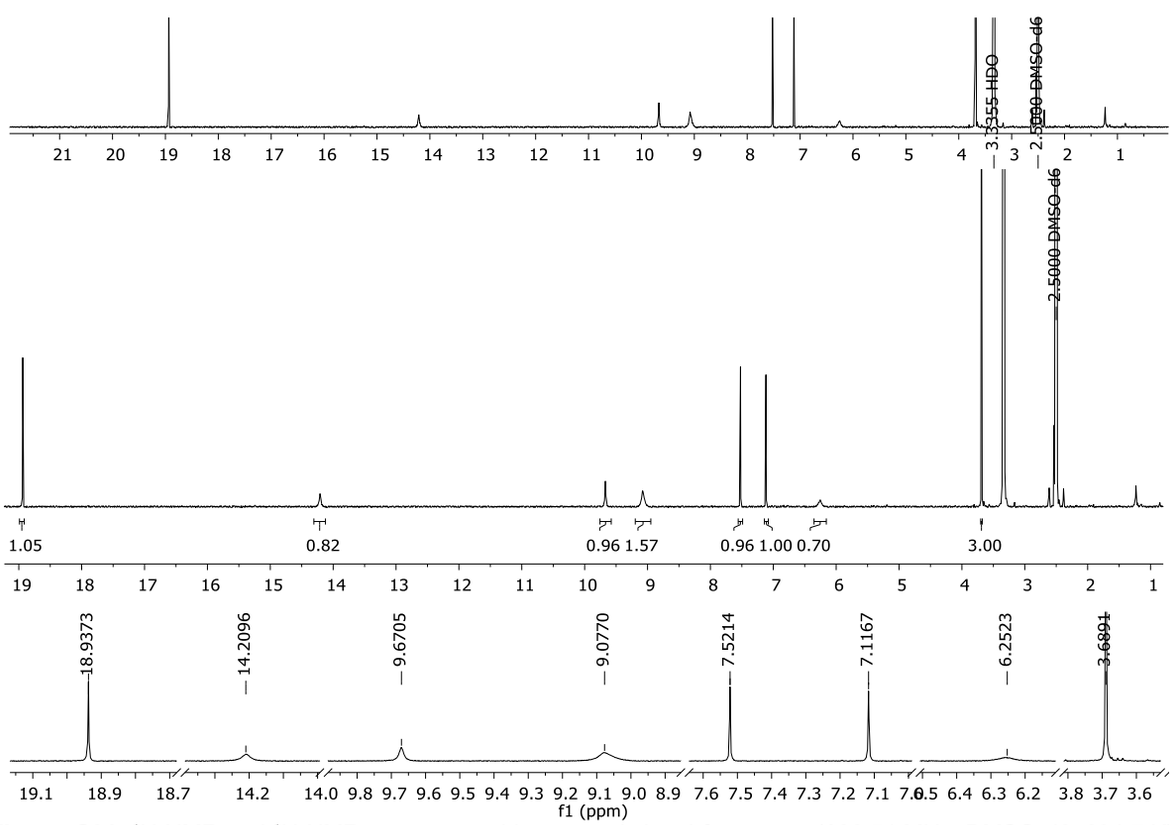

Figure. S96. ^{1}H-NMR and ^{1}H-NMR-spectrums with removed signal-free areas (600.51 MHz, DMSO-d6, 294.7 K).

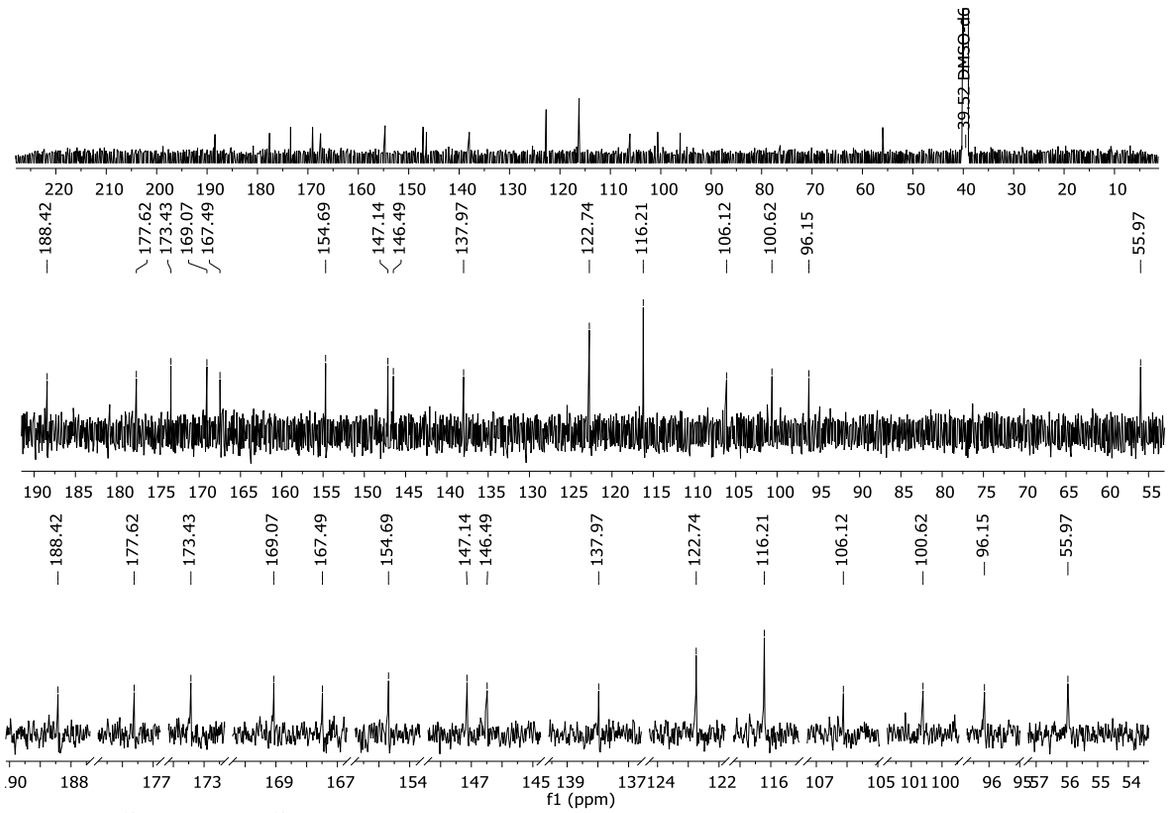

Figure. S97. ^{13}C-NMR and ^{13}C-NMR-spectrums with removed signal-free areas (151.01 MHz, DMSO-d6, 294.7 K).

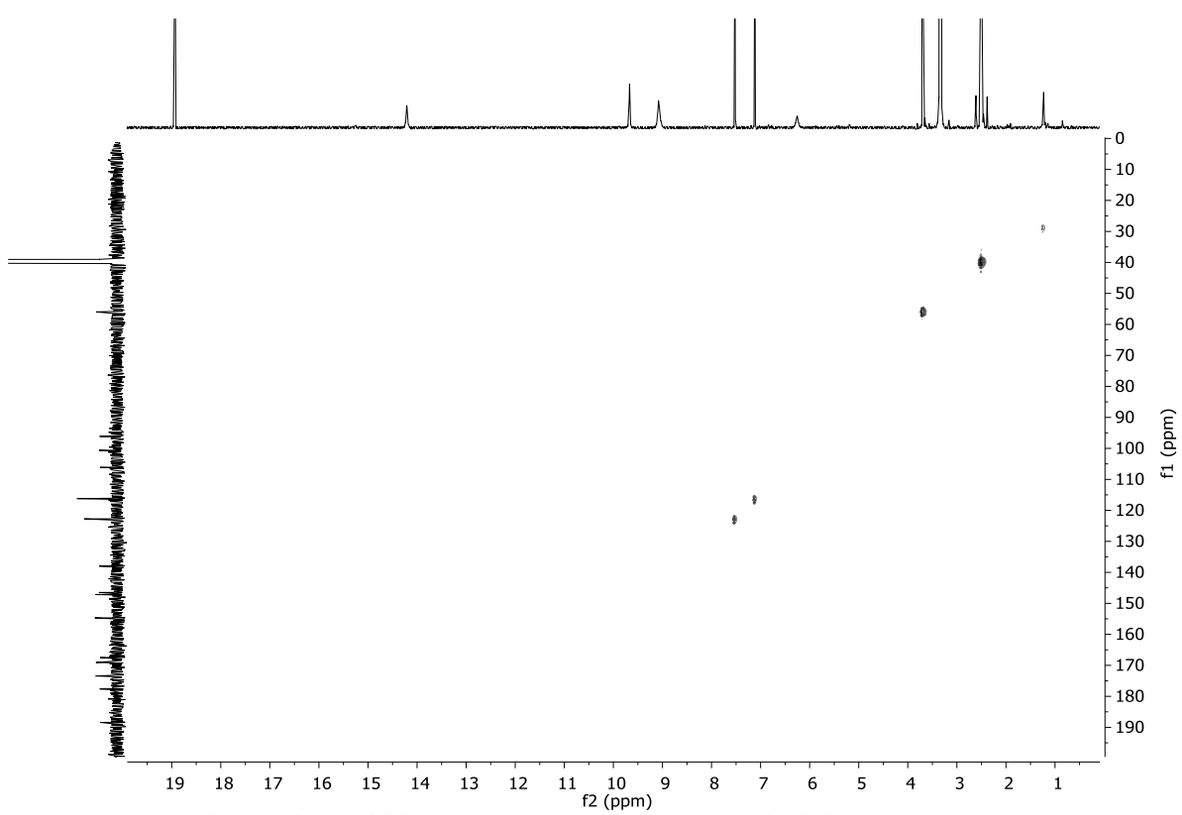

Figure. S98. HSQC-spectrum (600.51, 151.01 MHz, DMSO-d6, 294.8 K).

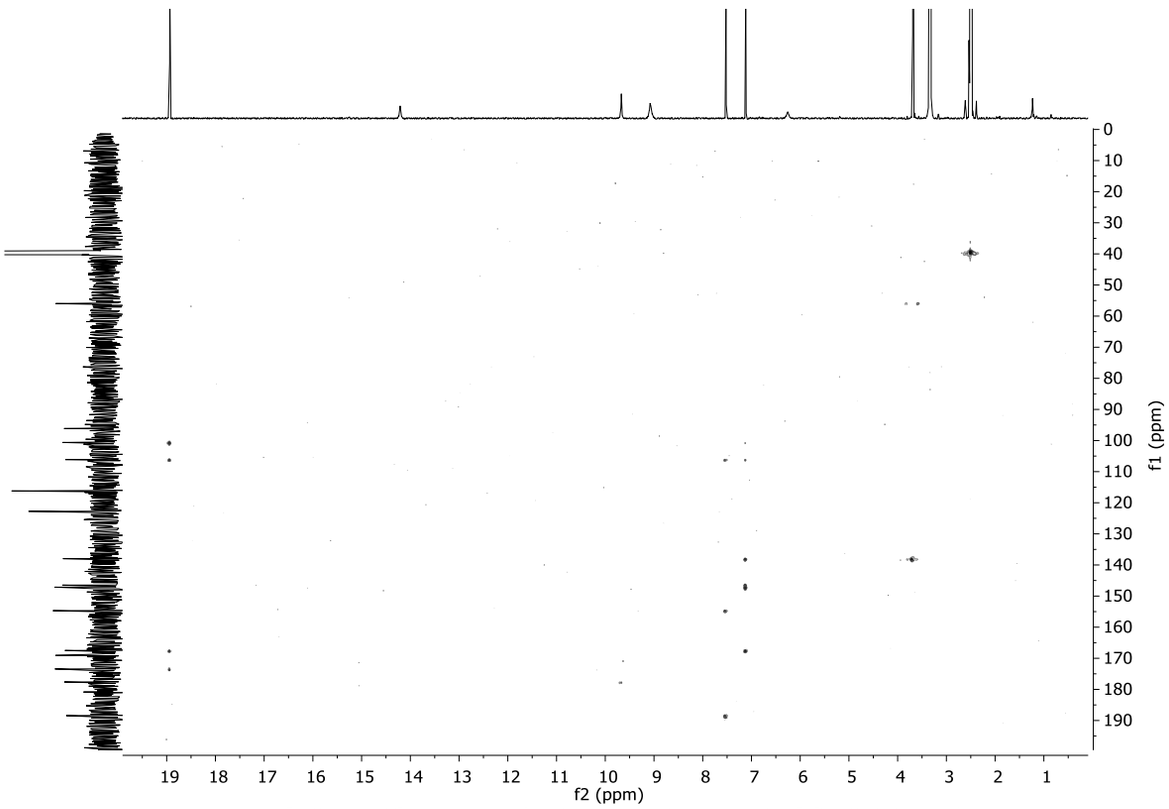

Figure. S99. HMBC-spectrum (600.51, 151.01 MHz, DMSO-d6, 294.7 K).

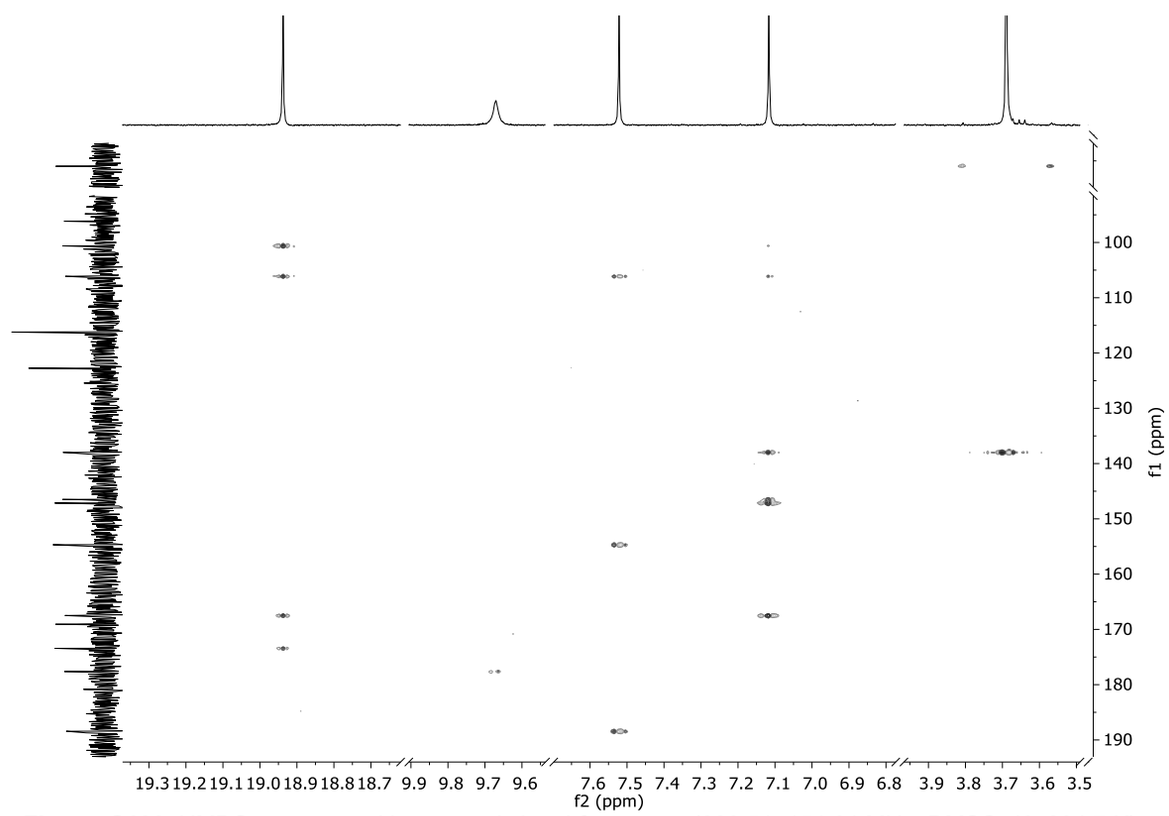

Figure. S100. HMBC-spectrum with removed signal-free areas (600.51, 151.01 MHz, DMSO-d6, 294.7 K).

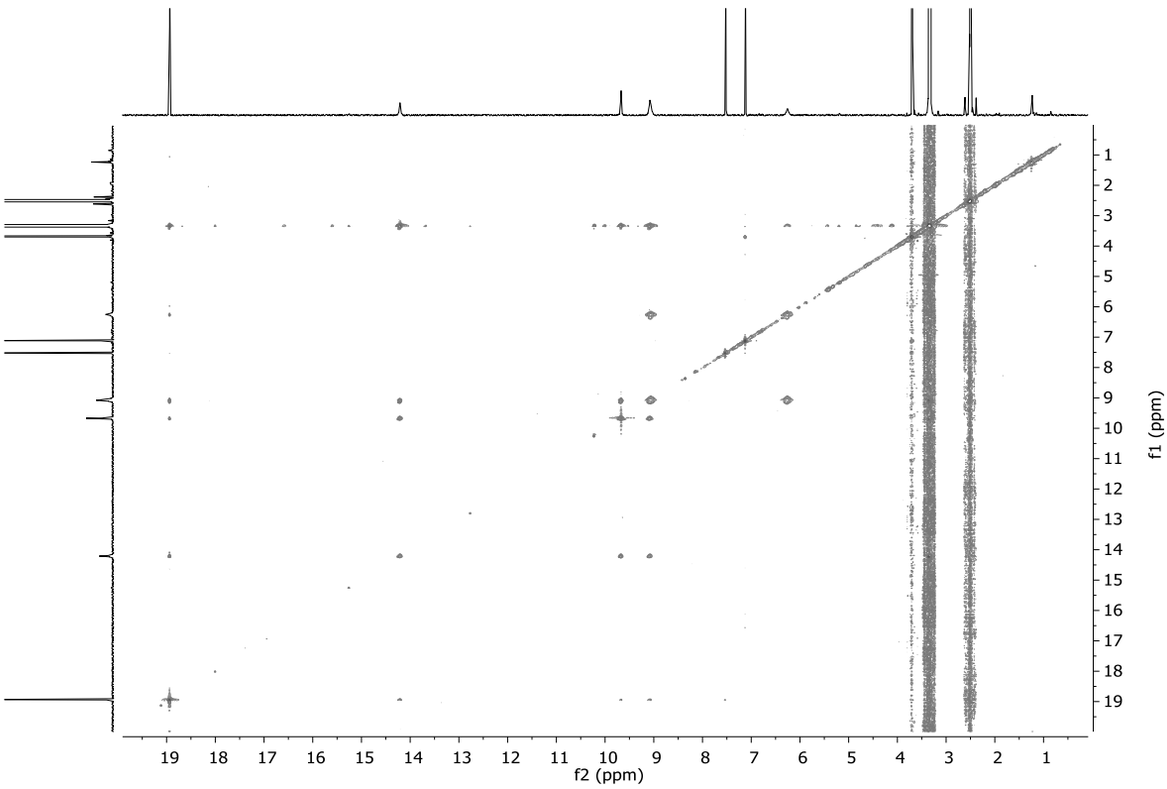

Figure. S101. NOESY-spectrum (600.51, 600.51 MHz, DMSO-d6, 294.7 K).

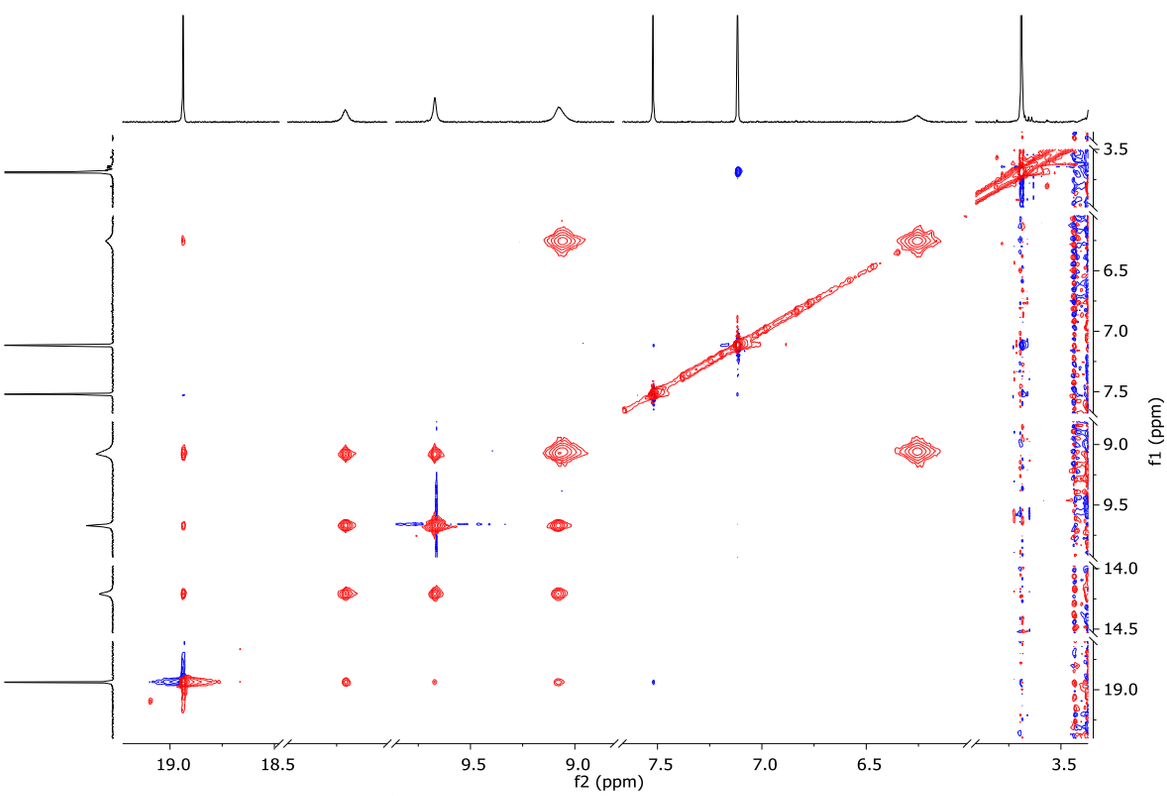

Figure. S102. NOESY-spectrum with removed signal-free areas (600.51, 600.51 MHz, DMSO-d6, 294.7 K).

9.19 Trivialine A (**47**)

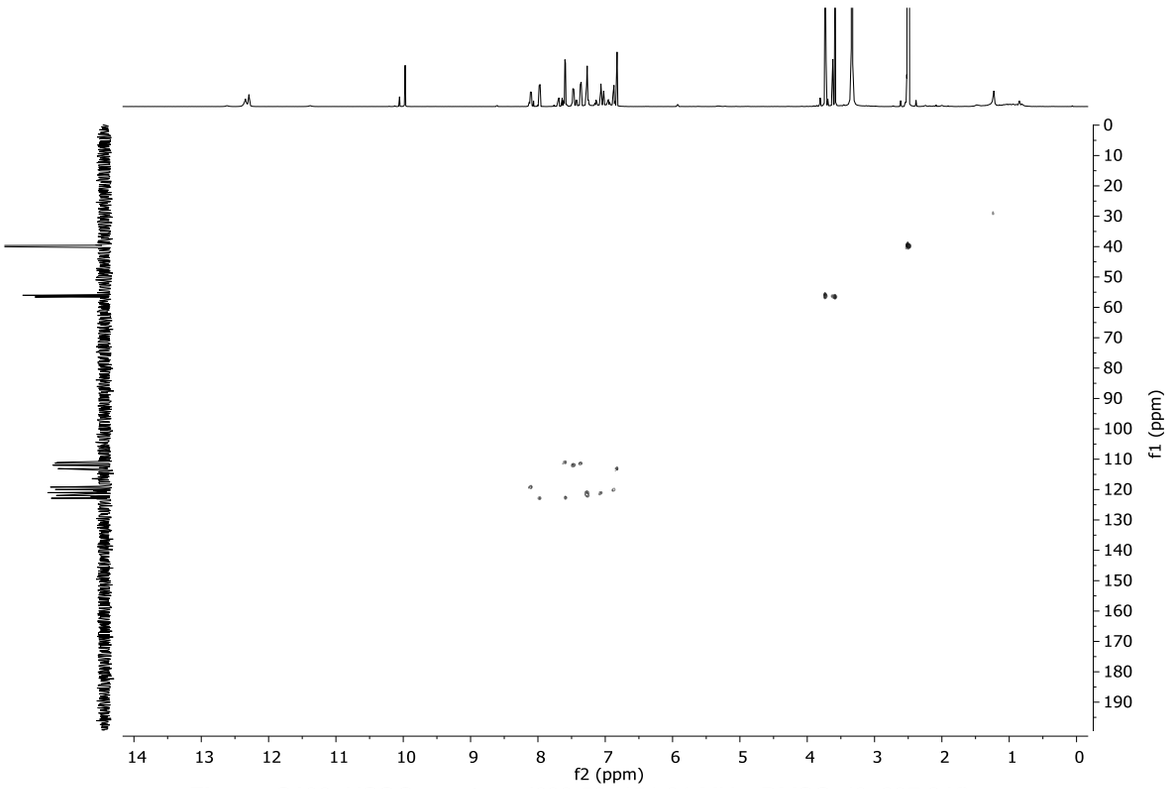

Figure. S103. HSQC-spectrum (600.50, 151.01 MHz, DMSO-d6, 297.2 K).

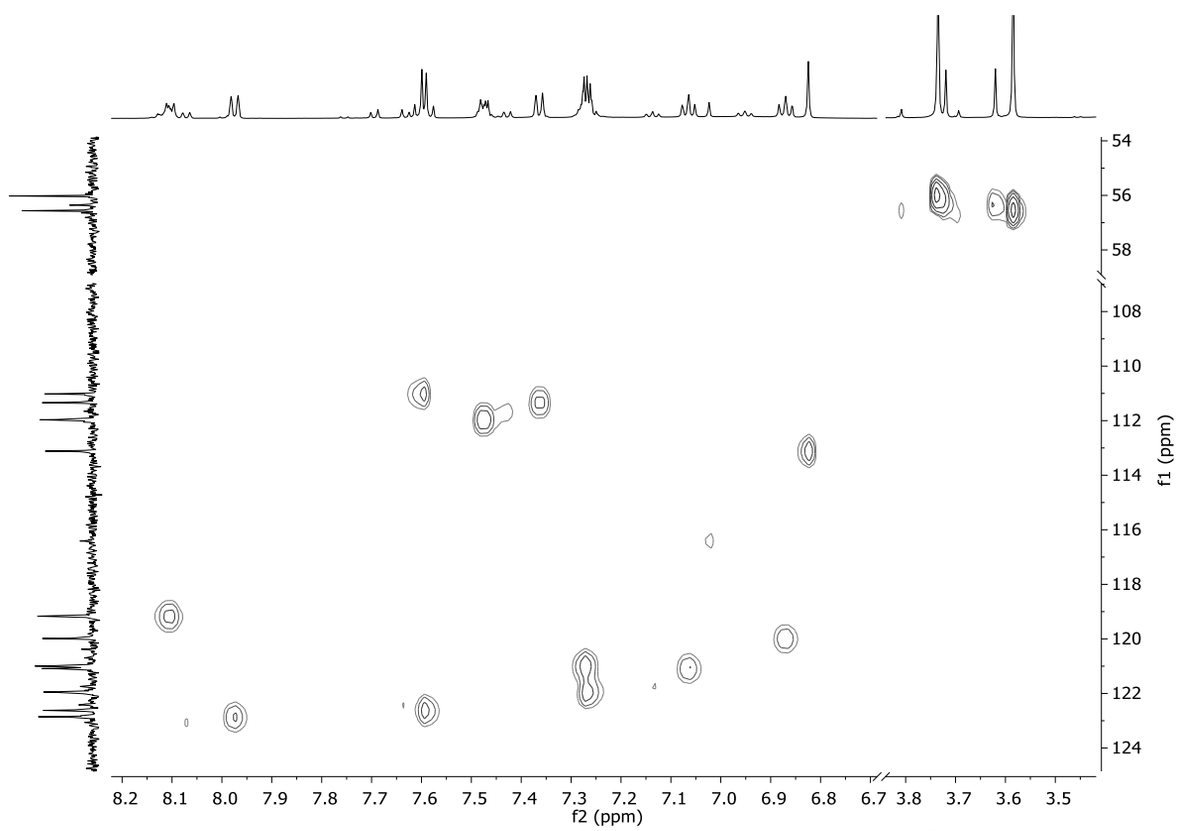

Figure. S104. HSQC-spectrum with removed signal-free areas (600.50, 151.01 MHz, DMSO-d6, 297.2 K).

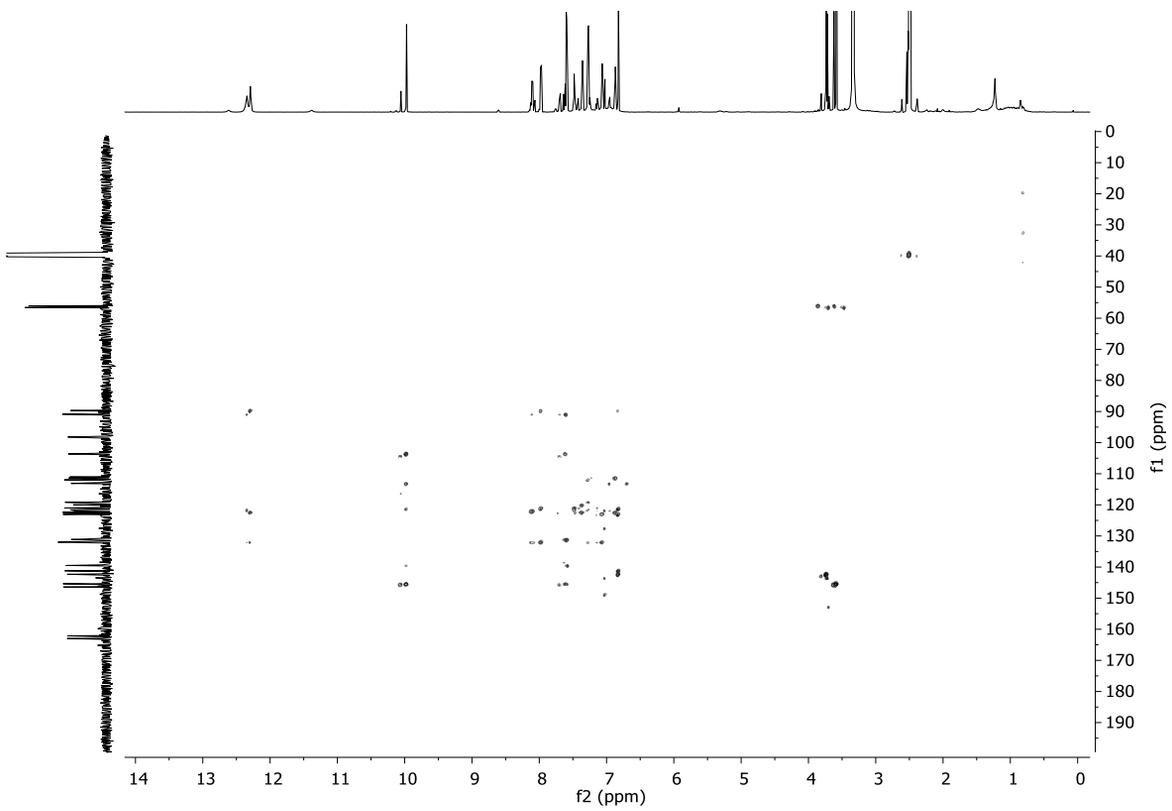

Figure. S105. HMBC-spectrum (600.50, 151.01 MHz, DMSO-d6, 297.1 K).

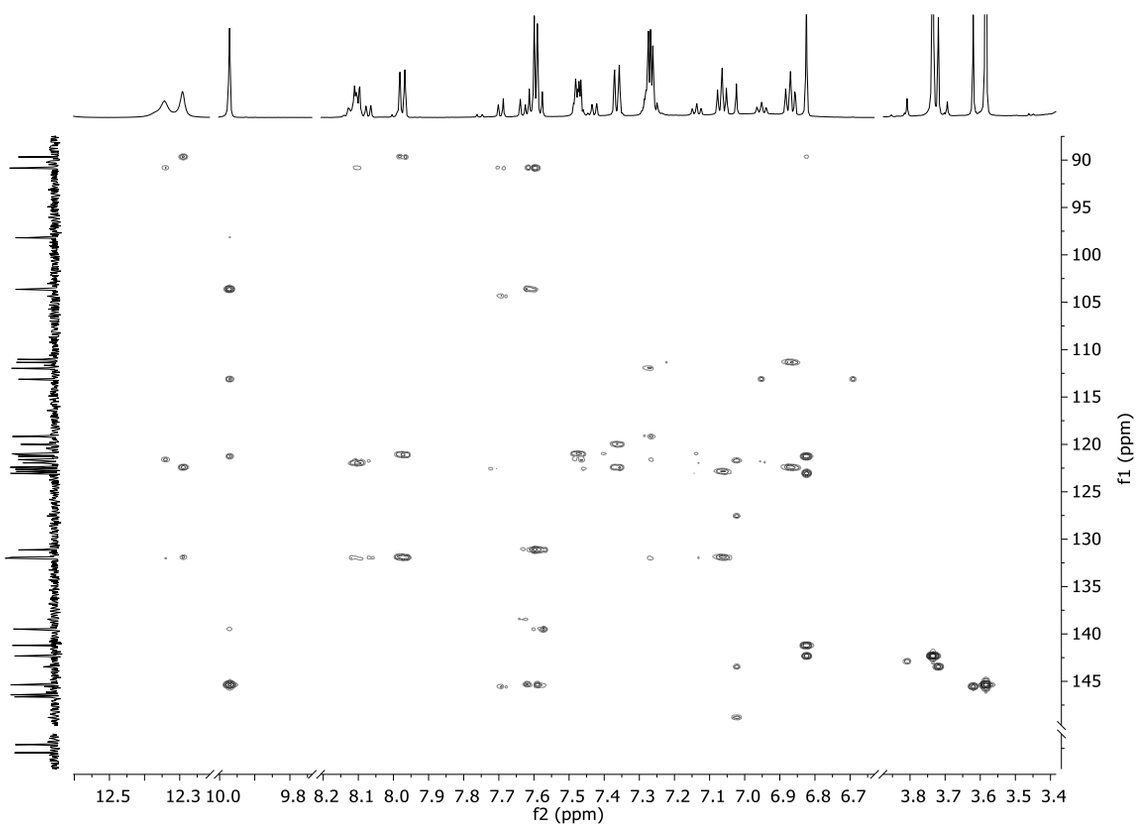

Figure. S106. HMBC-spectrum with removed signal-free areas (600.50, 151.01 MHz, DMSO-d6, 297.1 K).

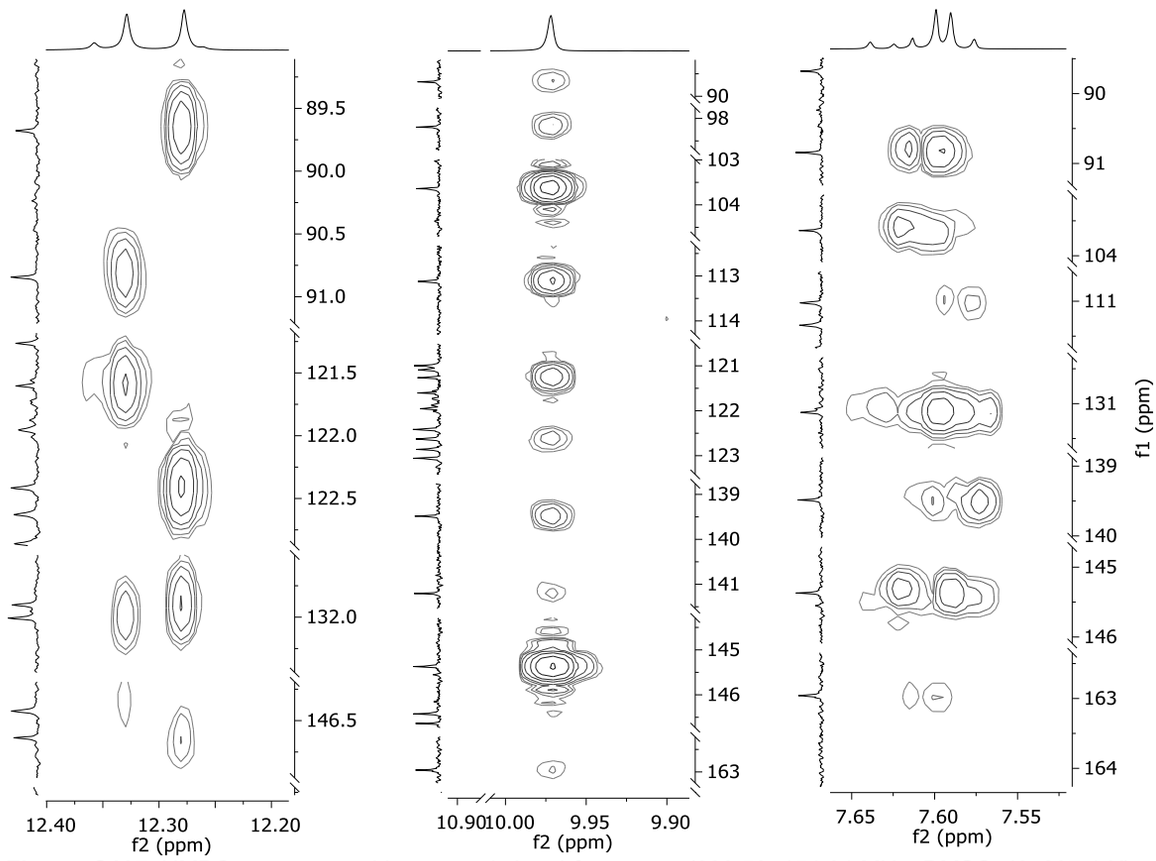

Figure. S107. HMBC-spectrums with removed signal-free areas (600.50, 151.01 MHz, DMSO-d6, 297.1 K).

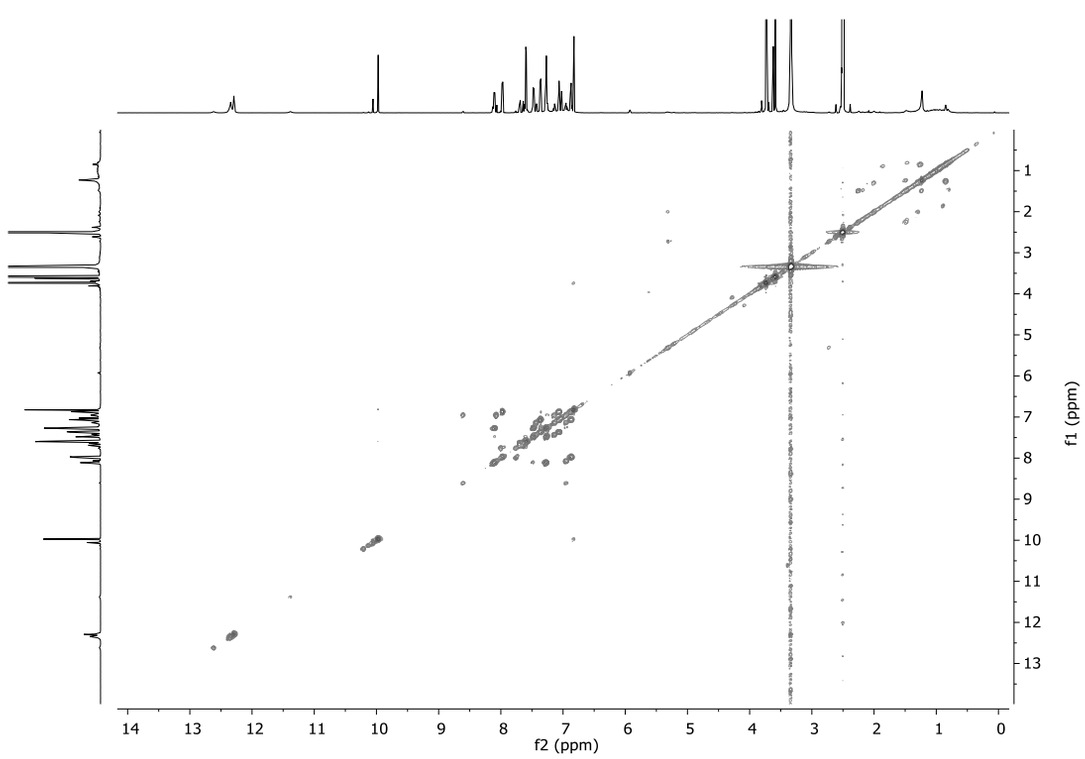

Figure. S108. COSY-spectrum (600.50, 600.50 MHz, DMSO-d6, 297.2 K).

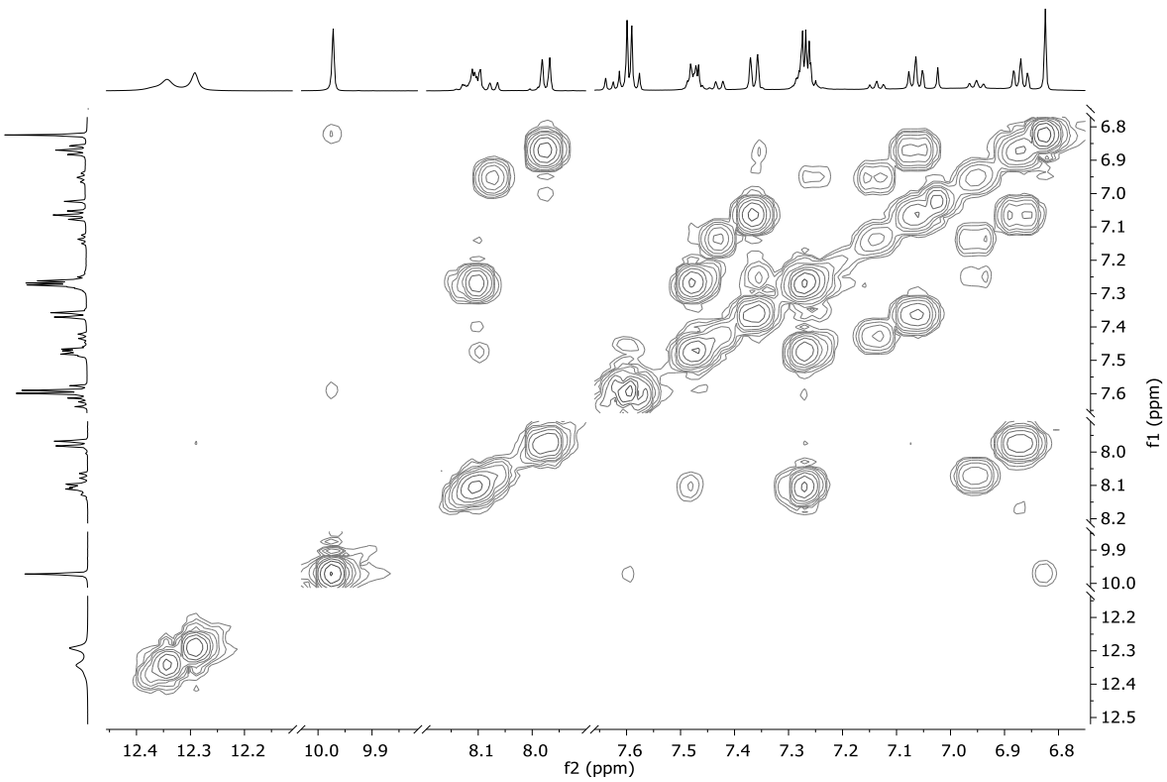

Figure. S109. COSY-spectrum with removed signal-free areas (600.50, 600.50 MHz, DMSO-d6, 297.2 K).

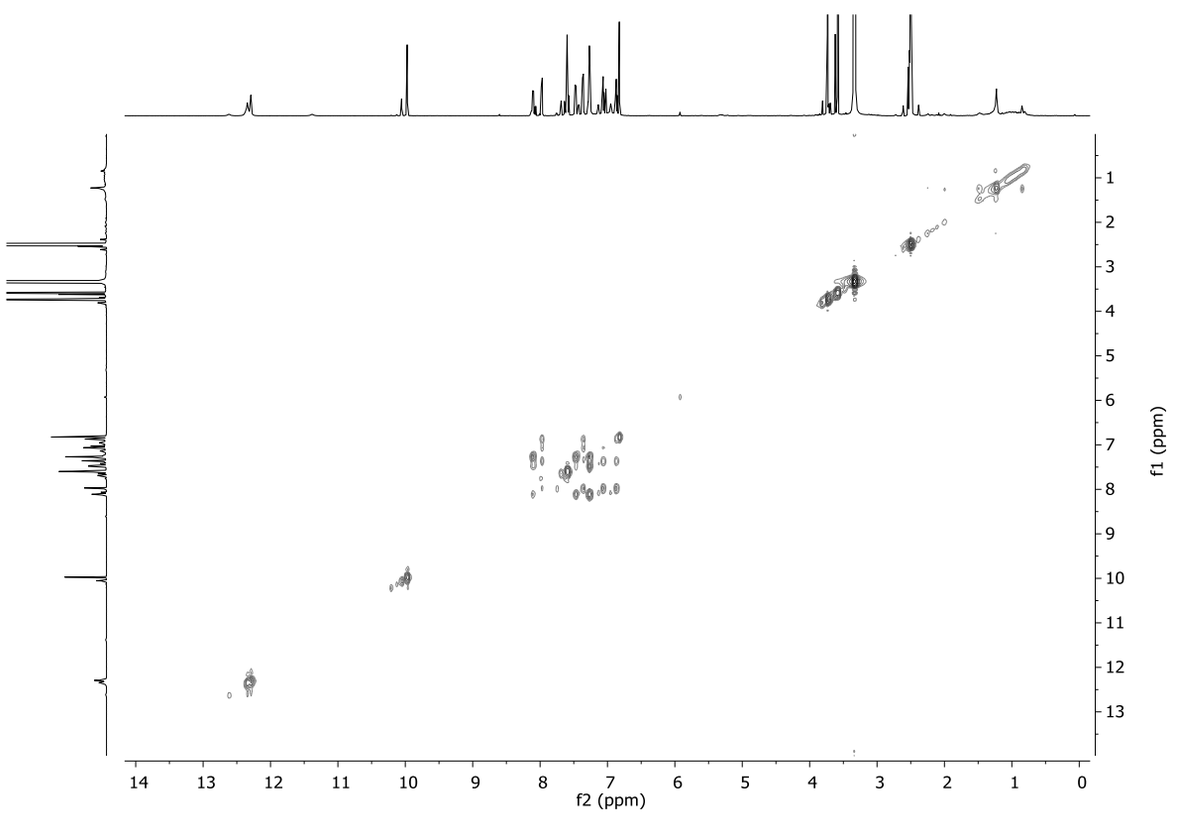

Figure. S110. TOCSY-spectrum (600.50, 600.50 MHz, DMSO-d6, 297.2 K).

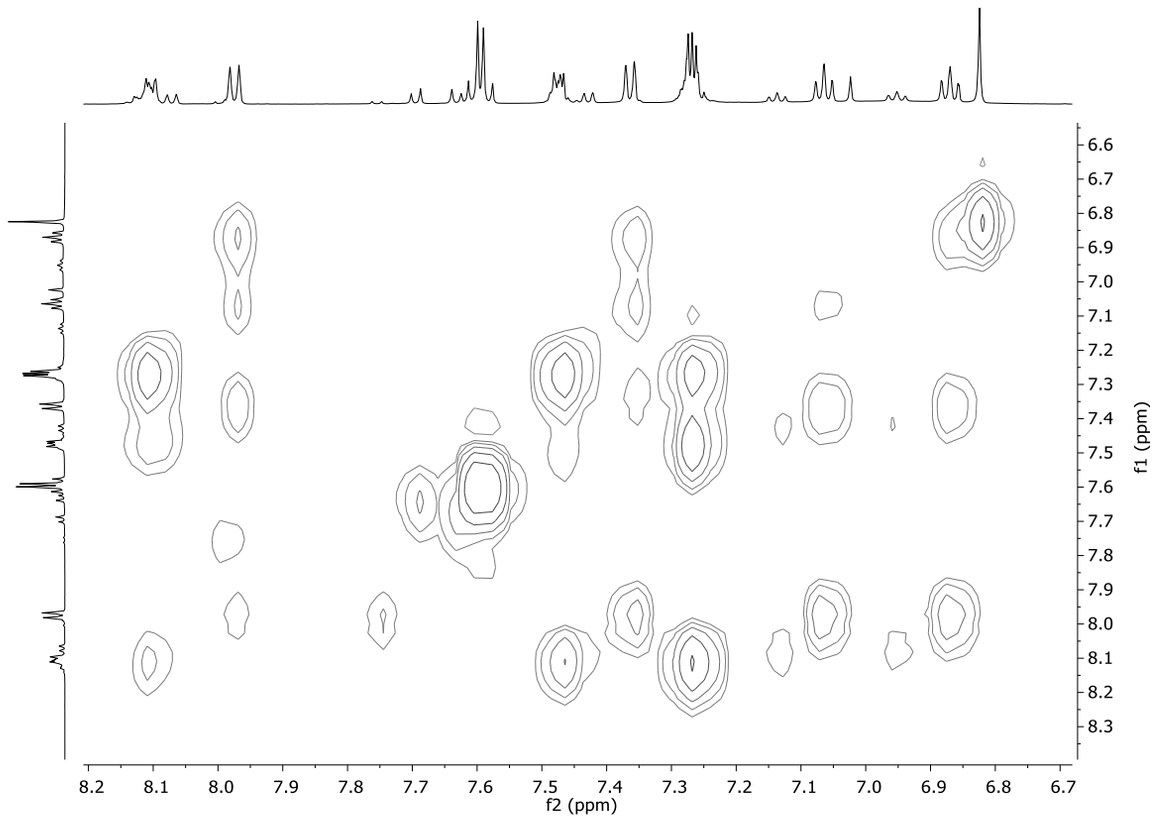

Figure. S111. TOCSY-spectrum with removed signal-free areas (600.50, 600.50 MHz, DMSO-d6, 297.2 K).

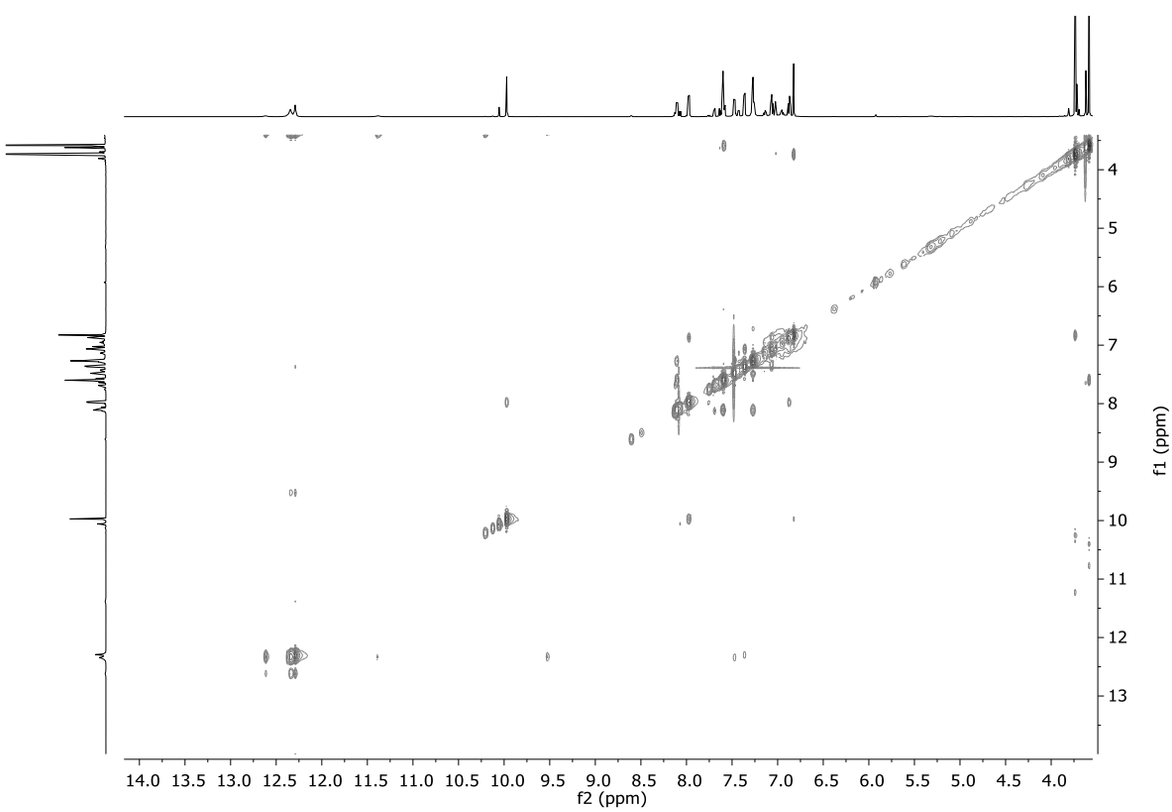

Figure. S112. NOESY-spectrum (600.50, 600.50 MHz, DMSO-d6, 297.2 K).

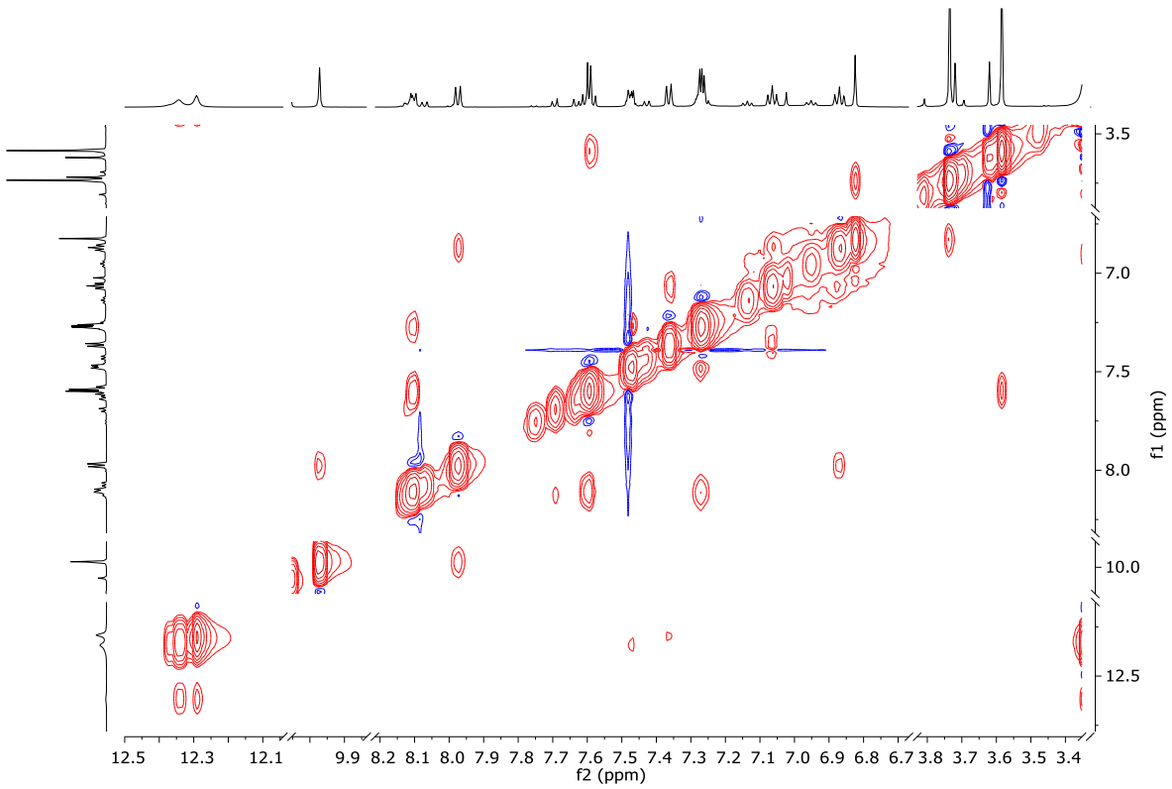

Figure. S113. NOESY-spectrum with removed signal-free areas (600.50, 600.50 MHz, DMSO-d6, 297.2 K).

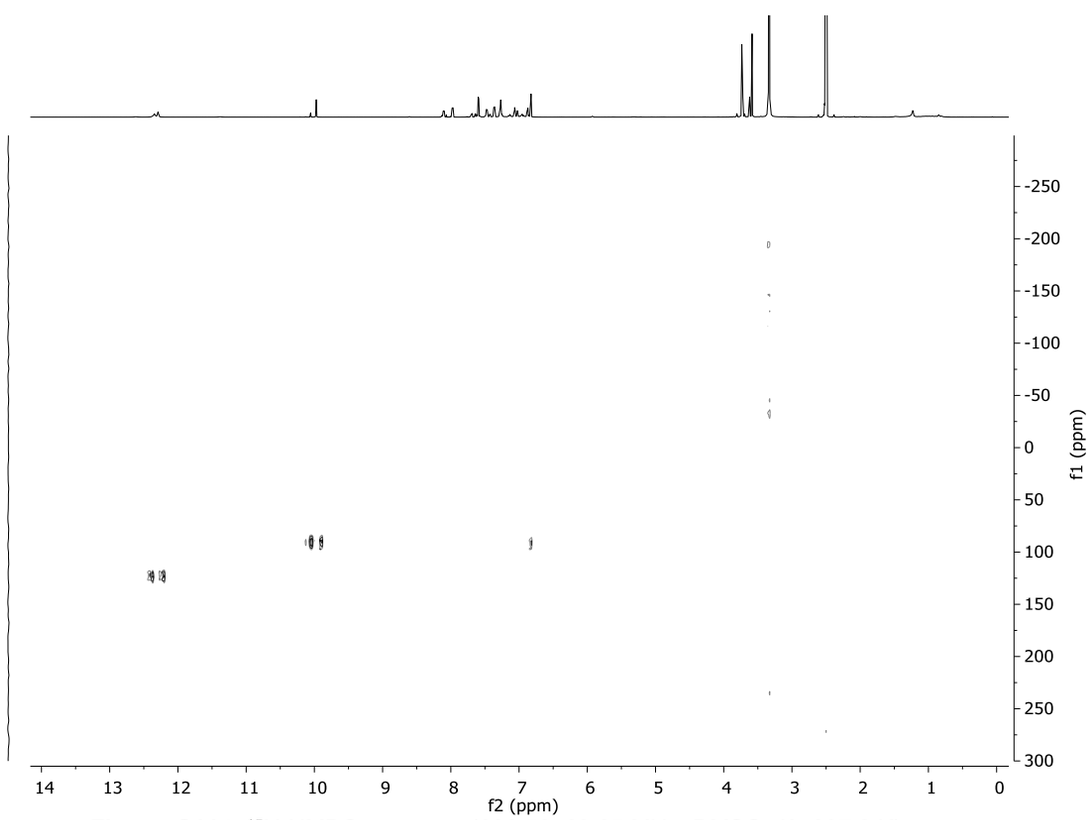

Figure. S114. ^{15}N-HMBC-spectrum (600.50, 60.85 MHz, DMSO-d6, 297.2 K).

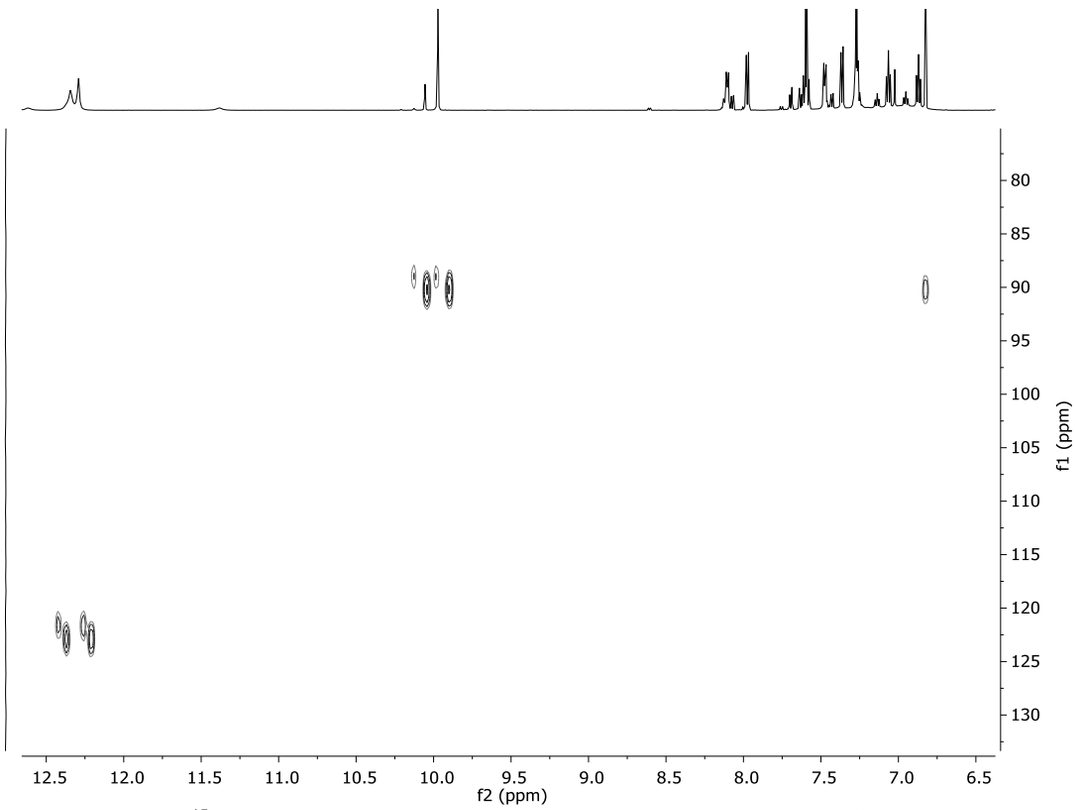

Figure. S115. ^{15}N-HMBC focused-spectrum (600.50, 60.85 MHz, DMSO-d6, 297.2 K).

9.20 Trivialine B (**48**)

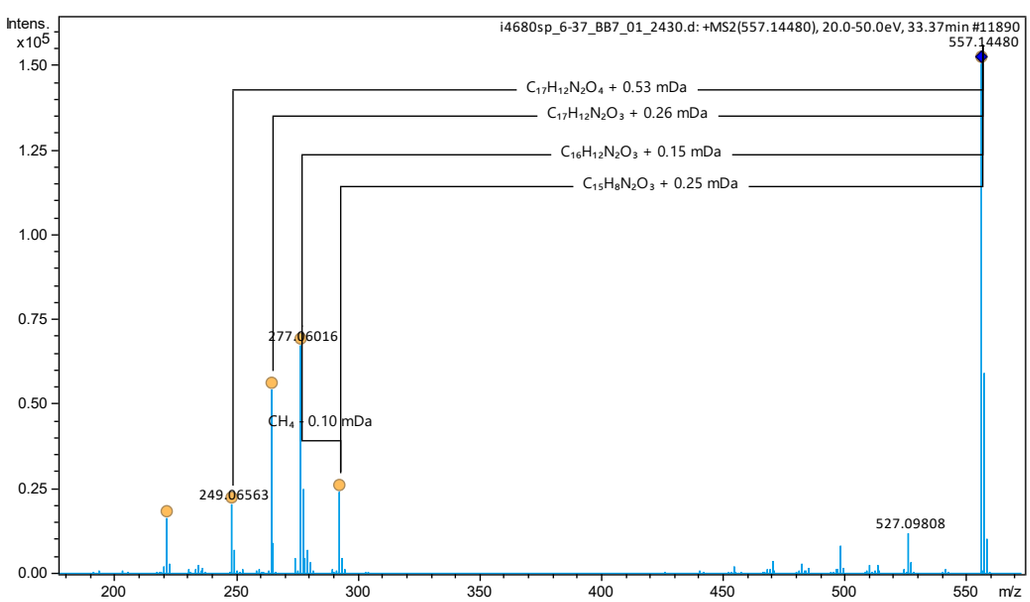

Figure. S116. HR-ESI-(+)-MS/MS-spectrum.

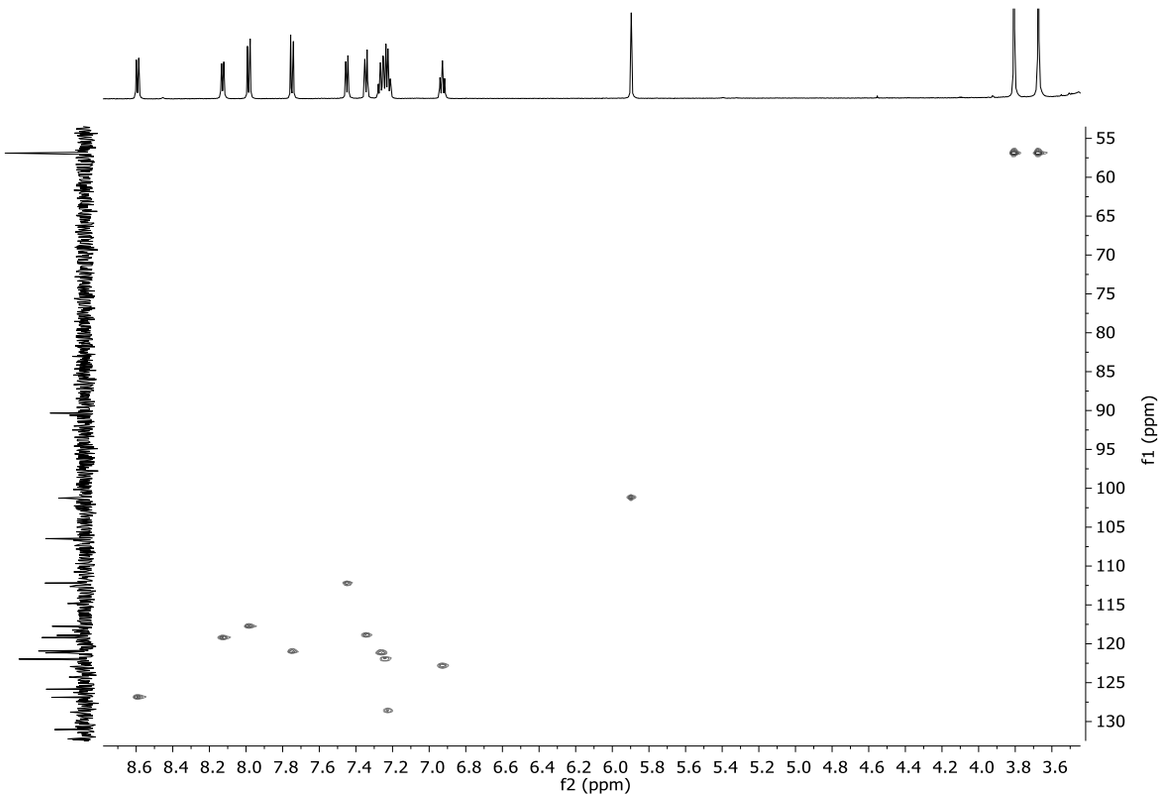

Figure. S117. HSQC-spectrum (600.51, 151.01 MHz, DMSO-d6, 297.2 K).

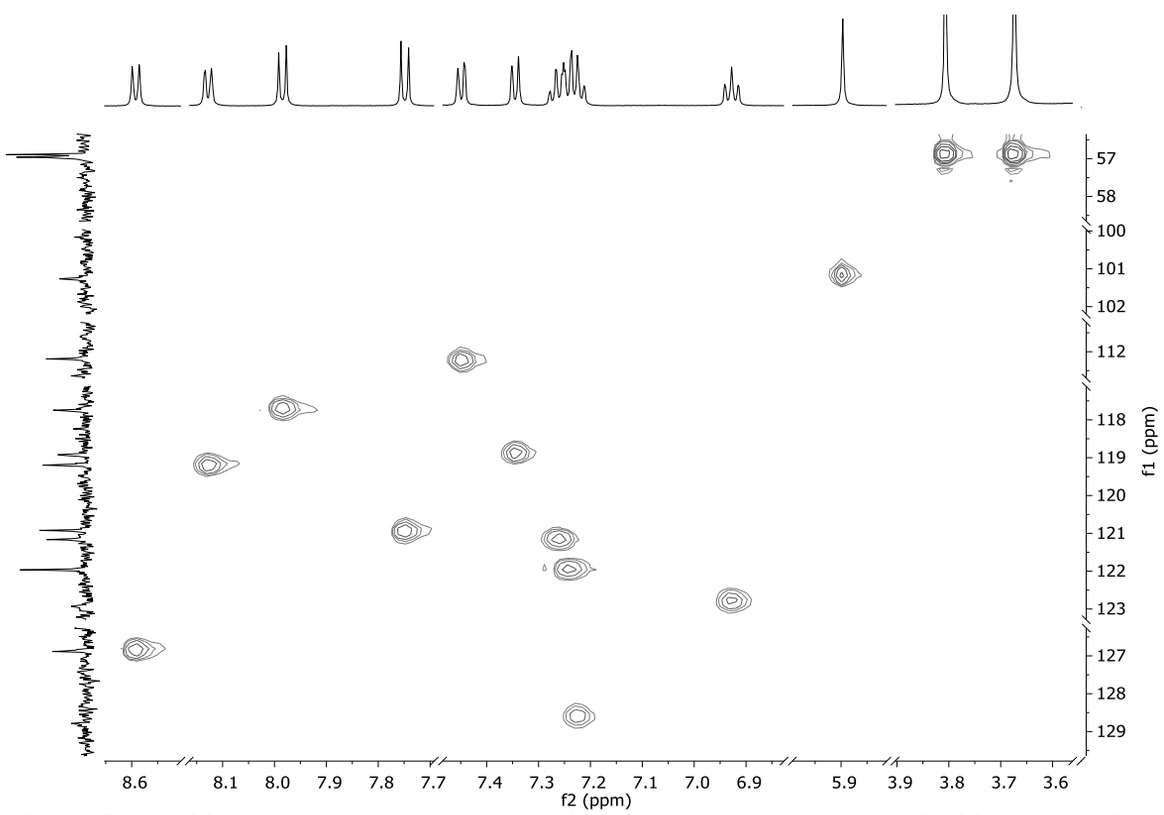

Figure. S118. HSQC-spectrum with removed signal-free areas (600.50, 151.01 MHz, DMSO-d6, 297.2 K).

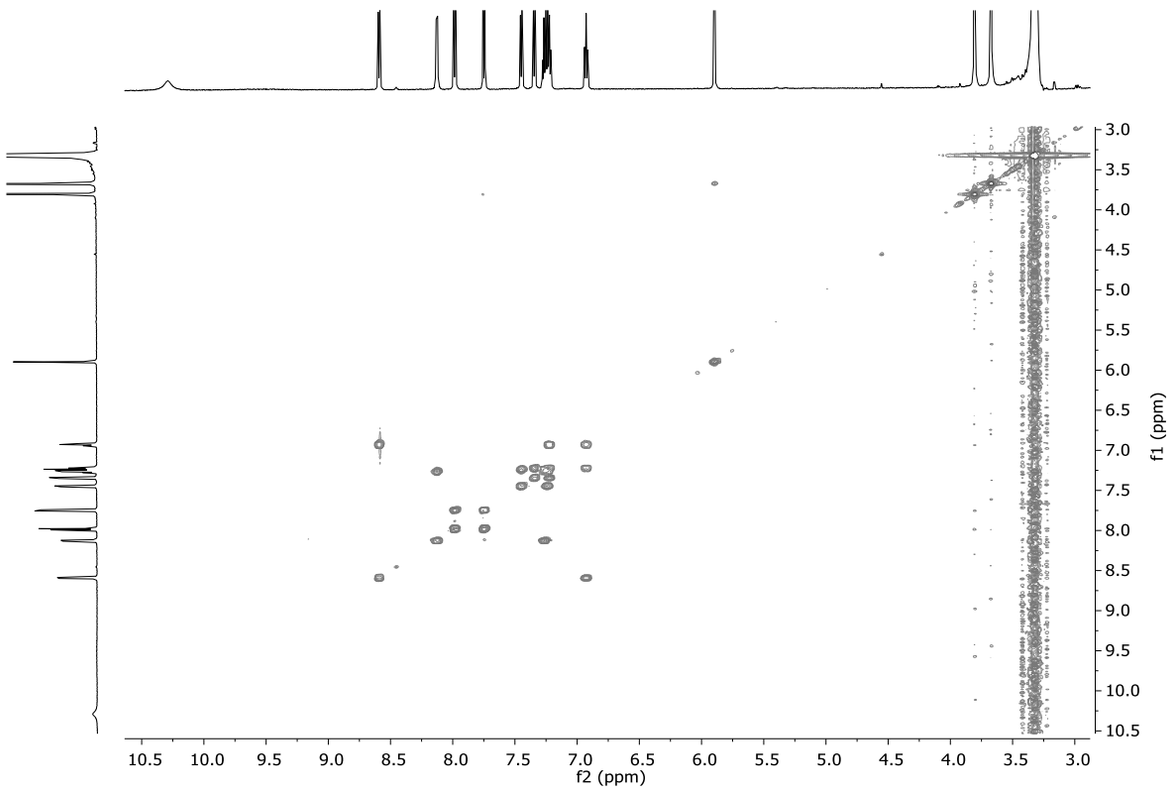

Figure. S119. COSY-spectrum (600.50, 600.50 MHz, DMSO-d6, 297.1 K).

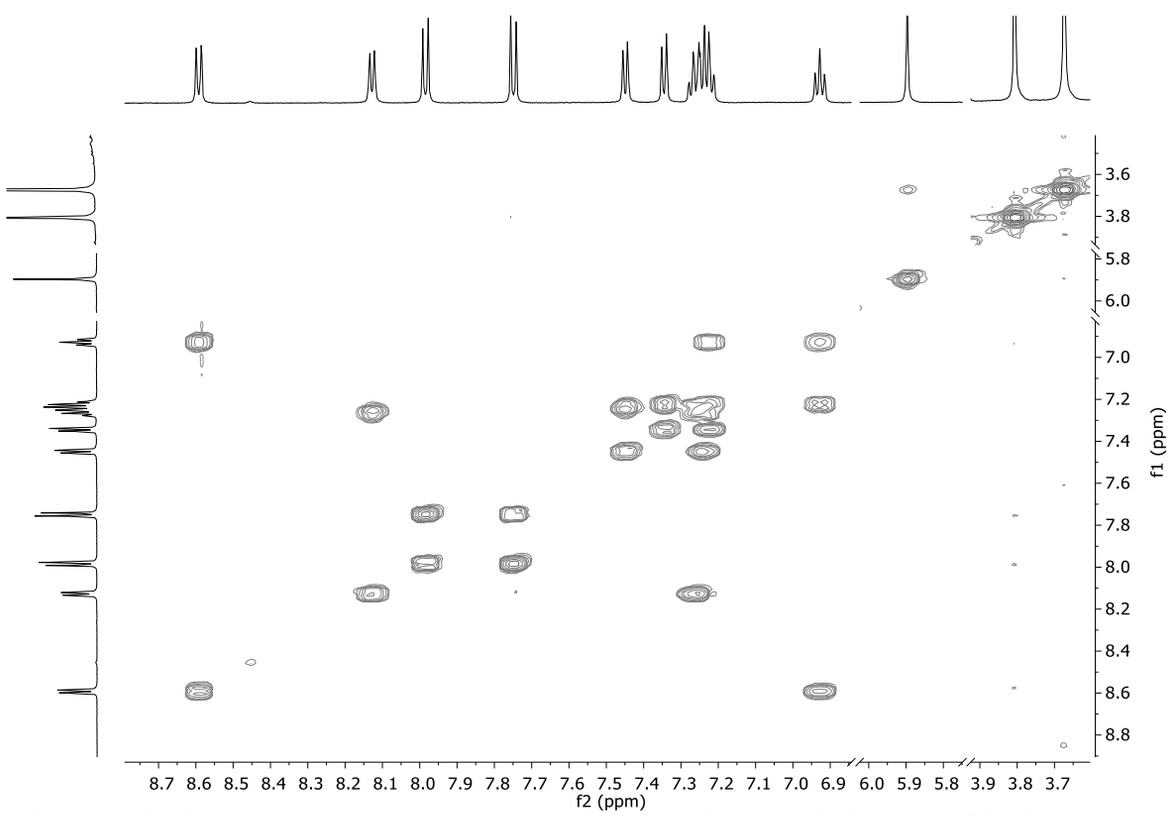

Figure. S120. COSY-spectrum with removed signal-free areas (600.50, 600.50 MHz, DMSO-d6, 297.1 K).

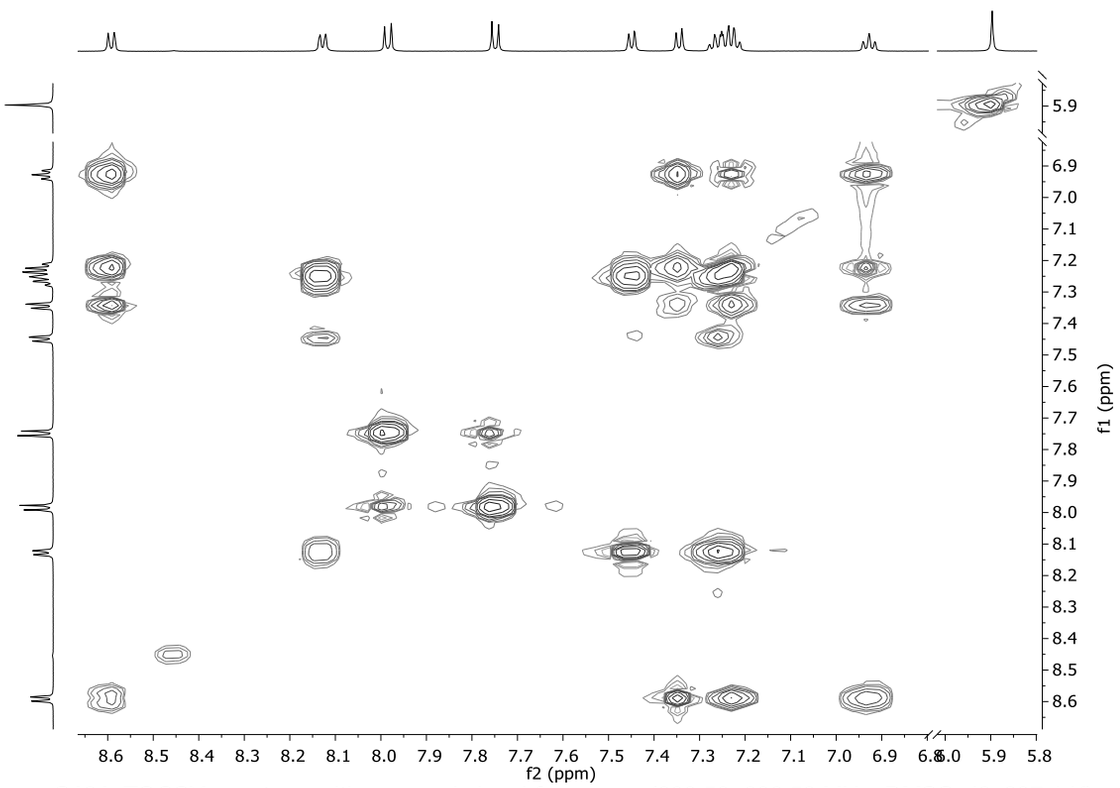

Figure. S121. TOCSY-spectrum with removed signal-free areas (600.50, 600.50 MHz, DMSO-d6, 297.1 K).

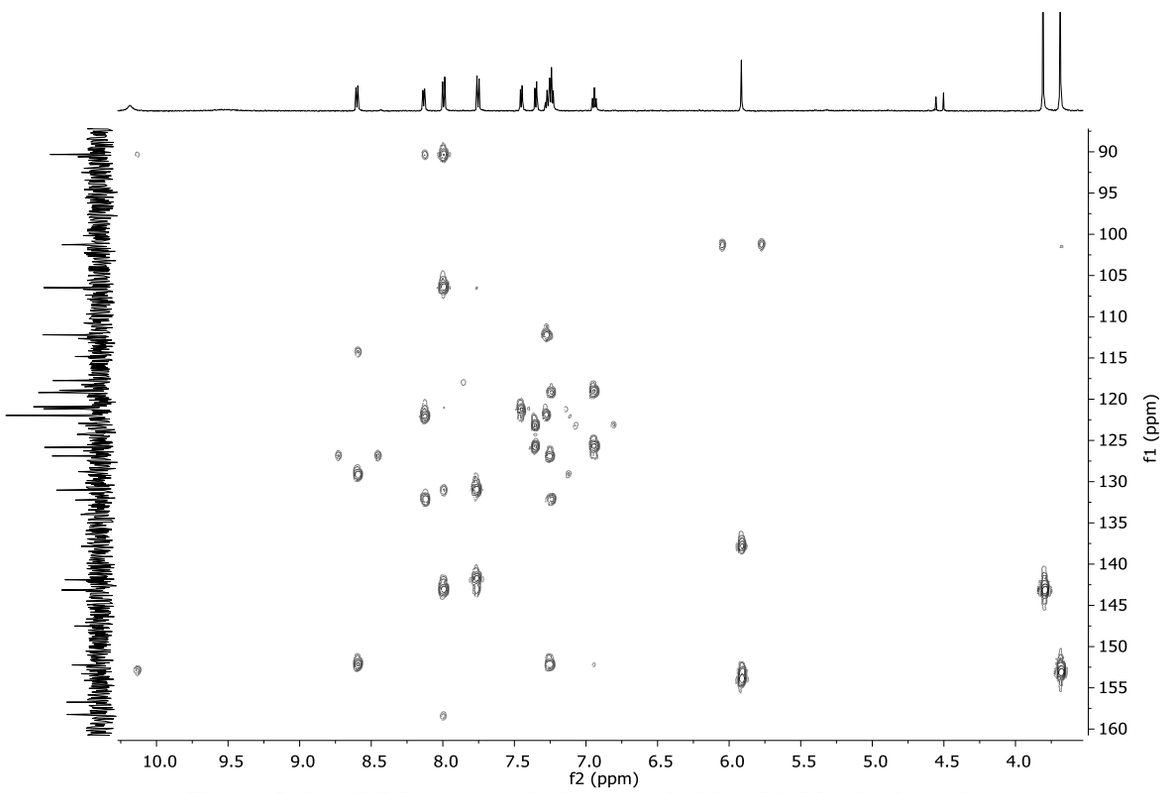

Figure. S122. HMBC-spectrum (600.50, 151.01 MHz, DMSO-d6, 297.2 K).

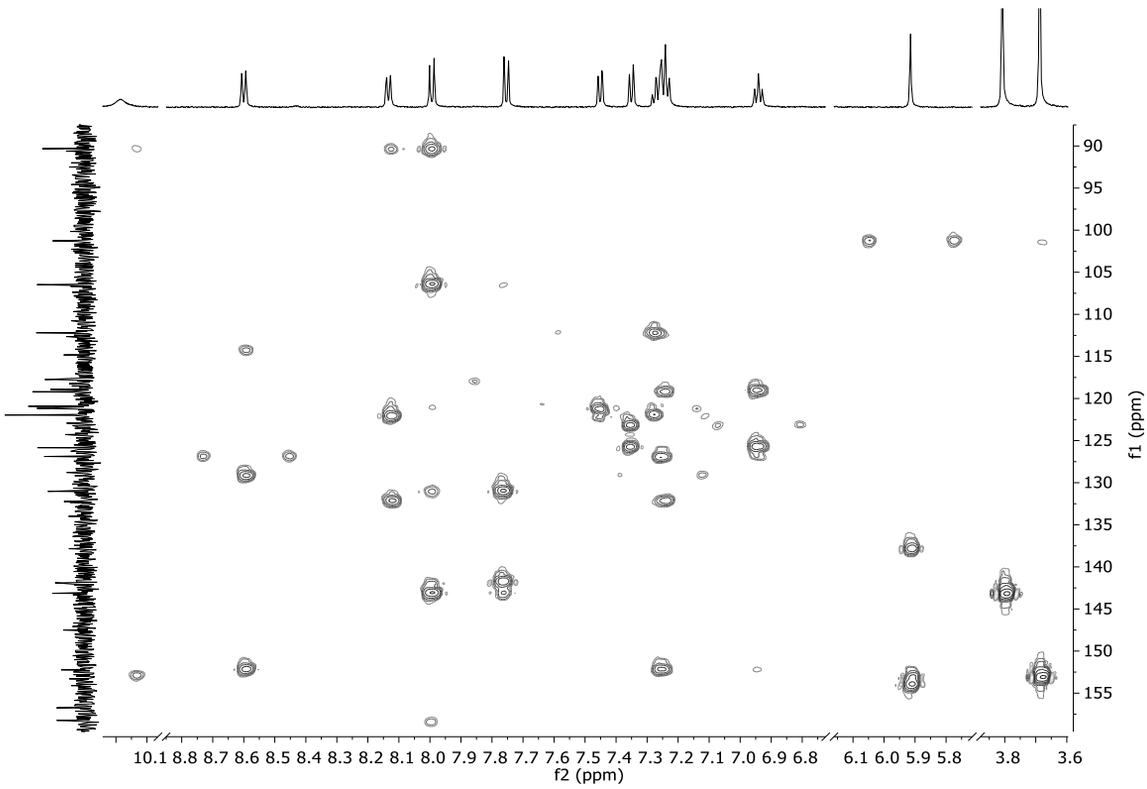

Figure. S123. HMBC-spectrum with removed signal-free areas (600.50, 151.01 MHz, DMSO-d6, 297.2 K).

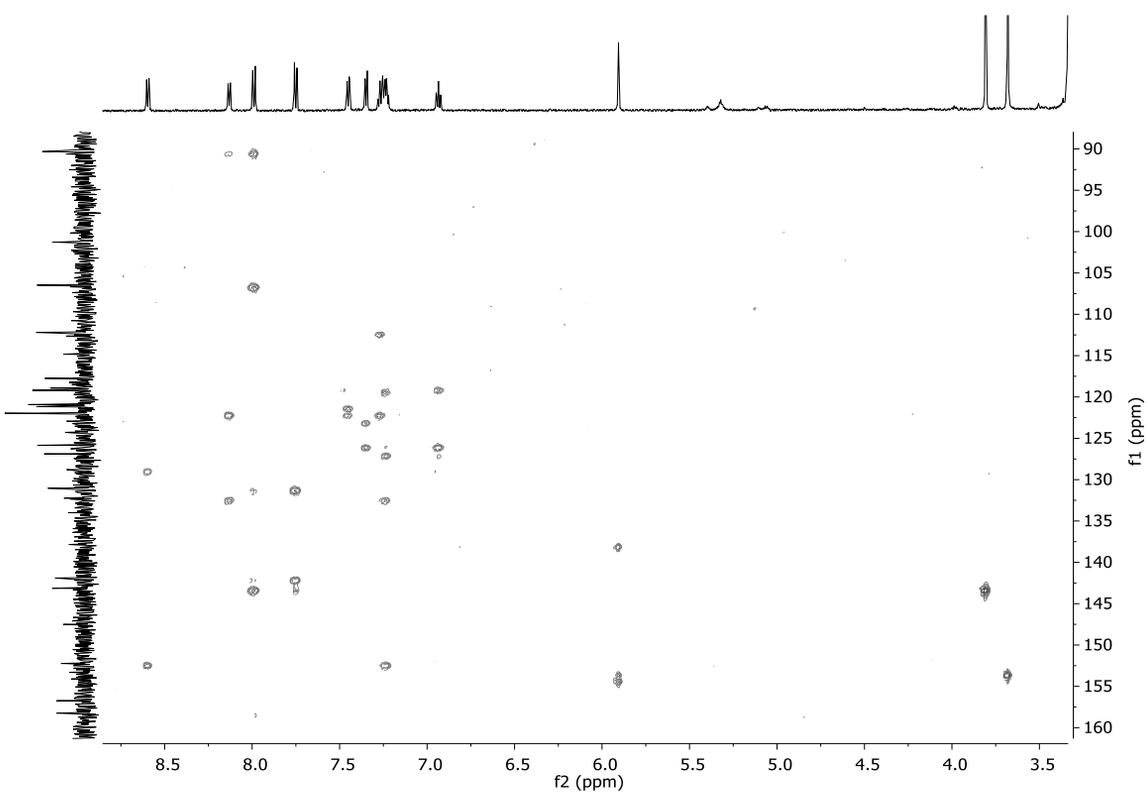

Figure. S124. HMBC-CT-spectrum (600.50, 151.01 MHz, DMSO-d6, 297.1 K).

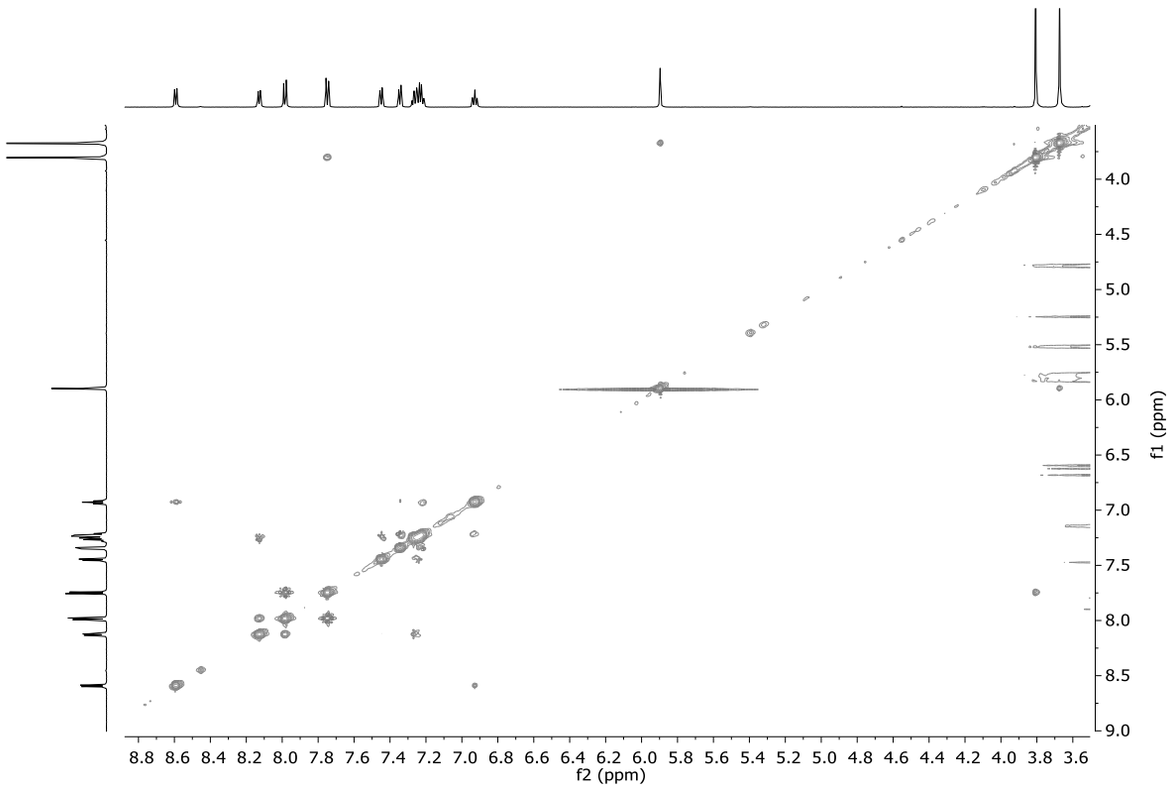

Figure. S125. NOESY-spectrum (600.50, 600.50 MHz, DMSO-d6, 297.2 K).

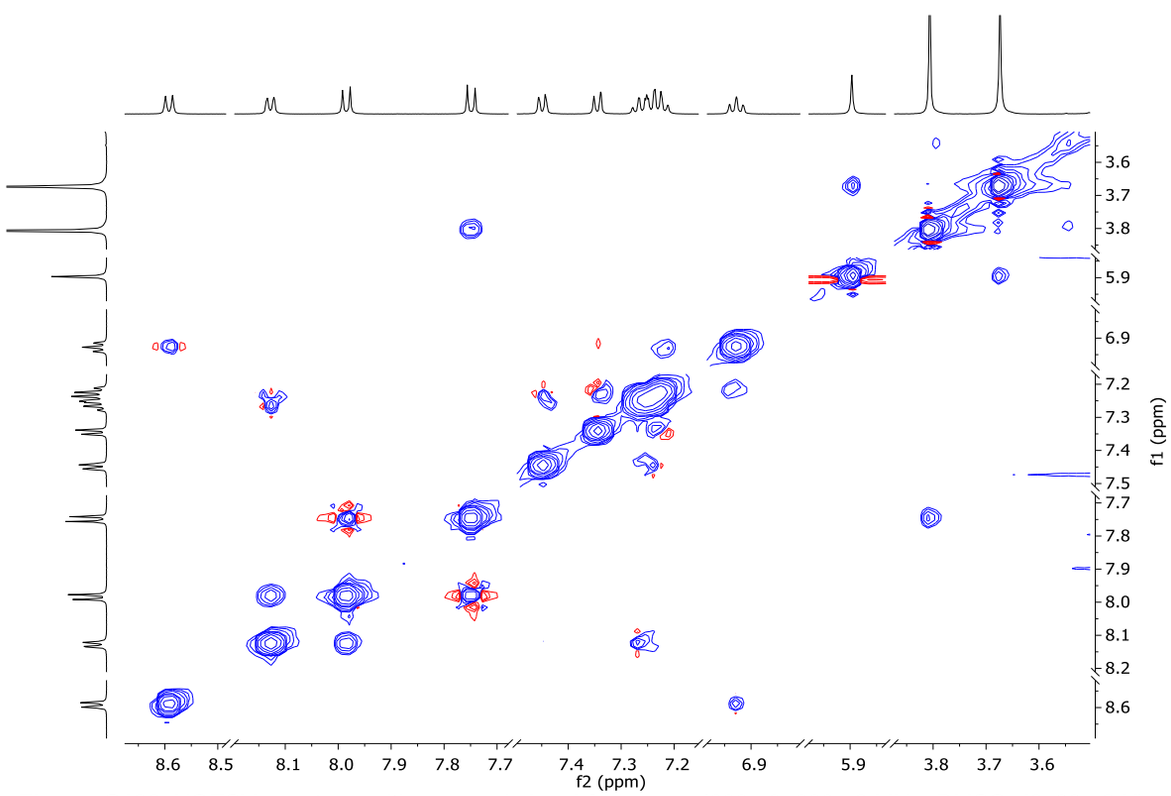

Figure. S126. NOESY-spectrum with removed signal-free areas (600.50, 600.50 MHz, DMSO-d6, 297.2 K).

9.21 Trivialine C (**49**)

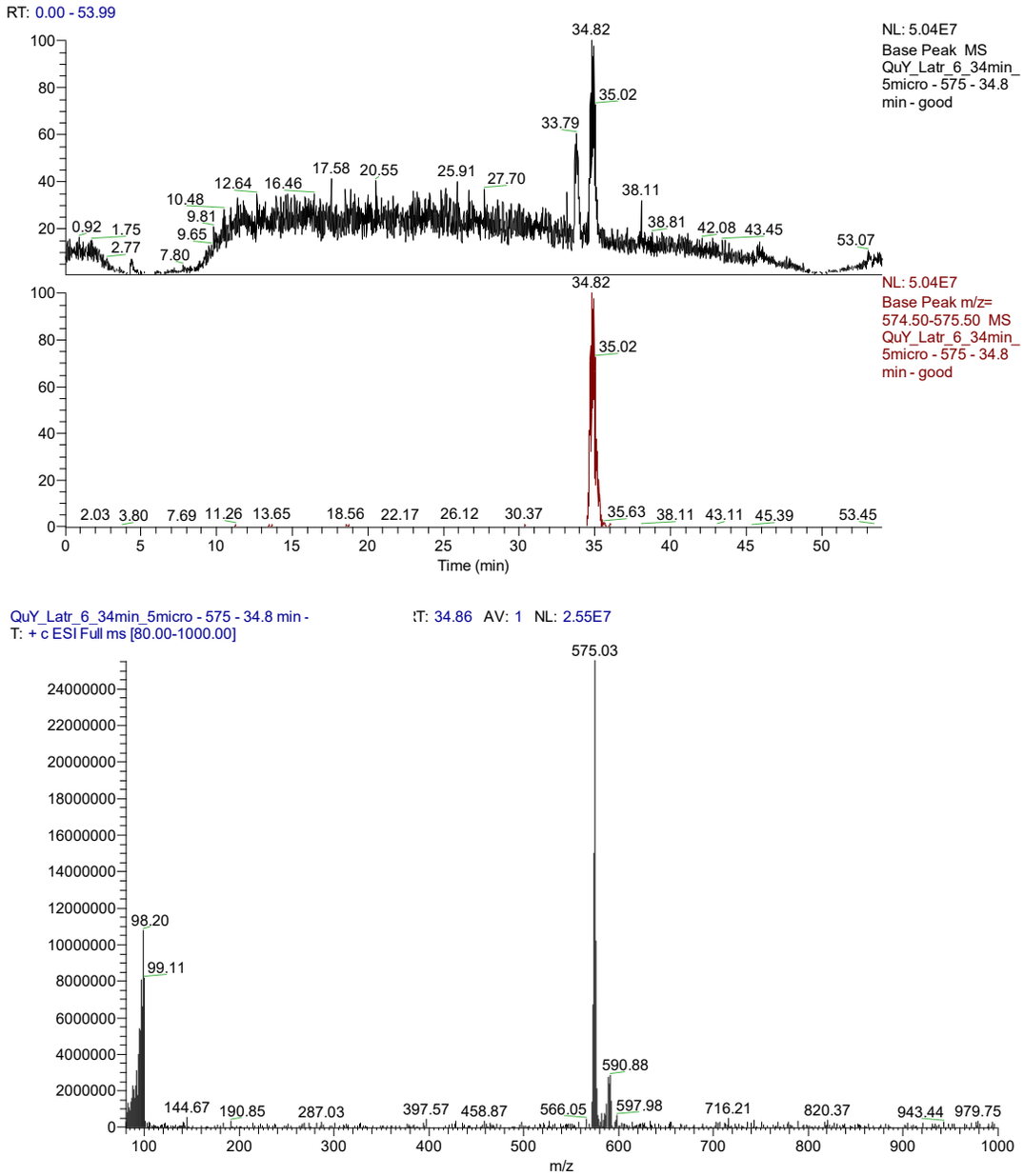

Figure. S127. (Up): LCESI-(+)-MS and excluded ion of 575 chromatograms, from up to down. (Down): Molecular mass of $[M+H]^+$ at *m/z* 575.03 at the R_t of 34.82 min. Gradient is in section 6.3.4.3.

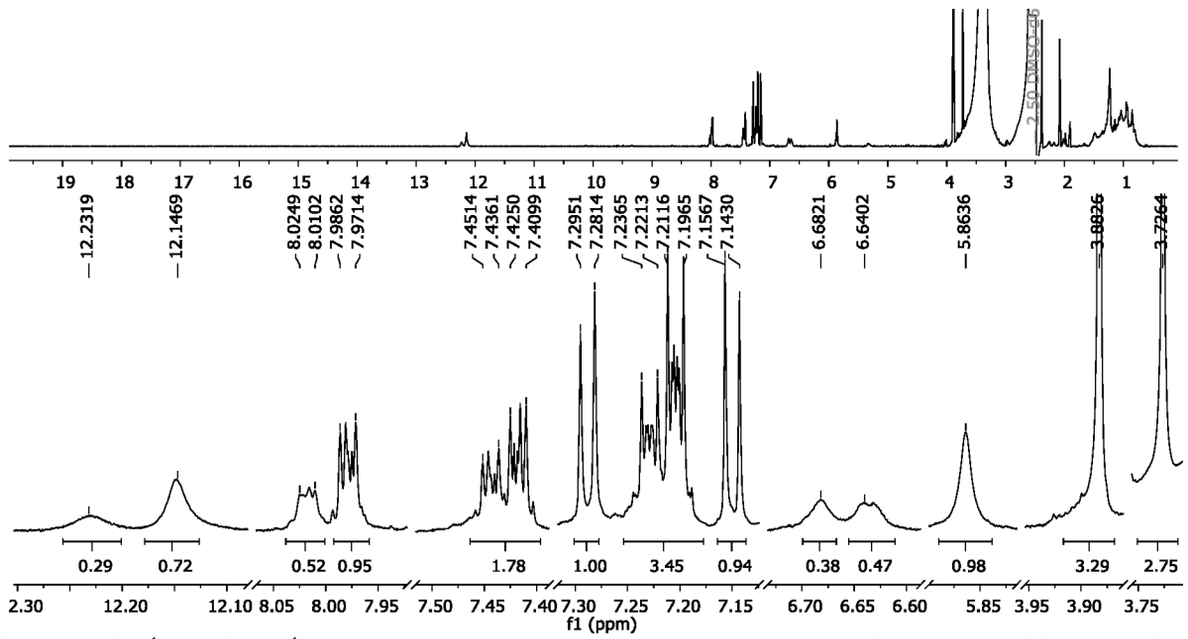

Figure. S128. ^{1}H-NMR and ^{1}H-NMR-spectrums with removed signal-free areas (600.51 MHz, DMSO-d6, 297.2 K).

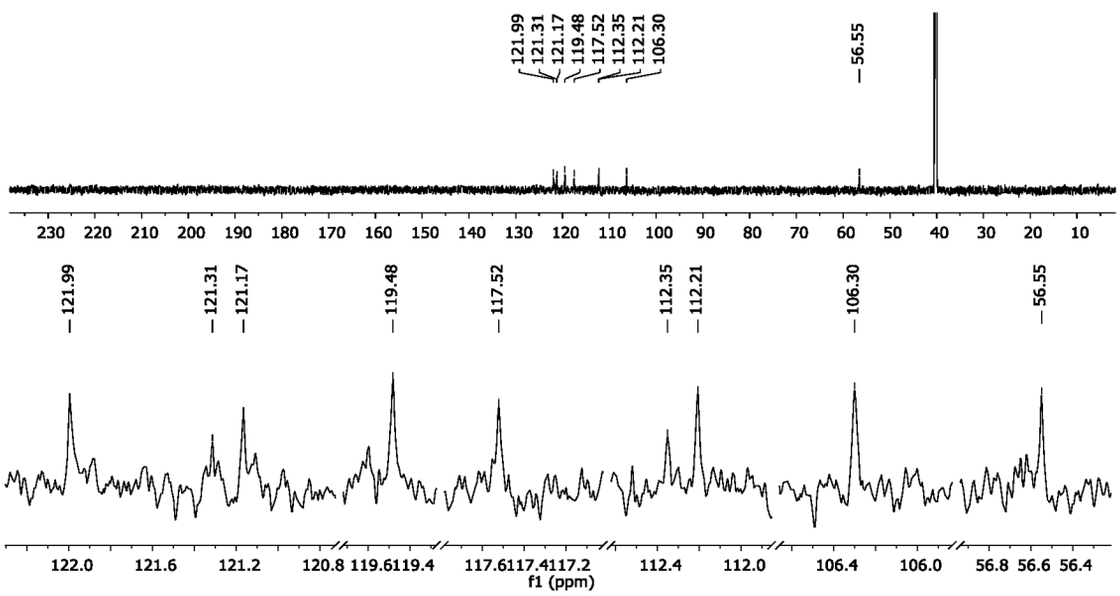

Figure. S129. DEPT135-spectrum (151.01 MHz, DMSO-d6, 297.1 K).

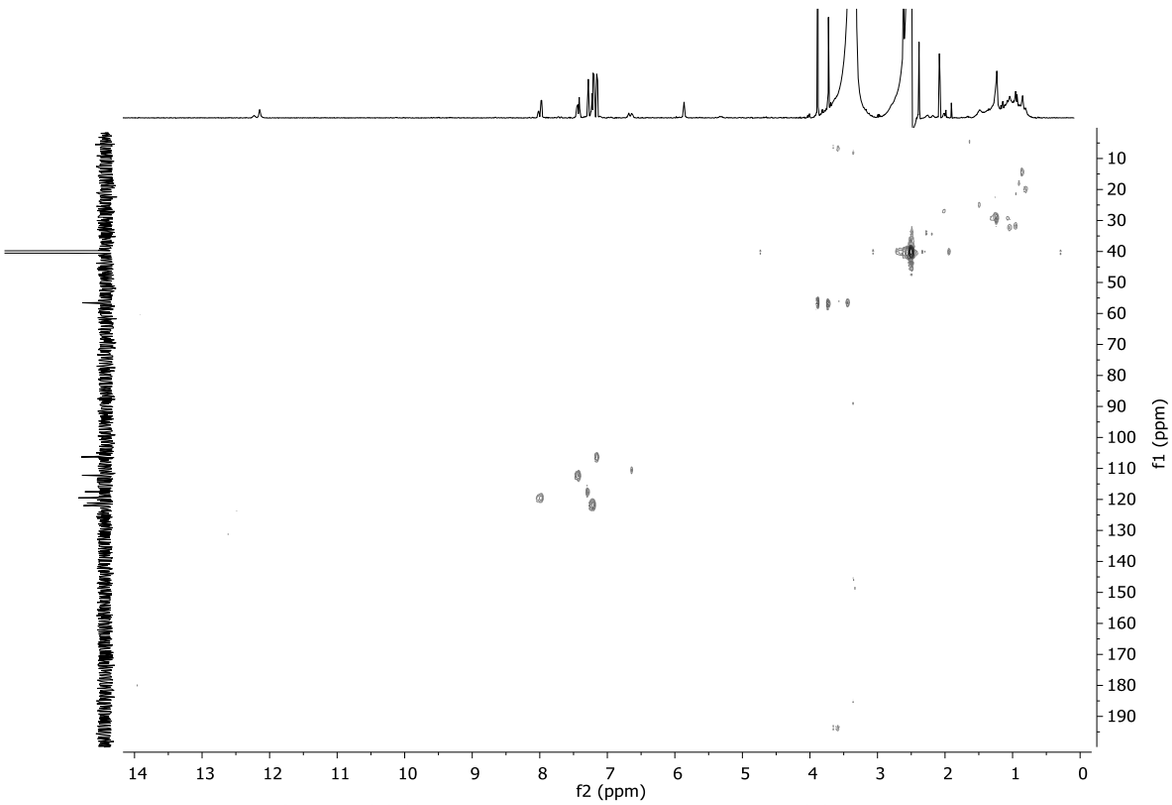

Figure. S130. HSQC-spectrum (600.50, 151.01 MHz, DMSO-d6, 297.1 K).

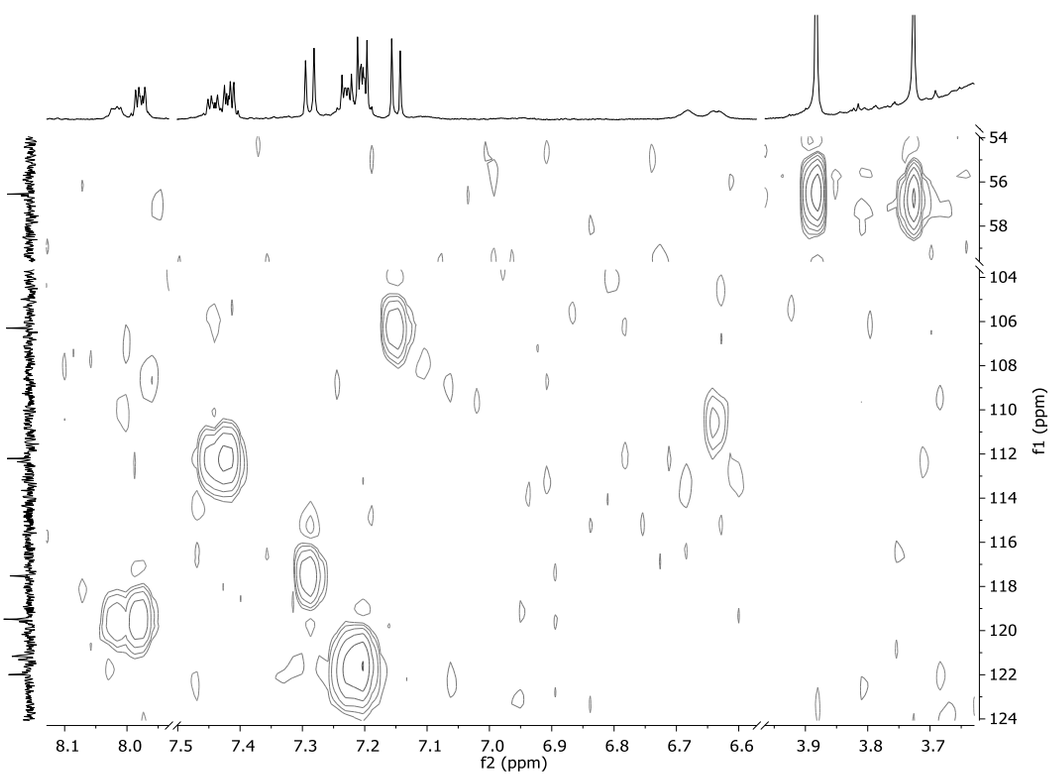

Figure. S131. HSQC-spectrum with removed signal-free areas (600.50, 151.01 MHz, DMSO-d6, 297.1 K).

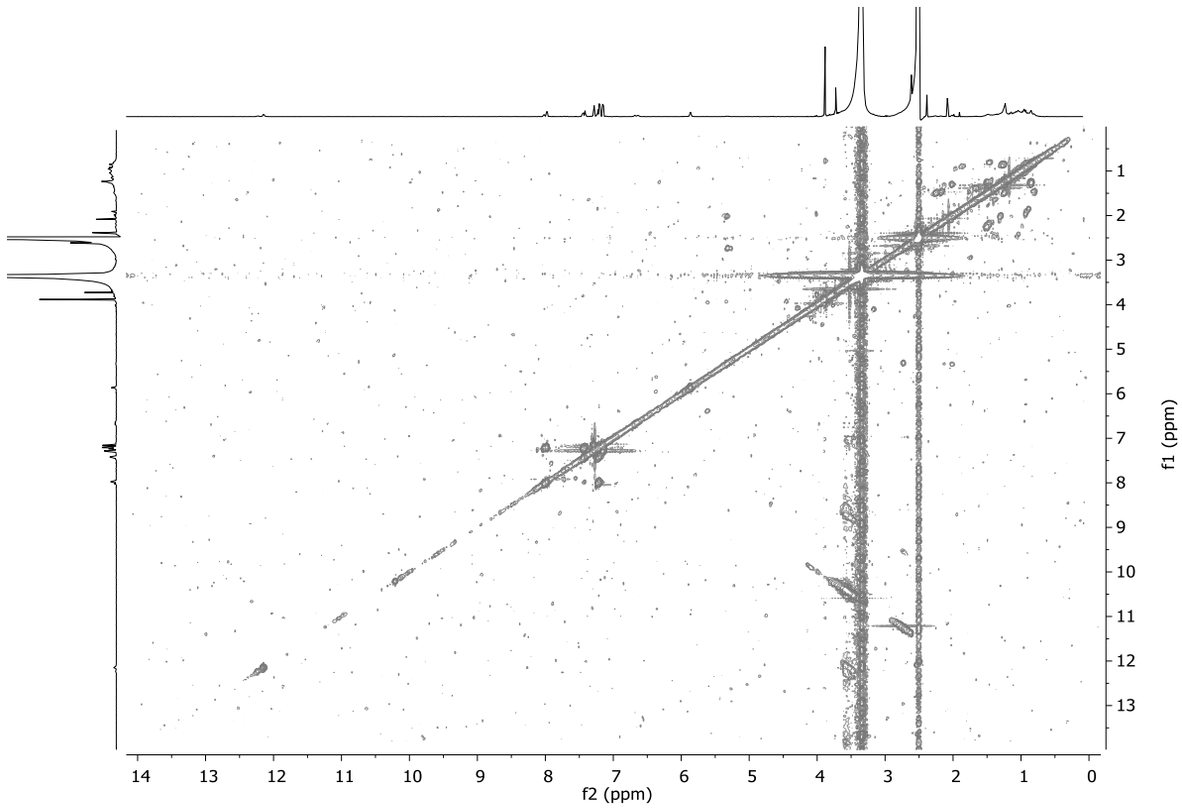

Figure. S132. COSY-spectrum (600.50, 600.50 MHz, DMSO-d6, 297.1 K).

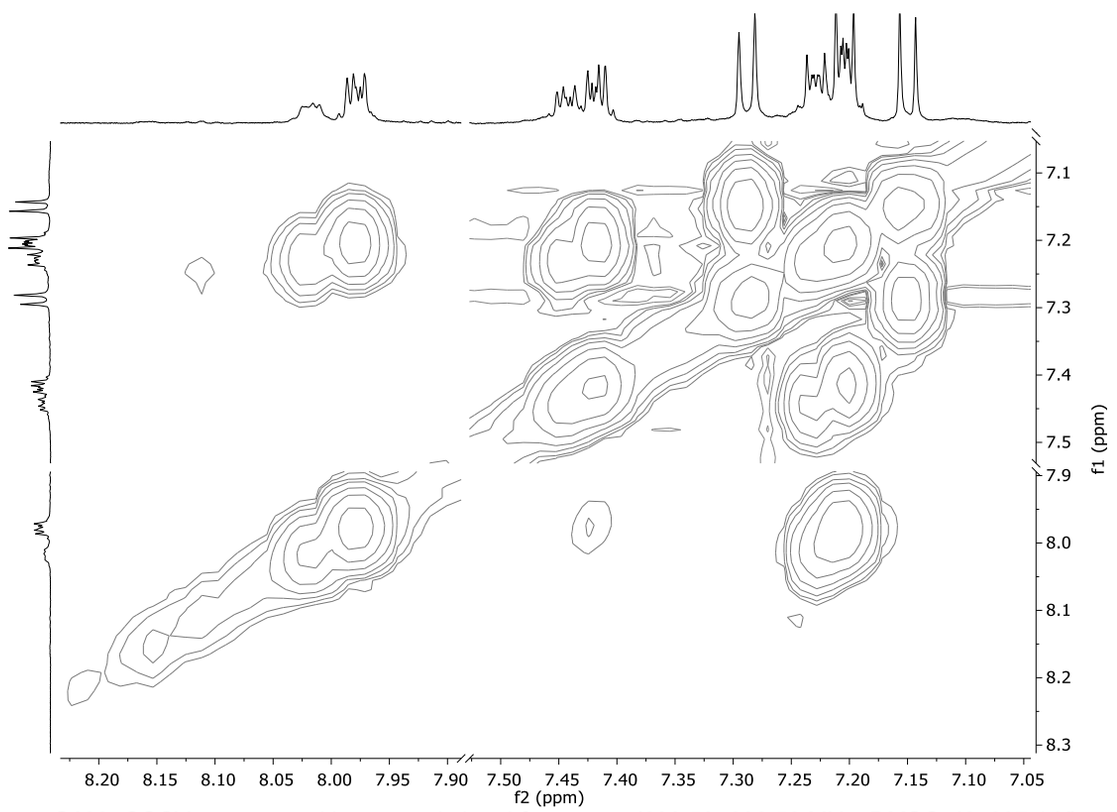

Figure. S133. COSY-spectrum with removed signal-free areas (600.50, 600.50 MHz, DMSO-d6, 297.1 K).

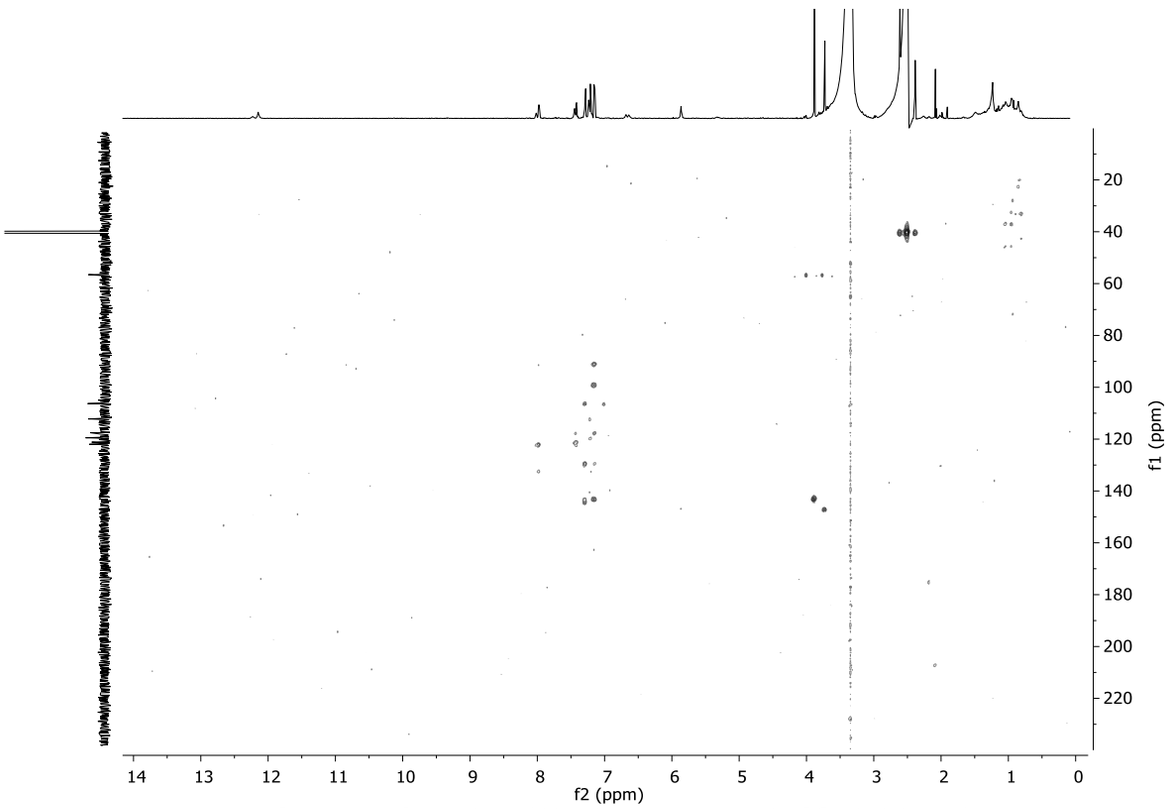

Figure. S134. HMBC-spectrum (600.50, 151.01 MHz, DMSO-d6, 297.2 K).

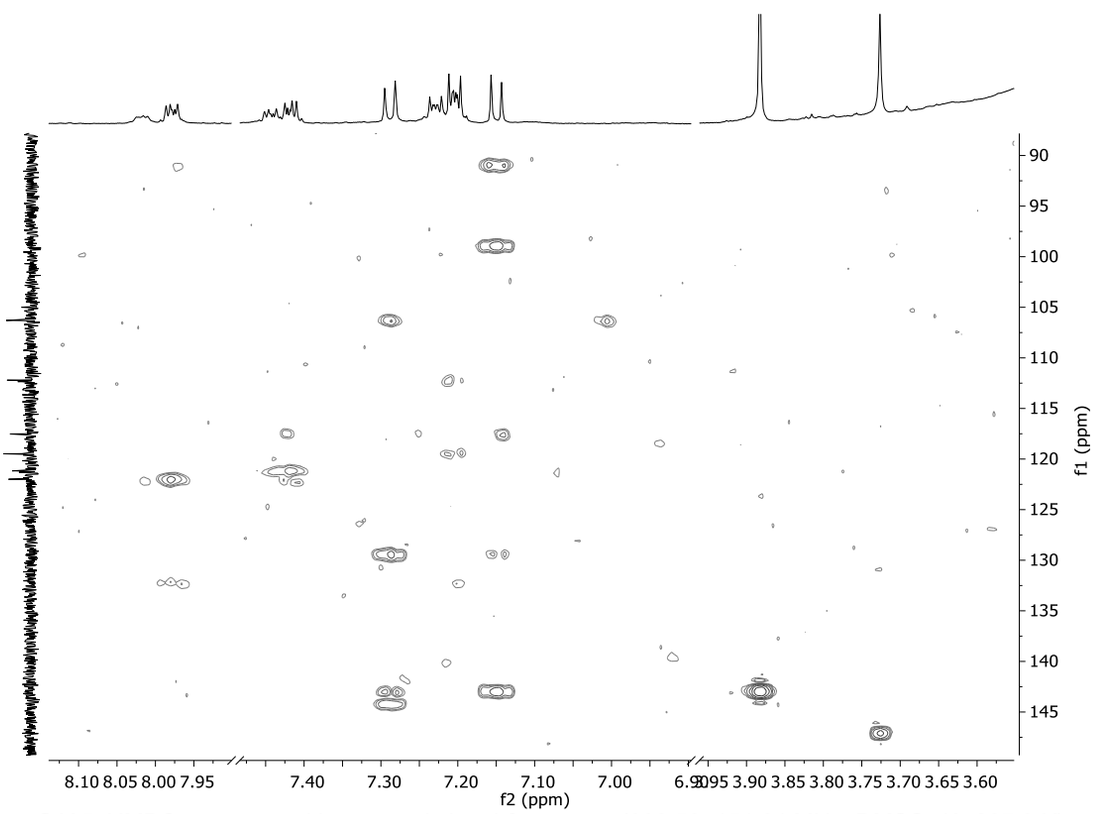

Figure. S135. HMBC-spectrum with removed signal-free areas (600.50, 151.01 MHz, DMSO-d6, 297.2 K).

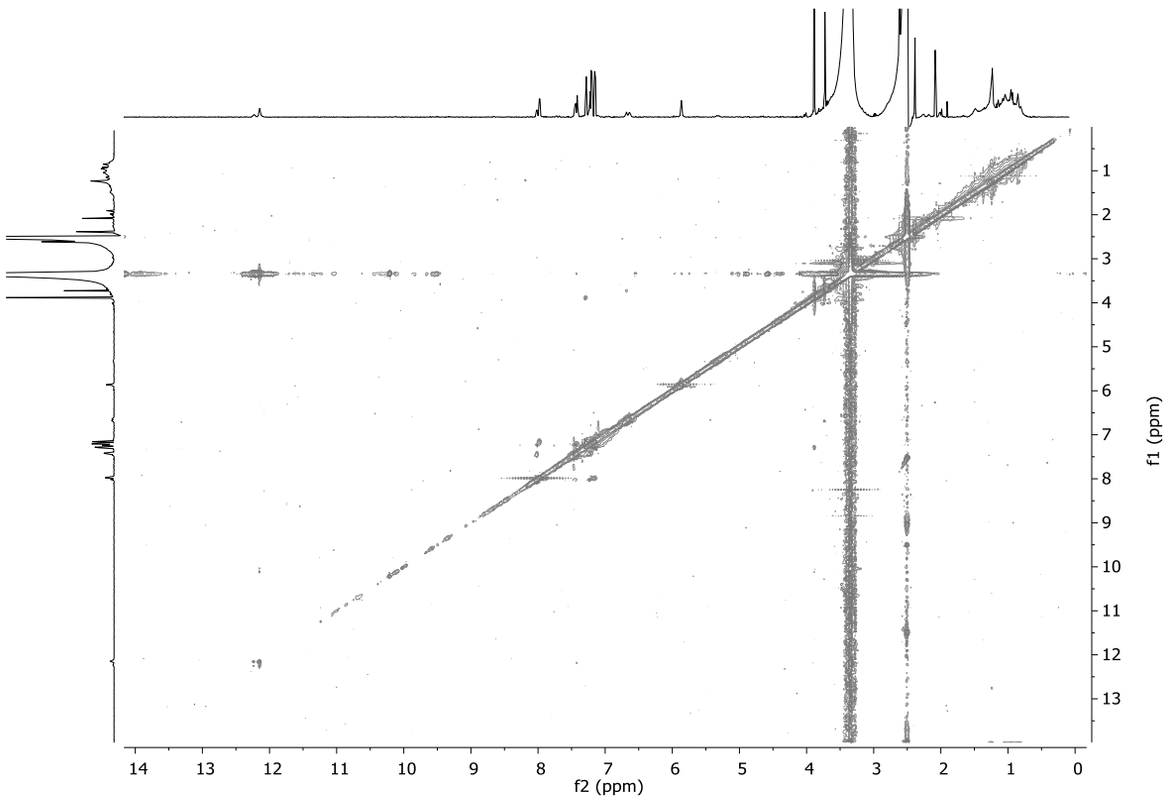

Figure. S136. NOESY-spectrum (600.50, 600.50 MHz, DMSO-d6, 297.1 K).

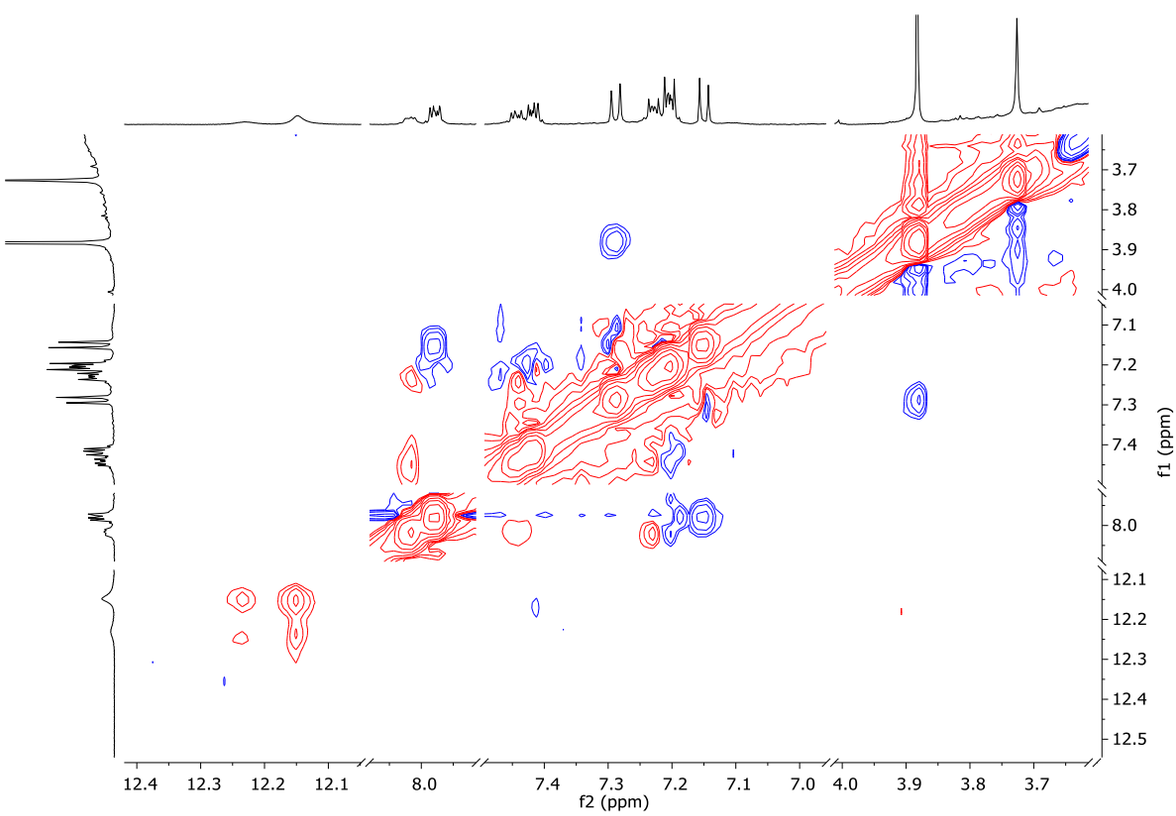

Figure. S137. NOESY-spectrum with removed signal-free areas (600.50, 600.50 MHz, DMSO-d6, 297.1 K).

9.22 Trivialine D (**50**)

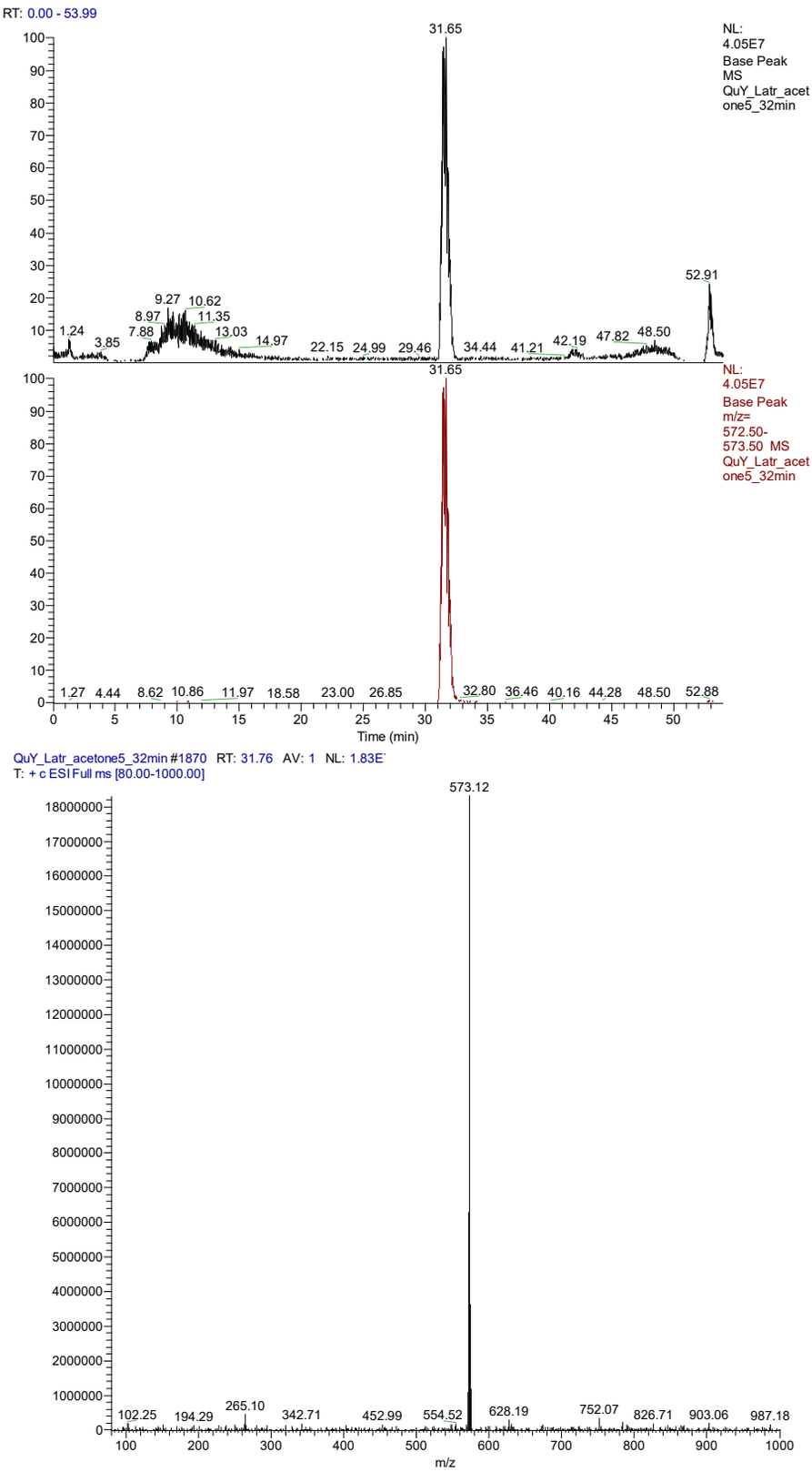

Figure. S138. (Up): LCESI-(+)-MS and excluded ion of 573 chromatograms, from up to down. (Down): Molecular mass of $[M+H]^+$ at *m/z* 573.12 at the R_t of 31.65 min. Gradient is in section 6.3.4.3.

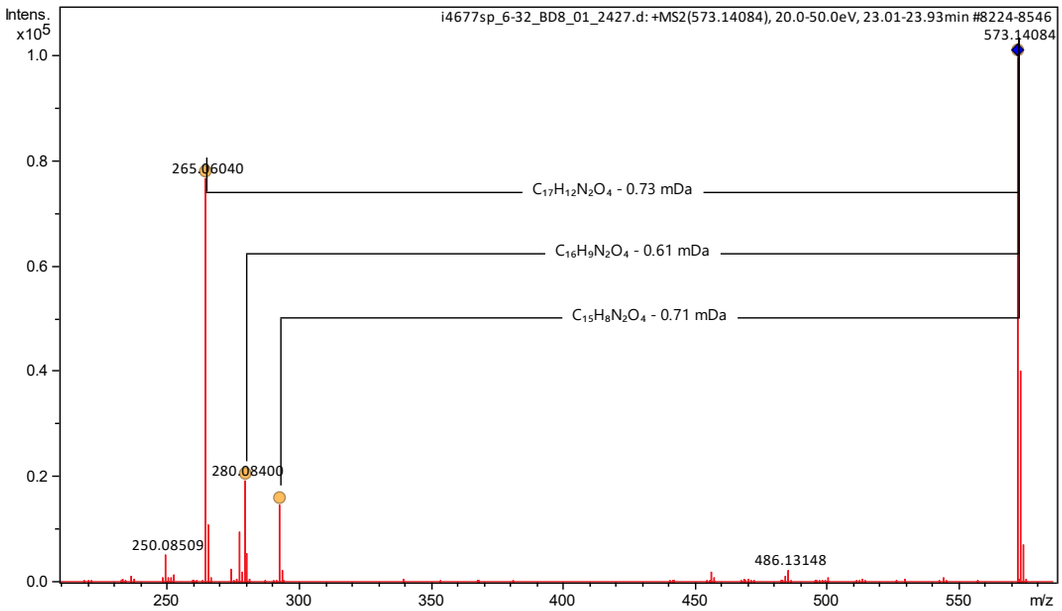

Figure. S139. HR-ESI-(+)-MS/MS-spectrum.

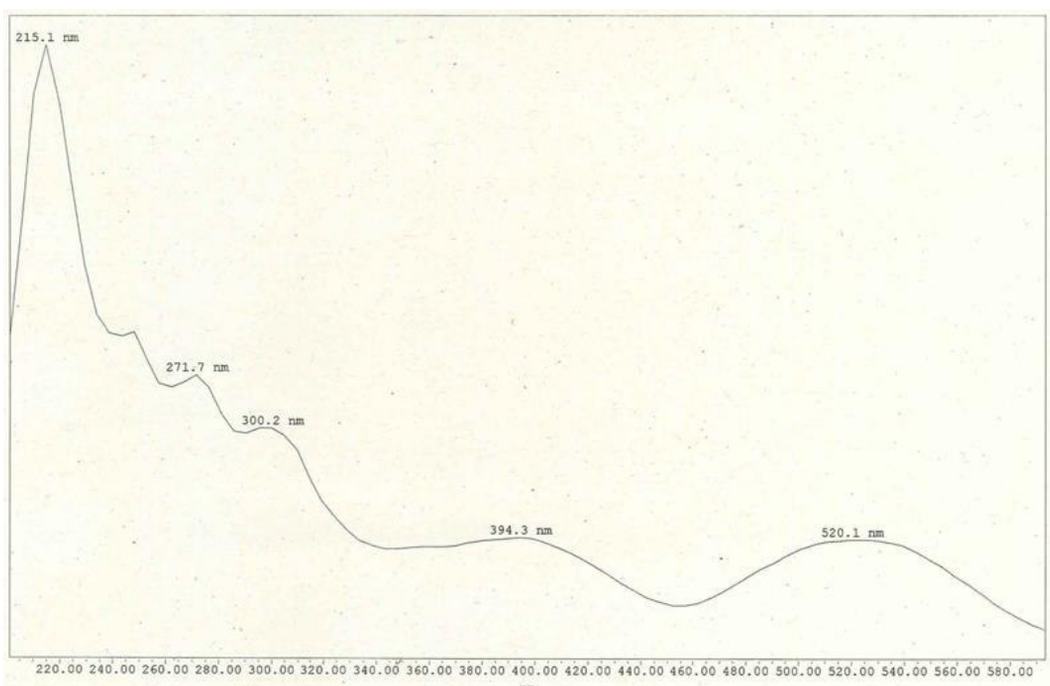

Figure. S140. UV/Vis-Spectrum. The spectrum was recorded from the semi-preparative HPLC, section 6.3.4.3.

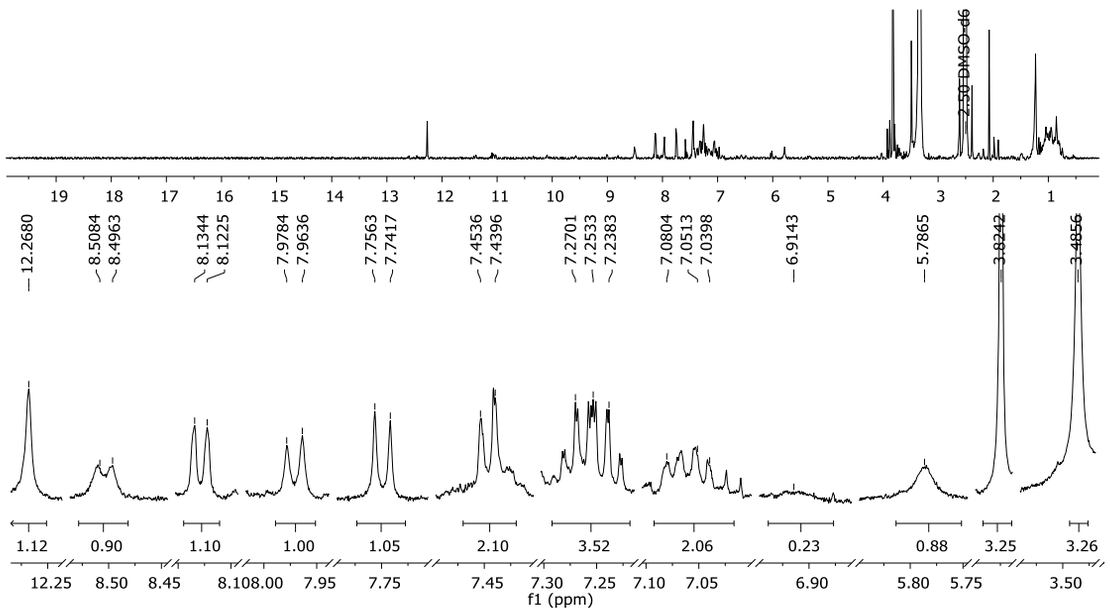

Figure. S141. [1]H-NMR and [1]H-NMR-spectrums with removed signal-free areas (600.51 MHz, DMSO-d6, 297.1 K).

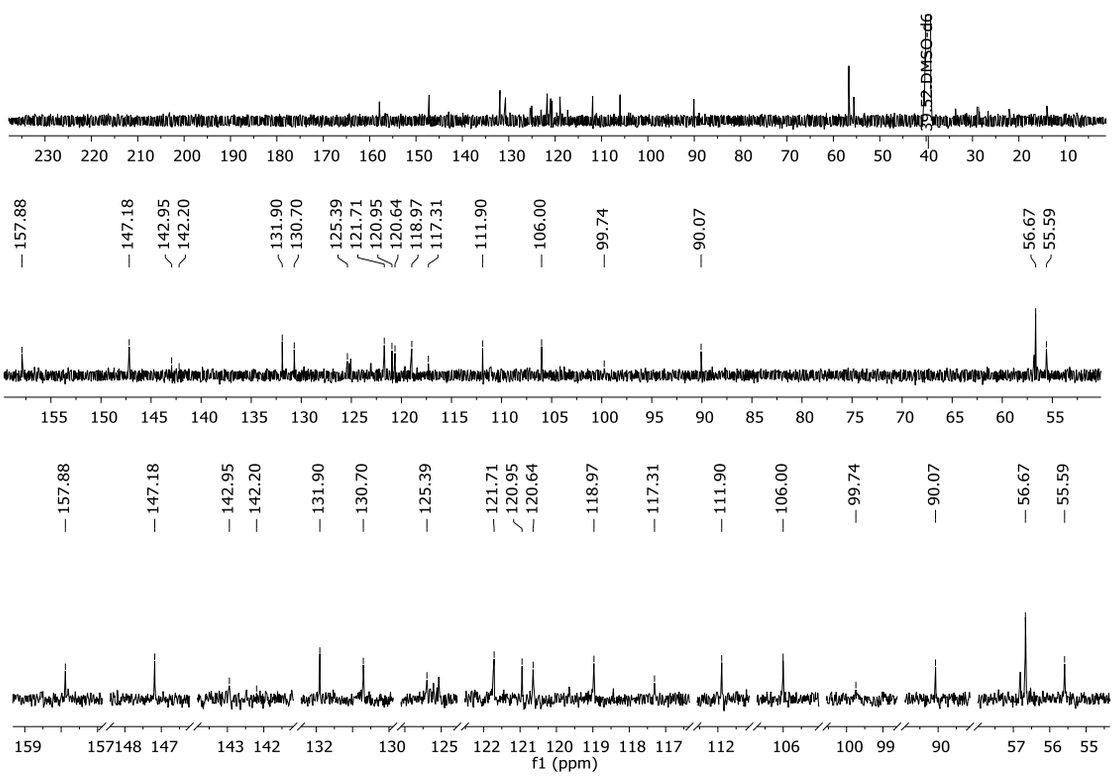

Figure. S142. [13]C-NMR, DEPT135 and [13]C-NMR-spectrums with removed signal-free areas (150.94 MHz, DMSO-d6, 297.2 K).

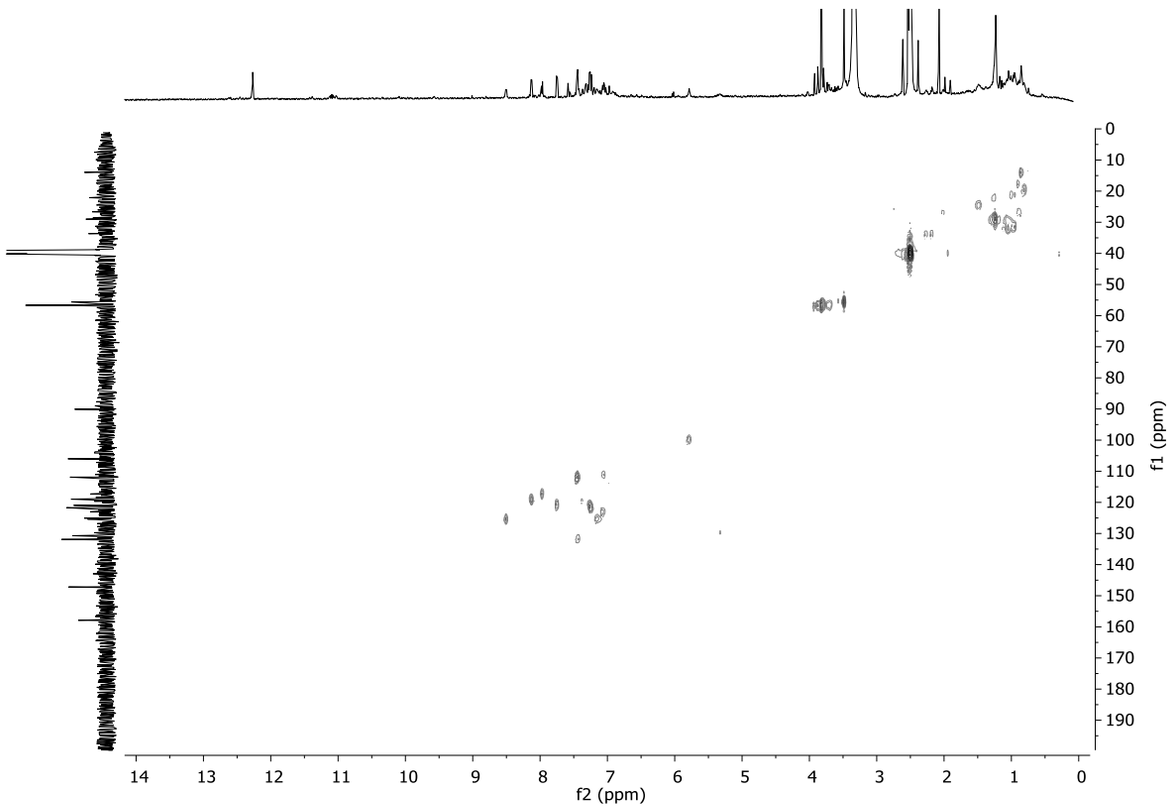

Figure. S143. HSQC-spectrum (600.50, 151.01 MHz, DMSO-d6, 297.2 K).

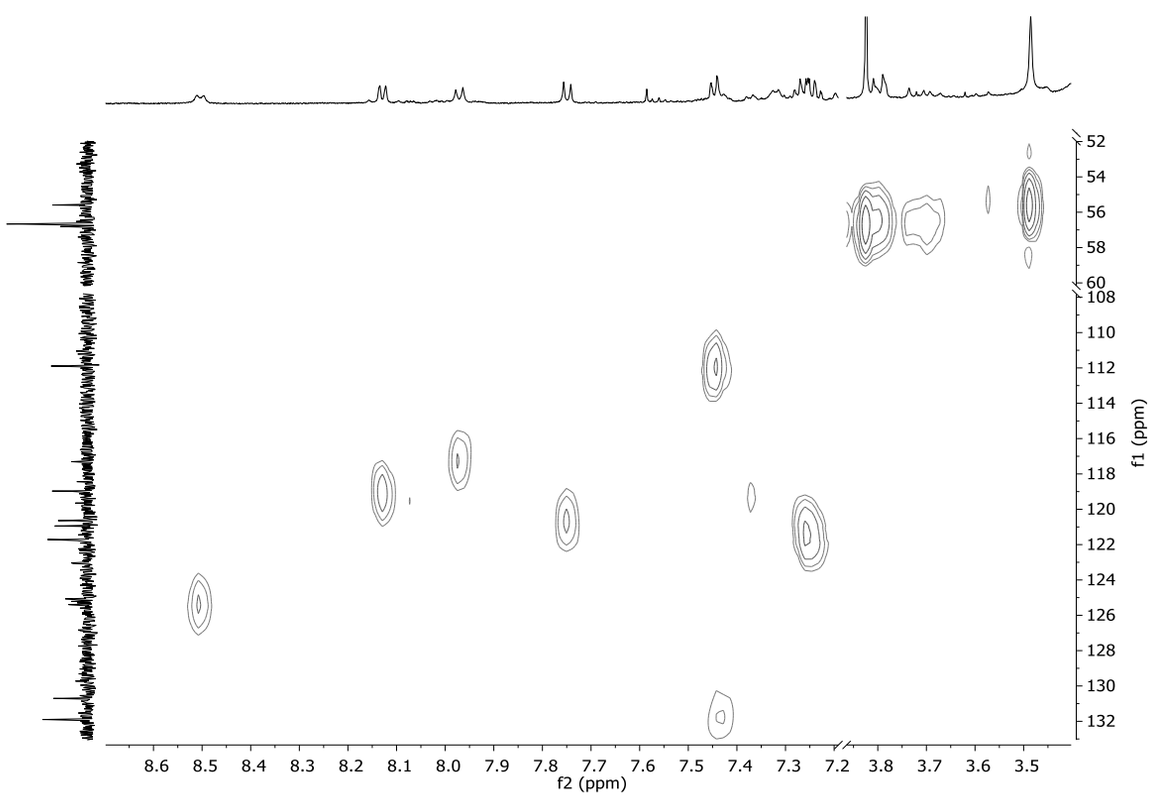

Figure. S144. HSQC-spectrum with removed signal-free areas (600.50, 151.01 MHz, DMSO-d6, 297.2 K).

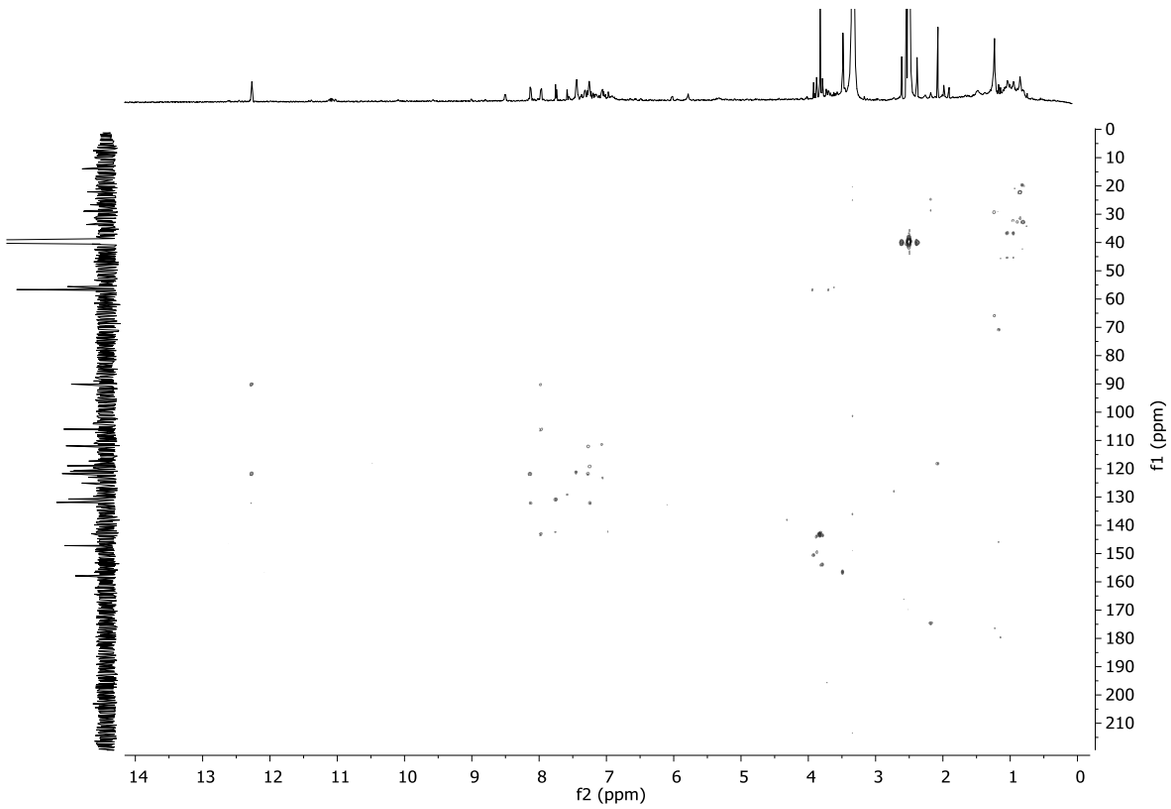

Figure. S145. HMBC-spectrum (600.50, 151.01 MHz, DMSO-d6, 297.2 K).

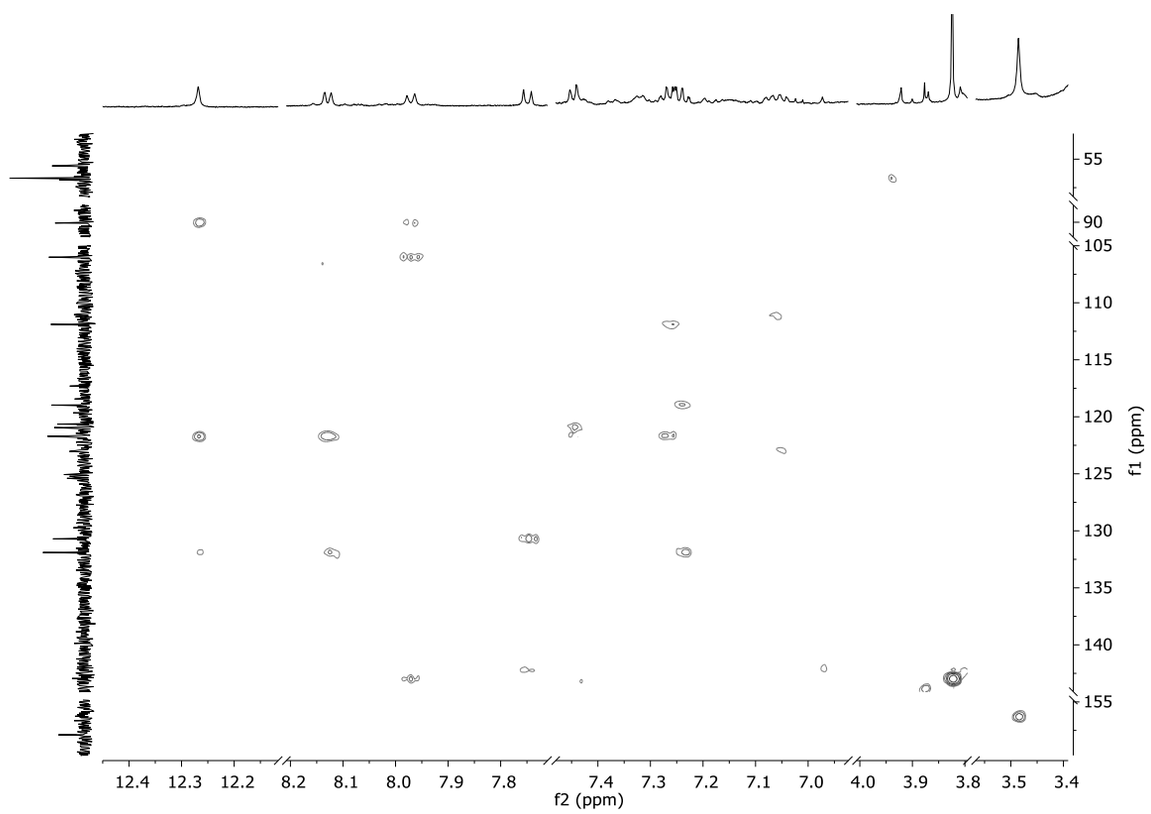

Figure. S146. HMBC-spectrum with removed signal-free areas (600.50, 151.01 MHz, DMSO-d6, 297.2 K).

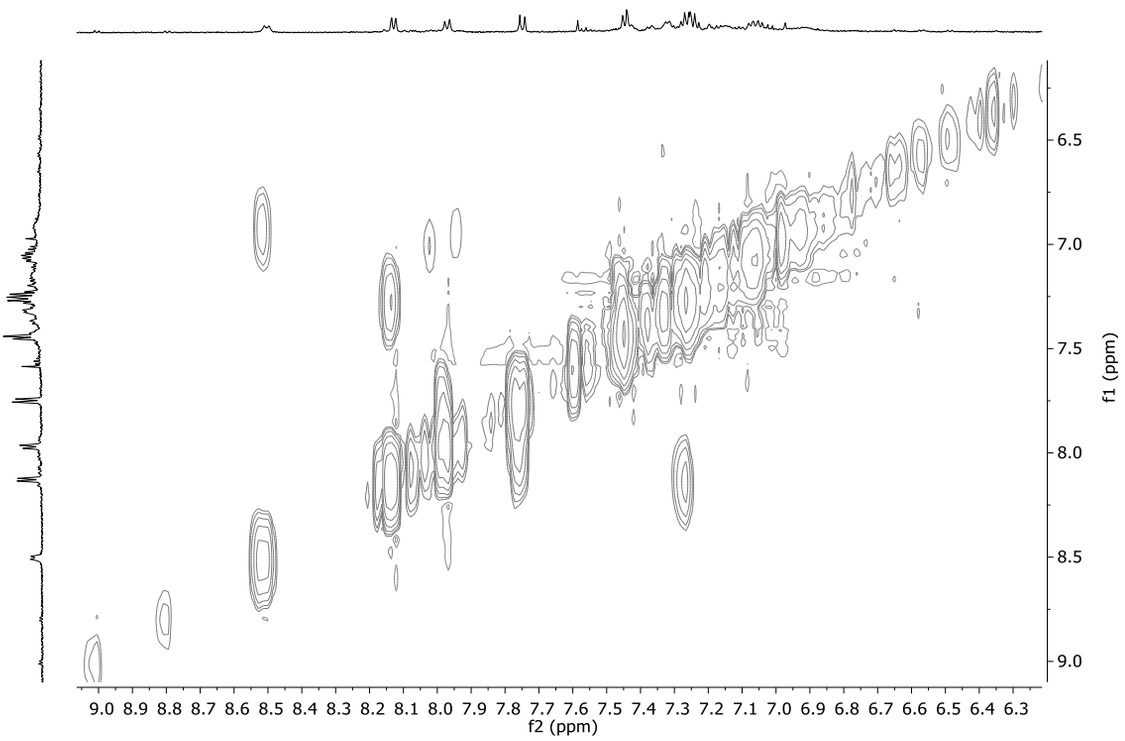

Figure. S147. Concentrated COSY-spectrum (600.50, 600.50 MHz, DMSO-d6, 297.1 K).

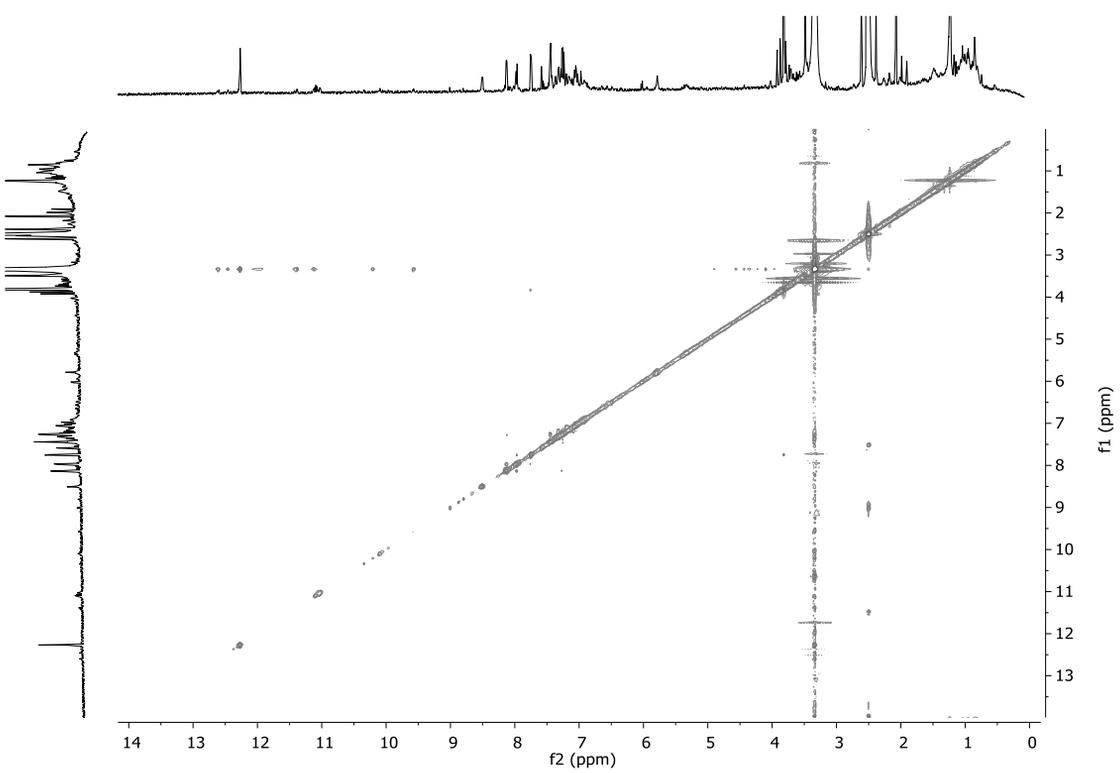

Figure. S148. NOESY-spectrum (600.50, 600.50 MHz, DMSO-d6, 297.2 K).

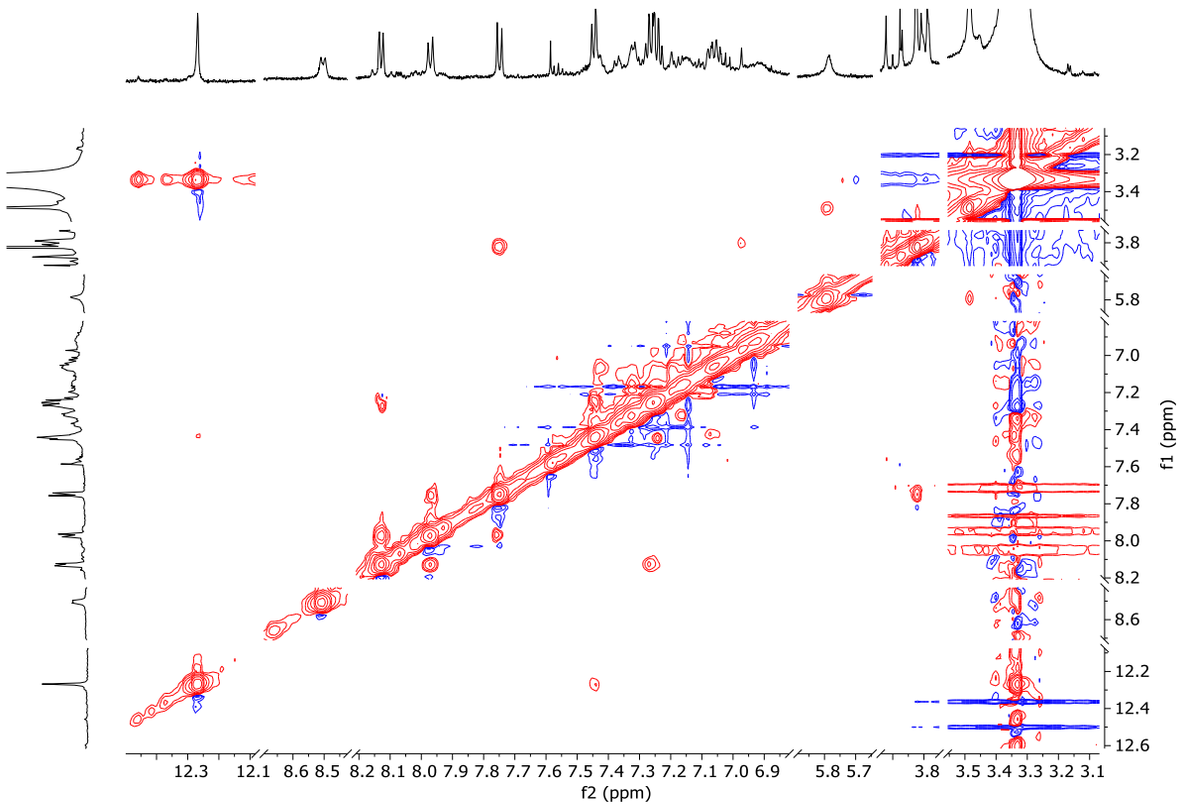

Figure. S149. NOESY-spectrum with removed signal-free areas (600.50, 600.50 MHz, DMSO-d6, 297.2 K).

9.23 Trivialine E (**51**)

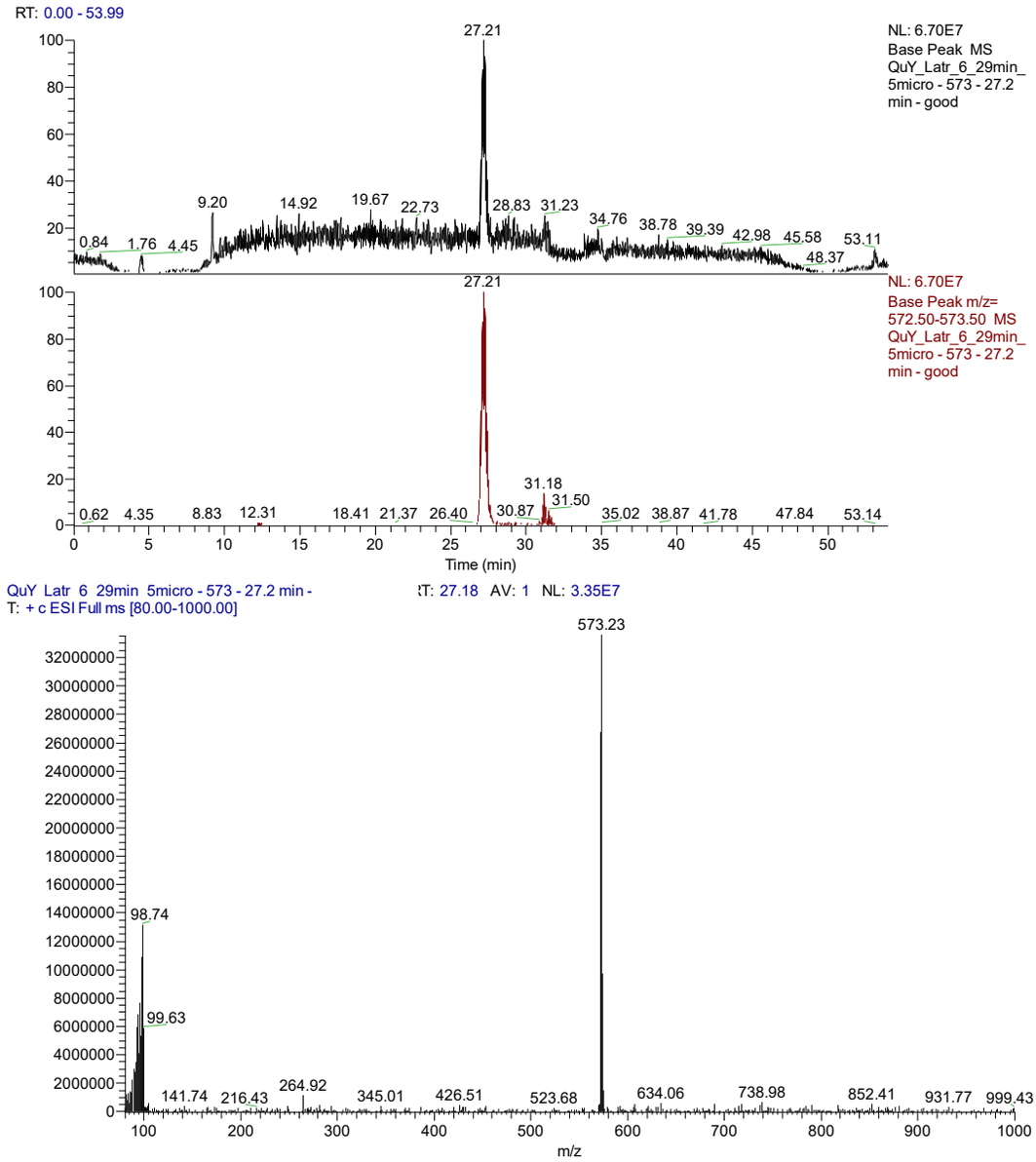

Figure. S150. (Up): LCESI-(+)-MS and excluded ion of 573 chromatograms, from up to down. (Down): Molecular mass of $[M+H]^+$ at *m/z* 573.23 at the R_t of 27.21 min. Gradient is in section 6.3.4.3.

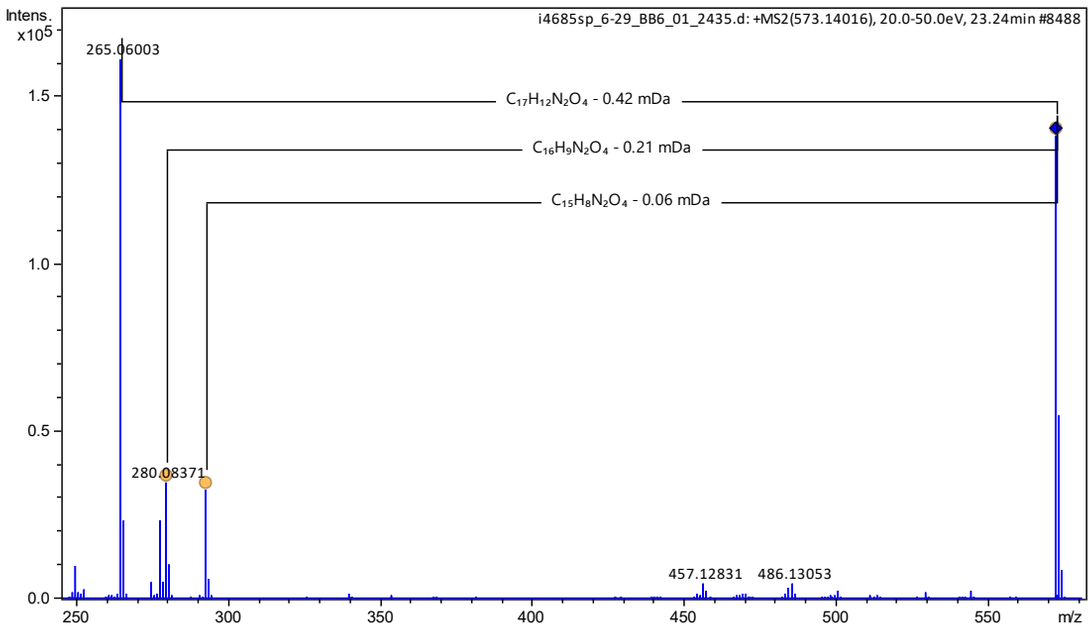

Figure. S151. HR-ESI-(+)-MS/MS-spectrum.

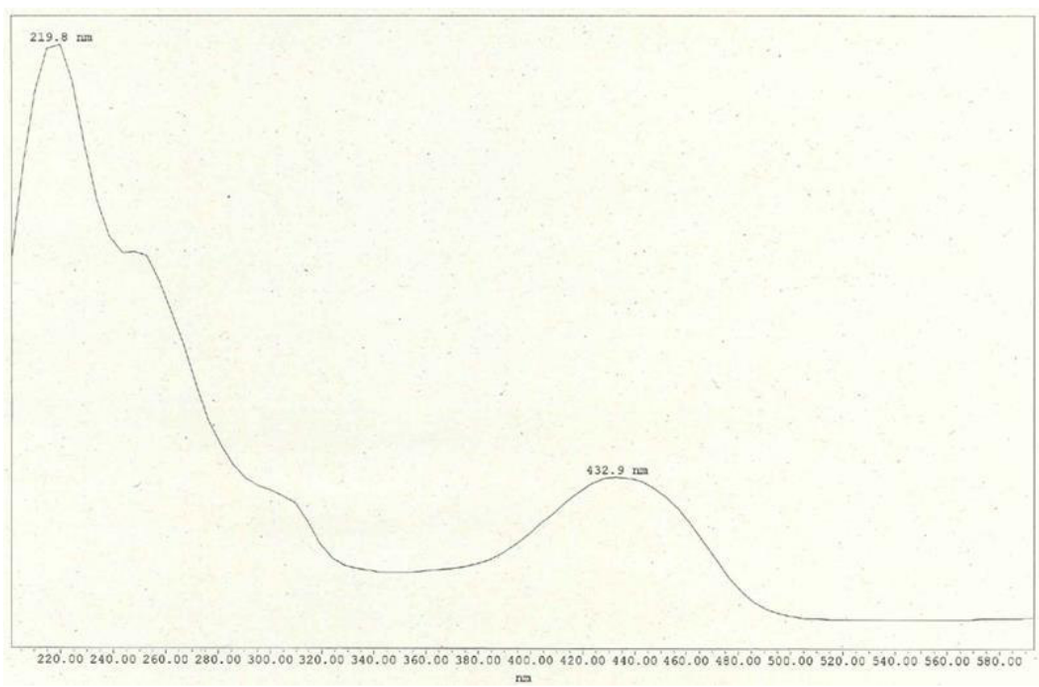

Figure. S152. UV/Vis-Spectrum. The spectrum was recorded from the semi-preparative HPLC, section 6.3.4.3.

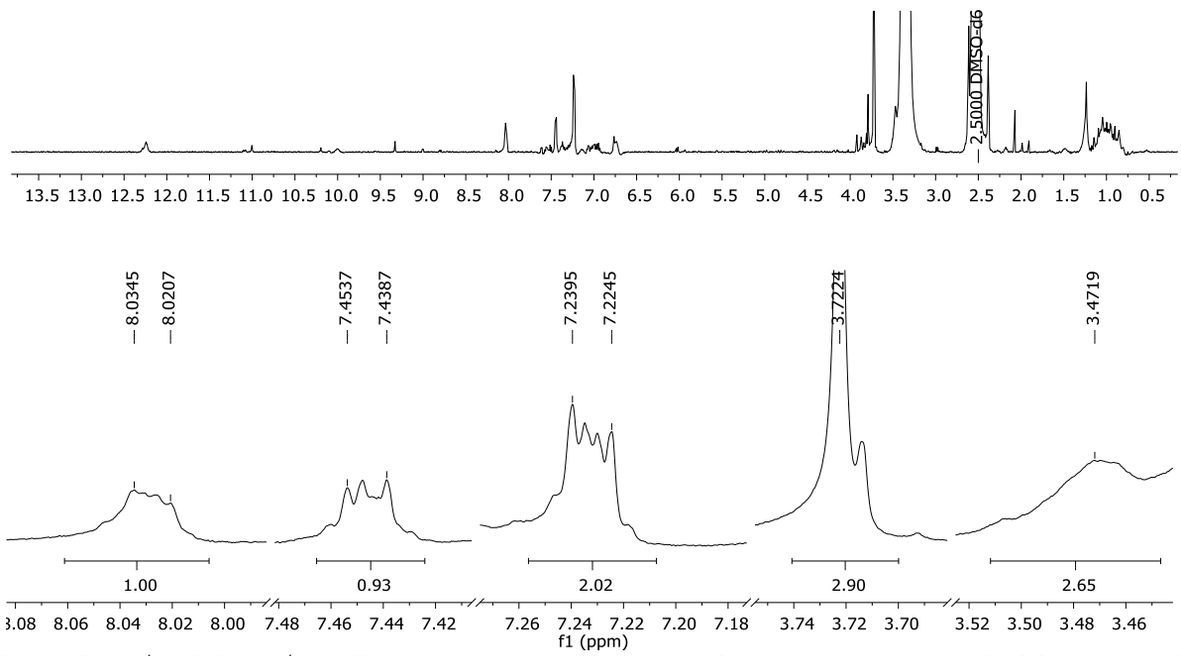

Figure. S153. [1]H-NMR and [1]H-NMR-spectrums with removed signal-free areas (600.22 MHz, DMSO-d6, 297.2 K).

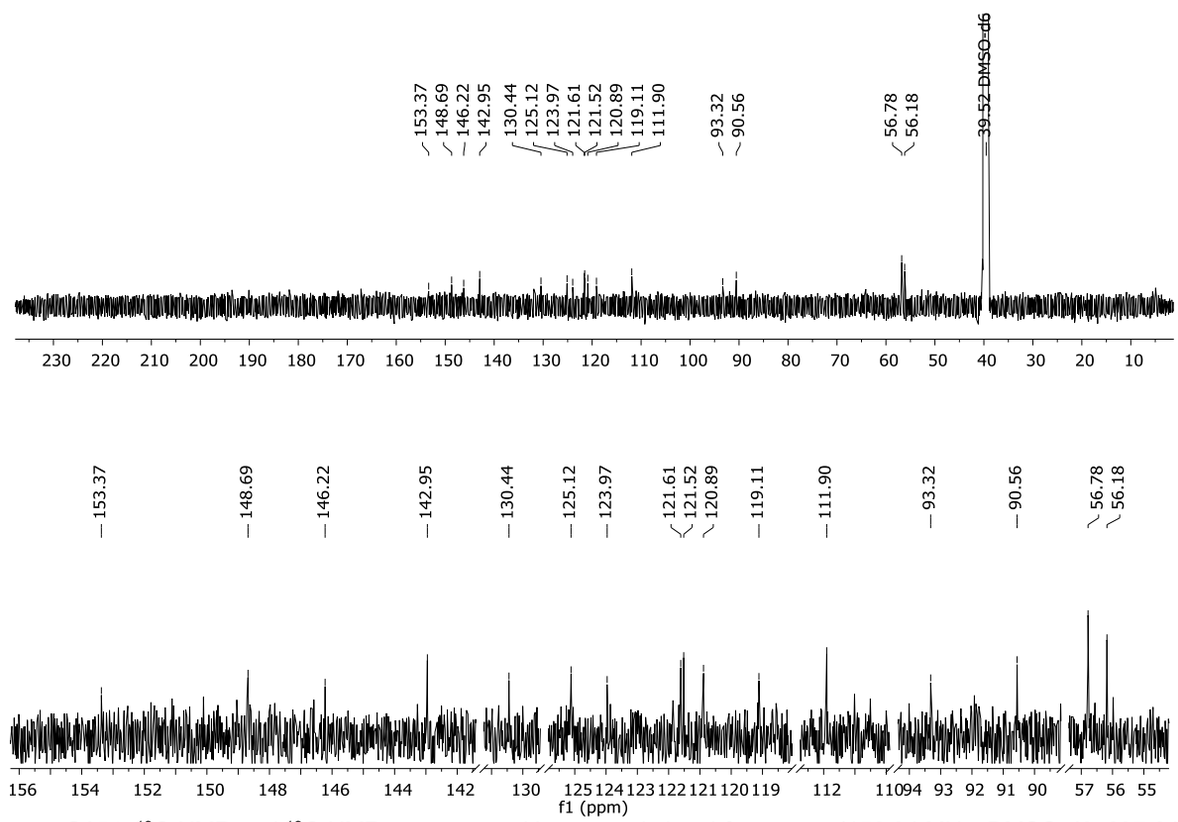

Figure. S154. [13]C-NMR and [13]C-NMR-spectrums with removed signal-free areas (150.94 MHz, DMSO-d6, 297.2 K).

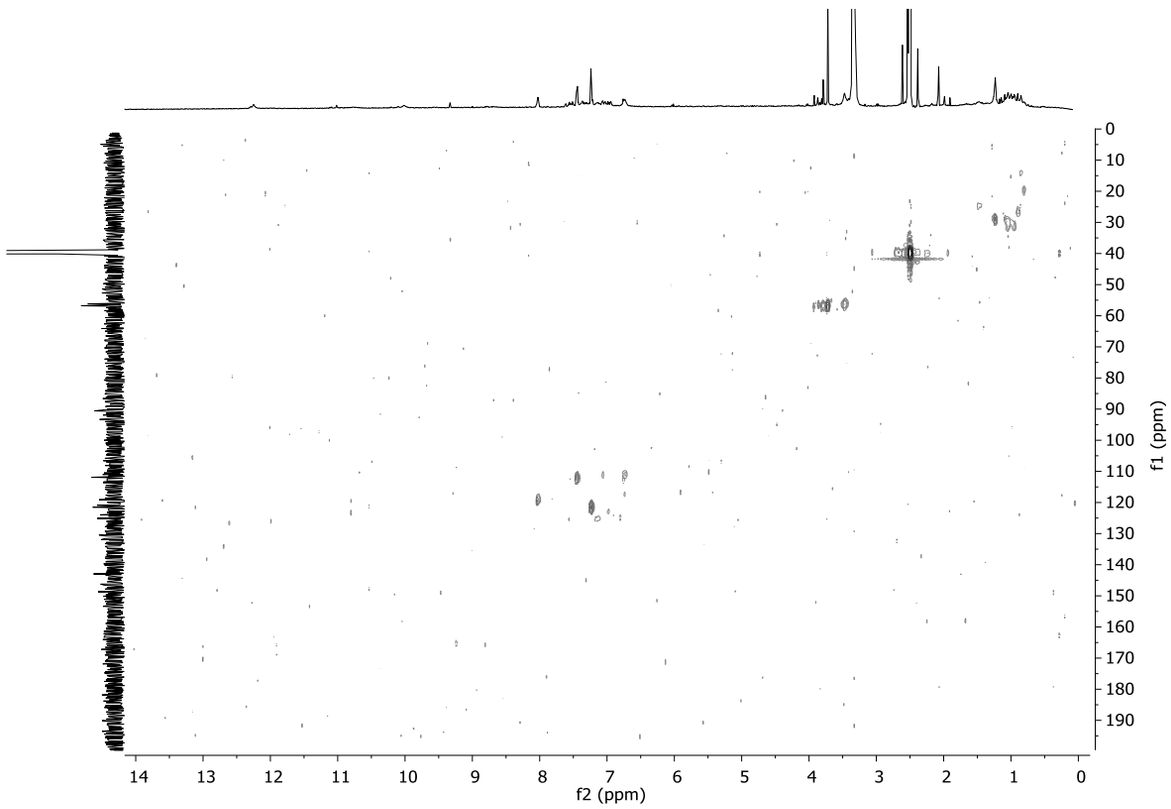

Figure. S155. HSQC-spectrum (600.50, 150.94 MHz, DMSO-d6, 297.1 K).

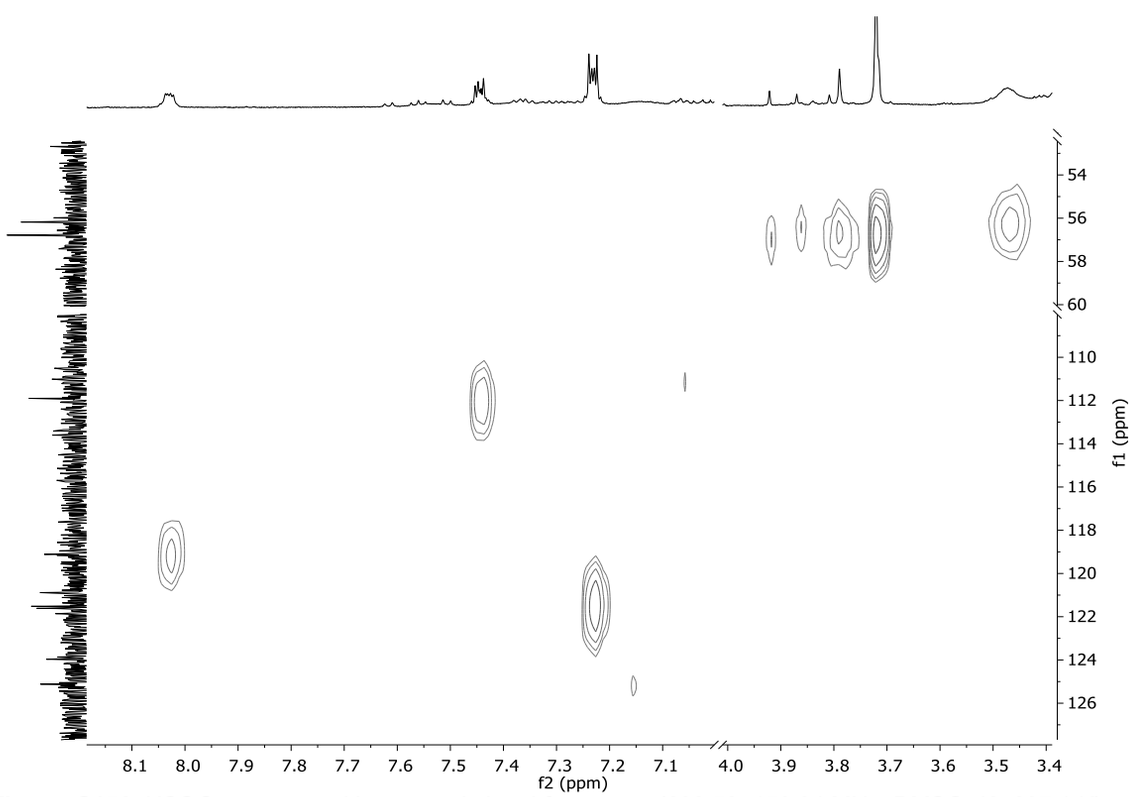

Figure. S156. HSQC-spectrum with removed signal-free areas (600.50, 150.94 MHz, DMSO-d6, 297.1 K).

9.24 N^5-isopentylglutamine (**54**)

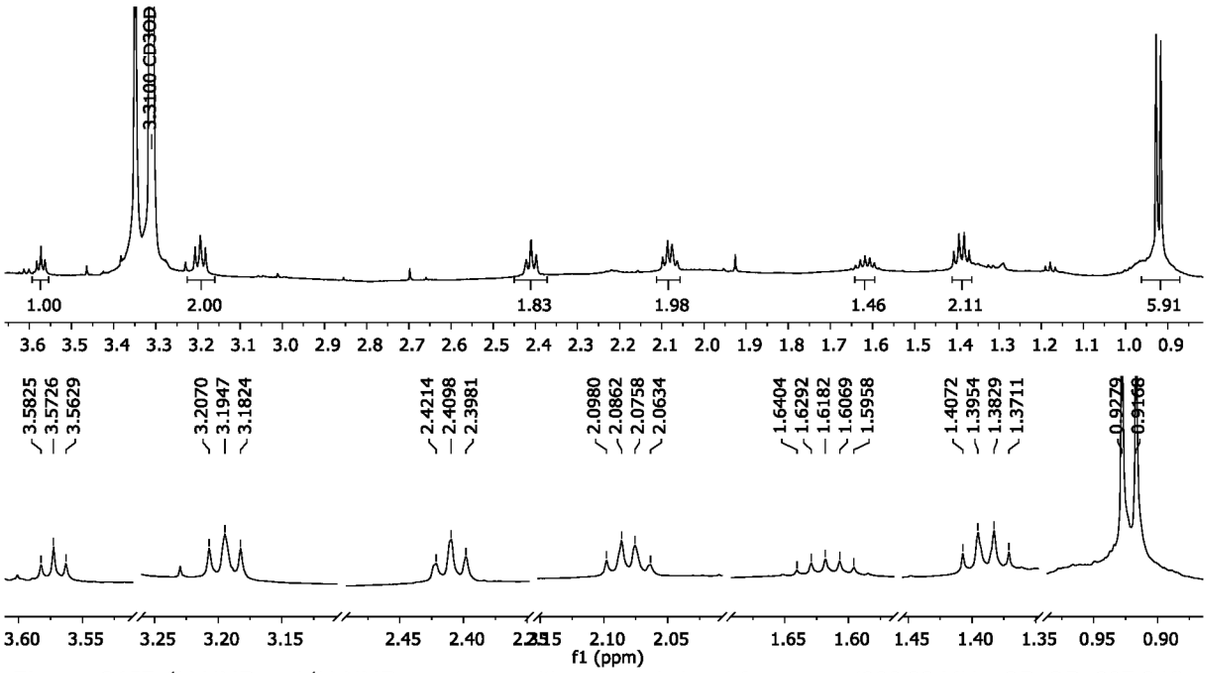

Figure. S157. ^{1}H-NMR and ^{1}H-NMR-spectrums with removed signal-free areas (600.22 MHz, CD_3OD, 297.2 K).

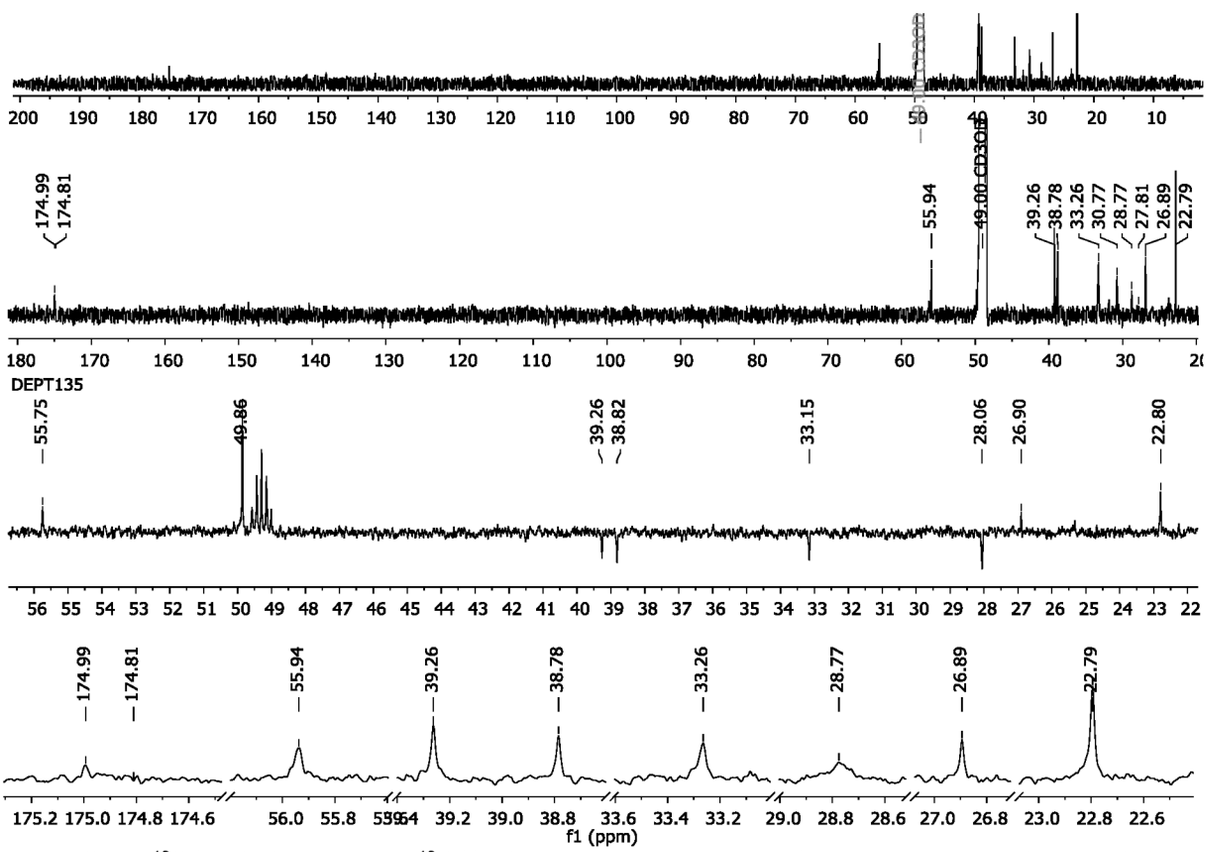

Figure. S158. ^{13}C-NMR, DEPT135 and ^{13}C-NMR-spectrums with removed signal-free areas (151.01 MHz, CD_3OD, 297.1 K).

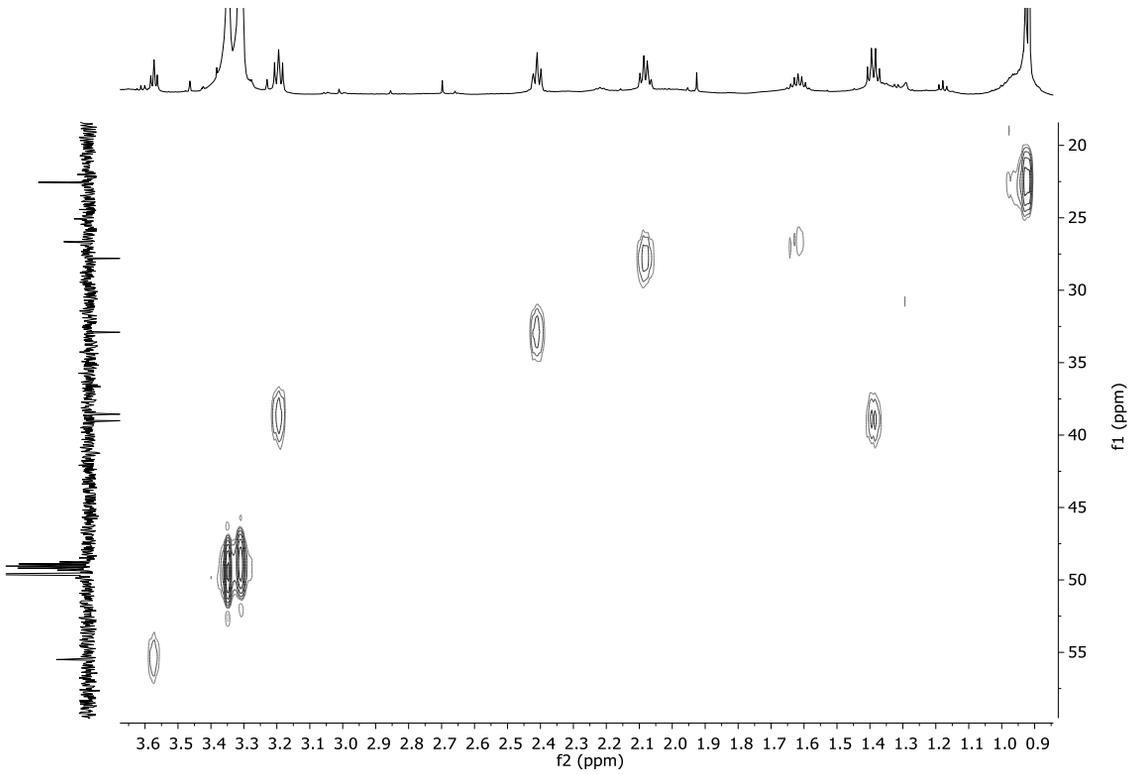

Figure. S159. HSQC-spectrum (600.50, 151.01 MHz, CD_3OD, 297.2 K).

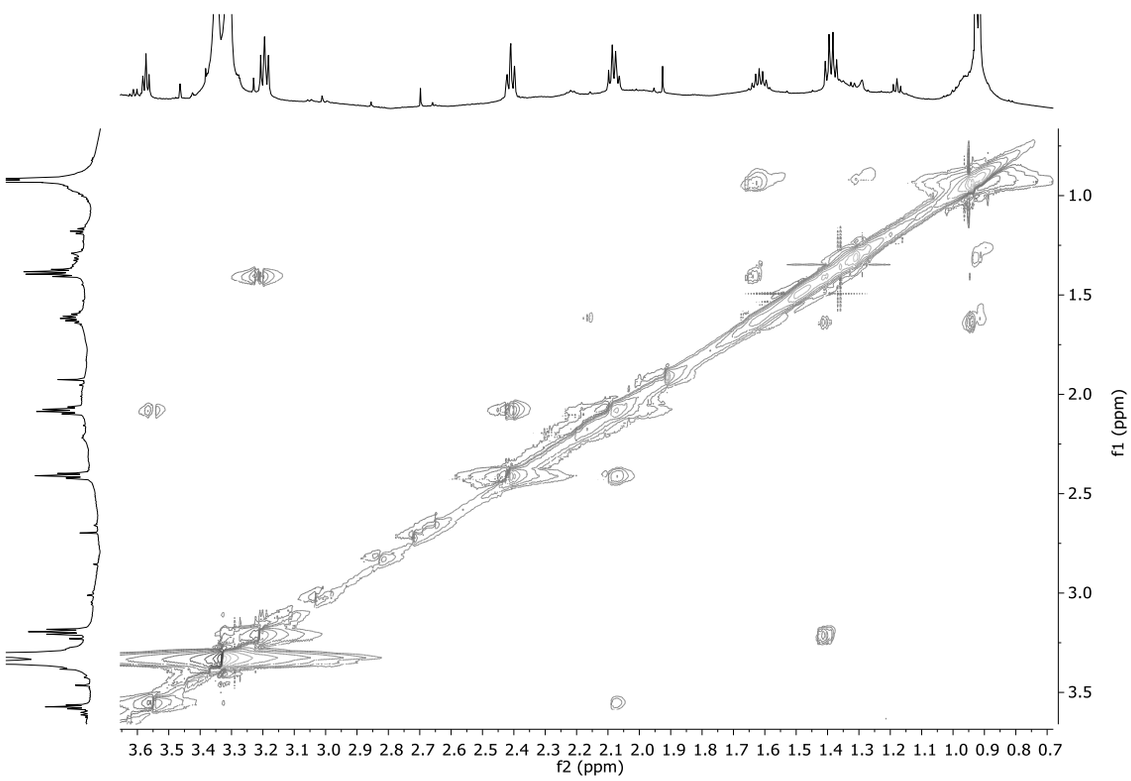

Figure. S160. COSY-spectrum (600.50, 600.50 MHz, CD_3OD, 297.2 K).

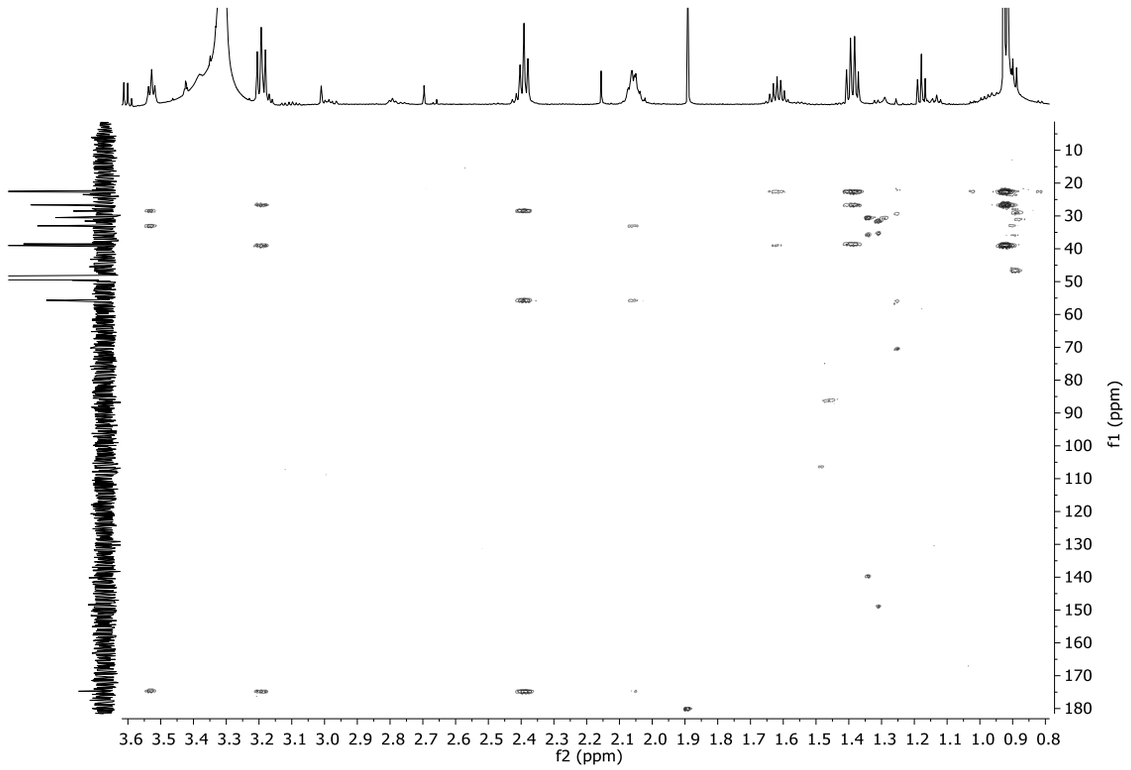

Figure. S161. HMBC-spectrum (600.50, 151.01 MHz, CD_3OD, 297.2 K).

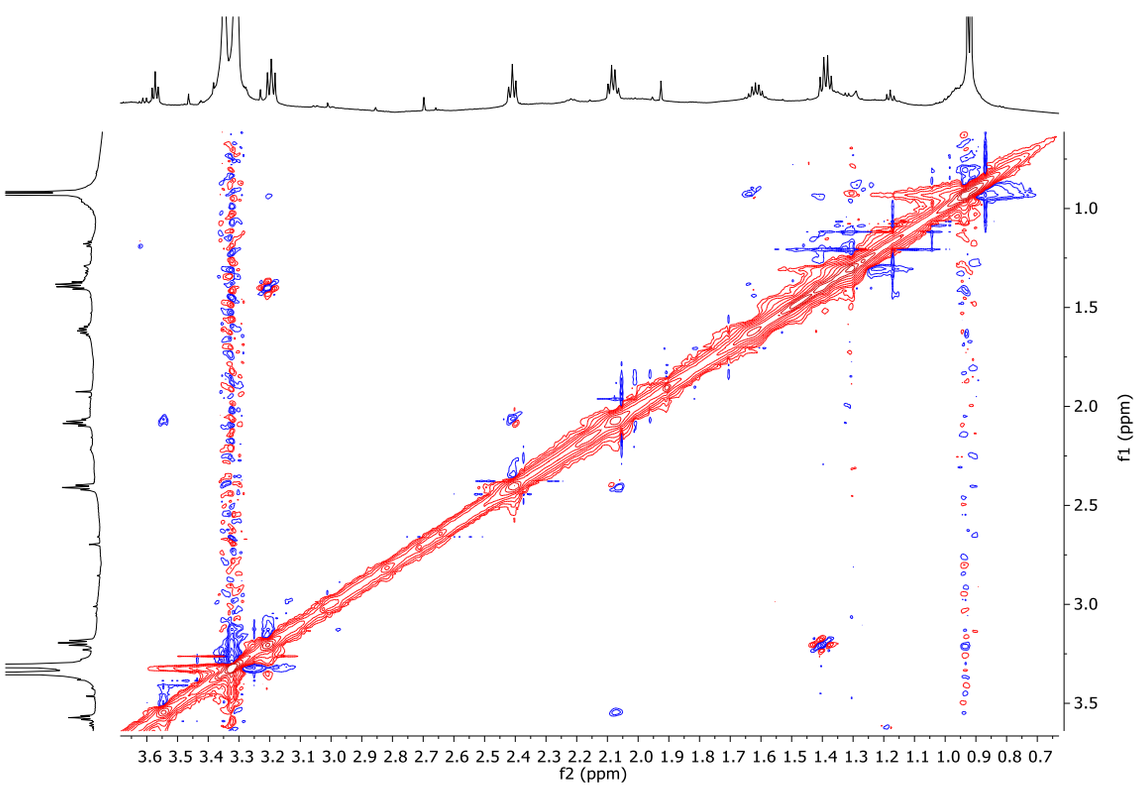

Figure. S162. NOESY-spectrum (600.50, 600.50 MHz, CD_3OD, 297.2 K).

9.25 N^5-2-methylbutylglutamine (**55**)

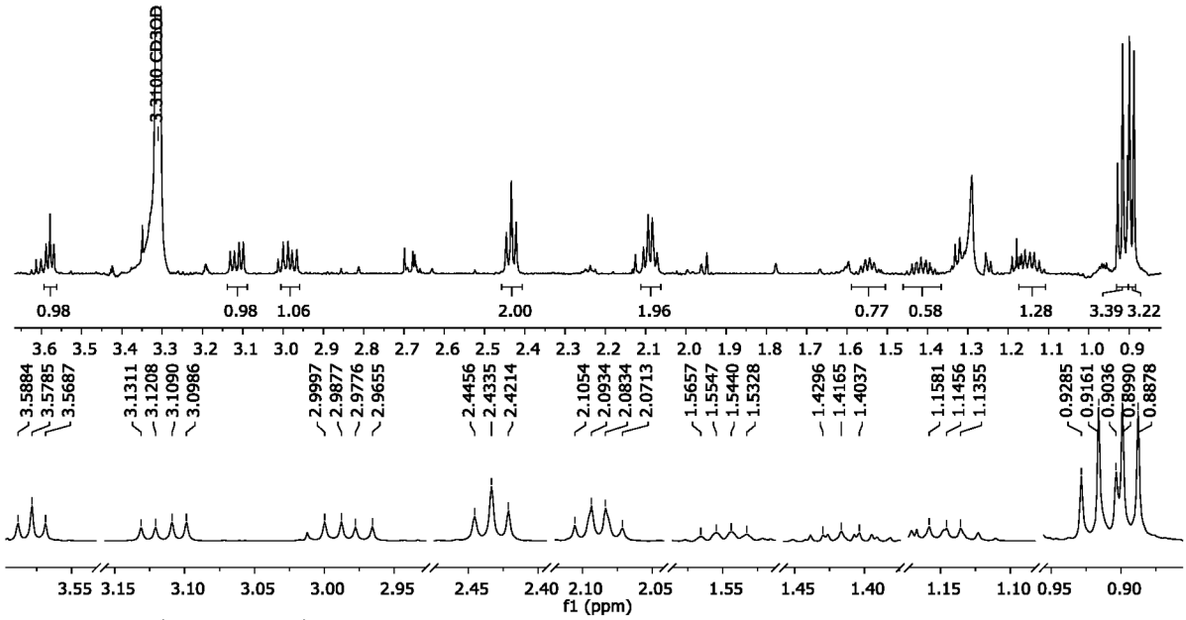

Figure. S163. ^{1}H-NMR and ^{1}H-NMR-spectrums with removed signal-free areas (600.50 MHz, CD_3OD, 296.1 K).

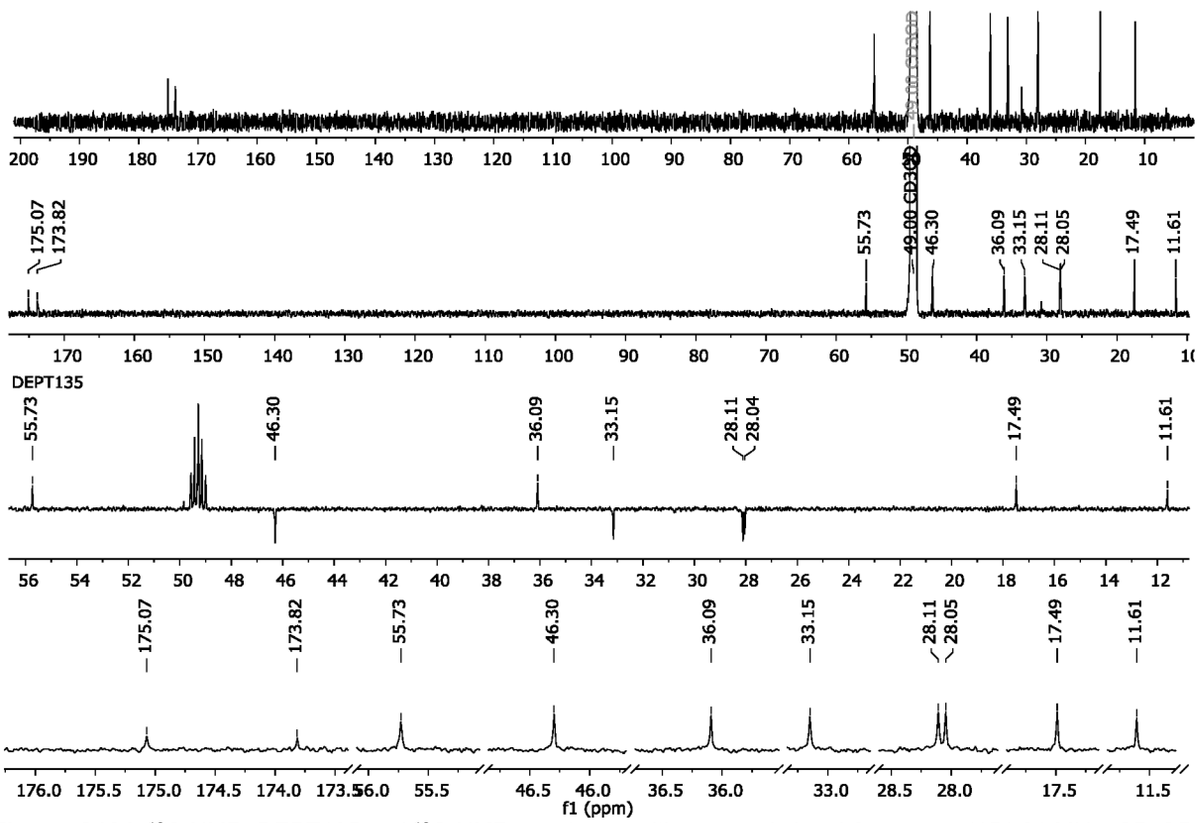

Figure. S164. ^{13}C-NMR, DEPT135 and ^{13}C-NMR-spectrums with removed signal-free areas (151.01 MHz, CD_3OD, 296.2 K).

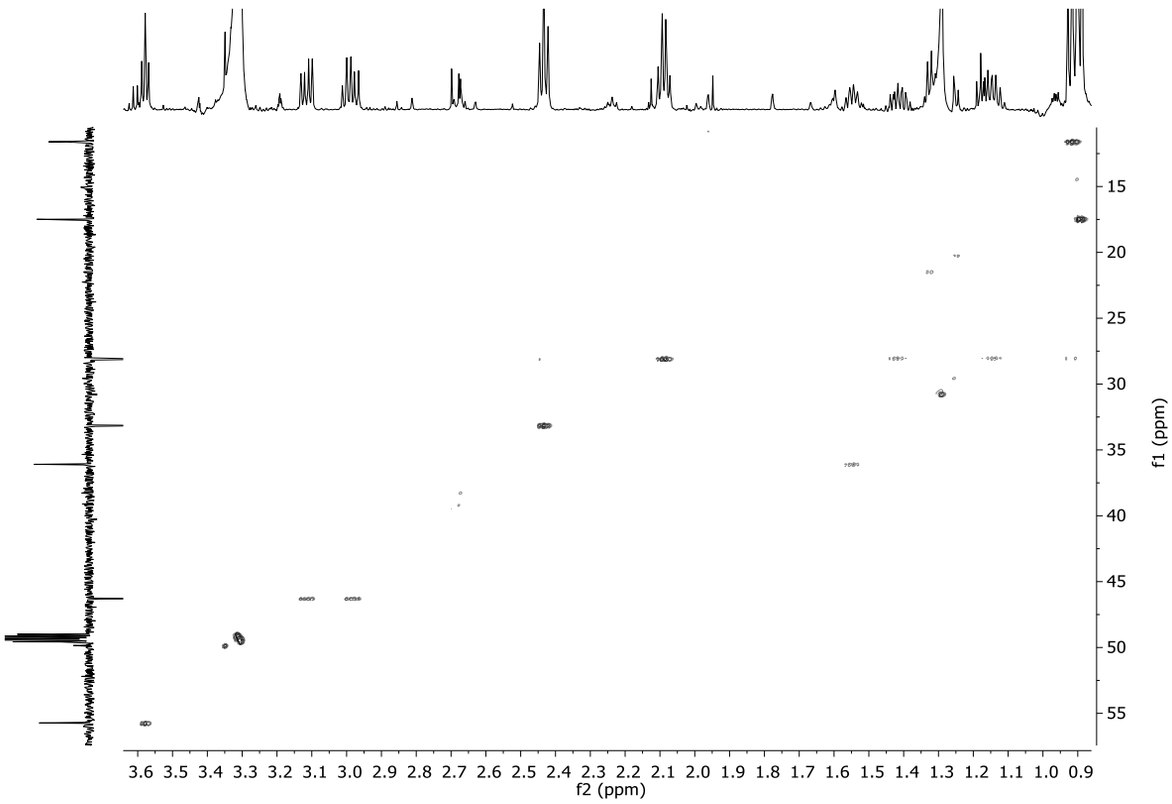

Figure. S165. HSQC-spectrum (600.50, 151.01 MHz, CD3OD, 296.1 K).

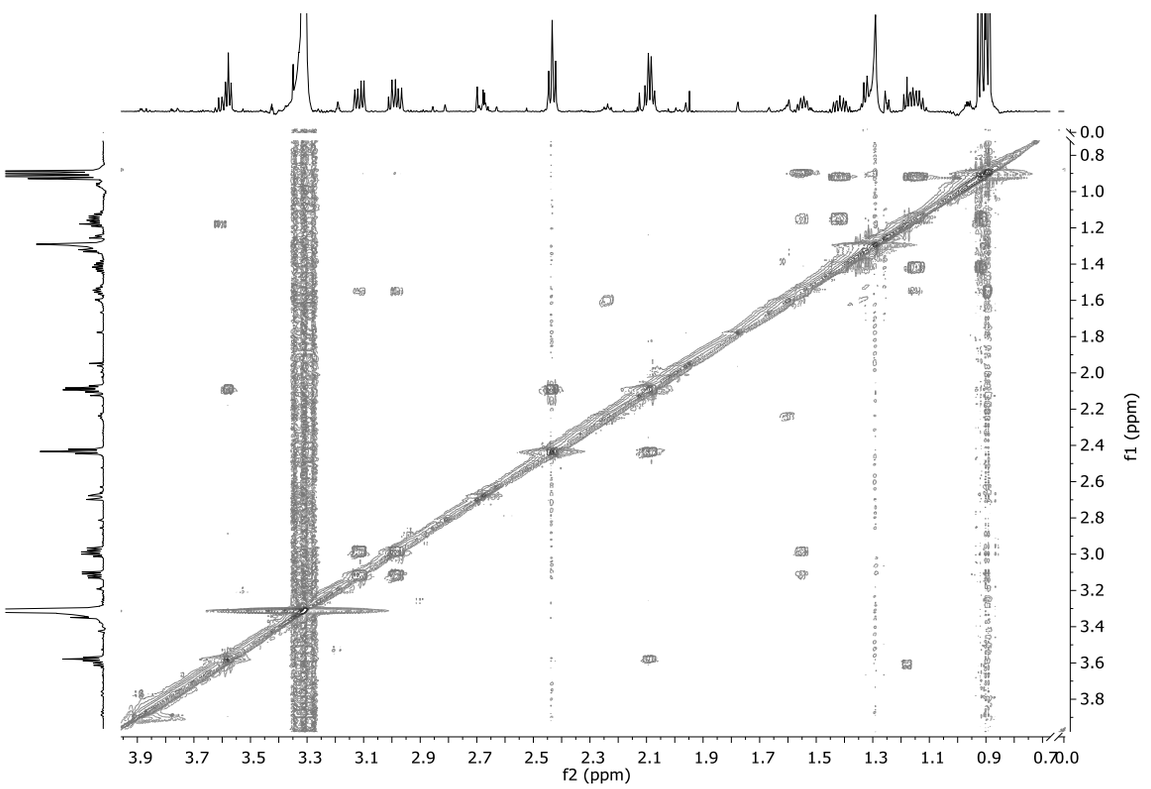

Figure. S166. COSY-spectrum (600.50, 600.50 MHz, CD_3OD, 296.1 K).

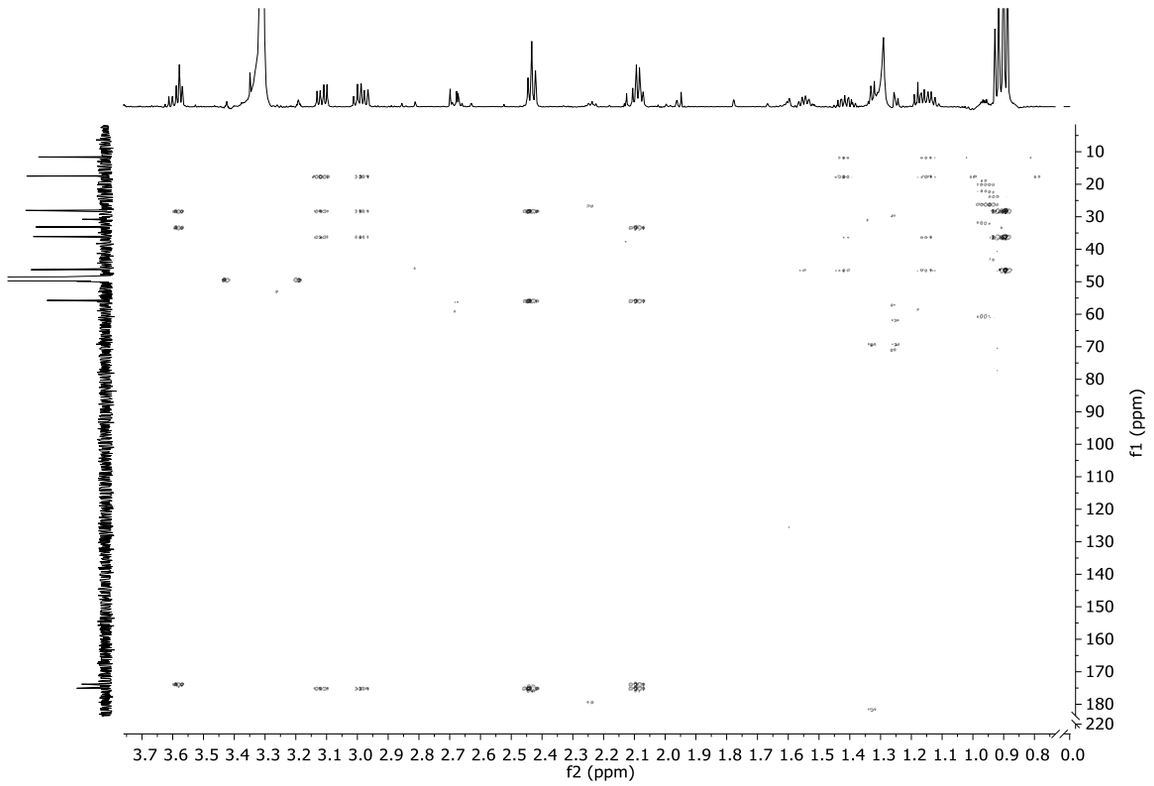

Figure. S167. HMBC-spectrum (600.50, 151.01 MHz, CD_3OD, 296.2 K).

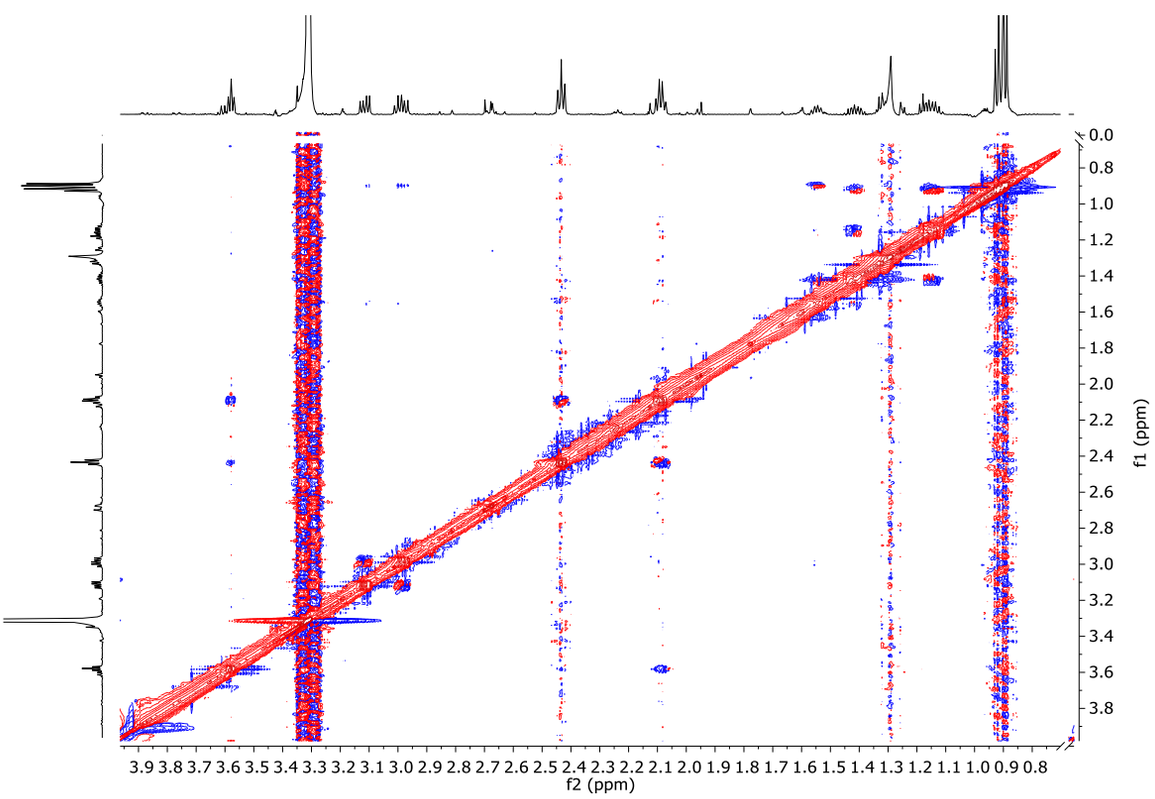

Figure. S168. NOESY-spectrum (600.50, 600.50 MHz, CD_3OD, 296.2 K).